2003 IEEE International Antennas and Propagation Symposium
and USNC/CNC/URSI North American Radio Science Meeting

# URSI Digest

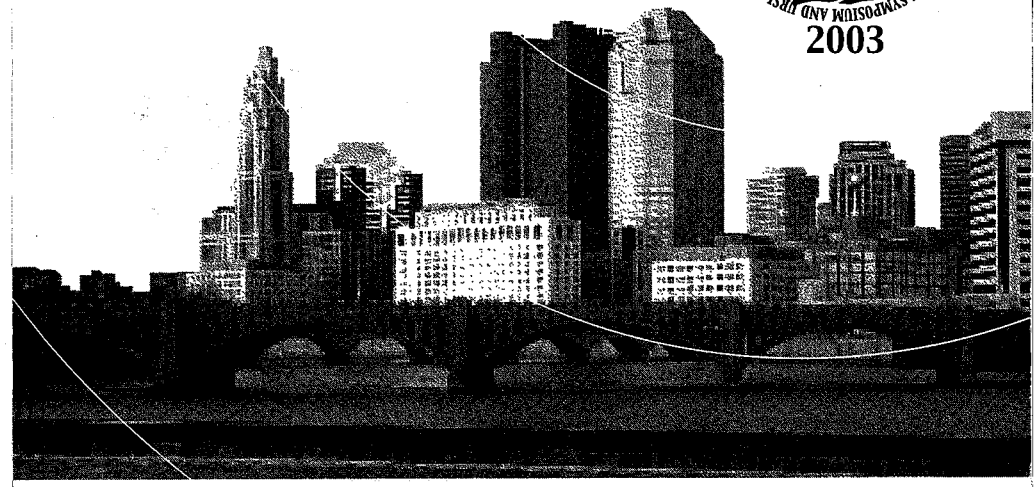

June 22-27, 2003
Columbus, OH

Our papers

81
178

56, 57, 58

80 85

168

608
611
615

W. L. STUTZMAN

# USNC/CNC/URSI
# North American Radio Science Meeting


June 22-27, 2003
Columbus, Ohio

## 2003 Digest

Held in conjunction with:
IEEE Antennas and Propagation Society
International Symposium

# IEEE Antennas and Propagation Society International Symposium 2003



For information about purchasing this four-volume set, write to the following address: IEEE Operations Center, 445 Hoes Lane, P.O. Box 1331, Piscataway, NJ 08855-1331.

| | |
|---|---|
| IEEE Catalog Number: | 03CH37450 |
| ISBN: | 0-7803-7846-6 |
| Library of Congress: | 90-640397 |

## *Chairman's Welcome*


### To all our friends and colleagues: Welcome to Columbus, Ohio!

It is privilege and pleasure, together and on behalf of the whole Steering Committee, to express to each of you our warmest welcome to the 2003 IEEE AP-S Symposium and North American Radio Science Meeting in Columbus, Ohio. This year is special because the North American Radio Science participation will provide papers and discussion on an even wider range of important topics, from Commissions A through K. We can assure you that you will be making a contribution to a great gathering, and you will be benefiting from discussions with many of your friends and colleagues on a large number of interesting topics.

The technical program co-chairs, Ron Marhefka and Jiti Gupta together, with Joel Johnson and Prabhakar Pathak, the URSI commission chairs, along with the 135 technical program committee members have put together a diverse and well-organized technical program. There are 164 total sessions and half-sessions for the 1575 papers to be presented. Roberto Rojas has organized 14 short courses, 7 on Sunday and 7 on Friday. Jin-Fa Lee is coordinating about 40 APS, URSI and joint APS/URSI special sessions. Our 2003 symposium will therefore be a very rich technical event! Also, you'll want to stop by the exhibitor's area, located right at the hub of the meeting area, which has been coordinated by Keith Shubert.

We are indeed proud to acknowledge that the entire ElectroScience Laboratory faculty, research scientists and staff contributed to making this conference a memorable one. In addition to those mentioned above for the technical program, we are pleased to acknowledge the enormous support we were fortunate to have from Frank Paynter on the electronic paper submission and web support. We are also pleased to acknowledge the leadership and support from Brian Baertlein, Bob Burkholder, Teh-Hong Lee, Rob Lee and Eric Walton.

We want to close this welcome with special thanks to our sponsors for their financial support. Northrop Grumman provided the funds for the Tote Bags and favors; Mission Research Corporation provided support for the Welcoming Reception, and the National Science Foundation provided support for the Student Paper Travel Grants.

On behalf of the entire steering committee we look forward to seeing you and greeting here in June. Have a pleasant trip!

Jonathan D. Young and John L. Volakis
Symposium Co-chairs

## *2003 APS/URSI Steering Committee*


***General Co-Chair***
Jonathan D. Young
Ohio State University
Phone: (614) 292-6657
Young.20@osu.edu

***General Co-Chair***
John Volakis
Ohio State University
PHone: (614) 292-5846
Volakis.1@osu.edu

***Special Sessions***
Jin Fa Lee
Ohio State University
Phone: (614) 292-7270
Lee.1863@osu.edu

***Technical Program***
Ronald J. Marhefka
Ohio State University
Phone: (614) 292-5752
Marhefka.1@osu.edu

***Tech Program Co-Chair***
Inder. J. Gupta
Ohio State University
Phone: (614) 292-5951
Gupta.11@osu.edu

***Short Courses/Workshops***
Roberto G. Rojas
Ohio State University
Phone: (614) 292-2530
Rojas-teran.1@osu.edu

***AP-S Liaison***
Prabhakar Pathak
Ohio State University
Phone: (614) 292-6097
Pathak.2@osu.edu

***URSI Liaison***
Joel Johnson
Ohio State University
Phone: (614) 292-1606
Johnson.1374@osu.edu

***Sponsors/Exhibitors***
Keith Shubert
Battelle Memorial Institute
Phone: (614) 424-4916
shubert@battelle.org

***Publications***
Teh-Hong Lee
Ohio State University
Phone: (614) 292-2043
Lee.52@osu.edu

***Publicity/Call for Papers***
Robert Lee
Ohio State University
Phone: (614) 292-1433
Lee.146@osu.edu

***Student Paper Contest***
Robert Burkholder
Ohio State University
Phone: (614) 292-4597
Burkholder.1@osu.edu

***Registration***
Brian Baertlein
Ohio State University
Phone: (614) 292-0076
Baertlein.1@osu.edu

***Local Arrangements***
Eric K. Walton
Ohio State University
Phone: (614) 292-5051
Walton.1@osu.edu

***Web Master***
G. Frank Paynter
Ohio State University
Phone: (614) 292-4946
Paynter.5@osu.edu

***Advanced Program***
Fernando Teixeira
Ohio State University
Phone: (614) 292-6993
teixeira.5@osu.edu


## *2003 APS/URSI Conference Facilitator*

***Three Dimensions***

Mary Ellen Vegter, Bonnie Grosek, Theodora Dirksen

## *2003 APS/URSI Technical Program Committee*

***Chair***
Ronald J. Marhefka

***Co-Chair***
Inder J. Gupta

Kenn Anderson
Y. Antar
Brian Baertlein
Constantine Balanis
E. A. Bering
Jennifer Bernhard
Wolfgang-Martin Boerner
Geoffrey Bower
Gary Brown
Jerry Burke
Robert Burkholder
W. Dennie Burnside
Gary Bust
Chalmers Butler
Filippo Capolino
John Carlstrom
Michael Carr
D. K. Chen
Zhi Ning Chen
Weng Chew
Christos Christodoulou
Peter Collins
R. Ted Compton
Anthea Coster
Steve Cummer
William A. Davis
Dan Dockery
Robert Dybdal
Romanus Dyczij-Edlinger
Samir M. El-Ghazaly
Steve Ellingson
Atef Z. Elsherbeni
Nader Engheta
Vakur Erturk
Heinrich Foltz
Gurudas Ganguli
Roland Gilbert
Allen W. Glisson
Julius Goldhirsh
Jaideva Goswami
Susan C Hagness
Jeffrey Herd
Kueichien Hill
Wayne Hocking
John Huang
Glen Hussey
Tamer Ibrahim
A Ishimaru
David Jackson
Gordon James
Dan Janning
Jianming Jin
Joel Johnson
Farzad Kamalabadi
David Kelley
Leo Kempel
Brian Kent
Per-Simon Kildal
Ozlem Kilic
Ahmed Kishk
Ira Kohlberg
Attila Komjathy
R. Kotiuga
Jeffrey Krolik
Y. Kuga
Ivan LaHaie
Kevin Lambert
Richard Langley
Jean-Jacques Laurin
Gianluca Lazzi
Jin-Fa Lee
Teh-Hong Lee
Hao Ling
Duixian Liu
Stuart A. Long
Anthony Martin
L. San Martin
John Mathews
Cliff Minter
Shantnu Mishra
Raj Mittra
Hossein Mosallaei
Ben Munk
Benoit Nadeau
Bob Nevels
Mike Newkirk
Edward Newman
Natalia Nikolava
Meers M Oppenheim
Hsueh-Yuan Pao
John Papapolymerou
Prabhakar Pathak
G. Frank Paynter
Andrew Peterson
Andrew Poggio
Ronald Pogorzelski
Omar M. Ramahi
Bodo Reinisch
Steve Reising
Roberto Rojas
David Routledge
John Sahr
Magdalina Salazar-Palma
Kamal Sarabandi
Tapan Sarkar
Stephen Schneider
B. Shanker
Michael Shields
Jiming Song
Gordon Staples
Jean-Pierre St-Maurice
W. Ross Stone
Chen-To Tai
Fernando Teixeira
Manos Tentzeris
Art Thansandote
Roberto Tiberio
Samir Trabelsi
Scott Tyo
Piergiorgio L. E. Uslenghi
Alejandro Valero
Guiseppi Vecchi
John Volakis
A. Voronovich
Parveen Wahid
Douglas H. Werner
James West
Ed Westwater
Brian Wilson
Kin-Lu Wong
Maj. William Wood
Jeffrey Young
Jonathan Young
Amir I. Zaghloul
Rick Ziolkowski

## *2003 APS/URSI Special Session Organizers*

E. A. Bering
Wolfgang-Martin Boerner
Geoffrey Bower
G. Brown
Gary Bust
F. Capolino
D. K. Chen
Zhi Ning Chen
Weng Cho Chew
R. Ted Compton
Steve Cummer
Dan Dockery
Romanus Dyczij-Edlinger
N. Eegheta
S.M. El-Ghazaly
N. Engheta
Vakur Erturk
R. Gilbert
Susan C. Hagness
Wayne Hocking
Glen Hussey
A. Ishimaru
D. R. Jackson
G. James
Jianming Jin
Farzad Kamalabadi
Per-Simon Kildal
Attila Komjathy
R. Kotiuga
Y. Kuga
Richard Langley
Gianluca Lazzi
Duixian Liu
L. San Martin
John Mathews
Cliff Minter
Raj Mittra
Hossein Mosallaei
Robert Nevels
Mike Newkirk
Meers M Oppenheim
Prabhakar Pathak
Omar Ramahi
B. Reinisch
Steve Reising
Roberto Rojas
John Sahr
Kamal Sarabandi
Motoyuki Sato
Chen-To Tai
F. Teixeira
Manos Tentzeris
Samir Trabelsi
Scott Tyo
P.L.E. Uslenghi
Guiseppi Vecchi
J.L. Volakis
A. Voronovich
Jim West
Ed Westwater
Brian Wilson
Kin-Lu Wong
R. Ziokowski

# *Antennas and Propagation Society 2003 Awards*

**2003 IEEE Electromagnetics Award**

Leo B. Felsen

*For innovative contributions to asymptotic and phase space methods for high frequency and short pulse electromagnetics in complex environments and interdisciplinary fields*

**Antennas and Propagation Society 2003 Awards**

**2003 Distinguished Achievement Award**

John D. Kraus

*For a career of outstanding innovation and invention in the field of antennas, and for the many students he has taught and inspired to excel in electromagnetics*

**2003 Chen-To Tai Distinguished Educator Award**

Chalmers M. Butler

*For outstanding contributions to electromagnetics education in the classroom and in graduate student supervision, and for his superlative communication of concepts in numerical electromagnetics.*

**2003 S. A. Schelkunoff Transactions Prize Paper Award**

R. Jean-Marc Cramer, Robert A. Scholtz, and Moe Z. Win

For the paper "*An Evaluation of the Ultra-Wideband Propagation Channel,*" May 2002

**2003 H. A. Wheeler Applications Prize Paper Award**

Jon W. Wallace and Michael A. Jensen

For the paper "*Modeling the Indoor MIMO Wireless Channel,*" May 2002

**2003 R. W. P. King Award**

Henrik Holter

For the paper "*On the Size Requirement for Finite Phased Array Models,*" co-authored with Hans Steyskal, June 2002

## *2003 IEEE Fellows*

Makoto Ando*
*For contributions to the design of high-gain planar waveguide arrays.*

Ercument Arvas*
*For contributions to the solution of electromagnetic scattering problems.*

Quirino Balzano
*For contributions to methodologies for assessing exposure to radiofrequency radiation from portable communication devices.*

Marek Edward Bialkowski*
*For contributions to the modeling, design, and testing of microwave guiding and radiating structures.*

Zoltan Joseph Cendes
*For contributions to the application of finite-element modeling to microwave guides, structures and circuits.*

Da Gang Fang
*For contributions to the development of the full-wave discrete complex image method and modified matched-layer absorbing boundary conditions.*

James Harvey
*For technical leadership in formulating and managing government research programs in science and technology.*

Kiyohiko Itoh
*For contributions to the development of small antennas and their applications.*

Ramakrishna Janaswamy*
*For contributions to numerical modeling techniques in radiowave propagation and electromagnetic scattering.*

Brian Michael Kent*
*For leadership in the development and application of radar cross section measurement.*

Randall William Kreutel*
*For contributions to antenna technology for satellite communications.*

Kwai-Man Luk*
*For contributions to the development of wideband microstrip-patch antennas and dielectric-resonator antennas*

Hiroshi Matsumoto*
*For contributions to the understanding of waves in nonlinear plasmas and microwave power transmission.*

Tung Sang Ng
*For contributions to signal processing techniques in spread spectrum communications.*

John William Rockaway*
*For technical leadership in the development and application of computational techniques for advanced antenna and electromagnetic system analysis.*

Brian C. Wadell
*For contributions to instrumentation applications.*

Tat Soon Yeo
*For contributions to scattering and synthetic-aperture radar.*

* evaluated by AP-S Fellows Committee

## *2003 APS/URSI Symposium Sponsors*

### *Platinum Level:*

Northrop Grumman, Electronic Systems

NORTHROP GRUMMAN

Electronic Systems

The Ohio State University

THE OHIO STATE UNIVERSITY

### *Gold Level:*

Mission Research Corporation

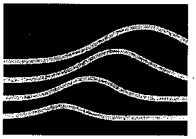

Mission
Research
Corporation

National Science Foundation

## Complex Media

**Co-Chairs:** V. V. Varadan
T. Wu

7:55 Opening Remarks



0-7803-7846-6/03/$17.00 ©2003 IEEE

# DYADIC GREEN'S FUNCTION FOR A GYRO-MAGNETIC MEDIUM

Abdullah Eroglu* and Jay Kyoon Lee
Department of Electrical Engineering and Computer Science
Syracuse University
Syracuse, New York 13244-1240 USA

In numerous electromagnetic applications such as remote sensing, wave propagation and scattering, monolithic integrated circuits and optics, it is necessary to compute the electromagnetic field inside the medium. When the dyadic Green's function (DGF) of the medium is known, it is relatively easy to find the electromagnetic field inside that environment. Because of this feature, the DGF method in electromagnetic applications still remains to be an attractive method for researchers over 50 years.

Many researchers have developed various techniques to obtain the DGFs for the isotropic and anisotropic multi-layered media. The most commonly used techniques include plane wave spectral representations of DGFs with vector wave functions, Fourier-transform domain representations with matrix analysis techniques, inverse operator technique, and characterizing each layer by an appropriate tensor and finding the Fourier transformed Green's function accordingly and the method of using transmission line network analog along the axis normal to the stratification.

The calculation of DGF for a magnetically gyrotropic or a gyro-magnetic medium such as a ferrite subject to a dc magnetic field requires special attention due to its Hermitian structured permitivity tensor. Y.A. Chow [*IEEE Trans. Antennas Propag.*, **AP-10**, 464-469, 1962] derived the dyadic Green's function of the gyro-electric-magnetic medium by extending F.V. Bunkin's [*Sov. Phys. JETP*, Engl. Transl., **5**, 277-295, 1957] tensorial Green's function technique which was only applied to an electrically gyrotropic or a gyro-electric medium. W.S.Weiglhofer [*Int. J. Electronics*, 73(4), 763-771, 1992] represented the DGF for a gyro-magnetic medium in terms of a single scalar Green's function which is a solution of a fourth order partial differential equation using duality between gyro-electric and gyro-magnetic medium.

In this paper, we derive the dyadic Green's function of a gyro-magnetic medium using a new formulation technique, which consists of a matrix method with dyadic decomposition in the k-domain and application of the principle of duality. Our work consists of two parts. In the first part, the DGF for a gyro-electric medium is derived. The system is transformed into the k-domain by taking the Fourier transform of the vector wave equation for DGF. In this domain, the representation of the DGF is reduced to find the inverse of an electric wave matrix. The inverse operation is accomplished by using the dyadic decomposition. As a final step, the DGF is constructed by expressing the adjoint of the wave matrix in terms of its wave vectors using the matrix method. In the second part, we apply the principle of duality to derive the relationship between the magnetic DGF of a gyro-electric medium and the electric DGF of a gyro-magnetic medium. This duality relationship is used to obtain the dyadic Green's function for a gyro-magnetic medium. It is shown that the dyadic decomposition greatly facilitates the calculation of an inverse operation, which is crucial in derivation of Green's function and the principle of duality makes it possible to find Green's function of a "dual" medium. An explicit and simple formulation presented here is useful in problems involving new types of advanced composite materials and magnetized ferrites which are widely used in high frequency electromagnetic and optical applications.

0-7803-7846-6/03/$17.00 ©2003 IEEE

# A novel method for the determination of the complex constitutive parameters of multilayer dielectric structures based on S-parameters measurements

Dr. Michael E. Baginski*, Dr. Manohar D. Deshpande†
and Daniel Lee Faircloth

Dept. of Electrical and Computer Engineering,
Auburn University, Room 423 Broun Hall, Auburn, Alabama, 36849, USA

**Abstract**

A novel method for the determination of the complex constitutive parameters of multilayer dielectric structures using X-band S-parameter measurements obtained using an HP-8510 Network Analyzer is presented here. It is assumed that the region of the section of the waveguide containing the sample consists of n-planar layers of uniform cross-sectional dimensions of the waveguide (X-band). Assuming only the dominate $TE_{10}$ mode propagates, the formulation of the scattering parameters for non-magnetic materials in terms of the unknown complex permittivities and geometric dimensions of the layered dielectric is done using the Method of Moments (MOM) yielding S-parameters (S = function($\epsilon$,geometry). Determination of the complex permittivities for each region is accomplished via a solution to an inverse problem where an error function (objective function) between predicted and measured values of the scattering parameters is minimized using a least squares error approach where the objective function error is defined by the equation $(error = s_{m,n(measured)} - s_{m,n(formulated)})$. Several alternative instrumentation and numerical approaches are also discussed in the presentation.

The resulting complex permittivities provide a 'best fit' to the input S-parameter measurements. Sensitivity of the method to both computational and measured errors was thoroughly investigated. The results indicate that the total error in the layered samples' complex permittivity value is primarily dependant on accuracy in sample construction (e.g., uniformity of layer thicknesses and cross-sectional dimensions). The results of the analyses of five representative multilayered samples are presented. Excellent agreement was found in a comparison of the predicated and known values of each layer's complex permittivity. In all cases considered, the overall accuracy of this technique is found to excellent ($error \sim 3-7\ \%$).

Previous work in this area relied on standard algorithms for determining the effective or "bulk" constitutive parameters of the entire layered material and neglected the possibility of parameter variations within the sample. If the permittivity of specific dielectric layers was required, the sample was typically physically dissected into several smaller samples where the material properties are assumed relatively constant and each subsection analyzed separately. Information obtained in this manner placed severe limitations on the usefulness of this technique. Samples are required to be of sufficient thickness so that material loss and damage during preparation can be minimized. However, many materials currently used are relatively thin and are intentionally fabricated with graded or layered electrical properties for specific purposes.

The results of this study have shown a highly accurate alternative solution of the problem where accuracy is due to errors in the sample fabrication process thus allowing individual layers to be characterized.

*Supported by a grant from NASA

†Research Scientist at NASA Langley, VA

0-7803-7846-6/03/$17.00 ©2003 IEEE

# Measurement of Circuit-Embedded Artificial Permeability Meta-Materials Utilizing Frequency Extended Perturbation Method

Kevin Buell, and Kamal Sarabandi
*Radiation Laboratory*
*Electrical Engineering and Computer Science*
*University of Michigan, Ann Arbor, MI 48109-2122*
*[kbuell and sarabandi]@umich.edu*

While low-loss dielectric materials offer a wide range of permittivity values, the availability of magnetic materials for microwave applications is woefully limited. Advanced artificial meta-materials which provide desirable bulk EM characteristics not available in naturally occurring materials have been developed, presenting a challenge to existing measurement methods. Such materials promise among other things, a wide range of selectable possible permeability values in the microwave region at low losses. Recently developed meta-materials provide highly desirable bulk properties including reactive impedance surfaces yielding greatly improved miniaturized patched antennas and embedded-circuit resonators yielding engineered selectable anisotropic or isotropic permittivity and permeability.

Potential applications of embedded-circuit resonators are numerous and promising, but before application, such materials must be fabricated and characterized to validate their theoretical permittivity and permeability. In order to measure these samples across a bandwidth a novel method for determining $\varepsilon_r$,and $\mu_r$ as a function of frequency from a single resonant method is presented. This technique has the benefit of high accuracy at the resonant frequency while simultaneously providing results across a bandwidth. This is particularly important for a dispersive medium such as this meta-material.

**Embedded-Circuit resonators for Engineered Permittivity and Permeability**

"Metamaterials" are engineered (nano) composites that exhibit superior properties that are not found in nature and not observed in the constituent materials. By embedding circuit elements which are very small relative to the operating wavelength, the electric or magnetic energy storage property of the circuit may be imparted to the larger bulk material. In natural materials atoms and molecules perform the role of electric and magnetic energy storage to determine the materials permittivity and permeability. In metamaterials, electromagnetically small circuits and engineered inclusions may be employed for this same purpose.

One of the simplest circuits to demonstrate this phenomenon is an LC resonator in a natural dielectric medium. Since the electric and magnetic storage of the embedded circuits are a consequence of the geometry of the microstrip elements, the bulk permittivity and permeability of this manufactured medium are independently controllable by adjusting the microstrip geometry.

In planar array medium of such elements the permittivity ($\varepsilon$) and permeability ($\mu$) exhibit anisotropic behavior such that the effective permeability and permittivity tensor are given by $\mu_y=\mu_{eff}$, $\mu_x=\mu_z=\mu_0$ and $\varepsilon_z=\varepsilon_{eff}$ while $\varepsilon_x=\varepsilon_y=\varepsilon_0$. Analytical formulations of $\varepsilon_{eff}$ and $\mu_{eff}$ as a function circuit geometry exist, but only experimentation can validate them. (K. Sarabandi, "Electro-Ferromagnetic Tunable Permeability, Band-Gap, and Bi-Anisotropic Meta-Materials Utilizing Embedded-Circuits" AP Symposium, 2003).

An engineered Meta-Material composed of embedded circuits to achieve artificial permeability is designed, fabricated, and measured.

**Frequency Extended Perturbation Method**

Traditional perturbation method is applied to determine $\mu_r$ or $\varepsilon_r$ with high accuracy at a single frequency. By placing a small sample in the null of the magnetic field of a resonant cavity and observing the resonant frequency shift $\varepsilon_r$ can be determined. At the E-field null $\mu_r$ can be measured.

In a more generally conception every point in the perturbed system responses frequency response is a point-to-point mapping of the unperturbed system response. The traditional perturbation method equations represent the frequency portion of the mapping algorithm applied at the resonant peak only. In the frequency extended perturbation method, frequency mapping is applied to determine $\mu_r$ or $\varepsilon_r$ across a bandwidth. To develop the magnitude mapping algorithm the sample losses and the compression/expansion of the spectral response must be accounted for as they will tend to narrow or widen the 3-dB bandwidth while raising/lowering the peak transmission coefficient. Luckily, if the change in 'Q' between perturbed and unperturbed cases and dispersion are minor, this difference can be ignored and the predicted system response easily obtained.

To validate this inversion method a small volume fraction (1%) non-dispersive dielectric of $\varepsilon_r$=2.17 with low loss (Tan$\delta$=0.001) was placed in a physical cavity and the perturbed and unperturbed system responses were measured, results validates the extended perturbation method is +/- 10% accurate over a 15% bandwidth.

# Free Space Characterization of Frequency dependent Metamaterials with Complex Electromagnetic Properties

Vasundara V. Varadan* and Anilkumar Tellakula+
* Center for the Engineering of Electromagnetic and Acoustic Materials & Devices, The Pennsylvanaia State University, University Park, PA 16802
+HVS Technologies, Inc., 309 Science Park Road, State College, PA 16803

ABSTRACT

A free space system for the measurement of complex effective permittivity and permeability of metamaterials is described here. Electromagnetic metamaterials are structured composites formed either from periodic or random arrays of scattering elements. The interesting aspect of metamaterials is that they can exhibit a frequency region in which either the real part of permittivity is negative or the real part of permeability is negative or both. The index of refraction can be negative in these materials (V. G. Veselago, Sov. Phys. Usp. 10, 509, 1968.)

We use a free space microwave measurement system, which is suitable for electromagnetic property measurements in the frequency range of 5.8 to 40 GHz (and extendible to 110 GHz). The frequency range is covered using a single connection, single sweep vector network analyzer, along with 3 pairs of spot focused horn lens antennas. This method is based on illuminating the sample with plane waves by focusing the microwave beam to a measurement plane. Hence, a single sample can be characterized over the entire frequency range, unlike other techniques that are limited to a narrow frequency band. Characteristics of metamaterials such as negative angle of refraction can be verified using the oblique incidence measurement capability provided by this setup. The complete system is calibrated using the TRL calibration method modified for free space measurements. The reflection and transmission coefficients (S-parameters) of the metamaterial are measured and inverted using closed form expressions to determine the complex permittivity and permeability. Electromagnetic properties of several metamaterial samples, fabricated by periodic placement of metallic wires in a dielectric medium, are evaluated as a function of frequency and the results will be presented. It is seen that only the real part of permittivity is negative in the frequency range of 5.8 to about 11 GHz. The real part of permeability is approximately 1. It is also observed that the plasma frequency (when permittivity=1) is about 12 GHz.

**Additional Information:**

1. Commission B (Fields and Waves), B2.Novel and complex media
2. A free space system is used to characterize complex metamaterials over a wide frequency band for the first time.
3. Previous work was mainly on modeling metamaterials and computing electromagnetic properties through simulations.

0-7803-7846-6/03/$17.00 ©2003 IEEE 

**Using FDTD To Illustrate the Behavior of Double Negative Materials**

Raymond J. Luebbers
Remcom Inc.
315 S. Allen St., Suite 222
State College, PA, 16801
rjl@remcom.com

There is strong interest in the behavior of metamaterials which have negative real parts for both permittivity and permeability. These are called by various names, including Negative Index Materials (NIM) and Double Negative Materials (DNG). It has been conjectured that these materials may have significant practical applications. Fully understanding their behavior is important to these potential applications. This understanding is initially challenging, since they behave in ways that appear to be contrary to intuition. For example, due to the negative index of refraction, the electromagnetic waves in DNG media may appear to defy causality and propagate toward the source. The ability to include these materials in full wave three dimensional solvers will be an important aid in using these materials in actual three dimensional designs.

The Finite Difference Time Domain (FDTD) method can be applied to these DNG materials ®. W. Ziolkowski and R. Heyman, Phys Rev E, Vol 64, 056625, October 2001) with good success. While several techniques for this exist, in this paper the recursive convolution method has been applied to both the permittivity and permeability. Both are modeled with Drude behavior, thus satisfying causality and allowing stable FDTD results to be obtained. Since calculations are made in the time domain, the results are determined by straightforward numerical methods. The ability of the time domain results to show the transient interaction of the electromagnetic fields with the DNG materials provides important insights into their characteristics, including the physical impact of negative phase velocities that can be superluminal. Results which seem to defy causality are readily observed. Investigation of these results is an important consideration of this paper.

0-7803-7846-6/03/$17.00 ©2003 IEEE 

# Analysis of Discontinuities of Double Negative (DNG) Slab Waveguide Sandwiched between Two Conventional Slab Waveguides

Hao Dong and Thomas X. Wu
School of Electrical Engineering and Computer Science
University of Central Florida,
Orlando, FL 32826

In 1968 [V.G. Veselago, *Soviet Phys. Uspekhi* **10**, 509, (1968)], Veselago theoretically investigated plane wave propagation in double negative (DNG) material whose permittivity and permeability were assumed to be simultaneously negative, and predicted that electromagnetic plane waves in such medium would propagate in a direction opposite to that of the flow of energy. The direction of the Poynting vector is antiparallel to the direction of phase velocity, contrary to the case of plane wave propagation in conventional simple media. Recently, renewed interests to DNG media appears. Ziolkowski [R.W. Ziolkowski and E. Heyman, *Physical Review E* **64**, 056625, (2001)] investigated the propagation of electromagnetic waves in DNG media from analytical, numerical and experimental point of view. Engheta [N. Engheta, *Digest of URSI-USNC National Radio Science Meeting*, 66, Boulder, (2002)] proposed the DNG waveguide and analyzed the dispersion diagram of DNG slab waveguide and found that the portion of the guided mode inside the slab has the Poynting vector antiparallel to the direction of phase flow of the mode and the portion of guided mode outside the slab has the Poynting vector parallel with phase flow. If a conventional slab waveguide is put next to a DNG slab waveguide, one can have the "anti-directional coupling" [A. Alu and N. Engheta, *2002 IEEE-Nanotechnology Conference*, Washington DC, 233, (2002)].

In this paper, we use the mode-matching method to analyze the discontinuity structure of a DNG waveguide sandwiched between two dielectric slab waveguides as shown in the Figure below. The field representations in the transverse direction and the scattering characteristics of discontinuities in the longitudinal direction are derived. Four cases with different height of the waveguide are considered and the results are discussed. For case 1, when all the modes in the DNG waveguide are cutoff, the percentage power of the transmitted $TM_0$ mode is 0. For case 2, if the guided mode in the DNG waveguide is at the critical point, the reflection of $TM_0$ mode and the backward radiation are the majority components except for the resonant points. At those resonant points, $TM_0$ mode has no reflection and most of the power becomes the transmitted $TM_0$ and forward radiation. For case 3, when the DNG waveguide is in the special region, there are oscillations in the reflected and transmitted power because of the coupling of the special two modes. The reflection of $TM_0$ mode is much smaller and the transmission takes the majority component. For case 4, when only one TM mode exists in the DNG waveguide, this mode is almost matched with the $TM_0$ mode in the dielectric waveguide. For this case, the reflected $TM_0$ and $TM_1$ mode, the transmitted $TM_1$, backward radiation and forward radiation are all very small. The transmitted $TM_0$ is the majority component.

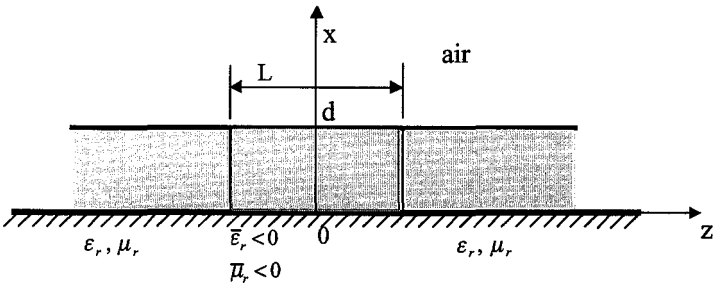

# A Generalized Fourier Transform Applied to Propagation in Irregular Stratified Chiral Media

Paul E. Crittenden*
Department of Mathematics and Statistics
University of Nebraska-Lincoln
Ezekiel Bahar
Department of Electrical Engineering
University of Nebraska-Lincoln

Generalized Fourier transforms appropriate for the expansion of the electromagnetic fields scattered at a rough interface between two chiral materials with laterally varying electromagnetic properties are derived. The transforms are used to obtain the generalized telegraphists equations for scattering in chiral media. The telegraphists equations are a set of coupled ordinary differential equations for the forward and backward wave amplitudes of the $z$-component of the magnetic field and the $y$-component of the electric field.

Schelkunoff (S. A. Schelkunoff, *Bell Syst. Tech. J.*, **31**, 784–801, 1952) derived a similar set of equations using a rigorous method of mode matching in irregular achiral waveguides. Unlike the discrete waveguide mode spectra, the spatial wave spectra in this work are continuous and discrete. A similar set of equations for achiral media, which also included discrete and continuous wave spectra, was derived by Bahar (E. Bahar, *Canadian J. of Phys.*, **50**, 3132–3142, 1972) and has been solved numerically and iteratively. From a solution to the generalized telegraphists, the field transforms can be found and inverted to find the diffusely scattered fields. Solutions to the generalized telegraphists equations could be obtained using assumptions appropriate for particular applications. In deriving the generalized telegraphists equations, no assumptions are made about the characteristics of the surface, the frequency of the source, or the location of the source and observation point. Therefore, they provide an advantageous starting point for deriving solutions to a very broad class of problems.

Chiral media are materials with a handedness. They interact differently to left and right circularly polarized electromagnetic waves, allowing one or the other to propagate with a faster phase velocity. The root cause of chirality is believed to be imbedded helical substructures (of either macromolecules, molecules, or DNA, depending on the wavelength). Manmade chiral materials have also been fabricated by imbedding conducting helices in an achiral host. With a rigorous solution for electromagnetic wave propagation in irregularly stratified chiral materials, the discrimination between different chiral media and the optimization of the electromagnetic characteristics of artificial chiral media is possible. Possible military applications include the detection of films of biological weapons sprayed on the surface of battlefields and the optimization of manmade chiral materials for stealth technology. Space exploration applications could include detecting life on other planets and the pre-screening of interplanetary space vehicles. The eye consists of layers of chiral media, that alternate between left and right handedness. This leads to an application in biology. Pharmaceuticals, food additives, and fertilizers, made from the same ingredients, can have vastly different properties if the molecular structures are left or right handed. In electrical engineering, waveguides with organic chiral cores are investigated for use in integrated optical devices, including polarization transformers, modulators and directional couplers (W. N. Herman, *J. of the Opt. Soc. of Am. A*, **18**, 2806–2818, 2001). In all of these settings, small variations in the cross sections could significantly affect electromagnetic wave propagation.

0-7803-7846-6/03/$17.00 ©2003 IEEE

# Natural Mode Description of the Transient Field Reflected by a Planar Layer of Debye Material

J. Oh and E.J. Rothwell*
Department of Electrical and
Computer Engineering
Michigan State University
East Lansing, MI 48824
rothwell@egr.msu.edu

Michael J. Havrilla†
Department of Electrical and
Computer Engineering
Air Force Institute of Technology
WPAFB, OH 45433

Layered materials are often applied to conducting surfaces for the purpose of reducing the scattered field strength within specific frequency bands. A wideband pulse may be used to interrogate the layered structure so as to characterize the materials or determine whether the materials have degraded. If the late-time behavior of the reflected field can be expressed as a natural resonance series, then techniques such as the E-pulse method (G.J. Stenholm, et. al., *IEEE AP-S Int. Symp.*, Boston, 2001) can be used to determine whether the material properties have changed compared to baseline values determined by previous measurements.

We have shown previously (E. Rothwell, et. al., URSI North American Radio Science Meeting, San Antonio, 2002) that the transient field reflected from a conductor-backed planar layer with frequency-independent material parameters (permittivity, permeability, and conductivity) has both an early-time and a late-time component. The early-time component consists of the reflection of the incident wave from the air-slab interface. The late-time component is produced by the ensuing multiple reflections within the slab, and is a pure natural resonance series. To show this it was necessary to identify the two branch points arising in the inverse Laplace transform of the frequency-domain reflection coefficient, and to show that there is no contribution from the integral around the branch cut. In this paper we analyze the transient field reflected by a conductor-backed slab of Debye material with frequency-dependent permittivity. The Debye material gives rise to a frequency-domain reflection coefficient with two pairs of branch points. We show that there is no contribution from the integral around the two associated branch cuts, and thus the late-time scattered field is again a pure natural resonance series.

Results computed using the resonance formulation are verified by comparison to the direct inverse Fast Fourier Transform. The distribution of resonance frequencies in the complex plane and their dependence on the Debye parameters are examined.

†The views of the co-author expressed in this article do not reflect the official policy of the U.S. Air Force, Department of Defense, or the U.S. Government.

0-7803-7846-6/03/$17.00 ©2003 IEEE

# SURFACE WAVE SUPPORTED BY A PLANAR SEMICONDUCTOR-DIELECTRIC INTERFACE AND ITS DISTRIBUTED CIRCUIT REPRESENTATION

Mohamed El-Dessouki and Thomas Wong*
Department of Electrical and Computer Engineering
Illinois Institute of Technology
Chicago, Illinois 60616

Surface wave interactions on a semiconductor distinguish themselves from others mediated by surfaces without free charges. The presence of mobile charges leads to both dissipation in the energy carried by the wave through conduction current and screening of the field from the interior of the semiconductor. The latter effect results in a more rapid decay in the transverse component of the electric field than that found in a surface wave guided by a dissipative dielectric having a similar loss tangent. Depending on the applications, such charge accumulation may be employed to provide controllable phase shift or it may be suppressed by external bias or otherwise to facilitate a low attenuation interconnect for components as found in RF integrated circuits.

A full-wave solution to the surface wave problem involving a semiconductor requires the coupling of the Maxwell's equations to the equations of motion of the charges in the semiconductor. Previous efforts have been made to identify the salient features of the resulting space-charge wave in the semiconductor but the formulation remains until today a computationally intense exercise. An investigation on a canonical structure aiming at obtaining a distributed circuit representation to enable the application of transmission line theory to the analysis and simulation of wave interactions in components on a semiconductor substrate would appear attractive.

In this work, the surface wave (TM) supported by a semiconductor-dielectric interface is analyzed in terms of the propagation constant, field and charge distribution, and the dependence of the wave impedance on the carrier concentrations and frequency. Considerations made on the results of analysis and the asymptotic behavior of computational outcomes led to the development of a distributed circuit representation for the structure in which each element can be justified by the physical process of charge-field interaction. An extension of the approach to the case of a metal-insulator-semiconductor structure was made to identify the features associated with a quasi-TEM wave that propagates along a semiconductor surface. Results of computation carried out for structures with typical material parameters will be presented. The assumptions and the range of validity of the distributed circuit representation will be discussed.

0-7803-7846-6/03/$17.00 ©2003 IEEE 

## Full-Wave Propagation of Short-Pulse Wavepackets in Ray-Chaotic Billiards

Vincenzo Galdi[1], Innocenzo M. Pinto[1], and Leopold B. Felsen[2]

*(1) Waves Group, Department of Engineering, University of Sannio, Benevento, Italy*

*(2) Dept. of Aerospace & Mechanical Eng., Boston University, USA (part-time)*
*Also, University Professor Emeritus, Polytechnic University, Brooklyn, NY USA*

During the last decade, there has been a growing interest in electromagnetic (EM) propagation environments featuring *ray-chaotic* behavior. Apart from intrinsic theoretical aspects (ray theory describes wave dynamics in the zero-wavelength limit), this interest is motivated by the possibility of designing novel devices and components (microlasers, resonators, etc.) where ray chaos has been demonstrated to play a key role (see, e.g., C. Gmachl *et al.*, *Science,* **280**, p. 1556, 1998). Since *ray chaos* implies *exponential* separation of nearby-originating *ray trajectories*, this concept *cannot* be used to describe *finite* (nonzero) *wavelength* dynamics; the *linear* wave equations *do not* exhibit exponential sensitivity to initial conditions in deterministic environments. Nonetheless, it is widely accepted that one should expect "signatures of ray-chaos" in some *wave* solutions.

In a recent investigation (V. Fiumara *et al.*, *Proc. ICEAA '99*, Turin, Italy, Sept. 13-17, 1999, p. 357), we have explored the possibility of utilizing the ray-chaotic properties of a stadium-shaped cavity excited by a pulsed (wideband) wavepacket to create a "pulsed reverberation enclosure," with potential applications as a testbed for EM interference (EMI) and/or EM compatibility (EMC). Ideally, equipment under test placed in such an environment should be exposed to pulsed illumination with nearly *uniform* distribution in arrival direction, *independent* of position and/or orientation of the target, thus allowing for assessment of figures of merit like shielding effectiveness, spurious emission, etc. Our preliminary analysis was based on the highly-idealized assumption that the wavepacket launched in the cavity behaves as a *nondiffracting bullet*, which preserves its shape and space-time localization while propagating inside the cavity and undergoing multiple reflections at the boundaries. This assumption allows for a purely *kinematic* (i.e., ray) qualitative analysis which confirms the above expectations.

In this paper, we go one step further by solving the *full-wave* propagation problem of a short-pulse wavepacket in a stadium-shaped enclosure, using a finite-difference time-domain (FDTD) code. In this connection, various field statistics (e.g., space-time correlations) are computed and analyzed. Furthermore, a wave-oriented *local spectral analysis* (in terms of pseudo-Wigner distributions) is performed in order to parameterize phase-space features of particular interest (e.g., the distribution of arrival angles). Preliminary results indicate the presence of distinct features in the field distribution and statistics, which are of potential interest in EMI/EMC applications. These features do not seem to have any resemblance to those found in "regular" (e.g., rectangular and circular) billiards, and may thus be viewed as *ray-chaos signatures* in the *full-wave* regime.

0-7803-7846-6/03/$17.00 ©2003 IEEE 

# The Distortion and Crosstalk of Wideband Pulse Waves Propagating in Some Cylindrical Coplanar Waveguides and Microstrip Lines

*W. Y. Yin, B. Guo, X. T. Dong, and Y. B. Gan*

Temasek Laboratories, National University of Singapore (NUS), 10 Kent Ridge Crescent, Singapore 119260, E-mail: tslyinwy@nus.edu.sg

***Abstract***: Coplanar waveguides (CPWs) have been widely used in radio frequency and monolithic microwave integrated circuits (RF(MM)ICs), due to their several advantages over conventional microstrip. Further, picosecond pulse propagation in some planar CPWs has been examined by some researchers in the past a few years, and the coupling among neighboring strips can be effectively reduced by optimizing the structure parameters of the CPWs. On the other hand, the dispersion characteristics of various cylindrical CPWs and microstrip lines have been studied by some researchers. Among these one should mention the work done by Wong *et al*, where the effective permittivity of the dominant mode and the characteristic impedance of different structures have been examined symmetrically using the Galerkin's method (R. B. Tsai, and K. L. Wong, *IEEE Trans. MTT*, 43, 1607-1610, 1995; H. S. Su and K. L. Wong, *IEEE Trans. MTT*, **44**, 2120-2122, 1996). These types of waveguide structures have some unique features and can meet certain requirements in advanced antennas and monolithic microwave integrated circuit designs.

In this work, we are focused on the propagation of wideband pulse waves propagating in some cylindrical coplanar waveguides and microstrip lines. The mathematical treatment is based on the Galerkin's method in the spectral domain and the fast Fourier transformation (FFT). Parametric studies are performed to show the hybrid effects of geometrical and material parameters on the pulse wave distortion and crosstalk (Fig. 1).

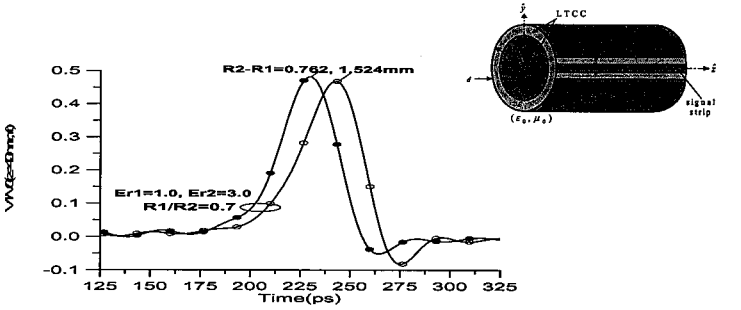


Figure 1. The Gaussian pulse wave response of a cylindrical CPW.

0-7803-7846-6/03/$17.00 ©2003 IEEE

# A PLASMA CYLINDER EMERGENCE EFFECT ON THE ELECTROMAGNETIC FIELD IN A WAVEGUIDE

Nataliya Sakhnenko, Alexander Nerukh
Kharkov National University of Radio Electronics
14 Lenin Ave., Kharkov, 61166, Ukraine
E-mail: nataliya_sakhnenko@rambler.ru

Investigation of an electromagnetic field transformation caused by a plasma cylinder appearance inside a waveguide at some moment of time is implemented using the Volterra integral equation approach.

We consider a flat waveguide between two parallel perfectly electric conducting plates. It is assumed that until zero moment of time the waveguide had been filled with some homogeneous dielectric medium. At zero moment of time, homogeneous time-varying cold plasma having a constant plasma frequency appears inside a cylinder of some finite radius that is co-axial with the driving current. A vertical driving line current that may have arbitrary time dependence excites the initial field. This current is considered as a sort of emitter model and can be turned on at arbitrary moment, either before or after plasma appearance.

We analyze the axially symmetric electromagnetic field in time domain. Here, the integral equation is formulated by virtue of the time-spatial Green's function in the cylindrical system of coordinates. This equation can be solved by the resolvent method, as it is a Volterra integral equation of the second kind. The exact and explicit expression for the resolvent operator of the integral equation has been derived for the case when the plasma density changes in time abruptly. The obtained resolvent operator allows considering an arbitrary time dependence of the plasma density that can be modeled by the step-like functions.

The resolvent operator consists of two terms. One of them corresponds to the similar problem when the whole waveguide is filled abruptly with homogeneous plasma. The other is caused by the influence of the cylindrical boundary of plasma only. In the case of excitation of the waveguide by the step current, the spectrum of oscillations has resonance peaks at the plasma frequency and at the eigenfrequencies of the plasma cylinder. Amplitudes of the peaks at the eigenfrequencies decrease with resonance number. No resonances are observed in the field outside the cylinder.

0-7803-7846-6/03/$17.00 ©2003 IEEE 

*Special Session*

## Metamaterials: Part I

**Organizer(s):** N. Engheta
R. Ziokowski

**Co-Chairs:** N. Engheta
R. Ziolkowski

7:55 Opening Remarks

4. 1 8:00 Numerical Analysis of a Tunable Magnetic Resonator ..... 17
*S.-W. Lee, Y. Kuga, A. Ishimaru, University of Washington, USA*

4. 2 8:20 Metamaterials Composed of Fractal Sphere Molecules ..... APS
*M. J. Facchine, D. H. Werner, Pennsylvania State University, USA*

4. 3 8:40 Experimental Results on Metamaterial Simulations using SRR-loaded Waveguides ..... APS
*J. Baena, R. Marqués, J. Martel, F. Medina, Universidad de Sevilla, Spain*

4. 4 9:00 Backward Wave Propagation in Waveguide Filled with Negative Permeability Meta Material ..... APS
*S. Hrabar, J. Bartolic, University of Zagreb, Croatia*

4. 5 9:20 Reflection, Transmission and Excitation of a Slab of Arbitrary Permittivity and Permeability ..... 18
*A. Ishimaru, J. R. Thomas, University of Washington, USA*

4. 6 9:40 Resonance Phenomenon in Paired Epsilon-Negative and Mu-Negative Bilayers ..... 19
*A. Alu, N. Engheta, University of Pennsylvania, USA*

4. 7 10:00 TAILORING DOUBLE NEGATIVE METAMATERIAL RESPONSES TO ACHIEVE ANOMALOUS PROPAGATION EFFECTS ALONG MICROSTRIP TRANSMISSION LINES ..... 20
*C. Cheng, R. W. Ziolkowski, University of Arizona, USA*

4. 8 10:20 Sub-wavelength Focusing and Dispersion Characteristics of Negative Refractive Index Transmission Line Media ..... 21
*A. Grbic, G. V. Eleftheriades, University of Toronto, Canada*

4. 9 10:40 Circuit Equivalence of "Growing Exponential" in Pendry's Lens ..... 22
*A. Alu, N. Engheta, University of Pennsylvania, USA*

4. 10 11:00 2D Distributed Meta-Structures with Negative Refractive Properties ..... 23
*A. Sanada, C. Caloz, T. Itoh, University of California, Los Angeles, USA*

4. 11 11:20 Resonance Cone Radiation from a Planar, Anisotropic Metamaterial ..... 24
*K. G. Balmain, A. A. E. Luttgen, G. V. Eleftheriades, University of Toronto, Canada*

4. 12 11:40 Photonic Crystals As Negative Index Materials ..... 25
*S. Enoch, D. Maystre, G. Tayeb, Institut Fresnel, France*

# Numerical Analysis of a Tunable Magnetic Resonator

Seung-Woo Lee, Yasuo Kuga*, and Akira Ishimaru
Department of Electrical Engineering
University of Washington, Box 352500, Seattle, WA 98195-2500
Tel: (206)543-0478, Fax: (206)543-6185, E-mail: ykuga@u.washington.edu

Since the split-ring resonator (SRR) was proposed by Pendry et al., it has been extensively investigated analytically, numerically, and experimentally. In our recent work, we proposed an efficient technique based on the quasi-static Lorentz theory to analyze a metamaterial composed of a 3-D array of small inclusions. This technique has been successfully applied for the analysis of media with a SRR and a stacked split-ring resonator (SSRR) which is a modified split-ring resonator and consists of two split-rings with one split-ring placed on the top of another. The previous research has supported the unique feature of this medium as a metamaterial, that is, it has negative permeability values at a certain frequency range which is due to its resonating structure, and its resonance frequency is determined by the size of the ring ($\approx 0.1\lambda$) and the spacings.

In this paper, a SSRR will be further modified by inserting auxiliary lumped elements, such as an inductor and/or a capacitor, between the split of each ring with the purpose of alternating the electric and magnetic dipole moments and improving the material characteristics. We will present numerical simulation results showing the effect of the auxiliary lumped elements. Through the numerical experiments, it will be shown that the resonance frequency of the proposed resonator structure can be controlled by adjusting the auxiliary lumped elements, and in addition, the size of the ring resonator can be reduced to an order of $0.01\lambda$ that is one tenth that of the split ring resonator by choosing the proper lumped elements. Further improvements, such as a wider bandwidth which may be able to be achieved by utilizing a variable capacitor, will be discussed.

0-7803-7846-6/03/$17.00 ©2003 IEEE

# Reflection, Transmission and Excitation of a Slab of Arbitrary Permittivity and Permeability

A. Ishimaru and J.R. Thomas
Department of Electrical Engineering
University of Washington
Campus Box 352500, Seattle, WA 98195-2500

We have examined reflection and transmission at the vacuum interface of a slab of material or metamaterial with arbitrary permittivity $\varepsilon$ and permeability $\mu$. Our objective is to understand the range of properties that could be provided by such materials. The material is assumed uniform and isotropic. Excitation sources include plane waves and the radiation from an idealized line source. Since the p-polarization and s-polarization cases can be treated as equivalent by interchanging permittivity and permeability (with allowance for a change in sign of reflection coefficient), we concentrate on the p-polarization case. For a line source, this is an idealized line of magnetic current. Then, we have categorized the small loss cases by studying reflection properties in the 2-dimensional plane of Real($\varepsilon$) versus Real($\mu$).

We present a systematic characterization of the poles, zeros, and branch points involved in the reflection coefficient from a semi-infinite half space of metamaterial. We divide the Real($\varepsilon$) — Real($\mu$) plane into a sequence of regions based on the magnitude of $S^2$ and the index of refraction. The complex quantity S is defined following Wait as $k_x/k_o$ at the pole of the reflection coefficient, where $k_x$ is the transverse propagation constant along the slab surface. S may also be regarded as a generalized sine of the angle of incidence. In each different region we find the asymptotic behavior from the poles and branch cuts. We classify these various contributions in the classical forms of primary wave, reflected wave, surface wave, Zenneck wave, and lateral wave. We have found unusual combinations such as a region with forward surface wave and backward lateral wave or with backward surface wave and backward lateral wave. We discuss the range of the parameters $\varepsilon$ and $\mu$ to give the conditions for the existence of forward or backward surface waves, forward or backward lateral waves, Zenneck waves, relations to Brewster's angle and the locations of the poles in the proper and improper Riemann surfaces.

0-7803-7846-6/03/$17.00 

# *Resonance Phenomenon in Paired Epsilon-Negative and Mu-Negative Bilayers*

Andrea Alu[1,2] and Nader Engheta[1]
[1]*University of Pennsylvania*
*Department of Electrical and Systems Engineering*
*Philadelphia, Pennsylvania 19104, U.S.A.*
[2]*Università di Roma Tre*
*Department of Applied Electronics*
*Rome, Italy*
*E-mail: andreaal@ee.upenn.edu , engheta@ee.upenn.edu,*
*URL: http://www.ee.upenn.edu/~engheta/*

Metamaterials with negative real effective permittivity and permeability are being studied by several research groups worldwide. These materials can exhibit interesting features that may lead to unconventional phenomena in guidance, radiation, and scattering of electromagnetic waves. These media are termed with various terminologies such as "double-negative (DNG) media", "left-handed (LH) media", "backward-wave (BW) media", etc.

Most of the work reported in the recent literature has been focused on the wave interaction with the DNG media, either by themselves or in juxtaposition with conventional "double-positive" (DPS) media. However, materials in which only *one* of the two parameters of $\varepsilon$ and $\mu$ has the negative real part, *not both,* may also exhibit unusual features when they are paired in a conjugate manner. Fredkin and Ron (*Applied Physics Letters*, vol. 81, pp. 1753-1755, September 2, 2002) have shown that such a combination can provide an effective group velocity that would be antiparallel with the effective phase velocity, and thus this combination may act as an equivalent LH medium. We have explored and analyzed thoroughly the wave interaction with a bilayer structure in which a slab of lossless material with negative real permittivity but positive real permeability (i.e., an epsilon-negative (ENG) medium) is paired with another slab made of a lossless material with positive real permittivity but negative real permeability (i.e., "mu-negative (MNG) medium), finding some interesting properties due to such juxtaposition of these "conjugate" layers. For instance, we have found that under certain sets of material parameters, the paired bilayer structure exhibits resonance phenomenon, and thus the wave can "tunnel" through completely, effectively making the pair transparent. We have analyzed the field distributions inside and outside such paired slabs, and obtained the reflection and transmission coefficients, while also focusing attention on the Poynting vector distributions. Furthermore, using equivalent transmission-line models with appropriate distributed series and shunt reactive elements, we can physically justify such effects and can describe the conditions on the slabs parameters for resonance, tunneling and transparency.

In this talk, some of the results of our analysis will be presented and discussed.

0-7803-7846-6/03/$17.00 ©2003 IEEE 

# TAILORING DOUBLE NEGATIVE METAMATERIAL RESPONSES TO ACHIEVE ANOMALOUS PROPAGATION EFFECTS ALONG MICROSTRIP TRANSMISSION LINES

*Ching-Ying Cheng* and Richard W. Ziolkowski*

Department of Electrical and Computer Engineering, University of Arizona,
1230 E. Speedway Blvd., Tucson, AZ 85721-0104

Department of Electrical and Computer Engineering
The University of Arizona
1230 E. Speedway
Tucson, AZ 85721-0104 USA

Tel: (520) 621-6173
Fax: (520) 621-8076
E-mail: ziolkowski@ece.arizona.edu, ccheng@ece.arizona.edu

In the past few years, there has been a renewed interest in using sub-wavelength structures to develop materials that mimic known material responses or that qualitatively have new response functions that do not occur in nature. These efforts include the realization of double negative (DNG) metamaterials, artificial materials whose effective permittivity and permeability are both negative. These DNG metamaterials exhibit an effective negative index of refraction that can be tailored to a specified frequency regime.

We have investigated the performance of microstrip transmission lines loaded with DNG metamaterials formed by embedding capacitively loaded strips (CLSs) and capacitively loaded loops (CLLs) in the substrate region. It has been demonstrated theoretically and experimentally that a suitable arrangement of these components in Roger's 5880 DUROID ($\varepsilon_r$=2.2) produces (theoretically and experimentally) a negative index of refraction in the X-band. Similar behavior has been demonstrated theoretically in an open waveguiding environment associated with a microstrip transmission line operating in the S-band.

The DNG metamaterial loaded microstrip transmission line problem will be reviewed in detail. Simulations based on Ansoft's High Frequency Structure Simulation (HFSS) tools will be used to characterize the S-parameter performance of this configuration. It will be shown that a matched metamaterial can be obtained that yields complete transmission in a specified frequency region (S-band). Furthermore, it will be shown that a transmission line lumped element model can be used to extract the effective permittivity and permeability in that regime. Cases will be shown that generate DNG values in the matching region and, hence, that have a negative index of refraction there. Potential applications to modify the shape of signals propagating along these DNG loaded metamaterial microstrip transmission lines will be described.

0-7803-7846-6/03/$17.00 ©2003 IEEE 

# Sub-Wavelength Focusing and Dispersion Characteristics of Negative Refractive Index Transmission Line Media

Anthony Grbic and G.V. Eleftheriades

The Edward S. Rogers Sr. Dept. of Electrical and Computer Engineering
University of Toronto
10 King's College Rd., Toronto
ON, M5S 3G4
Canada

Materials exhibiting simultaneously negative values of permittivity and permeability have received widespread attention in recent years. John Pendry's (J.B. Pendry, Phys. Rev. Lett., **85**, 18, 3966-3969, 2000) prediction that a perfect lens could be made of such materials has revived interest in media exhibiting a negative refractive index (NRI), which were initially investigated by V.G. Veselago in the 1960's. The first implementation of a NRI composite material employed metallic wires to achieve negative permittivity and split-ring resonators to achieve negative permeability (R.A. Shelby, D.R. Smith, S. Schultz, Science, **292**, 77-79, 2001). Recently, a periodic L,C loaded two-dimensional transmission line (TL) network was shown to exhibit electromagnetic properties associated with NRI media. This network consisted of transmission line sections loaded with shunt inductors and series capacitors. It has been referred to as a dual TL structure due to its high pass configuration, as opposed to the low pass representation of a conventional TL. Previous work experimentally demonstrated backward-wave radiation leakage (A. Grbic and G.V. Eleftheriades, J. Appl. Phys. **92**, 10, 5930-5935, 2002) and focusing at microwave frequencies using such dual TL structures (G.V. Eleftheriades, A.K. Iyer, and P.C. Kremer, IEEE Trans. Microwave Theory Tech., **50**, 12, 2702-2712, 2002).

In this work, we present a periodic (Bloch) analysis of the dual TL structure to explain its various passbands and stopbands. From the analysis, useful design equations are derived and expressions for the effective material parameters are found at frequencies of homogeneous and isotropic NRI operation. The issues of impedance matching, proper termination and excitation of finite size structures are also addressed. Moreover, the two-dimensional dispersion characteristics of dual TL media are examined. Based on this analysis, the criteria for sub-wavelength focusing using dual TL slabs are established and sub-wavelength focusing results using a lens consisting of a dual TL structure are shown.

0-7803-7846-6/03/$17.00 ©2003 IEEE

# *Circuit Equivalence of "Growing Exponential" in Pendry's Lens*

Andrea Alù[1,2] and Nader Engheta[1]
[1]*University of Pennsylvania*
*Department of Electrical and Systems Engineering*
*Philadelphia, Pennsylvania 19104, U.S.A.*
[2]*Università di Roma Tre*
*Department of Applied Electronics*
*Rome, Italy*
*E-mail: andreaal@ee.upenn.edu , engheta@ee.upenn.edu,*
*URL: http://www.ee.upenn.edu/~engheta/*

Pendry in his paper (*Physical Review Letters.*, vol. 85, No. 18, pp. 3966-3969, 2000) put forward an idea for a lens made of a lossless metamaterial with negative refractive index (also referred to in the literature as "double-negative (DNG) material), and he concluded that under certain parameter conditions such a lens can provide focusing with resolution beyond the conventional limit. In his analysis, the evanescent wave inside the slab of lossless DNG material is "growing", and thus it "compensates" the decaying exponential outside the slab. This issue of "growing exponential" has been the subject of debates among several groups interested in metamaterial research.

We have been interested to examine the issue of "growing exponential" in such a slab from the transmission-line viewpoint, and to analyze a set of distributed circuit elements representing evanescent wave interaction with a lossless slab of double-negative (DNG) medium. Considering the TM case as a case study, one can show that a TM evanescent wave in a conventional "double-positive (DPS)" medium can be treated with an equivalent transmission-line model with series capacitance and shunt capacitance, i.e., a C-C transmission line, while an evanescent wave in a DNG medium can be modeled as a transmission line with series inductance and shunt inductance, i.e., a L-L transmission line. So the equivalent TL model for the TM evanescent wave interaction with the DNG slab in Pendry's problem may consist of a finite segment of L-L line, representing the DNG slab for the evanescent wave, sandwiched between two semi-infinite segments of C-C lines, representing the outside DPS regions for the evanescent wave. We have analyzed such a lossless TL structure, and have examined the possibility of growing exponential term for the voltage and current distributions along a segment of this TL structure. Our analysis shows that under certain conditions the current in series elements and the voltage at the nodes may have the dominant increasing term in the L-L line segment and the dominant decreasing term in the C-C line segments, due to the suitable resonance in the lossless circuit.

In this talk, we will present some of the key features and results of our study on this TL analogy for evanescent wave interaction with metamaterials.

0-7803-7846-6/03/$17.00 ©2003 IEEE 

## 2D Distributed Meta-Structures with Negative Refractive Properties

Atsushi Sanada, Christophe Caloz, and Tatsuo Itoh

Electrical Engineering Department, University of California, Los Angeles, CA90095, sanada@ieee.org

The transmission line (TL) approach of left-handed (LH) or negative refractive index (NRI) metamaterials has lead to broadband and low-loss structures, whereas resonant-type configurations, such as the split ring resonators (SRRs) [1] and metal wires structure experimentally demonstrated by R. A. Shelby et al. [2], are intrinsically very lossy and narrow-band. C. Caloz et al., have successfully demonstrated a distributed one-dimensional (1D) microstrip line configuration [3] and characterized its dispersion relation by developing a new circuital theory of composite left/right-handed (CLRH) model, which takes into account the effects of parasitic series inductances and shunt capacitances [4]. In addition, a lumped-element 2D-NRI-TL has been proposed by G. V. Eleftheriades [5] et al. and demonstrated to exhibit focusing properties due to negative refraction when interfaced with a conventional material [6].

In this paper, 2D *distributed* periodic TL structures with LH fundamental mode are proposed. The unit cell is composed of a square mushroom-shaped structure on a ground plane [7] with 45°-rotated square metal caps just below the mushroom (see the inset in Fig.1). The dispersion diagram of the unit cell computed by the FEM is shown in Fig.1. The mushroom structure provides a shunt inductance to the ground and series capacitances to adjacent unit cells. The caps dramatically enhance the series capacitance and, as a result, contribute to drastic enhancement of the left-handedness of the TL in terms of negative slope in the $\omega$-$\beta$ diagram and LH bandwidth. This structure is *open* and the fundamental LH mode consequently couples with the surface wave (TM) mode at low frequencies.

A closed version of the distributed 2D-TL can be realized by combining symmetrically two open structures in a parallel-plate waveguide configuration with the mushrooms in the center. This structure can have a pure CRLH fundamental mode, which is characterized by left-handedness below a transition frequency $\omega_0$, where $\beta = 0$, and right-handedness above, as shown in the dispersion diagram in Fig.1. The frequency $\omega_0$ corresponds to the $\Gamma$-axis of the dispersion diagram where *perfect effectiveness* is achieved: $period/\lambda_g = 0$. It is essential to note that there is no gap between the LH and RH ranges; the $\omega_0$-point is therefore associated with a non-zero group velocity and the structure can be quasi-lossless at this point. The transition frequency is given as $\omega_0 = (\omega_L \omega_R)^{-1/2}$, where $\omega_L = (L_L C_L)^{-1/2}$ and $\omega_R = (L_R C_R)^{-1/2}$, $L_L$ and $C_L$ are the inductance and capacitance of the LH unit cell and $L_R$ and $C_R$ are the parasitic inductance and a capacitance, respectively [3].

Both the open and closed LH distributed structures described here can exhibit *negative refraction* effects in their effective frequency range when interfaced with conventional right-handed (RH) structures. This has been confirmed by full-wave simulations, which revealed unique phenomena such as the existence of *focusing and surface plasmons*. In the case of the open structure, a parallel-plate waveguide was used as the RH medium; in the case of the closed structure, the RH medium was a strip line structure. These effects have also been observed in sandwiched RH/LH/RH configurations analogous to the "superlens" presented in [6].

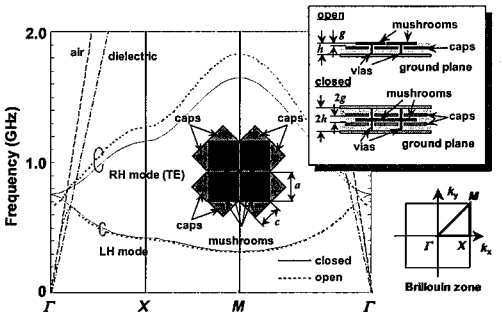


Fig.1 Dispersion diagram. $a$ = 32.6mm, $c$ = 16.1mm, $h$ = 1.697mm. $g$ = 0.127mm. The period of structure is 33.0mm, the permittivity of the substrate is $\varepsilon_r$ = 2.2, and the diameter of the via is 0.4mm.

[1] J. B. Pendry, A. J. Holden, D. J. Robins, W. J. Stewart, IEEE Trans. on Microwave Theory and Tech., vol. 47, no. 11, pp. 2075-2084, 1999. [2] R. A. Shelby, D. R. Smith, S. Schults, Science, vol. 292, No. 6, pp. 77-79, 2002. [3] C. Caloz, and T. Itoh, IEEE-APS Int'l Symp. Digest, vol. 2, pp. 412-415, June 2002. [4] C. Caloz, and T. Itoh, "Novel microwave devices and structures based on the transmission line approach of Meta-Materials", submitted to IEEE-MTT Int'l Symp., June 2003. [5] G. V. Eleftheriades, A. K. Iyer, and P. C. Kremer, IEEE Trans. on Microwave Theory Tech., vol. 50, no. 12, pp. 2702-2712, Dec. 2002. [6] J. B. Pendry, Phys. Rev. Lett., vol. 85, no. 18, pp. 3966-3969, Oct. 2000. [7] D. Sievenpiper, L. Zhang, R. F. J. Broas, N. G. Alexopólous, and E. Yablonovich, IEEE Trans. on Microwave Theory and Tech., vol. 47, no. 11, pp. 2059-2074, Nov. 1999.

0-7803-7846-6/03/$17.00 ©2003 IEEE

# RESONANCE CONE RADIATION FROM A PLANAR, ANISOTROPIC METAMATERIAL

*Keith G. Balmain, Andrea A.E. Lüttgen and George V. Eleftheriades
The E.S. Rogers Department of Electrical and Computer Engineering
University of Toronto, Toronto, Ontario, Canada
balmain@waves.utoronto.ca

The metamaterial under study is based on a square-celled, planar, wire-grid network that is series-loaded with capacitors in one direction and inductors in the orthogonal direction (or equivalently loaded with distributed elements). Further, this two-dimensional grid is positioned over a horizontal ground plane and parallel to it, and an inductor-loaded vertical wire is dropped from each grid-wire intersection to ground. For the computational simulation results to be discussed here, the overall configuration is square-shaped and excited by a voltage source located at one corner and inserted in a wire connected between the grid and ground. At this conference last year (2002 URSI Digest p. 45), and for a configuration similar to the present one but lacking the grid-to-ground inductive branches, it was found that the near fields were concentrated along radial lines called resonance cones extending outward from the corner source. For the present configuration, the resonance-cone high-field regions are still in evidence at similar angles. The key difference now is that the vertical inductive branches carry enough current to contibute significantly to the radiation fields, especially the vertically polarized ones that propagate in near-horizontal directions.

The corner-to-corner diagonal resonance cone provides useful examples of radiation patterns. The designs tried so far tend to be low-profile, with heights on the order of a twentieth of a wavelength. For a particular choice of parameters, the near-field phase is nearly constant along the resonance cone, producing a radiation pattern horizontal main lobe that is near-broadside with respect to the cone direction. A further benefit arises from the fact that the resonance cone near fields exhibit a rapid phase shift horizontally across the cone direction. This phase shift is sufficient to produce a near-null in the horizontal-plane radiation pattern, to one side of the cone, thus making the horizontal broadside radiation unidirectional. Still further, the radiated-field source distribution tends to be concentrated near the driven end of the array, a common problem with other types of leaky-wave antennas. Our solution is to employ graduated-height tapering of the array, which has so far proved to be satisfactory.

For other parameters, the near-field equiphase contours approximate straight lines cutting across the resonance cones at particular angles in the horizontal plane, such that the normals to these lines in the vicinity of the cones correspond to the directions of the radiation maxima. This translates into an opportunity for electronic beam steering.

0-7803-7846-6/03/$17.00 ©2003 IEEE 

# Photonic crystals as negative index materials

**S. Enoch *, D. Maystre, G. Tayeb**

*Institut Fresnel, UMR CNRS 6133, Faculté de Saint Jérôme, case 161, 13397 Marseille Cedex 20, France*

Negative index materials are the subject of a recent controversy. The first study of negative index materials (NIM) is due to V. Veselago (1964), who showed that a medium with both permittivity and permeability equal to -1 behaves as a medium producing negative refraction for plane waves. Recently, J.B. Pendry proposed a perfect lens using NIM, arguing that evanescent components of the electromagnetic field play a vital role in the perfect focusing process. Assuming that a material with such property exists, one can show that a slab of such a material can make a point image of a point source. This result has raised a polemical discussion.

First, we will show using a simple and rigorous demonstration that a homogeneous material having both permittivity and permeability equal to -1 cannot exist, even at a given wavelength.

On the other hand, it must be acknowledged that experimental results have evidenced the phenomenon of negative refraction in left-handed materials. Furthermore, we have shown from numerical data that purely dielectric photonic crystals can generate the same phenomenon. In these cases, the observed properties can be explained and it can be shown that such materials can be used to elaborate efficient (but not perfect) lenses which can go beyond the usual lenses.

We will give numerical illustrations of these results in the case of a two-dimensional dielectric photonic crystal. The physical insight of negative refraction is provided using dispersion curves of Bloch modes. We also estimate the limitations of a lens made of photonic crystals.

From our theoretical and numerical results, a critical appraisal of the recent results published elsewhere will be carried out.

0-7803-7846-6/03/$17.00 ©2003 IEEE 

## Calibration of Radiometers

**Co-Chairs:** T. Landecker
J. Welch

10:00 Opening Remarks

## The Flux Density Scale at the Very Large Array

Rick A. Perley*, Bryan J. Butler, National Radio Astronomy Observatory

The Very Large Array (VLA) is one of the world's premier radio telescopes. It is an interferometer composed of 27 telescopes of diameter 25 meters, each equipped with eight receiver bands covering frequencies from 74 MHz to 50 GHz. Baselines up to 35 kilometers allow sub-arcsecond resolution. The VLA is located on the plains of San Augustin, in New Mexico.

Since the VLA is extremely good at getting relative flux densities of sources (as long as they are not over-resolved by the interferometer), but not so good at getting absolute flux densities, the calibration of VLA data is obtained by observation of astronomical sources whose flux density is assumed to be known by other means. We have adopted the Baars et al. scale at frequencies less than 15 GHz, using Cygnus A as the primary calibrator at 74 MHz, and 3C295 at all other frequencies.

A set of secondary calibrators, including 3C48, 3C84, 3C123, 3C138, 3C147, 3C196, and 3C286, are monitored against 3C295 very carefully in each D-configuration of the VLA, or roughly every 16 months. This provides a set of sources for calibration of VLA data at the lower frequencies, as well as providing information on the intrinsic variability of these secondaries.

We have recently (in the last 5 years) engaged in an extensive program to attempt to determine adequate sources for calibration at frequencies greater than 15 GHz at the VLA. Along with the monitoring of the above listed secondaries (which we also observe at high frequency), we have also been monitoring several planets (Venus, Mars, Uranus, and Neptune), planetary nebulae (NGC 7027 and NGC 6572), and the evolved star MWC 349. We obtain good agreement between models and observations for Mars and NGC 7027, and the flux density scale at high frequencies (20 to 50 GHz) at the VLA is now based on these models and observations.

The current status of calibration and the flux density scale at the VLA will be presented, including results on variability of sources and the flux density scale at high frequencies.

0-7803-7846-6/03/$17.00 ©2003 IEEE

## Amplitude Calibration of ALMA

Bryan J. Butler, National Radio Astronomy Observatory

The Atacama Large Millimeter Array (ALMA) is a major ground based project for millimeter and submillimeter astronomy to be realized during this decade. It is an interferometer composed of 64 telescopes of diameter 12 meters, each equipped with ten receiver bands covering the atmospheric windows from 30 to 950 GHz. Baselines up to several kilometers will allow sub-arcsecond resolution. The ALMA array will be located on a high-altitude (5000 m) plateau in the Atacama Desert in Northern Chile. The project is a joint venture of Europe and North America (USA and Canada) with Japan intending to join later on.

The specification for amplitude calibration for ALMA is 1% at millimeter wavelengths and 3% at submillimeter wavelengths. This is significantly more precise than current millimeter and submillimeter instruments, and presents a significant design challenge. Major elements involved in the calibration of the amplitude include: focus, delay, pointing, bandpass, sideband gain ratio, atmosphere (including decorrelation), and receiver.

The atmosphere (excluding decorrelation) and receiver can be calibrated by an extension of the traditional chopper wheel method. There are several variants being studied, but the two most promising are the dual-load (current design has them in the subreflector), and the semi-transparent vane techniques. Each of these has advantages and disadvantages, and these are currently being studied, both theoretically, and by testing prototype systems at millimeter observatories.

I will discuss the current status of the amplitude calibration of ALMA, including all of the elements of the calibration framework, but focusing on recent developments and measurements involving the dual-load and semi-transparent vane calibration devices.

0-7803-7846-6/03/$17.00 ©2003 IEEE

# Instrumental Polarization across the Field of View of a Radio Telescope

T. Ng [1,2], T.L. Landecker[2], F. Cazzolato[3], A.D. Gray[2], B.G. Veidt[2], D. Routledge[1]

[1]Department of Computer and Electrical Engineering, University of Alberta, Edmonton, Alberta, Canada, T6G 2V4

[2]Dominion Radio Astrophysical Observatory, Herzberg Institute of Astrophysics, National Research Council, Penticton, B.C., Canada, V2A 6K3

[3]Département de Physique, Université Laval, Sainte-Foy, Québec, Canada, G1K 7P4

A radio telescope sees the sky through its beam. In aperture synthesis image processing it is commonplace to correct the total-intensity image for the primary beam, usually using a Gaussian function or some other simple mathematical form. The primary beam also has polarization properties that vary across the field of view. This paper presents computation of the instrumental polarization across the field of view of a paraboloidal reflector antenna, and investigates the contributions of reflector shape, feed cross-polarization, blockage by feed-support struts, and reflector roughness.

The computations use the GRASP 8 software, based on Physical Optics. The reflector is fed with a linearly polarized signal. Computed radiation patterns at four feed orientations from 0° to 135° in steps of 45° are averaged to provide a good approximation of the randomly polarized radio astronomy signal. Stokes parameters are calculated, and maps of Q/I and U/I are computed. These indicate the degree of conversion of I into Q and U by the telescope beam. The results of the computation are consistent with measurements made using unpolarized radio sources.

The computations show that the dominant source of instrumental polarization across the field is the cross-polarization of the feed. The next most significant effect is scattering by the feed struts. The differences between three-strut and four-strut configurations is quite obvious. Strut cross-section has a significant effect on polarization performance, and we show that struts of triangular cross-section give better polarization performance than circular struts. We present calculations of the Induced Field Ratio (the ratio of the size of the effective blockage caused by a strut to the blockage calculated from its physical size) for struts of various cross sections.

Surface roughness has relatively little effect in the main beam, but effectively randomizes the polarization of the sidelobes. This may be an advantage in an aperture synthesis telescope. Surface roughness introduces some spurious circular polarization because it introduces a small offset to the antenna geometry.

The computations show that the first and subsequent sidelobes are highly polarized, with levels of Q/I and U/I up to 50%.

0-7803-7846-6/03/$17.00 ©2003 IEEE 

# Accurate Antenna Gain Calibration

James Gibson & Wm. J. Welch
Radio Astronomy Laboratory
University of California
Berkeley, CA 94720

January 15, 2003

**Abstract**

The accurate measurement of radio source fluxes depends on precise knowledge of the antenna gain. We describe a scheme for accurate antenna gain measurement that depends on having a stable interferometer and a calibrated standard gain horn. The standard gain horn is fastened to the side of one of the interferometer antennas and connected to a switch so that either the main feed horn of the antenna or the standard horn drives the receiver of the antenna. The interferometer is set to observe a strong radio source, and as the switch is flipped, the correlator output is the product of either the normal antenna pair signals or the standard horn signal and the other antenna signal. The ratio of the two correlator signals is the voltage ratio of the standard horn to that of the normally fed antenna. The main antenna gain is then that ratio (in db) added to the gain of the standard horn. It can be readily measured to an accuracy of the order of one percent. With a similar accuracy for the standard horn, one obtains an overall accuracy of about one percent for the main antenna. A number of issues must be carefully considered, including antenna pointing accuracy, antenna gain stability with elevation, angular size of the radio source, correlator linearity, atmospheric extinction, and cable delays. In this experiment, one of the BIMA array antenna gains is measured at 28.5 GHz using the planet Jupiter to an accuracy of 1%, and the brightness temperature of Jupiter is measured to an accuracy of 1.5%.

0-7803-7846-6/03/$17.00 

# A DUAL-LOAD CALIBRATION SYSTEM FOR MILLIMETER-WAVE ASTRONOMY

Douglas C.-J. Bock
Radio Astronomy Laboratory
University of California, Berkeley
Berkeley, CA 94720, USA

Accurate radiometric calibration in millimeter-wave radio astronomy has been an elusive goal. Present instruments generally use a single-load system (the *chopper wheel method*), often in the optical path near the feed. Such a system allows convenient measurements by making the simple assumption that the load temperature is similar to the physical temperature of the absorbing sky. However, the resulting accuracies are at best a few percent. The next generation of millimeter and sub-millimeter interferometers (ALMA, CARMA, etc.) will require higher accuracy to improve the comparison of data with models, comparisons between data observed at various epochs and with various telescopes, and to give the best dynamic range and image fidelity.

A dual-load system with temperature-controlled and thermally isolated loads at the subreflector can provide calibration at the 1% level once an independent measurement of the opacity is available. Additional advantages include:

- the calibration signal can be small (a few Kelvin), allowing continuous calibration, and avoiding the difficulties of receiver saturation
- the system can be made to be wavelength and receiver independent
- the loads may be alternately presented sufficiently rapidly that receiver instabilities can be tracked in the presence of sky fluctuations
- the entire signal path may be calibrated.

In poor weather the system can function as an improved (continuous) chopper wheel method. We have constructed a prototype of such a system on one antenna of the Berkeley-Illinois-Maryland Association Array at Hat Creek, northern California.

In this paper, I will describe the prototype system, evaluate its performance, and outline the next steps that will allow it to be used in regular astronomical observations.

0-7803-7846-6/03/$17.00 ©2003 IEEE 

# Polarization Characteristics of the Green Bank Telescope

T. H. Troland*, University of Kentucky, Physics & Astronomy Department, USA
T. Robishaw & C. Heiles, Berkeley Astronomy Department, USA

Commission J4 – Antennas and antenna arrays

The 100m Green Bank Telescope (GBT), operated by the National Radio Astronomy Observatory in Green Bank, WV, is in its commissioning phase. This fully steerable radio telescope is currently equipped with receivers operating at 300 MHz to 50 GHz, operation above 100 GHz eventually expected. Receivers above 1 GHz are at the Gregorian focus of the telescope.

An innovative design feature of the GBT is its offset feed system. This system eliminates blockage of the aperture, resulting in very low sidelobes if aperture illumination is properly tapered. For example, the first sidelobe at L-band is approximately 30db below than the main beam.

We have recently conducted tests of the polarization performance of the GBT at L, C and X-bands. We perform scans across radio continuum sources in four directions and use a cross-correlation spectrometer to derive the beam characteristics out to the first sidelobe in all four Stokes parameters. At each band, we observe four separate sky frequencies to assess polarization properties as a function of frequency.

From our data, we derive *beam squint*, *beam squash* and telescope efficiencies. Beam squint is the difference in directions of the main beam in orthogonal polarizations. It is measured in arcsec. In the Stokes parameter Q, U, or V beam patterns, beam squint appears as a two-lobed pattern with lobes of opposite sign on opposite sides of beam center. Beam squint is expected in the Stokes V pattern owing to misalignment of the electrical axis of the feed with that of the reflecting surface. Beam squash is a deviation from circular symmetry of the primary beam cross-section in orthogonal polarizations. Beam squash is also measured in arcsec, it is the difference in beamwidth in orthogonal directions. In the Stokes parameter Q, U, and V beam patterns, beam squash appears as a four-lobed pattern with lobes of opposite signs on opposite sides of beam center. Beam squash is expected in Stokes Q and U patterns.

Preliminary analysis of our data at L-band reveals beam squint and beam squash in Stokes parameters Q, U and V. In the Stokes parameter V beam, we find squint of order 0.5 arcsec or less and squash of order 1 arcsec or less. These dimensions are very small fractions of the primary beamwidth of 540 arcsec. Therefore the circular cross polarization performance of the GBT is excellent. In the Stokes parameter Q and U beams, we find beam squint of order 2-4 arcsec and beam squash of up to 30 arcsec. Linear cross polarization of the telescope is significantly higher than circular polarization, as is usually the case in radio telescopes.

The circular polarization performance of the GBT indicates that it will be an excellent instrument for measurement of the Zeeman effect in radio frequency spectral lines. Such measurements involve detection of very small fractional polarizations in the lines.

0-7803-7846-6/03/$17.00 ©2003 IEEE

# FEEDS FOR THE EXPANDED VERY LARGE ARRAY TELESCOPE

S. Srikanth*
National Radio Astronomy Observatory
2015 Ivy Road
Charlottesville, VA 22903
Peter Napier
National Radio Astronomy Observatory
1003 Lopezville Road
Socorro, NM 87801

The Very Large Array (VLA) synthesis telescope is currently undergoing a major upgrade to improve its scientific capabilities by an order of magnitude in all key observational parameters. As a part of Phase I of the Expanded VLA (EVLA) project, the array will be outfitted with wideband receiver systems at the secondary focus, a state-of-the-art correlator, a fiber optic data transmission system and a new on-line control system. This paper discusses the feeds aspect of the expansion project. The VLA antenna has a 25-m diameter, shaped primary reflector. The secondary focus receivers are mounted on a circle, with a radius of 97.5 cm, around the reflector axis. An asymmetric shaped subreflector focuses the radiation into one of the six (L, C, X, Ku, K and Q) receivers. These receivers have narrow bandwidths of the order of less than 1.3:1. The lowest frequency of operation at the secondary focus is 1.3 GHz.

The EVLA will have eight wideband receivers providing continuous frequency coverage from 1.0 GHz to 50 GHz. In addition to increasing the bandwidth of the existing bands, two new bands (S and Ka) will be added. Gain/System temperature analysis was carried out at three frequencies (3, 10 and 30 GHz) in order to determine the feed taper at the edge of the subreflector for various bands. Limited space in the feed circle led to the selection of a smaller-than-required L-band feed, resulting in compromised performance at the low end of the band. Feeds for the L, C and S bands are compact, corrugated horns with 2:1 bandwidth ratio. The other bands will have linear-taper, corrugated feed horns. All the feeds use ring-loaded corrugations in the mode-converter section and have four corrugations per wavelength in order to keep the cost of machining at a minimum. Various manufacturing techniques will be used for the feeds, depending on the frequency. Comparison of performance between the new L-band feed and the existing feed will be presented.

0-7803-7846-6/03/$17.00 ©2003 IEEE 

*Special Session*

## Contributions of E. M. Kennaugh to Polarimetry

**Organizer(s):** Dr. Wolfgang-Martin Boerner, University of Illinois at Chicago
Motoyuki Sato

**Co-Chairs:** W. Boerner
J. Sarvas

7:55 Opening Remarks

8. 1 8:00 Contributions of the Late Professor Edward Morton Kennaugh (1921-1963) To "Radar Polarimetry"- Theory and Applications ..... 36
*W. Boerner, University of Illinois at Chicago, USA*

8. 2 8:20 Kennaugh and the Dual Space Approach To Radar Polarimetry ..... APS
*E. A. Lueneburg, EML Consultants, Germany, W. M. Boerner, UIC-ECE, USA*

8. 3 8:40 The Kennaugh's Concept of the Inversion Point Inside the Poincare Sphere Model of the Scattering Matrix and Further Developments of His Ideas ..... APS
*Z. H. CZYZ, Telecommunications Research Institute, Poland*

8. 4 9:00 Generalized Optimization of Polarimetric Contrast Enhancement ..... APS
*J. Yang, G. Dong, Y. Peng, Tsinghua University, China, Y. Yamaguchi, H. Yamada, Niigata University, Japan*

8. 5 9:20 Ground-Based Polarimetric SAR Systems for Environment Studies ..... APS
*Z. Zhou, M. Sato, Tohoku University, Japan*

8. 6 9:40 Fast Computing of the First Order Interaction Terms for Scattering Amplitudes in Polarimetric Remote Sensing ..... 37
*J. O. Sarvas, Helsinki University of Technology, Finland, L. Zurk, MIT, USA*

## Contributions of late Professor Edward Morton Kennaugh (1921 – 1963) to *"Radar Polarimetry"* – theory and applications

**Wolfgang-Martin Boerner**, University of Illinois at Chicago, Department of Electrical and Computer Engineering, Communications, Sensing & Imaging and Navigation Laboratory
UIC-ECE/CSN, m/c 154, 900 W. Taylor Street, SEL-W (607) – 4210, CHICAGO, IL/USA 60607-7018,
T&F: + [1] (312) 996-5480, E-mail: boerner@ece.uic.edu

**Abstract**

The Electrical Engineering profession and the electromagnetics discipline lost a great luminary and teacher with the death of Professor Edward M. Kennaugh at age 60 on March 11, 1983. Beyond the borders of the campus of his alma mater and that of the USA he became known and highly admired, specifically through his contributions to NATO Advanced Study Institutes and AGARD Workshops. Here we are gathering twenty years later honoring the contributions of this visionary – one of the greatest scientists of the past century who influenced most profoundly the progress made in electromagnetic imaging, antenna theory and practice until this very day

Coming to the Ohio State University in 1946 he stayed as a graduate student under Professor Victor Rumsey, and labored for 35 years on electromagnetic scattering theory, bringing international fame to himself and honor to the Electro-Science Laboratory in which he worked. His fundamental theory of the polarizing properties of radar scatterers, accomplished in the early 1950's while he was still a student, remains today the definitive work on this subject. His introduction in 1948of the *"Impulse Response"* concept for three-dimensional scattering obstacles brought new importance to the time-domain viewpoint in scattering theory and opened avenues of research which continue to branch even today. The large body of literature, which has been built upon this one concept, is overwhelming witness to the depth of Professor Kennaugh's insight into the scattering process. For twenty years, he and his students labored to refine the theory and contribute to this literature while proceeding to develop basic ideas in other directions. In the early 1960's he laid the foundations of antenna scattering theory and called attention to the importance of antennas in the modification and control of radar scattering. This work was in advance of its time and came to be widely appreciated only with the advent of low cross section aircraft. In the middle 1960's he inspired and fostered the development of modal descriptions of scattering by obstacles of arbitrary shape. In this fundamental work he displayed his genius for seeing common things in an uncommon way by bringing together the familiar ideas of power factor and eigenvectors, a union which continues to bear fruit even today. In the early 1970's, Professor Kennaugh took on the directorship of the Electro-Science Laboratory and remained at that post for three years while continuing his researches in scattering theory. His "retirement" in 1977 was one in name and not in fact, for he proceeded in the six years given to him since then to develop the so-called *"K-pulse"* concept which he formally introduced in 1981 and he was carrying forward at the time of his death. This concept crowns Professor Kennaugh's years of research in time-domain methods and, with its singular originator now gone, its development remains a formidable challenge to present and future investigators.

Here, in this overview and session mainly the fundamental contributions to *"Radar Polarimetry"* of this extraordinary luminary will be addressed.

Prepared for APS-URSI Special Session E.M. Kennaugh

0-7803-7846-6/03/$17.00 ©2003 IEEE 

# Fast Computing of the first Order Interaction Terms for Scattering Amplitudes in Polarimetric Remote Sensing

Jukka Sarvas* and Lisa Zurk†
*Electromagnetics Laboratory, Helsinki University of Technology, Finland
†MIT Lincoln Laboratory, Lexington, MA, USA

In polarimetric remote sensing of forest, the trunks and branches often are modeled as finite dielectric cylinders and in the resulting multiple scattering problem only the direct terms of single cylinders and the first order interaction terms of pairs are taken into account in computing the far field scattering amplitude. The far field and the scattering amplitude of a finite cylinder can be in a fast way computed by using a truncated infinite cylinder approximation (TICA). I this talk we present a new method how to compute the scattering amplitudes of the interaction terms also in a fast way by using TICA and the Rokhlin translation formula, well-known in the context of the fast multipole methods.

For incident polarization $\hat{\alpha}$ and direction $\hat{\boldsymbol{k}}_i$, the scattering amplitude $f^{V_2,V_1}_{\hat{\beta},\hat{\alpha}}(\hat{\boldsymbol{k}}_s,\hat{\boldsymbol{k}}_i)$ of the first order interaction term of cylinders $V_1$ and $V_2$ in the scattering direction $\hat{\boldsymbol{k}}_s$ and for the scattering polarization $\hat{\beta}$ can be given in the terms of the reaction integral of Chiu and Sarabandi as follows,

$$f^{V_2,V_1}_{\hat{\beta},\hat{\alpha}}(\hat{\boldsymbol{k}}_s,\hat{\boldsymbol{k}}_i)=\frac{i\omega\mu_0}{4\pi}\int \boldsymbol{E}_{\boldsymbol{J}_1}(\boldsymbol{r})\cdot\boldsymbol{J}_2(\boldsymbol{r})d\boldsymbol{r} \tag{1}$$

where $\boldsymbol{J}_1$ is the volume current in $V_1$ induced by the incident plane wave $\hat{\alpha}e^{ik_0\hat{\boldsymbol{k}}_i\cdot\boldsymbol{r}}$ when $V_2$ is not present, $\boldsymbol{J}_2$ is the volume current in $V_2$ induced by the incident plane wave $\hat{\beta}e^{-ik_0\hat{\boldsymbol{k}}_s\cdot\boldsymbol{r}}$ when $V_1$ is not present, and $\boldsymbol{E}_{\boldsymbol{J}}(\boldsymbol{r})$ is the electric field in vacuum due to a source current $\boldsymbol{J}$. The currents $\boldsymbol{J}_1$ and $\boldsymbol{J}_2$ can be computed by TICA in a fast way, but the integral in (1) is essentially 6-dimensional and usually slow to compute directly.

For a fast computing of this integral, we chop the cylinders $V_j$ and the currents $\boldsymbol{J}_j$ into short blocks $V_{j,m}$, $\boldsymbol{J}_{j,m}$, $m=1,\ldots,M_j$, $j=1,2$, and the integral in (1) gets the form

$$\sum_{n=1}^{M_1}\sum_{m=1}^{M_2}\int \boldsymbol{E}_{\boldsymbol{J}_{1,n}}(\boldsymbol{r})\cdot\boldsymbol{J}_{2,m}(\boldsymbol{r})d\boldsymbol{r}.$$

Next the fields $\boldsymbol{E}_{\boldsymbol{J}_{1,n}}$ are expanded about $V_{2,m}$ in plane waves by using the Rokhlin formula, and the resulting integrals are again efficiently computed by using TICA.

In this talk we show how this procedure can be organized into a fast algorithm which greatly reduces the cost of computing the integral in (1). Also numerical examples are presented.

0-7803-7846-6/03/$17.00 ©2003 IEEE

## Aperture Antennas

**Co-Chairs:** W. Imbriale
A. Petosa

10:00 Opening Remarks

**Real Time Distortion Compensation in Large Reflector Antennas: Algorithms for Estimating Distortion**

W. A. Imbriale
California Institute of Technology
Jet Propulsion Laboratory
Pasadena, CA 91109

Over the past decade, extensive work has been performed at JPL on the use of a Deformable Flat Plate (DFP) and Array Feed Compensation System (AFCS) to correct for the gravity-induced distortions on a large reflector antenna (Imbriale, *Large Antennas of the Deep Space Network*, John Wiley and Sons, 2003). The DFP is placed in the beam path and deformed in order to compensate for the gravity-induced distortions as the antenna moves in elevation. Actuators controlling the plate surface are driven via a look-up table. Values in the look-up table are derived using the measured antenna distortions, ray tracing, and a structural finite element model of the DFP. The Array Feed Compensation System (AFCS) consists of a small array of horns, low noise amplifiers, down converters, and digital signal processing hardware and software for optimally combining the signals received by the horns. Each system acting alone and a combined system consisting of both the DFP and the AFCS were demonstrated on the Deep Space Network (DSN) 70-meter antenna. The combined system worked better than either one of the systems acting alone. However, even in the combined experiment, each system was operated independently in that there was no feedback from the AFCS to the DFP.

Recent experiments (Imbriale, et. al., "Toward Real Time Compensation with a Combined DFP/AFCS System", 2002 IEEE APS Symposium, San Antonio, TX, 2002), carried out during tracks of Ka-band signals from the Cassini spacecraft, demonstrated the feasibility of real time compensation using the AFCS to update the DFP actuator positions. The combined system corrected, in real time, for intentionally introduced sub reflector offsets. This experiment also demonstrated that once the reflector geometry was know, the actuator positions could be computed and updated in less than 2 seconds. This was a precursor to a more complete system for compensating any time varying (not necessarily gravity dependent) deformations.

The purpose of this paper is to discuss algorithms for estimating the reflector distortions from the amplitude and phase of the signals received in the AFCS. A simple statement of the problem is; given the relative amplitude and phase of the signals received by an array feed in a distorted reflector, compute the reflector distortions required to produce the given signals. The problem is solved in two parts. First, the focal plane field is estimated by best fitting a postulated focal plane field with the given signals. Then, the focal plane fields are used to compute the distortions.

0-7803-7846-6/03/$17.00 ©2003 IEEE

# A LENS DESIGN USING THE HOLOGRAPHIC PRINCIPLE

A. Ittipiboon, A. Petosa* and S. Thirakoune

Communications Research Centre

3701 Carling Avenue, P. O. Box 11490, Station H, Ottawa,

Ontario, Canada K2H 8S2

E-mail: apisak.ittipiboon@crc.ca

High gain antennas have been vital components in various communication systems, where antennas such as lenses and reflectors have been widely employed. In a conventional design, antenna beam-forming characteristics have been achieved by applying Fermat's principle through geometrical constraint. For a system that requires multi-focal points, for multi-beam applications from a shared aperture, this can be a very challenging problem. A design based on the holographic principle is a promising alternative method, which can overcome this problem.

A zone plate has been recognized as a simple hologram (W. E. Kock, Microwaves, pp. 46-54, November 1968). The equivalence was demonstrated by a simple hologram of a pin hole using laser light and a photographic plate. A volume-type holographic antenna has also been reported in the literature (K. Iizuka, et al, IEEE Trans. Antennas Propagat., vol. AP-23, pp.807-810, November 1975). The holographic antenna was constructed from circular arcs of metal strips as a crude representation of a hologram. The antenna functions in a similar way to a traveling wave type where the beam scans with frequency. In this paper, a flat lens design using the holographic principle is presented. A method for efficiency enhancement will also be discussed. The proposed antenna should be attractive for millimeter-wave applications due to its low loss nature.

The proposed antenna configuration consists of a number of short dipoles arranged in a concentric ring pattern. The locations of the short dipoles are determined by applying the holographic principle. The two waves used to produce a hologram consist of a spherical wave from the feed and a plane wave propagating in the boresight direction, the desired direction of the antenna beam in this investigation. The location of the spherical wave is the focal point of the lens. For a single layer lens, the antenna produces two symmetrically beams located at the front and back. However, the back lobe radiation can be suppressed by using a multilayer configuration. Preliminary results of a two-layered lens achieve a gain increase of close to 6 dB with a significant reduction of the back lobe. The number of layers serves as a design parameter for antenna efficiency enhancement in addition to proper feed selection criteria. This investigation is confined to the boresight beam. However, the concept can be easily applied to the design of a lens with a tilted beam. Details of the study and a discussion will be presented at the conference.

0-7803-7846-6/03/$17.00 ©2003 IEEE

# Analysis & Optimisation of Holographic Antennas Using an Integral Equation Formulation

Pradiv Sooriyadevan* & Derek M$^{c}$Namara
University of Ottawa, 161 Louis Pasteur Street, Ottawa, Ontario, K1N6N5, Canada.
Aldo Petosa & Apisak Ittipiboon
Communications Research Centre Canada, Ottawa, Ontario K2H 8S2, Canada.

Antennas based on holographic principles have been proposed for (amongst other applications) multipoint wireless communications because of their flat profile and potentially high gain. Most published design work on holographic antennas (eg. K.Lévis, A.Ittipiboon, A.Petosa, L.Roy & P.Berini, *IEE Proc.-Microwav. Antennas Propagat.*, **148**, 129-132, 2001) has been based on approximate expressions and experimental experience. No attempt appears to have made to use some computational electromagnetics approach to model these antennas. Thus no numerical optimization has been possible.

One aspect that makes the modeling/optimization process difficult is that such holographic antennas are electrically large. For instance, the combined length of the finite-width conducting strips on the antennas in the above-mentioned reference can be more than $100\lambda_0$. In this paper we apply a two-dimensional analysis that allows one to determine the H-plane radiation characteristics of the holographic antenna. This analysis consists of a well-known integral equation formulation for a line source illuminating a structure consisting of conducting strips and dielectric material, and its solution using the method of moments (eg. X.Yuan, R.F.Harrington, & S.S.Lee, *JEWA*, **2**, 21-44, 1987). A similar approach has previously been used to model the principal plane patterns of horn antennas with complex flare geometries (eg. D.J.Heedy & W.D.Burnside, *IEEE Trans.*, **AP-33**, 1223-1226, 1985). We will show how it can be applied in the modeling of the holographic antennas in question. It is possible to model the holographic antenna's feedhorn, the holographic antenna proper, and its interaction with the feedhorn. In addition, we have integrated the electromagnetic analysis with numerical optimization algorithms, and will show what antenna geometries (such as the distribution of conducting strip widths) are obtruded by such algorithms as being optimum in some sense.

In order to apply numerical optimisation it is of course necessary to translate a set of practical requirements into mathematical expressions that define the objective functions to be minimized. We will illustrate how the optimal solutions for the holographic antenna design change with alterations to the possible objective functions.

0-7803-7846-6/03/$17.00 ©2003 IEEE 

# Multilevel Fast Evaluation of Radiation Patterns for Lens and Reflector Antennas

Amir Boag
Department of Physical Electronics
Tel Aviv University,
Tel Aviv 69978, Israel

Christine Letrou*
INT / SAMOVAR (CNRS FRE 2310)
9 rue Charles Fourier
91011 Evry cedex, France

Lens antennas are gaining popularity in the millimetric and submillimetric ranges, for applications as diverse as mobile broadband communication and radioastronomy. For these applications, lenses are especially useful for multibeam or shaped beam antennas, and they are used either in combination with horns, or in open structure configurations, where planar antennas are printed at the back of substrate-lenses. On the other hand, reflector antennas are well established in a variety of applications. Here, we refer specifically to lens antennas while the proposed approach is directly applicable to all aperture radiation cases, including reflector antennas and radomes. Conventionally, the radiation pattern of a lens antenna is evaluated by employing the physical optics integral while assuming that the tangential electric and magnetic fields on the outer surface of the lens have been already computed. The latter computation is often effected by the Method of Moments (MoM) analysis of the feed followed by a ray tracing procedure and will not be discussed any further. Due to the large electrical dimensions of lens antennas, the computation time is often dominated by the surface integration time.

In this paper, we address the issue of numerically efficient evaluation of the pertinent integrals. The number of field sampling points $N$ on the lens surface is proportional to its illuminated area (normalized to the wavelength squared). In order to sufficiently resolve the two-dimensional structure of the radiation pattern, the latter should be evaluated over a hemisphere at a number of points, also, proportional to the aperture area. Of course, the proportionality factors depend on the acceptable error level and the specific quadrature rule used, as well as, the desired level of oversampling of the radiation pattern. Thus, the computational cost of the straight-forward integration for $O(N)$ far-field directions each using $O(N)$ field samples amounts to $O(N^2)$ operations. On the other hand, the conventional Fast Fourier Transform (FFT) far field evaluation for planar apertures achieves an $O(N\log N)$ computational complexity. Recently, we proposed a novel domain decomposition approach aimed at achieving a high computational efficiency while removing the restrictions on the surface geometry (A. Boag and C. Letrou, *IEEE Trans. Antennas Propagat.*, vol. 51, no. 5, May 2003). This approach is based on the observation that the fields on the lens surface serving as the equivalent sources of radiation are sufficiently smooth, and we can safely assume that no "super-gain" distributions are present. Under these conditions, the radiation pattern can be "fully described" by its samples at a number of points proportional to the area of the surface domain comprising the equivalent sources. By "fully described" we mean that the pattern at an arbitrary point can be evaluated (with a prescribed error) by interpolation from the samples. Extending the proposed approach, we propose a multilevel computational algorithm based on a hierarchical domain decomposition of the aperture into subdomains. In this algorithm, the radiation patterns are first computed directly for the subdomains on the finest level of decomposition. The radiation patterns of the subdomains are evaluated over a very sparse grid of directions, thus providing the computational savings. Subsequently, the radiation patterns are progressively aggregated into the final pattern of the antenna as a whole. The aggregation steps involve phase correction, interpolation and addition. The multilevel algorithm attains the $O(N\log N)$ asymptotic complexity.

0-7803-7846-6/03/$17.00 ©2003 IEEE

# Improvement the Bandwidth of Microstrip Reflectarray Antenna for Use in Microsatellites

**Kiyan Keyghobad[1,2] and Homayoon Oraizi[1]**

**[1] Department of Electrical Engineering**
**Iran University of Science and Technology, Narmak, Tehran 16844, Iran**
**Tel: +98-21-7808022 Fax: +98-21-7454055 e-mail: h_oraizi@iust.ac.ir**

**[2] Advanced Electronic Research Center ,Tehran, P. O. Box 19585-836, Iran**
**Tel: +98-21-2549734 Fax: +98-21-2546895 e-mail:kiyan43@yahoo.com**

The advantages of microstrip reflectarray make it attractive for use in microsatellites to replace the conventional parabolic reflector antennas.These advantages are low profile, low volume and mass, easy deployability, scannable beam, low manufacturing cost, ability of dual and circular polarization, and dual band frequency. However, the main disadvantage of this antenna is its limited bandwidth.

There are two main methods for design and analysis of the microstrip reflectarrays. In both of them , the first step is to calculate the phase required for each microstrip patch element for a desired main beam angle. In one method the reflectarray is implemented by identical patches and the desired phases can be realized by varying the length of microstrip stubs (open or short circuit) attached to the patches ( J. Huang, Proc. ISAP 96, Chibo, Japan, 1177-1180, 1996 ). In another method the phases can be realized by an array with variable size microstrip patches. Full wave analysis of infinite arrays and the method of moment are then used for element phase determination ( D. M. Pozar, S. D. Targonski and H. D. Syrigos, IEEE- AP-45, No. 2, 287-296, Feb. 1997 ).

In this paper it is proposed to combine the two methods. The reflectarray antenna is a n×n microstrip patch elements planar array which reflects the incident fields radiating from a feed antenna.Each patch element introduces a phase change to the scattered fields.At first it is determined the phases required to be made by patches for radiation in a desired direction. These determined phases are implemented by varying both the size of patches and the length of attached stubs. A full wave analysis consisted of modeling an infinite array by Spectral Domain Electric Field Integral Equation ( SDEFIE) implemented to determine the phase shift effect of each stub loaded microstrip patch in the reflectarray. The Method of Moment is used for solving the SDEFIE and obtaining the current distribution on patch elements and open ended stubs. This current distribution is used for determining the far field radiation pattern of the reflectarray. The shape of open ended microstrip stubs are optimized by Least Square Method to improve the bandwidth characterestics of antenna.

In this way , it can be used the advantages of both methods mentioned above and omit the constraints of the antenna bandwidth.

0-7803-7846-6/03/$17.00 ©2003 IEEE 

## Design of Twin E Plane Sectoral Horns for Power Division

**Wendell A. Brokaw [1,2], Gary M. Briand [1], and Thomas X. Wu [2]**
[1] Harris Corporation, Melbourne, FL 32902
[2] School of EE and CS, University of Central Florida, Orlando, FL 32816

A simulated model and physical prototype is presented for the development of two E plane sectoral horns that will deliver directional and unequal power radiation for illumination of a cassegrain sub reflector and a primary feed horn from a WR42 waveguide within a frequency band of 20.22 GHz to 20.28 GHz. The two horns are designed to deliver a signal at 60 degrees and -70 degrees from a horizontal normal. The horn delivering the signal at -70 degrees is required to be –4 dB lower than the horn delivering signal at 60 degrees. The design of the device begins with an HFSS simulation of a straight section of WR42 waveguide that must divide the power as specified. A straight section of length 0.35 inches, accounting for waveguide attenuation of higher order modes, is modeled with an infinitely thin septum to achieve the necessary power division. Once the location of the septum is optimized, the septum is then modeled with a thickness that can be feasibly manufactured. The optimized septum width dimension is found to be 20 mils. The return loss of the straight WR42 waveguide section with the septum is seen to be less than -23 dB. As a result of the septum, the WR42 waveguide is divided into a large port and a small port. The two E plane sectoral horns must be matched to the reduced dimensions of the WR42 waveguide; this is done through a single step quarter wave transition [G. Matthaei, L. Young, and E. Jones, *Microwave Filters, Impedance-Matching Networks, and Coupling Structures* (1980)]. Each horn step transition is modeled, and the return loss is seen to be less than -45dB at the large port, and less than –43 dB at the small port. Two E plane sectoral horns are then designed to exhibit a pattern with side lobe levels of less than –8 dB below peak gain [C. Balanis, *Antenna Theory*, (1996)]. The horns are designed to match the same aperture dimensions, 0.112 inches by 0.42 inches. A full model is constructed consisting of the WR42 waveguide, septum, step transitions, and E plane sectoral horns. The return loss at the feed port is seen to be slightly less than -13 dB. To optimize the return loss of the entire system, HFSS is used iteratively to de-embed into the feed port of the system, and the impedance is viewed. It is found that at a distance of 0.13 inches the impedance can be matched using an inductive iris. Through iterative efforts using HFSS, an inductive iris of 40 mils by 35 mils by 420 mils is sufficient to yield a total system return loss of less than –37 dB. The prototype is fabricated as a mandrel that is processed through copper electro-formation. Figure 1 displays a wire frame view of the inner conductor geometry to which the prototype is fabricated. The radiation pattern of the prototype is measured in a primary focus antenna range. A comparison of the simulated and measured radiation patterns is displayed in Figure 2.

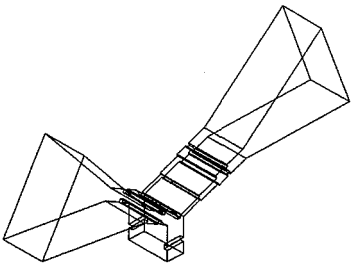

**Figure 1**

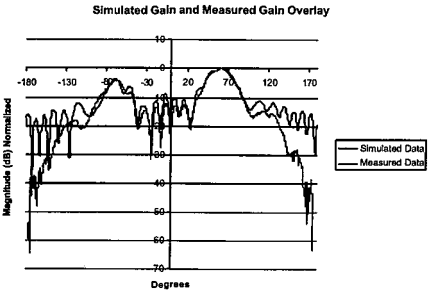


**Figure 2**

0-7803-7846-6/03/$17.00 ©2003 IEEE

***Special Session***

**Active Integrated Antennas**

**Organizer(s):** Roberto Rojas, ESL OSU
Vakur Erturk

**Co-Chairs:** R. Rojas
V. Erturk

7:55 Opening Remarks

10. 1 8:00 Integrated Antenna System for Wireless RFID Tag in Monitoring Oil Drill Pipe ..... APS
*B. Strassner, K. Chang, Texas A&M University, USA*

10. 2 8:20 Active Integrated Beam Scanning Microstrip Array ..... 48
*K. W. Lee, R. G. Rojas, The Ohio State University, USA*

10. 3 8:40 Active Quasi-Optics ..... 49
*D. B. Rutledge, Caltech, USA*

10. 4 9:00 Fault Tolerance Millimeter-Wave Spatial Power Amplifiers ..... 50
*A. Al-Zayed, North Carolina State University, A. Mortazawi, University of Michigan, USA*

10. 5 9:20 Developments in Active Integrated Antennas ..... APS
*K. M. Leong, T. Itoh, University of California, Los Angeles, USA*

10. 6 9:40 A Triangular Phased Array Excited by Oscillators Coupled on a Hexagonal Lattice ..... 51
*R. J. Pogorzelski, California Institute of Techology, USA*

# Active Integrated Beam Scanning Microstrip Array

K.W. Lee* and R.G. Rojas
Dept. Electrical Engineering, ElectroScience Laboratory
The Ohio State University
Columbus, Ohio 43212-1191, USA

Research on active integrated transmitting antenna arrays (AITAA) is a multidisciplinary endeavor because it requires expertize in antenna theory, electronic device modeling and nonlinear dynamics. Due to the highly nonlinear behavior of the system of coupled oscillators, AITAA have interesting properties that can be exploited in practical applications. One such application is in the area of active integrated phased arrays (Stephan, *IEEE Trans. Microwave Theory and Techniques*, **34**, 1017-1025, 1986, and York, *IEEE Trans. Microwave Theory and Techniques*, **41**, 1799-1809, 1993). Unlike traditional phased array design, where phase shifters are used for phase control of the array elements, the phase profile of the active integrated phased array can be manipulated by using nonlinear locking techniques. Hence, the amount of phase shifters used in the array can be significantly reduced.

Previous proposed schemes often suffer from a small beam scanning range and/or the array performance is sensitive to environmental changes. In this paper, an active integrated phased array scheme consisting of a phase-locked loop (PLL), an array of coupled VCO-antennas (voltage-controlled-oscillator active integrated antennas) and phase delay elements is presented. Rectangular microstrip antennas, which function as radiators and resonators, are integrated with transistors and voltage control varactors to form the VCO-antenna elements. The coupling structure between the two outer elements at each edge of a one dimensional array consists of two circulators and one phase shifter to provide non-reciprocal coupling, whereas, the inner VCO-antenna elements are coupled to their nearest neighbor with a reciprocal resistively loaded microstrip transmission line.

The basic idea of the scheme is that a phase-locked loop is employed to enhance stability of the array operating frequency while beam scanning is done by adjusting the delay elements. Design procedures, detail analysis and experimental results of the array will be presented. Recently, it came to the authors' attention that Hwang and Myung (*IEEE Microwave and Guided Wave Letters*, **8**, 191-193, 1998) had proposed a similar beam scanning technique. Their technique is also based on controlling the coupling angle of the coupling element at each of the two edges in a coupled oscillator array. However, their coupling structure is different from ours, because their coupling scheme at the two edges is reciprocal. In addition, they only have antenna elements for the inner oscillators and the antennas act as radiators only.

0-7803-7846-6/03/$17.00 ©2003 IEEE

# Active Quasi-Optics

David Rutledge
California Institute of Technoogy

There has been terrific progress in high-speed transistor technology, and this makes it possible to construct transistor amplifiers now for frequencies as high as 220GHz. However, the output power drops rapidly at the high frequencies for fundamental reasons. The gate length must be made short to make the transistor fast, and this limits the voltage. The gate width must scale with the length to maintain reasonable impedance, and this limits the current. The result is that the maximum power tends to drop off as frequency squared. Transistors produce hundreds of watts at 30MHz, but only a few milliwatts at 30GHz. This limits the introduction of millimeter-wave radars, high-speed point-to-point Internet connections, and high-speed millimeter-wave satellite uplinks. For these transmitters, we need to be able to combine the outputs of hundreds or thousands of transistors. However, the traditional transmission-line power combining technology using Wilkinson splitters and combiners is limited by transmission-line losses. Power loss on transmission lines follows an exponential law with distance, and that means that there is a maximum output power that can be achieved; adding more devices actually reduces the total power. Power combiners based on Wilkinson couplers typically have only 8 or 16 devices.

At Caltech, we have been studying power amplifiers based on spatial splitting and combining. The advantage of this approach is that the outputs of large numbers of transistors can be combined with low loss. We make periodic structures loaded with transistors that are called *grid amplifiers*. These are made as single gallium-arsenide integrated circuits with up to 500 transistors. The input is a beam that comes through the back of the chip, and the output comes out from the front. We measured a combining loss of only 1-dB for a 35-GHz grid amplifier. The output power was 5W. Early measurements were made with large 30-cm diameter plastic lenses, which are not suitable for applications outside of the laboratory, but recently we have developed compact waveguide mode converters for coupling to the grid amplifier [1]. In addition, we have built an indium-phosphide grid amplifier in waveguide that operates at 60GHz, but with a small 2-dB gain [2].

References

[1] "A Waveguide Mode-Converter Feed for a 5-W, 34-GHz Grid Amplifier," Chun-Tung Cheung, Jonathan B. Hacker, Gabor Nagy, David Rutledge, International Microwave Symposium, Seattle, June 2002.
[2] "V-Band Transmission and Reflection Grid Amplifier Packaged in Waveguide," Chun-Tung Cheung, Roger Tsai, Reynold Kagiwada, David Rutledge, submitted to the International Microwave Symposium, Philadelphia, June 2003.

This work was supported by the Army Research Office under the Quasi-Optic Power Combining MURI program.

## Fault Tolerance Millimeter-Wave Spatial Power Amplifiers

**Ayman Al-Zayed* and Amir Mortazawi**
***North Carolina State University, Department of Electrical and Computer Engineering, Raleigh, NC 27695, USA**
**University of Michigan, Department of Electrical Engineering and computer Science, Ann Arbor, MI 48109, USA**

Spatial power combined amplifiers have been maturing over the past few years, providing increased power output levels, power added efficiencies, and power combining efficiencies from an array printed antennas coupled closely with solid state devices. In this paper, modeling data and experimental results from a 49-elements Ka band spatial power amplifier array are presented; prospective view of this amplifier is shown in Fig. 1. In addition, system degradation versus device failure has been studied. Results for both simulated and measured cases will be discussed. As can be seen in Fig. 2 when 16% of the active devices fail across the array only 2.2 dB reduction in power was measured.

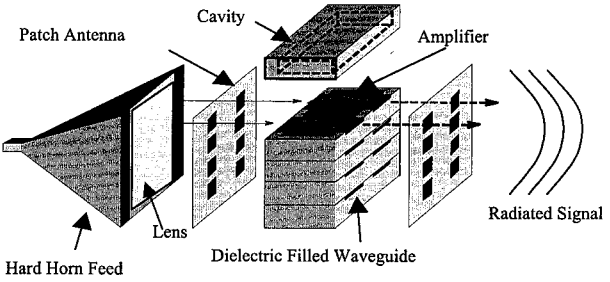


Figure 1: Prospective view of the perpendicularly-fed patch array structure.

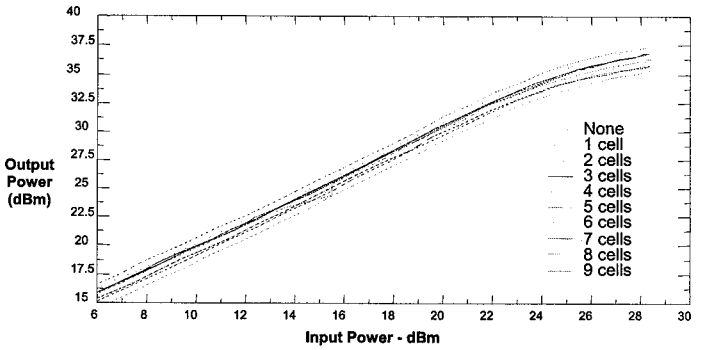


Figure 2: Measured power compression curves of the amplifier for various numbers of device failures.

# A TRIANGULAR PHASED ARRAY EXCITED BY OSCILLATORS COUPLED ON A HEXAGONAL LATTICE

Ronald J. Pogorzelski
Mail Stop 138-307
Jet Propulsion Laboratory
California Institute of Technology
4800 Oak Grove Drive
Pasadena, CA 91109-8099

When a set of electronic oscillators is coupled so as to mutually injection lock, it can be used to produce excitation signals for the elements of a phased array antenna which have a linear phase distribution over the array. [R. A. York, IEEE Trans., MTT-41, pp.1799-1809] [P. Liao and R. A. York, IEEE Trans., MTT-41, pp. 1810-1815] The slope of this phase distribution can be controlled by adjustment of tuning of the oscillators on the perimeter of the array. This has been studied both theoretically and experimentally over the past several years in the context of coupling on a Cartesian lattice with a rectangular aperture each oscillator being coupled to four nearest neighbors. [R. Ispir, S. Nogi, M. Sanagi, and K. Fukui, IECE Trans. Electron., E80-C, 1211-1220, Sept. 1997] [R. J. Pogorzelski, Microwave and Guided Wave Letters, 10, pp. 478-480.] [J. Shen and L. W. Pearson, 2001 Nat. Radio Sci. Mtg, Boston, MA] More recently, a triangular aperture was investigated in which the oscillators were coupled on a triangular lattice; that is, coupled to six nearest neighbors. [R. J. Pogorzelski, 2002 Nat. Radio Sci. Mtg, Boulder, CO]

In this paper, a triangular array is proposed with oscillators coupled on a hexagonal lattice. The analyses of such an oscillator array using the full nonlinear formulation based on a Van der Pol model of the oscillators, a linearized version of this formulation, and a continuum model of the array are outlined. It is shown that the response time of the array is scaled by a factor of four relative to the rectangular case making the steering rather slow. More importantly, and somewhat counter-intuitively, it is shown that, unlike the rectangular and triangular coupling schemes, for the hexagonal scheme, a planar phase distribution is not a solution of the differential equations describing the array dynamics for all azimuth angles. Thus, although approximately achievable, a planar aperture phase is theoretically not exactly achievable for arbitrary azimuth angle without adjustment of the tuning of all the oscillators, not just those on the array perimeter. The primary impact on the array performance is a small degradation in the gain. There are, however, discrete azimuth angles for which the planar distribution is in fact an exact solution of the equations and, thus, for these angles a planar distribution is achievable and there is no gain degradation.

0-7803-7846-6/03/$17.00 ©2003 IEEE

## Novel Antenna Designs

**Co-Chairs:** W. Pickens
E. Arvas

10:00 Opening Remarks

**High Aperture Efficiency Ka-Band Horn Using Hard Boundary Walls**

Wesley Pickens, Jet Propulsion Laboratory, California Institute of Technology

A prototype horn has been developed using dielectric-filled longitudinal corrugations in the vertical walls to create a hard boundary condition. The result is a field distribution in the horn aperture that is uniform in amplitude and phase. FEM modeling in Ansoft Corporations High Frequency Structure Simulator (HFSS) provided preliminary analysis of horns with an initial corrugation depth chosen based on the work presented by P.S. Kildal (*Elect. Let.*, vol. 24, pp168-170, 1988).

The horn is fed by a square waveguide with the corrugations increasing in depth until the desired field excitation is achieved. The depth increases along a cosine taper. The horn is fed by the transition piece shown in Figure 1. Preliminary results show that this geometry will provide a better impedance response than would a linear taper.

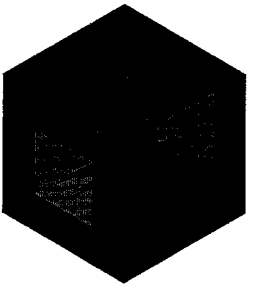

(a)

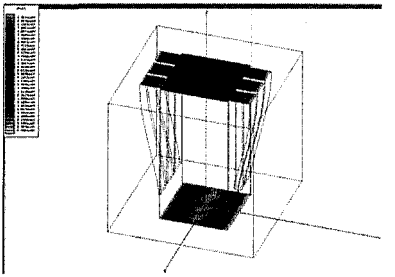

(b)

Factors considered in choosing the depth of the corrugations include the field distribution in the aperture, the S-parameter response and the value of the complex propagation constant. The values were obtained by simulating transition sections with varying corrugation depths. Through comparison of the results a design exhibiting the highest likelihood of success was chosen for fabrication.

Geometries employing more numerous and narrower corrugations were simulated and have shown even better field responses that could lead to higher aperture efficiencies. However, the manufacturing cost of such a design is prohibitive at this stage of development. Additionally, simulations have been run with a single dielectric slab using both linear and cosine tapers. Measured results will be compared to the simulations and presented for the chosen design.

0-7803-7846-6/03/$17.00 ©2003 IEEE

# A Hybrid Model of a Monopole with a Coaxial Shielded Load

Jeremy P. Rudbeck and Chalmers M. Butler*
Holcombe Department of Electrical and Computer Engineering
331 Fluor Daniel EIB
Clemson University, Clemson, SC 29634-0915 USA
jrudbec@clemson.edu cbutler@clemson.edu

The analysis of an antenna loaded with lumped circuit elements can be based on an efficient combination of Maxwell's equations (antenna) and circuit theory (loading circuit). But, if for example a wire antenna is loaded by a traditional thin-wire coil, the accuracy of the analysis may suffer due to the field coupling between the antenna members and the turns of the coil, which is not accounted for in either the antenna or circuit analysis per se. In such cases, the advantage in simplicity gained by using circuit theory to account for the presence of the lumped loading circuit elements is diminished by a loss in accuracy of the combined analysis. Shielding a coil, however, isolates its windings from the "stray fields," thereby ensuring coupling only at the terminals of the loading circuit and assuring the validity of computations based on the laws of circuit theory. Of course, there are other advantages realized by shielding tuning coils. The use of circuit laws to characterize load circuits, as opposed to appealing to Maxwell's equations to capture all significant effects, greatly simplifies analyses and reduces design efforts. But, on the other hand, the presence of the shield renders the characterization of a coil more complex. However, if the input impedance to a shielded load can be determined accurately, one may easily employ such loads for tuning purposes.

An accurate hybrid method is presented for analyzing a cylindrical antenna loaded with a shielded coil. The method consists of a computational procedure for solving the loaded cylindrical antenna integral equation and of a measurement procedure for accurately characterizing the shielded load. The structure of the shield ensures that the above mentioned accuracy-degrading effects of stray field coupling does not exist and the hybrid analysis technique fully accounts for the loading coil in the presence of its shield.

Measuring the input impedance of a shielded load presents several difficulties in practice, as standard connectors do not exist for interfacing the load with a network analyzer. A method to accurately measure the impedance looking into a shielded load, which involves interfacing the load with a measuring instrument by means of a two-port network, is described. The effects of the interfacing network on the measurements of the properties of a shielded load are removed from the data by invoking a simple transformation based upon two-port network theory and knowledge of the impedance parameters of the network. A calibration scheme is developed to determine the impedance parameters of the interfacing network. With data available to characterize the shielded load, one incorporates this load in the antenna integral equation and can obtain a solution that accurately accounts for the presence of loads in their shields along the antenna. Data from the hybrid solution are compared with those obtained from measurements made on a laboratory model. Accurate measurement of the input impedance of the model is facilitated by another de-embedding technique similar to that mentioned above.

0-7803-7846-6/03/$17.00 ©2003 IEEE 

# Turnstile/Cone Antenna Design and Analysis for UHF SATCOM Communications

T. G. Campbell, and Darius Romanek* and C. J. Reddy
Applied EM, Inc., Hampton, Virginia 23666
[tom_campbell, darius, cjreddy]@appliedem.com

**Abstract:**
Inexpensive, lightweight antennas are needed to provide omni directional, circularly polarized radiation patterns for UHF SATCOM applications. A turnstile/cone antenna was designed to meet UHF SATCOM requirements. The basic antenna concept consists of a canted turnstile, fed by a split-tube balun and is positioned over a truncated, slotted conical ground plane. This combination produces a broad beam, circularly polarized radiation pattern. Another design feature of this antenna concept is the opportunity to include a radial choke flange to attenuate the back lobe radiation. This antenna concept has a unique heritage. NASA used a similar design concept for the landing radar altimeter on the Viking Mars Lander Spacecraft that soft-landed on the Planet Mars in 1976. This antenna was redesigned and optimized for UHF SATCOM applications using very unique conductive coatings (www.unishield.com). Unishield is a water-based, highly conductive coating is used to reduce the weight of the antenna. Commercial EM analysis software, FEKO is used for this antenna design and optimization. The field computation is based on Method of Moments (MoM) formulation. The geometry of the turnstile/cone antenna was defined using FEKO's parametric geometry cards. With this capability, FEKO provided a 3D visualization of the surface currents on the antenna and resulting 3D radiation patterns. Optimization feature in FEKO (optFEKO) is applied extensively to optimize the design of the turnstile/cone antenna for UHF SATCOM communication applications. Input impedance and radiation pattern measurements are conducted to validate the design. Results of this analysis along with experimental measurement results are presented in this paper.

Turnstile cone
CP crossed dipoles

360 MHz

220 - 450 MHz covers all military Satcom, This one doesn't cover all that

0-7803-7846-6/03/$17.00 ©2003 IEEE


Space Act Agreement - make measurements at LaRC

L1 (GPS+GLONASS) 1588,5 ± 23,5 MHz ~3%
L2 (GPS 1227,6 ± 10 MHz

# A DUAL BAND DOUBLE LAYER PRINTED QUADRIFILAR HELIX ANTENNA FOR GPS, GLONASS AND GALILEO APPLICATIONS.

R. Cléquin[(1)], A. Sharaiha[(2)]
[(1)]MBD.A missile systems, "La Chaudronne" - RD 75, 41300 Selles Saint-Denis - France
r.clequin@dial.oleane.com
[(2)]IETR, Groupe Antennes § Hyperfréquences, UMR CNRS 6164
Université de Rennes 1, 263 Avenue Général Leclerc, 35042 Rennes cedex, France
ala.sharaiha@univ-rennes1.fr

In the last few years, the printed quadrifilar helix antenna (PQHA) has become an attractive candidate for use in mobile communication systems due to its features of circular polarisation, good axial ratio and low cost. However, the bandwidth of a conventional PQHA is typically equal to 5 to 8% and could be insufficient for such applications.

This article introduces a low cost dual band Double Layer Printed Quadrifilar Helix Antenna (DL-PQHA) for GPS, GLONASS and GALILEO applications. The dual frequency band behaviour is obtained by using the mutual coupling effect between the two PQHAs fitted into each other. This structure give a good impedance match in both GPS and GLONASS operating frequency bands.

This antenna is used for equipments of ground fixed station world-wide and is realised by MBDA Missile Systems. The antenna department of MBD.A performs research, design, and manufacturing in the field of communication antenna systems. In house production facilities are available for high quality production using advanced materials and processes. MBD.A is certified ISO 9001.

Typical products are Telemetry, Tracking, Control (TTC) and GPS antennae for satellites and launchers, data link, telemetry and GPS antennae for military applications, TTC and GPS antennae for the equipment of ground fixed stations.

The Antenna design : The DL-PQHA is composed of two PQHA where the four arms of each is printed on a thin dielectric substrate. The inner PQHA is wrapped around a cylindrical dielectric foam ($\varepsilon r \cong 1$) surrounded by a cylindrical spacer foam. This way, we obtain the first antenna which will be the cylindrical support of the outer PQHA wrapped around it. This structure is supplied with the same feeding network.

The Analysis : The antenna was modelled and optimised using moment-method formulation for arbitrary-shaped coated wire antenna. The computer modelling include the dielectric loading by transforming the printed antenna into an equivalent dielectric coated wire structure using quasi-static approximation.

Conclusion : A DL-PQHA for GPS and GLONASS was realised. The experimental results illustrated a good VSWR and an hemispherical radiation in the two receiving bands. The structure can also cover the GALILEO frequency band. This new low cost antenna is a promising candidate for GPS and GLONASS and all dual band applications.

Measured Gain (dBi) at 1227 MHz

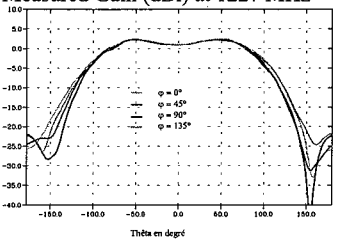


Measured Axial ratio (dB) at 1227 MHz

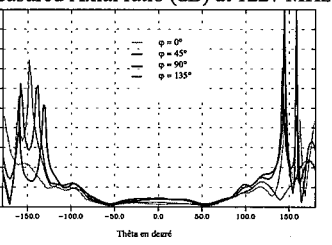




5-8% BW

## The Broadband Quadrifilar Helical Antenna

Samir Tozin[1*], Carl Gerst[2], Joe Mautz[1], Ercument Arvas[1]
1 *Syracuse University, Syracuse, New York*
2 *Anaren Microwave, East Syracuse, New York*

The quadrifilar helical antenna (QHA) has become increasingly popular in satellite based communication systems because of its ability to produce high gain and excellent circular polarization over wide beam angles. In this paper, the determinantal equation for the infinite tape QHA is reported, and used to analyze the QHA for its complete Brillouin, $(k-\beta)$, diagrams. We show that a QHA has four determinantal equations and four distinct $k-\beta$ diagrams. Each $k-\beta$ diagram is associated with a particular sequence mode, and each sequence mode is associated with a particular excitation. Of the four QHA sequence modes, we focus our attention on the two modes that produce circularly polarized radiated waves. Two basic radiation modes are exposed; a scanning mode and a fixed forward end-fire mode. These modes are similar in nature to Klock's (P. Klock: "A Study of Wave Propagation on Helices," Thesis, University of Illinois, March 1963.) unifilar modes. The effects of varying tape width, pitch angle and frequency are studied. A QHA model based on antenna array theory is developed, and used to investigate radiation patterns as well as operating bandwidth for each mode. One of the $\overline{k}-\beta$ diagrams for the QHA is shown below. The normalized wavenumber $\overline{k} = \frac{2\pi a}{cot\psi}k$, where $a$ and $\psi$ are the radius and pitch angle, respectively. Our first observation is that, for a given $\overline{k}$, it is possible to have two values of $\beta$. There are in fact many more $\beta$'s for a given $\overline{k}$, but some have been ruled out because of their non-physical nature. Mode 1, labeled with $*$, is the so called scanning mode; Mode 2, labeled with $o$, is the fixed forward end-fire mode. These modes are very similar to those described by Klock.

PSfrag replacements

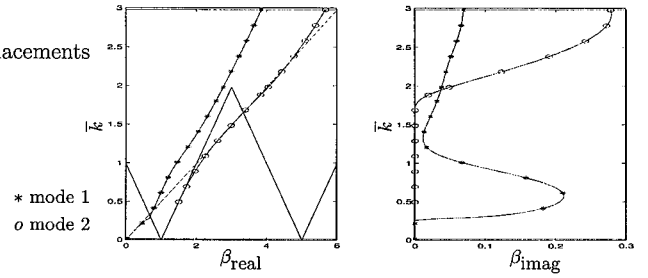


0-7803-7846-6/03/$17.00 ©2003 IEEE

*Special Session*

## Electromagnetic Interference with Complex Platforms I

**Organizer(s):**

**Co-Chairs:** M. Harrison
I. Kohlberg

7:55 Opening Remarks

## Introduction to EMI Effects on Complex Platforms

Piergiorgio L. E. Uslenghi
Department of Electrical and Computer Engineering
University of Illinois at Chicago
851 South Morgan Street, Chicago, Illinois 60607-7053, USA
Email: uslenghi@uic.edu

Electromagnetic threats on electrical systems and equipment include both ultrawide-band environments and narrow-band, high-power microwave sources. Complex platforms and the integrated circuits they carry are becoming electrically comparable to a wavelength; their resonances and coupling effects alter significantly the physics of electronic components, circuits, and systems. This work outlines a major, comprehensive effort to study such EMI effects analytically, numerically, and experimentally. Four major tasks are surveyed.

The first task is the characterization of coupling mechanisms responsible for guiding EMI energy from outside the platform down to electronic components. The platform is broken down into pieces that are studied individually and then connected topologically. Use is made of advanced frequency-domain and time-domain EM solvers. The codes are validated by comparison with each other and with some exact analytical solutions to boundary-value problems.

The second task is the characterization of the spurious waveforms at the ports of a digital system. A full-wave 3D analysis of linear passive systems converts the radiating and conducting EMI into sets of noise sources at the input ports of nonlinear active circuits. Circuit models for coupling paths are developed. A network-oriented nonlinear transient simulator is developed for small- and large-signal analysis of nonlinear electronics.

The third task is the determination of conditions for induced change-of-logic states and alterations of logic functions for digital circuits and computer systems. A fault-tolerance analysis is developed to determine, classify, monitor and control various system program errors under EM threat. The fourth task is to perform system, subsystem and component design and testing for the validation of EM penetration and coupling models, and of circuit and system fault models.

This comprehensive program is being carried out by groups of researchers at Clemson University, University of Houston, University of Illinois at Chicago, University of Illinois at Urbana-Champaign, University of Michigan, and Ohio State University, with the assistance of US Air Force personnel and DOD consultants.

0-7803-7846-6/03/$17.00 ©2003 IEEE 

**Analysis of a Coaxial Cavity with Cross-Section Dependent upon Axial Displacement**

John C. Young and Chalmers M. Butler*
Holcombe Department of Electrical and Computer Engineering
336 Fluor Daniel EIB
Clemson University, Clemson, SC 29634-0915 USA
johny@ces.clemson.edu cbutler@eng.clemson.edu

The field in a cylindrical cavity, comprising cascaded coaxial and circular-cylindrical sections, may be computed by expanding the field in each section in terms of the eigenfunctions of that section and enforcing continuity of the tangential field in the apertures in the planes at which the sections join. When a section's cross-section varies with axial displacement, the eigenfunctions of the section may not be known and, hence, another method must be devised to determine the field in that section. If the cavity is composed of a combination of sections with fixed cross-sections and sections with variable cross-sections, then the eigenfunction expansions may still be used to determine the fields in the fixed cross-section cavities.

In this paper, aperture theory is employed to determine the field in a cavity section with variable cross-section which is excited by the field in a sending-end uniform coaxial section and which is terminated by means of a receiving-end uniform coaxial section. In the usual way, the apertures are shorted and an equivalent magnetic current (related to the electric field in the aperture) is placed on the shorted apertures. Next, the pec walls of the cavity are removed and an equivalent electric current is placed on the surfaces formerly occupied by the walls. If this new (wall) surface (original walls plus shorted apertures) is a closed surface, then either the EFIE or the MFIE may be incorporated in the solution technique, but, if surface is not closed, e.g., the modeled wall has a baffle, only the EFIE is applicable. From the coupled integral equations formulated to satisfy boundary conditions, sending-end excitation, and receiving-end termination, one determines wall current and equivalent magnetic current (or aperture electric field), and, from these quantities, the cavity field can be readily found.

The time-harmonic integral equations, whose solutions may be used to compute all other quantities of interest, are solved numerically. For specified input signals and receiving-end terminations, the time history of reflection at the input and transmission to the receiving end are determined from frequency-domain data and the FFT. Models have been fabricated and experiments were conducted for a number of cavity configurations. Measured data allow one to corroborate computed values of quantities of interest. Computed and measured results are in very good agreement.

0-7803-7846-6/03/$17.00 ©2003 IEEE 

**Field in a Complex Cylindrical/Coaxial Cavity Subject to Time-Harmonic and Transient Excitation**

Charles L. Bopp, III,* and Chalmers M. Butler
Holcombe Department of Electrical and Computer Engineering
331 Fluor Daniel EIB
Clemson University, Clemson, SC 29634-0915
cbopp@clemson.edu cbutler@eng.clemson.edu

The field in a complex cylindrical cavity is investigated. We present a coupled-integral-equation method for calculating the field in a cavity constructed from multiple cascaded and overlapping coaxial and circular-cylindrical regions or sections. The regions may have different axial and radial dimensions and may be filled with material having different electrical and magnetic properties. The cavity walls are perfect electric conductors. The first and last sections are coaxial cavities whose dimensions are such that higher order modes are cutoff, leaving only the TEM mode to propagate. The source is taken to be a TEM mode in the sending-end (first section) coaxial guide. The field in a section is related to the field in apertures in planar conducting surfaces, which bound the section. One interface may contain more than one aperture and, hence, may be part of a boundary of more than two regions. A set of integral equations in matrix form is developed and solved by numerical methods. In order to illustrate the solution method and demonstrate its accuracy, a cavity is constructed and analyzed, and the results are compared with data obtained through measurement. Both frequency domain and time domain results are compared. The accuracy of the method is also verified by comparison of measurements and calculations of the current and charge on the center conductor. Special probes are used for measuring signals proportional to the current and charge at various points along the surface of the center conductor. The probes protrude through a slot in the inner tube and may be displaced axially along the center conductor. Results obtained from calculations compare very favorably with the measured charge and current on the inner cylindrical conductor.

0-7803-7846-6/03/$17.00 ©2003 IEEE 

**Analysis of Transmission of a Signal through a Complex Cylindrical/Coaxial Cavity by Transmission Line Network Methods**

Charles L. Bopp*, III, Chalmers M. Butler, and Frederick M. Tesche
Holcombe Department of Electrical and Computer Engineering
331 Fluor Daniel EIB
Clemson University, Clemson, SC 29634-0915
cbopp@clemson.edu cbutler@eng.clemson.edu fred@tesche.com

The transmission of time-harmonic and transient signals through a complex cylindrical cavity is investigated by methods akin to microwave circuit techniques. The complex cavity may be thought of as multiple cascaded and overlapping coaxial and circular-cylindrical regions or sections with perfectly conducting walls. The sections may have different axial and radial dimensions and may be filled with material having different electrical and magnetic properties. The first and last sections are coaxial cavities or guides in which only TEM modes exist, allowing one to readily perform measurements and accommodate excitation and termination of the complex cavity.

The adjacent sections constituting the cavity have common planar interfaces or boundaries with apertures that may be looked upon as junctions at which two or more waveguides or transmission lines join. An interface may contain more than one aperture and, hence, may be part of the boundary of more than two sections. The guides may support only TEM waves remote from these junctions, they may support higher-order modes, they may support both, or they may support no wave at all. If two guides having a common junction each support only one mode, the junction may be viewed as a two-port network. If additional modes are supported, the number of ports of a network increases. In any event, one can define scattering parameters for each junction in the complex cavity. And these S-parameters can be determined for each junction independently by formulating and solving relatively simple integral equations that account for the junction structure and the nature of the joining guides. Once the junctions have been identified and the scattering parameters for each determined, a composite waveguide or transmission line network can be developed and the overall input/output transfer function for the network representation of the complex cavity can be found by microwave circuit techniques. In addition, as a bit of lagniappe, the scattering parameter network description lends itself readily to the BLT transmission line analysis.

This method of analyzing a complex cavity is under investigation and the results are to be compared with those obtained from more traditional solution methods based on coupled integral equations with eigenfunction kernels. Scattering parameters for the junctions have been obtained and are being compared with measured values under the condition that the cavity is particularized to the simple junction plus an input and output section.

0-7803-7846-6/03/$17.00 

# Wire Antenna Attached to a Conducting Body and Coupled to an Enclosed Cavity

John C. Young and Chalmers M. Butler*
Holcombe Department of Electrical and Computer Engineering
336 Fluor Daniel EIB
Clemson University, Clemson, SC 29634-0915 USA
johny@ces.clemson.edu cbutler@eng.clemson.edu

In any evaluation of the immunity of a system containing sensitive electronic devices to deleterious effects caused by spurious signals, the characteristics of the offending signals at the inputs to the devices must be available. Often this signal originates from a source outside the system and couples into the system through an antenna. Ultimately it finds its way to the device via some path. A typical path may be along wires and cables, through enclosed regions, e.g., housings of components, and through apertures where one housing joins another. The influence of transmission paths on the shapes and magnitudes of signals as they pass through a system is important in any investigation of the possible alteration of the performance or output of an electronic device. If a signal of a specified form enters a system at a given point, one would like to be able to predict the characteristics of the signal at another location in the system where a susceptible circuit might be located. From an alternate point of view, one may be interested in a radiation problem instead of a penetration problem. In this case, the signal may originate at some device in the system, propagate through the system, and excite an antenna. Then, interest lies in how the system affects the signal as it propagates to the input of the antenna.

A structure comprising a conducting body that encloses an axisymmetric cavity is analyzed. The cavity is attached to the conducting body by a coaxial transmission line whose center conductor extends through a planar surface of the conducting body to form an antenna. For this investigation, the conducting body is also axisymmetric, but the antenna need not reside on the axis of the body. The transmission line is operated well below cutoff so that the antenna characteristics manifest themselves to the cavity in the form of a lumped load at the end of the transmission line. The "exterior" antenna-conducting body problem is solved independently of the cavity problem to determine the antenna input impedance. Then the cavity problem is solved with the determined antenna input impedance used as a load impedance. Data are presented for the radiation problem, where the source is located inside the conducting body. In particular, the measured and computed input admittance looking into an appropriate plane in the cavity is presented. Good agreement between measured and computed data is observed.

0-7803-7846-6/03/$17.00 ©2003 IEEE

**Penetration through an Aperture Backed by a Channel –Coupled Integral Equation Formulation with Specific Green's Functions**

Michael D. Lockard* and Chalmers M. Butler
Holcombe Department of Electrical and Computer Engineering
336 Fluor Daniel EIB
Clemson University, Clemson, SC 29634-0915 USA
mlockar@clemson.edu cbutler@eng.clemson.edu

Penetration through a backed slot in an infinite conducting plane is investigated. Coupled integral equations are formulated which may be solved for the field penetrating into a cavity or channel of arbitrary cross-section. This integral equation method is also applied to the special case of an elliptical-channel-backed slot where the materials interior and exterior to the cavity are isorefractive. Results are compared with data obtained from an analytic solution involving the summation of Mathieu functions [D. Erricolo, M. Lockard, C. M. Butler, this digest]. The general coupled integral equations are also used to analyze channel-backed slotted screen structures which are amenable to analysis by single integral equations with Green's functions specific to the channel geometry and material. Green's functions are developed for magnetic sources in cylinders of circular, sectorial, and rectangular cross-sections. Each Green's function is derived for the case of a magnetic line source as well as for a magnetic line dipole to account for an excitation that is TE or TM to the direction of the slot, respectively. Development of Green's functions with the use of a non-Lorentz gauge for radially-directed line dipoles is discussed and the advantages of such a Green's function are delineated.

The materials in the interior and exterior regions of the structure may be similar or dissimilar for all integral equations considered. Data comparisons are presented for cases of various materials in either region. An arrangement of terms in the coupled integral equations also allows the line source to be positioned in the interior of the channel. Data are presented that illustrate that reciprocity is upheld.

0-7803-7846-6/03/$17.00 ©2003 IEEE 

# Effects of Propagation Path on Transient Signals in Electronic Systems

Anthony Q. Martin*, Vivek Ramani, and Chaitanya Seerama
Holcombe Department of Electrical & Computer Engineering
Clemson University, Clemson, SC 29634-0915

The influence of the transmission path on the characteristics of a transient signal as it passes through an electronic system is of importance in discovering how the operation of digital circuits might be altered as a result of unexpected or spurious electromagnetic energy being incident upon, and propagating through, an electronic system. If a signal of a specified form enters a system at a given point, it is desirable to know the salient features of the signal that reaches some location within the system, where a susceptible digital circuit might be located. Moreover, it is useful to know if any of the features of the induced signal are primarily those peculiar to the entering signal, or if they are more influenced by the properties of the transmission path and/or environment. Addressing these issues should help one gain an appreciation for the nature of a spurious signal arriving at the input of a digital circuit embedded deep within a complex system that is subjected to high-power RF excitation originating outside the system proper.

In the present talk the influence of the transmission path (and environment) on the shape and magnitude of a transient signal will be addressed by numerically modeling the propagation of a signal through a variety of structures that contain certain features present in real-world systems. Structures that electromagnetically replicate only the important details of component configurations found in a typical real-world systems are considered. Examples of such systems include aircrafts, missiles, ground vehicles, personal computers, and electronic test equipment.

The structures considered in this talk are metallic rectangular cavities of different sizes with various types of apertures/openings for signal entry, as well as various interior features such as backplanes, wires, cable/trace runs, and discrete components. Signals having various waveforms are used to excite the structures at various entry points. The numerical analysis of the structures is handled both in the frequency domain, via the moment method, and in the time-domain, via the FDTD technique. The talk considers variations in structure and interior features as well as several transient waveforms, whose spectra span a frequency range from nearly DC to 2 or 3 GHz.

0-7803-7846-6/03/$17.00 ©2003 IEEE

# Aperture Excitation Of A Transmission Line In A Cavity

D. Negri*, D. Erricolo, P.L.E. Uslenghi
Department of Electrical and Computer Engineering
University of Illinois at Chicago
851 South Morgan Street Chicago IL 60607

Under consideration is the excitation in terms of currents and voltages of the two loads of a two-conductor straight transmission line system inside a rectangular cavity due to an external source of plane waves. The electromagnetic fields propagate from the source to the transmission line system through a rectangular aperture on the cavity wall facing the source. The problem is solved by applying the equivalence theorem: the aperture is replaced by a rectangular perfectly electric conductor and an equivalent magnetic surface current density is introduced. The problem is therefore split into an internal problem and external one.

The equivalent magnetic surface current density is strictly dependent on the value of the tangential component of the electric field on the aperture. The imposition of the continuity of the tangential magnetic field in the aperture allows to derive an integral equation to be solved using the method of moments (MoM).

The MoM is reduced to the evaluation of the admittance matrix of the aperture (R. F. Harrington, J. R. Mautz, IEEE Trans. Antennas Propagation, vol. AP-24, pp. 870-873, Nov. 1976). In this evaluation, the admittance matrix is split into two parts. One part does not consider the external scattering; the other part is a correction term recently introduced for taking into account the contribution of the external scattering. While the first part is easily obtainable and largely spread in literature; the evaluation of the second one exploits a heavy numerical technique, involving the use of the "generalized impedance matrix" (T. Wang, Ph.D. dissertation, Syracuse Univ., Syracuse, NY, 1989).

In the internal problem, the coupling between the cavity and the transmission line, in terms of radiation produced by the transmission line, may be either neglected in first approximation, or included in the formulation increasing the computational complexity of the MoM. If it is neglected, in order to overcome the previous approximation, the perturbation approach of the MoM may be applied, assuming that the problem under consideration is only slightly different (perturbed) from the one to be solved exactly. The perturbation approach reaches its end when it converges within an arbitrary tolerance. When the electromagnetic fields inside the cavity are known, the extended BLT equations may then be used. They provide the tool to solve the transmission line system problem to find the required excitation at the loads. Innovative elements of the present research are: the use of the above solving procedures for a cavity containing a transmission line and the application of the BLT equations inside a cavity.

0-7803-7846-6/03/$17.00 ©2003 IEEE 

# Network Analysis of Multiple Apertures on Cavity Enclosure s with Wire Penetrations

T. Yang[1], T. Ozdemir[1], E. S. Siah[1] and J. L. Volakis[1,2]
[1]Radiation Lab., EECS Dept., The University of Michigan, Ann Arbor, MI 48109
[2]ElectroScience Lab., The Ohio State University, Columbus, OH 43212

Increasing clock speeds and the need for compact electronic systems calls for Electromagnetic Interference and Compatibility (EMI/EMC) studies. In enclosures of electronic devices, there may be electromagnetic penetration and radiation through apertures such as ventilation slots, or interference among transmission lines. The goal is to cast the problem into a framework of network analysis, where individual structures involving apertures and wires are represented as macromodels generated from full-wave analysis. Macromodel generation requires multiple parameter sweep and efficient full-wave methods speed up the process.

We present an efficient solution for estimating coupling among arbitrarily shaped apertures on a rectangular metallic cavity (see Fig.1a). In our formulation, the fields across the apertures are approximated via the Method of Moments (MoM) using rooftop basis functions and Fig.1(b) shows the agreement with the measured data for a single aperture on a rectangular box. At the meeting, we will present approximate analysis for multiple apertures.

The presence of wires inside the cavity is treated through the field bouncing method. The interior field, expressed using modal Green's function, is first computed in the absence of wires. It is then used to illuminate the wires, and induced currents are computed using local approximations and the Transmission Line Theory. The currents are then reradiated into the cavity interior and the resulting total field is again interacted with the wires. The iteration continues until the steady state solution is reached.

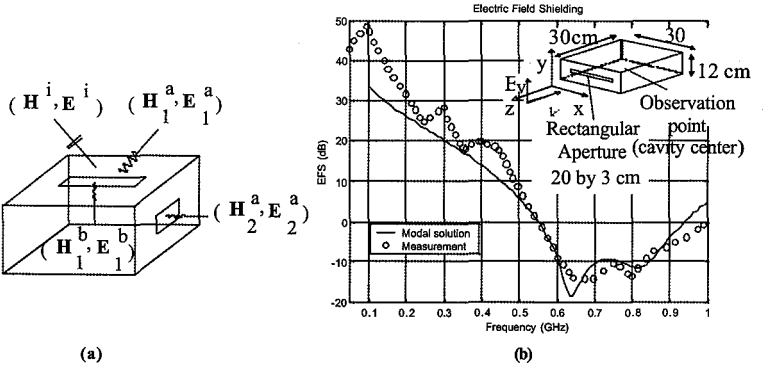


(a) (b)

**Fig. 1: (a) Multiple apertures on a rectangular metallic cavity, (b) Electric Field Shielding for single aperture case.**

# Coupling to a Printed Circuit Board Inside a Cavity from a Wire Penetrating an Aperture

David R. Jackson, Donald R. Wilton, and Chatrpol Lertsirimit

Applied Electromagnetics Laboratory
Department of Electrical Engineering, University of Houston
Houston, Texas 77204-4005

An important EMC problem that arises in various contexts is the electromagnetic coupling from an exterior field to a circuit component on a printed-circuit board (PCB) inside a conducting cavity (shield) via a direct connection from a wire or cable that penetrates an aperture in the cavity. This type of coupling mechanism can be very important in determining the signal levels on the PCB due to the coupling from an exterior field, and it may be the dominant coupling mechanism. Therefore, an accurate and efficient methodology for calculating this type of coupling is important.

One difficulty in the numerical analysis of such coupling problems is treating the disparate levels of feature size. The cavity dimensions may be on the order of a wavelength or more. However, on the circuit board the feature size is often much smaller than a wavelength. Furthermore, a complicated conductor trace pattern may exist on the PCB, requiring a fine level of discretization in a purely numerical scheme. Hence, a method that allows for an efficient analysis of the coupling to the component on the PCB without requiring a complete discretization of the entire problem is desirable.

In this presentation, a hybrid technique for calculating the signal level on the PCB due to an exterior field incident on the cavity is discussed. The technique separates the analysis of the cavity/wire from that of the conductor trace on the PCB, thus enabling an efficient calculation. The method allows a Thévenin equivalent circuit to be obtained at any point on the circuit board (a definable "port"), such as a point where the conductor trace meets a circuit component on the board. Hence, the voltage level at the input to a device on the PCB that results from the exterior incident field can be calculated.

To obtain the Thévenin port voltage, transmission-line theory is used to first obtain an equivalent input impedance seen by the coupling wire at its junction with the conductor trace when an open circuit is placed at the desired port. A full-wave analysis, which accounts for the effects of the cavity, is then used to obtain the current on the coupling wire with the PCB trace replaced by its equivalent impedance. The Thévenin voltage at the port is then found by summing the port voltages that arise from two contributions. The first contribution, which is found from transmission line theory, is the port voltage due to the direct current injection from the coupling wire at the contact point. The second contribution is the port voltage induced by coupling from the current on the wire to the PCB trace. This contribution is found from transmission-line theory, using a distributed source model. The Thévenin impedance can be found from a similar analysis, i.e., by placing a short circuit at the port and then determining the short-circuit current at the port.

Results will be presented to verify the accuracy of the proposed method for various PCB substrate thicknesses within realistic cavity sizes, and to study the effects of cavity resonances on the coupling to the PCB.

0-7803-7846-6/03/$17.00 ©2003 IEEE 

## Generalized FE-BI for solving mixed surface and volume geometries

[1]E.S. Siah, [1]R.W. Kindt, [2]K. Sertel and [1,2]J.L. Volakis
[1]Dept. of Electrical Engineering and Computer Science,
[1]The University of Michigan, Ann Arbor, Michigan 48109-2122
[2]ElectroScience Lab, Ohio State University, Columbus, OH 43212
{esiah, volakis}@eecs.umich.edu

Recent developments in fast computational electromagnetic simulation tools such as the multilevel fast multipole moment method (MLFMM) have enabled analysis of complex real-life problems in shorter solution times using less computer memory. Most realistic problem geometries require the treatment of both volumetric and surface regions concurrently. In this paper, we present a hybrid approach combining the finite element-boundary integral (FE-BI) method with exterior surface modeling through boundary integral coupling between the volume boundary and the surface geometry. Such formulation is intended to couple FE-BI, BI and surface integral methods into a single system. This allows two or more geometries to be modeled in the most efficient manner. For our specific application (Fig. 1), the microstrip circuit board with dielectrics is modeled with FE-BI whereas surface integral with curvilinear basis functions is used to model the PEC surfaces of the cavity and the automobile chassis.

The traditional approach for the FE-BI method involves solving the internal electric fields within the volume of the geometry and the surface electric and magnetic fields on the closed boundary. On the other hand, the solution of PEC structures with the traditional Method of Moments (MoM) using EFIE yields the currents flowing along open PEC surfaces. These two systems can be linked by coupling the surface fields along the volume boundary to currents on the PEC surface. A typical matrix system is given below where $I^n$ refers to the current coefficients along the PEC surfaces, $b^n$ and $b^e$ are the external incident fields on the exterior PEC surface and volume boundary respectively.

$$\begin{bmatrix} A^{VI} & A^{VS} & 0 & 0 \\ A^{SV} & A^{SS} & B & 0 \\ 0 & P & Q & L' \\ 0 & P' & Q' & L \end{bmatrix} \begin{Bmatrix} E^v \\ E^s \\ H^s \\ I^n \end{Bmatrix} = \begin{Bmatrix} b^i \\ b^s \\ b^e \\ b^n \end{Bmatrix} \tag{1}$$

The sub-matrix L' indicates the forward coupling of the surface PEC currents onto the surface fields along the volume boundary whereas sub-matrices P' and Q' denotes the reverse coupling. This generalized approach is applied to two problem geometries shown in figure 1. The EM induced effects at the output ports of the printed circuit in the presence of these surface enclosures, under external illumination, will be presented.

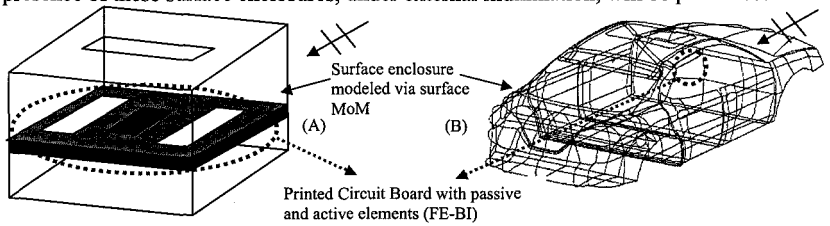


Fig 1: Geometry of PCB (A) within a cavity and (B) within an automobile chassis.

# Susceptibility Analysis of a Cavity with an Aperture and System Effects

Ronald Kollman and H.Y. David Yang
Dept. of Electrical and Computer Engineering
University of Illinois at Chicago
ron_kollman@ieee.org

Susceptibility of equipment to High Power Microwave (HPM) and Electromagnetic Pulse (EMP) attacks has been a serious issue for both military and commercial electronic systems. High-frequency HPM/EMP may cause equipment failure with disastrous consequences.

Much of the equipment of concern is housed in metal enclosures where apertures for ventilation and input/output lines are the avenues for coupling to the system. The radiated susceptibility due to the apertures and the conducted susceptibility due to the input/output penetrations are the concern here. Conducted susceptibility in this case is also due to the external field.

This paper will present analysis of a typical enclosure. Commercially available full-wave electromagnetic simulator is employed to provide data on the coupling to the system. Induced current or voltage at the system input port is determined and treated as noise to the system. System analysis based on signal-to-noise ratio provides the information of the overall effect. Radiated susceptibility will be due to an aperture and internal coupling is to electronics systems. In field modeling, the aperture size and transmission line types will be varied to analyze the HPM/EMP effect on the system. Conducted susceptibility analysis will use a single external wire penetrating the enclosure. Various lengths will be used for analysis. Finally the system effect will be analyzed to determine the worst case scenario and threshold limits for safe operation. Analysis will be shown for the effect on both analog and digital systems.

The results of this analysis will be later compared to empirical data to determine the accuracy of the model.

0-7803-7846-6/03/$17.00 ©2003 IEEE 

## Propagation Through Forest and in Urban Environments

**Co-Chairs:** K. Sarabandi
M. Casciato

7:55 Opening Remarks

# Scatter function characterization of microwave radio signals by vegetation forms

Authors: Harlem. St.michael [(1)], _and Dr. Ifiok Otung

[(1)] Electrical and Electronic Engineering Department. University of Glamorgan.
Pontypridd. CF371DL. Wales. United Kingdom.
**E-mail: hstmicha@glam.ac.uk phone:01443482587 fax:01443482541**

## Abstract:

Very significant progress has been made over the years in the area of radio propagation modeling and measurement. A traditional approach to modeling the excess loss experienced by radio waves propagated through paths obscured by vegetation is to assume that this loss increases exponentially with distance through the vegetation media. From a review of some of the available propagation models, the empirical models do over estimate the excess loss.

In this paper, the author's report on measurements conducted in a controlled environment at 20 GHz to characterize the scatter function of ficus and cornifer plants. To establish the scatter function of this plants, the forward scattered signal level emerging from the vegetation media in single and multiple formation and its dependence on the azimuth direction of the receiving antenna is investigated. Based on this investigation, a comparison is made on the behavior of the scatter function of the ficus and cornifer plants.

Experimental measurement results show that the forward scattered signal distribution is rather uniform around its azimuth direction, hence the scatter function for the ficus and cornifer plants is characterized using a total effective scattering cross-section per unit volume of the vegetation media.

A theoretical model based on the radiative energy transfer (RET) is used to interpret some of the complex phenomenon observed in the scatter function results. Observation from experimental measurement result show a strong forward scattering and reduced attenuation rate for an increased vegetation in signal path. At regions of reduced attenuation rate, the scattered beam broadens out, which suggests that the coherent field component is trying to disappear within the incoherent field component.

0-7803-7846-6/03/$17.00 ©2003 IEEE 

# MODELLING OF VHF RADIO PROPAGATION INSIDE FOREST USING A PARABOLIC EQUATION ALGORITHM

**Marc LE PALUD**
CREC St-CYR / French Ministry of Defense - 56381 GUER CEDEX - FRANCE
marc.lepalud@st-cyr.terre.defense.gouv.fr

## INTRODUCTION

The development of future telecommunication and detection systems requires accurate prediction models in order to obtain optimal performances. Our laboratory has been working since several years, both experimentally and theoretically, to improve the understanding of VHF ground propagation and transmission in forested environments.

## PROPAGATION MODELLING INSIDE FOREST

It is well known that the signal is highly fluctuating when the receiving antenna is immersed in the vegetation. This chaotic behaviour is due to the presence of multiple scatterers that are randomly located, causing strong multipath interference and deep fading (M. Le Palud et al., *IEEE RADAR 2000 Conf. Proc.*). It is yet interesting to be able to predict a mean signal level (i.e. a local spatial average) by replacing the vegetation bulk, which is a complicated mixture of air, wood and leaves, by a smoothly-varying equivalent medium. Following this approach, some important works (T. Tamir, *IEEE AP*, Vol 25, n° 4, 1977) have been achieved in order to obtain closed-form solutions, which allowed the discussion and interpretation of the phenomena; however, crucial hypothesis had to be made, like:

- homogeneous medium
- constant height of trees
- flat ground
- range-independent parameters

Our own goal was to compute the field inside a forest, without the preceding restrictions, for irregular-terrain situations like the one represented on figure 1.

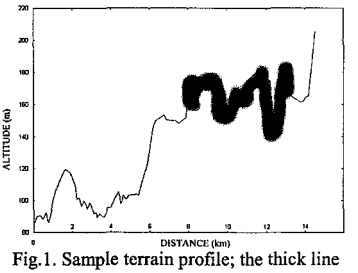

Fig.1. Sample terrain profile; the thick line corresponds to the forest

In previous works, we have used a parabolic equation algorithm to compute VHF propagation over the forest. The top of the trees was considered as the ground surface (lower boundary) with special values of electromagnetic parameters. With this approach the values of the field inside the forest cannot be obtain directly. So we have decided to modify our algorithm in the following way: the vegetation is know considered as the lower layer of the atmosphere and is characterised by a refractive index n and an attenuation factor A. These two parameters may vary with height and range. The results obtained by this method have been confronted with those given by other approaches and with experimental data. The influence of the vertical profile of the forest (i.e. variations of n and A with height) on the field distribution has also been investigated.

# Theory and Measurement of Millimeter-Wave Propagation Through Foliage

Feinian Wang, Il-Suek Koh, and Kamal Sarabandi,
Radiation Laboratory
Department of Electrical Engineering and Computer Science
The University of Michigan, Ann Arbor, MI 48109-2122

**Abstract**

The military demand for high data rate communication is on the rise. For this purpose wide-band communication at millimeter-wave frequencies is proposed. Urban and forested environments pose a signi£cant challenge for the operation of such systems. In order to assess the performance of communication device operating at millimeter-wave frequencies, characteristics of the channel such as path-loss, coherent bandwidth, fading statistics etc. must be determined. In this paper we investigate the characteristics of a forest channel at millimeter-wave frequencies. This problem is approached both theoretically and experimentally, and a comparison between measurement and theory will be presented at 35GHz.

An outdoor measurement was conducted for a pine tree stand. This stand included 13 pine trees occupying a 15m × 25m area with average distance of 5m between two adjacent trees. In this experiment path-loss due to the tree stand was measured at Ka-band (35GHz). Two identical high-gain horn antennas with a half-power beamwidth of 10° were used for the transmitter and receiver. The transmitter was located in a clear area, 20m away from the tree stand, illuminating it from the side. The antenna foot print at 20m is about 3m × 3m which is substantially smaller than the tree crown dimensions, ensuring a distributed target-type measurement. The receiver was £rst set up in front of the tree line for calibrating the systems, and then moved behind trees for path-loss measurements. After excluding the free space path loss between the reference point and the measured power beyond the stand, the path loss due to the tree cluster is obtained. To acquire the desired path-loss statistics, 84 independent spatial samples of transmitted signal through the pine stand were collected.

A coherent wave propagation model based on Monte Carlo simulation and realistic looking fractal trees is used to simulate propagation through the tree stand. The trees were generated with physical and structured parameters, such as tree density, height, mean trunk diameter, etc., similar to the experimental tree stand. The model uses Foldys approximation based on single scattering theory to calculate the coherent attenuation rate. It is known that single scattering is not suf£cient for the accurate estimation of attenuation rate of a dense and highly scattering medium. Foldy's approximation in conjunction with single scattering overestimates the attenuation effect. Hence to improve the accuracy of the coherent model partial multiple scattering occurred among the needles of highly dense leaf clusters is included for the estimation of the coherent attenuation. Incoherent scattering from the branches, leaf clusters, and tree trunks are calculated and added to the mean £eld for accurate estimation of the overall path-loss and £eld ¤uctuation statistics.

0-7803-7846-6/03/$17.00 ©2003 IEEE

**MLFMA Analysis of Wave Interaction with Multiple Trees: Validation of Ray Codes Used in Wireless Propagation**

Ling Li and Lawrence Carin
Department of Electrical and Computer Engineering
Duke University
Durham, NC 27708-0291

The multi-level fast multipole algorithm (MLFMA) is employed to analyze wave interaction from a large number of tree-like structures situated above a lossy half space (soil). A scalable MLFMA formulation is implemented. In one case all of the scatterers (trees) are analyzed simultaneously on a set of networked computers. In the other formulation wave interaction between the trees is analyzed iteratively, and each tree is analyzed separately on its on computer node. In the latter case multiple scattering is handled via inter-computer communication. The relative efficacy of these two scalable implementations is discussed, with regard to CPU and RAM requirements.

The MLFMA software is then used to analyze wireless propagation in a small forest, for validation of ray codes. This analysis allows consideration of a ray and MLFMA for identical scattering environments, thereby allowing calibration of the ray model. This direct comparison of a rigorous (MLFMA) and approximate (ray) analysis should be compared with previous comparisons of ray results to measured data, for which the exact scattering environment is rarely known exactly. Also note that for validation of the ray model, the rigorous model must be valid at high frequencies, thereby motivating MLFMA vis-à-vis the relatively low-frequency method of moments. We consider various approximations in the ray model, for example the number of inter-target interactions retained, the number of diffraction terms retained, and the inclusion of curved-body diffraction terms. Several example results and comparisons are presented.

0-7803-7846-6/03/$17.00 ©2003 IEEE 

# Long Distance Wideband Propagation Measurements in a Forested Environment

Mark D. Casciato* *Member, IEEE*, Leland Pierce *Senior Member, IEEE*, Adam Hartz, Brett Lyons, Wayne Walker, and Kamal Sarabandi *Fellow, IEEE*,

Radiation Laboratory
Department of Electrical Engineering and Computer Science
University of Michigan
Ann Arbor, MI 48109-2122 USA
email: casciato@eecs.umich.edu, saraband@eecs.umich.edu

Recent advancements in physics-based computer models for radio wave propagation in a forested environment, such as those developed at the University of Michigan's Radiation Laboratory, allow for the generation of accurate simulated data, under various scenarios, without the need for an extensive and costly measurements campaign. A more limited measurements campaign is needed however, in order to validate and improve on these physics-based codes. To capture the dispersive effects of the forest environment, including the frequency decorrelation effects of the forest, and to more completely validate the computer models, it is desired to conduct measurements over a broad bandwidth. As the decay rate of the mean field (attenuation constant) through a forest is a function of distance (for example the rate of decay of the mean field at large distances through a forest tends to decrease, as the surviving mean field is dominated by the effects of scattering from the tree structure), it is also desired to conduct the measurements over distances large enough to capture this effect. This however is a difficult task, as the higher system noise in such a wideband configuration reduces receiver sensitivity and does not allow for detection of the weaker signal over large distances.

To overcome the inherent difficulties in operating a wideband system over large propagation distances, a novel measurement system has been developed at the Radiation Laboratory. In this system two HP8753D vector network analyzers (NWA) are employed, one as the system transmitter, one as a low-noise receiver. The NWA provides the level of receiver sensitivity needed (as low as -100 dBm) for the long distances involved. Under normal operation, and NWA is used as a single unit, with all triggering done internally, and with a common LO determining the frequency of the transmitted signal, as well a the center frequency of the narrow-band receiver. When operating two separate units for a common through (S21) measurement, both the LO frequency and the timing of the frequency sweep must be very precisely matched. In order to achieve this level of precision, two synchronized rubidium atomic clocks, which control both the timing of the frequency sweep, as well as provide a stable LO reference for each NWA, are employed.

The discussed system was employed in a measurement campaign conducted at the Lakehurst Navel Air Station, Lakehurst, NJ. The Lakehurst site consists of varying plots of sand pine forests and open areas. Measurements were conducted over a frequency range from 30 MHz to 3 GHz and at distances of over one kilometer, through forest stands of up to 400 m thickness, the limiting factor on distance being available transmitter power. In this paper, data gathered at Lakehurst, in this measurements campaign, will be presented and analyzed, as well as compared to data generated by the physics-based codes discussed earlier. Data presented will include path loss, as well as the frequency decorrelation effects of the forest environment.

Frequency correlation decreases with increasing f due to multiple scattering

0-7803-7846-6/03/$17.00 ©2003 IEEE

# Foliage Attenuation Model for the Calculation of Forest Path Loss

Mark D. Casciato* *Member, IEEE* and Kamal Sarabandi *Fellow, IEEE*

Radiation Laboratory
Department of Electrical Engineering and Computer Science
University of Michigan
Ann Arbor, MI 48109-2122 USA
email: casciato@eecs.umich.edu, saraband@eecs.umich.edu

The ability to predict attenuation or path loss in a forest in a simple, and yet accurate and more general fashion, is greatly desired by the systems engineer. Physics-based computer models for forest propagation are accurate and more generally applicable, however they involve complicated mathematics and in order to capture the statistical nature of the propagation channel, time consuming Monte Carlo simulations are required. Other commonly used attenuation models are heuristic, based on measured data, and in some cases overly simplified electromagnetic formulations, with little correlation to the physics of the problem. Thus, while simple to implement, these models lack the desired accuracy and generality, in part due to the fact that they are based on a limited measured data set. An example of this is the Weissberger Foliage attenuation model. A heuristic model, based on measured data, the Weissberger model predicts path loss by using an exponential model, which is a function of frequency and distance through foliage in a forest. This model is limited to ranges under 400 m and uses a slightly different formulation for distances under 14 m. It is assumed to be accurate at frequencies through 95 GHz, however, it does not account for the effects of the tree structure, tree density or type, moisture content of leaves, branches, etc., or wave polarization. Also the accuracy of the Weissberger model has been questioned at higher frequencies (11.2 - 20 GHz). (A Generic Model of 1-60 GHz Radio Propagation through Vegetation-Final Report, Rogers, et. al, *Document produced by QinetiQ for the UK Radiocommunications Agency*, May 2002)

In order to significantly improve and expand upon heuristic models like the Weissberger model, while retaining their desired simplicity, a more complete data set is required, however the time and cost required to gather such an extensive data set by a field campaign is impossible. Recent accomplishments in physics-based computer modeling at the University of Michigan's Radiation Laboratory however, allow for the generation of a much more extensive data set, using computer simulations, based upon which, a simple, and more accurate and general macromodel of the mean power attenuation, for point to point propagation in a forest can be developed. The Michigan models, which have had significant validation, are as mentioned, physics-based models, and account for the effects of tree structure, frequency, polarization, distance, and tree density, on the propagating radio wave. These models include near-field effects, which are essential for accuracy, when the radio receiver is near a tree trunk or branch.

It is proposed in this work to develop an improved macromodel for path loss (power) in forested environments, with parameters which allow users to change tree density, and tree height. The model will be developed in a "heuristic" fashion, from data generated by the Michigan physics-based forest models. The proposed macromodel will be more complete than the Weissberger model and will account for polarization effects, tree density, range, and frequency, as well a tree type. Results from the macromodel will be shown and compared to the Weissberger model, measured data, as well as the simulated data set.

0-7803-7846-6/03/$17.00 ©2003 IEEE

# Low-to-Ground Wideband Channel Measurements over Line-of-Sight and Forested Paths at 300 MHz and 1.9 GHz

G.G. Joshi* [1], C.R. Anderson [2], C.B. Dietrich Jr. [1], W.G. Newhall [2], W.A. Davis [1]; J. Isaacs [3], G. Barnett [3]
(gajoshi@vt.edu, chanders@vt.edu, cdietric@vt.edu, newhall@vt.edu, wadavis@vt.edu; Jim.Isaacs, Gregory.Barnett@itt.com)
[1] Virginia Tech Antenna Group (VTAG),
[2] Mobile and Portable Radio Research Group
340 Whittemore Hall, Blacksburg, VA 24061-0111;
[3] ITT Aerospace/Communications Division
1919 West Cook Rd., Ft. Wayne, IN 46801

Wideband wireless communication with low antenna heights is vital to emerging military applications such as battlefield sensor networks and communication between dismounted soldiers. Similar capabilities can support public emergency services, search and rescue operations, utility meter monitoring, and other civilian and commercial applications. When channel conditions permit, wideband communication systems can exploit multipath signal combining to enhance the quality of service, as with a RAKE receiver. Reliable low-to-ground wideband radio applications require a detailed understanding of channel characteristics to optimize communication performance. Hence wideband measurements for a variety of channel conditions for low-to-ground applications are needed.

We present results of 300 MHz and 1.9 GHz radio wave propagation measurements of line-of-sight (LOS) channels and of forested paths with dense and light foliage, using low antenna heights. LOS and obstructed wide band measurements were performed for distances up to 2 km, using omnidirectional and directional antennas at varying heights. An additional set of wideband channel measurements was performed on a rainy day to study the effect of wet foliage on signal propagation at 1.9 GHz. Path loss as a function of distance was characterized based on narrowband and wideband measurements, and channel power-delay profiles were extracted from wideband measurements.

Virginia Tech's wideband Vector ImPulsE Response (VIPER) channel measurement system (W.G. Newhall et al., *RAWCON 2002*, 133-136) was used to characterize the multipath channel in terms of the channel impulse response given by power-delay profiles. The transmitter uses a field programmable gate array to generate a 10-80 MHz PN sequence for BPSK modulation of the carrier (300 MHz or 1.9 GHz). The wideband modulated signal is then transmitted. The receiver down converts the signal and samples at 1 Giga-samples/sec. Snapshots of the received signals are processed in software and are used to estimate the channel impulse responses. Cross-correlation between the received and transmitted signals are used to produce the power-delay profile.

Results for different transmitter/receiver heights, several combinations of omni-directional and directional transmitting and receiving antennas, and foliage conditions for distances up to 2 km are reported. Measurement results are compared to path loss models including the Egli, Weissberger, and ITU models to determine how well they represent low-to-ground conditions.. Implications for feasibility of wideband multipath combining are also discussed.

0-7803-7846-6/03/$17.00 ©2003 IEEE 

# Modelling and Comparison of the Propagation of 433 MHz, 868 MHz, 2.4 GHz and 5.0 GHz Electromagnetic Waves within a Simulation Construction

Leena Ukkonen*, Panu Ali-Rantala, Pasi Raumonen,
Lauri Sydänheimo, Markku Kivikoski
Tampere University of Technology, Institute of Electronics
Rauma Research Unit, Kalliokatu 2, 26100 Rauma, Finland
Phone: +358-3-3115 3347, email: leena.ukkonen@tut.fi

The propagation of 433 MHz, 868 MHz, 2.4 GHz and 5.0 GHz electromagnetic waves within a simulation construction was modelled by using a computer tool. The main aim was to model how the thickness of the wall and the wall material affect the attenuation of the electromagnetic waves. Research on electromagnetic wave propagation within a building has been going on at Tampere University of Techonology recently. (P. Ali-Rantala *et al.*: Indoor Propagation Comparison between 2.45 GHz and 433 MHz Transmissions, 2002, IEEE AP-S Interational Symposium) The research has considered modelling and measuring the wave attenuation in a building.

The wall materials used in the simulations were concrete and wood. The simulated thicknesses of both materials were 0.15 m, 0.2 m, 0.25 m, 0.3 m and 0.4 m. The electromagnetic properties that have the largest affect on the attenuation are conductivity $\sigma$, dielectric constant $\varepsilon_r$. (D. M. Pozar, Microwave Engineering, 22-27 and 38-46, 1990) These parameters were used in the simulations when modelling the propagation. For concrete $\varepsilon_r = 4$ and $\sigma = 0.05$ S/m. However, moisture content affects the electromagnetic properties of wood. Therefore wood was simulated by using different parameters. For example parameters $\varepsilon_r = 4.2$ and $\sigma = 1.0*10^{-5}$ S/m model the average wooden material and were therefore selected for further discussion. (Forest Products Laboratory, Wood handbook – wood as an engineering material, Chapter 3, 1999)

The length of the construction used in the simulations was 20 m, the width was 15 m and the height was 2.5 m. The construction was divided into seven rooms that were 2 – 4 m wide. The width varied between 2 and 4 meters so that the construction had similarities with real buildings (Figure 1). An omnidirectional antenna was used as a 1 mW power transmitter and it was placed in the middle of the centermost room of the construction and its height was 1 m. The gain of the antenna was about 2 dB.

It is seen from the simulation results that the attenuation properties of concrete depend not only on thickness of the wall but also on the system frequency because concrete consists of both conducting and insulating parts. It is also seen that the attenuation properties of wood depend only on system frequency because wood can be considered an insulator due to its low conductivity.

From the concrete simulation results it can be seen that for example at 868 MHz frequency when the thickness of the wall is 0.25 m in every wall and room the attenuation increases of about 15 dB (from – 20 dB to – 85 dB) (Figure 2). However, from the simulation results of the wooden wall it can be seen that at 868 MHz frequency when the thickness is 0.25 m the attenuation is about – 40 dB all over the construction.

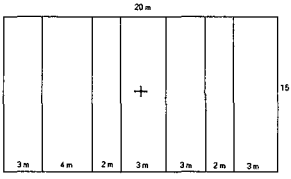


**Figure 1. The simulation construction**

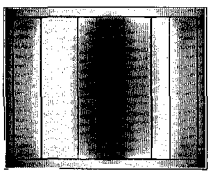

**Figure 2. A simulated picture of the wave attenuation in the 0.25 m thick concrete wall at 868 MHz**

0-7803-7846-6/03/$17.00 ©2003 IEEE

# *NO-WAVE-EQUATION RADIOPROPAGATION MODELS: EXPERIENCES WITH THE PERCOLATION THEORY*

**Maria Montepeloso**
D.I.E.I. Univ. of Perugia
bkxmon@tin.it

**Roberto Sorrentino**
D.I.E.I. Univ. of Perugia
sorrent@unipg.it

**Maila Strappini***
D.I.E.I. Univ. of Perugia
strappini@diei.unipg.it

**Luciano Tarricone**
D.I.I. University of Lecce
Via Monteroni 73100
Lecce - Italy
luciano.tarricone@unile.it

## *Abstract*

The use of accurate radiopropagation models is of paramount importance for a large variety of problems. Among them, the study of electromagnetic (EM) urban area propagation is probably one of the most relevant, because of its importance in the design of reliable wireless communication networks. Several models are available indeed, with different characteristics. Apart the trivial free-space (FS) approximation, it can be worth mentioning empirical models such as the Okumura-based model (OK), or the semi-deterministic Walfisch-Ikegami model (WI), or fully-deterministic methods such as ray-tracing. All these models, resulting from a research effort starting several decades ago, are far from fulfilling all the requirements. Some models are especially devoted to manage with specific geographical or urban characteristics, some others are too CPU-time demanding, others deserve a strong tuning effort before ensuring reliable predictions.

As a matter of fact, new models must be experienced, based on new formulations. Among them, percolation theory is quite promising. The model is based on the assumption that EM urban propagation can be assimilated to a fluid flowing through a percolative lattice (Franceschetti, Marano and Palmieri, IEEE Trans. Ant. Prop., 47, 9, 1999). Consequently, a modelling technique can be set up, without using the typical EM wave equations. In this work, the percolative approach (PA) is compared with more standard techniques, so that its potential perspectives and limitations are discussed into details.

In PA, an urban area is considered as a lattice. The lattice can be statistically described by the probability $p$ of a square to be empty (or full). The urban tissue can be identified by its "occupancy" degree $q=1-p$. A monochromatic EM wave is assumed to impinge with a certain angle $\theta$ on the upper bound of the p-lattice: by combining the theory of geometrical optics and Markov chain theory the ray power loss after the n-th reflection can be predicted. Consequently, once the average behaviour of EM propagation has been investigated for the ensemble of possible p-lattices, with given p and $\theta$, the probabilistic characterization of propagation is achieved.

The implementation of PA, as well as of other rough (FS) or sophisticated models, such as OK and WI models, allows a rigorous analysis of the PA performance. In Fig. 1 some results are proposed, demonstrating that the PA has a similar accuracy with respect to well renown models (OK and WI). Several other data also demonstrate the same conclusion.

Some current limitations must also be taken into account, such as the difficult management of wide-band sources, and the very relevant computational effort required to solve real three-dimensional problems. Nonetheless, the approach is quite promising, and the previous problems are challenging tasks for the immediate future.

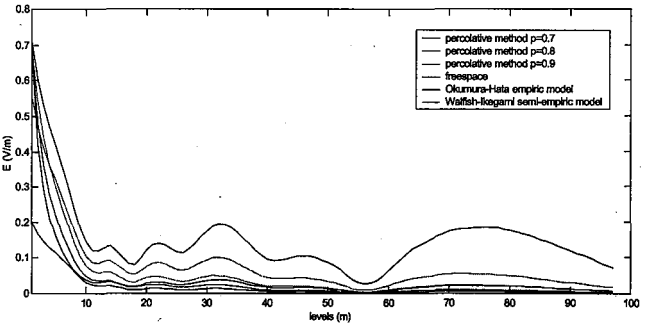


**Figure 1.** E mean value in a lattice with $\theta=30$

0-7803-7846-6/03/$17.00 ©2003 IEEE

# Indoor propagation: comparisons between simulations and measurements

M. AMEUR*, C. HUMBERT, M. SYLVAIN

ESYCOM – Université de Marne la Vallée, 5, boulevard Descartes, Champs sur Marne,77454 Marne La Vallée cedex 2 – France
e–mail: mameur@univ–mlv.fr – phone: (+33)1 60 95 72 79 – fax: (+33)1 60 95 72 14

submitted to URSI commission F1 (Propagation Modeling and Measurement)

This paper presents comparisons between indoor propagation channel wide band measurements and two simulations algorithms based on ray–optic approximation.

Measurements were made at 2.4 GHz (with a 400 MHz bandwidth) in the fourth floor of a modern building, both with and without line of sight propagation (Fig 1).

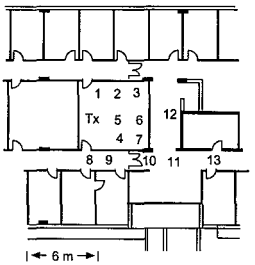


Fig 1 1...13: receivers Tx: Transmitter

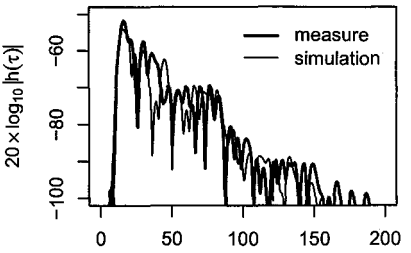


Fig 2

The measurements device was built around a vector network analyser. The sampled frequency response is Fourier transformed to give the impulse response.

Simulations are obtained by the image method and by the shooting ray method and compared with measurements. To get simulations presenting an acceptable agreement with measurements, several features have to be considered which are the matter of this paper:

1. Scene description accuracy;
2. The simulations give impulse response as a set of Dirac impulses and must be properly filtered;
3. due attention is paid to variation with frequency of the rays parameters (amplitude and phase). This point generally neglected in previous studies, globally increases agreement with experimental data. A frequency sweep is made in simulations to account this last point.

Agreement between simulated and measured impulse responses at point 4 of the scene is illustrated in Fig 2.

More results will be presented in the final paper, comparing impulse responses and derived parameters such as the rms delay spread, mean excess delay and local mean power.

# Simplified Analysis of Indoor Radio Wave Propagation at 2.4GHz Band

Ryoichi Sato [1]*, Kei Hayashi [1] and Hiroshi Shirai [2]

[1] Faculty of Education and Human Sciences, Niigata University
8050, 2-no-cho, Ikarashi, Niigata, 950-2181 Japan
[2] Faculty of Science and Engineering, Chuo University
1-13-27 Kasuga, Bunkyo-ku, Tokyo 112-8551 Japan

**Abstract**

According to the recent spread of wireless LAN systems based on IEEE802.11 at 2.4GHz band, it has been one of the most important research topics to investigate how radio waves propagate inside office environments, because local objects like pillars, walls, doors and windows may reduce the link performance of such low power wireless systems.

For outdoor environments like urban complex, ray tracing/shooting techniques based on Geometrical Theory of Diffraction (GTD) like the Vertical Plane Launch (VPL) method (H. L. Bertoni, *Radio Propagation for Modern Wireless Systems*, Prentice Hall, 2000) have been widely applied to the analyses of the wave propagation modelings, because the approximate ways provide easy and accurate propagation prediction with physical insight and give high computer efficiency for such large models. However, such ray based techniques may not be suitable to analyze indoor propagation models since there may be lots of transmitted fields through dielectric walls and glasses. One may be able to treat the reflected field contribution from the surface with the aid of the impedance boundary conditions, but not for the transmitted fields.

While, the Finite Difference Time Domain (FDTD) method, which is widely used for microwave and antennas analyses, may provide us an easy evaluation procedure for the complex propagation behavior of the fields inside the dielectric materials like walls and glasses. However, enormous memory size must be required for precisely modeling an office floor at 2.4GHz band, especially for 3D modeling.

In this paper, to avoid such large memory requirement, a simple and easy 2D-FDTD analysis for indoor propagation model at 2.4 GHz band is made an attempt. Here the $TM_z$ mode of the Yee's FDTD formulation (A. Taflove, *Computational Electrodynamics*, 2nd ed., Artech House, 2000) is utilized. A numerical experiment is done for a real indoor model, *i.e.* a 30×30 m floor space in the building of Niigata University. The analytical region includes four lecture rooms and one hallway. In this 30×30 m case, the 2D-FDTD does not require huge available memory size. While, by using the PC software, the simplified measurement of the signal strength in the wireless IEEE 802.11 system is executed along the hallway. In comparison between the numerical and the measured results, it is verified that very similar propagation tendency in the hallway region is observed, even though the reflection contributions from both the floor (lower) and the ceiling (upper) surfaces are not included in the simple 2D modeling. From some points of view, physical interpretation for this *strange tendency* of the propagation feature between them will be discussed.

This research was partially supported by a Scientific Research Grant-In-Aid (13650425, 2001) from the Ministry of Education, Culture, Sports, Science and Technology, Japan.

0-7803-7846-6/03/$17.00 ©2003 IEEE

**Session Topic:** **Commission F (Wave Propagation and Remote Sensing). F1. Propagation modeling and measurement.**

# Radiowave propagation model for cellular mobile communication systems using Genetic Algorithms.

** Lambros V. Skarlas, Stavroula D. Bouzouki and Spiridon D. Likothanassis*

**Abstract**

This work presents the results from the application of evolutionary computation techniques to a radio wave propagation measurements campaign for cellular mobile systems coverage characterization in urban areas. The experimental data was collected through a mobile measurement system and the results were compared with the most known coverage prediction models. A new path loss prediction model for urban areas is proposed using a genetic algorithm.

One of the problems that are of continual interest to the wireless system designers, is the estimation of the actual area coverage per cell. Bearing in mind, the cell planning aspect of the next generations of mobile cellular communication systems, the objective is to evaluate the coverage either before the system is handed over to the operator or after a system modification or cell site addition.

This propagation prediction model would satisfy the demands of the cell planning of the mobile cellular communication systems more efficiently and more easily. It can be adapted in the geographical area of interest, since less computational time is needed and more specific geographical information for the prediction of the coverage is given.

Using Friis Free space path loss model, that ignores phenomena like reflection, diffraction and scattering, the deviation between the measurements and the model's suggested prices was presumably, was found to be very high. Using OKUMURA's and modified HATA-OKUMURA's models, for frequency equal to 900MHz, their predicted values for the received power were closer to the actual experimental ones. The comparison of our suggested model with other models such as, the empirical HATA model (the first modified model which appeared in a CCIR report in attempt to extend the HATA model to cover greater distances), the ITU-R P.529-3 and the ERC REPORT68, shows that our model is the most suitable for general use. Moreover, it is worth mentioning that the adaptability of the model is such that it can accurately predict the radio wave's propagation in macro cell metropolitan urban areas and in micro cell suburban areas.

0-7803-7846-6/03/$17.00 ©2003 IEEE 

## Microstrip Antennas

**Co-Chairs:** R. Q. Lee
M. A. Saed

7:55 Opening Remarks

# Quasi-Analytical Model of an Infinite Leaky-Wave Slot Coupled to Microstrips

**S. Bruni [1], A. Neto [1], S. Maci [2], G. Gerini [1]**

(1) Radar Technology Group, FEL -TNO
Oude Waalsdorperweg 63, 2597 AK, Den Haag, The Netherlands
neto@fel.tno.nl, bruni@fel.tno.nl

(2) Dept. of Information Engineering, University of Siena,
Via Roma 56, 53100, Siena, Italy, macis@ing.unisi.it

In [A. Neto, S. Maci, IEEE Trans. on Antennas Propagat, Vol. 51, No. 6, 2003] the Green's function of an infinite slot printed between two different homogeneous dielectric media has been studied. There, the formulation is structured by deriving, under non-restrictive assumption, an analytical expression of the magnetic currents, providing next a uniform asymptotic approximation for the field radiated in every observation point. For that geometry, the exciting dipole was located on the slot, as needed for the analysis of coplanar-waveguide fed slot. This latter feed configuration has been analyzed in [A. Neto, P. de Maagt and S. Maci, , IEEE Trans. on Antennas Propagat, Vol. 51, No. 6, 2003] by constructing, via the previous Green's function based magnetic currents, suitable entire domain basis functions to be applied in the Method of Moments (MoM) solution. For the described geometry, the asymptotic dominant contribution in the denser medium is a conical leaky-wave field. This suggest to use this structure to realize a leaky wave antenna by covering the slot with a dielectric lens in order to provide the denser medium were the energy must leaks, while narrowing the conical beamwidth in the transverse plane.

In this paper, we continue the investigation by analyzing the same slot when fed by means of an electromagnetic coupled microstrip line. When using multiple microstrip feed arrangement, the leaky wave antenna is presently being designed and breadboarded at TNO-Fel for a multifrequency application in the millimeter wave range.

The problem is approached by first formulating an electric field integral equation on the microstrip domain. Inside the integral kernel we use the slot's Green's Function (GF) derived in [A. Neto, S. Maci, IEEE Trans. on Antennas Propagat, Vol. 51, No. 6, 2003] and extended to the present case to include the effect of the microstrip substrate. The integral equation is next solved by a method of moments (MoM). In this solution, a problem matched entire domain basis function is defined to represents the fringe (*i.e.*, non-modal) microstrip currents in vicinity of the microstrip-slot transition. This latter is obtained on the basis of the canonical microstrip GF problem. To this end, a minor modification of the GF formulation presented in [C. Di Nallo, F. Mesa, D. R. Jackson, IEEE Trans. on MTT, Vol. 46, no.8, pp 1062-1071, August 1998] has been applied.

The use of the slot GF in the integral equation kernel, accompanied by the microstrip-GF-based basis function for the MoM solution, leads to a quasi-analytical formulation, elegant, rich of physical insight, and accurate in a reasonable range of slot and microstrip widths. This accuracy has been successfully validated by a conventional full-wave analysis applied to a slot very long in terms of a wavelength.

0-7803-7846-6/03/$17.00 ©2003 IEEE

Numerical Analysis of Microstrip Square patch and Ring Antennas

Mohammad Zunoubi*
Department of Electrical and Computer Engineering
State University of New York
New Paltz, New York 12561-2499

**INTRODUCTION-** One of the most useful microstrip antenna structures is the rectangular patch. The antenna characteristics including resonant frequency, input impedance, and the quality factor have been studied both numerically and experimentally. By reconfiguring the rectangular patch to a ring, additional parameters are added to further control the aforementioned antenna's characteristics. The most comprehensive theoretical study of the rectangular microstrip antennas has been carried out by Bafrooei, P. M. and Shafai L., IEEE Trans. Antennas Propagat., Oct. 1999. A full wave approach using mixed potential integral formulation in conjunction with the method of moment is utilized to obtain antenna's characteristics. The objective of the present research is to develop a finite-difference time-domain technique to analyze both the rectangular microstrip patch and ring antennas. The proposed numerical analysis is simple, accurate and very efficient. By obtaining results for impedance bandwidth, resonant frequency, and cross polarization in the H-plane an optimum design for the antennas is proposed.

**FORMULATION AND NUMERICAL SOLUTION-** The geometry of the problem is depicted in Figure 1. Both rectangular patch and rectangular ring microstrip antennas are considered. The ring antenna is similar to a solid patch except that its central conducting part $W_2$ is removed. A 50-Ω coaxial cable is used to excite the antenna. Resonant frequency, input impedance, impedance bandwidth, cross polarization in the H-plane, and the effect of moving feed probe are all studied. Results are compared with the corresponding published theoretical and measured results. An optimum design for the rectangular microstrip antenna is presented. Results are obtained very accurately and efficiently.

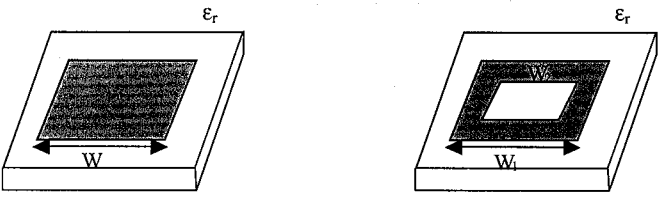


Figure 1. Geometry of printed microstrip patch and ring antennas.

0-7803-7846-6/03/$17.00 ©2003 IEEE

**Imbedded Microstrip and Helical Antennas as Sensors and Communicators:**
**Sane Application of Genetic Algorithms**

By: You Chung Chung**, Pitchitpong Soontornpipit*, Kamal Vasagiri**, Rama Devi**, Cynthia Furse*

Center of Excellence for Smart Sensors
University of Utah* and Utah State University**
50 S. Campus Drive4120 Old Main Hill
Salt Lake City, Utah 84112Logan, Utah 84322-4120

Many of today's biological sensors, medical implants, and emerging artificial vision, hearing, and muscle control electronics are sufficiently small that they can be imbedded in the human body. These imbedded sensors require communication systems to retrieve the data or control the device. Other applications for imbedded sensors include remote moisture, composition, and weather monitoring for precision agriculture, food processing, manufacturing, etc. This paper describes a set of sensors that have been developed for either remove sensing or communication or the combination of the two.

The genetic algorithm approach has been applied to optimize the designs of these antennas, resulting in improvements to existing designs and new designs as well. While the application of genetic algorithms has been shown in some cases to provide improved antenna designs, it remains a "scientists' tool" rather than a mainstream antenna design method. This is because the methods of applying the GA to a realistic problem, which has multiple facets of the antenna to be simultaneously optimized, requires significant expertise to adequately design the cost function and parameter space for convergence and effective GA design. In addition, the amount of computer time required becomes extremely large as the parameter space is increased in any meaningful way. The practical aspects of applying the GA to these problems is addressed, with the intention of providing a nearly "knowledge-free" application design program that allows a user who knows little or nothing about a GA to apply the method with reasonable success to an imbedded antenna design problem.

This method is demonstrated in the design of a wireless soil moisture sensor with both underground sensing antennas and above ground communication antennas in a complex environment.

0-7803-7846-6/03/$17.00 ©2003 IEEE 

## Recent Progress in Optically Transparent Antennas

Richard Q. Lee* and Rainee N. Simons
NASA Glenn Research Center
Cleveland, OH 44135

A class of optically transparent patch and slot antennas that consist of an optically transparent electrically conductive film deposited on glass or plastic substrates has been demonstrated from 2 to over 20 GHz. The antenna can be fabricated at low cost using conventional IC fabrication techniques. At these frequencies, these antennas offer potential NASA and commercial applications for wireless communications. Some advantages of these antennas include:

- Space reuse (terrestrial): the antenna ca be printed on the video display for compact packing and efficient integration in communications devices (palmtop computer, digital telephone, flat-panel display etc.) Recently, an example of such use has been reported (C. F. Huang and L. Chan, Electronics Letters, Vol. 38, No. 20, September 2002).
- Space reuse (spacecraft): the antenna subsystem saves weight by reusing space on photovoltaic or on Earth-facing sensors.
- Covertness or aesthetics: 'hidden' antennas blend with the background. Transparent antennas can be mounted unobtrusively on automobile windshields or other location for communications purpose.

This paper presents an overview of past works and most recent progress on optically transparent antennas development at NASA GRC. The types of antennas that have been investigated include patch, slot and ring antennas, as well as 2x2 arrays of patch and slot ring elements. In addition to return losses and pattern measurements, a close proximity video links has been demonstrated with these antennas in the laboratory environment. Preliminary results indicated that these types of antennas are capable of broadband operation, and therefore, have high commercial potentials. Detailed designs of different antenna types, their performance characteristics and fabrication technique will be presented and discussed.

0-7803-7846-6/03/$17.00 ©2003 IEEE

# Broadband Planar Antenna Using CPW-Fed Monopoles in a Rectangular Aperture

Dr. Mohammad A. Saed
Department of Electrical and Computer Engineering
Texas Tech University
Lubbock, Texas 79409-3102

Broadband planar antennas are highly desirable in many applications due to their low cost, lightweight, and amenability for integration with active devices. Using coplanar waveguides as feed transmission lines eases integration with active devices due to their uniplanar design. Improving the bandwidth of printed antennas, such as microstrip antennas, has been the subject of numerous research papers. The most common techniques include stacked multilayer configurations and parasitically coupled single layer configurations. Multilayer configurations improve bandwidth at the cost of increased complexity and overall thickness, which in turn increases loss due to surface waves. Parasitic configurations result in larger area and distortions in radiation patterns. Planar antennas fed with coplanar waveguides concentrated mostly on slot antennas using a single substrate or slot-coupled microstrip patches. In this paper, we introduce a new antenna design that uses a coplanar waveguide transmission line feeding planar monopoles in a rectangular aperture. The monopoles are extensions of the center conductor of the coplanar waveguide. A rectangular aperture surrounding the monopoles is formed in the ground planes of the coplanar waveguide. The entire design is uniplanar. This new antenna can achieve very broadband impedance behavior. Full wave theoretical simulations of an antenna with two monopoles forming a V-shape printed on a 1.27 mm thick substrate with 10.2 dielectric constant shows impedance bandwidth of about 40%. This bandwidth far exceeds bandwidths achievable using conventional microstrip or slot antennas on similar substrates. Effect of various dimensions, geometry, and substrate properties on input impedance and radiation characteristics are investigated theoretically and experimentally. The geometry, design techniques, and results for the proposed antenna will be presented.

0-7803-7846-6/03/$17.00 ©2003 IEEE 

# Reconfigurable and Broadband Microstrip Antennas Using Patches Of Various Shapes

Dr. Mohammad A. Saed
Department of Electrical and Computer Engineering
Texas Tech University
Lubbock, Texas 79409-3102

Microstrip antennas have been very popular due to their numerous advantages, which include being low cost, lightweight, low profile, conformal, and compatible with integrated circuits. Several patch shapes were investigated in the literature; however, the emphasis is on rectangular and circular patches. In general, microstrip antennas are narrowband due to their resonant nature. Several techniques for bandwidth enhancement have been explored in the literature. These techniques include stacked multilayer configurations, parasitically coupled single layer configurations, and single patches with shaped slots. There has also been a great deal of interest in designing reconfigurable antennas with multiband, multi-polarization capabilities. In this paper, we investigate the two aspects, broadband behavior and reconfigurability, of microstrip antenna designs using various patch shapes.

For bandwidth enhancement, we concentrate on parasitically coupled, single layer patches. The traditional configuration of this kind involves placing parasitic patches adjacent to an excited patch, all of the same shape. It has been applied mainly to rectangular patch antennas. This technique provides bandwidth enhancement at the cost of large area and distorted radiation patterns. In this paper, we investigate the use of mixed shapes in order to improve the bandwidth while reducing the occupied area and leaving the radiation patterns undistorted. In particular, we investigate circular/radial, rectangular/triangular, and triangular/triangular configurations with various feeding mechanisms to achieve our goal. For reconfigurable designs in terms of multiband and dual polarization capabilities, triangular patch shapes are used. Feed location and geometrical arrangement of these patches provide the desired performance. This research uses theoretical and experimental methods. Theoretical simulations are based on a full wave method of moment approach. For the experimental component, various antenna prototypes are designed, built, and tested.

0-7803-7846-6/03/$17.00 ©2003 IEEE

# Reconfigurable Planar Log Periodic Antenna

Brandon L. Nance* and Mohammad A. Saed
Department of Electrical Engineering
Texas Tech University
Lubbock, Texas 79409

Log periodic antennas have been around for many years and have been valued for their very broadband behavior. The self-complimentary toothed-planar version was one of the earliest log periodic antennas and has been explored much in broadband antenna literature. Here, we discuss methods of modifying this design so that its frequency band and polarization characteristics become reconfigurable. In order to allow room for modifications to the antenna geometry, the self-complimentary portion of the original antenna design was abandoned.

The central idea to the frequency reconfigurability modification is that by closing appropriately placed switches, the electrical lengths of all the teeth are halved. This doubles the frequency radiated by each tooth, and hence doubles the upper and lower band limits. The diodes require a biasing network which consists of narrow slots that extend a quarter-wavelength from the end of each tooth and then terminate into a large gap. To reconfigure the polarization, a copy of the original antenna pair must be rotated $90^{\circ}$ and added to the substrate. Diodes at the feed structure then provide the ability to switch between the two antenna pairs. With the incorporation of a phase shifter into one of the feeds, the antenna now has capability to change between linear, dual and circularly polarized configurations.

Theoretical simulations in Ansoft Ensemble have been used to optimize a microstrip-fed planar log periodic slot antenna and the bias network it requires in the frequency-reconfigurable design. Diodes were modeled in Ensemble as thin strips of copper placed appropriately along the teeth, and the results showed that lower and upper limits of the bandwidth indeed doubled. A microstrip-fed antenna with diode biasing network has been built using a milling machine on a 62 mil Duroid substrate of dielectric constant 2.33, and measured results are favorable.

Design details, theoretical simulations, as well as experimental results for both the frequency-reconfigurable and polarization-reconfigurable designs will be presented at the conference.

0-7803-7846-6/03/$17.00 ©2003 IEEE 

# Reconfigurable Circularly Polarized Dual-Band Stacked Microstrip Antenna

N. Surittikul*, R.G. Rojas and K.W. Lee
Dept. Electrical Engineering, ElectroScience Laboratory
The Ohio State University
Columbus, Ohio 43212-1191, USA

There are several types of reconfigurable antennas. In this paper we concentrate on antennas that can change their beamwidths in real time. Furthermore, in some applications, such as GPS, there is a need for dual band circularly polarized antennas. A new design for a three-layer reconfigurable circularly polarized dual band staked microstrip antenna is proposed. Figure 1 depicts a cross section of the dual band microstrip antenna. The antenna consists of two staked patches in the bottom two layers and a ring on the top layer. Note that the antennas are probe-fed and $\varepsilon_1 = \varepsilon_2 > \varepsilon_3$.

The effective width of the parasitic ring surrounding the antenna can be changed in real time by activating switches (diodes, transistors or RF MEMS). Adjusting the width of the ring can then change the beamwidth of the radiated field. The switches, diodes in this case, are assumed to have two states of operation, namely, *on* and *off*. Ideally, the *on* state allows the current to flow through the switches, while the *off* state does not. The change in the beamwidth is larger with this scheme (more degrees of freedom) than a previous scheme presented by these authors (K. W. Lee, N. Surittikul and R.G. Rojas, IEEE-APS/URSI Symposium, June 2002).

This study is being accomplished by means of analysis, computer simulations and implementation of prototypes. 2D and 3D models are being developed to understand the behavior of this class of antennas. Numerical techniques such as the Method of Moments (MoM) and the Finite Difference Time Domain (FDTD) are used to obtain numerical results of the radiation pattern, input impedance, polarization properties, etc.

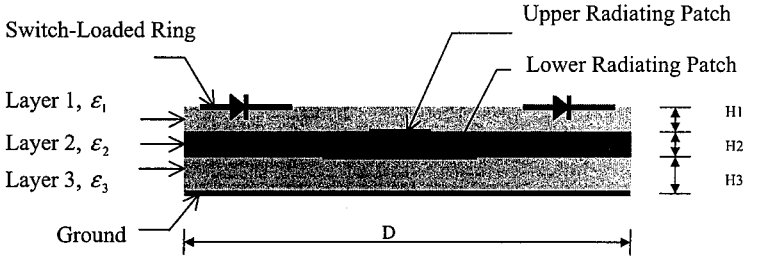


Figure 1: Cross Section of a Reconfigurable Dual Band Microstrip Antenna

0-7803-7846-6/03/$17.00 ©2003 IEEE

# MEMS Enabled Continuously Tunable Patch Antennas using Electrostatic Actuation: Design, Simulation, and Applications

**John P. Gianvittorio, Joe Zendejas, Yahya Rahmat-Samii, and Jack W. Judy**
*Department of Electrical Engineering*
*University of California, Los Angeles*
*Los Angeles, California 90095-1594*
*johng@ee.ucla.edu*

**Introduction:** The resonant frequency of a patch antenna can be controlled by adjusting the height of the patch. While the heights of most patch antennas are static due to a fixed substrate thickness, MEMS can be employed to design a patch antenna whose height can be adjusted to tune the resonant frequency. Furthermore, because the antenna does not rely on switches for its reconfigurability, the precision of possible tuning is limited to the precision which the height can be controlled.

**Patch Antenna Design:** The resonant frequency of the patch antenna changes as the height of the patch over the ground plane is changed due to the changing cavity size under the patch. A MEMS enabled patch that can achieve various heights can be fed with a microstrip feed through aperture coupling. Aperture coupling is chosen to minimize the metallic connections to the patch which could fracture after repeated actuations. The resonant frequency response has been determined using the Method of Moments (MoM) to simulate a patch antenna with varying heights over a ground plane. The resulting input impedance is shown on the left of Fig. 1. It can be seen how the resonant frequency shifts 2% by lowering the patch 33%. Over small ranges of height changes the bandwidth and far field patterns of the antenna remain stable.

**MEMS Design:** The patch antenna is suspended by a polysilicon membrane. A DC voltage applied to the patch electrostatically draws the patch closer to the ground plane. By balancing the forces between the applied DC electrostatic actuation force and the restoring forces of the polysilicon torsion beams, the patch antenna can be held at arbitrary fixed height. A 3D schematic concept drawing of the fabricated MEMS enabled patch is shown on the right of Fig.1.

**Applications:** Tunable patch antennas can be useful in the design of large antenna arrays. Reconfigurability can increase the versatility of these designs. A reconfigurability of 2% at 90GHz leads to potential tuning of 1.8GHz. Another potential application is in the design of phased arrays. Detuned elements have been shown to shift the radiated phase and eliminate the need for external phase shifters.

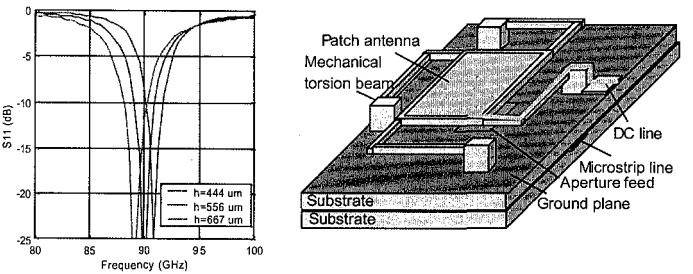


**Figure 1:** The simulated input match as calculated with MoM for a patch antenna of various heights showing the tunability is shown on the left. A 3D schematic of a potential MEMS design for the tunable patch antenna is shown on the right.

0-7803-7846-6/03/$17.00 ©2003 IEEE

## A Novel MEMS Reconfigurable Leaky Wave Antenna

Afroz Zaman*, Ramesh Ramadoss[1], Simone Lee[1], Richard Q. Lee, Y.C. Lee[1], and K.C.Gupta[1]

NASA Glenn Research Center
21000 Brookpark Road, MS 54-8
Cleveland, OH 44135
[1]University of Colorado
Boulder, CO 80309

A microstrip leaky wave antenna (LWA) is based on the leakage properties of a microstrip transmission line. The structure can be seen either as a long rectangular patch or as a large open circuited microstrip line. Such an antenna radiates when excited in its first higher order propagating mode and when its dominant transmission line mode is suppressed. It has been shown that it is possible to generate a narrow tilted fan beam in the H plane of a LWA through a single excitation (C.Luxey and J.Laheurte, *IEE Proc. Microwave Ant. & Prop.* vol. 144, No. 6, Dec. 1997). A simple LWA based array for a tilted pencil beam has been proposed for automotive transceiver application (C. Hu et al, *IEEE Trans. Antennas Propagat.* vol. 45, No. 11, Nov. 1997). LWAs as frequency scanned elements have been proposed as an alternative to achieving beam scanning without phase shifters. But the frequency bandwidth available usually limits the scan performance, if wide-angle coverage is required. By periodically loading the radiating edges of a LWA with capacitors and varying the capacitor DC bias, single beam steering at a fixed frequency was demonstrated (C.Luxey and J.Laheurte, *Electron Lett.* vol. 36, No. 15, July. 2000). A 2-beam, scanning LWA integrated with a varactor tuned voltage controlled oscillator was demonstrated where beam steering was achieved by tuning the oscillator frequency with DC bias voltage (C. Wang et al. *IEEE Trans. Antennas Propagat.* vol. 47, No. 8, Aug. 1999).

In this paper, a novel MEMS based 3-beam switchable Leaky Wave Antenna is proposed. The antenna consists of two leaky wave structures placed symmetrically on both sides of a rectangular patch antenna. In this configuration, the center patch provides a broadside beam and the leaky wave structures (with transverse slits to inhibit propagation of the dominant surface wave mode) provide two narrow tilted beams. The antenna beam switching is achieved by reconfiguration of the broadside patch structure into two leaky wave structures. This is accomplished by turning on any of the flexible circuit based MEMS actuator pairs located on either sides of the center patch. Thus the proposed configuration provides a broadside beam when the MEMS actuators are off, and can be reconfigured to provide a tilted beam by turning either the right or the left actuator pairs on through applied DC bias voltage. The antenna has been fabricated on 20 mil thick RT/Duroid 6002 substrate ($\varepsilon_r = 2.94$). The flexible circuit-based MEMS actuators (R. Ramadoss, S. Lee, V.M. Bright, Y. C. Lee, and K. C. Gupta, *IEEE Int. Microwave Symp. Dig.*, June 2-7, 2002) have been designed, fabricated, and integrated with the antenna, at University of Colorado at Boulder in collaboration with NASA Glenn Research Center. Preliminary data on S-parameter ($S_{11}$) and radiation pattern measurements of the LWA with the MEMS actuators on and off show the validity of the predicted performance. Details of the simulated and experimental results will be presented and discussed.

0-7803-7846-6/03/$17.00 ©2003 IEEE

## Array Antennas

**Co-Chairs:** L. W. Pearson
R. MacPhie

7:55 Opening Remarks

16. 1 8:00 Plane-Wave Synthesis by an Antenna-Array. Application To RCS Determination.....100
*B. Stupfel, S. Vermersch, CEA/CESTA, France*

16. 2 8:20 CONFORMAL ANTENNAS on a JOINED-WING AIRCRAFT.....101
*B. P. SMALLWOOD, A. J. Terzuoli, R. A. Canfield, Air Force Institute of Technology, USA*

16. 3 8:40 Efficient Impedance Interpolation and Pattern Approximation for Linear Microstrip Phased Arrays Using Neural Networks.....102
*J. A. Bossard, D. H. Werner, M. G. Bray, The Pennsylvania State University, USA*

16. 4 9:00 Array Far Field Synthesis with Near Field Control.....103
*R. Vescovo, Universita' di Trieste, Italy*

16. 5 9:20 Pattern Improvement by the Use of Coincident Multiplicative Arrays.....104
*R. MacPhie, T. Yoon, University of Waterloo, Canada*

16. 6 9:40 Power Combining by Means of Injection Locking.....105
*M. R. Kühn, E. M. Biebl, Technische Universität München, Germany*

16. 7 10:00 Achievable Coupled-Oscillator Array Performance.....106
*C. M. Tompkins, L. W. Pearson, Clemson University, USA*

16. 8 10:20 Defected Ground Structure for Use in Phase Scanning Microstrip Antennas.....107
*Leili Shafai, J. S. Wight, Carleton University, A. Petosa, Communications Research Centre, L. Shafai, University of Manitoba, Canada*

16. 9 10:40 Inverse Cosecant Square Beam Antenna Pattern by Unequal Power Divider.....108
*C. Jau-Wen, Da-Yeh University, Taiwan*

16. 10 11:00 Semi-Circular Microstrip Array on a Planar Reflector with Extended Beam-Scanning Range.....APS
*J. Freese, Darmstadt University of Technology, Germany, G. Tudosie, ETH Zürich, Switzerland, M. Schüßler, R. Jakoby, Darmstadt University of Technology, Germany*

16. 11 11:20 Broadband Millimeter-wave Suspended Microstrip Antenna Array.....APS
*N. Lau, R. Sloan, UMIST, United Kingdom*

# PLANE-WAVE SYNTHESIS BY AN ANTENNA-ARRAY. APPLICATION TO RCS DETERMINATION.

Bruno Stupfel and Sébastien Vermersch
CEA/CESTA, Commissariat à l'Énergie Atomique, B.P. 2, 33114 Le Barp, France

By its definition, Radar Cross Section (RCS) is a plane-wave (PW) concept, i.e., it is determined by the far-field scattering of an object when illuminated by a PW. RCS measurements of targets of about $2m$ in size performed in a $45m \times 13m \times 12m$ anechoic chamber are accurate for frequencies above, typically, 1GHz when employing the standard calibration technique with only one emitting antenna. For lower frequencies, this technique yields erroneous results essentially because the absorbers become ineffective and the field emitted by the antenna no longer satisfies the PW condition on the object – the size of the quiet zone decreases with the frequency.

A possible way to circumvent these difficulties is to use a phased array that synthesizes a PW in a bounded domain, called quiet zone (QZ), as proposed, e.g., in (M. P. Kestler et al., *Ultra-Wideband, Short-Pulse Electromagnetics 3*, pp. 295-304, 1997): The weights applied to each antenna are determined by requiring that the corresponding field is a PW in the QZ. However, this technique is ill-adapted to a closed, almost perfectly electrically conducting chamber. Also, a number of parameters, like the number of antennas or the array dimensions, need to be specified.

In this paper, we propose a calibration technique that allows an accurate RCS reconstruction of a target located in the near-field of the array, even when electrically conducting walls are present. A theoretical study of the problem at hand is presented, that allows us to specify clearly the hypothesis that are being made, and to identify the parameters that govern the accuracy of the RCS reconstruction. In particular, a far-field condition is derived, more realistic and much less constraining than the conventional $D^2/\lambda$ one. When the target-array, antenna-antenna and target-walls-target interactions are neglected, it is mathematically demonstrated that this calibration technique synthesizes a PW in the QZ if the calibration object is a monopole (2D) or a dipole (3D). Finally, 3D numerical simulations performed with a dipole antenna-array and taking into account all the previously mentioned interactions illustrate the efficiency of this technique when the array and conducting walls are a few wavelengths apart from the target.

0-7803-7846-6/03/$17.00 ©2003 IEEE

# CONFORMAL ANTENNAS ON A JOINED-WING AIRCRAFT

**Ben P. Smallwood,* Andrew J. Terzuoli, Jr., Robert A. Canfield**
**Air Force Institute of Technology, USA**

This paper presents the results of investigating antenna arrays that are structurally integrated into the wings of a joined-wing aircraft. The joined-wing aircraft has a large rear wing swept forward to join with the trailing edge of the front wing, thus creating a diamond shape when looking down on the aircraft from above. These antennas conform to the airfoil shape on the top and bottom surfaces of the wing. One antenna ensemble is placed in each wing of the diamond shape, thereby giving the aircraft a 360° field of view. These antennas are operating in the Ultra High Frequency (UHF) range (400-450 MHz). This paper focuses on the antenna analysis performed in this joined-wing study; the structural integration of the antennas will also be discussed briefly.

A simplified finite element model (FEM) of a conformal, load-bearing antenna is created. This model consists of an electromagnetically transparent top layer, a honeycomb core section, a load-bearing graphite epoxy layer, another honeycomb core section, and a second graphite epoxy layer. This layered material is then used in the full FEM of the joined-wing aircraft, replacing the aluminum skin material in the four sections of the wing surface where the antenna arrays are located. This process allows the antennas to become part of the optimized aircraft design.

Once the antennas are placed in the aircraft model, the antenna performance is investigated. To manage the scope of this research, half-wavelength, horizontally polarized dipole antenna elements with constant and cosine current distributions are used instead of the actual conformal, load-bearing antennas mentioned earlier. These dipoles have the same polarization as the actual antenna elements, and an analytical model can be developed and analyzed. The analytical model is then verified using a commercial Method of Moments software package. Two different cases are considered: an undeformed wing configuration, where the wings are rigidly trimmed, and a deformed wing configuration, where aerodynamic loads are applied to trim and deflect the wings.

For the case considering the undeformed wing, coordinate locations of the center points of each element in a chordwise array are read into a MATLAB routine. This code calculates the inter-element spacing and performs a far field sum of the electric field of each dipole. An array factor is then applied to this chordwise summation to create a rectangular array of 5 chordwise by 40 spanwise elements, and then polar plots are generated of the magnitude of the E-field off the leading edge of the wing.

For the deformed wing case, analysis similar to that of the previous case is performed except that an array factor cannot be used due to the rotation of the elements with respect to one another out the span of the wing. A central difference formula is used to approximate the curvature of the deformed wing, thus allowing tangents to be found at each of the element locations. These tangents define the direction of the dipoles. A second summation of the electric field is then performed to account for this rotation, and the magnitude of the E-field is once again plotted in polar form. The results of this deformed case are then compared to those of the undeformed case to quantify the effect that wing deformation has on the antenna performance.

0-7803-7846-6/03/$17.00 ©2003 IEEE 

# Efficient Impedance Interpolation and Pattern Approximation for Linear Microstrip Phased Arrays Using Neural Networks

J. A. Bossard*, D. H. Werner and M. G. Bray
The Pennsylvania State University
Department of Electrical Engineering
University Park, PA 16802
jab678@psu.edu, dhw@psu.edu and mgb144@psu.edu

Antenna array optimization techniques such as genetic algorithms require efficient evaluation of essential design parameters including driving point impedances and radiation patterns. Rigorous full-wave electromagnetic simulation techniques provide accurate impedance calculations. However, these simulations are often computationally intensive, thereby greatly increasing the time required to perform antenna array optimizations. This study attempts to lay the foundation for extending the technique developed in (M. G. Bray et al., Proceedings of *The 2001 IEEE AP-S Symposium*, Vol. 3, pp. 688-691, July 2001). This design synthesis technique was originally developed for dipole arrays and will be extended here to include linear microstrip antenna arrays. An efficient impedance representation is sought through neural network interpolation. The corresponding radiation pattern calculations are made using a cavity model. These efficient simulation techniques are then applied to the analysis of a linear microstrip antenna array as shown in Figure 1.

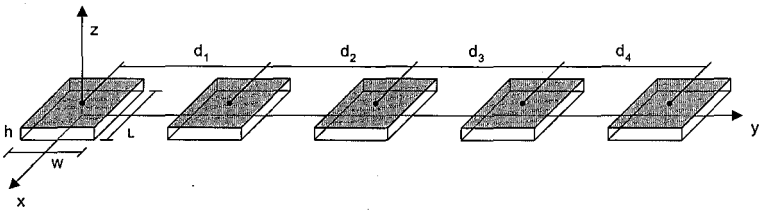


**Figure 1.** Example of Linear Microstrip Antenna Array Geometry.

Initially, a single microstrip antenna design with a given value of L, w, and h is chosen for use in the array. This single isolated antenna is simulated using a numerically rigorous full-wave method at multiple feed positions to find the corresponding self-impedance curves. Two patch antennas are then simulated at varying separation distances and feed positions to create a database of mutual impedances. Separate neural networks can then be trained to represent the self-impedance of a patch and the mutual impedance between two patches given specified feed positions and element locations. Using N-port network theory, the driving point impedances can be calculated from source excitations, self-impedances, and mutual impedances for each patch in an N-element array. Once the driving point impedances are known, the antenna array pattern is calculated using the cavity model for a single patch and applying pattern multiplication to find the radiation pattern for the entire array. The methods developed in this study are applied to the design of several five-element linear microstrip antenna arrays with comparisons made to full-wave electromagnetic simulations.

0-7803-7846-6/03/$17.00 ©2003 IEEE

# ARRAY FAR FIELD SYNTHESIS WITH NEAR FIELD CONTROL

Roberto Vescovo
Dipartimento di Elettrotecnica Elettronica ed Informatica - Università di Trieste
Via A. Valerio, 10 - 34127 Trieste – ITALY
E-mail: vescovo@univ.trieste.it

In some antenna problems it is important to reduce the field produced by an antenna array in an assigned region $V$ in the near-field zone, to the aim of reducing the electromagnetic coupling with the environment. However, the problem is to obtain such a reduction without an excessive distortion of the far field pattern.

Given an antenna array, let $\mathbf{I}=[I_1, I_2, \ldots, I_N]$ be the generic excitation vector, $F(\mathbf{I}, \theta)$ the corresponding far-field pattern in the direction $\theta$ and $\mathbf{E}(\mathbf{I},\mathbf{r})$ the electric field produced at the point $\mathbf{r}$. We assume that a mask $M$ for the far-field pattern is assigned (by $M$ we mean the set of all functions $G(\theta)$ such that $M_1(\theta) \le |G(\theta)| \le M_2(\theta)$, where $M_1(\theta)$ and $M_2(\theta)$ are two non-negative functions). We want to solve the following problem: *determine an excitation vector* $\mathbf{I}$ *such that* : (a) $F(\mathbf{I}, \theta) \in M$; (b) $|\mathbf{E}(\mathbf{I},\mathbf{r})| \le E_{max}$ for $\mathbf{r} \in V$, *where* $E_{max}$ *is a given threshold* and $V$ *is the assigned region.*

Denoting by $K$ the set of all vector functions $\mathbf{S}(\mathbf{r})$ satisfying condition (b), and by $A$ the Cartesian product $M \times K$, the problem can be formulated as follows: determine a pair ( $F(\mathbf{I}, \theta)$, $\mathbf{E}(\mathbf{I},\mathbf{r})$) belonging to the set $A$ (assuming that $A = M \times K$ is non-empty). Denoting by $B$ the set of all pairs $(F(\mathbf{I},\theta),\mathbf{E}(\mathbf{I},\mathbf{r}))$, where $\mathbf{I}$ is the generic excitation vector, a solution to the problem is any pair $(F(\theta),\mathbf{E}(\mathbf{r})) \in A \cap B$. This suggests the possibility of solving the problem by the method of alternate projections (O.M. Bucci, G. D'Elia, G. Mazzarella, and G. Panariello, " Antenna Pattern Synthesis: A New General Approach," *Proceedings of the IEEE*, Vol. 82, No. 3, Mar 1994, pp. 358-371). To this aim, we introduce the following norm $\|(G,\mathbf{S})\|$ of the generic pair $(G(\theta),\mathbf{S}(\mathbf{r}))$:

$$\|(G,\mathbf{S})\|^2 = \|G\|_1^2 + T\|\mathbf{S}\|_2^2$$

where $\|G\|_1^2 = \int_I |G(\theta)|^2 d\theta$, with $I$ the interval containing the space directions $\theta$, $\|\mathbf{S}\|_2^2 = \int_V |\mathbf{S}(\mathbf{r})|^2 dV$ and $T$ is an assigned real positive number. This allows introducing a distance between two pairs, so that the following two projectors can be defined: $P_A$, that associates with any pair $(F,\mathbf{E})$ a pair $(F_A,\mathbf{E}_A) \in A$ closest to $(F,\mathbf{E})$; $P_B$, that associates with $(F,\mathbf{E})$ the pair $(F_B,\mathbf{E}_B) \in B$ closest to $(F,\mathbf{E})$. If $(F,\mathbf{E})_0$ is a starting point, then we follow the iteration scheme $(F,\mathbf{E})_n = P_B\, P_A\, (F,\mathbf{E})_{n-1}$ $(n=1,2,\ldots)$. The elements $(F,\mathbf{E})_n$ belong to $B$ (that is, $F$ is an array pattern corresponding to an excitation vector $\mathbf{I}$ and $\mathbf{E}$ is the field produced by $\mathbf{I}$), and have progressively decreasing distances from $A$. An element $(F,\mathbf{E})_n$ sufficiently close to $A$ is considered as a solution to the problem.

In order to find a simple implementation of the projector $P_A$, we replace the above condition (b) by the stronger conditions: $|E_x(\mathbf{r})| \le E_{max}^x$, $|E_y(\mathbf{r})| \le E_{max}^y$, $|E_z(\mathbf{r})| \le E_{max}^z$, where $E_{max}^x$, $E_{max}^y$ and $E_{max}^z$ are such that: $(E_{max}^x)^2 + (E_{max}^y)^2 + (E_{max}^z)^2 = (E_{max})^2$.

Several tests showed the effectiveness of this method.

0-7803-7846-6/03/$17.00 ©2003 IEEE

# Pattern Improvement by the Use of Coincident Multiplicative Arrays

**Robert H.MacPhie*** and **Tae Ho Matthew Yoon**
Department of Electrical and Computer Engineering
University of Waterloo, Waterloo, ON N2L3G1 Canada
E-mail:r.macphie@ece.uwaterloo.ca

This paper considers a uniformly spaced linear receiving array where element output voltages are split into two distinct parts which are then combined additively to form two coincident array output voltages $V_A(t)e^{j\omega t}$ and $V_B(t)e^{j\omega t}$. The two voltages are then multiplied, passed through a low pass filter and time- averaged to give the output product pattern $P_o(u) = \mathrm{Re}\{A_o(u)B_o^*(u)\}$ Such a system has been used to obtain the principal solution (R.N. Bracewell and J.A. Roberts, Austral. J Phys.,7, 615-640, 1954)in radio astronomy (R.N.N.Utukuri and R.H.MacPhie, IEEE Trans. AP-15, 49-59, 1967). More recently, a thinned principal solution has been proposed (R.H.MacPhie, IEEE Trans, AP-51, to appear, 2003).

In this paper we first consider the case of two patterns of uniformly weighted coincident arrays which are shifted by $\pm \Delta\bar{u}/4$ where $\Delta\bar{u}$ is the beamwidth of the uniformly weighted array from the maximum to the first null. The resulting product pattern $P_o(u)$ has a narrower mainlobe and lower sidelobes than that of the power pattern of the uniformly weighted array. We next consider the product of the pattern $A_o(u)$ of a uniformly weighted array with the pattern $B_o(u)$ of an array with a linear amplitude taper. The product pattern $P_o(u)$ has the same beamwidth measured to the first null as the power pattern $|A_o(u)|^2$ of the conventional uniformly weighted array but has far sidelobes which are much lower.Other cases of pattern improvement with multiplicative coincident arrays will be given.

In summary, the multiplicative coincident array system has effectively twice the number of degrees of freedom as the conventional array with square-law detection since the patterns nulls of $A_o(u)$ and $B_o(u)$ can be chosen independently. This results in improved patterns with lower sidelobes and /or narrower mainlobes.

0-7803-7846-6/03/$17.00 ©2003 IEEE

# Power Combining by Means of Injection Locking

M.Kühn, E.Biebl
Technische Universität München

Power combining can be used to enhance the detecting distance with low expense. An increasing number of applications for the 24 GHz ISM-band like short range communication links and automotive radar systems demand for oscillators providing moderate power of a few mW and a moderate frequency stability of about 0.5%.

The maximum oscillation frequency of low-cost off-the-shelf transistors is not sufficient for stable operation of a fundamental 24 GHz oscillator. So, we designed a 24 GHz first harmonic oscillator. The power generated at the fundamental frequency (12 GHz) is reflected. This generates a high output power at the first harmonic in an effective way. We measured a power radiated by an integrated planar antenna of more than 1 mW. Though this oscillator provides better frequency stability compared to fundamental oscillator, for some application additional stabilization is required.

For a low-cost method, injection locking can be used to phase lock oscillators that provide sufficient stability in free running mode. Based on our harmonic oscillator concept injection locking has to be achieved at the first harmonic, because only the antenna is accessible for signal injection. We designed, built up and characterized an harmonic oscillator using the antenna as a port for injection locking. The locking range was measured versus various parameters. In addition, phase-noise improvement was investigated. A theoretical approach for the mechanism of first harmonic injection locking is presented.

For power combining, it is necessary that all oscillator are synchronised in frequency and phase. In this work the 3x1 array is optimised for power combining. The method of injection locking is used for synchronising in frequency and phase of each oscillator to the others. Besides increased radiated power in the far field the geometry of the beam lobe can be controlled by the distance of the antenna elements. So the maximum distance and the area of the detecting region can be selected. Furthermore the array can be locked to an external device by one of the two antennas at the periphery of the array. This extends the application possibilities because the array is synchronised to the stable external source.

0-7803-7846-6/03/$17.00 ©2003 IEEE

# Achievable Coupled-Oscillator Array Performance

C. M. Tompkins* and L. W. Pearson
Holcombe Department of Electrical and Computer Engineering
Clemson University
Clemson, SC 29634-0915
ctompki@clemson.edu
pearson@ces.clemson.edu

Coupled-Oscillator arrays (COAs) were introduced by Stephan (K. D. Stephan, IEEE Trans. Microwave Theory Tech., Oct. 1986, pp. 1017-1025) and a substantial knowledge base has been built by York (*e.g.*, R. A. York, P. Liao, and J. J. Lynch, IEEE Trans. Microwave Theory Tech., Nov. 1994, pp. 2040-2045). A few groups, including that of the present authors have elaborated upon this seminal work. Our primary interest has been the optimization of COAs to the end of low-cost deployable arrays at millimeter wavelengths. This presentation summarizes our current understanding of COA performance and presents theoretically extrapolated results for arrays of practical scale. (By necessity, experimentation to date has been on small-scale models—16 and fewer elements.)

The key to good array performance lies in fabricating individual oscillator cells with wide locking range and strong cell-to-cell coupling. An array designed in this way exhibits low random phase error among cells. A further fundamental consideration is the matching of the free-running frequencies among all of the cells. The frequency matching is difficult in light of the wide-locking-range goal. A recent Ph.D. thesis by Wang (Holcombe Department of Electrical and Computer Engineering, Clemson University, 2003) deals with simultaneous optimization of frequency sensitivity and locking range.

The use of wide locking range oscillators (or, crudely stated, low-Q oscillators) leads to an array whose output exhibits extremely poor phase noise properties. The COA phase noise may be brought close to that of an external source to which the array is injection locked, allowing independent control of the phase noise. We recently conducted an experimental study of COA phase noise under a number of different locking configurations. We present these new results in this presentation.

Computations from a complete model of a COA, comprising a Runge-Kutta solution to the equation developed by York, *et. al.*, are presented for cases of practical scale.

A promising COA architecture employs a mixer in the path between each oscillator element and its antenna. Consequently, one must be concerned with noise introduced in the mixing process. The computational model indicated in the forgoing paragraph is subjected to this mixer noise and the calculations are repeated, thereby providing the most complete model data possible for deployable-scale COAs.

0-7803-7846-6/03/$17.00 ©2003 IEEE

# DEFECTED GROUND STRUCTURE FOR USE IN PHASE SCANNING MICROSTRIP ANTENNAS

Leili Shafai*[1], J. S. Wight[1], A. Petosa[2], L. Shafai[3]

[1]Department of Electronics, Carleton University
1125 Colonel By Drive, Ottawa, ON K1S 5B6
lshafai@doe.carleton.ca, jsw@doe.carleton.ca

[2]Communications Research Centre
3701 Carling Ave, Ottawa, ON, CANADA K2H 8S2
aldo.petosa@crc.ca

[3]Department of Electrical and Computer Engineering, University of Manitoba
15 Gillson Street, Winnipeg, MB, CANADA R3T 5V6
shafai@ee.umanitoba.ca

In recent years, an increasing number of publications concerning the use of periodic structures in the form of photonic bandgap structures have been presented as a means to minimize surface wave excitation to enhance radiation characteristics of antennas and minimize losses within microwave circuits, or as alternatives to reduce the size within microwave circuits. A periodically defected ground plane is one such structure.

It is desired to investigate the phase scanning potential of a periodically etched structure in the ground plane beneath an antenna. Initial studies by the above authors involved the simulation of circular ground plane perforations beneath a microstrip patch. A phase shift of 80° in the far-field phase at the point of maximum gain was realized for the largest perforation radius. However, only a perforation size of 10% of the resonant length of the patch achieved a satisfactory return loss at the design frequency, corresponding to a 30° phase change at the point of maximum gain in the far-field (Leili Shafai, *et al.*, *ANTEM*, 471-474, 2002).

Multiple perforations in the ground plane beneath the patch in vertical ($y$-axis) and horizontal ($x$-axis) configurations produced increased phase change, but with differing results, indicating that the change in phase is dependent on the location of the perforation beneath the microstrip patch. Perforation combinations provide the greatest phase change in the far-field when placed where the current magnitude is greatest. Increasing the number of perforations along this direction consistently impinges along a new set of currents within its path, and thus has significant effects on the properties of the patch. In the orthogonal direction the effect was minimal.

When loading the patch with ground plane perforations, the resonance of the structure was affected. With a microstrip transmission line, this effect is equivalent to a change in propagation delay and thus a phase change. Extensive studies of perforations beneath a transmission line included variations in the dimensions of a single perforation, as well as studies involving dielectric constant, substrate thickness, line impedance, and frequency. With small non-radiating perforations, the maximum usable differential phase was 20°, and the insertion loss remained similar to that of the initial transmission line. Multiple ground plane perforations (or slots) provided increasing phase shifts, nearly proportional to their number. Since such a transmission line phase shifter structure does not alter the antenna radiation properties, and does not add to the complexity of an antenna array, it is now being investigated as a technique for implementing phased arrays and their beam scan. Details of the study will be provided during the presentation.

0-7803-7846-6/03/$17.00 ©2003 IEEE

# Inverse Cosecant Square Beam Antenna Pattern by Unequal Power Divider

Dau-Chyrh Chang, Jau-Wen Chen
Department of Electrical Engineering, Da-Yeh University
No. 112, Shanjiau Rd., Datsuen Shiang, Changhua, Taiwan 515
TEL: 04-8511888#2187 FAX: 04-8511200
E-mail: dcchang@mail.dyu.edu.tw

**Abstract:** For many base station antenna systems, inverse cosecant square beam pattern is required for near range for range power control. There are various ways in designing this kind of beam pattern. This research topic is a part of the four beams pattern with inverse $\csc^2$ capability. Fig.1 shows the prototype of $4 \times 4$ antenna elements array with four beams pattern capability. Fig2 shows the back of the array. A 4 to 1 Wilkinson power divider is applied to vertical BFN. In order to increase the directivity of the array, $4 \times 8$ antenna elements are arrayed for frequency between 1.7GHz to 2.2GHz. The vertical 8 to 1 BFN is unequal weighting 8 to 1 power divider as shown in Fig.3. The pattern simulation is shown in Fig.4 for frequency at 1.95GHz. The design and test results will be discussed during the presentation.

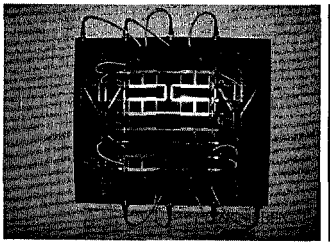

Fig1 Front of array

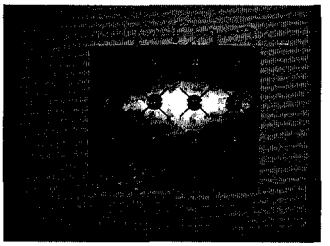

Fig2 Back of array

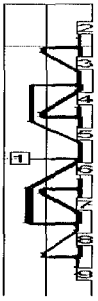

Fig 3 8 to 1 UPD of circuit

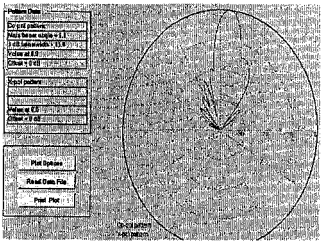

Fig 4 1.95GHz for polar pattern

## Fractal Antennas and Space Filling

**Co-Chairs:** J. Anguera
L. Carin

7:55 Opening Remarks

# Peano Antennas

Jinhui Zhu[1], Ahmad Hoorfar[1] and Nader Engheta[2]

*(1) Villanova University*
*Dept. of Electrical and Computer Eng.*
*Villanova, PA, 19085, U.S.A.*
*hoorfar@ece.villanova.edu*

*(2) University of Pennsylvania*
*Dept. of Electrical & Systems Eng.*
*Philadelphia, PA 19104, U.S.A.*
*engheta@ee.upenn.edu*

Space filling curves are of interests in many antenna applications since they provide a planar resonant structure that could have a very small footprint as one increases the step-order in iterative filling of a 2-D region. The most widely used of these curves is the one proposed by David Hilbert in 1891, and indeed several research groups in the last few years have studied the radiation properties of the antennas whose geometry are formed by using the Hilbert-curve algorithm [see e.g., Vinoy, *et al.*, *MOTL*, Vol 29, No. 4, pp. 215-219, May 2001; Anguera, *et al. Digest of the 2002 IEEE AP-S Internat. Symposium*, San Antonio, TX, pp. 546-549, vol. 4]. Like other electrically small antennas, Hilbert antenna has a small radiation resistance and a small input resistance, in the order of a few ohms, when it is center-fed at its point of symmetry. We have previously shown, however, that a properly chosen off-center feed point can always provide, regardless of how high $n$ is, a 50 ohm match at the structure's *lowest* resonant frequency [Zhu, *et al.*, USNC/URSI National Radio Science Meeting digest, p. 373, San Antonio, TX, June 2002].

In this work we have investigated the application of another family of space-filling curves, namely Peano curve, in design of small planar resonant antennas. It is noteworthy that Peano curve, proposed by G. Peano in 1890, was in fact the first demonstration of any space-filling curve [Hans Sagan, *Space-Filling Curves*, Springer- Verlag, 1994]. The first few step-order iterations of the Peano curve are shown in the figure below. By applying a moment-method-based simulation code we have performed a detailed parametric study of Peano antenna as the step-order increases from n = 1 to n = 4. We have found that, as in the case of Hilbert antenna, it is possible to locate an off-center feed point that results in an approximate input resistance of between 50 and 100 ohms and negligible input reactance for all the step orders investigated .The corresponding feed points for the step orders $n$ = 1 and $n$ = 2, for a 50-ohm match, and $n$ = 3, for a 75-ohm match, are shown in the figure below. A matched Peano antenna has far-field patterns that resemble those of a dipole antenna, as Hilbert antennas do, and has cross-polarization levels that decrease significantly as the step order, $n$, is increased. For a given footprint and a fixed step order $n$, the Peano antenna resonates at a lower fundamental resonant frequency and, therefore, results in an electrically more compact radiator than a comparable Hilbert antenna, albeit at the expense of a smaller input-impedance bandwidth. This is expected because of the relatively higher compression rate of the Peano-curve algorithm in filling of a 2-D region. A detailed parametric study of the radiation characteristics of the Peano antenna will be given in the presentation and compared with those of the Hilbert antenna.

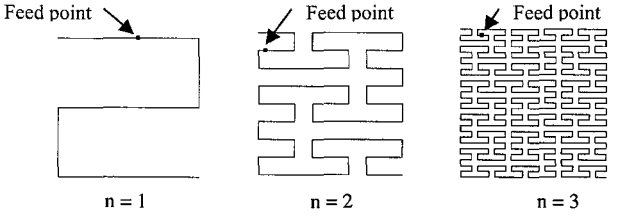


0-7803-7846-6/03/$17.00 ©2003 IEEE

# Characterization of fractal and space-filling monopole antennas using the box-counting dimension

**Jaume Anguera, Carles Puente, Carmen Borja, Jordi Soler**
*Technology Department*
*Fractus S.A. Avda. Alcalde Barnils 64-68, Ed. Testa - Módulo C.*
*Sant Cugat, 08190 Barcelona, Spain*
*jaume.anguera@fractus.com www.fractus.com*

In the last years, miniature monopole antennas have received much attention. Such antennas are attractive in environments where space is a constrain factor for example antennas integrated in handheld telephones, watches, $Bluetooth^{TM}$ applications,etc. In other situations, such antennas integrated in vehicles, miniature antennas offer the advantage of easy integrability with other components, aerodinamically performance, avoid thieves from robberies, easy to fix to the mechanical structure, etc.

Among the several techniques to reduce antenna size, namely, reactive loading, top loading mechanism, dielectrics, bending monopole arm, it is the last one that it is discussed in the present paper.

Given a monopole height, it is obvious that if the wire length is increased by bending the monopole arm, resonant frequency decreases, i.e, the antenna becomes electrically smaller. If one takes a straight monopole with the same wire length that such bent miniature monopole, one would obtain a lower resonant frequency. In other words, given a monopole of height $h$, if it is enlarged two times by bending its wire and at the same time maintaining the height $h$, the resonant frequency will not be $\frac{f}{2}$ but larger. That means that we need more wire length in order to obtain the same resonant frequency than that of a straight monopole with the same length. Therefore, it seems that bending a wire antenna is interesting because it offers the possibility to reduce antenna size, however, we need more wire length than expected. The question addressed in the present paper is then, is there any geometrical parameter that could help us to know if we need more or less wire length? To solve such question we use the box-counting dimension to study the relation between the geometrical properties of the curve defining the monopole and the resonant frequency [J.Anguera, E.Martínez, C.Puente, E.Rozan, "The Hilbert monopole: a two dimensional wire", Microwave and Optical Technology Letters, vol.36, $n^o$2, pp.102-104, Jan. 2003]. As an example, Fig. 1 shows three different curves based on fractal geometries each one with a different box-counting dimension.

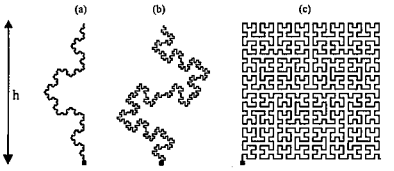


Fig. 1. Monopoles based on the fractal curve of a) Koch; b) 3/2 step; c) Hilbert [Space Filling Miniature Antennas, patent app. WO0154225 ]

0-7803-7846-6/03/$17.00 ©2003 IEEE

# Multiband Fractal Yagi Antennas: Design and Simulation

**John P. Gianvittorio and Yahya Rahmat-Samii**
*Department of Electrical Engineering*
*University of California, Los Angeles*
*Los Angeles, California 90095-1594*
*johng@ee.ucla.edu, rahmat@ee.ucla.edu*

**Introduction** Fractal antennas have been shown to increase the versatility of antenna designs. This work includes the design of a Yagi antenna array that can operate on multiple frequency bands. A multiband element based on the Sierpinski gasket is utilized in these arrays. The design involves the analysis of an element that operates at the various frequency bands of interest. This element is then incorporated into an array as parasitic elements that are fed via mutual coupling. The spacing and the size of each of the parasitic elements needs to be optimized to achieve the proper excitation phase to achieve maximum directivity.

**Sierpinski Fractal Antenna** The multiband response of a fractal Yagi array is based on the Sierpinski gasket fractal antenna. This antenna exhibits multiband behavior stemming from the multiple scales that is present inside the geometry. The antenna and its feed is very similar to a bowtie dipole. The simulated input impedance from a Method of Moments (MoM) analysis program developed at UCLA is shown in Fig. 1 and exemplifies the multiple resonances.

**Bowtie Yagi Array** The bowtie element is the zero order of the Sierpinski gasket and provides a good starting point for a multiband design. A three-element design incorporating bowtie dipoles in a Yagi configuration has been designed and simulated yielding front to back ratios of 8 dB.

**Fractal Yagi Array** The first piece of the design of a fractal Yagi array is an antenna element that operates at the desired bands of interest. The spacing and the size of each of the reflectors and directors should be optimized to achieve the highest directivity possible. The layout of a three-element design is shown in Fig. 2. Because each of the elements is fed via mutual coupling from the adjacent elements, the magnitude and phase of the excitation of each element cannot be designed independently as would typically be done with a phased array. A design has been initiated which includes two elements operating over two bands to show the feasibility of the concept. The Sierpinski gasket elements, where the director is 1.5 times larger than the driven element, are spaced $0.125\lambda$ and $0.45\lambda$ apart for the first and second bands, respectively. The simulated front-to-back ratio shows a better performance for the lower band than for the upper band. Further steps in the design include optimizing the spacing and the size to achieve good performance and similar patterns over all of the bands of interest.

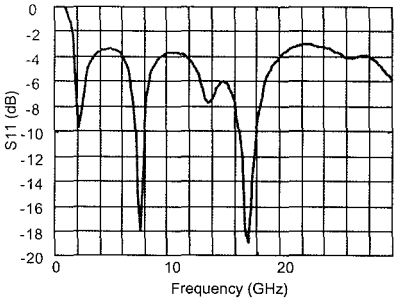


*Figure 1: Simulated input impedance for a multiband Sierpinski gasket element*

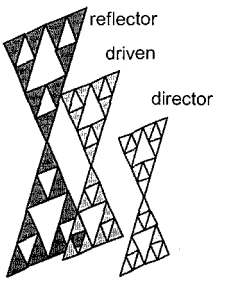


*Figure 2: Multiband Yagi array of Sierpinski gasket elements.*

# Results on a New Extended Analytic Model to Understand the Radiation Performance of Mod-P Sierpinski Fractal Multiband Antennas

J. Soler, C.Puente and J.Anguera

Technology Department, Fractus S.A.
c/ Alcalde Barnils 64-68. Edifici Testa
Mòdul C, 3ª planta. Parc Empresarial Sant Joan
08190 Sant Cugat del Vallès (Barcelona), Spain
jordi.soler@fractus.com www.fractus.com

Analytic models for antennas are specially attractive since they permit to understand the radiation principles of antennas. This understanding becomes more difficult when just using common antenna numerical analysis techniques. Multilevel structures are a set of geometries with a more flexible approach then early Sierpinski fractal designs, which provide a technological solution to built multiband antennas. However, multilevel-shaped antennas (Multilevel Antennas, Invention Patent WO0122528) feature such complex forms which makes difficult to develop analytic models to understand, calculate and predict their radiation performances. In (C.Puente, J.Soler, Analysis of Fractal-Shaped Antennas using the Multiperiodic Traveling Wave Vee Model, IEEE Antennas and Propagation Society International Symposium, Boston, July 2001) an analytic model was introduced for the calculation of the radiation performance of the classical Sierpinski-like monopole antenna. As it was previously reported by the author, the well-known Sierpinski-like antenna is a special case of a wider class of antennas and can be referred as the mod-2 Sierpinski gasket.

The original analytic model can be extended and improved; that is, the novel extension not only adds to the model the capability to calculate the whole radiation pattern, but also accounts for the self-scalability of the active current region in the antenna structure as a function of the frequency. The inclusion of this self-scalability in the formulation allows to improve the results from the original formulation in the calculation of the antenna patterns specially at the higher resonances. The novel extension of the analytic model is described in detail and the analytical results are compared with measured patterns for different mod-p Sierpinski-like multiband antennas.

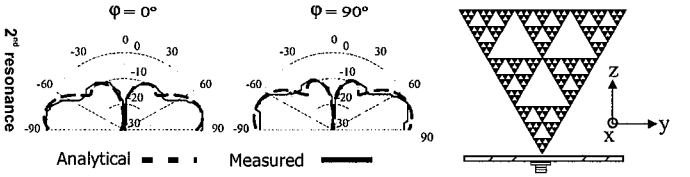


Fig 1 Comparison between measured and analytic main vertical cuts of the radiation pattern for the mod-3 Sierpinski-like monopole antenna at the second odd resonance. Analytical data is shown in dashed line.

0-7803-7846-6/03/$17.00 ©2003 IEEE

# Novel Combined Mod-P Structures: A Complete Set of Multiband Antennas inspired on Fractal Geometries

J. Soler, D.Garcia, C.Puente and J.Anguera

Technology Department, Fractus S.A.
c/ Alcalde Barnils 64-68. Edifici Testa
Mòdul C, 3ª planta. Parc Empresarial Sant Joan
08190 Sant Cugat del Vallès (Barcelona), Spain
jordi.soler@fractus.com www.fractus.com

One of the main challenges in the field of multiband antennas is the difficulty to find an antenna which can operate at more than two or three frequency bands. Most of antenna engineers would like to have an antenna design which could work at, for instance, DAB, TETRA, GSM900, DCS, UMTS and BLUETOOTH™, with similar radioelectric parameters at all these frequency ranges. Therefore, an antenna which could cover all these services should have the capability of including new bands by simply modifying the antenna geometry. Also, parameters such as the spacing between bands and the input resistances of the radiator could be adjusted by modifying part of the structure. Multilevel-shaped antennas (Multilevel Antennas, Invention Patent WO0122528) become a good and efficient solution to design multiband antennas. In (J.Soler, J.Romeu, C.Puente, "Mod-p Sierpinski Fractal Multiband Antenna", AP2000 Millennium Conference on Antennas and Propagation, Davos, 9-14 April 2000) it was first shown that the classical Sierpinski antenna, which features a spacing between bands of two, is in fact a special case of a wider class of structures, which are referred as mod-p Sierpinski antennas. The latter can provide spacings between bands higher than two. Also, a new frequency band can be easily included by just adding a new fractal iteration. However, by including a new fractal iteration the spacing between bands keeps constant; that is, for instance, for the mod-3 Sierpinski antenna the spacing between resonances is three for any fractal iteration.

In order to add new resonances to the antenna and also to change the spacing between the new resonances, the geometries of different mod-p structures can be combined, Fig.1. The strategy on how to build these novel combined antenna geometries is described and the results are compared with previous reported multiband antenna solutions.

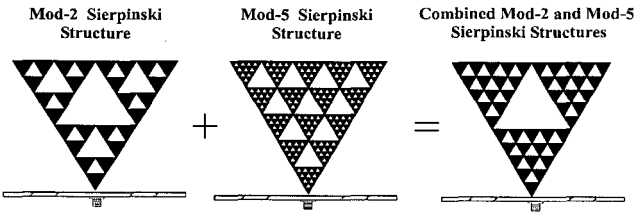


Fig 1 Concept description for the generation process of a new antenna geometry based, for instance, on the mod-2 and mod-3 Sierpinski structures to accommodate new resonances with variable spacings between bands.

0-7803-7846-6/03/$17.00 ©2003 IEEE

# Multifrequency Properties of Monopole Antennas using Multilevel Ground Planes inspired on the Sierpinski Fractal Shape

J. Soler, C.Puente and J.Anguera

Technology Department, Fractus S.A.
c/ Alcalde Barnils 64-68. Edifici Testa
Mòdul C, 3ª planta. Parc Empresarial Sant Joan
08190 Sant Cugat del Vallès (Barcelona), Spain
jordi.soler@fractus.com www.fractus.com

Some advanced antenna geometries can be used to design multiband and miniature antennas, such as those structures described in (Multilevel Antennae, Invention Patent WO0122528) and in (Space-filling Miniature Antennas, Invention Patent WO0154225). However, much attention and engineering efforts are devoted to the radiating element itself, rather than to the ground plane. Depending on the feeding scheme used for the antenna, the ground plane can become a useful contributor in the radiating process. Multilevel structures can be used to design a wide range of antennas and other elements with interesting properties. Multiband monopoles are described in (J.Soler, J.Romeu, C.Puente, "Mod-p Sierpinski Fractal Multiband Antenna", AP2000 Millennium Conference on Antennas and Propagation, Davos, 9-14 April 2000), small and high directivity antenna elements in (J.Anguera, C.Puente, C.Borja, R.Montero, J.Soler, "Small and High Directivity Bowtie Patch Antenna based on the Sierpinski Fractal", Microwave and Optical Technology Letters, vol.31, nº3, pp.239-241, November 2001) and frequency selective surfaces in (J.Romeu, Y.Rahmat-Samii, Fractal FSS: A Novel Multiband Frequency Selective Surface, IEEE Transactions on Antenna and Propagation, vol.48, no.7, pp.1097-1105, July 2000) to name a few.

In addition, these complex structures can improve the radiation performance of an antenna system when used as elements in the ground plane (Multilevel and Space-Filling Ground-Planes for Miniature and Multiband Antennas, Invention Patent PCT/EP01/10589) as it is depicted in Fig.1. The multifrequency properties of these novel antenna solutions with multilevel-shaped ground planes are analyzed and the main results and advantages are discussed.

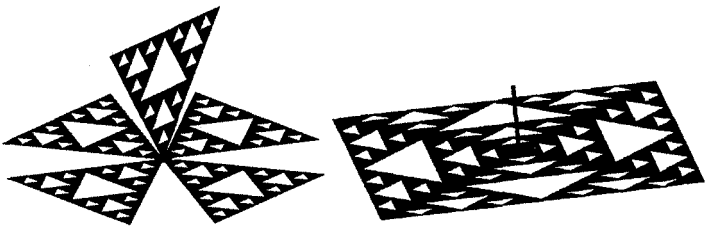

Fig 1 Mod-2 Sierpinski monopole using a multilevel-shaped ground plane with four mod-2 Sierpinski elements, on the left, and a straight monopole above a multilevel-shaped ground plane derived from four mod-2 Sierpinski gaskets, on the right.

0-7803-7846-6/03/$17.00 ©2003 IEEE

# Solutions to Tailor the Radiation Patterns of 2D and 3D Multiband Antennas based on the Sierpinski Fractal

J. Soler, C.Puente and J.Anguera

Technology Department, Fractus S.A.
c/ Alcalde Barnils 64-68. Edifici Testa
Mòdul C, 3ª planta. Parc Empresarial Sant Joan
08190 Sant Cugat del Vallès (Barcelona), Spain
jordi.soler@fractus.com www.fractus.com

There is a considerable interest in developing multiband antennas since they permit telecom operators to reduce their costs and to minimize the environmental impact. In base station networks, for instance, this implies that they reduce their costs, specially in terms of the logistic of introducing news bands (searching for new sites, applying for permissions to add the new antennas on top of the existing towers, etc). Therefore it is clear that a single-port unique-element multiband antenna represents an optimum solution for those sites where a similar coverage is simultaneously required at different frequency bands. Multilevel-shaped antennas (Multilevel Antennas, Invention Patent WO0122528) represent a good and efficient solution to design these type of multiband antennas.

Although it has already been reported how some Sierpinski fractal designs can be modified to adjust their input parameters, less work has been done on techniques to adjust the antenna patterns at the different frequency bands.

In (C.Puente, M.Navarro, J.Romeu, R.Pous, Variations on the Fractal Sierpinski Antenna Flare Angle, IEEE Antennas and Propagation Society International Symposium, Atlanta, June 1998) it was shown that a variation on the Sierpinski antenna's flare angle was translated into its input parameters, but also into the shape of its radiation patterns. As an extension of that work, a dual-band antenna design based on the Sierpinski fractal with a bi-directional pattern is described. The procedure design to find the optimum antenna geometry is also explained. Moreover, the antenna is mounted with a reduced-sized ground plane so as to provide a compact performance.

In addition, a 3D antenna structure using two planar elements derived from the classical Sierpinski gasket is presented, Fig.1. The results of this novel antenna show how a 3D geometry can be used to tailor the radiation patterns at the different frequency bands.

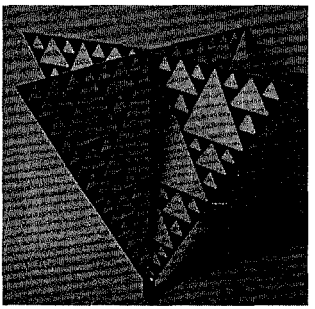

Fig 1 3D antenna solution used to tailor the antenna patterns at the different frequency bands. The antenna is built with two planar structures based on the Sierpinski fractal

0-7803-7846-6/03/$17.00 ©2003 IEEE

# Are prefractal monopoles optimum miniature antennas?

*J.M. González-Arbesú*, J. Romeu, J.M. Rius*
Universitat Politècnica de Catalunya
c/ Gran Capità s/n, D3, Campus Nord
08034 Barcelona (Spain)
email: jmgonzalez@tsc.upc.es

*M. Fernández-Pantoja, A. Rubio-Bretones, R. Gómez-Martín*
Facultad de Ciencias
Universidad de Granada
18001 Granada (Spain)
email: mario@ugr.es

Radiation efficiency and impedance bandwidth are reduced with the electrical size of the antennas. This makes small antennas inefficient by nature (low radiation resistances, high ohmic losses, high currents in the conductor, high energy stored in the near-field of the antenna). The inefficient performance of small antennas is summarized by the high values of the quality factor ($Q$), already predicted by the fundamental limit stated by Chu and reexamined by McLean. This limit starts from the hypothesis that an infinitesimally small antenna radiates only a $TE_{01}$ or $TM_{01}$ spherical mode and that depends on the electric size of the antenna $k_0a$, being $k_0$ the wave number at resonance, and $a$ the radius of the smallest sphere that encloses the antenna (and its image in the case of monopoles). However, real antennas do radiate more reactive modes contributing to higher $Q$ values.

Lowering the $Q$ of an electrically small antenna ($k_0a<1$) is only possible by a proper utilization of the volume that surrounds it in establishing a $TE_{01}$ or $TM_{01}$ mode, or by reducing the efficiency of the antenna ([R.C. Hansen, Proc. IEEE, 69, 170-182, Feb. 1981]). Altshuler ([E.E. Altshuler, TAP, 44, (6), 787 –791, June 1996]) used Genetic Algorithm optimization to search for 3D self-resonant wire antennas "that best utilize the volume within which the antenna is confined". Constraints posed in the analyzed structures were the number of wire segments connected in series contained in a cube of specified volume. Measurements assessed with simulations carried out with NEC. The optimization lied in the minimization of a figure of merit combining both resonance frequency and bandwidth of operation. Unfortunately, the absence of information about radiation efficiencies and ohmic losses unables any comparison on the efficiency of the technique for the design of small antennas but stated the potential of the method.

Being the electric size ($k_0a$) of the antenna who limits its performance in terms of $Q$, the purpose of this work is applying Genetic Algorithms optimization for the design of small bidimensional (inscribed in a plane) wire monopoles. A multiobjective optimization is used to optimize both quality factor and radiation efficiency at resonance for an specified electric size of the antenna. GA-optimized designs will be compared with prefractal structures showing that the same degree of miniaturization can be achieved with better performances. Preliminary results have been obtained (and also will be shown) from the analysis of Koch monopoles.

Conclusions from bidimensional wire monopoles can be extended to 3D antennas. Bidimensional wire monopoles are our objective antennas because they are easily manufactured using conventional techniques for the fabrication of printed circuit boards, and they do not need baluns to balance currents. Radiation efficiencies and quality factors are measured using the Wheeler cap method.

0-7803-7846-6/03/$17.00 ©2003 IEEE

## Rough Surfaces and Random Media

**Co-Chairs:** L. Carin
J. Anguera

10:00 Opening Remarks

**Time-Domain Simulation of Scattering by Two-Dimensional Random Rough Surfaces**

Traian Dogaru
US Army Research Laboratory
2800 Powder Mill Rd, AMSRL-SE-RU
Adelphi, MD 20783-1197

Xianyang Zhu and Lawrence Carin
Department of Electrical and Computer Engineering
P. O. Box 90291, Duke University
Durham, NC 27708-0291

The numerical analysis of electromagnetic scattering by rough surfaces is a subject of continued interest within the research community. Our work is particularly motivated by evaluating clutter levels in the context of using low-frequency, ultra-wideband ground penetrating radar for detection of objects placed at or under a rough air-ground interface.

Whereas many numerical tools for rough surface analysis are based on integral-equation solvers, we approach the problem in the time-domain, based on the multi-resolution time-domain (MRTD) method. The advantages of this technique include the possibility of handling arbitrary media and obtaining results over a wide band of frequencies in one time-marching run. The application of MRTD to modeling large two-dimensional rough surfaces (three-dimensional simulations) comes at a significant computational cost. Therefore, we implemented a parallel MPI version of our MRTD code that enables us to handle surfaces of tens of wavelengths on each side. The emphasis in this paper is on dielectric (penetrable) interfaces with Gaussian statistics, although the techniques can be applied to any other configuration.

The results are presented as radar cross-section (RCS) per unit surface area as a function of frequency, for different angles of incidence, polarizations and surface parameters. In order to make the results statistically meaningful, we perform a Monte Carlo analysis, by averaging the clutter levels over a large number of independent rough surface realizations. We address implementation issues such as the effects of the finite surface size and the staircase approximation of the interface. Also, we perform a comparison of our numerical results with theoretical rough surface analysis techniques.

0-7803-7846-6/03/$17.00 ©2003 IEEE 

**Scattering From Electrically Large Rough-Surfaces via a Scalable Fast Multipole Analysis**

James Thompson and Lawrence Carin
Department of Electrical and Computer Engineering
Duke University
Box 90291
Durham, NC 27708-0291

Studying the scattering features of three-dimensional randomly rough surfaces is a very important and challenging problem, of interest when sensing targets over the ocean and in the presence of rough terrain. We have implemented an efficient scalable multi-level fast multipole algorithm (MLFMA) for perfectly conducting and dielectric rough surfaces. The scalable software is implemented via the message-passing interface (MPI). We first demonstrate the efficiency and scalability of the MLFMA software, and then use it to analyze scattering from both perfectly conducting and dielectric interfaces. With regard to the perfectly conducting rough surface, we perform two distinct implementations for truncation of the surface. In one we truncate the surface and employ beam excitation. In the second we taper the finite rough surface into a flat interface, with this coupled to the perfectly conducting half-space Green's function. In this latter approach the rough surface is finite, but the surface is embedded within an infinite perfectly conducting half plane. We therefore employ plane-wave excitation in this latter case. In this talk we perform a detailed analysis of the distinctions between the results computed via these two approaches.

For the sea-surface problem we often employ a perfectly conducting surface, thereby necessitating an electric-field integral equation (EFIE). Finely detailed structure on the rough surface implies that we often require basis functions that are very small relative to wavelength. Under this circumstance the EFIE is typically poorly conditioned, thereby significantly slowing algorithm convergence via iterative solvers, such as the conjugate-gradient method. In this talk we also investigate a new formulation of the EFIE integral equation, which is better conditioned, thereby yielding significantly improved convergence of the numerical solution.

0-7803-7846-6/03/$17.00 

# FDTD Modeling of Correlation Functions for Scattered Light in Passive and Active Random Media Crossing from Weak to Strong Scattering Regimes

**Shih-Hui Chang[1]*, Hui Cao[2], Allen Taflove[1]**
[1]Department of Electrical and Computer Engineering
[2]Department of Physics and Astronomy
Northwestern University, Evanston, IL 60208

The recent discovery of lasing in random media has received considerable interest. This phenomenon has important potential practical applications, especially with regard to reducing the cost of commercial lasers. However, the physics involved is not yet well understood. Specifically, there is the question of how optical gain in random media can enhance light scattering while simultaneously leading to enhanced light confinement.

The speckle pattern of waves coherently transmitted through disordered media shows intensity fluctuation. In microwave experiments, the correlation function of this fluctuation exhibits enhanced long-range correlation in disordered media. However, in such experiments, the material absorption hinders electromagnetic wave localization, and further it is difficult to add gain media to the system.

In this paper, we apply the finite-difference time-domain (FDTD) method to study the correlation functions of scattered light in passive and active random media. The system in our calculation is a two-dimensional metal waveguide containing a random spatial distribution of material cylinders of fixed radius, fixed dielectric properties, and either zero optical gain or a fixed optical gain modeled by a macroscopic Lorentzian gain algorithm. An impulsive point source is placed in air immediately in front of one surface of the random sample, and the transmitted electric field waveform is recorded at the opposite surface. As the sample length increases, the system goes from a weak scattering regime to a strong scattering regime. We calculate the ensemble-averaged spatial and spectral field-field and intensity-intensity correlation functions of the transmitted signal along the sample surface in both scattering regimes.

For the passive random medium case, we find that the ensemble-averaged field-field correlation function is the same for all scattering regimes, but the intensity-intensity correlation shows a significant enhancement as the scattering strength increases. The spectral correlation function shows a reduced frequency correlation linewidth with an increase of the scattering strength. This indicates that the average lasing mode linewidth is reduced. When the averaged linewidth is smaller than the average mode frequency spacing, the sample enters the localization region.

For the active random medium case, we find that the spatial field-field correlation is unchanged from the passive case, but the intensity-intensity correlation is greater at long range. The spectral field-field correlation shows a reduction of the correlation linewidth due to the introduction of gain. This indicates that light confinement in an active random medium can be *enhanced* by optical gain.

0-7803-7846-6/03/$17.00 ©2003 IEEE

# Modeling of Electromagnetic Signal Propagation in Random Discrete Absorbing Media Inclusive a Semitransparent Spherical Object

V. G. Spitsyn
Department of Computer Engineering, Tomsk Polytechnic University,
84, Sovetskaya street, Tomsk, 634034, Russia,
Tel: +7 3822 418912, Fax: +7 3822 419149,
E-mail: spitsyn@ce.cctpu.edu.ru

The necessity of analysis of electromagnetic signal with arbitrary frequency spectrum propagation in the three-dimensional random discrete media requires the development of new methods of computation. In this paper we consider the stochastic model of electromagnetic signal multiple interaction with discrete inhomogeneities chaotically disposed in the stratified media. The media consist of the five layers and inclusive a spherical object, moving with constant velocity.

The method of solving this problem is based on the stochastic modeling of wave interaction with random discrete media (V.G. Spitsyn, *IEEE AP-S International Symposium*, 1, 288-291, 2002). Here is assumed that the wavelength of the wave is less than the sizes of the layers and scattering occurs incoherently by an image on statistically independent discrete inhomogeneities. The oscillator of electromagnetic signal is presented as a source of photons with corresponding diagram of radiation. The type of photons interaction with discrete inhomogeneities is determined according to set cross sections of absorption and scattering. There is computed the Doppler shift of electromagnetic signal frequency conventional of signal scattering on the moving discrete inhomogeneities (V.G. Spitsyn, *Modeling of radiowave scattering on the ionospheric plasma disturbances, created of space vehicle*, Tomsk: Publishing House "STT", 2002). In the result of computer imitation of researched process we receive the distributions in space of coordinates of energy scattering signal and energy of absorption signal into media. In addition to we received the transformation of electromagnetic signal frequency spectrum after multiply interaction with moving discrete inhomogeneities, contained in a semitransparent spherical object

Thus in the paper the stochastic model concerning electromagnetic wave propagation in the three-dimensional random discrete media is offered. The problem about passage of the wave through the random media with five layers and moving spherical object is solved. Dependencies of frequency spectrum and energies of scattering and absorption signals from the factors, describing the nonuniform of the structure of random discrete media are investigated.

0-7803-7846-6/03/$17.00 ©2003 IEEE 

## Radar Techniques

Steve Cummer, Duke University
E. A. Bering, University of Houston
**Co-Chairs:** J. Sahr
F. Lind

7:55 Opening Remarks

# Implementing Software Radar Systems at Millstone Hill

Frank D. Lind(1)*, Philip J. Erickson(1), Tom Grydeland(2), Bill Rideout(1), and John Holt(1)

(1)MIT Haystack Observatory, Route 40, Westford MA 01886
(2)Department of Physics, University of Tromsø, Tromsø, Norway

We have recently implemented a Software Radar System as the production data taking and control system for the Millstone Hill Incoherent Scatter Radar. In a Software Radar the traditional real-time hardware, control, and signal processing elements of a radar system are replaced by software running on general purpose computer systems and interconnected by a high speed and low latency data network.

From our efforts to develop this system we have identitified a number of key architectural elements which are important for achieving performance, modularity, and scalability in distributed systems of experimental radar instrumentation. These elements include global coherence, reference signal digitization, multicast interconnection, persistence management, and a large number of generic software patterns (channels, signal chains, distributors, listeners, recorders, replayers, filterers, triggers, bridges, proxies, schedulers, and weavers). We will discuss the role of these elements in the design of the Millstone Hill Software Radar. In particular we will focus on the structure and performance of our implementation and we will show example incoherent scatter radar data and control information from different stages in the data processing chain.

We will also discuss the design constraints on Software Radar scalability and performance in the context of implementing practical monostatic radars and more novel multistatic Coherent Radar Networks. As part of this discussion we will briefly describe the design of a Coherent Radar Network to provide complementary measurements for the Millstone Hill Incoherent Scatter radar. The ISIS Array (Intercepted Signals for Ionospheric Science) is enabled by Software Radar technology and will combine active radar, passive radar, beacon scintillation, and beacon tomography into a single distributed instrument design capable of observing wide regions of the ionosphere.

0-7803-7846-6/03/$17.00 ©2003 IEEE 

# An Ionosonde for the 21st Century

**J. W. Wright*, R. N. Grubb, and N. A. Zabotin**
*Cooperative Institute for Research in Environmental Sciences (CIRES), University of Colorado/NOAA, Boulder, CO, 80309-0216*
**M. T. Rietveld**
*EISCAT Scientific Association, Tromsø Norway*
**F. T. Berkey**
*Space Dynamics Laboratory, Utah State University, Logan, UT*
**R. C. Livingston**
*Scion Associates, Port Townsend, WA*

The ionosonde is as fundamental to monitoring and understanding the upper atmosphere as are the seismograph to the solid earth, the magnetometer to geomagnetism, the barograph to meteorology, the wave and tide recorder to oceanography, and sonar to marine-acoustic applications. Ionosondes have fulfilled their role from the time of primitive analog instruments nearly 80 years ago, until present-day digital systems. On average, about 200 ionosondes have been deployed globally under the administration of many government and academic institutions.

Modern ionosondes can and should face the challenges posed within the Space-Weather framework, and they must serve expanding research opportunities in geophysics, plasma and radio physics. No longer merely "devices for making ionograms", they enjoy the remarkable sensitivity of MF/HF radio to complex plasma structure, in turn exploiting the sensitivity of ionization to nearly every internal and external geophysical influence. Diagnostics in three spatial dimensions, with single-site resolution extending from tens of meters to hundreds of kilometers, with millisecond resolution and unlimited (and adaptive) temporal continuity, can now be demonstrated. Dynamic descriptions of irregular plasma structure are usefully statistical at less than about the Fresnel scale (a few km), and become usefully deterministic toward larger scales.

Fortunately, modern digital technology enables a cost-effective approach to the design of a modern ionosonde, while assuring rapid data processing, dissemination and archival tasks. A new system now in the engineering stage of development will be modular, with at least four parallel, identical, digital receivers, giving at least 20-bit I/Q echo processing with dynamic range exceeding 80 dB. Digital (programmable) definition of output waveform and receiver performance assure echo phase coherence and low RFI generation. An open-source operating system will permit continuing evolution of measurement capabilities for monitoring and research applications.

Extensive data analysis capabilities are demonstrated at present using the NOAA Dynasondes at EISCAT (Tromsø Norway) and the USU Bear Lake Observatory, and are available in real time on the Web (e.g., *http://dynamite.eiscat.uit.no/jww*).

0-7803-7846-6/03/$17.00 ©2003 IEEE

## Multiple Scattering Effects in Ionospheric Radio Sounding

**N. A. Zabotin* and J. W. Wright**
*Cooperative Institute for Research in Environmental Sciences (CIRES), University of Colorado/NOAA, Boulder, Colorado, 80309-0216*

We consider the problem of radio wave reflection from an optically thick, plane, monotonic layer of non-magnetoactive ionospheric plasma containing random field-aligned density irregularities, and investigate numerically the influence of multiple scattering on the averaged intensity and angular distribution of the received signal. Our approach uses a special form of the radiative transfer equation in invariant ray coordinates (Zabotin *et al.*, *Waves in Random Media*, **8**, 421-436, 1998). The mid-latitude case is treated in some detail, but we also examine the principal effects of latitude dependence, which result from the varying aspect presented by elongated irregularities. In vertical sounding, multiple scattering in the ionospheric "mirror" produces a diffuse image of the radio point source, with a specific angular-spectrum structure. Three distinct maxima are present: A sharp central peak is oriented along the "magnetic" meridian plane. Laterally, two wider but weaker peaks are located symmetrically relative to the meridian. The effect may be called "astigmatism of the ionospheric mirror" and arise from the orientation of the irregularities.

The case of slightly oblique sounding is also considered. As the distance between transmitter and receiver increases, the side peak closer to the undisturbed angle of arrival gradually becomes dominant; the other one practically disappears, but the former central peak (radiating vertically to the receiver) continues to play a noticeable role. This characteristic two-maxima structure of the obliquely scattered signal may be described approximately in terms of double refraction in some effective medium. Note that this effect is not magnetoionic; it is caused by multiple scattering.

Earlier versions of the theory showed a strong anomalous-attenuation effect; this is now confirmed, with quantitative adjustments. For very typical irregularity-amplitudes in the range $0.002 < \Delta N / N < 0.01$ at the scale length 1 km our calculations produce integral attenuation of the signal intensity between 5 and 22 dB. A special calibration procedure permits estimation of anomalous attenuation in practical dynasonde measurements. We discuss the application of our results to explain the ionogram phenomenon of spread F.

Our results for the polar ionosphere produce a peculiar arc-like shape of the radio reflection. They resemble some optical images of the artificial aurora obtained during heating experiments in Tromsø (M. J. Kosch *et al.*, *Proc. of the XXVIIth General Assembly of URSI, CD-ROM Edition*, Paper #1321, 2002). This suggests a common origin of the two phenomena, arising from multiple scattering of the heating signal within the ionospheric layer.

0-7803-7846-6/03/$17.00 ©2003 IEEE

# VHF Passive Radar Interferometer Calibration using Targets of Opportunity

Melissa G. Meyer, John D. Sahr, Chucai Zhou, Dawn M. Gidner
University of Washington Electrical Engineering, Seattle, Washington

January 14, 2003

Radar interferometry is a relatively new, powerful technique to be applied to studies of turbulence in the ionosphere. Coherent scatter radars collecting echoes on multiple antennas can, with a little extra signal processing, resolve the transverse structure of scatterers, and with the proper antenna arrangement, can locate targets in both azimuth and elevation angle. Imaging can also be done with systems of more than two antennas. We have recently demonstrated the use of interferometry with passive radar, determining uncalibrated azimuthal structure in E-region irregularities. Interferometer calibration requires care, and there are many parameters which deserve attention; we will focus on a few of them here.

An unknown phase shift is imposed on each received signal due to the transmission lines connecting the antennas and the receiver, where the data is recorded. The electrical length of these cables may be roughly determined, but a regular correction done using data from the instrument itself is desirable because of the temperature dependence of the cables and varying environmental conditions. Useful targets in this case are VHF transmitters in the area; these point targets are stationary at exactly known locations and thus their apparent "movement" in the interferometer beam can be used to calibrate the instrument. Area transmitters are also useful in determining exactly the baselines between the various antennas in the interferometer. In many cases baselines are more accurately measured by carefully observing data from the instrument itself, rather than trying to determine the exact electrical centers of the antennas and then physically measuring the distance between them.

Finally, other point targets such as aircraft, which we observe routinely, are useful in refining knowledge of the interferometer beam pattern. The width of a lobe at a certain range can be estimated by tracking commercial aircraft as they progress across it. Typically these airplanes maintain a constant velocity, and often they follow predictable courses in the sky. Thus, much can be learned by monitoring their Doppler velocity and phase progression.

Our objective is to develop a robust, effective instrument that can continuously recalibrate itself and operate reliably in the field, requiring minimal upkeep. Developing calibration techniques which utilize the data products themselves is a step in this direction. Here we will describe the abovementioned interferometer calibration techniques and demonstrate them with our VHF coherent scatter passive radar. We will also comment on the practicality of implementing these techniques and their usefulness in ionospheric radar applications.

0-7803-7846-6/03/$17.00 ©2003 IEEE

# Ionospheric Irregularity Diagnostics: The Relative Contribution of Different Scale Lengths, in the Phase Structure Function Method for the Dynasonde

**N. A. Zabotin and J. W. Wright**
*Cooperative Institute for Research in Environmental Sciences (CIRES), University of Colorado/NOAA, Boulder, Colorado, 80309-0216*

Drift of the ionospheric plasma permits a radio-sounding signal to pass through different irregularities of electron density, even at only slightly different times. For a series of successive sounding pulses, this causes temporal phase variations which may be characterized statistically by the structure function. We have proposed (N. A. Zabotin and J. W. Wright, *Radio Sci.*, **36**, 757-772, 2001) a new diagnostic method for ionospheric irregularities based on this effect, which is applicable to Dynasonde sounding data. In the present paper, we consider the range of the irregularity scales accessible by the phase structure function method. Our approach involves representation of the phase structure function as an integral over the irregularity spectrum; we can investigate numerically the contribution of different spectral bands into the integral. We show that for a two-dimensional irregularity power spectrum index $2 \lesssim \nu \lesssim 3$ (which is quite typical for ionospheric conditions), the phase structure function in the region of small temporal lags is sensitive to irregularities in a broad band of scales extending from several meters to several kilometers.

According to our analysis, small-scale irregularities are sufficiently represented in the ionosphere if the index $\nu$ of their power spatial spectrum $\Phi(\kappa_\perp) \propto \kappa_\perp^{-\nu}$ is less than three. In this case, a specific estimate for the minimum detectable scale length is given by the expression $L \simeq 2V\tau$, where $V$ is the horizontal drift speed of the ionospheric layer and $\tau$ is the temporal lag of the phase structure function. In the opposite case ($\nu > 3$) where small-scale irregularities are very weak, advantage may be taken of a further result from our study, showing increased sensitivity for ray paths close to the direction of the geomagnetic field. This option is of practical value owing to the dynasonde's ability to measure the direction of arrival of ionospheric radio echoes.

We present our most recent results of the ionospheric irregularity diagnostics by the phase structure function method.

0-7803-7846-6/03/$17.00 ©2003 IEEE

## A Study of the Distribution of High Latitude Absorption

**Amin Aminaei** Research student in Communication Systems Department of Lancaster University
**Farideh Honary** Professor in Communication Systems Department of Lancaster University - UK
**Andrew J. Kavanagh** Researcher in National Center for Atmospheric Research,Boulder,CO-USA

Since September 1994 IRIS (Imaging Riometer for Ionospheric Studies) has been operating at high latitude (Kilpisjarvi, Finland, 69.05° N) providing measurements of cosmic radio absorption in the D layer of the Ionosphere. This paper presents some results of modelling absorption based on the statistical distribution of data taken by IRIS (at 38.2 MHz) in different Magnetic Local Time (MLT) sectors. A high latitude absorption model based on solar wind parameters will be discussed and compared with previous models based on the Kp index. The results of our study indicate:

-Distribution of absorption in the zenithal beam of IRIS (epoch 1995-2001) for different magnetic local time sectors (e.g. Fig.1) follows the Log-Normal distribution as suggested by Foppiano and Bradley (Journal of Atmospheric and Terrestrial Physics, Vol.46, No.8 pp.689-696, 1984).
-Distribution of solar wind pressure (nPa) from 1995 to 2001 inclusive (Fig.2) and the distribution of solar wind speed (km/s) at 10-minute resolution (Fig.3) are also best fit by a Log-Normal distribution.
-Distribution of the 3-hour Kp in the same epoch as well as the occurrence of Kp in the four individual seasons is best modelled with a Weibull distribution.

***Key Words:***
High Latitude Absorption, Kp index, Solar Wind Parameters, Log-Normal Distribution and Weibull Distribution

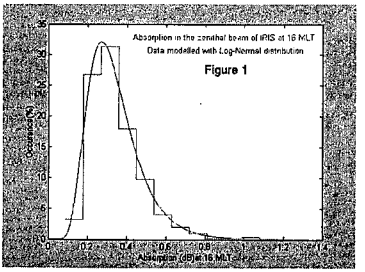


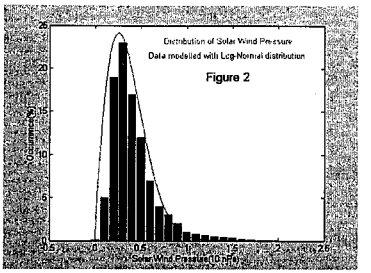


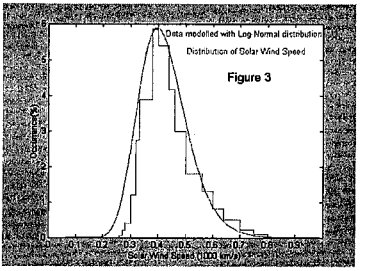


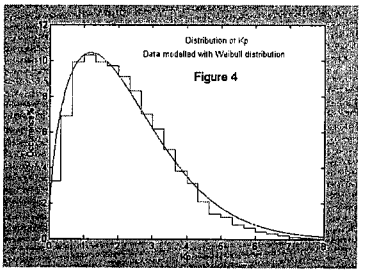

*Special Session*

## Meteor Physics

**Organizer(s):** John Mathews, Penn State University
Wayne Hocking

**Co-Chairs:** J. Mathews
W. Hockings

10:00 Opening Remarks

# Radio Science Issues Surrounding HF/VHF/UHF Radar Meteor Studies

J. D. Mathews
Communications and Space Sciences Laboratory, The Pennsylvania State University, University Park, PA 16802-2707 USA, JDMathews@psu.edu

Classical meteor radars depend on coherent (Fresnel) scattering from a meteor trail oriented perpendicular to the radar wave-vector at closest approach to the radar. Meteor trails viewed in this manner are described as "classical" radar meteors with under/over-dense trails. While meteor "head-echoes" are rarely seen with classical low-power, wide-beam HF meteor radars, they are essentially always seen by large aperture (narrow-beam), high-power VHF/UHF radars. We discuss the expected radar scattering cross-sections (RCSs) of head- versus trail-echoes and how equilibrium concepts such as plasma frequency are of limited use in describing the results. Particular attention is given to the frequency dependence of the RCS and how the frequency dependence may yield considerable new information regarding the plasma distribution in the "coma" surrounding the meteoroid. As the head-echo is directly associated with the meteoroid, instantaneous (single-pulse) Doppler observations are possible. In the case of classical trail-echoes, the time evolution of the RCS as a function of frequency may provide new information on the plasma diffusion rate and thus on atmospheric density and temperature. Information from the time evolution of the trail must however be considered in light of new results showing that the trail rapidly B-field-aligns in a manner apparently driven by plasma instabilities that develop in 10-100 msec after trail deposition. It is in the context of instability-driven B-field alignment of the trails that we discuss anomalous trail-echoes. The anomalous trail-echo is a range-spread chaotic (non-classical) trail-echo derived from a meteor that travels at an arbitrary angle relative to the radar wave-vector. We present numerical simulations illustrating these concepts.

0-7803-7846-6/03/$17.00 ©2003 IEEE 

## UHF and VHF Meteor observations using the Arecibo and MU radars

Qihou H. Zhou[1*], D. Janches[2,3], T. Nakamura[4], J. D. Mathews[3], Y. T. Morton[1], T. Stover[1]

1. School of Engineering and Applied Science, Miami University, OH 45056;
2. NAIC, Arecibo Observatory, Arecibo, PR 00979.
3. CSSL, Penn State University, University Park, PA 16802
4. Radio Science Center for Space and Atmosphere, Kyoto University, Kyoto, Japan.

This paper reviews and updates the meteor observations made at the Arecibo observatory as well those made using the Japanese Middle and Upper (MU) atmospheric radar over the past decade. We also discuss potential scattering mechanisms associated with the Arecibo and MU observations and their potential implications.

The first Arecibo meteor results were reported by Zhou et al. (*J. Atmo. Terr. Phys.*, **57**, 421, 1995) using the time-integrated data collected for the background ionosphere. Despite that the early observations could not resolve the time-duration, it is clear that the Arecibo radar sees meteors as faint as visual magnitude +16, the faintest meteors observed by any ground based instrument. Subsequent meteor observations at Arecibo have been using the raw-data taking mode to resolve the time resolution to a milli-second and height resolution to 150 m (Mathews et al., *ICARUS*, **126**, 157, 1997; Zhou and Kelley, *J. Atmo. Terr. Phys.*, **59**, 513-521, 1997). The evolution of meteor observations and signal processing techniques was reported by Mathews et al. (*J. Atmos. Solar-Terr. Phys., submitted, 2002*). Simultaneous meteor observations have also been made of the Arecibo 430 MHz and 47MHz radars (Zhou et al., *Radio Sci.*, **33**, 1642, 1998). Janches et al. reports accurate measurements of meteor deceleration with a single feed (Janches et al., *ICARUS* **143**, 347, 2000) as well as with the more recently available dual beam (Janches et al., *J. Geophys. Res.* Submitted, 2002).

Dedicated meteor observations made by the MU radar operated by the Kyoto University reveal the existence of field-aligned irregularities (FAI) within each meteor trail (Zhou et al., *Geophys. Res. Lett.*, 2000). Because of the ubiquitous presence of FAI echoes, they potentially may affect extraction of winds and ambipolar diffusion coefficient from meteor trails. We also discuss some theoretical calculations of the aspect sensitivity of meteoric FAI echoes.

0-7803-7846-6/03/$17.00 ©2003 IEEE

# Meteoroid plasma density, mass and velocity determination using a new 3D full-wave scattering method applied to head echoes

S. Close[1,2], S. Hunt[1,2], M. Oppenheim[2], A. Coster[1]

[1] *MIT Lincoln Laboratory, Lexington, Massachusetts*
[2] *Boston University, Center for Space Physics, Boston, Massachusetts*

Large-aperture radars have the ability to detect the high-density plasma that forms in the vicinity of the meteoroid and moves with the meteoroid's velocity; reflections from these plasmas are called head echoes. To determine the head echo plasma density and configuration, we have modeled the interaction of a radar wave with the head echo plasma without assumptions relating to wavelength or plasma density; this solution is referred to as the "full-wave" scattering method. This presentation contains the results of a 3D full-wave scattering method applied to head echo data detected by ALTAIR at both VHF and UHF during the Leonid 1998 storm. Head echoes are modeled as reflections from sphere-like plasmas with frequencies near the radar frequency and radii that scale with the atmospheric mean free path. The head echo plasma density was determined by applying the full-wave solution to each head echo's radar-cross-section (RCS), and indicates that head echo RCS will be maximized when the head echo plasma achieves the best balance between plasma density and size. Head echo plasma density is highly dependent upon meteoroid velocity, mass and detection altitude and will be maximized at low altitudes, where densities can exceed $10^{17}$ el/m$^3$.

We used three methods to validate our full-wave method. First, we used the 3D method to compare VHF plasma densities with UHF plasma densities. Second, we converted the maximum plasma density from each VHF head echo to electron line density and compared these values with those obtained from a meteoroid ablation model. Finally, we calculated the electron line density at each frequency from a single head echo detected simultaneously at VHF and UHF in order to compare its meteoroid mass at both frequencies. Our results indicate that the full-wave method produces consistent results across frequencies and agrees remarkably well with the ablation model.

0-7803-7846-6/03/$17.00 ©2003 IEEE 

# The Linear Plasma Theory of Meteor Trails and Implications for Radar Measurements

M. M. Oppenheim*, L. P. Dyrud, S. Close, S. Hunt, L. C. Ray and K. Mcmillon
Center for Space Physics, Boston University
725 Commonwealth Ave, Boston, MA 02215
(e-mail: meerso@bu.edu)

Radars probing the atmosphere between 75 and 130 km frequently receive echoes from plasma trails left by ablating micron-sized meteors. These echoes have proven useful in characterizing meteors and in estimating wind velocities and temperatures. Two distinct types of radar echoes return from meteor trails. First, strong "specular" echoes occur when the radar pointing direction lies perpendicular to the meteoroid's trajectory. Second, weaker "non-specular" echoes are measured by large-aperture, high-gain, radars when not pointing perpendicular to the trail's orientation but when the radar points perpendicular to the geomagnetic field. Figure 1 shows an example of a head echo (the line at the left of the image) followed by a non-specular trail.

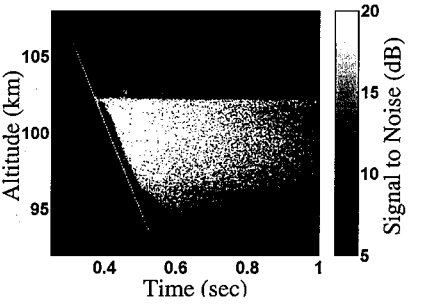


Figure 1: Example of a trail echo recorded by the VHF ALTAIR radar at the Kwajalein missile range as a function of altitude and time.

This paper further develops the plasma physics of meteor trail irregularities and compares the results of theory, simulations and observational data. This study helps us use radar data to better understand the composition of meteor trails and their interactions with the surrounding atmosphere. In particular, we can evaluate: (1) the criterion for the onset of the instability as a function of altitude, atmospheric temperature, and meteor trail composition and density; (2) the nature of the instability and the resulting waves as measured by radars; (3) anomalous cross-field diffusion will occur only within this limited altitude range with consequences for calculating diffusion rates and temperatures with both specular and non–specular radars. This analysis should enable us to better use meteor radar data to characterize meteors and the upper atmosphere.

**Commission:** G/H Meteor physics - invited talk

**New knowledge contributed:** Developing models of meteor trail turbulence allows a more accurate analysis of radar measurements of meteors.

**Relationship to previous work:** This research builds on previous work, particularaly in using non-specular trail characteristics to evaluate meteoroid characteristics.

0-7803-7846-6/03/$17.00 ©2003 IEEE

# Meteor Detection With the HAARP VHF Radar

Frank T. Djuth
Geospace Research, Inc., 550 N. Continental Blvd., El Segundo, CA 90245

In May 2001, a new VHF radar system was installed at the HF Active Auroral Research Program (HAARP) site in Gakona, Alaska. The radar transmitter is capable of operating from 135 to 143 MHz. However, from a practical standpoint, the radar is typically tuned to frequencies clear of interference. In this regard, 139.3 MHz is the most common transmission frequency. The radar antenna consists of an array of 32 × 24 collinear, coaxial dipoles. The maximum and minimum pulse widths are 2 milliseconds and 0.5 microseconds, respectively, and the maximum duty cycle is 10%. As currently configured, the radar employs sixteen transmitter modules to generate 40 kW peak power. The purpose of the radar is to monitor naturally occurring phenomena in the atmosphere/ionosphere above HAARP as well as modifications to the ionosphere brought about by the HAARP high-power, high-frequency modification facility. The first extended duration observation runs with this radar took place beginning in July 2002 and ending in September 2002. Although the radar observation program was optimized for the detection of Polar Summer Mesospheric Echoes, a rich variety of meteors were detected as part of the geophysical background. Many of the observations were made in the time frame of the Perseids shower (August 12), but observations at the peak of the shower were curtailed by a power blackout. Because the radar beam is directed vertically, meteor head echoes are most commonly observed in the main beam. However, strong meteor trails and perhaps geomagnetic field-aligned trails are detected through the sidelobes of the antenna. Meteors are commonly observed at ranges from 150 km to 450 km and beyond. In this presentation, we explore the plasma physics involved in meteor ablation in the atmosphere. Investigations indicate that the plasma processes can be quite turbulent depending on the size and nature of the meteor.

0-7803-7846-6/03/$17.00 ©2003 IEEE 

# VHF Passive Bistatic Radar Observations of Meteor Trails

J. D. Sahr, M. G. Meyer, D. M. Gidner, C. Zhou
Department of Electrical Engineering Box 352500
University of Washington, Seattle WA 98195-2500

The Manastash Ridge Radar is a completely passive bistatic VHF radar designed to observe the scatter of commercial FM broadcasts from ionospheric E-region irregularities. The altitude of these irregularities is comparable to that of meteor decay, and meteor trail scattering cross sections are frequently large enough to be observed with this 100 MHz instrument. Our radar is not sufficiently sensitive to detect head echoes.

At 100 MHz we expect that the meteor trails are primarily underdense, and that the scattering cross section is enhanced by coherent scatter from field-aligned meter-scale plasma irregularities (Dyrud *et. al.*, GRL v28 p2775, 2001). We can determine the slant range ($\Delta r \sim 1.5$ km) and Doppler spectrum ($\Delta v \sim 2$ m/s). We also have interferometric capability, which produces an angular resolution of about 0.1° for strong meteor echoes. Meteor targets are moderately overspread at 100 MHz, however the radar detection algorithm is based upon time series analysis rather than correlation-based estimates. The useful sample rate for these time series is approximately 500 Hz, so that the temporal resolution is a few milliseconds.

We will present a variety of examples of meteor detections, including range-Doppler observations, high time-resolution observations, time series, and interferometric observations. The Doppler and interferometric information are consistent with the notion of the meteor trail formed in the midst of a thick mesospheric wind field which creates shears that distort the observed trails. Although the overall Doppler width may be large (about 100 m/s), the interferometric information suggests that the Doppler spectra are narrow at a particular location along the trail, and the overall Doppler velocities are consistent with the expected winds in the mesosphere. In other words, the plasma waves which are presumably responsible for the VHF scatter apparently have relatively little phase velocity with respect to the plasma column on which they form.

0-7803-7846-6/03/$17.00 ©2003 IEEE

# Meteor Orbital Parameters using CMOR

A. R Webster, P. G. Brown, and J. Jones,
The University of Western Ontario'
London, Ontario.
Canada

The Canadian Meteor Orbit Radar (CMOR) is a relatively new system designed to determine the orbital parameters of meteors detected by the back-scatter radar. The transmitter is of reasonably high power (6kWpeak) and the pulse-repetition frequency variable up to a maximum of 2000pps. This feeds a single 3-element Yagi antenna.

The heart of the receiving system is a 5-element array of 2 orthogonal 3-element arrays with common center element each consisting of a 2-element Yagi antenna. This part of the system has been operatonal for a few years and has been used in the recent observations of the Leonid meteor shower from 1998 to 2002. This core system is capable of determining the azimuth and elevation of a given meteor with considerable accuracy (better than $0.5^0$ for s:n > 10dB).

A recent development adds two out-rider stations each with a single receiving antenna and at a distance ~ 8km. These two stations are located from an approximate right angle with the main base station allowing the determination of velocity and direction in space of the meteor. Approximately 30% of the meteors observed on the main station are also observed on these two added receivers.

Results are presented from the operation of the system on a routine basis over a period of several months. This includes observations of sporadic and several shower meteors.

0-7803-7846-6/03/$17.00 ©2003 IEEE

# New Atmospheric Parameters deduced with Meteor radars

W.K. Hocking
Dept. of Physics, University of Western Ontario, N6A 3K7
*email: whocking@uwo.ca*
Ph: +1 (519) 661 3652 Fax +1 (519) 661 2033

Because of fast, modern computers, it is now easy to identify meteor signals digitized by radars and discriminate them from other impulsive phenomena like lightning, ionospheric signals, and man-made noise. Very specific algorithms have been developed which allow such identification with well over 99% success rates. This has meant that new generations of meteor radars can produce extremely clean (uncontaminated) data sets, which has in turn permitted new procedures to be developed with much greater reliability than in the past.

These new developments have not only allowed better estimates of mesospheric winds, but have also allowed a variety of newer parameters to be determined. Examples including mesopause temperatures, mesopause temperature tides, ambipolar diffusion coefficients, and mesopause pressures. Additional astronomical parameters can also be deduced, including shower radiants, meteor entrance speeds, meteor angles of arrival, and ionic recombination coefficients. The variance in the recombination coefficient (which relates to the variability in metallic composition of meteors) can also be measured.

The principles behind these various techniques, as well as examples of their application, will be discussed and demonstrated.

0-7803-7846-6/03/$17.00 ©2003 IEEE

# Comparison of meteor radar and Na Doppler lidar measurements of winds in the mesosphere above Maui, HI

S. J. Franke, A. Z. Liu, X. Chu, G. R. Swenson, C. S. Gardner, W. Hocking

Simultaneous meteor radar and Na Doppler lidar measurements of horizontal winds were obtained in the mesosphere (80-100 km) over Maui, HI during July 7-17, 2002. These observations were carried out under the Maui Mesosphere and Lower Thermosphere (Maui/MALT) initiative. Comparisons of hourly-averaged winds with height resolution of 3 km show that the meteor radar and Na lidar horizontal wind components exhibit height-dependent rms differences ranging from approximately 8-10 m/s at altitudes near 90 km, where the data quality from both instruments is the highest, to 20 m/s at the upper and lower edges of the 80-100 km altitude range. Overall, meteor radar and lidar winds data are highly correlated, with correlation coefficient of approximately 0.9. The statistical distribution of wind shears measured by the lidar and radar will also be discussed and compared.

0-7803-7846-6/03/$17.00 ©2003 IEEE

*Special Session*

## Physical Models for Transient Radiation, Reception, and Scattering

**Organizer(s):** Scott Tyo, University of New Mexico
**Co-Chairs:** J. S. Tyo
E. Heyman

7:55 Opening Remarks

21. 1 8:00 New Developments in IRAs: Shaped Reflectors, Unbalanced Feeds, and Sidelobe Suppression ..... 144
*E. Farr, S. Bigelow, L. Atchley, L. Bowen, Farr Research, Inc., S. Tyo, University of New Mexico, D. Lawry, Air Force Research Laboratory / DE, USA*

21. 2 8:20 Application of the Shielded Loop Antenna for Measurements of UWB Signals ..... 145
*A. G. Yarovoy, TU Delft, Netherlands*

21. 3 8:40 Network-Oriented Dyadic Short-Pulse Field Representations for Periodic Arrays ..... 146
*F. Capolino, University of Siena, Italy, L. B. Felsen, Boston University, USA*

21. 4 9:00 Axial Backscattering from a Wide Angular Sector ..... 147
*C. E. Baum, Air Force Research Laboratory, USA*

21. 5 9:20 Some Fundamental Aspects on Scattering of EM-pulses ..... 148
*A. R. Karlsson, Lund University, Sweden*

21. 6 9:40 Off-Boresight Radiation from Impulse Radiating Antennas ..... APS
*J. S. Tyo, University of New Mexico, E. G. Farr, L. H. Bowen, Farr Research, Inc., J. S. Schoenberg, AFRL/DEHP, USA*

**New Developments in IRAs: Shaped Reflectors, Unbalanced Feeds, and Sidelobe Suppression**

Everett G. Farr*†, W. Scott Bigelow†, Lanney M. Atchley†, Leland H. Bowen†, J. Scott Tyo§, and Dean I. Lawry‡
†Farr Research Inc., 614 Paseo Del Mar NE, Albuquerque, NM, 87123
§Electrical and Computer Engineering Department, University of New Mexico Albuquerque, NM 87131-1356
‡Air Force Research Laboratory / Directed Energy Directorate 3550 Aberdeen Ave. SE, Kirtland AFB, NM 87117-5776

We consider here a number of new developments in the theory and practice of Impulse Radiating Antennas (IRAs). These devices, consisting of a paraboloidal reflector and a broadband feed, have demonstrated two decades of bandwidth in a compact package.

First, we have tested a shaped reflector that eliminates the portion of the reflector that contributes destructively to the radiated field. It was predicted by J. S. Tyo that eliminating a portion of the reflector would provide improved gain, and we can report here the first experimental confirmations of that effect. This becomes important in configurations of the IRA where the feed arms are constructed out of a flexible material, and have to be displaced toward the center of the reflector to keep the feed arms under tension.

Next, we have tested the IRA with a simplified feed configuration, using a single 50-ohm feed cable. This contrasts with the splitter balun that is normally used, in order to provide optimal impedance matching. The splitter balun consists of two 100-ohm cables that are connected in parallel at the 50-ohm cable port and in series at the focus of the reflector to feed the 200-ohm feed arms. The unbalanced feed configuration is forced upon us in a number of situations where either the voltage is too high for the splitter balun, or there is insufficient space for it. This may occur, for example, in the Para-IRA. We have found that there is remarkably little deterioration in antenna performance with the simplified feed, especially at the low end of the frequency spectrum.

Finally, we discuss our efforts to build UWB antennas with low sidelobe level, which is an important characteristic for radar applications. This is a considerable challenge in reflector-based IRAs, because of the high aperture fields near the feed arms. To address the problem, we are studying IRAs based on lenses. These have a more uniform aperture field, and initial results appear to be promising.

0-7803-7846-6/03/$17.00 ©2003 IEEE

# Application of the shielded loop antenna for measurements of UWB signals

A.G. Yarovoy
International Research Centre for Telecommunications-Transmission and Radar
Delft University of Technology
Mekelweg 4, 2628 CD Delft, The Netherlands
Phone: +31-15-278-2496, Fax: +31-15-278-4046, e-mail: a.yarovoy@its.tudelft.nl

Measurements of short electromagnetic (EM) pulses in time domain require utilization of ultra wideband sensors for electromagnetic field (M. Kanda, *Time-Domain Measurements in Electromagnetics*, Van Nostrand Reinhold Company, New York, 122-174, 1986). The majority of commercially available sensors are so-called B-dot or D-dot sensors, which measure time derivative of B or D component of EM field correspondingly (J.P. Castillo and L. Marin, *Time-Domain Measurements in Electromagnetics*, Van Nostrand Reinhold Company, New York, 268-295, 1986). To recover the EM-waveform field from data obtained with these sensors, numerical integration is needed. For weak signals with small signal-to-noise ratio (this is a typical situation with B-dot or D-dot sensors) this integration causes numerous artifacts. That is why recently several non-differentiating (replicating) sensors have been developed based on TEM-horn (E. Farr and L. Bowen, *Book of Abstracts, Euro Electromagnetics'2000*, 65, 2000) or on dipole with curved arms (S. Tyo and J. Buchenauer, *Book of Abstracts, Euro Electromagnetics'2000*, 66, 2000). Providing large sensitivity and ultra-wide band performance these sensors suffer from large (in comparison with the smallest wavelength in their bandwidth) physical dimensions.

Over years we successfully use the shielded loop antenna (A.G.Yarovoy, R.V. de Jongh, and L.P.Ligthart, *Electronics Letters*, **36**, 1679-1680, 2000) for antenna measurements in time domain. This sensor is a compact sensor with almost replicating behavior. The relative bandwidth of this sensor is typically 20:1 (on –10dB level). We use this sensor for far-field antenna measurements as well as for near-field antenna measurements. We also use this sensor in a test range for Ground Penetrating Radar. In the latter case the sensor is used to recover the waveforms of electromagnetic field in the ground.

The developed theoretical model of the sensor allows to optimize the probe for desirable bandwidth and sensitivity. Using this theoretical model we have developed and manufactured in house a number of different modifications of this sensor, which are used in different bands (particularly, we are interested in 300MHz-3000MHz and 1GHz-6GHz bandwidth). These sensors are calibrated and the probe compensation techniques have been developed. The latter have been tested on basic antennas; it was found excellent agreement with measurement results in frequency domain and results of numerical simulations. The probe compensation technique for the measurement in the ground (dry sand) has been developed and successfully tested as well. This probe compensation technique is based purely on theoretical model.

Finally we have successfully used the probe in Ground Penetrating Radars dedicated for landmine detection (R.V. de Jongh, A.D. Schukin, A.G. Yarovoy, L.P. Ligthart, and I.L.Morrow, *patent WO 01/38902 A2*, 2001). For such radar it is essential not only to detect the scattered by the object field, but correctly record the waveform of this field. This waveform is used later on for classification and identification of detected targets.

0-7803-7846-6/03/$17.00 ©2003 IEEE

# Network-Oriented Dyadic Short-Pulse Field Representations for Periodic Arrays

**F. Capolino[1] and L. B. Felsen[2]**

1) Dept. of Information Engineering, University of Siena, 53100 Siena, Italy. Email: capolino@dii.unisi.it
2) Dept. of Aerospace and Mech. Engineering, Boston University, Boston, MA 02215, USA (part time). Also University Professor Emeritus, Polytechnic University, Brooklyn, NY 11201, USA. Email: lfelsen@bu.edu

Wide-band and short-pulse radiation from actual rectangular phased array antennas, infinite and truncated periodic structures, frequency selective surfaces and related applications is a topic of increasing interest. Our planned research agenda so far has dealt with investigations of basic canonical time domain (TD) dipole-excited Green's functions for infinite [L.B. Felsen and F. Capolino, *IEEE Trans. AP*, **6**, 921-931, 2000] and truncated [F. Capolino and L.B. Felsen, *IEEE Trans. AP*, **1**, 31-41, 2002] periodic line arrays, and of infinite and semi-infinite periodic planar arrays [F. Capolino and L.B.Felsen, *IEEE Trans. AP*, **12**, 2002, and *Radio Science*, in print]. The radiated field has been expressed and parameterized in terms of TD Floquet waves (FW). The Green's function for the infinite planar array of dipoles has been used advantageously in a fast TD method of moments algorithm for wide band analysis of periodic structures [N. Chen, M. Lu, B. Shanker, F. Capolino and E. Michielssen, *this conference*]. Here, a network oriented dyadic Green's function is formulated for the infinite sequentially excited planar dipole array (Fig.1). The advantage of the network approach is (a) that E (TM) and H (TE) polarized TD-FW modes are treated individually, with their field expressed in terms of TD transmission line (TL) Green's functions (Fig.2) that obey standard network theory; (b) that plane-stratified inhomogeneous media can be accommodated by the same formalism. Causality issues pertaining to the E and H mode decomposition are treated in detail. It is found that, individually, each *pq*-indexed E and H mode is noncausal, and can obtained in closed form via convolution between an auxiliary frequency domain formulation that involves characteristic noncausal functions, and the causal TL Green's functions (Fig.2). Causality on the total vector FW field is recovered by summing the E and H mode contributions. We show how the transverse TD-TL vector mode functions are defined using modal-FW scalar potentials $\phi_{pq}$ and $\psi_{pq}$, with voltage and current TL Green's functions $\hat{Z}_{pq}$ and $\hat{T}^I_{pq}$ (Fig.2) represented in terms of Bessel functions and incomplete Lipschitz-Hankel integrals. We also exhibit here some properties, such as orthogonality and completeness, pertaining to the TD-FW as basis sets. Asymptotic inversion from the FD yields the instantaneous frequency behavior which parameterizes the constituent TD-FWs. The localization of the synthesizing frequency spectrum around instantaneous frequencies is due to the periodicity-induced dispersive FW behavior. Numerical examples of radiation from infinite planar arrays of dipoles with short-pulse band-limited excitation are presented to demonstrate the accuracy of the TD-FW algorithm and to illustrate the rapid convergence of the (TD-FW)-based field expansion since only a few terms are required for describing the off-surface radiated field.

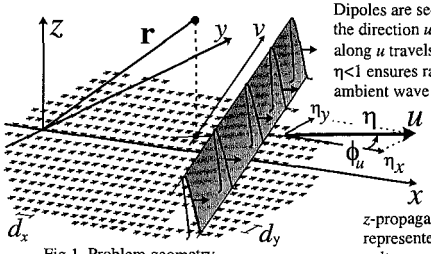


Fig.1. Problem geometry

Dipoles are sequentially excited along the direction $u$. The excitating wavefront along $u$ travels with speed v=c/η. where η<1 ensures radiation and $c$ is the ambient wave speed.

$z$-propagation for each TD-FW is represented by an equivalent TD-TL voltage and current Green's function.

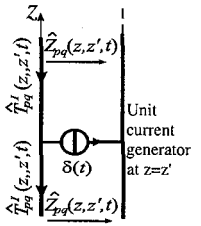


Fig.2. TD transmission line Green's Functions

# Axial Backscattering from a Wide Angular Sector

Carl E. Baum
Air Force Research Laboratory
Directed Energy Directorate
Kirtland AFB, NM

In testing the physical-optics (PO) approximation for axial backscattering from cones it has been observed that for a circular perfectly conducting cone the PO result is quite good, at least asymptotically for small (near zero) and wide (near $\pi/2$) cone angles. [C. E. Baum, "The Physical Optics Approximation and Early-Time Scattering," Interaction Note 563, October 2000] [J. J. Bowman, T. B. A. Senior, and P. L. E. Uslenghi, *Electromagnetic and Acoustic Scattering by Simple Shapes,* Hemisphere Publishing (Taylor & Francis), 1987]. However, for noncircular cones the disagreement can be large as shown for the thin angular sector (perfectly conducting), and more generally for the thin elliptic cone (perfectly conducting) [C. E. Baum, "Axial Scattering from Thin Cones," Interaction Note 565, November 2000]. The present paper (using a completely different technique) considers the wide angular sector for $\psi$ near $\pi/2$ ($\psi'$ near 0). The angular sector lies on the $xz$ plane (y=0) with the $z$ axis as the sector bisector (symmetry axis).

The solution here has some interesting properties. It is proportionality to $\cot(\psi')$. This can be contrasted to the $\cot^2(\psi')$ dependence for the wide circular cone. The difference between these two can be ascribed to the fact that the angular sector has an integral over the surface current density using only one transverse coordinate, while the circular cone has an integral over two transverse coordinates. As an alternate view consider that for $\psi' \rightarrow 0$ the angular sector tends to a half plane which scatters field proportional to $r^{-1/2}$ while the circular cone tends to a plane which scatters field proportional to $r^0$ (which requires a more singular behavior of the $r^{-1}$ term as $\psi' \rightarrow 0$).

So now we have solutions for the axial backscattering from both thin and wide perfectly conducting angular sectors. This leaves the intermediate angles $\psi$ to be solved. There exists a solution in terms of an infinite series of eigenfunctions. However, this does not give simple analytic insights. Further development of "exact" analytical and numerical results would be helpful.

0-7803-7846-6/03/$17.00 ©2003 IEEE

# Some fundamental aspects on scattering of EM-pulses

Anders Karlsson
Electroscience, Lund University
Box 118
SE-221 00 Lund
Sweden
Phone:+46-46-2224089, e-mail: anders.karlsson@es.lth.se

This contribution discusses some fundamental results for the scattering of electromagnetic pulses from objects with finite size and also for pulses transmitted from antennas. The results are obtained from the Jefimenko's equation, the optical theorem, reciprocity and causality.

The Jefimenko's equation is a time domain volume integral representation of the electric field in terms of its sources, i.e., current and charge densities. From this representation it is possible to derive some necessary conditions for the wave field that is scattered from an object and also for the wave field that is transmitted from an antenna. As an example a pulse with Gaussian time dependence does not satisfy these conditions.

The optical theorem in the time domain is obtained from its frequency domain counterpart by the use of Parseval's relation. The time domain theorem implies a number of interesting results for the scattered power when a plane electromagnetic pulse of finite length is scattered from an object. Many of these results have been published earlier by the author. Here they will be discussed from a physical point of view and they will also be applied to receiving antennas.

The reciprocity theorem in the time domain can be applied to the case of a plane wave that is scattered from a reciprocal object. It implies that one may exchange the direction of observation for the direction of incidence and still get the same far field. In combination with the optical theorem, the reciprocity theorem leads to useful results for the scattered power.

Some of the results have been verified numerically by the utilization of Mie scattering from spheres.

0-7803-7846-6/03/$17.00 ©2003 IEEE 

## Reconfigurable Antennas and Circuits Using RF-MEMS

**Co-Chairs:** J. Papapolymerou
J. Bernhard

1:15 Opening Remarks

25. 1 1:20 Reconfigurable Miniature Three Dimensional Fractal Tree Antennas ..... APS
*J. S. Petko, D. H. Werner, Penn State University, USA*

25. 2 1:40 Re-configurable Sierpinski Gasket Antenna using RF-MEMS Switches ..... APS
*D. Anagnostou, University of New Mexico, USA, M. T. Chryssomallis, Democritos University of Thrace, Greece, J. C. Lyke, Air Force Philips Laboratory, C. G. Christodoulou, University of New Mexico, USA*

25. 3 2:00 Measurement and FEM Modeling of a Reconfigurable-Patch Antenna for Use in the Wideband Gapfiller Satellite System ..... APS
*A. W. Lee, University of California Los Angeles, S. K. Kagan, United States Airforce, Los Angeles Airforce Base, M. Wong, Raytheon Inc., R. S. Singh, E. R. Brown, University of California Los Angeles, USA*

25. 4 2:20 Behavior of Pattern and/or Frequency Reconfigurable Antennas in Small Arrays ..... 151
*G. H. Huff, J. Feng, S. Zhang, J. T. Bernhard, University of Illinois at Urbana-Champaign, USA*

25. 5 2:40 Simulation of the Effects of a Ground Plane on the Radiation Characteristics of Self-Complementary Arrays ..... APS
*X. Dardenne, C. Craeye, Université catholique de Louvain, Belgium*

25. 6 3:00 Microwave Laminate PCB Compatible RF MEMS Technology for Wireless Communication Systems ..... APS
*B. A. Cetiner, J. Qian, H. Chang, M. Bachman, G. Li, F. De Flaviis, University of California, Irvine, USA*

25. 7 3:20 Fabrication and Modeling of an SP3T RF MEMS Switch ..... APS
*M. Daneshmand, R. R. Mansour, University of Waterloo, Canada*

25. 8 3:40 RF MEMS Capacitive Switches for Integration with Printed Circuits and Antennas ..... APS
*R. Ramadoss, S. Lee, K. C. Gupta, Y. C. Lee, V. M. Bright, University of Colorado at Boulder, USA*

25. 9 4:00 Design, Implementation and Measurement of 26.6GHz Patch Antenna using MEMS Technology ..... APS
*M. Abdel-Aziz, H. Ghali, H. Ragaie, Ain Shams University, H. Haddara, MEMScAP - EGYPT, Egypt, E. Larique, B. Guillon, MEMScAP, P. Pons, LAAS, France*

25. 10 4:20 Reconfigurable Dual-Band Dipole Antenna on Silicon using Series MEMS Switches ..... APS
*J. E. Kiriazi, H. A. Ghali, H. F. Ragaie, Ain Shams University, Faculty of Engineering, H. Haddara, MEMScAP, Egypt*

25. 11 4:40 Reconfigurable Microstrip Antenna Design Based on Genetic Algorithm ..... APS
*S. Xiao, B. Wang, X. Yang, Institute of Applied Physics, University of Electronic Science and Technology of China, China, G. Wang, Intpax Inc., 6 Results Way Cupertino, CA 95014, USA*

25. 12 5:00 A Novel Reconfigurable Discrete Antenna ..... APS
*W. Chen, M. Fan, Z. Feng, Tsinghua University, China*

# Behavior of Pattern and/or Frequency Reconfigurable Antennas in Small Arrays

G. H. Huff*, J. Feng, S. Zhang, and J. T. Bernhard
Electromagnetics Laboratory
Department of Electrical and Computer Engineering
University of Illinois at Urbana-Champaign
Urbana, IL 61801
jbernhar@uiuc.edu

Novel antenna designs capable of reconfiguring their radiation characteristics and/or frequency responses will play an increasingly important role in both civil and military sectors in response to the demanding tasks presented by high speed data communication. Individually reconfigurable antenna elements can be integrated onto devices or into arrays to meet these challenges. The switching of simple tuning elements within these individual antennas provides variable directionality and multi-band operation that can greatly enhance the overall effectiveness of the system. In both single element and array settings, the ability to alter directionality as well as frequency selectivity can generate extra degrees of freedom to better enable data intensive applications as well as operation in harsh or noisy electromagnetic environments. These new degrees of freedom can also lead to a decrease in the peripheral electronics needed to achieve array beam steering, as well as provide reductions in spatial dimensions from the use of a single antenna for multi-band operation.

This study reports on the theory and measurement of small arrays consisting of novel pattern and/or frequency reconfigurable antennas. The antenna being considered (G.H. Huff, J. Feng, S. Zhang, and J.T. Bernhard, *IEEE Microwave and Wireless Components Letters*, **2**, 2003) is a single-turn Archimedean square microstrip spiral capable of both broadside and endfire radiation within two well-spaced frequency bands. To characterize the functionality of an array comprised of this new breed of antenna, parameters such as the array spacing are examined to determine the benefits and limitations arising from the pattern reconfigurability and relative spacing of the operating frequency bands. Along with factors surrounding array spacing and beamforming constraints, operation of the individual antenna elements will be studied to determine the effects of spacing and orientation on radiation and impedance bandwidths, as well as the inter-element coupling. Electromagnetic visibility studies on the packaging and integration of reconfigurable antennas have shown a strong dependence on the performance of the device based on its integration position. Therefore, in addition to parameters directly related to the antenna, the possible effects from packaging will also be considered. Measurements of the radiation characteristics, impedance, 2:1 VSWR bandwidth, inter-element coupling, and array gain will be provided and compared with theoretical results.

0-7803-7846-6/03/$17.00 ©2003 IEEE 

*Special Session*

## Memorial Session Honoring Professor Y.T. Lo

**Organizer(s):** Weng Cho Chew, University of Illinois at Urbana-Champaign
Jianming Jin, University of Illinois at Urbana-Champaign

**Co-Chairs:** W. Chew
J. M. Jin

1:15 Opening Remarks

**Preliminary Remark – Part 1**

Weng Chou Chew
Center for Computational Electromagnetics and Electromagnetics Laboratory
Dept. of ECE, University of Illinois at Urbana-Champaign, Urbana, IL 61801

**Content of this paper will be presented at the Symposium.**

0-7803-7846-6/03/$17.00 ©2003 IEEE

## Preliminary Remark – Part II

S.W. Lee
Center for Computational Electromagnetics and Electromagnetics Laboratory
Dept. of ECE, University of Illinois at Urbana-Champaign, Urbana, IL 61801

**Content of this paper will be presented at the Symposium.**

0-7803-7846-6/03/$17.00 ©2003 IEEE

# Small, Broadband Meanderline Loaded Inverted-L Antenna

Roland A. Gilbert
BAE SYSTEMS, Nashua, NH 03061

Abstract

This paper describes a very small, efficient, inverted-L antenna that operates over a decade bandwidth in two modes: 1) a resonant, tuned mode for low band and 2) an instantaneous broadband mode for the high band. The antenna consists of a vertical plate structure fed by a probe through the ground plane and a horizontal top plate structure that is capacitively connected to the top end of the vertical plate. A set of length-adjustable meandering transmission lines are connected in series with the top plate and the vertical plate. At the high end of the frequency band, the meanderlines behave as a choke thereby sending all current through the vertical and horizontal plates. Wideband operation is attained since the antenna appears large in terms of wavelength at the high end of the operational band. The pattern and impedance behavior is representative of a top loaded monopole antenna. Because the horizontal plate is offset and carries significant current, there is also a horizontally polarized component contributing to the antenna pattern.

At low frequencies the meanderlines behave as a frequency dependent lumped inductance which tunes out the capacitive reactance of the plates. The current flowing through the resonant structure becomes larger than that through the feed itself. As a result, the the feed point appears to shift to the gap between the top and vertical plates. In this mode, the antenna behaves as a vertical dipole, thereby reducing coupling to the ground plane. For this reason, the antenna exhibits a higher efficiency than the tuned short monopole or loop antennas.

0-7803-7846-6/03/$17.00 ©2003 IEEE 

# The Two Sphere Scattering Problem

Dr. John H. Bruning
President, CEO
Corning Tropel Corporation
60 O'Connor Road
Fairport, New York 14450
E-Mail: bruningjh@corning.com

In this talk, I will talk about the two-sphere scattering work, YT's inspiration and how that has influenced my work in other areas along with some highlights.

0-7803-7846-6/03/$17.00 ©2003 IEEE

# Input Impedance of Antenna—Its Calculation and Meaning

Weng Cho Chew
Center for Computational Electromagnetics and Electromagnetics Laboratory
Dept. of ECE, University of Illinois at Urbana-Champaign, Urbana IL 61801
(wchew@uiuc.edu)

*(Dedicated to the memory of Professor Y.T. Lo)*

The calculation of the input impedance impedances of an antenna is a topic of long interest. The work goes back to the formulation of Hallen's integral equation, and has been a topic of intense interest pursued by R.W.P. King for many years. The author has had the opportunity to discuss some of these issues with the late Professor Y.T. Lo.

The paper will delve into the history of various ways to compute the input impedance of an antenna, and elucidate the physical meaning of these various calculations. We will also discuss the measurability of an input impedance calculation. In the antenna input calculation, we often have to arrive at a theoretical model for the calculation. However, many of these theoretical models are not realizable in the real world. Namely, no true experiment can be set up to verify the manner or the model on which the calculation has been based.

Various formulas, methods, and models are available to calculate the input impedance of an antenna. There are the power method, the induced-EMF method, the reaction formula, the delta-gap model, the magnetic frill model, the electric current-source model, and so on. We will discuss these different ways to obtain the input impedance.

The impedance is a concept that belongs to the world of circuit theory, while an antenna is an electromagnetic device. Hence, the input impedance is a parameter that we use to interface between the world of electromagnetic devices and the world of circuit theory. Also, in order for the concept of impedance to hold true, the model on which the impedance is defined has to be such that the world of circuit theory, which is based on quasi-static electromagnetics, holds true. Hence, it is not sensible to have feed points of an antenna that is sizeable compared to wavelength, and yet to insist on defining an input impedance with respect to the feed point.

Also, the world of theoretical modeling is often idealized, and is quite different from anything realizable in an experimental measurement. Hence, what is measured in the laboratory is often not what is been calculated. We will discuss the ramification of the discrepancies between a theoretical model setup and an experimental setup, and ways to reduce this gap.

0-7803-7846-6/03/$17.00 ©2003 IEEE

# The Cavity Model for Microstrip Antennas Revisited

Constantine A. Balanis*

Department of Electrical Engineering, Telecommunications Research Center
Arizona State University, Tempe, AZ 85287–7206

There are many models that can be used to analyze microstrip antennas. These models span from the simplest, such as the transmission–line model, to the more complex, such as the integral equation model. Advantages and disadvantages are associated with each one of them, including simplicity, physical insight, complexity and accuracy. One model that is simple, accurate and sheds physical insight is the cavity model developed by Prof. Y. T. Lo and his graduate students. This model treats the microstrip antenna as a cavity whose field configurations/modes underneath the patch can be easily obtained by treating it as a boundary–value problem with the appropriate boundary conditions. The boundary conditions proposed by Prof. Y. T. Lo and his students are those that treat the upper and lower sides of the cavity as PEC (perfect electric conducting) and those around the periphery as PMC (perfect magnetic conducting). These boundary conditions lead to very good field configurations for both rectangular and circular cavities, as well as for other canonical geometries. The edges of the cavities are slightly extended to account for fringing. This model has also been used to study microstrip microwave resonators.

The microstrip antenna cavity model leads to very good results in terms of input impedance, when the cavity is fed by a probe, as well as amplitude radiation patterns. To determine the amplitude patterns, the fields around the periphery of the cavity are assumed to be the same as those of the ideal cavity with PMC walls. The equivalent current densities associated with these fields are then formed, which, in turn, are used to determine the patterns. The computed amplitude patterns based on these current densities lead to very good results when compared with measurements as well as with other methods. Because the cavity model assumes that the bottom wall of the cavity is PEC, the predicted patterns for practical microstrip antennas based on this model for the E–plane do not vanish or nearly vanish, as expected, near grazing angles. This shortcoming of the cavity model near grazing angles can be remedied by supplementing the formulation of the cavity model in the E–plane with a reflection coefficient of a lossy surface instead of that of a PEC for the bottom wall. The reflection coefficient used for the E–plane is that of a vertical polarization for a lossy surface. The patterns predicted based on this simple extension of the cavity model lead to very good results for the E–plane. The H–plane patterns based on the cavity model agree quite well with measurements. Therefore, in the H–plane, the formulation for the patterns does not need to be modified because the boundary conditions of the ideal cavity model and those of the actual antenna are very similar.

In the oral presentation of this paper, the cavity model as developed by Prof. Y. T. Lo and his graduate students, and its extension, will be reviewed. Simulations will be presented for both rectangular and circular microstrips, and the results will be compared with measurements and/or other available data.

0-7803-7846-6/03/$17.00 ©2003 IEEE

# A Revisit of Random Arrays and Some Recent Applications

Hao Ling*
Department of Electrical and Computer Engineering
The University of Texas at Austin
Austin, TX 78712-1084

and

Yuanxun Wang
Electrical Engineering Department
University of California at Los Angeles
Los Angeles, CA 90095

It is well known that to design antenna arrays with uniformly spaced elements, the element spacing must be kept below half a wavelength to avoid the appearance of grating lobes. In his pioneering work nearly four decades ago, "A Mathematical Theory of Antenna Arrays with Randomly Spaced Elements" (*IEEE Trans. Antennas Propagat.*, **15**, 257-268, 1964), Professor Yuen-Tze Lo showed that a highly thinned array with an average spacing much greater than half a wavelength could achieve the same beamwidth performance as that of a uniformly spaced array while overcoming the grating lobe problem. It was also shown explicitly that the price for a large reduction in the number of elements is the sidelobe level of the array.

In this paper, we discuss several recent applications of the concept of random arrays, or more generally, non-uniformly sampled functions, to problems related to antennas, computational electromagnetics and radar imaging. First, the random array idea is applied to ultra-wideband aperture design. It is shown that by using a multi-frequency, random aperture, it is possible to achieve constant beamwidth over a very wide bandwidth. Design studies using quasi-random apertures involving identical random subarrays are also considered.

Second, the non-uniform sampling idea in random arrays is applied to accurately interpolate coarsely computed electromagnetic prediction data in frequency and aspect. In order to overcome the high sidelobes produced by the coarse, random sampling, a CLEAN-based iterative technique is applied to achieve an accurate and sparse parameterization. Results are demonstrated using the computation data from the fast multipole computer code FISC.

Finally, the concept of non-uniform sampling is applied to the problem of radar image formation from measurement data. It is shown that radar data from a maneuvering target resemble the random array problem in the target pose dimension with respect to the radar. By using the iterative CLEAN-based technique, it is shown that two- and three-dimensional images of targets can be successfully constructed.

0-7803-7846-6/03/$17.00 ©2003 IEEE 

***Special Session***

## Metamaterials: Part II

**Organizer(s):** N. Engheta
R. Ziokowski

**Co-Chairs:** N. Engheta
R. Ziolkowski

1:15 Opening Remarks

28. 1 1:20 BANDWIDTH of a MICROSTRIP PATCH ANTENNA ON a MAGNETO-DIELECTRIC SUBSTRATE ..... 163
*S. Yoon, R. W. Ziolkowski, University of Arizona, USA*

28. 2 1:40 OPTIMUM DESIGN and FABRICATION of VOLUMETRIC GRADED SUBSTRATE for a BROAD_BAND MINIATURE ANTENNA ..... APS
*G. Kiziltas, Y. Koh, University of Michigan, J. L. Volakis, Ohio State University, N. Kikuchi, J. Halloran, University of Michigan, USA*

28. 3 2:00 Patch Antenna Above Hilbert High-Impedance Surface ..... 164
*J. A. McVay, Villanova University, N. Engheta, University of Pennsylvania, A. Hoorfar, Villanova University, USA*

28. 4 2:20 Arrays of Sparse Sources using Artificial Materials ..... 165
*F. Capolino, University of Siena, M. Albani, R. Gardelli, University of Messina, Italy*

28. 5 2:40 Effective Medium Properties of Finely Periodic Substrates ..... APS
*X. Gong, University of Michigan, L. P. Katehi, W. J. Chappell, Purdue University, USA*

28. 6 3:00 Distributed Periodic Structures: Bragg Diffraction and Long-Wavelength Left-Handed Refraction ..... 166
*Christophe Caloz, Atsushi Sanada, Tatsuo Itoh, UCLA, USA*

28. 7 3:20 Wave Types Guided by the Interface Between Air and a Semi-infinite Periodic Structure ..... 167
*S. T. Peng, National Chiao-Tung University, Taiwan, A. A. Oliner, Polytechnic University, USA*

28. 8 3:40 Dispersion Properties of Periodic Grounded Structures Via Equivalent Network Synthesis ..... APS
*S. Maci, M. Casaletti, M. Caiazzo, C. Boffa, University of Siena, Italy*

28. 9 4:00 The Synthesis of Metamaterial Ferrites for RF Applications Using Electromagnetic Bandgap Structures ..... APS
*D. J. Kern, D. H. Werner, The Pennsylvania State University, USA*

# BANDWIDTH OF A MICROSTRIP PATCH ANTENNA ON A MAGNETO-DIELECTRIC SUBSTRATE

*Seongho Yoon and Richard W. Ziolkowski*

Department of Electrical and Computer Engineering
The University of Arizona
1230 E. Speedway
Tucson, AZ 85721-0104 USA

Tel: (520) 621-6173
Fax: (520) 621-8076
E-mail: ziolkowski@ece.arizona.edu, seonghoy@email.arizona.edu

The bandwidth of a microstrip patch antenna is a commodity that is constantly in demand. There are many commercial applications that could use more if it were available. Many schemes have been devised to increase it. In a very interesting paper, R.C. Hansen and Mary Burke ("Antenna with Magneto-Dielectrics", *Microwave Opt. Tech. Lett.*, **26**, 2000, 75-78, 2000) predicted that the best substrate to use to increase the bandwidth of a basic microstrip patch antenna (MPA) was one in which $\varepsilon_r = 1.0$ and $\mu_r \gg 1.0$. The Hansen and Burke result is based on a first-order approximate model for the MPA. On the other hand, with the excitement associated with metamaterials, artificial materials that mimic known material responses or that qualitatively have new response functions that do not occur in nature, there have been alternate claims that a substrate with $\varepsilon_r \gg 1.0$ and $\mu_r \gg 1.0$ will actually produce a better bandwidth result (e.g., H. Mossallaei and K. Sarabandi "Periodic meta-material structures in electromagnetics: Concept, analysis, and applications," 2002 IEEE APS International Symposium Digest, vol. 2, San Antonio, TX, 380-383, 2002). The issue is clouded somewhat in the metamaterial case because the large positive permittivities and permeabilities are achieved with a complex mixture of electrically small inhomogeneities that are loaded into the substrate in a specific periodic arrangement and an electromagnetic bandgap response may be affecting the overall results.

Because these two results are contradictory, it was felt that a more in-depth analysis was required to settle the issue. In this paper we will review the derivation of the bandwidth of MPAs on a magneto-dielectric substrate. The substrate is assumed to have both the relative permittivity ($\varepsilon_r$) and permeability ($\mu_r$) greater than or equal to one. The radiation process of the antenna was carefully investigated with a complete cavity model and the bandwidth has been expressed as a function of both $\varepsilon_r$ and $\mu_r$. These results will be reviewed; they show that the optimal substrate to achieve the widest bandwidth with a single coaxial-fed patch antenna operating at its dominant mode is the one predicted by Hansen and Burke, i.e., one in which $\varepsilon_r = 1.0$ and $\mu_r \gg 1.0$. Using ANSOFT's High Frequency Structure Simulator (HFSS,), it will be shown that these more complete simulation results agree very well with the analytical results. Additional results for MPAs on DNG metamaterial substrates will be discussed if completed in time.

0-7803-7846-6/03/$17.00 ©2003 IEEE 

# *Patch Antenna above Hilbert High-Impedance Surface*

John McVay[1], Nader Engheta[2] and Ahmad Hoorfar[1]

*(1) Villanova University*
*Dept. of Electrical and Computer Eng.*
*Villanova, PA, 19085*
*hoorfar@ece.villanova.edu*

*(2)University of Pennsylvania*
*Dept. of Electrical & Systems Eng.*
*Philadelphia, PA 19104*
*engheta@ee.upenn.edu*

As known in the mathematics literature, Hilbert curve is an example of family of curves known as space-filling curves [Hans Sagan, *Space-Filling Curve*, Springer-Verlag, NY, 1994], and it is a continuous mapping from a normalized [0,1] interval to a two-dimensional regions, $[0, 1]^2$ that passes through every point in the region. As iteration order of Hilbert curve is increased, longer line can be compacted into a small 'surface" area, and therefore as an electromagnetic scatterer, conducting wires shaped as Hilbert curves may have resonant wavelength much longer than its footprint. In our previous work, we have shown that a metamaterial surface made of 2-D periodic arrangement of "Hilbert-curve" inclusions, closely placed above a highly conducting ground plane, can attain high surface impedance at certain frequencies, causing it to effectively behave as a magnetic wall with reflection coefficient $R = +1$ [J. McVay, N. Engheta and A. Hoorfar, "High Impedance Metamaterial Surface Using Hilbert Inclusions", *2002 USNC/URSI National Radio Science Meeting*, San Antonio, TX, p. 226, June 2002]. We also explore the radiation characteristics of a resonant wire antenna above such a high-impedance surface [McVay, *et al.*, submitted for presentation at the *2003 IEEE MTT-S International Microwave Symposium* (IMS'2003), Philadelphia, PA, June 8-13, 2003].

In the present study, we examine numerically the performance of another class of antennas, i.e., a probe-fed patch antenna, located above such a Hilbert high-impedance ground plane (See Figure). The operating frequency of this patch antenna is chosen to be near the frequency of operation of Hilbert surface. We explore the effects of Hilbert iteration order, separation from the ground plane, and probe location for patch antenna on the input impedance, impedance bandwidth, directivity, and efficiency of such patch antennas. We also explore the role of small foot print of Hilbert inclusion as "compact resonator" on the performance of the patch antennas.

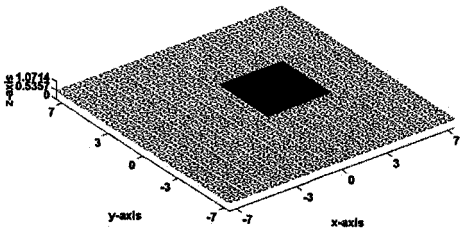


In this talk, we will present some of our numerical results and will discuss physical insights and intuitive remarks on mathematical findings.

# Arrays of Sparse Sources Using Artificial Materials

Filippo Capolino[1], Matteo Albani[2], and Renato Gardelli[2]

[1] Dept. of Information Engineering, Univ. of Siena, Siena, Italy. capolino@dii.unisi.it
[2] Dept. Matter Physics and Advanced Technologies, Univ. of Messina, Italy. malbani@ingegneria.unime.it

High directivity antennas are often obtained using arrays of elementary sources. In general each elementary source does not exhibit a high directivity and in order to avoid strong secondary lobes arrays antennas are designed with periodicity distances less than a wavelength. This requires in general array antennas with several individual radiators, and the inter-sources spacing to be slightly larger than the sources dimension, that does not always permits to accommodate the feeding network, implying complicated and expensive feeding lines, often developed out of the radiators plane. These problems become more critical when a dual polarization is required because it necessitates two distinct feeding networks (e.g., TV-SAT rx). It is also for this reason that we have investigated the possibility to obtain sparse arrays of elements with higher directivity to avoid grating lobes. In this arrangement, the elementary radiators are placed far apart from each other, resulting in an array antenna with lesser elements requiring a simpler feeding network and thus lower costs. This larger inter-element distance provides better and easier design solutions for the feeding network, especially in the dual polarization case.

Here we present possible implementations consisting of array of radiators placed within/under an artificial material such as a photonic band gap (PBG) structure (e.g., see the geometry in Figure), working in the transition between its transmission and stop bands. There, the material offers interesting phenomena and can be equivalently modeled as a material with low dielectric constant. This causes interesting refractive properties that are used to build highly directive source radiators [B. Gralak, S. Enoch, G. Tayeb, *J. Opt. Soc. Am. A*, **17**, 1012-1020, 2000].

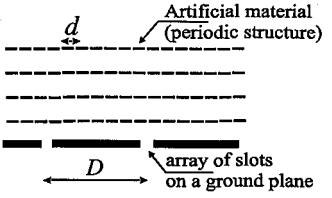


The array antenna radiation pattern is obtained using the reciprocity principle, that states that an antenna has the same radiating/receiving performances, and this is independent of the complexity of the antenna system. Therefore, we will assume a plane wave illuminating the antenna system and, due to the periodicity of the artificial material, a periodic method of moments (PMoM) is used to determine the near field at the various elementary source locations. Then, simple algebraic manipulation leads to a simple formula that describes the array radiation pattern. This is achieved multiplying the data provided by the full wave method by an analytic simple formula that describes the far field interfering recombination of the array radiator contributions. When modeling the periodic artificial material by the PMoM, significant saving in the computation time is achieved when using a fast representation for the periodic Green's function to fill the impedance matrix of the PMoM, making this method advantageous also for design purposes. Particular simplified formulas for the field pattern are obtained when the periodicities of the array $D_1$ and $D_2$ are integer multiples of the periodicity integers of the artificial material $d_1$ and $d_2$, i.e., when $D_1=N_1d_1$, and $D_2=N_2d_2$. This permits to deal with the standard array factor for the sparse array multiplied by the data furnished by the PMoM. The possibility to obtain beam scanning phased arrays with such configurations is also investigated showing the limits arising from the high directivity of each array element.

0-7803-7846-6/03/$17.00 ©2003 IEEE

# Distributed Periodic Structures: Bragg Diffraction and Long-Wavelength Left-Handed Refraction

Christophe Caloz, Atsushi Sanada and Tatsuo Itoh

Electrical Engineering Department, University of California, Los Angeles, CA 90095, caloz@ee.ucla.edu

Our group has been developing a **transmission line approach of metamaterials,** which include left-handed (LH), right-handed (RH) and composite left-right-handed (CRLH) structures (C. Caloz, H. Okabe, T. Iwai, and T. Itoh, "Transmission Line Approach of Left-Handed (LH) Materials", USNC/URSI National Radio Science Meeting, vol. 1, p. 39, San Antonio, TX, June 2002) and demonstrating **novel microwave applications** (including tight/broadband couplers, backfire-to-endfire leaky-wave antennas, phase-conjugation negative meta-interfaces) based on this approach (C. Caloz, and T. Itoh, "Novel Microwave Devices and Structures Based on the Transmission Line Approach of Meta-Materials", *to be published in IEEE-MTT Int'l Symp.,* Philadelphia, PA, June 2003).

In general, the **LH structures** investigated by most of the groups so far were **periodic** (one exception is I. Lin, C. Caloz, and T. Itoh, "Transmission Line Approach of Left-Handed (LH) Non-Uniform Transmission Lines (NTL)", Asia-Pacific Microwave Conference, vol. 3, pp. 1501-1504, Kyoto, Japan, November 2002) because of convenience: it is easier to analyze and fabricate a periodic than an aperiodic structure.

**Photonic band-gap (PBG) structures** operate in the **Bragg regime** (period $a \approx \lambda/2$), where the emergence of photonic band-gap is a consequence of constructive interferences of the waves reflected from the different **diffraction** sites. Since such interference phenomena are a direct consequence of periodicity, periodicity is an essential attribute of PBGs. In contrast, in an **effective-medium** (average distance between "atoms" $\bar{a}/\lambda \to 0$), EM waves are "myopic" to the microscopic texture of the material, which is "seen" as an isotropic/homogeneous medium; periodicity is therefore not necessary and **refraction** effects are possible. However, **practical implementations** of LH structures necessarily exhibit an average period between those of PBGs and effective media ($0 < \bar{a} < \lambda/2$), and the frontier between the Bragg and long-wavelength effects is not so clear: in a **LH mode** (negative $\omega$-$\beta$ slope), **effectiveness** is obtained at the highest frequencies, which are close to the $\Gamma$**-point** ($a/\lambda=0$) of the dispersion diagram; in contrast, the ***X*-point** ($a=\lambda/2$) intercepted by the mode at lower frequencies is clearly a **Bragg** point; for frequencies, between the $\Gamma$ and $X$ points, we have a progressive evolution, from effective medium to non-effective Bragg medium. As a rule of thumb, we may consider that the condition $a<\lambda/4$ ($1^{st}$ half of the $\Gamma$-$X$ segment) is satisfying for effectiveness in practical applications.

It should also be noted that any **practical LH structure** is de facto of **CRLH** nature; it exhibits LHness at lower frequencies and RH at higher frequencies with infinite guided wavelength at the transition frequency. This is because parasitic series-L/shunt-C necessarily become dominant over the designed series-C/shunt-L at high frequencies and also because the series-C/shunt-L cannot be considered lumped anymore if frequency is too high.

In particular, **distributed 2D periodic LH structures** have different nature depending on whether they are **open or closed:** if they are **open** they **cannot be purely LH,** because they appear as a simple PEC plate open to air when frequency decreases to DC and the mode becomes RH and TM-like at the lowest frequencies; in contrast, a **closed** structure can have **a fundamental pure LH mode.** But even in the open case, LHness can be dominant and **focusing effects** can be observed. Different structures are presented and compared. **Isotropy** is also discussed and shown to be maximal at the highest frequency of the LH band. Focusing is demonstrated as illustration.

0-7803-7846-6/03/$17.00 ©2003 IEEE

# Wave Types Guided by the Interface Between Air and a Semi-Infinite Periodic Structure

**S. T. Peng* and A. A. Oliner**

*National Chiao-Tung University, Taiwan; Polytechnic University, Brooklyn, NY

During the early 1990s the optical physics community rediscovered the concept that a wave can be guided in the space between a pair of periodic structures if the periodic structures are operated in their stop bands (called photonic bandgaps by them). That community was unaware that the ***identical concept*** was published many years before in the microwave community (R. P. Larsen and A. A. Oliner, "A New Class of Low Loss Reactive Wall Waveguides," Int. Microwave Symp. Digest, pp. 17-22, 1967). The specific structure that was analyzed rigorously and also measured consisted of an air space $W$ between two periodic structures with period $d$, each comprised of parallel dielectric slabs, as shown in Fig. 1.

The structure in Fig. 1 is infinite and uniform in the $y$ and $z$ directions, and the wave propagates in the $z$ direction. The field decays exponentially away from the central air region in the transverse ($x$) direction in both of the periodic arrays. At too low a frequency the lowest guided mode is below cutoff, but at frequencies above that cutoff the field in the central region is trigonometric in the $x$ direction. At higher frequencies the field variation in the central region changes from trigonometric to hyperbolic, although the field remains exponentially decaying in the periodic structures throughout the whole frequency range. All these field behaviors were known from calculations made in the original 1967 publication.

When the periodic structure on one side in Fig. 1 is removed, producing an ***interface*** between a semi-infinite periodic structure on one side and a semi-infinite air region on the other side, as shown in Fig. 2, we have a new canonical structure that has not been studied previously. Our recent detailed calculations demonstrate that waves can be guided along that interface, and also show that the type of guided mode depends on the frequency range. At higher frequencies the wave is a ***surface wave***, with exponential field decay away from both sides of the interface, but the surface wave experiences a cutoff as the frequency is lowered. If the periodic structure is made finite in width, new physical results can be obtained below the cutoff frequency of the surface wave, including leaky waves with interesting properties. The novel behavioral features will be described, and the correspondences with the various propagation ranges in the waveguide in Fig. 1 will be presented.

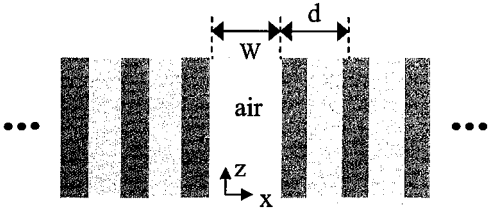


Fig. 1 A waveguide with periodic side walls that was analyzed and measured in 1967.

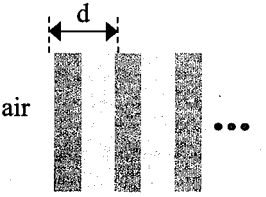


Fig. 2 Waves can be guided along the interface in this structure.

0-7803-7846-6/03/$17.00 ©2003 IEEE

2003 National Radio Science Meeting (Columbus, OH), June 2003

# APPLICATION OF DOUBLE NEGATIVE MATERIALS TO MODIFY THE PERFORMANCE OF ELECTRICALLY SMALL ANTENNAS

*Richard W. Ziolkowski* and Allison D. Kipple*

Department of Electrical and Computer Engineering
The University of Arizona
1230 E. Speedway Blvd.
Tucson, AZ 85721-0104

Tel: (520) 621-6173
Fax: (520) 621-8076
E-mails: ziolkowski@ece.arizona.edu, kipplea@ece.arizona.edu

In the past few years, there has been a renewed interest in using structures to develop artificial materials that mimic known material responses or that qualitatively have new response functions that do not occur in nature. The effective response functions of these "metamaterials" are often generated by artificially fabricated, extrinsic, low dimensional inhomogeneities that are electrically small and are loaded into a substrate in a periodic fashion. A number of electromagnetic structures that exhibit both effective negative permittivity and permeability properties have been designed. Experiments on these so-called double negative (DNG) metamaterials have been performed and have confirmed their expected properties. We have begun a study of how these DNG metamaterials may impact the performance of various antenna systems.

The effect of surrounding an electrically small dipole antenna with a shell of double negative (DNG) material ($\varepsilon_r < 0$ and $\mu_r < 0$) has been investigated both analytically and numerically. The results of these investigations will be reported. The problem of an infinitesimal electric dipole embedded in a homogeneous DNG medium will be treated; its analytical solution shows that this electrically small antenna acts inductively rather than capacitively as it would in free space. We will then show that a properly designed dipole-DNG shell combination increases the real power radiated by more than an order of magnitude over the corresponding free space case. The reactance of the antenna will be shown to have a corresponding decrease. Analysis of the reactive power within this dipole-DNG shell system indicates that the DNG shell acts as a natural matching network for the dipole. An equivalent circuit model that confirms this explanation will be introduced and discussed. The results obtained from several parameter studies of the dipole-DNG shell system will be used to illustrate its performance. The difficult problem of interpreting the energy stored in the dipole-DNG shell system and, hence, of calculating the radiation Q when the DNG medium is frequency independent will be discussed from several points of view.

0-7803-7846-6/03/$17.00 ©2003 IEEE 

# NANOSTRUCTURE MODELING AND APPLICATIONS

**Richard W. Ziolkowski***
Department of Electrical and Computer Engineering, University of Arizona, Tucson, Arizona, USA, ziolkows@ece.arizona.edu

**Mike Potter**
Department of Electrical and Computer Engineering, University of Calgary, Calgary, Alberta, Canada, mpotter@ieee.org

The nanotechnology area holds much promise for the realization of ultra-small devices with a variety of interesting applications. The optical sector is an immediate beneficiary of nanotechnologies because of the wavelengths associated with optical devices. For instance, 1.5 μm represents a well-known optical communications wavelength. If one wants to structure a material or an environment to modify the behavior of the propagation of light, for instance with a photonic bandgap (PBG) structure, one needs to arrange features with spacings that are less than half that wavelength in size, or 750 nm, and to create the features themselves that are even smaller yet.

We will review several nanotechnology areas that we have been modeling. These will include PBG structures, optical data storage devices, and metamaterials for microwave applications. We have selected the finite difference time domain (FDTD) approach for much of this modeling effort. Its versatility in the choices and configurations of materials and structures makes it an excellent candidate for studying the behavior of these ultra-small systems.

One significant issue for PBG structures is the process of how one will insert light into them. Several groups have recently presented designs for this application. We will review the designs we have modeled and contrast them to others. One significant optical data storage application is the use of nanostructured features for very high capacity systems. The focus of our research has been to examine the benefits of excellent densities of features obtained through imprint nano-lithography or some other such process, and the ability to read data in parallel. Sub-wavelength surface-relief structures (binary and non-binary) have been investigated and will be described. These nanostructures are amenable to low-cost manufacturing processes and facilitate near-field parallel readout with optical power detectors. Several proposed double negative (DNG) metamaterial applications for antenna structures in the microwave regime have been shown to require nanometer feature sizes. Thin shells of DNG metamaterials can be used to enhance the performance of ultra-small radiators. Results for this metamaterial-antenna application will also be presented.

0-7803-7846-6/03/$17.00 ©2003 IEEE

## Statistical Signal Processing with Applications to Subsurface Sensing, Communications, and Radars

**Co-Chairs:** J. Krolik
E. Miller

1:15 Opening Remarks

# A Fast 3-D Inverse Scattering Method for Objects in Layered Media

Zhong Qing Zhang and Qing Huo Liu
Department of Electrical and Computer Engineering
Duke University
Box 90291
Durham, North Carolina 27708

Ground penetrating radar (GPR) and electromagnetic induction (EMI) are two important modalities for the detection and discrimination of landmines and unexploded ordnance. Several signal processing algorithms have been successfully developed and are widely utilized. However, current processing algorithms for these measurements are far from being satisfactory. The major difficulties with these processing arises because of the presence of the layered earth.

To improve the processing schemes, we propose a 3-D inverse scattering method to process electromagnetic induction and ground penetrating radar data for buried target detection and discrimination. Unlike the conventional signal processing schemes, this inverse scattering method is based on the full physics of wave-material interactions. This method has the capability of imaging the subsurface structure of the buried objects and their surrounding environment. Therefore, it can be a useful complement to the existing signal processing methods.

Our algorithm is based on the nonlinear inverse scattering method. It incorporates the physics of multiple wave field interactions with the buried objects as well as the layer interfaces to unravel the complex subsurface phenomena, and thus gives a clear image of the objects. To account for the reflections from the ground surface and subsurface interfaces, we incorporate a dyadic Green's function for a general multilayered medium in the inverse scattering method. A novel method is developed for the inversion so that there is no need to perform time-consuming forward iterations during the inversion. Several convincing examples will be demonstrated to show the merit of this new technique.

0-7803-7846-6/03/$17.00 ©2003 IEEE

# Some Applications of Curve-Evolution Techniques to Inverse Scattering

Vincenzo Galdi[1], Haihua Feng[2], David A. Castañon[3], W. Clem Karl[3], and Leopold B. Felsen[3,4]

*(1) Waves Group, Department of Engineering, University of Sannio, Benevento, Italy*

*(2) The MathWorks Inc., Natick, MA, USA*

*(3) Dept. of Electrical and Computer Engineering, Boston University, USA*

*(4) Dept. of Aerospace and Mechanical Engineering, Boston University, USA (part time) Also, University Professor Emeritus, Polytechnic University, Brooklyn, NY 11201, USA*

In many inverse scattering applications, aimed at retrieving geometrical and constitutive properties of targets embedded in complex environments, *object-based* reconstruction techniques are rapidly emerging as an attractive alternative to traditional *pixel-based* approaches. The motivation behind object-based techniques is to focus on robust *global* features of the target (e.g., shape, contrast, etc.), instead of trying to image the target *pointwise*. Besides mitigating the *ill-posedness* of the inverse scattering problem, these methods typically yield better estimation of key features of the target image (such as *edges*) which is highly desirable in localization/classification procedures. An important class of object-based imaging techniques is represented by *curve evolution* (CE) techniques (J. Shah, *J. Visual Comm. Image Representation*, **11**, p. 142, 2000), where a *gradient flow* is designed which attracts initial closed curves to the target boundary. Numerical implementation of such techniques is usually carried out via the *level set* method (A.D. Litman *et al.*, *Inverse Problems*, **14**, p. 685, 1998).

Our application is concerned with subsurface imaging of mine-like targets in the presence of moderately rough air-soil interfaces, for both frequency-stepped and pulsed excitations. For *low-contrast* targets, we have recently explored an *adaptive* approach based on the use of Gaussian beam fast forward scattering models. In this approach, a prior (coarse-scale) interface estimation problem is solved, with the resulting reconstructed interface profile used to correct the raw backscattered field data observed at the receivers so as to compensate for the corresponding clutter. The subsurface *target imaging* is subsequently performed by inverting a Born-approximate forward scattering model. In this connection, the use of object-based CE reconstruction techniques is explored and compared with traditional pixel-based approaches. For *high-contrast* targets, we have explored the use of CE-based imaging techniques in conjunction with the contrast source inversion method proposed in (P. van den Berg and R.E. Kleinman, *Inverse Problems*, **13**, p. 1607, 1997). Preliminary results, so far restricted to the simplest case of *homogeneous* background (i.e., no interface) look promising.

0-7803-7846-6/03/$17.00 ©2003 IEEE

# Object-Based Dynamic Tomography

Yongang Shi and William C. Karl

Multdimensional Signal Processing Laboratory
Department of Electrical and Computer Engineering
Boston University

Many tomographic-type inverse problem applications are focused on the extraction of information pretaining to a discrete set of objects in the field of view. Further, these applications often have limited or poor quality data. Often the interest is primarily in the localized physical properties of the underlying target objects, such as size, shape, location, density, permittivity, etc and less in the distributed behavior of the field as a whole. A further challenges arise when the underlying objects also evolve as the data are being acquired. Typical approaches to these problems are sub-optimal, performing a pixel-based reconstruction followed by object boundary extraction and often ignoring the dynamics of the scene.

In this work, we present a unified variational framework for reconstruction of 3-D dynamic objects from tomographic observations. We focus on problems where the interest is in primarily in object geometry or shape and where intensity is either less important or reasonably captured through low order parametric models. We assume that the scene is assumed to be composed of a discrete set of objects and capture this through a series of continuous surface boundaries. Thus, we use a fundamentally geometric scene model. Object dynamics are are treated by using separate intensity and shape evolution models, which capture our prior knowledge of the temporal evolution of the scene. Finally, a prior model on spatial shape based on boundary area is used. These models are then combined in a unified variational framework which incorporates the observation data, shape and intensity dynamics, and prior information on object spatial behavior. To incorporate the shape dynamics we define a new distance measure between surfaces based on a function of their signed distance functions. This new measure is computable, leads to tractable optimization problems, and avoids the need to establish object boundary correspondence. The sequence of object surfaces and corresponding intensity values are estimated jointly as the minimizer of the resulting energy function. A coordinate descent algorithm based on surface evolution is developed to solve this nonlinear optimization problem. Efficient level set methods are used to implement the algorithm. This approach evolves the surfaces from their initial position to the final solution and handles topological uncertainties automatically.

0-7803-7846-6/03/$17.00 ©2003 IEEE 

# Exploiting Noisy Transient Response Using the Fractional Fourier Transform

Seongman Jang, *Tapan K. Sarkar

Department of Electrical Engineering and Computer Science
Syracuse University, 121 Link Hall, Syracuse, NY 13244
Email: sejang@mailbox.syr.edu; tksarkar@mailbox.syr.edu

The goal of this paper is to obtain the electrical properties of the target from the received transient noisy time domain waveforms. Because of their aspect independence, complex resonant frequencies of a conducting object are used as a signature of the object to discriminate it from others for the purpose of target identification. The singularity expansion method (SEM) proposed by Baum [1] has been applied to express electromagnetic response in an expansion of complex resonances of the system. It has been shown that the dominant complex natural resonances of a system are a minimal set of parameters that define the overall physical properties of the system. So, a transient scattering response is analyzed in terms of the damped oscillations corresponding to the complex resonant frequency of the scatterer or target. Since the resonance describe global wave fields that encompass the scattering object as a whole, the SEM series representation encounters convergence difficulties at early times when portions of the objects are not yet excited. Early time response is strongly dependent on the nature of the source, the location of the source, and the location of the observer. Usually the early time response shows impulse-like characteristics. Because of this difficulty, most previous techniques such as Prony's method and Matrix pencil method (MPM) used just late time signals only. It is necessary to include 'entire function' to represent early time impulse-like components. The 'entire function' is subset of the analytic function but it doesn't have any singularities.

In this paper, the transient noisy electromagnetic response is considered in the time domain and in the fractional Fourier transform (FrFT) domain. The whole time domain data set is used to test. Fractional Fourier transform (FrFT) is a generalized Fourier transform. Using the FrFT it is possible to discriminate an impulse-like component from the other components of the signals. Because of this property, impulse-like early time components can be separated from the damped exponentials. To describe the early time response a Gaussian pulse is selected. Gaussian pulse is an entire function and is quite adequate to describe pulse-like components in early time. Complex exponentials are used to describe the late time signals. The concept of a 'Turn-on time' is utilized to consider a time when the fully excited resonance can be used, formally. The results for wire scattering element and finite closed cylinder with various SNR show that if SNR is greater than 30dB it is possible to get meaningful parameters using proposed techniques.

0-7803-7846-6/03/$17.00 ©2003 IEEE

# Nonlinear Inverse Scattering with Diffuse Light

John C. Schotland

*Department of Bioengineering, University of Pennsylvania, Philadelphia, PA*

We consider the inverse scattering problem for diffuse light. In previous work we have developed the scattering theory of diffusing waves in inhomogeneous media, established conditions under which the existence and uniqueness of solutions to the linearized inverse problem are guaranteed, constructed the singular value decomposition (SVD) of the forward scattering operator under conditions of weak scattering, and used these results to obtain explicit inversion formulas for the case of the linearized ISP. In this paper we extend these results to the nonlinear case. In particular, we construct a formally exact analytic solution to the nonlinear ISP. This solution, which we refer to as the inverse scattering series, has the form of a functional series expansion for the scattering potential in powers of the scattering data. The first term in the expansion corresponds to the pseudoinverse solution to the linearized inverse problem. The higher order terms may be interpreted as nonlinear corrections to the SVD inversion formulas. We have also shown that summing the inverse scattering series to all orders is equivalent to solving the ISP by the Newton-Kantorovich method. We have investigated the effects of sampling and limited data in the computation of the inverse scattering series. We have implemented the first nonlinear correction and are working to improve the computational efficiency of computing corrections to higher order.

0-7803-7846-6/03/$17.00 ©2003 IEEE 

# DOA Estimation Using Temporal and Spatial Processing Based on Direct Data Domain ($D^3$) Approach.

**Kyungjung Kim and Tapan K. Sarkar**

**Department of Electrical Engineering & Computer Science**

Syracuse University

Syracuse, NY 13244-1240

Email: kkim08@mailbox.syr.edu

tksarkar@mailbox.syr.edu

**ABSTRAT**: The purpose of this paper is to estimate the direction of arrival (DOA) of the signal of interest (SOI) in the presence of both coherent and noncoherent interferences multipaths and utilizing a combined temporal and spatial DOA estimation technique based on a direct data domain approach. The number of the signals impinging on the array can be greater than the number of antenna elements in the phased array. In this paper we use the concept of cyclostationarity utilizing the temporal information of the SOI to separate it from the interferences. By exploiting the concept of cyclostationarity we can extract signals with the same cycle frequency and null out the co-channel interferences and additive noise. Hence, the signal detection capability can be significantly increased. Next the spatial processing is implemented to differentiate the various coherent/noncoherent multipaths of the same signal while have the same cycle frequency. The main contribution of the paper is that by combining temporal and spatial processing based on a direct data domain approach one can handle multipath signals under the conditions that the number of signals impinging on the array at all the frequencies can be greater than the number of antenna elements. However, the number of multipaths has to be less than approximately half the number of antenna elements. Since we do not form a covariance matrix of the data, this method is quite suitable for short data lengths or when the environment is quite dynamic. Hence, in the proposed algorithm, while the estimation of the cyclic array covariance matrix is avoided, we develop a new matrix form using extremely short data samples. As a result, the computational load in the proposed approach is relatively reduced and the robustness of the estimation of signal of interest (SOI) is significantly improved when the number of available snapshots is extremely limited. Numerical results are presented to illustrate the efficiency and accuracy of this method.

0-7803-7846-6/03/$17.00 ©2003 IEEE 

# Comparison of Array Configurations for Optimum Beamforming in Terms of Signal Spatial Signature Angle Difference, Angle of Arrival Difference, and Polarization Angle Difference

C.B. Dietrich Jr.*, K. Dietze, W.L. Stutzman,
(cdietric@vt.edu, kai@ee.vt.edu, stutzman@vt.edu)
Virginia Tech Antenna Group (VTAG)
Bradley Dept. of Electrical and Computer Engineering
340 Whittemore Hall, Blacksburg, VA 24061-0111

The optimum beamformer output signal to interference-plus-noise ratio (SINR) with one desired and one interfering signal can be expressed in terms of signal spatial signatures and noise power (Dietrich, et al., *AP-S Int'l Symposium*, 640-643, 2002). The expression can be written as a function of the angle between the spatial signature vectors of the desired and interfering signals. This presentation expands on that work with applications to typical array configurations used for beamforming and radio channels of practical interest.

First, we present an analytical and simulation-based evaluation of canonical co- and multi-polarized array configurations in terms of the SINR achieved in a variety of single-interferer scenarios. Free-space and multipath channels are considered, as are multiple cases of angle of arrival relative to array geometry.

Next, we present measurement results for specific physical angles of arrival, polarization angles, and array geometries, and compare these with the modeled cases. Measurements conducted at 2.05 GHz in Virginia Tech's anechoic chamber and in rural and campus multipath channels are presented. In the multipath channels, the effect of variations in both angle of arrival and polarization angle on beamformer performance are significantly reduced.

Based on the above analytical, simulated, and measured results, the interrelationships between SINR, spatial signature angle, physical angle of arrival, polarization angle, and element spacing are investigated. Spatial signature angle is shown as a function of physical angle for several array configurations and element spacings. This provides a particularly useful and intuitive measure for comparison of array configuration performance.

Finally, the implications of the spatial signature-based approach for, and potential for extending it to model, multiple-interferer cases and wideband signals are discussed.

0-7803-7846-6/03/$17.00 ©2003 IEEE 

# ESTIMATION OF FREQUENCY SELECTIVE WIRELESS CHANNELS FOR LAYERED SPACE-TIME SYSTEMS

M. F. SIYAU P. NOBLES R. F. ORMONDROYD

Communication and Wireless Networks Group, Cranfield University
Royal Military College of Science, Shrivenham, Swindon, SN6 8LA, UK
Tel: +44 (0) 1793 785722, email: v.siyau@rmcs.cranfield.ac.uk

Submit to: *URSI* **Commission C**- C8 or C9.

**Abstract**:
Space-time techniques for multiple-input multiple-output (MIMO) channels potentially provide vast increases in capacity compared to traditional wireless communication systems. A number of MIMO approaches have been proposed for both narrowband and wideband channels. In order to achieve the quoted capacity gains in the MIMO systems, the multiple channel impulse response and its fading coefficients must be known or estimated. Thus far, existing MIMO channel estimation schemes have been limited to either the narrowband case or cater specifically for coded space-time systems e.g. space-time block codes system or MIMO-OFDM system.

In this paper, we extend the layered space-time receiver architecture described in (*A. Lazono, C. Papadias, IEEE Trans. On Communication, Vol.50, 65-73, No.1 2002*) and present a novel MIMO channel estimation scheme for an uncoded layered space-time system operating in a wideband frequency selective fading environment. The proposed MIMO channel estimation scheme uses the orthogonal pilot sequences obtained from the Paley's construction of the Hadamard matrix and combines the following concepts to perform channel estimation in the MIMO frequency selective channel:

1) A pilot matrix transmitted as a sequence of pilot symbols is used to jointly estimate the fading coefficients of the individual channel impulse responses between the multiple transmit and receive antennas, as opposed to using a series of individual pilot symbols by an adaptive algorithm (*M. F. Siyau, P. Nobles, R. F. Ormondroyd, WPCM'01, Vol.3, 1451-1456, 2001*).

2) The Hadamard's property is utilised where the pilot sequences are made to be orthogonal and assigned to individual transmit antenna in order to resolve the multiple transmitted/received signals and the inter-symbol interference for each transmitted signals.

3) The Toeplitz structure of the Paley-Hadamard matrix is exploited to allow the length of the pilot sequence to be minimised for a given length of channel impulse response and thus maximise the effective data throughput.

The pilot sequences are periodically transmitted in block within frames of data that enable the channel estimation process to reconstruct the complete MIMO channel matrix. The key to the proposed MIMO channel estimation scheme is the ability to extract the orthogonal information carried by the received signals corresponding to the pilot sequences sent by the transmitter where the MIMO channel matrix can be obtained by applying a simple matrix operation to these pre-arranged received signals matrix at the receiver. We will also demonstrate how to design these pilot sequences. Results will be presented to demonstrate the accuracy of the proposed channel estimation scheme and its performance in layered space-time system with different system configurations.

0-7803-7846-6/03/$17.00 ©2003 IEEE 

# Large-Scale Electromagnetic Characterization of Urban MIMO Communication Systems

Kapil R. Dandekar*[1] and Robert W. Heath, Jr.[2]

[1] Drexel University, Philadelphia, PA 19104-2875, USA
Telephone: 1-215-895-2004, Fax: 1-215-895-1695, Email: dandekar@ece.drexel.edu
[2] The University of Texas at Austin, Austin, TX 78712-1084, USA
Telephone: 1-512-232-2014, Fax: 1-512-471-1856, Email: rheath@ece.utexas.edu

Multiple-input multiple-output (MIMO) wireless communication systems are of increased interest due to their high spectral efficiency and substantial diversity. Full characterization of the MIMO channel is very important, yet remains a challenge due to the complex electromagnetic interactions between the antenna elements and the environment. We use computational electromagnetics (CEM) to study the performance of MIMO links, and present large-scale simulation results in an outdoor urban environment. We examine the impact of the location of the antenna array in the environment, the average received power, and the angle spread on the average mutual information (AMI) of the MIMO channel. We find that locations closer to the base transceiver station (BTS) correspond to higher AMI, especially when these locations receive line-of-sight (LOS) rays. However, if perfect transmit power control is used, MIMO systems have higher capacity in non-line-of-sight (NLOS) regions due to increased spatial modes in the channel.

Our approach combines two different CEM techniques for the modeling of electromagnetic interactions: the Method of Moments (MoM) and Electromagnetic Ray Tracing (ERT). Combining both the near-field interaction of the array structures and the far-field propagation channel requires a hybrid approach of both ERT and MoM. MoM is used to model the near-field interaction among the array elements, while the far-field interaction between the antenna array and the environment is modeled by ERT. This is important because it allows us to isolate the influence of both near-field and far-field propagation parameters in AMI computations.

In Fig. 1(a) we plot the AMI for a 7 x 7 MIMO system making use of uniform circular antenna arrays in a center-excited urban microcell at 1.8 GHz as a function of position throughout the streets of a computer model corresponding to Austin, Texas. AMI is highest near the BTS and decays as a function of distance from the BTS. Locations close to the BTS have higher signal strength due to the limited path-loss, hence receive a larger capacity than positions further away from the BTS. In Fig. 1(b), we remove the effect of path-loss on AMI. Comparing with Fig. 1(a), we detect that there is an inverse trend with respect to LOS rays. Locations with NLOS rays seem to have AMI that is higher than those with LOS. In particular, there is a hotspot that appears in the upper area of Fig. 1(b) which corresponds to a group of tall buildings within the same proximity to the MTS. Our expectation is that this hub of tall buildings causes more diffractions, as well as a larger variation in the angle spread and therefore contributes to high AMI.

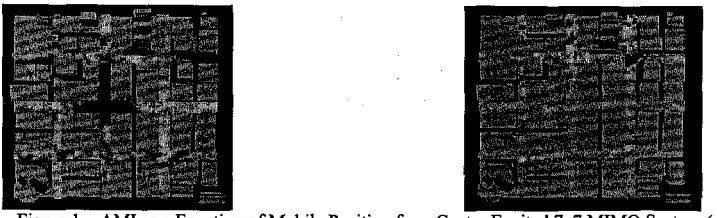

Figure 1 – AMI as a Function of Mobile Position for a Center Excited 7x7 MIMO System (A) With and (B) Without Path Loss Effects

0-7803-7846-6/03/$17.00 ©2003 IEEE

# EFFECTS OF IMPERFECT POWER CONTROL, FREQUENCY &TIMING OFFSET ON LS-DRMTA AND LS-DRMTCMA ALGORITHMS.

Ercüment H. Zorlu and İbrahim Tekin

Sabancı University,
Faculty of Engineering and Natural Sciences.
34956-Tuzla, İstanbul -Turkey
Tel: +90 216 483 95 51, Fax: +90 216 483 95 50
ercument@sabanciuniv.edu

**Abstract**

The CDMA and smart antennas are two promising approaches to increase system capacity and spectrum efficiency for mobile communication services. In a DS-CDMA system, frequency offset between local oscillator and the carrier of impinging signal, timing offset between local generated PN sequence and received PN sequence, imperfect power control may exist and this degrades the performance of the smart-antenna algorithms. In this paper, the effects of imperfect power control, frequency and timing offsets on smart antenna algorithms will be presented. A smart antenna system has been set up to implement blind adaptive algorithms for DS-CDMA in a laboratory environment. The blind adaptive algorithms implemented on the smart antenna system are Least- Squares Despread-Respread Multi Target Array (LS-DRMTA) and Least- Squares Despread-Respread Multi Target Constant Modulus Algorithm (LS-DRMTCMA). Since both LS-DRMTA and LS-DRMTCMA algorithms utilize user's PN sequence, they have several advantages compared to other blind adaptive algorithms for DS-CDMA. BER and beamforming performances of LS-DRMTA and LS-DRMTCMA algorithms in a two-user and three- element-antenna array system will be evaluated for systems with timing offset, frequency offset and imperfect power control. The smart antenna system consists of two-signal generators and transmit antennas, three receiver-chains with half wavelength spaced three-element antenna array and a computer to process captured data in Matlab. Signal generators generate BPSK modulated signal for two users at 1,92 Mchips, at carrier frequency of 2.125 GHz. The receiving module includes three microstrip inset patch antennas, three -receiver chains that makes the conversion from RF to baseband and sends the samples to computer for post processing in Matlab.

**(1) ID of Commission:** C (Signals and Systems)
**Session Topic:** C1.Beamforming and matched field processing.

**(2) Relation of this work to previous work**

LS-DRMTA and LS-DRMTCMA are first introduced by Rappaport and Rong. Using computer simulations they have shown that for DS-CDMA, LS-DRMTA and LS-DRMTCMA performs best in frequency and timing offset conditions by comparing BER vs. Number of Users curves for different algorithms.

**(3) New knowledge contributed by this paper**

In this paper, in addition to frequency and timing offsets the effects of imperfect power control condition on LS-DRMTA and LS-DRMTCMA will be examined using smart-antenna test bed in a laboratory setting.

0-7803-7846-6/03/$17.00 ©2003 IEEE 

# Signal Design and Processing for Orthogonal Netted Radar System

Hai Deng
Department of Electrical Engineering
The University of New Orleans, New Orleans, LA 70148

The netted radar systems through a central control unit will greatly improve the radar detecting and automatic tracking performances by information fusion. The conventional netted radar systems normally operate multistatic mode, i.e., one radar system operates as the transmitter and the rest operate as the receivers. If all radar stations in the netted system can transmit and receive simultaneously at the same carrier frequency, the netted radar system is coined as the orthogonal netted radar system. However, the waveforms used by the netted system must be carefully designed to avoid the self-interference and detection confusion. If the system transmits the waveforms from a special coding waveform set in which each of the waveforms has the nearly ideal aperiodic auto-correlation property and any two of them have no cross-correlation, it can adaptively operate, based on the environments, in regular monostatic mode or in bistatic or even multistatic mode with the same carrier frequency. The key to the feasibility of the orthogonal netted radar system is to design a set of the special coding waveforms of the unique properties as described above. The polyphase coding waveforms have increasingly become favorable alternatives to the traditional binary coding waveforms due to the maturity of digital signal processing and VLSI. Assuming that the waveform set used by an orthogonal netted radar system consists of $L$ polyphase coding signals with each signal consisting of $N$ complex numbers, we represent the frequency-hopping waveform set as: $\{s_l(n) = e^{j\phi_l(n)}, m = 1,2,..N\}, l = 1,2,...,L$ where $0 \le \phi_l(n) < 2\pi$ is the phase value of subpulse $n$ of waveform $l$ in the waveform set. For the orthogonal waveforms each of the waveforms has nearly ideal noise-like autocorrelation property and any two of them have no cross-correlation, therefore,

$$\frac{1}{N}\sum_{k=0}^{N-1-|m|} s_l^*(n)s_l(n+m)\begin{cases}=1, & m=0\\ \approx 0, & m\neq 0\end{cases} \quad l = 0,1,...,L-1 \tag{1}$$

and

$$\frac{1}{N}\sum_{k=0}^{N-1-|m|} s_p^*(n)s_q(n+m) \approx 0 \quad p \neq q, \quad p,q = 0,1,...,L-1 \tag{2}$$

The polyphase code set design with properties in (1) and (2) can be implemented with algebraic construction method or more practically, numerical methods. The following figure show the auto-correlation (a, b, c) and cross-correlation (d, e, f) properties for a designed polyphase code set by simulated annealing with $L$=3 and $N$=128. The processing of the polyphase coding signal is normally implemented with digital correlators. The processing results can be further improved by using CLEAN algorithms to remove the sidelobe and cross-correlation interferences..

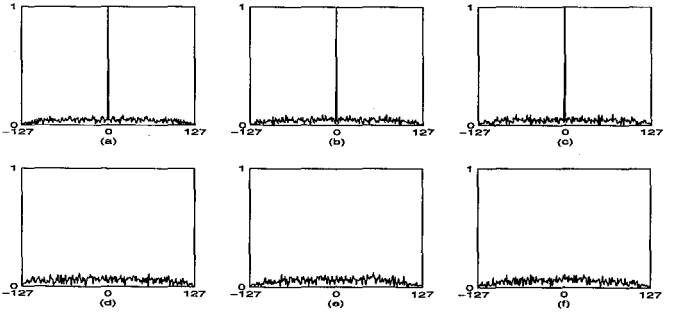


0-7803-7846-6/03/$17.00 ©2003 IEEE

## Numerical Analysis of Circuits and Waveguides

**Co-Chairs:** N. Nikolova
Q. H. Liu

3:20 Opening Remarks

# Analysis and Applications of Compact ADI-FDTD Method for Guided Wave Structures

Muhu Wang* and Ji Chen
Department of Electrical and Computer Engineering
University of Houston
Houston, TX 77204

Feng Liu
Synopsys Inc.
700 E. Middlefield Road
Mountain View, CA 94043-4033

The signal propagation on integrated circuit (IC) interconnects are of importance to both microwave/RF circuit designers and high-speed digital circuit engineers. The accurate characterization of interconnects frequency dependent behavior is often required in order to optimize a circuit design. To efficiently extract interconnect frequency dependent behavior, numerical simulations are often used. The compact finite difference time domain (FDTD) method has been successfully used to perform such extractions for general guided wave structures. However, the time step size constrain of this algorithm has limited its application to electrically small IC interconnects.

To improve the computational efficiency of the ADI-FDTD algorithm, an alternating-direction-implicit FDTD algorithm has been proposed. The algorithm is unconditional stable and the computational overhead is on the same order of the traditional FDTD algorithm. Recent work has shown that although the ADI-FDTD method is unconditional stable, its accuracy degrades as its time step size increases. There exists a maximum step size for ADI-FDTD method in order to maintain the same accuracy level as traditional FDTD method.

In this work, we will first investigate the accuracy level associated with the compact ADI-FDTD method. Since typical IC structures are electrical small and the boundary condition may have significant effect on the accuracy of the simulations, we will investigate both the dispersion errors associated with this algorithm and the error introduced by boundary reflections. We will also apply the non-uniform grids to further increase the spacing between the absorption boundary and IC interconnects. Based on the results of our accuracy analysis, we will apply this technique to study several interconnect structures.

0-7803-7846-6/03/$17.00 ©2003 IEEE 

# Modeling Microstrip Feeds using the Finite Element-Boundary Integral Method

Pedro Barba*, Arjun Jayaraman, and Leo Kempel

The Wireless Integrated Microsystems (WIMS) Center
Department of Electrical and Computer Engineering
Michigan State University

Electromagnetic interference (EMI) is an increasingly important issue for high-speed, mixed-signal circuit applications. The high data transfer rates in modern circuitry leads to new modes of signal coupling amongst circuits. Mixed-signal circuits are especially vulnerable to EMI due to the physical proximity of digital, analog, and radio frequency (RF) circuit components and interconnections between the elements. Interactions can occur via substrate, surface wave, and circuit-to-package-to-circuit couplings as well a host of other more complex routes. It is important to understand the phenomenology of the sources of EMI within complex circuits to minimize the impact of EMI. In the past, low-frequency approximations have sufficed to account for EMI routes within low-speed circuits. However, with increasing speed and hence bandwidth, models that account for distributed effects are increasingly important. One approach has involved the use of microwave circuit parameters, e.g. S-parameters, in a cascade network. This is suitable for design of microwave systems; however, it is difficult to use for EMI analysis. Other methods, involving various hybridizations of S-parameters and the popular circuit design tool SPICE have been used. The best approach, as the frequency of operation increases, is a full-wave model. Since modern mixed-signal circuits are tremendously complex, it is impractical to use a full-wave model for the entire circuit and package volume. Hence, the need to investigate each source of EMI to understand how emissions from one point in a circuit couples into another point. One area of particular interest is EMI emissions from pins that connect transmission lines or components to a circuit board.

Microstrip structures are some of the most basic transmission lines, or signal routing paths, in use for high-speed (e.g. wide bandwith) signals in mixed-signal devices. In this paper, a finite element-boundary integral (FE-BI) method is used to investigate the electric fields in the near vicinity of a feed pin for a microstrip line. The FE-BI method permits volumetric evaluation of the electric field. Once the field structure in the immediate vicinity of the pin is understood, an improved feed model will be developed that is more efficient that current methods and hence will enable more complex models, necessary for assessing the near vicinity interactions in a circuit.

0-7803-7846-6/03/$17.00 ©2003 IEEE

# Pseudospectral Beam Propagation Method and Finite Element Method: A Hybrid Technique in Computational Photonics

Imran Deshmukh* and Qing Huo Liu
Electrical and Computer Engineering
Duke University
Durham, North Carolina 27708
Email: qhliu@ee.duke.edu

The application of pseudospectral method for strongly guiding and longitudinally varying waveguides has shown that this method is superior to the classical beam propagation method (also known as the split step beam propagation method) and a widely used variation based on the finite element method (FE-BPM). In the light wave analysis of more sophisticated optical devices such as beam splitters and couplers, earlier beam propagation methods have been combined with conventional methods such as finite element method to solve for sharp inhomogeneities encountered in these structures.

In this work, we develop a hybrid technique comprised of the pseudospectral beam propagation method and finite element method to study the propagation of light in optical waveguiding structures with sharp inhomogeneities. Such a mixed-scale problem is divided into two parts: (a) the slowly varying waveguides are treated by the pseudospectral beam propagation method (Deshmukh and Liu, IEEE Photon. Technol. Lett., Jan. 2003); (b) the strong inhomogeneities (such as a coupler) are treated by the finite-element method. As an illustration of the utility of this technique we apply the following technique to an optical beam coupler. Essentially this structure consists of a 4-port junction connected to optical waveguides at each of the ports. The interface of the junction with waveguides at each of the ports represents the sharp inhomogeneity in the complete optical waveguiding setup. The exponentially accurate pseudospectral beam propagation method is applied to each of the waveguides attached to the junction. The junction is analyzed using the finite element method. The propagation solutions obtained from the pseudospectral beam propagation method and finite element method are reconciled by applying the boundary conditions at the each of the interfaces of the 4-port optical beam coupler. This hybrid method is superior to earlier methods employing combinations of beam propagation methods and conventional finite element methods.

0-7803-7846-6/03/$17.00 ©2003 IEEE 

# A Fast Simulation Method for 3D Photonic Crystals

Jianguo* Liu and Qing Huo Liu
Department of Electrical and Computer Engineering
Duke University
Box 90291
Durham, North Carolina 27708

The novel properties of photonic crystals, the artificial photonic structures whose refractive indices vary periodically on the scale of the wavelength of light, have attracted active research in the design of such new materials. For infinite periodic structures, under certain conditions a photonic crystal possesses a photonic bandgap (PBG) in which light propagation in any direction is prohibited. The design of photonic crystals with various bandgap properties calls for fast and accurate simulation of light interacting with complex dielectric structures. Ongoing efforts focus on the finite-difference time-domain (FDTD) method, pseudospectral time-domain (PSTD) method, finite-element method, and plane wave expansion method. Although such methods prove highly useful for infinite periodic structures (where only one period needs to be simulated) and for small truncated periodic structures, they are still very time consuming for large-scale truncated periodic structures where no periodicity conditions can be used to reduce the computational domain to a single period.

In this work, we propose to develop a fast simulation method for photonic crystals with the newly proposed volume adaptive integral method (VAIM). The VAIM is a fast integral equation method for electromagnetic scattering from 3D inhomogeneous objects (Zhang and Liu, *IEEE Antennas Wireless Propagat. Lett.*, vol. 1, no. 6, pp. 102–105, 2002). By projecting the unknown induced current density within an arbitrary element in the inhomogeneous object onto a fictitious uniform grid, this method accelerates the calculation of the far-zone interactions of basis and testing functions through the fast Fourier transform, thus greatly reducing the memory requirement to $O(N)$ and CPU requirement to $O(N \log N)$, where $N$ is the number of unknowns. The numerical results have been validated by the method of moment. Application to photonic crystals will be illustrated to show the efficacy of this method.

0-7803-7846-6/03/$17.00 ©2003 IEEE

# Matching of narrow-band photonic crystal filters and waveguides to free space and dielectric waveguides

Amir Boag, Ben Z. Steinberg*, and Orli Bushmakin
Faculty of Engineering, Tel-Aviv University, Tel-Aviv 69978 Israel
boag@eng.tau.ac.il, steinber@eng.tau.ac.il

It is well known that micro-cavities formed by local defects within an otherwise perfect photonic crystal structures can trap light at wavelengths within the stop-band of the background crystal. Since the micro-cavities resonate at a well-defined frequency with an ultra-narrow bandwidth, they can potentially be used as high Q filters. An array of equally spaced identical micro-cavities forms the Coupled Cavity Waveguide (CCW) - a narrow band waveguide whose central frequency and bandwidth are determined by the micro-cavities nature and their inter-spacing, respectively. Such devices can be used as optical or millimeter wave filters, routers, and multiplexers/demultiplexers with obvious applications in RF and optical communication systems.

A fundamental condition for the practical efficacy of micro-cavity filters and CCWs as sub-systems in a realistic multi-component system, is the ability to match them to structures external to the background photonic crystal, such as free space, dielectric slab waveguides, or optical fibers. This matching problem can be formulated as an optimization problem by which one seeks the minimum of a properly defined Standing Wave Ratio (SWR), with respect to limited variations of the dielectric structure/geometry in the neighborhood of the interface between the sub-system (micro-cavity, CCW) and the external structure. Formally, however, it is clear that the entire sub-system structure has to be accounted for to provide a proper solution of the wave-problem. This naturally calls for a sub-structuring procedure. The sub-system impedance matrix and its inverse are computed a-priori and remain unchanged during the optimization process, while the much smaller impedance matrix associated with the interface neighborhood (which constitutes the optimization search domain) and its inverse are re-calculated at every search step.

In this work, we use the sub-structuring methodology to match CCW devices. Several matching configurations are demonstrated and their corresponding performances are discussed.

0-7803-7846-6/03/$17.00 ©2003 IEEE

*Special Session*

## Electromagnetic Interference with Complex Platforms II

**Organizer(s):** P.L.E. Uslenghi, University of Illinois at Chicago
**Co-Chairs:** R. Gardner
C. Baum

1:15 Opening Remarks

# EMI Coupling to Cable Bundles

J. Pincenti*
Motorola, and University of Illinois at Chicago

P.L.E. Uslenghi
Department of Electrical and Computer Engineering
University of Illinois at Chicago
851 South Morgan Street, Chicago, Illinois 60607-7053, USA
Email: uslenghi@uic.edu

This work consists of two parts. In a first part, the different analytical, numerical and experimental methods employed in the study of electromagnetic interference on cable bundles inside an enclosure such as an aircraft are reviewed and critically compared, in order to determine the best available tools to predict the influence of EMI on signals propagating along the conductors in the bundle. The study is conducted in the frequency domain, and takes into account a variety of parameters including the effectiveness of insulating materials and metallic screens, the position of the cable bundle with respect to floor and walls of the platform, the presence and state of operation of neighboring bundles. Both deterministic and statistical approaches are examined. The scattering parameters of conductor pairs inside the bundle are analyzed.

In a second part, a detailed study is conducted on the influence of an external field on the propagation of signals inside a multi-conductor cable, by utilizing a distributed Green's function approach akin to that proposed by Schelkunoff (*Electromagnetic Waves*, chapter 7. New York: Van Nostrand, 1943) and previously utilized by Uslenghi and Bridges (*Alta Frequenza*, vol. 49, no. 2, pp. 172-178, 1980) to study the penetration of electromagnetic fields through the shield of a coaxial cable. The incorporation of these results into an extension of the BLT equation is considered.

0-7803-7846-6/03/$17.00 ©2003 IEEE 

## Coupling Among Multi-Conductor Transmission Lines and Complex Structures

***Y.Bayram[1], T.Ozdemir[2], J. L.Volakis[1,2]**
[1] ElectroScience Laboratory, EE Dept., The Ohio State University, Columbus, OH 43212
[2] Radiation Laboratory, EECS Dept, The University of Michigan, Ann Arbor, MI 48109-2122

This work focuses on generalizations and improvements of methods used to analyze field-excited (external radar excitation) multi-conductor transmission lines surrounded by arbitrary complex structures. The typical challenge with such analyses deals with the large size of the surrounding structure in presence of cable bundles that require extreme geometrical details for their modeling and characterization. Consequently, it is instructive to consider modeling of the cable bundle separately from the large nearby structure (aircraft or automobile) and to subsequently interact the two structures via field bouncing.

Methods for field-excited multi-conductor transmission lines in the presence of structure have been proposed by Taylor (C.D.Taylor et al., IEEE Trans. Antennas Propag., November 1987), Aggrawal (A.K.Agrawal et al., IEEE Trans. Electromagnet. Compat., May 1980) and Rachidi (Rachidi, IEEE Trans. Electromagnet. Compat., August 1993) . However, these approaches are only valid for those cases where the transmission line is close to conducting surfaces -- in other words, where quasi-TEM conditions are valid. Nevertheless, such methods have been widely used for characterizing the coupling between transmission lines and nearby structures even though they provide poor accuracy when the quasi-TEM condition is violated.

To carry out trustworthy field analysis of the coupling between multi-conductor transmission lines, in this paper we propose the integration of rigorous computational techniques for the analysis of surrounding structures in conjunction with multi-conductor cables. In our analysis, transmission lines are segmented into small sections and scattering information from each of them is used to develop inductance and capacitance parameters. The incident field along these lines is included by introducing distributed voltage sources using Aggrawal's approach. To take into account the scattering effects from other segments throughout the transmission lines, a field bouncing technique is carried out. In other words, the field radiated by the transmission lines is subsequently used to excite the nearby structures analyzed using rigorous computational methods such as the Moment Method. In this manner, interactions between the cables and the structure can be iterated until a desired accuracy is attained. A similar study was done by Tkatchenko et.al. (IEEE Trans. Electromagnet. Compat., November 1995) for a single open ended wire above an infinite ground plane and analytical expression were obtained for this case. In this work, we develop a completely general approach for the field coupling among multi-conductor cables in the presence of complex structures.

0-7803-7846-6/03/$17.00 ©2003 IEEE

**Analytical formulas and integral equation methods: a study of penetration, radiation, and scattering for a slotted semielliptical channel filled with isorefractive material**

Danilo Erricolo(1), Michael Lockard(2), Chalmers M. Butler(2) and Piergiorgio L.E. Uslenghi(1)

(1) Dept. of ECE, University of Illinois at Chicago, Chicago, IL 60607 USA.
Email derricol,uslenghi@ece.uic.edu
(2) Dept. of ECE, Clemson University, Clemson, SC 29634 USA.
Email: mlockar@clemson.edu,chalmers.butler@ces.clemson.edu

We consider a novel two dimensional problem for which an analytical solution is available and compare the theoretical results with those obtained using integral equation methods. The purpose of this work is to validate computer codes that are developed to study electromagnetic fields in complex structures.

The structure of interest is a slotted conducting plate backed by a semielliptical channel. The metallic plane is slotted along the interfocal strip of the semielliptical channel. The channel is filled with a material isorefractive to the material in the exterior half-space above it. In particular, the two materials may be the same, e. g. air. The primary source may be a plane wave obliquely incident on the structure from the exterior region and either E- or H-polarized, or an electric or magnetic line source parallel to the channel axis and located inside or outside the channel. Exact solutions for all these boundary-value problems have been developed in terms of expansions in series of products of radial and angular Mathieu functions (P. L. E. Uslenghi, "Exact penetration, radiation and scattering for a slotted channel filled with isorefractive material", IEEE Trans. Antennas Propagat., submitted)

The comparison is carried out by plotting the total electric and magnetic field along the plane of symmetry from the interior wall of the semielliptical channel to a few wavelengths outside the channel. The analytical solution is computed from Mathieu series expansions. The numerical solution comes from integral equations that have been developed to study the penetration into a generic cavity. Different approaches are considered. First, for a finite ground plane and TM polarization, the scatterer and Schelkunoff's methods are developed. Then, for an infinite ground plane, two coupled integral equations, for TE and TM polarizations, are considered.

The results show that in all cases the agreement between analytical and numerical solutions is excellent, thus providing a new validation for the integral equation methods.

0-7803-7846-6/03/$17.00 ©2003 IEEE 

# Exact Analysis of a 3D Cavity-backed Aperture With an Isorefractive Lens

C. Berardi, D. Erricolo, P.L.E. Uslenghi(*)
Department of Electrical and Computer Engineering
University of Illinois at Chicago
851 South Morgan Street, Chicago, Illinois 60607-7053, USA
uslenghi@uic.edu

The exact solution to an electromagnetic boundary-value problem involving a semi-oblate spheroidal cavity with metallic walls flush-mounted under a metallic ground plane and coupled to the half-space above the plane via a circular hole is considered. The material filling the cavity is separated from the free-space above the ground plane by a lens that occupies the circular hole and separates the cavity interior from the half-space above the cavity; both lens surfaces are coordinate surfaces in the oblate spheroidal coordinate system. The material inside the cavity and the lens material are both isorefractive to free space. The exact solution is in terms of series expansions involving oblate spheroidal wave functions. The expansion coefficients may be evaluated exactly, thereby leading to a canonical solution of the problem.

The primary source is an antenna located on the axis of symmetry of the structure and axially oriented. An exact formula is given for the electric and magnetic fields at any location inside or outside the cavity, or inside the lens. By invoking the reciprocity theorem, the fields on the axis of symmetry due to a primary radiator located elsewhere are given exactly.

The series representing the exact solutions are evaluated numerically, and the results are compared to those obtained by applying general frequency-domain computer codes to the problem at hand, thereby providing an independent validation of such codes. In particular, issues such as the evaluation of fields and surface currents near the edge of the coupling hole, and the effects of ground-plane truncation in the application of general computer codes, are analyzed in detail.

0-7803-7846-6/03/$17.00 ©2003 IEEE 

# Broadband Antenna System for Uniform Field Generation

Joseph D. Brunett* and Valdis V. Liepa
Radiation Laboratory, Electrical Engineering and Computer Science Department,
The University of Michigan, Ann Arbor

An antenna system operating from DC to over a GHz has been constructed for the purpose of inducing wideband uniform fields across an object. This system is a practical implementation of a similar antenna system analyzed previously (C. Cheon, *PhD. Thesis*, University of Michigan, 1992). The figure below shows a sketch of the antenna system and the instrumentation used in creating the uniform field. The antenna is of V-design with carbon loaded absorbing cones and resistors placed at the terminating end of the structure to minimize field reflections. The system has been constructed in a shielded semi-anechoic chamber above a metal ground plane. Because of the systems T.E.M. design, the antenna's low frequency cutoff is essentially 0 Hz (d.c.) while the high frequency cutoff of the system is limited only by the physical accuracy of the feed region construction. Although the carbon foam RF energy absorbing cones located at the terminated end of the field prove ineffective below 100 MHz, the antenna system works within the wide spectrum noted due to the addition of simple loading resistors on the terminating ends of the antenna. These resistors allow for low frequency operation. The maximum field strength in the uniform field region is limited by the breakdown voltage between the antenna structure and the ground plane at the feed location, the power handling ability of the resistors, and the capabilities of the sources and amplifiers used. The system we currently have constructed is capable of generating field up to 100 V/m over the range of 10 kHz to 1 GHz. The main applications of this antenna system include radiated electromagnetic immunity testing for CE EMC requirements and the generation of uniform plane-waves for aperture coupling measurements.

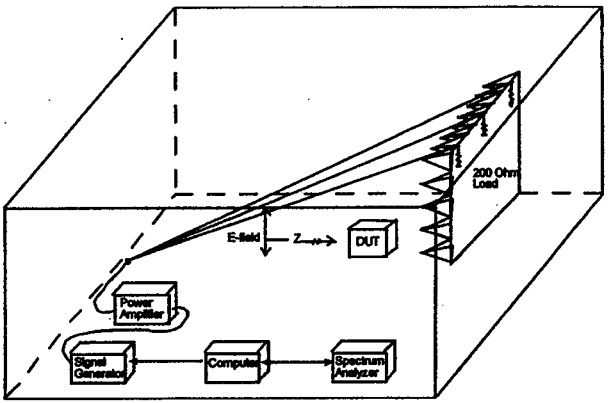


0-7803-7846-6/03/$17.00 ©2003 IEEE

## Plane wave illumination effects onto circuit topologies

[1]E.S. Siah, [1,2]J.L. Volakis , [1]D. Pavlidis and [1]V.V. Liepa
[1]Dept. of Electrical Engineering and Computer Science,
[1]The University of Michigan, Ann Arbor, Michigan 48109-2122
[2]ElectroScience Lab, Ohio State University, Columbus, OH 43210
{esiah, volakis, pavlidis}@eecs.umich.edu

**Extended Summary**

With the increasing use of wireless devices and services, the impact of electromagnetic coupling and interference on active circuits in the presence of ambient radiation should be carefully investigated. This interference can be intentional or unintentional and could result in distortion of the output signal for analog devices and their improper functionality leading to digital circuit logic errors. In this paper, we propose a hybrid finite element boundary integral (FE-BI) method for the analysis of EM coupling from external plane wave on passive circuit elements such as a microstrip interdigital filter and a coupled microstrip line filter. The input and output ports of both the microwave interdigital filter and the coupled microstrip line filters are terminated with 50Ω resistive loads. An induced voltage of 3.65 mV and 13 mV are respectively computed at the output of the microstrip interdigital filter and the microstrip line coupled filter. In both cases, the illuminating plane wave has an amplitude of 1V/m and the resonance, where the maximum induced voltage is computed, is close to the designed resonance of the microwave filter circuits. These induced voltages can therefore be significant when a 100 V/m plane wave intensity is considered.

This analytical study is further extended to a low noise amplifier (figure1) operating with a gain of 11 to 12 dB from 8 to 12 GHz. Induced voltages at the gate and drain terminals of the FET are computed with the FE-BI method at various levels of plane wave illuminations. Next, these voltages are modeled as extraneous sources with a single-tone harmonic balance simulation to evaluate the effect on the LNA gain due to external plane wave illuminations. We observed that as the amplitude of the plane wave increases, the distortion at the LNA output increases. When the LNA is connected to other digital and analog circuits, such EM interference and coupling may therefore result in bit errors at the output. A study on the degree of non-linearity introduced to the LNA circuit is also performed. In this study, the LNA operates at 10 GHz ($f_1$) while a 9.5 GHz ($f_2$) 50V/m external plane wave with the same orientation and polarization as before is used to illuminate the LNA. A two-tone harmonic balance simulation using the induced voltages at the gate and drain of the LNA indicates that the plane wave can introduce significant non-linearities within the LNA circuit with an IP3 intercept point at 40 dBm instead of infinity for an ideal linear amplifier (in the absence of radiation).

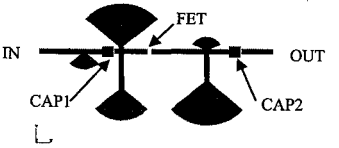


Fig 1: Layout of the LNA used for studying plane wave illumination effects.

# Conducting EMI Effects on RF Active Circuits

H. Y. David Yang
Dept. of Electrical and Computer Engineering
University of Illinois at Chicago, Chicago, IL 60607
hyang@ece.uic.edu

Recently, there is increasing effort to understand and model the effects of UWB (ultra wide band) pulse and HPM (high-power microwave) interactions with electronic circuits and systems at all scales. There has been significant EM simulation effort in a large scale to determining the field coupling from UWB and HPM sources into the circuits and systems at the pin levels. An aim of this paper is to investigate the effects of the induced EMI source to the circuit components and as a result, to the overall systems.

The HPM source is characterized as a series of pulses with fixed duration and off time. Its frequency characteristics will be used to determine both the EM and circuit model for analysis.

For analog or mixed-signal communication systems, we investigate the EMI source injected into the system front end, particularly the low noise amplifier (LNA). When the EMI source is sufficiently smaller or comparable to the normal receiving signals, the EMI source is treated as noise and its effect to the overall system is determined through the bit-error rate (BER). When the EMI source is modestly larger than the normal received signals, it has additional effect of introducing higher-order harmonic (IP3) due to the nonlinearity of the voltage gain. The bias point at transistor (CMOS) gate may also vary by the EMI source resulting in unstable transconductance and severe circuit mismatch. If the EMI source level is even higher, the CMOS transistor may be biased into saturation and the circuit is no longer functional. In this paper, we will quantify the EMI source level as related to the three possible scenarios.

In addition, we will discuss the EMI effect on the digital circuits. The emphasis is to determine the EMI source level at the gate such that the transistor logic is altered. Several examples of HPM coupling through apertures will be used to evaluate its threat to the electronics communication systems.

0-7803-7846-6/03/$17.00 

# An Improved Fast Algorithm for Transient Simulation of Microwave Circuits with Nonlinear Electronics

Jun Meng, Kemal Aygun, and Eric Michielssen
Department of Electrical and Computer Engineering,
University of Illinois at Urbana-Champaign,
1406 W. Green St., Urbana, IL 61801, U.S.A.

The computational analysis of electromagnetic field coupling into, or radiation from, shielded circuitry calls for an integrated full-wave simulation environment that allows for the simultaneous modeling of slotted enclosures, printed circuit boards, and nonlinear circuitry. Time domain electromagnetic analysis techniques—whether differential- or integral equation-based (e.g. the finite difference/element or marching-on-in-time (MOT) methods)—are prime candidates for driving the basic computational engines of such environments. Indeed, they (i) provide wideband information with a single program run and (ii) can be easily coupled to nonlinear circuit analysis tools.

Previously, we described a fast time domain integral equation solver that used a plane wave time domain-(PWTD) accelerated MOT kernel to model coupling of electromagnetic energy into complex systems comprising conducting surfaces/wires/junctions, potentially inhomogeneous finite dielectrics, and nonlinear loads (K. Aygun, B. Fischer, A. Cangellaris, E. Michielssen, "Fast time domain analysis of nonlinearly loaded printed circuit board structures," National Radio Science Meeting, University of Colorado at Boulder, January 9-12, 2002, Boulder, CO). During each simulation step, this PWTD-augmented MOT solver classically accounts for "near-field interactions". "Far-field interactions", in contrast, are calculated by the PWTD algorithm, viz., by expanding radiated fields into time domain plane waves. Linear/nonlinear lumped circuits in the system are modeled by coupling modified nodal analysis equations to the electromagnetic analysis environment.

Here, further improvements to this solver are presented that aim to increase its efficiency when analyzing realistic geometries that are both electromagnetically large and contain many geometric details. Previously, it was observed that, especially when modeling densely meshed geometries, a significant fraction of the overall CPU time and memory went towards the computation and storage of near-field interactions. The two major improvements to the above referenced solver proposed and described in this presentation are (i) the incorporation of a new prolate-type temporal basis function with superior stability properties compared to polynomial-type basis functions previously used and (ii) a singular value decomposition- (SVD) based compression scheme that significantly reduces the computational time and memory requirements when characterizing near-field interactions. The development and implementation of this SVD-based compression scheme with prolate-type temporal basis functions, all within a PWTD-accelerated MOT framework, constitutes the main contribution of this study. Results that demonstrate the efficiency of the resulting algorithm will be presented.

0-7803-7846-6/03/$17.00 ©2003 IEEE 

# A Hybrid Methodology for Efficient Electromagnetic Interference Modeling of High-Density Printed Circuit Boards

J. Morsey, M. J. Choi, V. Okhmatovski, and A. C. Cangellaris
Center for Computational Electromagnetics, ECE Department
University of Illinois at Urbana-Champaign
1406 W. Green Street, Urbana, IL 61801, USA
E-mail: cangella@uiuc.edu

Electromagnetic modeling for the anticipation of both external and internal electromagnetic interference and compatibility difficulties in integrated electronic systems is rapidly emerging as one of the key enabling technologies in the quest for virtual prototyping of multi-functional, performance-driven electronic products. Despite their usefulness and versatility as point tools for RF/microwave component design and modeling of fairly small-size portions of an integrated electronic system, state-of-the-art electromagnetic field solvers today do not exhibit the computational efficiency required for tackling numerical electromagnetic modeling and simulation at the system level. Thus, in their current form they are not suitable for use as computer-aided design (CAD) tools for the EMI/EMC-related system level modeling and simulation studies discussed in the previous paragraph.

To address this shortcoming of state-of-the-art EM modeling CAD tools, the electrical modeling and simulation community has been exploring hybrid modeling and simulation methodologies that, through the use of physical model complexity reduction, attempt to blend together different electromagnetic models for different portions of the integrated system for the purpose of enabling system-level electromagnetic performance assessment. To date, these efforts have focused primarily on the so-called "signal integrity" portion of the intra-system EMI/EMC problem, where the emphasis is on the prediction of crosstalk-related signal degradation in the interconnect structure and the simultaneous switching noise effects associated with power distribution. However, no systematic approaches have been put forth toward the extension of such a hybrid modeling methodology to encompass radiated emissions and radiated susceptibility.

In this paper, an approach is described toward the establishment of an enhanced hybrid electromagnetic modeling framework that extends the aforementioned signal integrity-driven modeling and simulation methodology to a more comprehensive EMI/EMC-driven one. The proposed approach is capable of tackling the complexity of state-of-the-art integrated electronics while at the same time providing the accuracy needed to support and facilitate product design. The modeling versatility and computational efficiency of the proposed methodology are based on the introduction of reduced physical models for the shielded portion of the signal network as well as the power distribution network. The approximations used for the construction of the proposed reduced models are motivated by the geometric attributes of the printed circuit board environment. A careful development of the hybrid model leads to accurate electromagnetic analysis of printed circuit boards of complexity that cannot be handled by state-of-the-art electromagnetic field solvers.

0-7803-7846-6/03/$17.00 ©2003 IEEE

# Design and Simulation of an EM-Fault-Tolerant Processor with Micro-Rollback, Control-Flow Checking and ECC

Franco Trovo, Shantanu Dutt* and Hasan Arslan
Dept. of Electrical & Computer Engr., University of Illinois at Chicago

Electromagnetic (EM) radiation can cause significant disruption to computer systems as demonstrated in previous works. Previous research dealing with fault detection and tolerance in digital and computer systems have typically considered one to two random faults occurring at a time, arising mainly from operational problems like electromigration, transistor malfunction due to, say, heating, and random noise events. For such disruptions, single or double random faults are indeed a reasonable fault assumption and also makes its analysis and simulation tractable. While data on the fault-extent and fault-pattern caused by EM disruption is not completely available, we postulate that most EM disruptions will result in multiple clustered faults, and further that external (i.e., off-chip) wiring, like, memory address and data buses, and input/output buses are most vulnerable to such disruptions. With these assumptions, we have developed and simulated a processor system that can withstand such fault patterns to a reasonable degree.

The core of our error detection mechanisms are: 1) Hamming error-correcting coding (ECC) of data/address on the memory data/address buses; 2) Control-flow checking (CFC) of the program under execution by a simple watchdog (WD) processor; 3) Reasonableness checks of addresses on the address bus by the WD; 4) Inherent processor detection of invalid instructions and other exceptions (e.g., divide-by-zero). The fault tolerance (FT) mechanism we have used is *microrollback*. In this technique, the "commitment" of the processor state (internal special registers, register file, cache and main memory contents) after each instruction execution is delayed via FIFO buffers interfacing with these storage entities by a maximum of $d$ instruction cycles. Two of the above four detection techniques (ECC and CFC) are coupled to the microrollback , and when either detects an error, the microrollback unit rolls back the processor states to the one existing $i$ instructions earlier, where $i$ is the maximum error detection latency of the particular scheme that detected the error (the maximum rollback distance $d$ is chosen to be the maximum of the maximum error latencies of the two detection mechanisms). The processor thus resumes execution from a point just prior to the fault event that caused the error. We believe this can be an effective FT technique for EM disruptions, because "malignant" EM radiation is characterized by short-duration repeating pulse trains. Each such pulse train can cause transient errors in the data/address on the memory buses which can be recovered from via the microrollback mechanism if the errors are detected by the above methods.

We implemented the above fault detection and tolerance mechanisms in VHDL for the Motorola 68040 processor. We simulated a variety of fault patterns and numbers on both memory buses ranging from two random faults to 4-bit cluster faults that we believe could be typical of fault patterns caused by EM radiation. We also simulated various frequencies of EM pulse-train repetition ranging from the most disruptive (one pulse train every bus clock cycle) to a low disruptive one (one pulse train every 100 bus clock cycle). Our current simulation results (we are in the process of tuning and improving our techniques) reveal that the program we ran (matrix multiplication) completed correctly under these fault environments and the above fault detection and tolerance methods between 67-100% of the time. The program finishes incorrectly only 0-16% of the time, while for the rest of the runs it does not finish; most probably this is due to the program getting into an infinite loop, and this can be detected by a timeout mechanism and the program can be stopped in a "fail-safe" manner. These results are promising and demonstrate that our techniques could be effective in protecting computer systems from actual EM disruptions.

0-7803-7846-6/03/$17.00 ©2003 IEEE 

# Functional and Communications Theory Models in Susceptibility Analysis

I. Kohlberg*
Institute for Defense Analyses, 1801 N. Beauregard, Alexandria, VA 22311
703-578-2744, Email: ikohlber@ida.org

R. L. Gardner, Consultant
6152 Manchester Park Circle, Alexandria, VA 22310
703-924-9370, Email: Robert.L.Gardner@verizon.net

Modeling the failure of electronic systems from incident electromagnetic wave is a challenging enterprise that requires the combination of several disciplines including very complex boundary value problems along with models of the function of the electronics. Various digital systems are of interest. In particular, those systems consist of processors that communicate with each other over a variety of means including computer buses and network links. The analysis of their susceptibility to unwanted electromagnetic signals differs greatly, depending, for example, on structure, protocols, bandwidth, and electromagnetic environment. In this paper, we will consider two approaches to that model. The first is the use of information theory to look at the consequences of interruption of the information flow in the system. In the second, we will consider the consequences of functional or block failure in a system. The latter is important in systems that cascade information or function such as SCADAs and digital control systems.

Bus systems are a critical part of any digital system. Information flow on those systems is critical to their function and can be interrupted by noise on the bus system. Buses are sufficiently large that the form effective antennas and enhance coupling. In this analysis, the buses are treated as discrete dynamic systems excited by continuous variable dynamic systems. The complexity of the analysis is increased by error correction techniques used to protect the integrity of these systems.

In extended electronic systems, particularly real time systems, data is first retrieved from a remote sensor or processor. That data is processed, decisions made, and control signals are sent out to remote parts of the system, including the original sensor or processor. Any of the various subsystems can fail with often complex consequences. Analysis of the susceptibility of the subsystems can be simpler than the system as a whole, so the division contributes to the ability of the analyst to make a failure prediction.

0-7803-7846-6/03/$17.00 ©2003 IEEE

# Engineering Trades For Combining Coupling Models and Empirical Effects Data in Susceptibility Analysis

R. L. Gardner, Consultant*
6152 Manchester Park Circle, Alexandria, VA 22310
703-924-9370, Email: Robert.L.Gardner@verizon.net

I. Kohlberg
Institute for Defense Analyses, 1801 N. Beauregard, Alexandria, VA 22311
703-578-2744, Email: ikohlber@ida.org

C. A. Ropiak
Envisioneering, Inc., Suite 46, 4485 Danube, King George, VA 22485
540-653-2717 Email: CRopiak@earthlink.net

When dealing with susceptibility predictions, the analyst must, at some point, resort to empirical results to complete the analysis. One limit is to use the empirical results for individual device failure and use various analysis techniques to perform the coupling calculation to the device level. This process places severe strain on the coupling analysis requiring predictions to the sub millimeter level that would require knowing the geometry to that level. At the other limit, one can perform the entire effects analysis empirically, with an observation of failure for a particular set of test conditions. This empirical process can require an unaffordable number of tests to complete a useful experiment matrix.

Digital systems consist of a number of building blocks. These building blocks consist of two processing and storage devices that take data, process and send it over a bus to another similar unit. Upset can occur if the communication is interrupted, the processing is corrupted or the stored data is changed. Buses consist of long (compared to the devices) conductors and hence act as antennas for coupling. The processing and storage devices are form a nonlinear, time dependent and sometimes active load on each of the elements of the line.

There are two compromise approaches that lie between the device level and system level empirical approaches. One of these approaches uses a functional model of the electronics to predict failure for a set of calculable conditions. There are a variety of functional models that are most applicable to predicting upset in a complex digital system. The other approach is to use analytical techniques to predict the currents at ports and use current injection for the empirical part.

In this paper, we will compare and contrast each of these approaches by estimating the cost and potential benefit of each one.

0-7803-7846-6/03/$17.00 ©2003 IEEE 

## Propagation Modeling

**Co-Chairs:** M. Newkirk
R. Janaswamy

1:15 Opening Remarks

# Refinement of Helicopter-Based Evaporation Duct Calculations

G.D. Dockery and M.H. Newkirk*

The Johns Hopkins University Applied Physics Laboratory
11100 Johns Hopkins Road
Laurel, MD 20723

For the past 20 years, the Johns Hopkins University Applied Physics Laboratory (JHU/APL) has been continually developing a set of helicopter instrumentation that is used to collect environmental data needed to calculate refractivity profiles that vary in range and height. These refractivity profiles are important inputs to propagation models, as the mechanism to include the effects of ducting and other non-standard conditions on electromagnetic propagation. More recently, the system was given additional capability by including sensors that are appropriate for measuring the parameters needed for evaporation duct calculations. This new system is currently being built to replace the older JHU/APL-built system that has been used for more than ten years by the Naval Air Warfare Center (NAWC) at Pt. Mugu, CA, to support US Navy radar system testing at several sites around the country. As this new system is transferred to the Navy for regular use, an assessment of its capabilities for estimating evaporation duct is warranted.

Building on the work in this area that was presented at the 2002 USNC/URSI Winter Meeting, this presentation will describe the sensor and data collection systems, along with the procedures used to collect data for the evaporation duct and vertical profile applications. In addition, the algorithms necessary to reduce these data to the bulk parameters needed by evaporation duct models will be described. The JHU/APL project boat *Chessie* recently collected data specifically for this purpose during planned helicopter operations, and these data will be used to compute benchmark evaporation duct heights against which the helicopter-derived estimates will be compared. The Liu-Katsaros-Businger (LKB), Constant Virtual Temperature (CVT) and Paulus-Jeske (PJ) models will be used for these comparisons. Finally, a brief discussion will be given on how these helicopter-derived evaporation duct parameters are used in the processing of this system's traditional vertical profile data.

0-7803-7846-6/03/$17.00 ©2003 IEEE

# Efficient FDTD Technique for Calculating Diffraction by Infinite Three-Dimensional Material Wedges

**Jiuan-Her Grace Chang* and Allen Taflove**
Department of Electrical and Computer Engineering
Northwestern University, Evanston, IL 60208

Wireless communication systems ideally provide contiguous coverage for mobile users in the geographical areas served. A combination of software planning tools and on-site measurements is used to determine the location and type of radio equipment that is required to achieve this goal. In urban environments, where cells are small, planning tools usually employ deterministic prediction models. Here, scattering objects such as building walls, wall corners, and rooftops are fairly well defined, and the accurate estimation of radio wave diffraction from such scattering objects becomes very important.

To this end, we have developed the generalized total-field/scattered-field (G-TF/SF) formulation of the finite-difference time-domain (FDTD) method. This technique permits modeling an infinite material wedge inside a compact three-dimensional (3-D) FDTD grid to efficiently obtain numerical diffraction coefficients. The G-TF/SF boundary is located in part within the perfectly matched layer (PML) absorbing boundary region of the FDTD grid. This allows: (1) sourcing a numerical plane wave with an arbitrary incident angle traveling into, or originating from, the PML; and (2) terminating the infinite wedge inside the PML with negligible reflection.

To validate our approach, we compare analytical diffraction coefficients for an infinite, 3-D right-angle PEC wedge obtained using the geometrical theory of diffraction (GTD) with numerical results obtained using the G-TF/SF formulation of FDTD. Then, we apply the G-TF/SF formulation to calculate numerical diffraction coefficients for a 3-D infinite right-angle dielectric wedge, covering a wide range of incident and scattering angles. Finally, we show means to compactly store the FDTD-calculated diffraction coefficients in a manner which permits: (1) easy interpolation of the results for arbitrary incidence and observation angles; and (2) straightforward interfacing with cellular planning software.

0-7803-7846-6/03/$17.00 ©2003 IEEE 

# Electromagnetic Scattering Analysis from the Terrain Profiles Using BiConjugate Gradient Method

Barış Babaoğlu*, Ayhan Altıntaş, Vakur B. Ertürk
Dept. of Electrical-Electronics Engineering
Bilkent University, TR-06533, Bilkent, Ankara, Turkey

Many propagation models have been introduced in the last three decades. Geometrical theory of diffraction (GTD) is a high frequency based method and concerns the wedge diffraction of the objects. Although the computed results using this method agree well with the experimental data, modeling the terrain profile is very complicated resulting a considerably long computation time. Another proposed approach is the parabolic wave equation (PWE) depending on the Helmholtz equations. This method provides fast computational analysis at the cost of accuracy such that it gives importance to the forward propagating fields and neglects the backscattered ones. An alternative propagation model is an integral equation (IE) method that is based on a method of moments (MoM) formulation. An IE is formed by applying the boundary conditions on the scattered surfaces and is solved via MoM. However, MoM type solutions suffer from both storage and CPU time requirements, since a very large number of unknowns N is required for the recognition of the terrain profile of interest. The conventional MoM requires an operation count of $O(N^3)$ for matrix inversion, whereas iterative techniques such as Bi-Conjugate Gradient (BiCG) have a computational complexity $O(N^2)$ for matrix-vector product per iteration. In order to reduce the computational cost and storage requirements, a novel scheme, named novel spectral acceleration (NSA) is proposed, (J. T Johnson and H-Chou, *Radio Science*, vol. 33, no. 5, 1277-1287, 1998) which accelerates the matrix-vector products and is based on the spectral representation of 2D Green's function. Although NSA is well suited for the forward backward method (FBM) that it proceeds the forward and backward sweeps of the propagating fields, it can also be used in any standard iterative method like BiCG algorithm.

The purpose of this study is to obtain an efficient and accurate simulation tool that can handle wave propagation over the terrain profiles in the rural areas. For the reliability, the results will be compared with ITU-R 1546 curves scanning a distance from 1 to 1000 km. The numerical algorithm is based on BiCG method in conjunction with NSA so that the operation count is reduced to $O(N)$. Some preliminary results for slightly rough surfaces with height deviations small compared to $\lambda_0$ ($\lambda_0$ being the free-space wave length) are given and compared with a conventional MoM approach ($\lambda_0$ = 1m & pulse width = $\lambda$ / 10). Results to more general terrain profiles and their comparisons with the measurements will be presented at the conference. The aim is to reach large distances at UHF / VHF bands. This study on the terrain profiles has also been treated in the literature (J. A. Lopez, M.R. Pino, F. Obellerio, and J. L. Rodriguez, *J. Electromagn. Waves and Appl.*, vol. 15, no. 8, pp. 1049-1074, 2001) with FBM but BİCG has never been applied to such a system. Although the number of iterations to reach to the exact solution is larger than the FBM, BiCG is more robust in many situations and endures divergence problem. Especially in transverse electric (TE) case, the residual error stays fixed after a few iterations for FBM. BiCG, however, still decreases the error at each iteration.

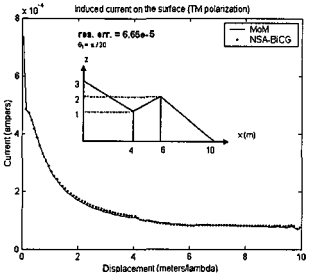


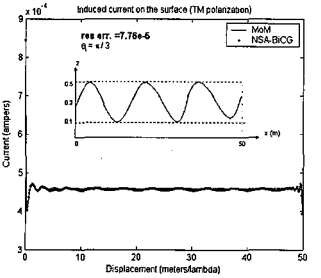


0-7803-7846-6/03/$17.00 ©2003 IEEE

# Efficient Method of Moments Approach for Propagation Over a Rough Surface

A. R. Hayslip and J. T. Johnson
ElectroScience Laboratory, The Ohio State University

Predicting electromagnetic (EM) propagation over terrain or sea surfaces is essential in many practical areas. EM rough surface scattering is of sufficient complexity that a robust analytic solution has yet to be discovered. Hence to solve such a problem it is often necessary to turn to numerical methods. Traditional numerical electromagnetic codes based on the method of moments would require a sample spacing of approximately $\lambda/8$, where $\lambda$ refers to the incident field's wavelength. This requirement places a limitation on the size of the problem that can be solved, even for recent more efficient algorithms.

A method of moments algorithm seeks to solve the field integral equations by assuming the unknown current embedded in the integral can be expanded into a series of basis functions. The sampling requirement is necessary to minimize the error in the series representation from the actual current. If the actual current were a relatively smooth varying function on the surface then fewer basis functions would be needed, which means fewer points per wavelength. The parabolic wave equation method suggests that surface currents should be slowly varying on rough surfaces containing only large-scale features if the incident field phase is removed. Thus, as in (Voronovich and Zavoronty, *IEEE Trans. Geosci. Remote Sens.*, **38**, 366-373, 2000), the following form shall be assumed for the currents

$$J\left(\vec{\rho}\right) = \sum_n c_n e^{j\vec{k}\cdot\vec{\rho}} p_n\left(x\right)$$

where the $p_n(x)$ represent pulses define to be unity on the $n^{th}$ segment of a rough surface divided into $N$ pieces and zero elsewhere. The vector $\vec{k}$ is the incident wave vector $\vec{\rho}$ and is the cylindrical spatial coordinate, while $x$ is the rectangular spatial coordinate. Using this choice for the basis functions it is possible to get accurate representation for the currents while sampling the surface much more sparsely. It is necessary, however, to perform integrations to obtain the matrix elements, and then proceed to invert the matrix either iteratively or directly.

Results from a numerical code will be used to observe propagation effects on electromagnetic signals over both terrain and sea surfaces. Analysis of this method's efficiency as compared to other approaches will also be discussed.

0-7803-7846-6/03/$17.00 ©2003 IEEE

# Use of Complex Refractive Index for Domain Termination in Split-Step PE Solutions

Zhiguo Lai* and Ramakrishna Janaswamy
Department of Electrical & Computer Engineering
215-D Marcus Hall, University of Massachusetts
Amherst, MA 01003-9292, USA
Email: zhlai@ecs.umass.edu; janaswamy@ecs.umass.edu

The parabolic equation (PE) technique is widely used in the study of wave propagation over earth and inhomogeneous atmosphere. One of the unresolved challenges is the proper truncation of the domain in the split-step Fourier solution of the PE, particularly for wide angles of propagation such as encountered over irregular terrain or with ground-to-air terminals. Most of the previous studies have used shaping windows in the spatial and wavenumber domains to accomplish this (M. Levy, "Parabolic Equation Methods for Electromagnetic Wave Propagation", IEE, 2000), although the use of a complex refractive index has been mentioned in (F. B. Jensen, *et al.*, "Computational Ocean Acoustics", AIP, 1994). In this work we consider a complex refractive index to gradually attenuate the fields at large altitudes and study its performance on the overall solution. The refractive index in most of the computational domain is equal to the actual refractive index, while an artificial imaginary part is added near the upper boundary. This lossy layer is uniform in the range direction ($x$-axis) but has a varying profile in the vertical direction ($z$-axis). Three different vertical profiles (linear, quadratic, and exponential model) for the modified refractivity are compared. The results show that all of them work well when the maximum magnitude of the modified refractivity is about two orders of magnitude or more. Furthermore the absorption layer needs to have a height of ¼ of the maximum atmosphere height. Instead of adding complex part to the refractive index, a Hanning window may also be used in the $z$-domain. The results show that in most cases use of the complex refractive index is superior to the Hanning window. A Gaussian beam antenna with variable beam-width and scan-angle and both narrow- and wide-angle PEs are considered in the study.

0-7803-7846-6/03/$17.00 ©2003 IEEE 

# Validation of the ABT scattering prediction method for the analysis of complex environment.

E. Di Giampaolo[1], F. Mioc[2], R. Chovanec [3], F. Bardati[3], M. Sabbadini[4], L. J. Foged[2]

[1] *DIEL, Università dell'Aquila, Monteluco, 67100 L'Aquila, Italy*
[2] *SATIMO, Via di Trigoria 86, 00128 Roma, Italy*
[3] *DISP, Università di Roma Tor Vergata, via del Politecnico 1, 00199 Roma, Italy*
[4] *European Space Agency, ESTEC, Keplerlaan 1, P.O. Box 299, AG Noordwijk ZH, The Netherlands*

Characterising antenna performances in real environments is a need in most applicative areas and the capability of assessing the effects of antenna interaction with the environment during design phases is becoming crucial in several of them. In particular, for space applications the problem of assessing interference levels on platforms are often addressed by resorting to lengthy measurement campaigns taking place in the later stages of the satellite development resulting in high costs and significant programmatic risks or on dedicated models when the information is needed during antenna development.

A new approach to the problem, based on the tight combination of measurement and prediction tools has been developed by combining fast and relative inexpensive near field measurements capabilities (P.O. Inversen, *et al., IEEE Antennas an Propagation Magazine*, 43, 90-94, 2000 ) with an efficient algorithm for GTD analysis (E. Di Giampaolo *et al., J. Electromagnetic Wave Applications*, 15, 439-460, 2001). The Astigmatic Beam Tracer (ABT) is a forward ray racer technique based on a complete angular partition of 3-D space with beams able to trace the propagation of radiated energy starting from the description of outgoing waves on a closed surface surrounding the sources of the electromagnetic field.

This approach offers the possibility to obtain almost real time numerical assessment of the antenna behaviour in its final operational complex environment from near field measurement of the isolated real antenna. Fundamental aspects to be assessed in this context are the accuracy of the system predictive component and the time efficiency of the combined process (measurement + analysis).

Accuracy and time efficiency aspects are validated by measurements on appropriate breadboards. In order to achieve the desired objective these breadboard models are designed to probe the most delicate aspects of GTD/UTD based algorithms, rather than focusing only on overall accuracy in a realistic reconstruction of typical operational environments. In this way it is possible to individually assess the various sources of error, compare it with error estimates based on the algorithm characteristics and use this information to build an overall error budget, also including the measurement error.

In the frame of this work the methodology and results of the validation activity will be presented.

0-7803-7846-6/03/$17.00 ©2003 IEEE

# Propagation and Coverage Analysis over Terrain Profiles comparing Empirical Approaches with Exact Solutions

Celal Alp Tunç*, Ayhan Altıntaş, Vakur B. Ertürk
Dept. of Electrical-Electronics Engineering
Bilkent University, TR-06533, Bilkent, Ankara, Turkey

Mobile radio planning requires the accurate prediction of electromagnetic field strengths over large areas and in a wide variety of environments. There are empirical, intuitive and deterministic approaches for predicting field patterns such as ITU curves, diffraction loss methods, UTD, GTD and parabolic wave equation method. All approaches to the radio propagation prediction present a similar behavior, although they do not give numerically or analytically exact results. In this regard, the problem is concerned with finding solutions and direct approaches to Maxwell's equations, such as integral equation based approaches. Since the numerically exact propagation models could be used to check solutions as a reference, integral equation based methods become desirable. The Forward-Backward method is a powerful numerical technique which is proposed by Holliday *et al.* (*IEEE Trans. Antennas and Propagat.*, vol. 44, pp. 722-729, May 1996) for ocean-like surfaces. Although the Forward-Backward method obtains very accurate results after few iterations, the computational cost for the method is $O(N^2)$. A spectral acceleration algorithm was proposed by Chou and Johnson (*Radio Science,* vol. 33, no. 5, 1277-1287, 1998) for perfectly electrical conducting and impedance ocean-like rough surfaces reducing this cost to $O(N)$. Since the original acceleration becomes not suitable for very undulating geometries, it is modified and adapted to the wave propagation over very undulating surfaces such as terrain profiles by López et al. (*J. of Electrmagn. Waves and Appl.*, vol. 15, No. 8, pp. 1049-1074, 2001). The operational count is reduced to $O(N)$ for undulating surfaces by this modified acceleration algorithm.

In this paper different radio propagation prediction approaches will be compared with reference solutions for larger distances at UHF frequencies. Propagation prediction models are applied over terrain profiles with the help of a computer tool developed at the Bilkent University Communications and Spectrum Management Research Center. The tool is an integrated spectrum engineering and planning software for the simulation, planning and analysis of radio spectrum from 10 kHz to 40 GHz. The coverage analysis of any terrain profile can be made due to empirical, heuristic and deterministic techniques. Various propagation models can be employed for different frequency bands. In the VHF and UHF bands, ITU propagation curves, Okumura–Hata, Walfish-Ikegami or ITU Rec. 529 and 1146 models can be readily employed. Diffraction correction to some of these models can also be chosen. Epstein–Peterson, Deygout and Vogler methods are available for the diffraction correction. The studies are done on a circular sector around the transmitter which is formed by radial paths. In order to improve the accuracy of these propagation models, propagation and coverage analysis results over different terrain profiles will be compared with reference solutions obtained using FB/SA. For certain terrain profiles which this method can not handle, the Generalized FB/SA method will be used.

0-7803-7846-6/03/$17.00 ©2003 IEEE

# IMPROVEMENTS OF THE *PIRAM* BULK MODEL TO CALCULATE REFRACTIVITY PROFILES WITHIN THE MARINE SURFACE BOUNDARY LAYER.

**Jacques CLAVERIE**
LESTP & IETR –CREC St-Cyr - 56381 GUER CEDEX - FRANCE
Email : jacques.claverie@st-cyr.terre.defense.gouv.fr

## INTRODUCTION

Within the Marine Surface Boundary Layer (MSBL), the vertical refractivity profile is rarely standard. At radiofrequencies (RF), the evaporation duct strongly modifies the low altitude radar coverage diagrams. At optical wavelengths, the most frequent propagation mechanism is subrefraction which limits the detection range of electro-optical (EO) sensors and leads to mirage effects.

## REFRACTIVITY PROFILES MODELING

The French *PIRAM* model uses a *bulk* method based upon Monin-Obukhov similarity theory (J. Claverie et al., *AGARD-CP-567*, pp 29-1/29-11, 1995). From in situ simple meteorological measurements, it computes the vertical refractivity profiles for RF bands, as well as for optical bands. Without any major difficulty, the method can be extended to determine the refractive index structure constant ($C_n^2$) vertical profiles within the MSBL.
PIRAM generally leads to very satisfactory agreements between propagation modeling and measurements concerning radar data (H.J.M. Heemskerk, *5th Int. Radar Conf. Proceedings*, Brest (FR), 1999) and EO data (J. Claverie et al., *RTO-MP-1*, pp 5-1/5-13, 1998).

## IMPROVEMENTS OF THE PIRAM MODEL

For some particular experimental data sets, the results provided by the actual PIRAM version did not match very well with the observed values (J. Claverie and Y. Hurtaud, *AP200 Conf.*, Davos (CH), 2000). Significant improvements of the model have been achieved by :

- Changing the stability functions needed in the vertical profiles expressions and changing also the roughness lengths calculation.
- Modifying the *bulk* profiles near the sea surface, in order to take into account the interactions between the lower atmosphere and the wave field.

As the PIRAM model concerns the first tens of meter above the sea surface, it is of major interest to be able to link our computed profiles with upper air data. These upper air data may come from radiosondes measurements or from meteorological mesoscale models. So, our actual modifications of the PIRAM model, also concerns the feasibility of generating what we could call *hybrid vertical refractivity profiles*.

0-7803-7846-6/03/$17.00 ©2003 IEEE

# MatLab Software Package for Propagation Data Pre-Processing

Armando Rocha*, Prof, University of Aveiro, arocha@det.ua.pt
José Pinto,Eng., Anacom, Lisbon
Miguel Matos, Eng, PT, Aveiro

## Abstract

Hydrometeors, gases and refractive index inhomogeneities cause the main propagation impairments on microwave terrestrial or satellite links. While the interactions of the wave are well known, a full statistical description of static and dynamic parameters of attenuation, depolarisation and scintillation require long term measurements and extensive data analysis due to climatic factors.

Following our participation on Olympus propagation campaign we prepared also for the already failed STENTOR campaign (STENTOR was destroyed on recently Ariane V launch) by developing a tool for pre-processing data analysis. The software tool is quite intuitive software developed in MatLab that allows an easy conversion of daily raw acquired data to attenuation and XPD time series.

Presentation is structured according the following mainlines:

- The requirements of the software tool ranging from data display, user interaction with the data and main facilities to be implemented are highlighted
- The software modules and procedures developed mainly:
  - Data loading and calibration
  - Inspection, classification and repairing
  - XPD and attenuation templates extraction using several approaches
  - Bias removal and data quality assessment
  - Data archiving oriented from several points of view: full data, events, etc
- Results and performance

Conclusions show that this software approach, using Matlab graphical facilities and a modern PC, is an excellent tool to perform data pre-processing tasks. These tasks were often made on a per event basis time-consuming sessions or with programs difficult to tailor to user needs or to debug and with a poor interface.

0-7803-7846-6/03/$17.00 ©2003 IEEE

# Effects of Out-of-Plane Terrain Slopes on Tropospheric Radar Propagation – Theory and Modeling

R. S. Awadallah*, J. Z. Gehman, J. R. Kuttler, and M. H. Newkirk
Johns Hopkins University Applied Physics Laboratory
Laurel, MD

Numerical simulation of long-distance tropospheric radar propagation is usually performed by marching the propagating field forward from the source to the receiver using either Fourier transform or finite difference techniques. The equation governing the field is a one-way parabolic wave equation subject to the terrain boundary condition in addition to an absorption condition, which is enforced on the boundaries of the numerical domain to prevent reflection artifacts.

In order to facilitate efficient propagation calculations over long distances (hundreds of kilometers), several approximations of the original problem have been proposed. An important approximation among these is the assumption that the lateral terrain variations along the great circle connecting the transmitter and the receiver are negligible. This approximation effectively reduces the original vector 3D problem into a scalar, efficiently solvable 2D problem. The latter problem is then transformed from the original spherical geometry to a Cartesian geometry via the appropriate conformal map and solved via one of the aforementioned marching techniques. It is obvious that such an approximation amounts to ignoring the effects of the lateral (cross-range) terrain slopes on the propagating field. These effects, which include depolarization, lateral diffraction and shadowing, may become prominent for steep cross-range terrain slopes.

In this paper we describe a 3D vector propagation model (VEMPE) that was developed to investigate the effects of lateral terrain variations on radar coverage. In this model, the parabolic wave equations governing the three Cartesian components of the vector electric (magnetic) field, and the terrain boundary condition, which couples these field components, are discretized using the finite-difference method. Close to the terrain, the coupled system of equations is solved using an efficient sparse-matrix bi-conjugate gradient method. Away from the terrain, the field components are independent and the solution is carried out via the alternating direction implicit method (ADI). Perfectly matched layers are used to prevent reflection artifacts from numerical boundaries.

We conclude by describing a common approach for generating quasi-3D results using a 2D propagation code. This approach propagates several 2D fields to create vertical slices that sample the 3D environment. Slices emanate radially from the source position, and each slice's 2D source field represents a different cut through the 3D source distribution. In our implementation, azimuthal separation between slices and 2D-propagation range/altitude calculation increments are selected to make the quasi-3D solution grid as coincident as possible with the VEMPE solution grid.

0-7803-7846-6/03/$17.00 ©2003 IEEE 

# Effects of Out-of-Plane Terrain Slopes on Tropospheric Radar Propagation – Results and Applications

J. Z. Gehman*, R. S. Awadallah, J. R. Kuttler, and M. H. Newkirk
Johns Hopkins University Applied Physics Laboratory
Laurel, MD

The two dimensional (2D) parabolic equation has become a powerful tool for modeling radar propagation over terrain. The efficiency afforded by a 2D approximation allows one to model propagation over hundreds of kilometers using Fourier split-step marching techniques; however, the cost is that effects of lateral terrain slopes are ignored. While this limitation is well known, its implications have not yet been adequately quantified.

In this paper we use our recently-developed Vector Electromagnetic Parabolic Equation (VEMPE) code to investigate the effects of lateral terrain variations on radar propagation. These effects are assessed by comparing VEMPE's 3D results to results from our popular 2D propagation code, the Tropospheric Electromagnetic Parabolic Equation Routine (TEMPER). Quasi-3D results are obtained from TEMPER by generating 2D solutions across multiple slices in azimuth. Because this quasi-3D approach is a common way of representing realistic environments in practical radar simulations, lessons learned from our comparisons have direct implications for current radar clutter and radar performance models.

Numerical examples that involve simple urban-like terrain are presented. Full 3D modeling of propagation through rectangular structures reveals salient 3D scattering effects, such as horizontal interference patterns, that are absent from the quasi-3D results. We then present cases involving propagation over realistic terrain environments that have been created from digital elevation maps (DEM's). Numerical issues involved in performing these realistic terrain calculations, such as DEM resolution, terrain slope limitations and domain size, are discussed. Results from these cases are then examined and related to potential improvements in practical radar clutter modeling.

0-7803-7846-6/03/$17.00 ©2003 IEEE

# MULTIPATH RADAR PROPAGATION MODELING: ASSESSMENT OF THE MILLER-BROWN APPROXIMATION

D. E. Freund*, N. E. Woods, H.-C. Ku, and R. S. Awadallah
Johns Hopkins University Applied Physics Laboratory
11100 Johns Hopkins Road
Laurel, MD. 20723

In order to reliably predict over the horizon radar coverage within an ocean environment, one must accurately account for the effects of ocean roughness on radar propagation. The method often referred to as the Miller-Brown approximation is currently one of the most widely used techniques for computing the coherent field reflected by a rough surface and it is often incorporated into sophisticated numerical propagation models such as the Fourier split step algorithm of the parabolic wave equation. Nevertheless, the accuracy and region of validity of the Miller-Brown approximation has never been systematically and rigorously assessed for realistic scenarios of interest to shipboard radars. We present here a first step toward this assessment by using an exact numerical method of moments (MoM) solution to compute the propagation factor, $\eta$, for a rough ocean surface and then compare the exact MoM results with the corresponding predictions for $\eta$ obtained using the Miller-Brown approximation. The particular MoM technique used here combines an accelerated spectral (steepest decent path) method and a multigrid iterative approach and will be referred to simply as the multigrid iterative approach (MGIA).

All calculations were performed at $S$ band ($f = 3$ GHz) using a horizontally polarized line source (cylindrical wave) for the incident field. A Monte-Carlo approach was used for the MGIA calculations in which the ensemble average of the propagation factor is computed for 50 rough sea surface realizations. Specifically, for each of three different wind speeds, 50 1-D realizations of rough sea surfaces were generated using the 1-D Bjerkaas-Riedel surface-wave spectrum. A temperature and salinity-dependent Debye relaxation model was used to assign all surfaces dielectric properties that are in accord with seawater. Comparisons between $\eta_{MGIA}$ and $\eta_{MB}$ are presented as a function of elevation angle at fixed ranges of 1km and 5km from the source.

0-7803-7846-6/03/$17.00 ©2003 IEEE 

*Special Session*

## Advanced Finite Methods in Electromagnetics

**Organizer(s):**
**Co-Chairs:** R. Dyczij-Edlinger
D. K. Sun

1:15 Opening Remarks

37. 1 1:20 Ultra-fast Finite Element Simulation of Planar Electromagnetic Structures ..... APS
*J. E. Bracken, S. Polstyanko, Z. J. Cendes, Ansoft Corp., USA*

37. 2 1:40 Perfectly Nested Finite Element Spaces using Generalized Hanging Variables ..... APS
*V. Hill, O. Farle, R. Dyczij-Edlinger, Saarland University, Germany*

37. 3 2:00 P-adaptive FE-BI Analysis of Homogeneous, Lossy Regions for SAR- and Far-field Calculations ..... APS
*M. M. Botha, D. B. Davidson, University of Stellenbosch, South Africa*

37. 4 2:20 Speed Up the Hybrid FEM+IE Formulation using a Low-rank Matrix Approximation ... APS
*M. Vouvakis, S. Lee, J. Lee, OSU, USA*

37. 5 2:40 Jacobi-Davidson-Type Algorithms with Interior Multigrid-Scheme for the Simulation of Electromagnetic Resonator Structures with Gyromagnetic Materials ..... APS
*M. Clemens, S. Feigh, R. Schuhmann, T. Weiland, Technische Universität Darmstadt, Germany*

37. 6 3:00 The Transfinite Element Time-Domain Method ..... APS
*D. Sun, J. Lee, Z. Cendes, Ansoft Corp., USA*

37. 7 3:20 Unstructured-Grid Spectral Method for 3D Maxwell's Equations with Well-Posed PML ..... APS
*T. Xiao, Q. Liu, Duke University, USA*

37. 8 3:40 Conformal Perfectly Matched Layers for the Time Domain Finite Element Method ..... APS
*T. Rylander, J. Jin, University of Illinois at Urbana-Champaign, USA*

37. 9 4:00 Stable Waveguide Ports for the Time Domain Finite Element Method ..... APS
*T. Rylander, J. Jin, University of Illinois at Urbana-Champaign, USA*

37. 10 4:20 Numeric Dispersion Analysis of 3D Envelope-Finite Element (EVFE) Method ..... APS
*W. Yao, Y. Wang, University of California, Los Angeles, USA*

37. 11 4:40 A FIT Matrix Formulation for the Application of Global Boundary Conditions in Frequency Domain ..... APS
*A. Skarlatos, R. Schuhmann, T. Weiland, TU-Darmstadt , Germany*

37. 12 5:00 A MGCR Multiple RHS Preconditioned Solver Applied To the Resolution of a FE-BI Equation with FMM Acceleration .....218
*J. Simon, V. Gobin, ONERA, France*

# A MGCR Multiple RHS Preconditioned Solver Applied to The Resolution of a FE-BI Equation With FMM Acceleration

Jerome Simon, Vincent Gobin*
jerome.simon@onera.fr vincent.gobin@onera.fr
ONERA, Centre de Toulouse, 2 avenue Belin, BP 4025,
31055 Toulouse CEDEX 4, France

Among the various numerical techniques to solve Maxwell Equation, Integral Equations (IE) are one of the most popular and widely applied to study antennas, stealth objects, and the EM Compatibility of systems. The objet mesh is parameterized with N basis functions developing the unknowns electric and/or magnetic currents. The fundamental principal with IE is to evaluate the interaction between each couple of basis functions, leading to a full linear system of size N. With classical algorithm (such as LU), the storage requirement and the CPU time needed to solve the problem scales respectively to $O(N^2)$ and $O(N^3)$. The method is quite insensitive to the number K of right hand sides (RHS) representing the various EM excitations of the object under test, because after factorizing the matrix, the resolution process scales to $O(KN^2)$.

In recent years, the Fast Multilevel Multipole method (FMM) is gaining a wide success in EM computing. The key point is a specific algorithm with allows the evaluation of a matrix vector product scaling to O(NlogN) (it is $O(N^2)$ with standard products). To benefit of FMM speed, one as to replace a classical solver with an iterative solver involving matrix vector products. Unfortunately with multiple RHS, the iterative process as to be restart from beginning with each RHS.

To overcome this problem, we use a GCR (Generalized Conjugate Residual) algorithm because at each iteration the descent vector is evaluated from the residual (with GMRES the residual isn't calculated at each iteration) at there is a explicit perpendicularity of the directions of descent. With a MGCR solver, we solve several RHS simultaneously ; at each iteration the vector of descent is built from a different RHS, for example the one with a maximum residual. With a single matrix-vector product per iteration, MGCR algorithm applied nicely to full matrix, the product been accelerated with FMM. As for any iterative solver a preconditioner can optimize the convergence. In our implementation we use a right side preconditioner.

The MGCR solver has been implemented and tested in two situations : PEC objects and mixed PEC and dielectric objets solved with a FE-BI technique. First, we show that with a single RHS, MGCR converges with a speed equivalent to the widely used GEMRES algorithm. With multiple RHS, various applications illustrate the benefit of MGCR and we obtain a reduction of a factor 6 with MGCR versus independent resolution for each RHS. It has to be noted that this benefit is sensitive to EM nature of the excitations. For example if the excitation is set of plane waves with varying incidences, CPU time reduction is obtained for RHS with the same polarisation (phi or theta). With RHS mixing polarization, the orthogonality of the excitations doesn't lead to any gain and the results are equivalent with 2 separated groups of RHS having same polarisation. Nevertheless, practical application with varying incidences, the MGCR is a quite promising technique.

0-7803-7846-6/03/$17.00 ©2003 IEEE 

## Guided Waves

**Co-Chairs:** R. Nevels
G. Hanson

1:15 Opening Remarks

38. 1 1:20 Dyadic Green's Functions for Circular Waveguide-Based Spatial Power Combining Applications ..... 220
*V. A. Klymko, A. B. Yakovlev, A. A. Kishk, A. W. Glisson, The University of Mississippi, USA*

38. 2 1:40 Discrete Complex Spectrum of 3D Open Omega Waveguides ..... 221
*A. L. Topa, C. R. Paiva, A. M. Barbosa, Instituto Superior Técnico, Portugal*

38. 3 2:00 An Integral Equation Technique for the Determination of Modal Fields in Arbitrary Cross-section Waveguides ..... 222
*G. B. Leal, L. C. Da Silva, Catholic University of Rio de Janeiro, Brazil*

38. 4 2:20 A Generalized ZY Smith Chart for Solving Nonreciprocal Transmission Line Problems ..... 223
*D. TORRUNGRUENG, ASIAN UNIVERSITY OF SCIENCE AND TECHNOLOGY, Thailand*

38. 5 2:40 Finite-Element Solutions with Complimentary Bases Applied To Waveguides ..... 224
*W. A. Davis, Virginia Tech, K. Sitapati, Kollmorgen, USA*

38. 6 3:00 Leaky Wave Effects on Source Driven/Terminated Three-Dimensional Interconnects ..... 225
*G. W. Hanson, University of Wisconsin-Milwaukee, A. B. Yakovlev, The Univeristy of Mississippi, USA*

38. 7 3:20 An Alternative Interpretation of Resonance of Two-aperture Irises in Rectangular Waveguide ..... 226
*J. A. Ruiz-Cruz, J. M. Rebollar, Universidad Politecnica de Madrid, Spain*

38. 8 3:40 Multi-layered Microstrip Line with an Electronically Controlled Phase-Shifter ..... 227
*C. Shin, R. Nevels, Texas A&M University, USA*

38. 9 4:00 Double-Layer Rectangular-Waveguide Structure for Butler Matrix using Slit Coupling on the Broad Walls ..... 228
*J. Hirokawa, Tokyo Institute of Technology, N. Goto, Takushoku University, K. Tsunekawa, NTT DoCoMo Inc., Japan*

38. 10 4:20 A Waveguide Switch using Microwave Photonic Bandgap Substrates ..... 229
*W. Kim, Korea University, Korea*

38. 11 4:40 A Multilayer Active Power Divider using Pseudo Hybrid-Ring and Ground-Slot Coupling Technique ..... 230
*S. C. Hui, B. Ooi, M. S. Leong, B. Wu, National University of Singapore,*

# Dyadic Green's Functions for Circular Waveguide-Based Spatial Power Combining Applications

V.A. Klymko*, A.B. Yakovlev, A.A. Kishk, and A.W. Glisson
Department of Electrical Engineering
The University of Mississippi
University, MS 38677-1848, USA
Phone/Fax: (662) 915-7231
Email: vick@olemiss.edu, yakovlev@olemiss.edu, ahmed@olemiss.edu, aglisson@olemiss.edu

The work described here was motivated by the necessity to develop a modeling environment for the analysis and design of circular waveguide-based amplifier antenna arrays for spatial power combining. In this design, an array of dielectric resonators or printed antennas inside a circular waveguide fed by a hard horn is coupled to MMIC amplifiers by coaxial probe feeds, which eliminates the multimoding effects in amplifier networks and efficiently isolates the receive and transmit antenna arrays. The analysis is based on the integral equation formulation for induced surface current density with dyadic Green's functions of a circular waveguide resulting in a generalized scattering matrix for coupled waveguide transitions.

Traditionally, dyadic Green's functions for closed-boundary circular waveguides are obtained in terms of eigenfunction expansion using Hansen vector wave functions *L*, *M*, and *N*. For the waveguide-based scattering/radiation problem described above, it is convenient to use the eigenmode expansion in terms of TE and TM modes of a circular waveguide. Here we present a procedure of deriving electric-type dyadic Green's functions for an infinite or terminated circular waveguide due to an arbitrarily-oriented electric point source. The components of Green's dyadics are obtained in a series form, where the transverse (cross-sectional) eigenvectors of TE and TM modes are normalized by power and the longitudinal part along the waveguiding direction is obtained in a closed form subject to the fitness condition at infinity or the appropriate boundary condition at a termination. This formulation allows for modeling three-dimensional current sources in a circular waveguide environment and provides a physical insight into the hybrid nature of the scattered field. The numerical experiments on the excitation of different waveguide modes were performed by varying the position, orientation, and amplitude of the point sources, and the convergence of Green's functions was studied in the near-field and far-field regions for a single-mode and overmoded waveguide. The numerical analysis of scattering and radiation characteristics of printed and dielectric resonator antennas operating in a circular waveguide will be shown and discussed in the presentation for a few representative structures.

0-7803-7846-6/03/$17.00 ©2003 IEEE 

# Discrete Complex Spectrum of 3D Open Omega Waveguides

**António L. Topa, Carlos R. Paiva, and Afonso M. Barbosa**

*Instituto de Telecomunicações* and *Instituto Superior Técnico*
Technical University of Lisbon
Av. Rovisco Pais 1, 1049-001 Lisboa, Portugal.
E-mail: antonio.topa@lx.it.pt

Unconventional complex media have new interesting electromagnetic properties that suggest its application in the design of devices and components for microwave and millimeter wave frequencies. The omega medium is obtained by doping a host isotropic medium with omega-shaped conducting microstructures, where the electric and magnetic fields induce both electric and magnetic polarizations perpendicular to each other.

The analysis of planar omega waveguides has been a topic of research in the past (N. Engheta, *Proc. Asia-Pacific Microwave Conference*, 99-111, Yokohama, 1998; A. L. Topa, C. R. Paiva, and A. M. Barbosa, *Progress In Electromagnetic Research*, **18**, EMW Publishing, 85-104, 1998). Emphasis has been put on the analysis of discrete real and complex modes on 2D structures (A. L. Topa, C. R. Paiva, and A. M. Barbosa, *Recent Advances in Electromagnetics of Complex Materials and Metamaterials*, Kluwer, 2003).

The present paper deals with the analysis of 3D omega waveguides. The analysis of 3D omega waveguides requires the characterization of step discontinuities. This problem was analyzed by the present authors using an approximate method, where a limited number of surface modes has been assumed to propagate in each region, coupling to each other at the step sides (A. L. Topa, C. R. Paiva, and A. M. Barbosa, *Proc. PIERS*, 95, Cambridge, 2000).

In this paper we extend the method of Peng and Oliner (S.-T. Peng and A. A. Oliner, *IEEE Trans. Microwave Theory Tech.*, **MTT-29**, 843-855, 1981), which has been used for common dielectric waveguides, to omega waveguides, following the procedure of discretizing the continuous spectrum with a perfect conducting wall placed far above the waveguide. Two types of discrete modes are considered in the uniform planar regions: surface and higher order non-surface waves (some propagating and the remainder nonpropagating). To derive the modal equation of the hybrid modes propagating in the waveguide, the transverse resonance method was applied.

The numerical results show the effect of the inclusion of the omega particles in the propagation constant of the first leaky wave modes. Curves for the phase and leakage constants, as a function of the strip width, are presented for several values of the media parameters.

0-7803-7846-6/03/$17.00 ©2003 IEEE 

# An Integral Equation Technique for the Determination of Modal Fields in Arbitrary Cross-section Waveguides

Gustavo Bevilacqua Leal and Luiz Costa da Silva
Catholic University of Rio de Janeiro
Rua Marques de Sao Vicente 225, Gavea, RJ, Brazil

Several techniques have been applied to the determination of modal fields and cutoff frequencies of arbitrary cross-section waveguides, such as variational methods, finite element method and integral equations. In a typical formulation by integral equations, the metallic walls of the waveguide are replaced by electric current densities in free space, appropriate boundary conditions are applied, and the values of the current densities are calculated by the moment method.

In the present work, it is presented an alternative formulation of the integral equation method, based on dyadic Green's functions of parallel plate waveguides and the moment method. The advantages of the proposed formulation are that it avoids numerical integrations (all integrals are performed analytically) and the modal fields are represented by a single series over orthogonal functions (trigonometric functions). The waveguide under consideration is initially replaced by an equivalent structure where it is circumscribed by a parallel plate waveguide, with horizontal plates, and has its contour approximated by a polygon. It is assumed that a modal wave, with propagation constant $\beta_o$, is propagating inside the arbitrary cross-section waveguide. The surface current density induced on the walls of the waveguide is determined by the moment method. TE and TM modes are considered independently. For the case of TM modes, the induced current flows only in the direction of propagation (z direction), and is expanded into a summation over pulse basis functions: $\vec{J} = \sum_i \alpha_i J_i e^{-j\beta_o z} \hat{a}_z$, where $J_i$ are the pulse functions, $\hat{a}_z$ is the unit vector in the z direction, and $\alpha_i$ are coefficients to be determined. The coefficients $\alpha_i$ are computed by the Galerkin's method. In this computation, the electric fields corresponding to each basis function are determined by with the help of the dyadic Green's functions of the parallel plate waveguide. Due to the functional dependence on z of the basis functions and of the dyadic Green's functions, all the necessary integrations can be performed analytically (using the residue theorem), avoiding approximations and numerical integrations inherent to the use of free space Green's functions. In the case of TE modes, it is assumed that $\beta_o = 0$ (cutoff frequency). The magnetic field has only a z component, and the induced surface current density is transverse to the z direction, $\vec{J} = \sum_i \alpha_i J_i e^{-j\beta_o z} \hat{a}_T$, $\hat{a}_T$ being a unit vector perpendicular to $\hat{a}_z$. The moment method is applied to the determination of $\alpha_i$, considering the boundary condition: $\sum_i k_i H_i = \alpha_j J_j$, here $H_i$ is the magnetic field, due to the ith component of $\vec{J}$, at an observation point on the walls of the waveguide. $\kappa$ is equal to 0.5 (unless $H_i$ is generated by a vertical current density ). This coefficient is necessary since the magnetic fields are expressed as a Fourier series (modal fields of the parallel plate waveguide) of a function with a discontinuity on the surface of the arbitrary cross-section waveguide (the value of the magnetic field changes from $J_j$ to zero). Application of this method to triangular, elliptical and circular waveguides produced good results, with errors less than 0.3% for the first six modes.

0-7803-7846-6/03/$17.00 ©2003 IEEE

# A Generalized $ZY$ Smith Chart for Solving Nonreciprocal Transmission Line Problems

D. Torrungrueng
Asian University of Science and Technology
Dept. of Electrical Engineering
89 Moo 12 Highway 331
Banglamung, Chon Buri, 20260
Thailand
Tel: (6638)754-450 (Ext. 2750)
Fax: (6638)754-460
Email: dtg@asianust.ac.th

The *standard* Smith chart has shown to be a very useful tool when solving *reciprocal* transmission line problems, especially for visualizing transmission line phenomenon. Note that the reciprocal transmission line possesses the *same* propagation constant, $\beta$, and the *same* characteristic impedance, $Z_o$, for propagation in the forward and reverse directions. However, the standard Smith chart needs to be modified for *nonreciprocal* transmission lines, where they possess different propagation constants, $\beta^+$ and $\beta^-$, with corresponding characteristic impedances, $Z_o^+$ and $Z_o^-$, for propagation in the forward and reverse directions, respectively. An example of such a line could be a microstrip transmission line on a magnetized ferrite substrate. In this paper, the standard $ZY$ Smith chart is generalized for nonreciprocal transmission lines.

First, the analysis of nonreciprocal transmission lines terminated in the load impedance $Z_L$ will be given. It can be shown that the reflection coefficient at the load, $\Gamma_L$, is a function of $Z_L$, $Z_o^+$ and $Z_o^-$. Once $\Gamma_L$ is obtained, the equations of resistance and reactance circles can be found analytically, and the *generalized Z* Smith chart can be constructed graphically by plotting a family of those circles on the reflection coefficient complex plane ($\Gamma$ plane). Similarly, the *generalized Y* Smith chart can be constructed by plotting a family of the conductance and susceptance circles on the $\Gamma$ plane, where the equations of these circles can be found from the expression of $\Gamma_L$. It can be shown that the generalized $ZY$ Smith chart reduces to the standard $ZY$ Smith chart when $Z_o^+ = Z_o^- = Z_o$, as expected. Some properties of the generalized $ZY$ Smith chart will be discussed as well. Finally, several cases will be examined to verify the validity of the generalized $ZY$ Smith chart. It is found that results obtained from the generalized $ZY$ Smith chart agree very well with those obtained from direct calculation of associated formulas.

0-7803-7846-6/03/$17.00 ©2003 IEEE

# Finite-Element Solutions with Complimentary Bases Applied to Waveguides

**Dr. William A. Davis*, K. Sitapati**
wadavis@vt.edu, ksitapati@kollmorgen.com
The Bradley Department of Electrical Engineering
Virginia Tech, Blacksburg, VA 24061-0111

This paper describes a new method of obtaining solutions to the modes of propagating electric and magnetic fields of arbitrarily shaped wave-guides loaded with multiple dielectrics. Currently, a large number of solutions to waveguide problems via the finite element method use the vector Helmholtz equation to obtain the modes as well as the electric and magnetic fields. The vector Helmholtz equation is used to obtain either the electric or magnetic field. A new approach to this problem is presented in this paper using a dual equation approach that provides solutions to both the electric and magnetic fields simultaneously as well as the modes.

The required equations for the finite element method are obtained directly from Maxwell's equations using variational principles. Basis functions that are complimentary in nature similar to the complimentary nature of Maxwell's equations are applied to these equations to develop the finite element solution. The vector Helmholtz equation is compared to the complementary variational approach. The variational solution is obtained using the complementary bases to solve for both the fields simultaneously. Several combinations of the complementary basis functions are possible and this paper provides results using different sets of complementary basis functions. A comparison with the solution via the vector Helmholtz equation for the electric field is provided for a circular waveguide. The eigenvectors obtained in the solution represent the fields, with the field patterns shown for several modes.

Previous articles by the authors introduced the complementary bases and its application to magnetostatics. This article provides the extension into dynamics. Specific information regarding the advantages and disadvantages of using the complimentary bases are not covered as it is left to future publications by the same authors.

0-7803-7846-6/03/$17.00 ©2003 IEEE

# Leaky Wave Effects on Source Driven/Terminated Three-Dimensional Interconnects

George W. Hanson*
University of Wisconsin-Milwaukee
3200 N. Cramer Street
Milwaukee, WI 53211
george@uwm.edu

Alexander B. Yakovlev
The University of Mississippi
University, MS 38677
yakovlev@olemiss.edu

Over the past two decades a considerable amount of effort has been devoted to understanding leaky waves on two-dimensional transmission lines integrated into inhomogeneous, planarly-layered media. It is now recognized that virtually all such printed transmission lines can support modes that leak energy into space-waves, surface-waves, or both types of waves. This energy leakage is often considerable as undesirable, resulting in poor transmission quality and spurious coupling, crosstalk, and radiation. There are also applications where this energy leakage is desirable, such as in the design of novel couplers, and in leaky-wave antennas.

Leaky waves on three-dimensional interconnects have received much less attention. In particular, from the two-dimensional analysis it is evident that the exact nature of the current density on the line, together with the value of the propagation constant, plays a critical role in determining if a mode will be leaky or not. However, it is not clear what types of excitations and terminations will lead to currents on three-dimensional interconnects that leak energy. For example, if an interconnect excitation and termination is such that a true transmission line mode is established on the structure, and the interconnect is sufficiently long, energy leakage should correlate well with the effects predicated by the two-dimensional analysis. However, if the interconnect is short, or the current on the structure does not resemble a transmission line mode, leakage effects on the three-dimensional interconnect may be quite different than that predicted by the two-dimensional analysis. In this paper we will investigate several three-dimensional interconnect geometries, with realistic excitations and terminations, to study the correlation between two-dimensional transmission line effects and three-dimensional interconnect phenomena.

0-7803-7846-6/03/$17.00 ©2003 IEEE

# An alternative interpretation of resonance of two-aperture irises in rectangular waveguide

J.A. Ruiz-Cruz and J.M. Rebollar*
Grupo de Electromagnetismo Aplicado y Microondas
ETSI de Telecomunicación, Ciudad Universitaria s/n, 28040, Madrid,
SPAIN
E-mail: jmrm@etc.upm.es

The multiple aperture irises present some interest for the design of low cost bandpass filters with some improved stopband attenuation. Approximate estimation of the rejection resonance position based on circuit theory modelling, joint to a circuital interpretation was proposed by (N.G. Paterson, *Electron Lett*, 592-594, 1976). An accurate electromagnetic estimation of such rejection resonance was presented at (R. Yang, *IEEE Trans. MTT*, 1369-1373, 1993). An interpretation of the nature of this resonance for two-aperture in terms of a pair of natural oscillations in the open-waveguide type structure was presented at (A.A. Kirilenko, *IEEE Trans. MTT*, 1419-1421, 2000). Application for a new type of bandstop filter with three-aperture irises was presented at (L. Mospan, *VIII Int. Conf. MMET*, 503-505, 2000).

In this paper, we present and alternative interpretation of resonance of two-apertures iris in terms of the excitation of the TEM mode of the structure. The mentioned TEM mode considers the strip between the two irises as one conductor and the wide walls of rectangular waveguide as the second conductor of the transmission line. This transmission line is short-circuited at both ends and its total length is approximately the wide of the iris. An accurate fullwave electromagnetic simulation joint to a visualisation of the electric and magnetic field vectors in the structure are employed to discuss and validate this interpretation. We consider that this alternative interpretation is very simple and useful from the designer point of view, specially to prevent spurious resonance in a variety of devices that use the mentioned multi-aperture iris structure.

Quantitative results of resonance frequency positions and field plots at these frequency points for different structures will be presented.

0-7803-7846-6/03/$17.00 ©2003 IEEE

# Multi-layered Microstrip Line with an Electronically Controlled Phase-Shifter

Chang-Seok Shin and Robert Nevels*
Department of Electrical Engineering
Texas A&M University
College Station, TX 77843-3128

Abstract

A microstrip is one of the most commonly used transmission lines. The design procedure for parameters such as characteristic impedance, effective dielectric constant, and the propagation constant is well defined in terms of $w/h$ and $\varepsilon_r$. Since the propagation constant is proportional to the effective dielectric constant, a microstrip transmission line with an electronically controlled propagation constant can be achieved if $w/h$, the dielectric constant, or the area of the dielectric material where the signal is guided can be electronically proscribed.

A silicon modulator has been realized by introducing impurities into a strip of N-type silicon to produce a $p^+$ region in the middle and $n^+$ region on each side (C-S Shin and R. Nevels, "Electronically Controllable Transmission Line Design for Traveling Wave Array Antenna Feed Network," 2002 USNC/URSI National Radio Science Meeting, San Antonio, Texas June16-21, 2002). Figure 1 shows the cross sectional view of a proposed multi-layered microstrip line. In this configuration, adjusting the external dc bias between the doped regions controls the conductivity of the silicon. An increase in the bias voltage causes an effective upward and lateral growth in the conductive region, which is seen as an increase in the width (w) of the upper conducting plate by the wave propagating in the microstrip line, thus producing a change in the phase constant of the guided wave. Depending on the dielectric constant of the substrate ($\varepsilon_{r1}$) compared to that of the silicon ($\varepsilon_{r2}$), the effective dielectric constant increases or decreases, as the conductive region (w) becomes wider.

In this paper we will present results for the phase shift obtained with the silicon controlled microstrip line phase-shifter pictured in the figure below. It will be shown that the silicon controlled phase shifter accomplishes electronic scanning of an eight-element aperture coupled microstrip patch antenna array. Our results are compared to those obtained with an Ansoft HFSS 3D simulation with a width equal to the average effective width of the biased silicon strip.

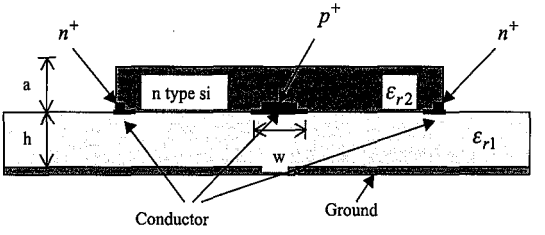


Figure 1. Cross sectional view of a multi-layered microstrip line with electronically controlled phase constant.

0-7803-7846-6/03/$17.00 ©2003 IEEE

# Double-Layer Rectangular-Waveguide Structure for Butler Matrix using Slit Coupling on the Broad Walls

Jiro Hirokawa[(1)], Naohisa Goto[(2)] and Koichi Tsunekawa[(3)]
[(1)]Tokyo Institute of Technology, [(2)]Takushoku University and [(3)]NTT DoCoMo

The authors proposed full double-layer configuration using rectangular waveguides of Butler matrix, where the hybrids are used with broad-wall slot coupling and the layers are changed only at places for the phase shifters as shown in Fig.1 (J.Hirokawa et al., Proc. 32nd European Microwave Conf., M36-3, 2002). This paper proposes to use slits all over the broad-wall to get wide bandwidth not only in the hybrids (F.Arndt at al., IEEE Trans. Microwave Theory Tech., 33, 95-104, 1985) but also in the phase shifters. The configuration is modified as shown in Fig.1 by including the phase progression in the hybrids and the phase delay in the phase shifters.

Fig.1 shows the block diagram of Butler matrix, for 8 beams as an example. The name of the input ports at the bottom express the beam direction (L: left, R: right, 1: smaller tilting angle – 4: larger one) (J.Butler and R.Lowe, Electron. Des., 9, 170-173, 1961). In the broad-wall coupling for the hybris, the output port at the differenet waveguide has 90-degree phase progression in comparison with that in the same waveguide in principle. However the phase shiter using the silts all over the common broad-wall of two shorted rectangular waveguides as shown in Fig.2 gives only some delay. It is difficult for it to give phase progression. Blocks of required phase shifts (+45, +45, 0, 0) in degrees in the conventional configuration should be replaced with (0, 0, –45, –45) as shown at Part (a) in Fig.1. The full double-layer configration can be still kept after this replacement. Other blocks of required phase shifts (+67.5, 0, 0, +22.5) should also be replaced with (–22.5, –90, –90, –67.5) as shown at Part (b) in Fig.1. –90-degree phase shiters will be obtained by installing corrugations at the bottom in a rectangular waveguide.

The phase shifter in Fig.2 is analyzed using the mode matching method. A –45-degree model is designed to supress the reflection below –40dB and to have a change of 4.8 degrees in the transmission phase over 3.9 – 4.1GHz as shown in Fig.3 by using genetic algorithm and modiled Powell method together (M.Okamoto et. Al, Math. Comp., 91, 63-72, 1998).

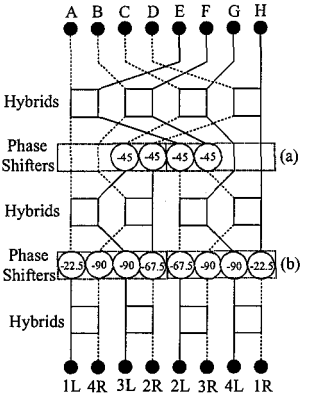


Fig.1: Block diagram of Butler Matrix (Solid: upper layer, dotted: lower one)

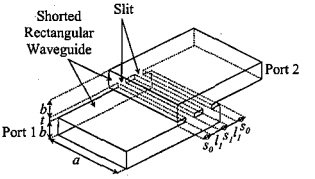


Fig.2: Phase shifter

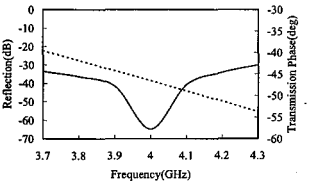


Fig.3: Reflection (solid) and transmission phase (dotted)

0-7803-7846-6/03/$17.00 ©2003 IEEE

## A Waveguide Switch Using Microwave Photonic Bandgap Substrates

*Won-Ho Kim[1], B. Park[1], M. Kim[1], J. Ryu[2], Y. Kim[2]

[1]Korea University, EE Department, Seoul, 136-701 Korea, korea98@korea.ac.kr
[2]Seoul National University, School of Mechanical and Aerospace Engineering, Seoul, 151-742 Korea

Waveguide components offer a solution for convenient system integration in millimeter-wave frequencies. For example, a waveguide duplexer providing a high isolation between the transmit and receive channels could be attached directly to a horn antenna without requiring waveguide-to-microstrip transitions. Previously, Xin *et. al.* demonstrated a 35GHz band-rejection waveguide filter using photonic bandgap (PBG) substrates as the covers for the top and bottom surfaces of a standard rectangular waveguide. As shown in Figure 1, these PBG covers consist of the outside metal ground plane and metal strips, facing toward the inside of the waveguide and lined up orthogonal to the direction of propagation. The conducting vias connect two sides that are separated by a thin dielectric substrate. The gap size between the metal strips determines the PBG resonant frequency at which the large surface impedance prevents $TE_{10}$ mode from propagating in the waveguide. A simple modification on the PBG cover design can improve the filter performance. HFSS simulations indicate that by varying the gap size between strips, thus changing the resonant frequency at different locations of the PBG cover, we can substantially increase the filter rejection bandwidth. The waveguide filter could be transformed into a switch by adding switching devices, such as RF MEMS switches or diodes, between the PBG strips. Because the PBG covers are conveniently located on the outside of the waveguide, dc-bias lines for the switching devices can be implemented without difficulty. Efforts are currently being made to fabricate MEMS-switchable PBG substrates at 40GHz.

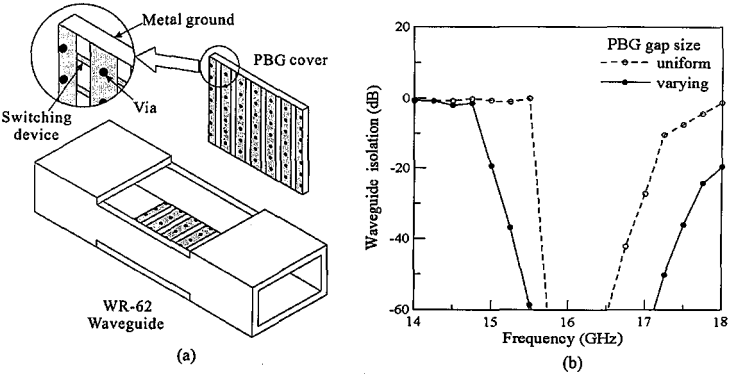


**Figure 1.** (a) Drawing of a waveguide switch, and (b) HFSS simulation results showing an increase in filter bandwidth when non-uniform gap sizes were used on the 23.7 mm-long PBG cover. Uniform gap size PBG cover was designed to produce an open surface impedance only at 16GHz while the varying gap size cover has three equally-divided sections to achieve an open impedance at 15, 16, and 17 GHz, respectively.

0-7803-7846-6/03/$17.00 ©2003 IEEE

**A Multilayer Active Power Divider Using Pseudo Hybrid-Ring And Ground-Slot Coupling Technique**

*S.C. Hui*, Ban-Leong Ooi, M.S. Leong and Bin Wu
Department of Electrical and Computer Engineering, National University of Singapore, Singapore 119260

A multilayer active power divider is presented for the Commission B under Guiding Structures and Circuits in URSI.

A broadband power divider in the form of five-ports hybrid-ring has been reported (G. F. Mikucki and A. K. Agrawal, "A broad-band printed circuit hybrid ring power divider," *IEEE Trans. Microwave Theory and Tech.*, vol. 37, no. 1, pp. 112-117, Jan. 1989). It is useful in sum mode operation and can divide the power for the realization of phase-array antenna systems. For the ground aperture technique, it is widely used in microstrip antenna design, and can also be applied to couple energy and/or to match impedance between microstrip lines. Here the proposed multilayer power divider uses a modified hybrid-ring structure and a ground-slot coupling technique to guide and couple signal between microstrip lines on the top and the bottom of printed circuit layers as shown in Fig. 1. With this coupling arrangement, two amplifying units can be placed on the bottom layer to boost up the coupled signal. The overall combination forms a multilayer structure which is broadband, compact and versatile.

The ground slots are carefully designed and optimized for a broadband performance while two Fujitsu HEMT (FHC40LG) transistors are used for the amplifying circuits. The power divider is designed and tested to operate in C-band with 35% 3dB-bandwidth, 9dB gain and 10dBm output P1dB. The output ports 2 and 3 have an identical response and a high isolation for a broadband frequency. In addition, their phase difference is less than 2 degrees which is mainly due to the transistors used being not identical. However, even with this slight phase difference, this design is still suitable for phase array antennas.

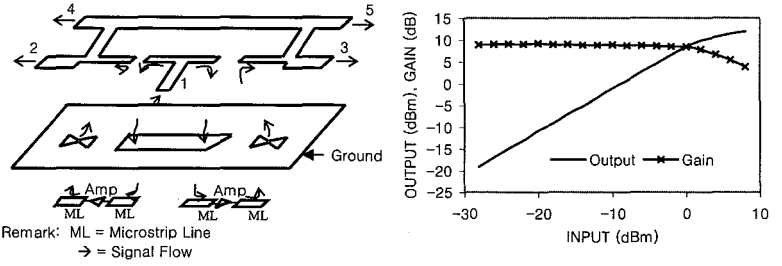


Fig. 1. Overall topology of the multilayer power divider, and output level and gain for different input level at 5.5GHz.

0-7803-7846-6/03/$17.00 ©2003 IEEE

*Special Session*

## Ionospheric Sounding with GPS

**Organizer(s):**
**Co-Chairs:** A. Komjathy
R. Langley

1:15 Opening Remarks

40. 1 1:20 On High-Resolution TEC Derivation from Regional GPS Networks: Feasibility Study ..... 232
*P. Wielgosz, D. A. Grejner-Brzezinska, I. Kashani, The Ohio State University,*

40. 2 1:40 Testing a 3D Ionosphere Model During 2001 Solar Maximum Period ..... 233
*Z. Z. Liu, Y. Gao, University of Calgary, Canada*

40. 3 2:00 GPS Observations of Tongues of Ionization in the Polar Cap ..... 234
*A. J. Coster, J. C. Foster, P. J. Erickson, MIT Haystack Observatory, F. J. Rich, AFRL/VSBXP, J. Ruohoniemi, Johns Hopkins Applied Physics Laboratory, USA*

40. 4 2:20 Detection of Ionospheric Perturbations using Dense GPS Arrays ..... APS
*E. Calais, J. S. Haase, Purdue University, B. Minster, Scripps Institution of Oceanography, USA*

40. 5 2:40 Summary of GPS Scintillation Observations in Brazil ..... 235
*E. R. De Paula, F. S. Rodrigues, National Institute for Space Research (INPE), Brazil, P. M. Kintner, Cornell University, USA*

40. 6 3:00 Studies of the GPS Signal Scintillation and Loss of Lock During Ionospheric Irregularities ..... 236
*L. F. C. de Rezende, E. R. De Paula, I. J. Kantor, National Institute for Space Research - INPE, Brazil*

40. 7 3:20 Low Latitude Ionospheric Observations with IOX and CORISS ..... 237
*P. R. Straus, P. C. Anderson, The Aerospace Corp., USA*

40. 8 3:40 Degradation of Signals and Operation Failures of Radio Engineering Satellite Systems During Geospace Disturbances Accompanied by Abrupt Changes in the ..... 238
*E. L. Afraimovich, Institute of Solar-Terrestrial Physics SD RAS, Russia*

40. 9 4:00 Traveling Wave Packets of Total Electron Content Disturbances As Deduced from Global GPS Network Data ..... 239
*E. L. Afraimovich, S. V. Voyeikov, N. P. Perevalova, Institute of Solar-Terrestrial Physics SD RAS, Russia*

# On High-Resolution TEC Derivation from Regional GPS Networks: Feasibility Study

P. Wielgosz (1,3)*, D. Grejner-Brzezinska (1), I. Kashani (1,2)

(1) Department of Civil and Environmental Engineering and Geodetic Science, The Ohio State University
(2) Technion - IIT - Israel Institute of Technology
(3) Institute of Geodesy, University of Warmia and Mazury in Olsztyn, Poland
wielgosz.1@osu.edu

GPS technique proved to be a powerful tool for studying Earth's ionosphere. Currently, many GPS analysis centers provide global ionosphere maps (GIM) on a daily basis. However, the resolution of these products is not sufficient to study local ionospheric structures. GIMs available on the Internet show routinely 15-minute temporal resolution at best, based on standard International GPS Service (IGS) data with 30-second sampling rate. Spatial resolution is around several degrees in latitude and longitude. Thus, GIMs cannot be used in detecting short-lasting processes with duration of about 1–10 min, much less in detecting virtually simultaneous disturbances on a global scale. Dual-frequency GPS carrier phase observables can be measured with high accuracy, allowing TEC estimation with a relatively small error less than 1 TECU (TEC unit) with possible uncertainty in the initial value. Even though an initial uncertainty may exist, the epoch-by-epoch TEC change can be determined with a high accuracy.

In this study, a zero-difference approach will be used for TEC determination from double frequency GPS data collected by a dense GPS CORS network (70 to 40 km station separation, 1Hz sampling rate). In order to demonstrate the capability of these data to detect local ionospheric features, we compare 1-second TEC data from Ohio CORS to the results obtained with standard IGS 30-second sampling rate. Sample periods of geomagnetic quiet and disturbed conditions are selected for demonstration purposes. For an undisturbed ionosphere, dual frequency GPS receiver observations show a flat TEC signature. When disturbances appear in the ionosphere, the calculated TEC will fluctuate reflecting the quick variations in the received carrier-to-noise ratio.

The contribution of this paper is a technology demonstration, which we believe, will enable detection of medium to small scale ionospheric irregularities, especially medium to small scale traveling ionospheric disturbances (TIDs), supporting nowcasting and forecasting of space weather, vital to radio-navigation, communication and surveillance.

0-7803-7846-6/03/$17.00 ©2003 IEEE

# Testing a 3D ionosphere model during 2001 solar maximum period

Zhizhao Liu, Yang Gao
Department of Geomatics Engineering, The University of Calgary, 2500 University Drive N.W., Calgary, Alberta, Canada, T2N 1N4 e-mail: zzliu@ucalgary.ca
Tel :1-403-220-4916 Fax :1-403-284-1980

The ionospheric refraction error is currently the most prominent error source in GPS measurements. To date, all ionosphere models that have been developed are essentially two-dimensional in nature so they are unable to fully characterize the ionosphere field. In this paper, a three-dimensional (3D) ionosphere model is described based on the tomography approach. Such a 3D model could provide a full dimensional description of the ionosphere field and outperform the 2D models in terms of modeling accuracy. The model performance was tested using data acquired during the 2001 solar maximum from 15 IGS stations. The geomagnetic Kp index value reached to 9 during the period and significant ionosphere variations were observed. The proposed model has been used to perform short-term (120 seconds) ionospheric TEC predictions and it was assessed through a comparison to directly GPS-inferred TEC values. The results indicated that the accuracy of the short-term vertical TEC predictions was about 6 TECU over a 24-hour period and the accuracy would be further improved if the prediction interval were shorter. The prediction computations have been implemented in a near real-time (NRT) mode so it meets the WAAS's ionosphere message update interval requirement (5 minutes). The obtainable accuracy of the vertical TEC prediction using the proposed model also satisfies the WAAS's ionospheric correction accuracy requirement of about 1.5 m for the Category (CAT) I precision approach in aircraft navigation.

0-7803-7846-6/03/$17.00 ©2003 IEEE 

# GPS Observations of Tongues of Ionization in the Polar Cap

**Anthea Coster [1], John Foster [2], Phil Erickson [3], Frederick Rich [4], J. Michael Ruohoniemi[5]**

*[1,2,3] MIT Haystack Observatory, Atmospheric Sciences, Off Route 40, Westford, MA 01886, USA*
*Tel: 781-981-5658, Fax: 781-981-5766, Email: ajc@haystack.mit.edu*
*[4] AFRL/VSBXP, [5] Johns Hopkins Applied Physics Laboratory*

During geomagnetic disturbances, intense storm-time electric fields of magnetospheric origin extend across mid-latitudes and the sub-auroral polarization stream is established. Ionospheric plasma is advected across both latitude and local time from a low-latitude source in the dusk sector to the dayside auroral region and the polar cap. Associated with such regions of storm enhanced density (SED), strong increases and sharp spatial gradients in total electron content (TEC) are observed in maps of TEC generated from multiple GPS receivers distributed throughout North and South America. Recent studies (e.g. Foster et al, GRL 2002) have shown the repeatability and global characteristics of these features at mid and auroral latitudes and their relationship to the erosion of the plasmasphere by the disturbance (SAPS) electric field. This analysis extends the GPS observations to high polar latitudes, and is based on data from ~ 180 GPS receivers during the 11 April 2001 storm. We focus on the tongue of ionization that forms across the polar cap as the TEC plume enters the polar region, and show its interconnection with the SED plume of plasmaspheric material observed over the continental US. The tongue of ionization correlates well with observations of discrete regions of strong HF backscatter observed by the SuperDARN radars and with polar cap enhancements of topside ionization observed by the DMSP satellites. Polar tongues of ionization formed in this way constitute a strong source of high-latitude space weather effects and radio scintillation.

*This work is sponsored by the Air Force under Air Force Contract AF19628-00-C-0002 Opinions, interpretations, conclusions, and recommendations are those of the author and are not necessarily endorsed by the United States Air Force.*

0-7803-7846-6/03/$17.00 ©2003 IEEE

It is well accepted that worst scintillation cases are expected to occur at low latitude regions close the nighttime Equatorial Anomaly (EA) peak. L Band scintillation is caused by intermediate-scale size (100-1000m) irregularities that usually are found to be embedded on large-scale (10's of km) plasma depletions, also referred as ionospheric plasma bubbles. During high solar activity years plasma bubbles develop more frequently at the magnetic equator, rise till high altitudes and reach low latitudes through the magnetic field lines. Since 1997, INPE has operated a Global Positioning System (GPS)-based scintillation monitor developed by Cornell University in São José dos Campos - SJC (23° S, 45°W, -18.07° dip latitude) to investigate characteristics of intermediate-scale irregularities occurrence and determine characteristics of the scintillation magnitude in the EA peak region. Besides SJC, GPS scintillation observations have also been carried out at several other observation sites in Brazil in such way that combination of collected data can give information about the temporal and spatial characteristics of irregularities/scintillations occurrence over the Brazilian region. In this work we present first analysis results of 5 years of scintillation observations at SJC. Data analysis shows the seasonal variation (September to April) of the intermediate-scale irregularities for the Brazilian region, occurrence frequency versus local time for different solar flux conditions and the solar flux effect over the magnitude of scintillations. During the 1997/1998 period (F10.7 = 99) the 5% average occurrence frequency started at about 20:30 LT and lasted till about 01:00 LT. However, during higher solar activity years the 5% average occurrence frequency started at about 19:30 LT and lasted till about 02:00 LT. The maximum average occurrence frequency reached 17% during the 1997/1998 period and 68% during the 2000/2001 period. Stronger scintillations were observed during higher solar activity years and equinoctial months (September/October and March/April) and higher occurrence frequency was observed during November, December and January months. Combination of data collected by several GPS scintillation monitors make possible to construct scintillation (based on the $S_4$ scintillation index) maps for Brazil that indicate regions where stronger scintillations are observed. Results can be used as input parameters in empirical or semi-empirical models for scintillation and/or ionospheric irregularity occurrence and also as reference for implementation of GPS Augmentation Systems in the Caribbean-South American region.

0-7803-7846-6/03/$17.00 ©2003 IEEE

# STUDIES OF THE GPS SIGNAL SCINTILLATION AND LOSS OF LOCK DURING IONOSPHERIC IRREGULARITIES

L. F. C. DE REZENDE, E. R. DE PAULA, I.J. KANTOR

INPE, São José dos Campos, SP, Brazil

The ionospheric irregularities give origin to amplitude and phase scintillations on the GPS receiver signal with larger amplitudes under the Equatorial Anomaly. These scintillations can cause loss of lock of the GPS signal with consequent reduction of reliability and accuracy in the navigation. In this work it was analysed 50 Hz L1 band amplitude GPS data at Cachoeira Paulista (23° S, 45 ° W, -18.07 ° dip latitude), that is under the Equatorial Anomaly, using a GEC Plessey Builder –2 GPS card, and with elevation angles larger than 10°. The data cover the solar maximum activity years of 2000 and 2001. The scintillation percentage of occurrence increased with the solar flux growth, and it was larger for summer solstice. During equinoxes it was observed larger scintillation amplitudes. The losses of lock were determined in function of the S4 scintillation index and the autocorrelation half width (Ax). Larger loss of lock occurrences for S4 between 0.2 and 0.3, and for autocorrelation width ranging from 1 to 2s, was observed for equinoxes and summer solstice, however with lower probability than for larger S4. Almost no loss of lock for winter solstice, when there are few scintillations, was observed. The ionospheric scintillation effects over the GDOP was also analysed.

0-7803-7846-6/03/$17.00 ©2003 IEEE

Low Latitude Ionospheric Observations with IOX and CORISS

Paul R Straus and P. C. Anderson

GPS occultation sensors have the potential to provide us with new insights into the physics of the low latitude ionosphere. Of particular interest are the possibility of globally distributed measurements of F-region parameters (peak density, altitude, topside scale height), height-resolved observations of ionospheric scintillation, and measurements of the E-region before and after sunset. The strengths of the occultation technique are its excellent vertical resolution and high inherent precision. Its primary weakness arises from difficulties in data interpretation associated with the convolution of its limb-viewing geometry and ionospheric structures. Data from the Ionospheric Occultation Experiment (IOX) will be used to illustrate these strengths and weaknesses. IOX is a dual-frequency GPS receiver similar to the Orsted and SunSat GPS instruments, but having better L2 performance. IOX has been making ionospheric occultation measurements since November 22, 2001 from a 67 degree inclination, 800 km altitude orbit on September 30, 2001. Most occultation measurements are made at a 1 Hz (so-called medium rate) cadence, but some high rate (50 Hz) observations at ionospheric tangent altitudes are also made. In addition to specific examples, a brief overview of the IOX database will be presented. IOX observations provide a preliminary sense of the types of analyses that will be enabled by the next occultation sensor with an exclusively ionospheric mission focus: the C/NOFS Occultation Receiver for Ionospheric Sensing and Specification (CORISS). A part of the Air Force's Communication/Navigation Outage Forecasting System (C/NOFS), the CORISS instrument is expected to be launched into an equatorial (13 degree inclination) orbit in early 2004, enabling continuous monitoring of the equatorial ionosphere. Because ionospheric morphology is ordered by the earth's magnetic field, occultation observations made from an equatorial orbit are expected to have a somewhat different character from those in a high-inclination orbit.

0-7803-7846-6/03/$17.00 

# Commission G, Session G6

## Degradation of signals and operation failures of radio engineering satellite systems during geospace disturbances accompanied by abrupt changes in the geomagnetic field

E. L. Afraimovich
Institute of Solar-Terrestrial Physics SD RAS,
p. o. box 4026, Irkutsk, 664033, Russia,
fax: +7 3952 511675; e-mail: afra@iszf.irk.ru

**Abstract**

With the development of progress, our civilization is becoming increasingly dependent on technological navigation and radar systems whose performance is to a certain extent governed by geospace conditions. Degradation of transionospheric radio signals and operation failures during geospace disturbances constitute a crucial factor of space weather influence on radio engineering satellite systems performance (along with other factors such as spacecraft surface charging, etc.). The objective of this report is to demonstrate how ionospheric disturbances during magnetic storms contribute to the degradation of signals and failures of the GPS system. We used automated software complex GLOBDET for global GPS detection and monitoring of ionospheric disturbances has been developed at the ISTP SB RAS. GLOBDET makes it possible to automate the acquisition, filtering and pretreatment process of the GPS data received via the Internet. The study is based on using Internet-available selected data from the global GPS network, with the simultaneously handled number of receiving stations ranging from 100 to 300. The analysis used 35 days from the period 1998–2002, with the values of the geomagnetic field disturbance index *Dst* from 0 to -300 nT. We found that ionospheric disturbances during magnetic storms contribute to signal degradation and GPS system malfunctions not only at the equator and in the polar zone but also even at mid-latitudes. During strong magnetic storms, the errors of determination of the range, frequency Doppler shift and angles of arrival of transionospheric radio signals exceeds the one for magnetically quiet days by one order of magnitude as a minimum. This can be the cause of performance degradation of current satellite radio engineering navigation, communication and radar systems as well as of superlong-baseline radio interferometry systems. The relative density of phase slips at mid-latitudes exceeds its mean value for magnetically quiet days at least by the order of 1 or 2, that makes a few percent of the total density of GPS observations. Furthermore, the level of phase slips for the GPS satellites located at the sunward side of the Earth was 5-10 times larger compared to the opposite side of the Earth.

0-7803-7846-6/03/$17.00 ©2003 IEEE

# Commission G, Session G6

## Traveling wave packets of total electron content disturbances as deduced from global GPS network data

Afraimovich E. L., Voyeikov S. V., Perevalova N. P.
Institute of Solar-Terrestrial Physics SD RAS,
p. o. box 4026, Irkutsk, 664033, Russia
fax: +7 3952 511675; e-mail: afra@iszf.irk.ru

**Abstract**

We identified a new class of mid-latitude medium-scale traveling ionospheric disturbances (MS TIDs), viz. traveling wave packets (TWPs) of total electron content (TEC) disturbances. For the first time, the morphology of TWPs is presented for 105 days from the time interval 1998-2001 with a different level of geomagnetic activity, with the number of stations of the global GPS network ranging from 10 to 300. The radio paths used in the analysis total about 700000. These data were obtained using the GLOBDET technology for global detection and monitoring of ionospheric disturbances of natural and technogenic origin from measurements of TEC variations acquired by a global network of receivers of the navigation GPS system. The GLOBDET technology was developed at the ISTP SD RAS. Using the technique of GPS interferometry of TIDs we carried out a detailed analysis of the spatial-temporal properties of TWPs by considering an example of the most conspicuous manifestation of TWPs on October 18, 2001 over California, USA. It was found that TWPs are observed no more than in 0.1-0.4% of all radio paths, most commonly during the daytime in winter and autumn at low geomagnetic activity. TWPs in the time range represent quasi-periodic oscillations of TEC of a length on the order of 1 hour with the oscillation period in the range 10-20 min and the amplitude exceeding the amplitude of "background" TEC fluctuations by one order of magnitude, as a minimum. The radius of spatial correlation of TWPs does not exceed 500–600 km (3–5 wavelengths). The velocity and direction of TWPs correspond to those of mid-latitude medium-scale traveling ionospheric disturbances (MS TIDs) obtained previously from analyzing the phase characteristics of HF radio signals as well as signals from geostationary satellites and discrete cosmic radio sources.

0-7803-7846-6/03/$17.00 ©2003 IEEE

*Special Session*

## Remote Sensing Applied to Climate Research

**Organizer(s):** Ed Westwater
Steve Reising

**Co-Chairs:** E. Westwater
S. Reising

7:55 Opening Remarks

48. 1 8:00 The GPM Mission, Cloud Resolving Models, and Microwave Precipitation Retrieval ..... 243
*S. A. Braun, E. A. Smith, NASA, USA*

48. 2 8:20 Cloud Phase Determination in the Arctic from Downwelling Infrared Radiance Spectra ..... 244
*D. D. Turner, S. A. Ackerman, CIMSS/SSEC, University of Wisconsin-Madison, USA*

48. 3 8:40 Recent Improvements in Cloud Liquid Water Path Retrievals Using Two-Channel Microwave Radiometer Measurements from the ARM Sites ..... 245
*E. E. Clothiaux, The Pennsylvania State University, S. A. Clough, Atmospheric & Environmental Research Inc., J. C. Liljegren, Argonne National Laboratory, K. Cady-Pereira, S. Boukabara, E. J. Mlawer, Atmospheric & Environmental Research Inc., USA*

48. 4 9:00 An Assessment of Microwave Absorption Models and Retrievals of Cloud Liquid Water using Clear-Sky Data ..... 246
*R. Marchand, Pacific Northwest National Laboratory, USA*

48. 5 9:20 A 95 GHz Solid State Cloud Radar for Cloud Research from Unmanned Aircraft ..... 247
*S. Sekelsky, J. Roman-Nieves, N. Majurec, University of Massachusetts, T. Tooman, W. Bolton, Sandia National Laboratory, USA*

48. 6 9:40 Production of an Enhanced Blended Infrared and Microwave Sea Surface Temperature Product ..... 248
*G. A. Wick, NOAA Environmental Technology Laboratory, USA*

48. 7 10:00 Design and Calibration of the Miniaturized Water Vapor Profiler ..... 249
*S. C. Reising, F. Iturbide-Sanchez, R. W. Jackson, University of Massachusetts at Amherst, USA*

48. 8 10:20 Experimental Evaluation of Four Microwave Radiative Forward Models Based on Ground-based Radiometer Data Near 20 and 30 GHz ..... 250
*D. Cimini, University of L'Aquila, Italy, E. R. Westwater, University of Colorado, S. J. Keihm, NASA, Y. Han, NOAA, USA, F. S. Marzano, P. Ciotti, University of L'Aquila, Italy*

# The GPM Mission, Cloud Resolving Models, and Microwave Precipitation Retrieval

*Scott A. Braun & Eric A. Smith*
NASA/Goddard Space Flight Center, Code 912, Greenbelt, MD 20771
Tel: 301-614-6316; Email: braun@agnes.gsfc.nasa.gov
Tel: 301-286-5770; Email: easmith@pop900.gsfc.nasa.gov

**Abstract**

The GPM mission is currently planned for start in the 2007-08 time frame. Its main scientific goal is to help answer pressing scientific problems arising within the context of global and regional water cycling. These problems cut across a hierarchy of scales and include climate-water cycle interactions, techniques for improving weather and climate predictions, and better methods for combining observed precipitation with hydrometeorological prediction models for applications to hazardous flood-producing storms, seasonal flood/draught conditions, and fresh water resource assessments. The GPM mission will expand the scope of precipitation measurement through the use of a constellation of some 9 satellites, one of which will be an advanced TRMM-like "core" satellite carrying a dual-frequency Ku-Ka band precipitation radar and an advanced, multifrequency passive microwave rain radiometer with vertical-horizontal polarization discrimination. The other constellation members will include new dedicated satellites and co-existing operational/research satellites carrying similar (but not identical) passive microwave radiometers. The goal of the constellation is to achieve 3-hour sampling at any spot on the globe -- continuously. The constellation's orbit architecture will consist of a mix of sun-synchronous and non-sun-synchronous satellites with the "core" satellite providing measurements of cloud-precipitation microphysical processes, plus calibration-quality rainrates to be used with the other retrieval information to ensure bias-free constellation coverage.

GPM is organized internationally, involving existing, pending, projected, and under-study partnerships which will link NASA and NOAA in the US, NASDA in Japan, ESA in Europe and additional space agency partners. Moreover, the program is actively pursuing agreements with other international collaborators and domestic sister institutions, as well as individual scientists from academia, government, and the private sector to fulfill mission goals and to pave the way for what ultimately is expected to become an internationally-organized operational global precipitation observing system. Notably, the broad societal applications of GPM are reflected in the United Nation's identification of this mission as a foremost contributor to peaceful uses of space.

An overview of the GPM mission design is given, followed by an explanation of its scientific agenda as an outgrowth of making improvements in rain retrieval accuracy, microphysics dexterity, sampling frequency, and global coverage. All of these improvements offer new means to observe variability in precipitation and water cycle fluxes, to improve water budget closure at regional and global scales, and to leverage these improvements in achieving improved predictability of weather, climate, and hydrometeorology. Specifically, the scientific agenda of the GPM mission is being designed to leverage the measurement improvements to improve prognostic model performance, particularly quantitative precipitation forecasting and its linked phenomena at short, intermediate, and extended time scales. In this context, the talk will focus on how GPM measurements will be used to improve the fidelity of mesoscale cloud resolving models (CRMs) and how in turn, CRMs will be used to improve the microwave algorithms designed to retrieve GPM satellite rainrates.

0-7803-7846-6/03/$17.00 ©2003 IEEE 

# Cloud Phase Determination in the Arctic from Downwelling Infrared Radiance Spectra

**D.D. Turner*[1,2] and S.A. Ackerman[1]**
[1]CIMSS/SSEC, University of Wisconsin-Madison, Madison, WI
[2]Pacific Northwest National Laboratory, Richland, WA

In the Arctic, longwave energy lost to space over an annual cycle is much larger than the shortwave energy absorbed. However, energy from the mid-latitudes is transported into the region via the ocean and atmosphere, and thus the cooling of the Arctic serves to cool the planet in general and makes the Arctic one of the primary heat sinks for the Earth. Clouds can have large impacts on the radiative transfer, and thus the energy budget, depending on the optical properties of the clouds (i.e., optical depth, single scatter albedo, and scattering phase function). These optical properties are dictated by the physical properties of the cloud such as its thermodynamic phase, particle size, number density, temperature, and geometrical thickness. Cloud phase is very important, as the refractive indices of ice and liquid water are different across most of the EM spectrum. However, until recently, there have been precious few cloud property data sets collected in the Arctic, and none of them covered a large enough time range from which seasonal statistics could be inferred.

The Department of Energy's Atmospheric Radiation Measurement (ARM) program has established a long term (>10 yr) site at Barrow, Alaska (71.3°N, 156.6°W) in 1998. This site has a broad range of in-situ and remote sensing instrumentation to measure and infer atmospheric and cloud properties. While it has active sensors such as a millimeter cloud radar and lidar, neither have polarization diversity to provide information on cloud phase. We have developed an algorithm that determines cloud phase from downwelling high-spectral resolution radiance observations made by the Atmospheric Emitted Radiance Interferometer (AERI) at the ARM site. This algorithm takes advantage of the distinct differences in the absorption coefficient of ice and liquid water at 12 μm (where the ice is more absorbing than water) and at 18 μm (where the opposite is true). Simulations were used to characterize the performance of the algorithm, demonstrating that the cloud phase was accurately determined for all cases, with the only exceptions occurring when the fraction of the optical depth due to liquid water was over 70%. This algorithm was applied to AERI data collected during the Surface Heat Budget of the Arctic Ocean (SHEBA), during which a co-located polarization diverse lidar was available to evaluate the skill of the AERI's phase determination algorithm. Case studies and monthly statistics on cloud phase from the two methods will be presented and discussed.

Building upon the success of the phase determination algorithm, we have also developed an algorithm to physically retrieve the optical depth and effective particle sizes of the water and ice components of Arctic clouds from the observed AERI radiance spectrum. Retrievals from simulated AERI data were used to demonstrate the accuracy of the algorithm and its sensitivity to various perturbations. Results from several case studies will also be shown and discussed.

*Corresponding Author: Dave Turner, dturner@ssec.wisc.edu

0-7803-7846-6/03/$17.00 ©2003 IEEE

**Recent Improvements in Cloud Liquid Water Path Retrievals Using Two-Channel Microwave Radiometer Measurements from the ARM Sites**

Eugene E. Clothiaux, *The Pennsylvania State University*
Shepard A. Clough, *Atmospheric & Environmental Research Inc.*
James C. Liljegren, *Argonne National Laboratory*
Karen Cady-Pereira, *Atmospheric & Environmental Research Inc.*
Sid Boukabara, *Atmospheric & Environmental Research Inc.*
Eli J. Mlawer, *Atmospheric & Environmental Research Inc.*

The first sets of statistically-retrieved cloud liquid water paths using two-channel microwave radiometer measurements collected by the US Department of Energy (DOE) Atmospheric Radiation Measurements (ARM) Program in the mid- to late-1990s exhibited too little accuracy to be of value in detailed atmospheric radiative transfer studies above the ARM sites. In particular, the use of monthly-mean climatological coefficients in the first retrievals was not sufficient to model important atmospheric thermodynamic state variability and the resulting errors in the retrieved cloud liquid water paths were significant. Since these early retrievals, further work by a number of investigators has led to improvements in the retrievals, a better understanding of the uncertainties in the model physics embedded in the retrievals, and improved characterization of the radiances input to the retrievals. Incorporating these improvements into a physical retrieval with a first-guess provided by a statistical retrieval that is based on instantaneously varying retrieval coefficients has led to the development of a new set of retrieved cloud liquid water paths. The relevance of these more recent retrievals to radiation studies over the ARM sites is considered and the remaining problems in the current retrieval are summarized.

0-7803-7846-6/03/$17.00 

# An Assessment of Microwave Absorption Models and Retrievals of Cloud Liquid Water using Clear-Sky Data

Roger Marchand and Thomas Ackerman
Pacific Northwest National Laboratory

Ed R. Westwater
Cooperative Institute for Research in Environmental Sciences
University of Colorado/NOAA Environmental Technology Laboratory
325 Broadway MS R/E/ET1 Boulder, CO 80303 USA

Shepard A. Clough and Karen Cady-Pereira
Atmospheric & Environmental Research
131 Hartwell Avenue Lexington, MA 02421

James C. Liljegren
Environmental Research Division
Argonne National Laboratory

*Abstract* – Passive microwave radiometers have a long history in the remote sensing of atmospheric liquid and water vapor. Retrievals of these quantities are senstitive to variations in pressure and temperature of the liquid and water vapor. Rather than use a statistical or climatological approach to account for the natural variability in atmospheric pressure and temperature, additional information on the atmospheric profile at the time of the radiometer measurements can be directly incorporated into the retrieval process. Such an approach has been referred to in the literature as "physical-iterative" solution. This paper presents an assessment of the accuracy of the column liquid water path that can be expected using such an iterative technique. It is shown that the retrieval accuracy is influenced by the accuracy of the instrument measurements and the quality of the atmospheric profiles of temperature and pressure, as one would expect. But also critical is the uncertainty in the absorption coefficients used in the underlying microwave radiative transfer model. The uncertainty in the absorption coefficients is particularly problematic in that it may well bias the liquid water retrieval. The differences between 3 absorption models examined in this presentation are equivalent to a bias of 15 to 30 g/m$^2$, depending on the total column water vapor. An examination of typical liquid water paths from the Southern Great Plains region of the United States shows that errors of this magnitude have significant implications for shortwave radiation and retrievals of cloud effective particle size.

0-7803-7846-6/03/$17.00 ©2003 IEEE 

# A 95 GHz Solid State Cloud Radar for Cloud Research from Unmanned Aircraft

Stephen M. Sekelsky*, Jorge Roman-Nieves, Ninoslav Majurec
University of Massachusetts at Amherst
Amherst, MA 01003

Tim Tooman, Will Bolton
Sandia National Laboatory
Livermore, CA

The Microwave Remote Sensing Laboratory (MIRSL) at the University of Massachusetts (UMass) has developed the first compact low power cloud radar designed to operate from high altitude unmanned aircraft. The Compact Millimeter-wave Radar (CMR) has recently flown as part of a suite of cloud and radiation sensors on the NASA Proteus Aircraft during engineering test flights in the Mojave Desert and in a U.S. Department of Energy sponsored cirrus experiment in Oklahoma. After a series of three planned flight series on the manned Proteus aircraft CMR and other sensors flown on the Proteus will be reinstalled on the U.S. Department of Energy Atmospheric Radiation Measurement Unmanned Aerospace Vehicle Program (ARM-UAV) Altus unmanned aircraft.

CMR is specifically designed as a compact low power radar for cloud studies from high altitude aircraft. CMR differs significantly from prior klystron tube transmitter based 95 GHz radar systems operated from the ground and from larger medium altitude aircraft. First, the klystron tube is replaced with a small array of solid state diode amplifiers whose outputs are combined to achieve a final peak output power of approximately 1 W. Use of the solid state transmitter eliminated the need for pressurizing the klystron's high voltage power supply and any other portion of the hardware. Next, frequency modulation (FM) chirp pulse compression is used to reclaim sensitivity lost by the use of such a low peak power transmitter. Here a direct digital synthesizer generates a low frequency version of the output waveform. Received waveform pulse compression is achieved in a stand-alone digital receiver/pulse-pair signal processor that is implemented in relatively low power reconfigurable logic.

Initial data from the 2002 flight series is presented, which verifies CMR's anticipated pulse compression gain, and proves that the radar operated reliably during 50+ hours of flight time. Calibration measurements and inter-comparison of cloud data with previously developed sensors having well established characteristics are also presented.

0-7803-7846-6/03/$17.00 ©2003 IEEE

**Production of an Enhanced Blended Infrared and Microwave Sea Surface Temperature Product**

Gary A. Wick
NOAA Environmental Technology Laboratory, Boulder, CO

The simultaneous availability of infrared and passive microwave satellite sensors provides highly complementary information enabling the creation of an improved all-weather, high-resolution sea surface temperature (SST) product. Infrared sensors provide high resolution and high accuracy estimates of the SST but the measurements are completely obscured by clouds. Passive microwave sensors, in contrast, have poorer resolution but are able to obtain measurements through non-precipitating clouds. We are preparing a blended SST product using infrared data from the AVHRR and passive microwave data from the TRMM Microwave Imager (TMI). The product consists of daily, global SST fields at 0.25 degree resolution along with an estimate of the amplitude of the diurnal cycle.

This paper will introduce the new product and describe the techniques used in its preparation. We first describe significant spatial differences that exist between the individual products and examine these differences as functions of such quantities as wind speed, water vapor, SST, and residual cloud effects. We next discuss the procedures used to compensate for diurnal warming effects and the different satellite measurement times while producing a single nighttime-representative product. We then explore different techniques for merging the data sets making use of their derived error characteristics. These techniques range from simple compositing methods to optimal interpolation. Finally, accuracy statistics of the blended products relative to independent in situ buoy measurements are presented and compared with the accuracy of the independent products.

0-7803-7846-6/03/$17.00 ©2003 IEEE 

# The Design of Miniaturized Water Vapor Profilers for Three-Dimensional Measurement of Atmospheric Water Vapor

S. C. Reising*, and F. Iturbide-Sanchez, Microwave Remote Sensing Laboratory, University of Massachusetts, Amherst, MA 01003-4410, USA
(Email: reising@ecs.umass.edu, fiturbid@ecs.umass.edu)

R. W. Jackson, Laboratory for Millimeter Wave Devices and Applications, University of Massachusetts, Amherst, MA 01003-4410, USA (Email: jackson@ecs.umass.edu)

Knowledge of the temporal and spatial distribution of water vapor is fundamental for short-range prediction of precipitation and severe weather. The paucity of current observations of wind, temperature and humidity in pre-storm environments limits the improvement of forecast skill for these events. Currently, measurements of precipitable water vapor in the troposphere are limited to twice-daily radiosonde launches, costly and limited clear weather lidar techniques and networks of GPS receivers measuring wet delay. Measurements of the water vapor field at higher spatial and temporal resolutions, as well as 3-D variational assimilation into numerical weather prediction models, are needed to improve short-range weather forecasting. Networks of water vapor profiling radiometers and associated analysis techniques are needed to address these shortcomings.

A large fraction of today's ground-based and airborne microwave remote sensing instrumentation was built using waveguide-based and discrete microwave components, aging technology that is still economical in this niche market, based on quantities of one or a few copies of an instrument. In contrast, analog microwave circuits in the wireless communications and some defense sectors are based increasingly on microwave monolithic integrated circuits (MMIC), yielding a higher level of integration and lower production costs, and often higher reliabilty. The demand for components in selected wireless communication frequency allocation bands has driven down the price of commercial off-the-shelf components, such as low noise amplifiers, to the $10 range. As a result, producing a unique, "one-off" design based on commercially available MMIC components is expected to be lower than that of waveguide-based systems. MMIC-based radiometer designs enable a reduction in total volume of one-to-two orders of magnitude and a reduction in total weight and power consumption of at least one order of magnitude, as compared with waveguide-based systems.

This paper describes the design and calibration of the Miniaturized Water Vapor Profiler (MWVP) at the University of Massachusetts (UMass) Amherst. The MWVP has the advantages of low cost and power consumption, as well as high reliability for long-term operation in the field. The MWVP design permits two-point radiometric calibration using both internal and external techniques. In this design, water vapor profiles are retrieved from brightness temperature measurements at a set of frequencies near the 22.235 GHz water vapor resonance chosen to optimize the vertical resolution of the profiler. The complete RF section of the MWVP occupies less than 50 $cm^3$ (3.1 $in^3$). The entire radiometer system has a volume smaller than 1800 $cm^3$ (110 $in^3$). This substantial reduction in size, weight, cost and power consumption of the MWVP, relative to existing ground-based water vapor profiling radiometers, is expected to allow flexible deployment in ground-based networks and aboard unpiloted aerospace vehicles (UAVs).

0-7803-7846-6/03/$17.00 ©2003 IEEE

# Experimental evaluation of four microwave radiative forward models based on ground-based radiometer data near 20 and 30 GHz.

D. Cimini[1], E. R. Westwater[2], S.J. Keihm[3], Y. Han[4], F. S. Marzano[1], and P. Ciotti[1]

[1] CETEMPS, University of L'Aquila, via Vetoio 1, Coppito, L'Aquila, 67010, ITALY.
[2] CIRES, University of Colorado/NOAA, Environmental Technology Laboratory, 325 Broadway, Boulder, CO, 80305, USA.
[3] Jet Propulsion Laboratory, California Institute of Technology, Pasadena, CA, 91109, USA
[4] NOAA/NESDIS, 5200 Auth Rd, Camp Springs, MD, 20746, USA)

## Abstract

In this work we study the differences in brightness temperature (Tb) as computed using a variety of four commonly used microwave absorption models. Furthermore, we compare theoretical predictions with ground-based radiometer measurements, in order to evaluate the ability of each model to reproduce the actual behaviour of the atmosphere. The four models we consider are from Liebe and Layton (NTIA Rept.87-24,1987), Liebe et al. (AGARD Conf. Proc. 542,1993), Rosenkranz (*Radio Sci.,* **33,** 919-928,1998) and MONORTM model of S. Clough (Turner et al., *J. Atmos. Oceanic Technol..*, in press ). By processing three appropriate historical datasets of radiosonde observations with these models, we computed the main Tb for each model in three contrasting environments, at tropical, medium and arctic latitudes. Then, we discuss the difference in computed Tb between the four models. We focus on the spectral range 20-30 GHz, which is commonly used for ground-based estimates of atmospheric water vapor by microwave radiometers, and for which routine measurements are often available. Both remotely sensed and in situ data were collected during the Water Vapor Intensive Operating Period, held in September/October 2000 at the Atmospheric Radiation Measurement (ARM) Southern Great Plains (SGP) site, near Lamont, Oklahoma, USA. Three microwave radiometer (MWR) units were deployed, with a total of seven channels from 20.6 to 31.65 GHz. In addition to radiometric observations, during the WVIOP2000 there were three-hourly radiosonde launches, deploying two different types of Vaisala humidity sensors, the RS80 and RS90. Since RS90 are believed to reduce the *"dry-bias"* affecting the RS80 (Wang et al., *J. Atmos. Oceanic Technol.*, **19(7),** 981-1002, 2002), the WVIOP2000 provided a unique opportunity of having high quality atmospheric profiles and ground-based observations. Thus, we show the comparison of Tb computed from RS90 measurements using the four models with Tb observations from the MWR units, and discuss a possible choice between the considered models.

0-7803-7846-6/03/$17.00 ©2003 IEEE 

# Ka-band Polarimetric Radiometer Calibration: Results from Recent Field Measurements

S. C. Reising*, M. A. Aziz, and K. A. Horgan, Microwave Remote Sensing Laboratory, University of Massachusetts, Amherst, MA 01003-4410, USA
(Email: reising@ecs.umass.edu, aziz@mirsl.ecs.umass.edu, kevin@mirsl.ecs.umass.edu)

The Ka-band Polarimetric Radiometer (KaPR) was designed and fabricated at the University of Massachusetts for ground- and platform-based brightness temperature measurements of geophysical media. This radiometer is fully polarimetric, i.e. it measures all four Stokes parameters. This paper reports the techniques for calibration of KaPR's brightness temperature measurements. The two receiver channels measuring horizontally and vertically polarized brightness temperatures are considered to be linear. The relationship between the input and output power of the radiometer is calibrated using two reference sources, a cold source and a hot source. The cold source is obtained through a tipcurve measurement to obtain the cosmic background radiation, considered to be 2.7 K (isotropic) in this frequency band. A quantitative measure of tipcurve goodness was developed to estimate the accuracy of the cold source measurement. An ambient load consisting of microwave absorber of nearly unity emissivity is used as a hot source reference. To ensure accurate calibration, the cold source and hot source measurements are both performed before the thermal conditions in the radiometer change significantly. Long-term gain variations of the system are corrected through frequent external calibration using tipcurve and ambient load measurements.

The stability of the radiometer's internal temperature is also crucial since many radiometer subsystems are sensitive to temperature variation. Very good temperature stability in the system is achieved by employing a thermoelectric heat/cool system. However, in most weather conditions short-term gain variations still exist. Internal reference noise source measurements are used to correct short-term gain variations, on the time scale of tens of seconds or less (I. Corbella et al., *IEEE Trans. Microwave Theory Techniques*, **50**, 1816-1820, 2002).

The calibration circle technique is used to calibrate U and V, the third and fourth Stokes parameters (A. Camps et al., *Radio Science*, **32**, 1821-1832, 1997). In this procedure, an internal reference noise source is input to both channels, and the phase in one of the receiver channels is varied from 0 to 360 degrees using a programmable phase shifter. The output obtained is an ellipse due to several potential error sources. A small change in the path length of one receiver channel with respect to the other introduces significant phase errors. The measured "calibration circle" is modeled by a best-fit ellipse using the least squares method. The gains of the U and V channels are calculated using the reference noise source input power and the axes of the best-fit ellipse. Finally, offset and phase errors are calculated from the ellipse.

During field measurements, platform pitch and roll motions introduce errors in the brightness temperature measurements due to incidence angle variation and polarization basis rotation. A correction algorithm is used to compensate for these fluctuations (I. Corbella et al., *IEEE Trans. Geosci. Remote Sensing*, **39**, 193-195, 2001). Results are presented from three experiments to measure the polarimetric emission of the ocean surface, including the FAIRS Experiment aboard the R/V FLIP in the eastern Pacific Ocean in 2000 and the POEWEX Experiment during October 2002.

0-7803-7846-6/03/$17.00 ©2003 IEEE 

# Rapid Calculation of Incremental Profiles for Satellite Radiometer Data Assimilation

A.G. Voronovich, A.J. Gasiewski, and R.J. Hill

NOAA/Environmental Technology Laboratory
325 Broadway, Boulder, CO, 80305-3328
alexander.voronovich@noaa.gov

Assimilation of microwave radiometric data from satellite- and airborne sensors under all weather conditions is an important challenge in numerical weather prediction. Microwave radiances upwelling from the atmosphere depend strongly on frequency and carry a wealth of information on moisture and temperature profiles as well as clouds, rain, and surface parameters. Such sub-cloud top information is not available using infrared and optical wavelengths that are opaque over to clouds.

Microwave brightness temperatures generally depend on the electromagnetic scattering properties of hydrometeors through a process well described by the radiative transfer. Statistically optimal retrieval of the environmental parameters requires accurate calculation of the derivatives of the brightness temperature with respect to variations of all atmospheric and surface parameters. To accommodate the dense data stream from modern passive microwave satellites one requires calculations times of ~0.1 msec per profile or better. This talk will present an algorithm addressing these problems and some results obtained with it for Hurricane Bonnie (1998) simulations.

In our approach the atmosphere is represented as a stack of homogeneous horizontal layers. The differential radiative transfer equation (RTE) used models processes of photon generation and absorption by gases and particles as well as scattering by particles. Symmetry properties of scattering are very essential for building a fast solution, and the RTE is first cast into an explicitly symmetric form. Each layer is characterized by transmittance and reflection matrices that provide a complete description of the layer as far as its interaction with other layers is concerned. Accurate and stable calculation of those operators for arbitrary layer parameters represents a non-trivial task since the opacity and scattering coefficients vary over a wide range. Moreover, the layer can be fairly transparent at steep incident angles and opaque at grazing angles. Computationally, this problem results in the need to invert ill-conditioned matrices. We solve the inversion problem by first analytically factoring the matrix to be inverted into a product of five matrices. Four of them are regular, and only one diagonal matrix remains ill-conditioned. After explicit inversion the result includes only benign matrices and works well in all cases.

Once the transmittance and reflectance operators for all layers are known, the overall brightness temperature field is easily built using the method of slab doubling via two profile sweeps. Calculation of incremental profiles generally requires only one extra sweep. Thus, the number of operations required is directly proportional to the number of layers, and not to this number squared, as it would be for straightforward divided difference calculation.

0-7803-7846-6/03/$17.00 ©2003 IEEE

## Design of IRMA III, the latest Infrared Radiometer for Millimeter Astronomy

David A. Naylor, Brad G. Gom, Robin R. Phillips, Ian M. Chapman
Physics Department, University of Lethbridge, Alberta, Canada

The performance of astronomical interferometer arrays operating at (sub)millimeter wavelengths is seriously compromised by phase distortions resulting from rapid fluctuations in atmospheric water vapor content. Unless corrected, these phase distortions, which vary rapidly in time and from antenna to antenna, greatly reduce the sensitivity and image quality of these arrays. The Atacama Large Millimeter Array (ALMA) interferometer, with 64 antennae and multi-kilometer baselines, will present a very difficult phase correction problem. This talk presents the productions model design and anticipated performance of IRMA III, a third generation Infrared Radiometer for Millimeter Astronomy, which we propose as a potential phase correction solution for ALMA. Building on the success of two initial prototypes (IRMA I and II), two IRMA III devices have been built and will be deployed for testing a Llano de Chajnantor, the future ALMA site in the Atacama desert of Chile. Since there is presently limited infrastructure at the Chilean site, the design must pay careful attention to all aspects of remote operation.

The challenging phase correction requirements for ALMA necessitate special instrumentation and modeling techniques. The IRMA III system is based on a cryocooled, 20 $\mu$m MCT detector system which monitors a large number of water lines in a well defined band near the peak of the Planck curve. Due to the high brightness of the 20 $\mu$m sky, this approach provides extremely high sensitivity with a small, relatively inexpensive, passive instrument. IRMA III system consists of a compact cryocooler and detector unit, Ethernet enabled embedded microcontroller, custom data acquisition electronics, calibration source, and 100 mm off-axis parabolic reflector, all in a weather-proof enclosure roughly the size of a toaster. The two initial test systems will include Alt-Az mounts, and will be positioned on a 300 m baseline to allow novel turbulent layer height and speed measurements, as well as correlation studies with the existing NRAO 12 GHz test interferometer. Members of our group have also developed an atmospheric model which has been used to verify the results from the first prototypes, and to predict the performance of IRMA III at the ALMA site.

0-7803-7846-6/03/$17.00 

# Water Vapor Phase Correction at OVRO

David Woody* and John Carpenter
Caltech
Owens Valley Radio Observatory, Big Pine, CA 93513

Correction of tropospheric phase errors is a major challenge for the next generation of millimeter and sub-millimeter interferometers. While the longest baselines at millimeter wavelengths have a nominal resolution of 0.01 arcsec, the fluctuations in water vapor in the atmosphere often limits the seeing to 0.1 arcsec or worse at even the best sites. It is important to remove the effect of these fluctuations if these instruments are to reach their full potential.

OVRO has had an ongoing program to use three channel radiometers observing the 22 GHz water vapor line to measure and correct the wet component of the tropospheric phase fluctuations. Each of the six 10 m diameter antennas in the millimeter interferometer array has cooled Water Line Monitor (WLM) which uses the full 10 m aperture to produce a pencil beam that is closely aligned with the millimeter astronomy beam.

The initial studies show that a large fraction of the water vapor induced phase fluctuations can be corrected and improved images obtained. The correction of the decorrelation on the five minute time scale is straightforward. It has also been demonstrated that linking the phase of the calibrator to the target source along with differential WLM phase correction can dramatically improve the astronomical images in bad seeing conditions. The challenge has been to develop robust imaging algorithms that can cope with the varying weather conditions and imperfections in the radiometers. The instabilities of the radiometers on the time scale from a few minutes to a few hours has been the most challenging aspect of the system.

This paper will report on the algorithms developed for processing the WLM and astronomy data and the degree to which they can correct for the tropospheric phase fluctuations.

0-7803-7846-6/03/$17.00 ©2003 IEEE

*Special Session*

## Frontiers in FDTD Theory and Applications

**Organizer(s):** Susan C. Hagness
Gianluca Lazzi

**Co-Chairs:** S. Hagness
G. Lazzi

7:55 Opening Remarks

# Two Emerging Multiphysics FDTD Applications from the Megameter Scale at 3 Hz to the Nanometer Scale at 300 THz

**Allen Taflove,* Jamesina Simpson, and Gilbert Chang**
Department of Electrical and Computer Engineering
McCormick School of Engineering, Northwestern University
Evanston, IL 60208

We foresee that, as computer and algorithm capabilities expand, finite-difference time-domain (FDTD) modeling will often be performed in the context of multiphysics simulations involving the simultaneous solution of the Maxwell's equations of classical electrodynamics and other fundamental equations of physics. Two examples of such multiphysics problems will be discussed in this paper. These examples "book-end" the spectrum from the megameter scale at ~3 Hz to the nanometer scale at ~300 THz.

- Example 1: Coupling of the Earth's seismic activities to its global electromagnetic environment at extremely low frequencies (ELF).

  Three-dimensional (3-D) finite-element models of the mechanics of plate tectonics, deformation, and fracturing will provide data for subterranean current sources due to piezoelectric and related effects which transduce changes in rock stresses to time-dependent electric signals. FDTD will then be applied to model the generation and propagation of electromagnetic waves due to these sources. 3-D FDTD models will account for the inhomogeneous dielectric properties of the entire global Earth-ionosphere waveguide system, including the lithosphere, oceans, and ionosphere within at least ±100 km of the Earth's surface. The end result of such modeling may be means to anticipate large-scale seismic events, if unique precursory signatures can be detected above the natural ELF noise background.

- Example 2: Coupling of the quantum behavior of electrons in multi-level atomic systems to photonic feedback systems.

  Systems of equations that describe electron populations within, and transitions between, multiple energy levels in atomic systems will be coupled to 3-D FDTD models of electromagnetic wave propagation within deterministic and random photonic feedback structures containing the atoms. There is emerging evidence that random arrangements of such atoms can yield lasing behavior at thresholds about as low as for deterministic arrangements, but with much lower manufacturing costs. More broadly, the synthesis of classical and quantum computational electrodynamics will assist in the development of a variety of 21st-century electronic and photonic devices engineered at the nanometer scale.

We expect that these and similar multiphysics FDTD applications will yield significant benefits for our society in areas as diverse as computing, telecommunications, and public health and safety.

0-7803-7846-6/03/$17.00 ©2003 IEEE 

# Toward the Creation of a Magic Time Step in Three-Dimensional FDTD Algorithms

C. L. Wagner* and J. B. Schneider
School of Electrical Engineering and Computer Science
Washington State University, Pullman, WA 99164-2752, USA
E-mail: clwagner@eecs.wsu.edu, schneidj@eecs.wsu.edu

When operated at the Courant stability limit, the one-dimensional (1D) Yee algorithm is a numerically exact differential equation solver—the only errors are due to the finite precision of digital computer arithmetic. The stability limit in 1D is obtained when the temporal step size is equal to the product of the spatial step size and the speed of propagation. Since this temporal step size yields zero errors, it is termed the "magic" time step. Unfortunately there is no magic time step in the classic Yee algorithm in higher dimensions.

However, for hyperbolic systems of coupled first-order equations (such as Maxwell's equations or the small-signal acoustics equations), volumetric (as opposed to point) gradient, divergence, and curl operators can be derived which allow the construction of an algorithm that has a magic time step in three-dimensions. Theoretically, this magic time step can be arbitrarily large, but the temporal step size is tied to a spatial integration which also increases in size as the temporal step size increases. Other than requiring that fields be staggered in time, the proposed algorithm is not tied to any specific grid. The algorithm requires the calculation of single-variable derivatives of multi-variable integrals of fields but it does not dictate the way in which these calculations are performed. Thus, fields may be offset or collocated. In a computer implementation of the algorithm the underlying calculations use sampling and reconstruction theory where the operators reduce to volumetrically summing the product of weighting coefficients and field values. Although the update coefficients can be precomputed prior to a simulation, obtaining them for any particular space-time grid is computationally expensive.

To demonstrate the method, an approximate version of the proposed algorithm is used to solve a rectangular resonator problem. As will be shown, even this simple (though certainly somewhat brute-force) implementation of the algorithm provides a good prediction of the true resonant frequencies up to the sampling limits imposed by the discretization of time and space. Results are also compared to, and shown to be superior to, those obtained using the standard Yee algorithm. As will be discussed, the computational expense of the global operators used in the algorithm is large since these operators are volumetrically global (as opposed to an algorithm such as PSTD which employs operators which are one-dimensionally global).

0-7803-7846-6/03/$17.00 ©2003 IEEE 

# A Novel PML Implementation for the ADI-FDTD Method with Reduced Reflection Error

Shumin Wang* and Fernando L. Teixeira

ElectroScience Laboratory and Department of Electrical Engineering
The Ohio State University, 1320 Kinnear Road, Columbus, OH 43212, U.S.A
e-mail: wangs@ee.eng.ohio-state.edu

The Alternating-Direction Implicit Finite Difference Time Domain (ADI-FDTD) method has been shown to be an attractive alternative to the standard FDTD in some problems due to its unconditional stability with moderate computational overhead. The ADI-FDTD can be particularly useful for problems involving devices with fine geometric features that are much smaller than the wavelength(s) of interest. In order to be applied for unbounded domain problems, the ADI-FDTD requires the use of appropriate absorbing boundary conditions, such as the perfectly matched layer (PML). The PML has been extended to the ADI-FDTD method previously and it has been shown that while the PML can still provide very small reflections at small Courant numbers, its performance gradually deteriorates for large Courant numbers.

Because the ADI-FDTD method is most useful for large (greater than unity) Courant numbers, a PML implementation that does not deteriorate for large Courant numbers is highly desirable. Here we introduce a novel PML implementation for the ADI-FDTD for this purpose. The proposed PML relies on successively applying forward and backward differencing in time for the conduction terms in the ADI-FDTD update, instead of center difference scheme used in the traditional PML implementation for the ADI-FDTD. As a result, the proposed PML maintains almost the same low level refection error for large Courant numbers.

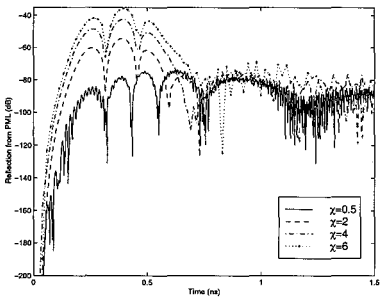


Fig. 1. Reflection error from the PML-ADI-FDTD method with traditional PML implementation.

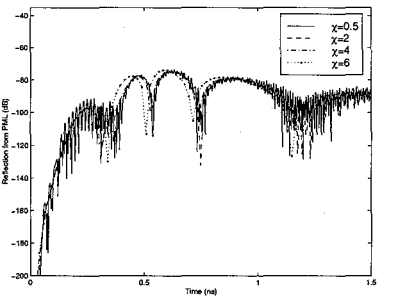


Fig. 2. Reflection error from the PML-ADI-FDTD method with improved PML implementation.

0-7803-7846-6/03/$17.00 ©2003 IEEE

# Specific Absorption Rate (SAR) Computation Using the D-H Unconditionally Stable ADI-FDTD Method

Stefan Schmidt* and Gianluca Lazzi

Department of Electrical and Computer Engineering,
North Carolina State University, Raleigh, NC 27695-7914, USA

As more and more applications of wireless devices in the personal space are emerging, the interaction of electromagnetic energy and biological objects has become increasingly important to researchers and the public. Due to the fear and awareness that health damage may be caused by the use of wireless equipment, it is important to minimize the electromagnetic interaction of wireless designs with the human body. Repetitive prototyping and measurements for specific absorption rate (SAR) minimization often can be too expensive and time consuming; hence, efficient and fast numerical methods are a very attractive alternative.

Electromagnetic problems, involving inhomogeneous dispersive media, are easily solved using the finite-difference time-domain (FDTD) method. For explicit FDTD methods, the fine geometric detail given in anatomical models, which is often far smaller than the wavelength under investigation, would dictate rather small time steps due to the CFL stability bound. This would lead to a large number of necessary computations and lengthy simulations. In contrast, an unconditionally stable FDTD method can alleviate the time step constraint and lead to an efficient method for bioelectromagnetic problems.

Our objective is to apply an unconditionally stable alternating direction implicit (ADI) method to the simulation of bioelectromagnetic problems and the computation of the SAR. To this end, a material independent D-H field formulation of the perfectly matched layer (PML) absorbing boundary condition is used. This choice leads to an efficient and simple implementation, which allows the truncation of dispersive material models. Furthermore, this formulation is easily extended to $n^{th}$ order dispersive materials. The D-H ADI FDTD method is tested on spherical geometries where the SAR distribution is computed. Results are compared to the explicit FDTD method and previously published experimental results.

0-7803-7846-6/03/$17.00 ©2003 IEEE

# One-step algorithm to solve the time-dependent Maxwell equations

H. De Raedt*, K. Michielsen, J.S. Kole, and M.T. Figge
Applied Physics - Computational Physics
Materials Science Centre
University of Groningen, Nijenborgh 4
NL-9747 AG Groningen, The Netherlands
http://www.compphys.org

We discuss a unified framework to construct and analyze finite-difference time-domain (FDTD) algorithms to solve the time-dependent Maxwell equations for systems with current sources and spatial variations in both the permittivity and the permeability. The basic idea of this approach is to use (variants of) the Lie-Trotter-Suzuki product-formula to approximate the formal solution, i.e. the time evolution matrix, of the Maxwell equations.

The conventional Yee algorithm naturally fits into this framework and we demonstrate that, by minor modification of the original Yee algorithm, second-order and fourth-order time-accurate schemes can be constructed that do not require the use of staggered-in-time fields, nor extra memory to store intermediate results.

In the case that the energy of the electromagnetic (EM) fields is a conserved quantity, the time evolution matrix is the matrix exponential of a skew-symmetric matrix. Approximations to the time evolution matrix that preserve this symmetry take the form of products of orthogonal transformations. The resulting numerical algorithms are unconditionally stable by construction. Replacing each of the matrix exponentials by its (1,1) Padé approximation (Cayley form) yields the unconditionally stable alternating-direction-implicit time-stepping algorithms proposed by F. Zheng and co-workers and T. Namiki.

In practice, to maintain a reasonable degree of accuracy during the time integration (and stability in the case of Yee-type algorithms), the time step in FDTD calculations has to be relatively small. Then, the amount of computational work required to propagate the EM fields for long times may be prohibitive for a class of important applications, such as bioelectromagnetics and VLSI design. Therefore it is of interest to explore alternative approaches that improve the accuracy and/or efficiency of the time integration.

One such possibility is to approximate the time evolution matrix by a Chebyshev polynomial of the skew-symmetric matrix that represents the (discretized) spatial part of the Maxwell equations. The result of this approach is a one-step algorithm that solves the time-dependent Maxwell equations for (very) large time steps but does not provide information about the EM fields for intermediate times.

Based on results of numerical experiments and rigorous error analysis, we discuss the virtues and shortcomings of the different algorithms. For applications where the long-time behavior is of main interest, we find that the one-step algorithm may be an order of magnitude more efficient than present multiple time-step FDTD algorithms.

0-7803-7846-6/03/$17.00 ©2003 IEEE 

# A LOOK AT THE CAUSE OF INSTABILITY PROBLEMS IN FDTD HYBRIDIZATION SCHEMES–AND A PROPOSED REMEDY

R. Mittra, M. Marrone and Wenhua Yu
EMC Lab, 319 EE East
Pennsylvania State University
e-mail: mittra@engr.psu.edu

Enforcing the Courant condition on the time step is a reliable approach to guaranteeing, in most part, the stability of the Yee-FDTD algorithm on a uniform or non-uniform but Cartesian grid. However, the same cannot be said about the hybridized version of the FDTD scheme, where in one uses a sub-grid or an unstructured mesh for instance, in a sub-region embedded within the FDTD computational domain. In a recent paper Railton and his co-workers have shown that certain conformal FDTD algorithms suffer from instability problems because they violate reciprocity, and have also suggested a way to rectify the situation by modifying the CFDTD algorithm. However, it is not obvious how a similar analysis can provide a clue as to the origin of the instability problems that frequently arise in hybrid schemes, which combine the conventional FDTD either with explicit sub-gridding algorithms, or with FETD and ADI schemes that are implicit in nature. The problem of instability in the above hybridization schemes has been examined by a number of researchers and it has been observed that the spurious reflections introduced by the interface of the FDTD and the inner sub-region not only corrupts the solution, but also causes the hybrid scheme to be unstable. While the above observations regarding the interface mismatch is indeed correct, it neither provide a convenient indicator for detecting the instability phenomenon in advance of running the FDTD program, nor does it provide a systematic and reliable approach to eradicating the problem.

In this paper we examine the issue of instability on a theoretical basis and show that a systematic indicator, based on the eigenvalues of certain system matrix can serve as a reliable indicator for the instability problem, assuring the stability of the hybrid algorithm if all the eigenvalues are located within the unit circle. This approach not only enables us to establish *a priori* that the algorithm is stable, but also provides us a clue as to how we might attempt to rectify the problem, and re-test the stability using the eigenvalue-spread criterion.

To illustrate the application of approach described above, we consider two scenarios shown in the figures below.

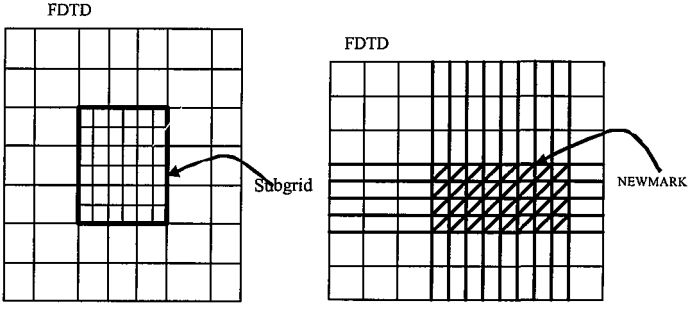


We consider both the cases illustrated above; *viz.*, hybridization of coarse grid FDTD scheme with the ADI or the Newmark-beta algorithm, on: (i) fine Cartesian grid; (ii) non-Cartesian grid, such as a triangular one.

The formulation of the stability problem is based on the Cell Method recently introduced by Marrone and his co-workers in a number of recent papers.

0-7803-7846-6/03/$17.00 ©2003 IEEE

# FDTD for Parametric Modeling of Nano-Structured Surface Relief Profiles for an Alternate Mode of Optical Data Storage

**Mike Potter***
Department of Electrical and Computer Engineering, University of Calgary, Calgary, Alberta, Canada, mpotter@ieee.org

**Richard W. Ziolkowski and Mark A. Neifeld**
Department of Electrical and Computer Engineering, University of Arizona, Tucson, Arizona, USA, ziolkows@ece.arizona.edu, neifeld@ece.arizona.edu

Current generation memory devices generally rely on one of two technologies, magnetic or optical storage. Examples would be hard drives for the former, and CD-ROMs for the latter. Both methodologies have provided very high capacity, and research continues in the improvement of both approaches. Classical resolution scales typically limit current optical memories to structures on the order of half a wavelength. Holography has been used to extend memories into the third dimension to capitalize on density. Demonstrations have shown faster access time than a hard disk for holographic random access memory, and 40Mbits/cm$^2$ capacity has been demonstrated in a working holographic read-only memory system. However, a limit is eventually reached where adding extra holograms will distort existing ones due to interference effects

Sub-wavelength topographical features created by imprint lithography can also be used as data that can be read using atomic force microscopy. Work in this area has demonstrated significantly enhanced storage densities, i.e., on the order of 400Gbits/in$^2$. One of the limitations with such a method is that each feature is read serially, and the time scale of the reading process introduces non-trivial latency effects.

The focus of our research is to gain the benefits of both methodologies: an excellent density of features obtained through imprint lithography or some other such process, and the ability to read data in parallel. Sub-wavelength surface-relief structures (binary and non-binary) are being investigated for this data storage application. These structures are amenable to low-cost manufacturing processes and facilitate near-field parallel readout with optical power detectors.

A variety of candidate structures have studied using the finite-difference time-domain (FDTD) method: simple relief patterns with low and high index refractive materials, high index materials with low index backfill, and low index materials with high index backfill. The high index profile with low index backfill appears to provide the best discrimination of the data readout vectors. The flexibility of the materials and geometries accessible to modeling with the FDTD approach has proved beneficial to testing these structures. Preliminary parameterizations have yielded storage densities of more than 5 bits per wavelength. A second objective of our studies has been to determine how varying nearby structures randomly (neighboring cells) affects each data vector, i.e., to determine the crosstalk between storage elements. For a given configuration $k$ and associated data vector, varying the neighbors creates an ensemble of data vectors associated with that $k$. We then determine whether *every* element in the ensemble $k$ will be distinguishable from every other element (in the sense that it is read as $k$ or as some other value) in all other ensembles. If it is distinguishable, then this configuration can represent a valid memory state. The number of distinguishable configurations (states) determines our capacity, and hence our memory storage density.

The bulk of the progress made in the past year has revolved around parameterizing and optimizing structures, according to metrics such as the height of features, the gap between cells, and the material constants. The storage density of these structures has approached 10Gbits/cm$^2$. This result should be compared with the approximately 5Gbits that a CD-ROM now holds. Several of these metrics, the resulting storage density results, and anticipated improvements will be discussed.

0-7803-7846-6/03/$17.00 ©2003 IEEE

# PSTD Modeling of Nonlinear Electrodynamics

**Tae-Woo Lee* and Susan C. Hagness**
Department of Electrical and Computer Engineering
University of Wisconsin-Madison
1415 Engineering Drive, Madison, WI 53706
(email: tae-woo@cae.wisc.edu, hagness@engr.wisc.edu)

Frequency conversion processes in nonlinear materials are extremely sensitive to the phase velocities of interacting electromagnetic waves. In order to accurately model such problems using FDTD, extremely fine grid resolutions are required to minimize the effects of numerical dispersion. We have recently shown that PSTD methods with second-order (PSTD-2) and fourth-order (PSTD-4) accuracy in time offer significant improvements in computational efficiency and accuracy for modeling electromagnetic wave interactions in frequency-independent $\chi^{(2)}$ nonlinear optical materials (T. W. Lee and S. C. Hagness, *IEEE Antennas and Propagation Society International Symposium*, vol. 3, pp. 232-235, San Antonio, TX, June 2002). However, accurate simulations require not only minimizing numerical dispersion, but also incorporating the material dispersion characteristics inherent in optical media.

In this paper, we present an algorithm extension of our previous work. Specifically, we incorporate the physics of material dispersion into the nonlinear PSTD-4 method using an auxiliary differential equation (ADE) technique. The dispersion model used in this study is that of a Lorentz medium. The ADE approach offers the ability the model the linear susceptibility of the Lorentz dispersion and the instantaneous nonlinear susceptibility. The ADE approach used here differs from previous techniques (for example, see P. M. Goorjian, A. Taflove, R. M. Joseph, and S C. Hagness, *IEEE J. Quantum Electronics*, 28: 2416-2442, 1992) in that it is developed for PSTD rather than FDTD and is applied to a second-order nonlinearity rather than a third-order nonlinearity. Also, it does not require iteratively solving a nonlinear constitutive relation.

In this talk, the computational features of the PSTD-4 algorithm will be discussed. The accuracy and computational efficiency are evaluated by modeling second harmonic generation in a simple nonlinear waveguide with a quasi-phase matched grating. The results show that even though a second-order-accurate time discretization is applied in the ADE approach, PSTD-4 still provides accurate results with a relatively large time step compare to PSTD-2. In some cases, it is found that the stability limit becomes sensitive to the choice of Lorentz dispersion parameters. This sensitivity is impacted by how the central differencing is implemented in the ADE.

In addition, we will present a few application examples illustrating the use of the PSTD-4 algorithm for modeling frequency conversion processes in nonlinear dispersive media. The first-principles modeling tool developed in this study can help provide invaluable insights about the complex wave phenomena inherent in photonic nonlinear-micro/nanostructures such as nonlinear photonic crystals.

0-7803-7846-6/03/$17.00 ©2003 IEEE 

# An Investigation of the Coupling between Extremely Compact Microstrip Patch Antennas in a Link for Biomedical Implants

Keyoor Gosalia* [1], Wentai Liu [1,2], James Weiland [3], Mark Humayun [3] and Gianluca Lazzi [1]

[1] Department of Electrical and Computer Engineering, NC State University, Raleigh, NC
[2] Department of Electrical Engineering, UC Santa Cruz, Santa Cruz, CA
[3] Retina Institute, Doheny Eye Institute, Keck School of Medicine of USC, Los Angeles, CA

Data communication between the external and internal components for biomedical prosthetic devices has traditionally been accomplished via low frequency (1-20 MHz) inductive links between two coils. In this approach, the low frequency power carrier is modulated by an information signal. This imposes a limitation on the achievable data bandwidth, which is dependent on the power carrier frequency. In data intensive biomedical implants such as a visual prosthesis, lack of adequate bandwidth may prove to be a significant functionality constraint in the efficient operation of the entire prosthetic system. In such cases, data communication at microwave frequencies (1–3 GHz) using a pair of external and internal microstrip patch antennas is a viable alternative and can provide a much larger bandwidth.

This work addresses the design of appropriately sized patch antennas and their coupling issues for a visual prosthetic device. Two frequency bands of operation were considered at 1.35–1.45 GHz and 2.35–2.45 GHz. For both the frequency bands, the external (transmitting) antenna size was restricted to $25 \times 25$ mm. Size of the receiving antenna was to be restricted to $6 \times 6$ mm. Hence, to reduce the surface area, size reduction techniques such as shorting posts, high dielectric constant and maximizing the current path (by incorporating slits) were employed to design the receiving antennas and restrict their size to $6 \times 6$ mm for both the frequency bands. Optimal design of the antennas was carried out using an in house FDTD code and then the transmit–receive pairs were implemented to resonate at the same frequency in both the frequency bands.

A parametric analysis of the free space coupling as a function of separation, spatial relative orientation and spatial angle of orientation was carried out at both the frequency bands. Due to their eventual intended application in a retinal prosthesis, the maximum separation distance was fixed at 35 mm. Within this distance the coupling exhibits near field behavior and it is observed that the antenna performance characteristics (resonant frequency, impedance) are sensitive to their relative proximity. It is further observed that the receiver antenna which exhibits a mixed polarization characteristic (due to shorting posts and several slits), is sensitive to a particular polarization of the transmitter antenna even in the near field region. Detailed account of the antenna design issues and a comprehensive investigation of parametric analysis of the coupling between the two antennas in both the frequency bands will be presented.

0-7803-7846-6/03/$17.00 ©2003 IEEE

# A Combination of the FDTD Method and Signal Processing Techniques: Fast FDTD/ARMA Approach

Fan Yang and Yahya Rahmat-Samii
ygfn@ee.ucla.edu, rahmat@ee.ucla.edu
Electrical Engineering Department
University of California at Los Angles
Los Angeles, CA 90095

The finite difference time domain (FDTD) method is a powerful and versatile numerical tool to analyze various electromagnetic structures. It has been widely used in the guided waves, radiation, and scattering analyses. The electromagnetic fields are calculated in the time domain using the Yee's algorithm and the frequency domain properties of the analyzed structure can be readily obtained through the Fourier transform. However, a relatively long time sequence needs to be computed for accurate characterizations of complex structures.

**Traditional fast algorithms.** The traditional fast algorithms start with a general complex exponential model for the FDTD time domain data as below:

$$h(n) = \sum_{k=1}^{K} C_k e^{(-\alpha_k + j2\pi f_k)dt \cdot n} \qquad n = 1,2,\cdots N \tag{1}$$

The coefficients can be determined by the Prony method or the generalized pencil-of-function method.

**Novel FDTD/ARMA approach.** From the signal processing viewpoint, the time domain data of the FDTD simulation can be defined as an impulse response (IR) of a linear time invariance system with an autoregressive moving average (ARMA) transfer function (A. K. Shaw and K. Naishadham, *IEEE Trans. Antennas Propagat.*, 49(3), 327-339, 2001):

$$H(z) = \frac{a_0 + a_1 Z^{-1} + a_2 Z^{-2} + \cdots + a_q Z^{-q}}{1 + b_1 Z^{-1} + b_2 Z^{-2} + \cdots + b_p Z^{-p}} \tag{2}$$

It is noticed that if one takes $z$ transform on both side of (1):

$$H(z) = \sum_{k=1}^{K} \frac{C_k}{(1 - (-\alpha_k + j2\pi f_k) \cdot Z^{-1})} = \frac{a_0 + a_1 Z^{-1} + a_2 Z^{-2} + \cdots + a_{p-1} Z^{-(p-1)}}{1 + b_1 Z^{-1} + b_2 Z^{-2} + \cdots + b_p Z^{-p}} \tag{3}$$

Thus, Eq. (1) is a special case of Eq. (2) when $q = p-1$. The coefficients of Eq. (2) can be determined through an iterative optimization process.

**Antenna analysis using the FDTD/ARMA method.** Several microstrip antennas are analyzed using both the FDTD/ARMA method and the traditional FDTD/Prony method. It is observed that the error of the ARMA model is smaller than that of the Prony method. Additionally, for a given error criterion the order of the ARMA model appears to be much smaller than that required by the Prony method.

0-7803-7846-6/03/$17.00 ©2003 IEEE

# Advances in FDTD Acceleration

Ryan N. Schneider *
ryan.schneider@ieee.org

Michal M. Okoniewski
michal@enel.ucalgary.ca

Laurence E. Turner
turner@enel.ucalgary.ca

Dept. of Electrical and
Computer Engineering
University of Calgary
Calgary, Alberta CANADA

The Finite-Difference Time-Domain (FDTD) Method has been widely and successfully applied to the modelling of complex electromagnetic behavior. The method is both flexible and accurate for a wide range of problems. The major drawback of FDTD is that it is computationally intensive and, hence, simulations can run for hours to days on multiprocessor supercomputers. Drastically reducing the runtime of FDTD simulations would greatly benefit FDTD users and open up new avenues of research. The primary goal of the research is to achieve an order of magnitude acceleration for existing FDTD software, as compared to a current personal computer (PC), by using (i) custom, programmable hardware, (ii) fine-grained parallelism and (iii) integer arithmetic. It is also desirable that this level of acceleration is achieved at a lower cost than current "accelerated" implementations.

Traditionally, FDTD has been accelerated by using parallel processing implementations, namely multi-processor, shared-memory architectures and distributed message-passing architectures. More recently, other research has been performed into hardware accelerators for FDTD. Marek, *et al*, predict a five- to nine-fold acceleration of the main FDTD update equations and PML equations, respectively, using a simulated hardware description language (HDL) design targeted for the Sparc workstation. Placidi, *et al*, describe a simulated VLSI design intended for FDTD computations on the PC platform. This work was again limited to simulation of the hardware and they predict a four-fold acceleration of the FDTD update equations.

For our research digital circuits that compute one- and two-dimensional FDTD update equations are implemented and measured on field-programmable gate-array (FPGA) hardware. Table I depicts the acceleration achieved compared to a reference PC.

TABLE I
HARDWARE ACCELERATION OF ONE- AND TWO-DIMENSIONAL FDTD

| Simulation Method | Runtime† (ms) | Acceleration |
|---|---|---|
| Software - 1D | 71 | |
| Hardware - 1D | 8.49 | 8.4X |
| Software - 2D | 230 | |
| Hardware - 2D | 12.5 | 18.4X |

†10,000 time steps

This method implements every single cell of the simulation in hardware. The computations are performed using a bit-serial, pipelined architecture and 2's-complement, integer arithmetic. A larger simulation requires more hardware, but also yields greater acceleration. Other methods are also discussed which reuse a smaller amount of hardware to achieve the desired acceleration.

0-7803-7846-6/03/$17.00 ©2003 IEEE

*Special Session*

## EBG Surfaces 1: Realizations

**Organizer(s):** Per-Simon Kildal
N. Eegheta
**Co-Chairs:** N. Engheta
P. S. Kildal

7:55 Opening Remarks

54. 1 8:00 A Novel Artificial Reactive Impedance Surface for Miniaturized Wideband Planar Antenna Design: Concept and Characterization ..... APS
*H. Mosallaei, K. Sarabandi, The University of Michigan, USA*

54. 2 8:20 Easily Designed and Constructed High Impedance Surfaces ..... APS
*K. W. Whites, B. Glover, T. Amert, South Dakota School of Mines and Technology, USA*

54. 3 8:40 AMCs Comprised of Interdigital Capacitor FSS Layers Enable Lower Cost Applications ..... APS
*S. Rogers, W. McKinzie, G. Mendolia, Etenna Corporation, USA*

54. 4 9:00 Design of High-Impedance Screens by using Multilayered Frequency Selective Surfaces ..... APS
*A. Monorchio, L. Lanuzza, G. Manara, University of Pisa, Italy*

54. 5 9:20 A Robust GA-FSS Technique for the Synthesis of Optimal Multiband AMCs with Angular Stability ..... APS
*L. Lanuzza, A. Monorchio, University of Pisa, Italy, D. J. Kern, D. H. Werner, The Pennsylvania State University, USA*

54. 6 9:40 A Multi-Band Artificial Magnetic Conductor Comprised of Multiple FSS Layers ..... APS
*W. McKinzie, S. Rogers, Etenna Corporation, USA*

54. 7 10:00 Active Negative Impedance Loaded EBG Structures for the Realization of Ultra-Wideband Artificial Magnetic Conductors ..... APS
*D. Kern, D. Werner, The Pennsylvania State University,*

54. 8 10:20 Magnetic Loading of Artificial Magnetic Conductors for Bandwidth Enhancement ..... APS
*R. Diaz, Arizona State University, V. C. Sanchez, E. Caswell, A. Miller, Titan - Aerospace Electronics Division, USA*

54. 9 10:40 How To Transform an EBG Surface To a Soft or Hard Surface and Thereby Improve Its STOP or GO Characteristics ..... 269
*P-S. Kildal, Chalmers University of Technology, Sweden*

54. 10 11:00 Low-Loss Tunable Monolithic Electromagnetic Crystal Surfaces with Planar GaAs Schottky Diodes ..... APS
*Hao Xin, H. Kazemi, Rockwell Scientific Company, A. W. Lee, UCLA, J. A. Higgins, M. J. Rosker, Rockwell Scientific Company, USA*

**How to transform an EBG surface to a soft or hard surface and thereby improve its STOP or GO characteristics**

Per-Simon Kildal, Fellow IEEE, www.kildal.se
Department of Electromagnetics, Chalmers University of Technology
41296 Gothenburg, SWEDEN

Sometimes electromagnetic bandgap (EBG) surfaces are used to reduce coupling or remove surface waves, which we herein refer to as a STOP characteristic. In many such cases the performance will be better if the EBG instead was made anisotropic like a soft surface, because the soft surface has STOP characteristics for all polarizations. Other times opposite walls of a rectangular waveguide are made of EBG surfaces to make them support quasi-TEM waves, herein being referred to as a GO characteristic. In such cases the performance will be better if the EBG walls (or preferably all walls) were made like hard surfaces, because the hard surface has GO characteristics for all polarizations. In both these two cases the EBG is normally behaving like an artificial magnetic conductor, whereas the soft or hard surface always can be represented by a PEC/PMC strip grid oriented transversely or longitudinally, respectively, with respect to the propagation direction of the wave along the surface. The purpose of the present paper is to define the STOP and GO characteristics of high impedance EBGs that are realizations of artificial magnetic conductors (AMCs), and soft/hard surfaces. We will also show by computation and measurements how to transform an AMC to a soft/hard surface.

We have taken a dual layer high impedance surface (i.e. an AMC) of mushroom type and measured the transmission between two vertical monopoles and two horizontal dipoles located on top of it. The measurements were repeated on a metal surface (i.e. PEC) of the same size, and on the AMC when this was provided with thin parallel metal strips (Aluminum tape) to obtain a soft/hard surface. We could then easily verify that the STOP characteristics are generally better for the soft surface than for the AMC, and that the GO characteristics are better for the hard surface. In the former case there is an exception, namely suppression of TEM waves between parallel plates, which is normally better with an AMC than a soft surface.

We have also computed the couplings with three moment method codes for the ideal cases of PEC, PMC, soft and hard surfaces. This could not easily be done, because commercial codes cannot normally model PMCs of finite extent and arbitrary shape, and certainly not soft and hard surfaces by a PEC/PMC strip grid. We have, however, built the latter model into an in-house code. It is desirable that commercial codes get these possibilities as well. The results are generally in agreement with the measurements, but not in detail, because we did not try to model the frequency behavior of the EBG. When working with EBGs, AMCs and soft/hard surfaces it is always desirable to know the performance that can be obtained for the ideal cases, before starting the laborious work of realizing the EBG. Therefore, commercial codes should be extended to allow such computations, which also are much faster than modeling the surfaces in all details.
More about measurements and computations of these surfaces and applications can be found in (P-S. Kildal and A. Kishk, invited lecture in plenary session at ACES Conference, Monterey, March 2003, to appear in a special issue of the ACES journal).

0-7803-7846-6/03/$17.00 ©2003 IEEE 

# Metallodielectric Electromagnetic Band Gap (MEBG) Surfaces with Tunable Characteristics

J. C. Vardaxoglou*, A. Chauraya and A. P. Feresidis
Wireless Communications Research Group
Loughborough University, Loughborough, LE11 3TU, UK
Email: J.C.Vardaxoglou@lboro.ac.uk

Metallodielectric Electromagnetic Band Gap (MEBG) surfaces are prime candidates for yielding controlled band gap performance due to their resonant nature. Here we present the performance of optically tunable MEBG surfaces formed by printed dipole arrays with several configurations. Photonic tuning is achieved by utilising the photoconductive properties of silicon. High resistivity (typically $\rho > 6$ k$\Omega$-cm) silicon microswitches are positioned appropriately in order to allow the dimensions of the resonant elements to be altered. This is achieved by switching between the on or off state, thus yielding a reconfigurable band gap. Low power LEDs are placed directly above the switches and emit a uniform optical beam of about 5mW and 7.5mW when driven at 0.5 Amps and 2 Amps respectively. Figure 1 shows results measured during dynamic tuning of a dipole MEBG array achieved by switching on and off defects in the array. Figure 2 presents simulation results showing the effect of tuning the resonant length, and hence the band gap, of a dipole array.

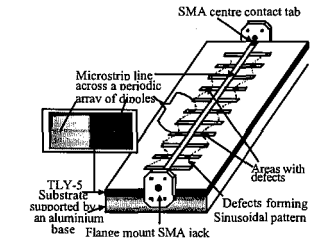


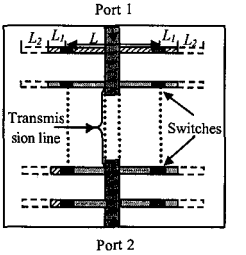


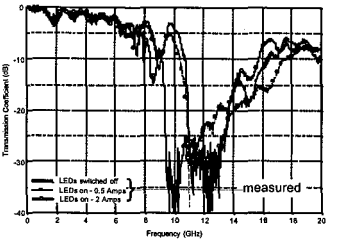


**Figure 1**

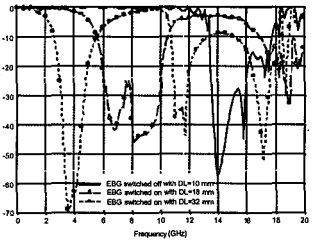


**Figure 2**

## Vehicle Electromagnetics and Inverse Scattering

**Co-Chairs:** D. Thiel
E. Rothwell

7:55 Opening Remarks

# SIMULATION OF A FM BAND SELF-STRUCTURING ANTENNA IN AN AUTOMOBILE ENVIRONMENT

B. T. Perry*, E.J. Rothwell, L.C. Kempel
ECE Department
Michigan State University
East Lansing, MI 48824
rothwell@egr.msu.edu

J. E. Ross
John Ross & Associates
422 N. Chicago Street
Salt Lake City, Utah
johnross@johnross.com

L.L. Nagy
Delphi Research Labs
51786 Shelby Pkwy
Shelby Township, MI

Antennas are often placed in environments where their interaction with surrounding objects effects their overall performance. Some are deployed in environments where the designer is unsure of the effect on the performance of the antenna. This is especially true in automotive applications where the car body, as well as other components of the vehicle, play a role in the functionality of the antennas. Self-structuring antennas (SSAs) are subject to this uncertainty during their design and analysis. For this reason, a simulation-based assessment of a self-structuring antenna placed in the rear window of an automobile was undertaken.

Using GA-NEC, a software package developed by John Ross & Associates, the states of the self-structuring antenna are chosen by way of a genetic algorithm. Chromosomes used in the GA consist of the states of switches residing on the self-structuring antenna template. Variations in the switch states give rise to changes in the electrical shape of the antenna, as described in previous work on the subject of SSAs. Analysis is done using NEC in the FM band (88-108MHz). Performance criteria such as input impedance, VSWR, and gain are used in the determination of the fitness of a certain SSA state.

The simulation of SSAs presented here is meant to provide a cost effective approach to the design of self-structuring antennas in environments that are not optimal for performance of an antenna. This study helps to provide a framework for a simulation-based approach to the study of self-structuring antennas in various environments, including automotive applications. As a specific example, an SSA placed in the upper rear window of a vehicle is considered. The results are compared to the simulation of a passive backlight antenna placed in the same environment.

0-7803-7846-6/03/$17.00 ©2003 IEEE

# A COMPARISON OF SEVERAL SELF-STRUCTURING ANTENNA TEMPLATES

B. T. Perry*, J.A. Nanzer
E.J. Rothwell, L.C. Kempel
ECE Department
Michigan State University
East Lansing, MI 48824
rothwell@egr.msu.edu

J. E. Ross
John Ross & Associates
422 N. Chicago Street
Salt Lake City, Utah
johnross@johnross.com

L.L. Nagy
Delphi Research Labs
51786 Shelby Pkwy
Shelby Township, MI

Successful operation of a self-structuring antenna (SSA) depends both on the large number of available antenna states, and the underlying characteristics of the antenna template. For example, if an antenna template is too small, an SSA likely won't perform well for low frequency applications, regardless of the switch states. Another possibility is that an SSA template is of appropriate size; in this case, the performance of the antenna depends on both the switch states and the configuration of the antenna elements. Up to this point, the effect of the underlying characteristics of the antenna template, i.e., the configuration of the antenna elements, has not been thoroughly studied. This paper looks to characterize the effect of the SSA template layout, using measured data such as standing wave ratio (SWR), antenna patterns, and input impedance. By finding the effect of template layout on the performance of the SSA, guidelines can be created by which future layouts can be designed. Through this process, self-structuring antenna templates can be custom designed to better fit particular applications.

This paper uses measured performance criteria to compare and contrast several SSA template designs. These designs include a "standard", linearly spaced SSA template, as described in previous work, a variation based on a log-periodic design, and several templates that are fairly application specific. The application specific templates are configured such that all switches and control hardware are aligned along one edge of the template. This allows the SSA to be used in applications where the placement of both the feed network and the switches are desired to be hidden away.

0-7803-7846-6/03/$17.00 ©2003 IEEE 

# A New 3-D MoM-Based Code for Solution of EMC Problems in Vehicle Design

F.G. Bogdanov[1], *R.G. Jobava[1], S. Frei[2]

[1]EMCoS, Tbilisi, Georgia, email: roman.jobava@emcos.com
[2]EMC Center, AUDI AG, Ingolstadt, Germany, email: stephan.frei@audi.de

EMC problems have become recently one of the most important problems in vehicle design. This is due to the dramatic increasing of the number of antennas, electronic devices and cables in the modern vehicles resulting in extra EM radiation and interference between the signals. An examination of vehicle EMC performance has become therefore mandatory both to evaluate the proper operation of vehicle EM tools, and to protect the vehicle driver and passengers from undesired radiation and electronic fails.

Numerical simulation of EMC problems is nowadays the more and more realistic alternative to the expensive experiments. The Method of Moments (MoM) is now the most popular technique for EM treating of 3-D structures. However, the usual MoM-based 3-D EM packages, such as MININEC, NEC, ESP, CONCEPT, FEKO, are not specialized, or only partially oriented to analyze specific EMC problems, especially those for structures having combination of large and extremely small dimensions (i.e. car body and cable harness). In most such cases circuit-level considerations are also important to model realistic situations, and EM code should have interfaces for hybridization with circuit solvers.

In this contribution, a new 3-D MoM based code named TriD with both EM and EMC features is supposed to ensure EMC calculations in vehicle design, especially in those encountered in automotive industry. EM core of TriD is based on MoM solution of Electric Field Integral Equations (EFIE) for surfaces and wires using well-known Rao-Wilton-Glisson triangular basis functions on triangular patches, axial triangular basis functions on wire segments, modified transition basis functions on wire to triangles junctions, and special basis functions on grounded wire segments.

TriD EM features allow treating of arbitrary, in principal, 3-D geometry exposed by excitation sources, with accounting for finite conductivity of wire segments. TriD EMC features allow performing multi-frequency field calculations and MoM hybridization with Multi-conductor Transmission Line (MTL) technique using frequency decomposition/ assembling procedures and multi-frequency description of excitation amplitudes.

The created code has been validated both on experimental and comparison data with other codes for the particular EM problems on canonical and realistic geometries. The possibilities of TriD to effectively solve the fundamental EMC problems on the construction of the modern car will be demonstrated. The features of MoM hybridisation on car susceptibility (immunity), cross talk (coupling), radiation (emission), and antenna engineering problems will be discussed.

0-7803-7846-6/03/$17.00 ©2003 IEEE

# Using the Fast Multipole Method to Calculate the Fields inside a Motor Vehicle due to Communication Antennas

Johann J. van Tonder* and U Jakobus

EM Software & Systems-S.A., Stellenbosch, South Africa, jvtonder@emss.co.za

The multilevel fast multipole method (MLFMM) is used with the electric field integral equation (EFIE) to determine the near fields inside a motor vehicle. These near fields are calculated for communication devices in modern cars, with operating frequencies including TETRA (380-440MHz), GSM (876-915MHz, 1710-1910MHz) and Bluetooth (2400-2485MHz). The numerical calculation of near fields inside vehicles has two main practical applications: a) To assess human exposure to RF and microwave fields; b) predict electromagnetic compatability (EMC) and interference (EMI).

For efficient modeling of arbitrarily shaped 3-D geometries, the metallisation is discretised using the triangular patches of Rao, Wilton and Glisson, and the EFIE is solved with the Method of Moments (MoM). In the traditional MoM computer resources increase dramatically with the frequency (memory scales as $N^2$). For a standard passenger car at 915MHz we have approximately $N = 37,000$ unknowns (traditional MoM will require 20GB memory), at 1910MHz we have $N = 100,000$ (150GB with traditional MoM), and at 2485MHz we have $N = 200,000$ (610GB for traditional MoM). The MLFMM was therefore implemented that scales no worse than $N * log^2(N)$. The computational box is subdivided into eight equal boxes, and this subdivision continues until the smallest boxes are approximately half a wavelength. Only non-empty cubes are stored in a tree-like manner. Since the EFIE has a worse condition number than the combined field integral equation (CFIE), we must use a good preconditioner to ensure convergence in the interative solver (e.g. CGS). The CFIE cannot be used in this case, because the geometry under investigation is not closed (the windows of the car are modeled as free-space).

In the MLFMM (fast matrix-vector product) we compute a sparse near field matrix corresponding to the close interactions in the MoM impedance matrix. We will use an ILU(0) preconditioner with the same sparsity pattern as this near-field matrix (ILU preconditioning with fill-in will increase the convergence, but at the expense of memory). More implementation details, e.g. a fast spherical filter for the interpolation and filtering steps, will be discussed.

After implementation, the MLFMM was verified with the full MoM solution (out of core) at GSM 900MHz. In previous work the MLFMM was mainly used to predict far-field patterns (RCS) of closed structures for which the CFIE is better conditioned. In this paper we concentrate on the near fields inside geometries which are open structures. The near fields, human exposure levels and EMC/EMI implications for various communication antennas inside a motor vehicle will be presented up to Bluetooth frequencies.

0-7803-7846-6/03/$17.00 ©2003 IEEE

# A Comparison of 3-D Antenna Measurement with Hybrid Electromagnetic Simulation for Vehicle Antenna Development

M.R. Markey, L. C. Kempel and E.J. Rothwell
ECE Department
Michigan State University
East Lansing, MI 48824
rothwell@egr.msu.edu

R. P. Kronberger
Infineon Technologies
Secure Mobile Solutions
IC FFI
Kastenbaurstr. 2
81677 Munich,
Germany

H.G. Schuering
Fuba Automotive
Tec Center
D-31162 Bad
Salzdetfurth,
Germany

It is a prime concern for antenna designers to determine the impact of antenna placement on a vehicle. Traditionally, antennas are designed in a free-field environment and then placed on a vehicle. The resulting performance can vary significantly from the theoretical predictions. Time honored practices of place-and-test have been used to determine the impact of antenna placement in a search for the best site on the vehicle. This is time consuming and consequently expensive. Rather, it would be desirable to predict installed performance using a numerical model *a priori* to testing. This raises the question: "How good is the agreement between predictions and actual test data in terms of commercially meaningful metrics?"

A good comparison of measurement to simulation using Method of Moments (MM) based software has been achieved with a vehicle antenna for the FM band of frequencies ranging from 76-108 MHz. As the customer demand for infotainment in a vehicle rises, so also does the need for an increased number of complex antennas on the vehicle. Clearly, many of these services operate at frequencies greater than 108 MHz. As automakers look to meet these needs while lowering design costs and time, simulation becomes a necessity. Unfortunately, using MM based software can be very expensive in terms of RAM requirements and computing time for higher frequencies. This has led to the development of hybrid methods of simulation. Hybrid methods utilize the accuracy of a MM solution at critical locations such as near the feed point while using other methods elsewhere on the vehicle. Recent developments in simulation have allowed the use of hybrid methods of simulation to reduce the required RAM and computation time while maintaining an acceptable tolerance of error from a full MM solution.

This paper compares measurement to simulation using hybrid methods for a vehicle. An antenna is mounted on a simplified simulation model of a vehicle measuring roughly 3.6 x 1.5 x 1.5 meters. The 3-D radiation pattern and input impedance measurements are taken in an outdoor free-field range facility. These measurements are then compared to a hybrid MM simulation for higher frequencies ultimately up to 1 GHz. The many problems faced while using these hybrid methods and the trade off to taking measurements is discussed.

0-7803-7846-6/03/$17.00 ©2003 IEEE

**Inverse Scattering and Superresolved Lithography**

Michael A. Fiddy
Center for Optoelectronics and Optical Communications,
University of North Carolina, Charlotte, NC 28223
mafiddy@uncc.edu; 704 687 6057

In the first Born approximation, it is well known that a Fourier transform relation exists between the far field scattering pattern and the relative permittivity fluctuations associated with the scattering object. The first Born approximation requires weak scattering but if this is not the case, a Fourier relation can still be written between the far field and the product of the permittivity distribution with the total field within the scattering volume. This product is sometimes referred to as the secondary source.

For a scatterer of finite volume, the far field pattern is an entire function of exponential type and can be described using a product of factors representing the function's (complex) zeros or roots. An interesting fact is that the asymptotic zero distributions, i.e. at larger scattering angles, are at locations determined by the overall extent of the scatterer rather than its detailed internal structure. Based on this it is possible to construct a function to represent a scattered field which has prescribed asymptotic zero locations and can therefore be the scattered field from an object of well-defined size. Non-asymptotic zero locations determine the internal structure of the scatterer. In some lithography applications it is desirable to generate a scattering pattern that originates from an object or aperture of known size but which exhibits an extremely narrow or superresolved central intensity peak. This is easily achieved by redistributing the zeros of an entire function so that their density is increased thereby generating a narrow feature in one region of the scattering domain, while the absence of zeros leads to spatially broad and high intensity regions elsewhere. The inverse problem, or more precisely the inverse synthesis problem in the first Born approximation, defines the scattering object by inverse Fourier transformation of this superresolved scattered field. The resulting diffractive element necessarily contains high spatial frequency features but not sub-wavelength structures. Conversely, the extended superresolved diffraction pattern could represent the field emerging from a diffracting structure satisfying the first Born approximation and this does include sub-wavelength structures. The consequences of this are discussed.

0-7803-7846-6/03/$17.00 ©2003 IEEE 

**Scalable Three-Dimensional Inverse Scattering of a Dielectric Target Embedded in a Lossy Half Space**

Yijun Yu and Lawrence Carin
Department of Electrical and Computer Engineering
Duke University
Box 90291
Durham, NC 27708-0291

A modified iterative-Born method is applied for three-dimensional low-frequency inversion of a lossless dielectric target embedded in a lossy half space. The forward solver employs a modified form of the extended-Born method and the half-space Green's function is computed efficiently via the complex-image technique. Example results are shown, with all scattering data based on a computational model, utilizing a rigorous forward solver distinct from that employed in the inversion. In addition, distinct gridding schemes are used in the forward and inverse solvers. Simple Tikhonov regularization is found to yield adequate results, for inversion of noisy data.

To allow consideration of large problems, the forward and inverse software have been implemented in a scalable framework via the message passing interface (MPI). Algorithm scalability is addressed in this talk, considering . In addition, using the scalable software we consider three-dimensional inversion of large and realistic subsurface-sensing problems.

In addition to the iterative-Born inversion method, we also consider regression algorithms for inversion of subsurface targets. In particular, we extend the recently developed relevance-vector machine (RVM) algorithm to vector regression. The RVM algorithm was first developed for scalar regression. Here the vector components are the parameters of the subsurface target. Vector regression is considered for inversion, the results from which are then used to initialize the more-general iterative-Born formulation.

0-7803-7846-6/03/$17.00 ©2003 IEEE

# Detection of Hard Targets Camouflaged Under Foliage Using Millimeter-wave Radars

K. Sarabandi[1], A. Nashashibi[1], E. Burke[2]
1- Radiation Laboratory, The University of Michigan
saraband@eecs.umich.edu, (734) 936-1575
2- The Army Research Laboratory

Over the past decade significant amount of effort have been devoted towards development of a reliable technique for detecting ground vehicles camouflaged under foliage. Because of foliage penetration capability of microwave signals, especially at low frequencies, ultra-wideband radar systems operating over the range of 50 MHz to about 500 MHz have been proposed for this purpose. Despite significant progress in system architecture, signal processing and automatic target recognition algorithms, the initial optimism in foliage-covered target detection has not yet led to the development of an operational system that satisfies the required false alarm rate and the probability of detection. These difficulties arise from the false alarms generated by tree trunk-ground interactions that may produce backscatter levels comparable to the hard targets in the scene. Besides, VHF-UHF ultra-wideband systems require large and non-dispersive antennas capable of operating over multi-octave frequency bands and there are always the issue of interference with TV, radio, and other wireless services that degrades the backscatter signal integrity.

Having recognized the aforementioned challenges and difficulties associated with the existing foliage penetrating side-looking radars, we reexamined the problem and considered millimeter-wave (MMW) radars for this application. It is noted that electromagentic signals at millimeter-wave (MMW) frequency can penetrate a few layers of foliage with some finite attenuation and the fact that there are considerable number of holes through most foliage covers. Furthermore, very high resolution and far more compact radar systems can be designed at millimeter-wave frequencies that can easily be mounted on a tactical UAV. Design of a nadir looking, wideband MMW, SAR with a 1-D phased-array antenna spanning the wings of the UAV and capable of scanning in cross-track direction is conceived. With such system a 3-D radar map of the terrain under the flight path can be produced. Isolating the radar returns of a hard targehut from those of vegetation, a 3-D high resolution height profile of the target can be obtained. To demonstrate the feasibility of this approach, extensive foliage penetration experiments at Ka- and W-band were conducted over two well-characterized sites. Backscatter measurements over rectangular regions with a spatial resolution of about 1 m were conducted with and without vehicles throughout the growing season using a boom truck. Foliage attenuation measurements were also carried out using an array of trihedrals. An algorithm is developed that classifies the radar return and isolates the radar return from hard targets. This algorithm is applied to the measured data and the feasibility of foliage-covered target detection and identification at millimeter-wave frequencies is demonstrated.

0-7803-7846-6/03/$17.00 ©2003 IEEE

# Nondestructive evaluation of embedded structures in concrete: Modeling and imaging

K.J. Langenberg*
K. Mayer
A. Zimmer
C. Kohl
T. Krylow
Dept. Electrical Engineering and Computer Science
University of Kassel
34109 Kassel, Germany
langenberg@uni-kassel.de

Steel reinforcements and metallic tendon ducts are typical structures embedded in concrete to be detected and located with microwaves, i.e. Ground Probing Radar (GPR) systems. Since propagation and scattering of electromagnetic waves by such complex geometries is rather intricate, numerical modeling techniques can help considerably to understand received signals physically. We utilize the Finite Integration Technique as realized as a commercially available code (Microwave Studio by CST) to model microwave propagation through steel reinforcements either in reflection or transmission. These results are compared with experimental data in order to understand measured arrival times.

Regarding microwave imaging we rely on the FT-SAFT algorithm (Fourier Transform Synthetic Aperture Focusing Technique) as a frequency diversity diffraction tomographic solution of linearized inverse scattering; the essence of this technique is SAR via the spatial Fourier space of the scatterer. We apply FT-SAFT in either a monostatic or a bistatic mode to experimental data obtained from a GPR system as well as to laboratory data upscaled in frequency: The possible extension of FT-SAFT to polarimetric data can the be evaluated in detail. Previously, this new polarimetric linear inverse scattering algorithm has been successfully applied to synthetic data, and now it will have to demonstrate its superiority over the corresponding scalar version against experimental data.

0-7803-7846-6/03/$17.00 

# Near Field Radiation Exposure Calculations from ill-defined Antenna Structures

Harald Ebersbach, David Thiel*, Radio Science Laboratory, Griffith University, Nathan, Queensland, Australia 4111, d.thiel@griffith.edu.au and
Mark Leckenby, Icomms Pty Ltd, Brisbane, Australia. mark.leckenby@icomms.com.au

**Abstract:** Increasing RF infrastructure requirements and community concern about RF exposure has led legislators to consider methods of advising the community about radiation levels surrounding telecommunications towers and building locations. One method of approach in Australia is to provide web-based access to paying customers. The essential elements of the software include:

Geographic location of all radiators
Antenna structures and maximum radiated power
Three-dimensional layout of all antennas and reflecting surfaces on the tower
Calculation engine for total exposure levels
Graphical representation of radiation levels

The classification of the radiating structures into aperture (including reflector antennas such as parabolic dish antennas), panel or wire type antennas is usually available from the current database in Australia. In some cases, details about the physical structure of the antennas are not available. Often the only radiation information stored by the central regulatory authority is two perpendicular planes of far field radiation pattern. From this limited information a significant problem lies in the efficient computation of the near fields.

In the case of a single wire dipole, the use of a three-point radiator representation has been shown to be effective in near field calculations (Ebersbach & Thiel, Australian Antenna Symposium 2003). This theory has now been extended to both Yagi-Uda antennas and dipole arrays with satisfactory accuracy. This approach requires knowledge of the wire structure of the antenna.

In this paper, techniques to deduce the structure of wire antennas from the far field radiation patterns, and the subsequent calculation of the near field strength are presented. A comparison with NEC based calculations verifies this approach. Similar techniques are also under development for aperture and panel antenna types. These techniques lie at the core of the calculation engine for near field exposure limits available to the public.

0-7803-7846-6/03/$17.00 ©2003 IEEE 

**Analysis of Electrical Large Targets with Adaptive Basis Functions**

Zhijun Liu and Lawrence Carin
Department of Electrical and Computer Engineering
Duke University
Box 90291
Durham, NC 27708-0291

There has been significant progress made recently in the integral-equation analysis of scattering from complex targets. For example, the multi-level fast multipole algorithm (MLFMA) has been developed to significantly reduce the memory and computation time required of method-of-moments-like solvers. In particular, for N unknowns the MLFMA requires order N log N memory and CPU. In most problems general basis functions are applied, such as the well-known Rao-Wilton-Glisson (RWG) triangular-patch basis functions. While these basis functions are very general for electrically large targets they often result in a large number of basis functions (and unknowns N). For large targets there are often extended regions of relatively smooth shape, and simpler extended basis functions may be applied. For example, there has been previous work on developing high-frequency localized basis functions, such accounting for physical-optics as well as diffraction-induced currents. Unfortunately these previous studies have required significant a priori knowledge of the properties of these extended basis functions, and therefore this technique has only been applied to simple targets.

We here use the MLFMA with RWG basis functions to compute the currents induced on large targets. We use the RWG up to the highest frequency possible with available computer memory. A signal processing technique, termed matching pursuits, is then used to adaptively and autonomously represent the RWG-defined currents into simpler and extended constituents, characteristic of general diffractive scattering. These simper basis functions result in far fewer unknowns, thereby reducing memory requirements. These new basis functions are now used in the scattering analysis, to carry the computations to higher frequencies.

The MLFMA is extended for the case of such physically and geometry motivated basis functions. In addition, iterative techniques are developed to address the effects of poor conditioning.

0-7803-7846-6/03/$17.00 ©2003 IEEE

# Radar Cross Section Control of Metallic Targets Using Physical Optics and Genetic Algorithms

M. Modarresi and K. Barkeshli*
Electrical Engineering Department
Sharif University of Technology
Azadi Avenue, P.O.Box 11365-9363, Tehran, Iran

**Abstract**

We propose a method to minimize the radar cross section (RCS) of large metallic targets using physical optics and shape optimization based on genetic algorithms. In order to compute the RCS of the target, its surface is discretized into triangular patches. The physical optics scattering from a metallic triangular patch is known analytically. The scattered electric field is computed at the observation point using superposition. The genetic algorithm is then used for the shape optimization within applicable geometrical constraints. As a simple example, the radar cross section of a small metallic target is examined in Fig. 1 at 10 GHz and 10 degree grazing angle. The RCS of the original design is shown in the lower part while its RCS after shape reconfiguration with genetic algorithm is shown in the upper part. It is observed that the peak and the average backscattered RCS have been reduced considerably. We are also including the triangular impedance patches in the code to account for the coated metals.

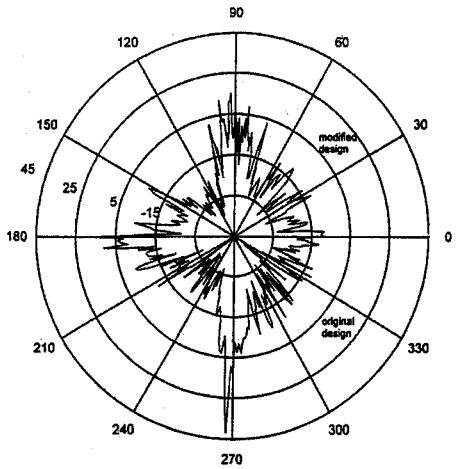


Fig. 1 - Comparison of the RCS before and after shape optimization.

0-7803-7846-6/03/$17.00 ©2003 IEEE

*Special Session*

## Ionospheric Imaging

**Organizer(s):**
**Co-Chairs:** G. Bust
F. Kamaladabi

7:55 Opening Remarks

# IDA3D Analysis of a Synoptic Scale Magnetosphere-Ionosphere Coupling Event

G. S. Bust* T. W. Garner and T. L. Gaussiran II
Applied Research Laboratories, The University of Texas at Austin

Submitted to Commision G (Ionospheric Radio and Propagation)
G2. Ionospheric modeling and data assimilation

The Ionospheric Data Assimilation Three Dimensional (IDA3D) objective analysis method has been applied to analyze a short lived high-latitude event ($<$ 30 min.). This event occurred on Dec. 12, 2001 at $\sim$ 0540 UT. The spatial region analyzed by IDA3D occurred at $\sim$ 3 MLT and spanned a region of about 5° of latitude and longitude. The resulting IDA3D electron density map shows a very steep depletion ($<$ 3 TECU) at $\sim$ 72° geomagnetic latitude, confined to less than $\sim$ 2° in both latitude and longitude. At the same time period, convection maps provided by SuperDarn, show a large ($\sim$ 1 km/s) counter-clockwise vortex in the same spatial region. The duration of the vortex is $<$ 30 minutes. This event study is part of a larger IDA3D analysis for the 24 hour period on December 12. For the 24 hour study, the data sources available to IDA3D includes over 50 GPS stations, tomography arrays in Greenland and Alaska, 7 ionosondes and GPS occultation data from CHAMP and IOX. IDA3D accepts all the above data sources and performs an objective analysis on the electron density, using either IRI95 or PIM as the background climatology. The 0540 event had a tomography pass over the spatial region of interest, providing an excellent two-dimensional image of this region. For the 0540 event, in addition to the usual maps of horizontal and vertical slices of electron density, 2D conductance maps were created by combining the IDA3D electron density map with a model of the electron collision frequency. Figure 1 shows the 2D Pederson conductance.

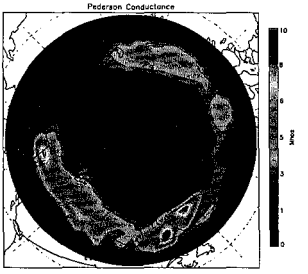


In addition to the conductance maps, we have taken the convection maps from SuperDarn and combined them with the conductance maps to obtain 2D maps of the horizontal currents. Finally, by appealing to divergence free current densities, we have estimated the parallel current. The results show that the low conductivity region is co-located with the large counter-clockwise convection pattern, and that a large Pederson current flows from high to low latitudes over a 5° region of latitude. The parallel current analysis shows a strong downward current flow of 2.2 $\mu A/m^2$ in the vortex region and a weaker upward current of 1 $\mu A/m^2$ in the high conductance region.

0-7803-7846-6/03/$17.00 ©2003 IEEE

# Estimating plasma fluxes in the equatorial ionosphere using tomographic images

V. E. Kunitsyn, E. S. Andreeva, S. J. Franke, K. C. Yeh

Time derivatives of F-region electron density are estimated from a series of radio tomographic (RT) cross-sections obtained from close in time satellite passes during Autumn 1994 in the region of equatorial anomaly (EA). Typical examples of temporal variations are described and shown. Derivatives of the morning cross-sections are mostly positive and evening sections derivatives are negative except for postsunset enhancement cases. Determination of time derivative from experimental RT data allows the calculation of fluxes in the F-region after taking into account appropriate boundary conditions and data about photochemical reactions that can be obtained from model calculations and/or by another independent method. In some cases the effect of photochemical reactions and boundary fluxes can be neglected which greatly simplifies the problem. In particular, at altitudes higher than 300 km the influence of photochemical reactions is insignificant. During morning and evening hours the vertical components of fluxes noticeably exceed the horizontal ones, therefore one can neglect the integral flux through side boundaries compared to the flux through the bottom boundary. The flux through the top boundary (about 1000 km) is also much less than the flux through the bottom. For morning and evening hours a method is proposed for calculation of vertical integral or average fluxes. Examples are given of determination, from experimental data, of average vertical fluxes in the meridional cross-section in the region of equatorial anomaly. A technique is also proposed for calculation of two-dimensional potential fluxes from experimental RT data. Examples are presented illustrating the determination of two-dimensional plasma fluxes in meridional cross-section in the region of EA from experimental data. These methods make it possible to carry out a comparison of the fluxes calculated from models and those calculated from experimental data. In the future it seems promising to develop combinations of complementing each other approaches that are based on the analysis of experimental RT data and model approaches with mutual verification.

0-7803-7846-6/03/$17.00 ©2003 IEEE

# RADIO TOMOGRAPHIC IMAGING OF SPORADIC-E LAYERS

P.A. Bernhardt[1], C.A. Selcher[2], C.S. Siefring[1], M. Yamamoto[3], S. Fukao[3]
[1]Plasma Physics Division, Naval Research Laboratory, Washington, DC 20375
[2]Information Technology Division, Naval Research Laboratory, Washington, DC 20375
[3]Radio Atmospheric Science Center, Kyoto University, Kyoto

During the SEEK 2 (Second Sporadic-E Experiment over Kyushu) two-dimensional images of Sporadic-E layers have been produced using computerized ionospheric tomography (CIT). Two rockets were launched from the Kagoshima Space Center (KSC) on August 3, 2002 at 23:24:00 JST (14:24:00 UT) and 23:39:00 JST (14:39:00 UT). Each of the two SEEK 2 rockets carried a two-frequency radio beacon that transmitted to receivers located at four ground sites. Two of the sites, Uchinoura and Taramizu were in the plane of the rocket trajectories. The rockets flew through sporadic-E layers located near 105 km altitude. The apogees of the two rockets were 151.9 and 116.6 km, respectively. The TEC measurements were obtained using differential phase from the 150 and 400 MHz carrier signals from the beacon. Because the rocket trajectory provided continuous tracking of phase absolute TEC was obtained. Data correction was required to eliminate rocket spin effects, which produced a constant differential phase, offset along with spin modulation of the phase. The latter was eliminated using a 1 Hz low pass filter. The initial data interpretation provided electron density profiles when passing through E-Layer and vertical TEC mapped to 105 km altitude along the propagation path. As the radio beacons penetrated the E-layers, sharp increases in total electron content (TEC) was observed. These data were differentiated with change in slant path to yield profiles of apparent electron density as a function of rocket altitude (see Figure). With these profiles as basis functions, tomography was used to reproduce the structure of the sporadic-E layers as a function of both altitude and horizontal range along the trajectory. Two other receivers located at Tanagashima and Tasaki were located 50 km on either side of the rocket trajectory. The data from these sites will be used to determine the three-dimensional structure of the sporadic-E layers. This experiment demonstrated the utility of a rocket-borne radio beacon sensor to detect irregularities along the propagation path between the radio beacon and a network of ground receivers.

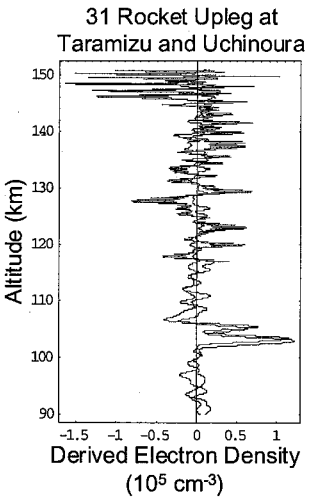

# Ionospheric Image Reconstruction Using a Combination of Convex Projections and Regularization Theories

Behzad Sharif, Romina Nikoukar, Farzad Kamalabadi

Department of Electrical and Computer Engineering and Coordinated Science Laboratory, University of Illinois at Urbana-Champaign

Remote sensing measurements of the ionosphere, regardless of the specific physical process under investigation, are often of a line-of-sight integrated nature (e.g., photometric brightness, and TEC). Theory and modeling, as well as monitoring systems, however, are generally concerned with intrinsic volumetric variables, such as wavelength-specific photon volume emission rate or ionospheric electron density. Tomography provides a framework for the estimation of such multi-dimensional parameters from their corresponding one-dimensional observables.

Examples include radio tomography whereby a set of overlapping TEC measurements are utilized, and optical tomography whereby a collection of spectroscopic measurements are inverted to form a multi-dimensional electron density map. The inherent non-ideal acquisition geometry of such remote sensing observations, however, often results in limited-angle tomographic inverse problems that are both ill-posed and ill-conditioned. Furthermore, the intrinsic presence of noise imposes severe challenges on conventional reconstruction methods. To overcome these limitations, we approach the solution of these inverse problems by incorporating a priori information in the form of combined regularization and convex projections.

Regularization theory addresses the limitation of conventional least squares techniques in the presence of noise by replacing a given ill-conditioned problem with a well-conditioned one whose solution is an acceptable approximation to the solution of the original problem. The method of Projection onto Convex Sets (POCS) allows for the incorporation of a priori knowledge in the form of convex constraints, represented formally as:

$$f_{k+1} = P_m P_{m-1} ... P_1 f_k \qquad k = 0, 1, 2, ...$$

where $f_{k+1}$ is the updated image at the $kth$ iteration and $P_i$ is the corresponding projector for the convex constraint set $C_i$ which corresponds to one piece of the *a priori* knowledge of the image to be recovered. Examples of common constraints used in image reconstruction are: image function spatial support, image function amplitude range (e.g., positivity), energy constraint, reference constraint and similarity constraint.

In the proposed method, the two theories are combined in the following manner. At each iteration, first the regularized solution is computed. Next, several convex projections are performed. The first projector, which is usually the positivity projector, takes the regularized image as its input and projects it onto the set of positive images. The projected output is then fed to the next projector. Finally, the output of convex projections is fed to the next iteration of the algorithm which is then used as an initial guess for computing the next regularized image. Experiments show promising results that are superior to conventional Algebraic Reconstruction Technique (ART) and standard regularization methods.

0-7803-7846-6/03/$17.00 ©2003 IEEE

# Neural Networks for automated classification of HF radar returns

S. Wing

The Johns Hopkins University Applied Physics Lab.

Simon.wing@jhuapl.edu/Fax:240-228-1641

The classification of HF radar returns from the ionospheric irregularities (sometimes called clutters) into those suitable, or not, for further analysis, is a time-consuming task that has typically required human intervention. We tested several different feedforward neural networks on this task, investigating the effects of network type (single-layer vs. multilayer) and number of hidden nodes upon performance. As expected, the multilayer feedforward networks (MLFNs) outperformed the single-layer networks. The MLFNs achieved performance levels of 100% correct on the training set and up to 98% correct on the testing set. Comparable figures for the single-layer networks were 94.5% and 92%, respectively. When measures of sensitivity, specificity, and proportion of variance accounted for by the model are considered, the superiority of the MLFNs over the single-layer networks is much more striking. Our results suggest that such neural networks could aid many HF radar operations such as frequency search etc.

0-7803-7846-6/03/$17.00 

# Dayside high latitude UV imaging of the ionosphere

Clayton Coker[1], Kenneth F. Dymond[2], Gary S. Bust[3], Stefan E. Thonnard[2], Erin E. Henderlight[1]
[1]*Praxis Inc.,* [2]*Naval Research Laboratory, Washington, DC 20375, USA*
[3]*Applied Research Laboratories, University of Texas, Austin, TX 78713, USA*

Special Sensor Ultraviolet Limb Imager (SSULI) is an optical limb scan imager developed by the Naval Research Laboratory (NRL) for the Defense Meteorological Satellite Program (DMSP). Retrieval algorithms will be used to image ionospheric electron density and atmospheric composition. As a prototype to SSULI, Low Resolution Airglow/Auroral Spectrograph (LORAAS) was flown on the Advanced Research Global Observation Satellite (ARGOS) beginning in 1999. This paper examines the performance of the dayside electron density retrieval algorithm at high latitudes using the 911 Å spectral line.

High latitude retrievals of dayside electron density from LORAAS UV limb scans are compared to retrievals of electron density from radio beacon receivers. Four beacon receivers, located along the west coast of Greenland, provide coverage in the polar cap and subauroral ionosphere. Since the ARGOS satellite carries a beacon transmitter and an aft-looking, UV limb scan imager, the retrievals resulting from the two techniques are reasonably close in time and space. Additional ionospheric diagnostics in the region are employed when available. These include additional beacon-satellite passes, incoherent scatter radar at Sondrestrom and ionosondes. While the first objective is to validate the limb scan dayside retrieval algorithm, the benefit of multiple sensors specifying the plasma distribution over a large area near the dayside cusp is also discussed. The operational version of this UV limb scan imager will provide many years of high latitude plasma imaging and significant opportunities for research.

0-7803-7846-6/03/$17.00 

## Imaging the Earth's Ionosphere with FUV and GPS Occultation Instrumentation

P. R. Straus, L. J. Paxton, G. Crowley, S. Henderson, Hyosub Kil, D. Morrison, C. Swenson, A. B. Christensen

Flight of new ionospheric remote sensors during recent years has resulted in a wealth of new data becoming available to support ionospheric studies. Two of the most important new technologies in this area are far ultraviolet (FUV) imaging and GPS occultation sensors. Measurements from two instruments that fall into these categories will be presented. The two instruments are the Global Ultraviolet Imager (GUVI) on the TIMED satellite and the Ionospheric Occultation Experiment (IOX) on the PICOSat spacecraft. The optically thin 135.6 nm emission is generated by radiative recombination of oxygen ions and electrons, providing a radiance that is proportional to the line-of-sight integral of the electron density squared. GUVI limb observations of this nightside emission can be used to infer electron density profiles, while disk observations can provide information on F-region peak densities and total electron content (TEC) below the TIMED spacecraft. These observations provide substantial information on ionospheric morphology not available from other sources. On the other hand, the IOX instrument provides line-of-sight TEC observations between PICOSat and up to 8 GPS satellites. Electron density profiles can be inferred using the Abel transform from TEC-tangent altitude plots obtained during Earth-limb occultation events. Because the distribution of occultations is driven by the time-varying geometry of the GPS-PICOSat spacecraft and is therefore pseudo-random in nature, it is easier to evaluate this type of data statistically through comparisons to climatology. However, direct comparisons with the GUVI instrument are also possible during time periods for which the PICOSat and TIMED orbit planes are aligned.

0-7803-7846-6/03/$17.00 ©2003 IEEE 

## Simultaneous Imaging of $O^+$, $Mg^+$, and $Fe^+$ Ion Densities In the E- and F-region Ionosphere

K F Dymond, S A Budzien, A C Nicholas, E. O. Hulburt Center for Space Research, Naval Research Laboratory, Washington, DC 20375-5352, Tel.: (202)767-2816, FAX (202) 767-9388, e-mail: kenneth.dymond@ nrl.navy.mil

R P McCoy, Office of Naval Research, Code 321SR, 800 N. Quincy Street, Arlington, VA 22217-5660 Tel.: (703) 696-8699, e-mail: mccoyr@onr.navy.mil

The High Resolution Airglow and Aurora Spectroscopy (HIRAAS) experiment was launched from Vandenberg AFB, CA aboard the *Advanced Research and Global Observation Satellite (ARGOS)* on 23 February 1999 at 2:29:55 AM Pacific Standard Time. The ARGOS is in a sun synchronous, circular orbit at an altitude of 843 Km. The ARGOS operated from mid-May 1999 through March 2002. The HIRAAS experiment contains the Low Resolution Airglow and Aurora Spectrograph (LORAAS) and the Ionospheric Spectroscopy and Atmospheric Chemistry (ISAAC) instruments. Both instruments gathered limb scans over the 750–100 Km altitude range. The LORAAS observe limb profiles of the 911 Å emission during the daytime; this emission is produced by radiative recombination of F-region $O^+$ ions and electrons and therefore are useful for characterizing the ion density distribution in the F-region. The ISAAC instrument observed the middle ultraviolet passband 1800-3200 Å at 3.8 Å resolution; of interest here are the $Mg^+$ emissions at 2800 Å and the $Fe^+$ emission near 2600 Å. The Mg+ and $Fe^+$ ions are produced by meteor ablation below 90 km and are transported into the F-region where they persist for several days. These ions are excellent tracers of dynamics in the E and lower F-region. Maps of the densities of these species show compact structures, ~1-10 km thick, that may either be small scale patches or blobs. Some of these compact structures have been observed well into the F-region.

We present the first latitude versus altitude maps of the densities of all three species. The $O^+$ maps are produced by tomographically inverting the O I 911 Å radiance profiles. The species densities of the meteoritic ions are determined by scaling the radiance maps, as the viewing geometry minimized overlap between contiguous limb scans.

0-7803-7846-6/03/$17.00 ©2003 IEEE

## Simultaneous Inversion of TEC and UV Radiance Data to Produce F-Region Electron Densities

K F Dymond, S E McDonald, S E Thonnard, S A Budzien, A C Nicholas, E. O. Hulburt Center for Space Research, Naval Research Laboratory, Washington, DC 20375-5352, Tel.: (202)767-2816, FAX (202) 767-9388, e-mail: kenneth.dymond@ nrl.navy.mil

P A Bernhardt, Beam Physica Branch, Plasma Physics Division, Naval Research Laboratory, Washington, DC 20375-5352

C A Selcher, Transmission Technology Branch, Information Technology Division, Naval Research Laboratory, Washington, DC 20375-5352

R P McCoy, Office of Naval Research, Code 321SR, 800 N. Quincy Street, Arlington, VA 22217-5660 Tel.: (703) 696-8699, e-mail: mccoyr@onr.navy.mil

The High Resolution Airglow and Aurora Spectroscopy (HIRAAS) experiment was launched from Vandenberg AFB, CA aboard the *Advanced Research and Global Observation Satellite (ARGOS)* on 23 February 1999 at 2:29:55 AM Pacific Standard Time. The ARGOS is in a sun synchronous, circular orbit at an altitude of 843 Km. The ARGOS operated from mid-May 1999 through March 2002. The HIRAAS experiment contains the Low Resolution Airglow and Aurora Spectrograph (LORAAS). The LORAAS gathers limb scans over the 750–100 Km altitude range, covering the 800–1700 Å passband at 17 Å resolution. The LORAAS observes limb profiles of the 911 Å emission during the daytime and the O I 1356 Å at night; these emissions are both produced by radiative recombination of F-region $O^+$ ions and electrons and therefore are useful for characterizing the ion density distribution in the F-region. The Coherent Electromagnetic Radio Tomography (CERTO) radio beacon also flew on the ARGOS. The CERTO is a coherently radiating radio beacon operating at 150 and 400 MHz. The slant total electron content (TEC) between the ARGOS and the ground was measured, using the CERTO emissions, by a receiver located at the Naval Research Laboratory during early 2001.

We present a comparison of the UV derived TEC and the radio beacon derived TEC over the NRL during January – April of 2001. Additionally, we present the electron densities derived by simultaneously inverting both the UV radiances and the radio derived TEC. These results are validated against ionsondes.

0-7803-7846-6/03/$17.00 ©2003 IEEE 

# Comparison of TEC Derived Ultraviolet Limb Scans to TOPEX TEC Data

Erin E. Henderlight (Praxis, Inc.)*, K. F. Dymond, S. E. Thonnard (Naval Research Laboratory), C. Coker (Praxis, Inc.), S.E. McDonald, A. C. Nicholas, S.A. Budzien (Naval Research Laboratory), and R.P. McCoy (Office of Naval Research)

In February of 1999, the Air Force Space Test Program launched the *Advanced Research and Global Observations Satellite* (*ARGOS*) into an 830 km altitude, near-polar sun-synchronous orbit with a 14:30 ascending node local time. On board the *ARGOS* satellite is a suite of remote-sensing instruments that measure density, composition, and temperature of both the thermosphere and ionosphere. The Low Resolution Airglow and Auroral Spectrograph (LORAAS) aboard ARGOS monitors upper atmospheric airglow in the far-ultraviolet and extreme-ultraviolet passband. LORAAS is identical to the Special Sensor UV Limb Imager (SSULI) instrument whose mission will be starting with the launch of the next Defense Meteorological Satellite Program (DMSP) satellite and continuing on the next four DMSP satellites. Limb scans, atmospheric radiance profiles, in the satellite's orbital plane are collected every ninety seconds. At night, the altitude distribution of the OI 1356 Å emission can be used to determine variations in the vertical electron density distribution.

The study presented here is a continuation of previous research into the comparison of total electron content (TEC) derived from LORAAS UV limb sensing techniques to total electron content derived from TOPEX data of the nightside ionosphere used to assess the accuracy of the UV inversion. It is necessary for a validation effort to be performed to estimate the quality of the two-dimensional nightside ionosphere algorithm based using the LORAAS data set. An earlier comparison using data from November 1999 and December 2000 showed promise for this research endeavor. Although there was a small sampling for 1999, all indications are that there is very good agreement with regard to TOPEX TEC and the LORAAS UV TEC measurements. This would indicate that our algorithm is working properly and that the sensitivity coefficient derived from the previous stellar calibration is correct. Upon first glance at the 2000 data, it was noted that there seemed to be a bias in the LORAAS UV data. A simple recalculation showed that the sensitivity coefficient needed to be updated for this time period, and was calculated based on the TOPEX results to range between 0.14 and 0.20.

With the continuation of this work here, our objectives include the inclusion of additional valid scans, a reduction in regularization in an attempt to better capture the Ionospheric variations in the UV reconstruction, and an analysis of data from December 2001 to increase our sample. Another priority is to evaluate the decrease in instrument sensitivity as a function of time. By doing this the threshold signal to noise value can be determined, allowing for quantification of the errors associated with the density retrieval.

0-7803-7846-6/03/$17.00 ©2003 IEEE

*Special Session*

## Integration of Antennas on RF/Wireless Packages

**Organizer(s):** Manos Tentzeris, Georgia Institute of Technology
**Co-Chairs:** M. Tentzeris
J. Bernhard

1:15 Opening Remarks

62. 1 1:20 Integration of Electronics and Antennas ..... APS
*K. Leong, T. Itoh, UCLA, USA*

62. 2 1:40 LTCC Multilayer Based CP Patch Antenna Surrounded by a Soft-and-Hard Surface for GPS Applications ..... APS
*R. Li, G. DeJean, M. Tentzeris, J. Laskar, J. Papapolymerou, Georgia Institute of Technology, USA*

62. 3 2:00 Design of a Wideband Planar Volcano-smoke Slot Antenna (PVSA) for Wireless Communications ..... APS
*J. Yeo, Y. Lee, R. Mittra, Electromagnetic Communication Laboratory, USA*

62. 4 2:20 Embedding Antennas into Concrete for Sensing Applications: A Packaging Adventure..... 299
*J. T. Bernhard, E. C. George, K. Hietpas, P. Lee, A. Zoeteman, J. Hill, University of Illinois at Urbana-Champaign, USA*

62. 5 2:40 Optically Driven CPW Fed Slot Antennas and Arrays for Wireless Communications .... APS
*G. Tzeremes, M. Khodier, University of New Mexico, T. S. Liao, P. K. Yu, University of California, C. G. Christodoulou, University of New Mexico, USA*

62. 6 3:00 DC Bias Effects on Bulk Silicon and Porous Silicon Substrates ..... APS
*I. Itotia, R. F. Drayton, University of Minnesota, USA*

62. 7 3:20 Design and Analysis of a 6 GHz Chip Antenna on Glass Substrates for Integration with RF/Wireless Microsystems ..... APS
*P. M. Mendes, J. H. Correia, University of Minho, Portugal, M. Bartek, J. N. Burghartz, Delft University, Netherlands*

62. 8 3:40 Analysis of Conformal Automobile Antennas, Theory and Experiment ..... APS
*Y. Horiki, E. K. Walton, The Ohio State University, USA*

62. 9 4:00 Some Antenna Devices Based on PBG Systems ..... APS
*R. Zaridze, A. Bijamov, D. Karkashadze, K. Tavzarashvili, V. Tabatadze, I. Paroshina, Tbilisi State University, Georgia, C. Hafner, D. Erni, Swiss Federal Institute of Technology, Switzerland*

62. 10 4:20 Effects of Bonding-wire Interconnect on Electrically Tunable Microstrip Antennas ..... APS
*Y. Park, Y. Hussein, S. El-Ghazaly, Arizona State University, V. Nair, H. Goronkin, Motorola Inc., USA*

62. 11 4:40 The GTRI Prototype Reconfigurable Aperture Antenna ..... APS
*L. N. Pringle, P. H. Harms, S. P. Blalock, G. N. Kiesel, E. J. Kuster, P. G. Friederich, R. J. Prado, J. M. Morris, GTRI, G. S. Smith, Georgia Institute of Technology, USA*

62. 12 5:00 Design of a 26 GHz Base Station Phased Array Antenna Element ..... APS
*G. Mitropoulos, R. Makri, M. Gargalakos, N. Uzunoglu, National Technical University of Athens, Greece*

# Embedding Antennas into Concrete for Sensing Applications: A Packaging Adventure

J. T. Bernhard*, E. C. George, K. Hietpas, P. Lee, A. Zoeteman, and J. Hill
Electromagnetics Laboratory, Department of Electrical and Computer Engineering
University of Illinois at Urbana-Champaign, Urbana, IL 61801
jbernhar@uiuc.edu

The nation's civil transportation infrastructure of structural concrete bridges is aging and deteriorating – principally as a result of the corrosion of the steel reinforcement that gives these structures their tensile strength. State Departments of Transportation officials are faced with the challenge of determining which structures need to be rehabilitated or replaced and when to do so. Assessing the condition of the steel reinforcement is not simple, since the steel is typically buried beneath 1 to 2 inches or more of concrete. Currently, these assessments are based primarily on qualitative visual inspections and anticipated design lives. This subjective and empirical information has proven insufficient for developing cost-effective asset management and operating strategies. In the hands of decision-makers, advanced, accurate information about the internal condition of steel reinforcement and the effectiveness of new materials and rehabilitation methods could save the nation billions of dollars annually.

Certainly, the industrial and academic communities have already moved to address this nationwide problem. Several non-destructive external sensing methods have been developed to assess the condition of the hidden steel. Unfortunately, none of these solutions has been integrated into a useful, viable system, since they often require prohibitive effort and expense to install and maintain. Moreover, the data collected from embedded sensors often fail to provide a quantitative description of deterioration such as extent of loss in bond or reduction in the cross-sectional area of the tendon.

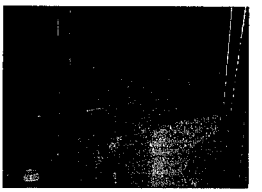

Figure 1: Antenna embedded in concrete cylinder.

As part of a multi-disciplinary effort to develop a wireless embedded sensor system to examine corrosion of tendons in prestressed concrete girders, we have designed, fabricated, and tested antennas operating in the 2.4 GHz and 5.8 GHz ISM frequency bands embedded in concrete samples. The antenna is intended strictly for communication purposes while the actual sensing mechanism will use ultrasonics. The presentation will detail the electromagnetic characterization of a number of concrete mixes considered for bridge girders and the implementation of this data into the antenna design procedure. The antenna design, based on a U-slot microstrip patch antenna (S. Weigand et al., *IEEE Trans. on Antennas and Propagat.*, **2**, 2003) takes several factors into account. One set of factors is the anticipated range of conductivity and permittivity of the surrounding concrete as its water content changes over time and with seasons. Another consideration is the size limitation of the antenna/radio/sensor system imposed by the desire to maintain the girder's structural integrity. Measurements and simulations of antenna behavior in a number of embedded scenarios (one depicted in Fig. 1 above) will be presented and discussed in the context of the anticipated communication link budget for the "girder network."

0-7803-7846-6/03/$17.00 ©2003 IEEE

## Frequency Selective Surfaces

**Co-Chairs:** B. Munk
D. Janning

1:15 Opening Remarks

65. 1 1:20 FSS Equivalent Circuit Extraction Techniques ..... APS
*J. H. Meloling, Space and Naval Warfare Systems Center San Diego, R. J. Marhefka, The Ohio State University, USA*

65. 2 1:40 A Fast Technique for the Analysis of Infinite Frequency Selective Surfaces ..... APS
*N. Huang, R. Mittra, The Pennsylvania State Univeristy, USA*

65. 3 2:00 Analysis of FSS Composites Comprising of Multiple FSS Screens of Unequal Periodicity ..... APS
*J. Ma, R. Mittra, N. Huang, The Pennsylvania State University, USA*

65. 4 2:20 A New Method with Exponential Convergence To Evaluate the Periodic Green Function ..... APS
*M. G. Silveirinha, Universidade de Coimbra, C. Fernandes, Instituto Superior Técnico, Portugal*

65. 5 2:40 Analysis of Curved Frequency Selective Surfaces using the Hybrid Volume-surface Integral Equation Approach ..... APS
*C. Yu, C. Lu, University of kentucky, USA*

65. 6 3:00 Analysis of Radius-Periodic Cylindrical Strucures ..... APS
*H. Boutayeb, K. Mahdjoubi, A. Tarot, IETR-Institut d'Electronique et de Telecommunicati, France*

65. 7 3:20 A New Class of Bandpass Frequency Selective Structures ..... APS
*A. Abbaspour-Tamijani, B. Schoenlinner, K. Sarabandi, G. M. Rebeiz, University of Michigan, Ann Arbor, USA*

65. 8 3:40 Enhanced Transmission Through Periodic Subwavelength Hole Structures ..... APS
*V. Lomakin, N. W. Chen, E. Michielssen, University of Illinois at Urbana Champaign, USA*

65. 9 4:00 Analysis and Applications of Dielectric Frequency-Selective Surfaces Under Plane-Wave Excitation ..... APS
*A. Coves, Universidad Miguel Hernandez, B. Gimeno, M. V. Andres, Universidad de Valencia, A. A. San Blas, Universidad Miguel Hernandez, V. E. Boria, J. Morro, Universidad Politecnica de Valencia, Spain*

65. 10 4:20 A CLOSELY SPACED WAVEGUIDE PHASED ARRAY INTEGRATED with a FREQUENCY SELECTIVE SURFACE MODELING and DESIGN ..... APS
*S. Monni, N. Llombart Juan, A. Neto, G. Gerini, TNO-FEL, Netherlands*

# ARBITRARY SHAPED APERTURE/PATCH FSS'S IN PLANAR PHASED ARRAYS. FULL-DOMAIN AND SUB-DOMAIN BASIS FUNCTIONS.

**G. Gerini[(1)], S. Monni[(1)], L. Zappelli[(2)]**

*[(1)] TNO-Physics and Electronics Laboratory, P.O. Box 96864, 2509 JG The Hague, The Netherlands. Tel.: +31 70 3740000, E-mail:gerini@fel.tno.nl*
*[(2)] Automatics and Electronics Department, University of Ancona, Via Brecce Bianche, 60131 Ancona, Italy. Tel.: +39 071 2204893, E-mail: l.zappelli@ee.unian.it*

## Abstract

The use of Frequency Selective Surfaces (FSS) is becoming more and more frequent in the design of antennas for complex warship platforms. From the antenna point of view, the main challenge is the capability of designing antennas with high performances, integrated in complex platforms with low Radar Cross Section (RCS) and a high number of different antenna systems mounted on the same support. This clearly requires the capability of improving the frequency and angular selectivity of the antenna, keeping at the same time under control the dimensions and shapes of the antenna itself. The solution to these requirements is the design of array antennas integrated with FSS panels with different frequency/angular filtering behavior.

In previous works, we have already presented an efficient and flexible approach to this kind of problem based on a Multi-mode Equivalent Network (MEN) method (G. Gerini, L. Zappelli, *Conference Proceedings 31st European Microwave Conference*, 2001, pp. 321-324), (S. Monni, G. Gerini, A. Neto, *XXVII URSI General Assembly*, 2002). This technique allows the derivation of an accurate multi-mode impedance matrix representation of the overall structure including array, arbitrary shaped FSS's and radomes placed on the top of the array itself.

A crucial aspect in terms of accuracy and efficiency is the choice of the expanding functions for the unknown electromagnetic quantities. Hence, in order to investigate this aspect, in this contribution we analyze the effects of expanding the unknown electromagnetic quantities in terms of different basis. We have considered both piece-wise sinusoidal expanding functions and full-domain modal representations obtained by the BCMM (boundary contour mode matching) method (F. Giese, J. M. Reiter, F. Arndt, *IEEE MTT'S Digest*, 1995, pp. 1359-1362).

These different expansions have been applied to dual problems like metallic patches and screens of infinitesimal thickness and arbitrary cross-section.

In general, piece-wise sinusoidal functions have a very simple analytical form and offer a great flexibility in terms of shapes that can be analyzed. On the other end, their large spectral content is such that a very large number of terms (proportional to the scalar product of the expanding functions with the Floquet's modes) have to be summed up in the kernel of the integral equation. This would lead to a relatively large CPU time, unless efficient acceleration techniques are applied in the summation of the series. On the contrary, full domain basis functions are less flexible for the analysis of complex shapes and often require the solution of an eigenvalue problem for the eigenmodes determination. Nevertheless, a relatively smaller number of functions are necessary to describe the unknown fields in complex geometries and furthermore their spectral content is such that the kernel of the IE is more rapidly converging.

A comparison between results for the same problem obtained with the two expansion sets will be presented at the conference, together with a detailed trade-off study in terms of accuracy and computing time.

0-7803-7846-6/03/$17.00 ©2003 IEEE

## New Millimeter Wavelength Arrays

**Co-Chairs:** B. Butler
A. Wootten

1:15 Opening Remarks

66. 1 1:20 The Atacama Large Millimeter Array (ALMA) ..... 306
*A. Wootten, National Radio Astronomy Observatory, USA*

66. 2 1:40 The ALMA at Chajnantor ..... 307
*S. J. E. Radford, NRAO, USA*

66. 3 2:00 ALMA Prototype Antennas ..... 308
*J. S. Kingsley, National Radio Astronomy Observatory, USA, S. Stanghellini, European Southern Observatory, Germany, N. Ukita, National Astronomical Observatory Japan, Japan*

66. 4 2:20 Plans and Progress in the Construction of Receiver Systems for ALMA ..... 309
*C. Cunningham, Herzberg Institute of Astrophysics, National Resea, Canada, G. Tan, European Southern Observatory, Germany*

66. 5 2:40 Band 3 Receiver for ALMA ..... 310
*S. Claude, C. Chin, P. F. Dindo, D. Erickson, F. Jiang, K. Yeung, National Research Council, Canada*

66. 6 3:00 The Baseline ALMA Correlator ..... 311
*J. C. Webber, R. P. Escoffier, C. M. Broadwell, J. Greenberg, R. Treacy, National Radio Astronomy Observatory, USA*

66. 7 3:20 The Submillimeter Array ..... 312
*K. Young, Smithsonian Astrophysical Observatory, USA*

66. 8 3:40 CARMA ..... 313
*R. L. Plambeck, University of California, USA*

66. 9 4:00 CARMA Software Development and Data Archiving ..... 314
*M. W. Pound, University of Maryland, USA*

66. 10 4:20 The Sunyaev-Zel'dovich Effect ..... 315
*J. E. Carlstrom, University of Chicago, USA*

66. 11 4:40 Polarization Studies of Interstellar Clouds ..... 316
*B. C. Matthews, University of California, Berkeley, USA*

66. 12 5:00 Measurements of Atmospheric Vapor Above Mauna Kea using an Infrared Radiometer ..... 317
*D. Naylor, I. Chapman, B. Gom, R. Phillips, University of Lethbridge, Canada*

## The Atacama Large Millimeter Array (ALMA)

Alwyn Wootten, National Radio Astronomy Observatory, 520 Edgemont Rd, Charlottesville, Virginia 22901 USA

The Atacama Large Millimeter Array, or ALMA, is an international telescope project which will be built over the coming decade in Northern Chile. With over 7000 $m^2$ of collecting area comprised of 64 12m antennas arrayed over baselines up to 14 km in extent, ALMA will provide images of unprecedented clarity and detail. One revolutionary feature of ALMA will be its ability to combine interferometric and single telescope data, providing complete flux recovery. ALMA will cover a spectral wavelength range from 7mm to 0.3 mm or shorter wavelengths, providing astronomy with its first detailed look at the structures which emit millimeter and submillimeter photons, the most abundant photons in the Universe.

Construction funding was approved by the major partners during 2002. Approved by both the U. S. National Science Board and by the European Southern Observatory Council, the project entered full construction. The first of two prototype antennas was constructed at the ALMA Test Facility in New Mexico, near the NRAO Very Large Array. This antenna, built by VertexRSI, achieved first light on 2003 January 14. A second antenna, built by a consortium led by Alcatel, is being assembled at the same site. Meanwhile, development of the site at Llano Chajnantor near San Pedro de Atacama, Chile, is expected to begin before the end of 2003.

Construction will continue with the first production antennas due by the end of 2005. Early Science is expected to commence by the end of 2007. Observers will interact with the instrument through Regional Support Centers (RSCs). One of several RSCs will be located at NRAO, with others located as the ALMA partners deem appropriate. Through these RSCs, new equipment will be developed for deployment on ALMA as the construction phase gives way to an operations phase as this decade ends.

0-7803-7846-6/03/$17.00 ©2003 IEEE

# The ALMA at Chajnantor

Simon J. E. Radford
National Radio Astronomy Observatory
949 North Cherry Avenue, Tucson, Arizona 85721

The international Atacama Large Millimeter Array will be constructed on the high (5050 m) plateau southwest of Cerro Chajnantor, Chile, about 40 km east of the village of San Pedro de Atacama. Measurements since 1995 have demonstrated this is a premier site for observations at millimeter and submillimeter wavelengths, with exceptional atmospheric conditions, i. e., transparency and stability.

The ALMA will consist of sixty four antennas, each 12 m diameter. These antennas are transportable so the array can be reconfigured to provide a variety of observational capabilities. Instead of discrete configurations, the ALMA will use a flexible reconfiguration scheme. By moving a few antennas, the array size can be increased or decreased slightly in a self-similar manner. In operation, the array will be reconfigured continuously, cycling from the smallest to the largest configuration and back with a schedule adjusted to meet scientific demand. In total, the ALMA configurations will have more than 225 antenna stations and span a 100:1 dynamic range from 150 m to 14 km effective diameter. The most compact configuration is designed for maximum surface brightness sensitivity, the intermediate configurations, about 250 m to 4 km diameter, are designed for high quality imaging with Gaussian synthesized beam shapes to minimize sidelobes and reconstruction errors, and the largest configuration is designed for maximum resolution.

Only the actual components of the ALMA telescope, i. e., the antennas, the receivers, the associated electronics, and the necessary infrastructure will be installed at the high altitude site. As far as possible, the array will be operated and maintained from a lower altitude (2900 m) Operations Support Facility about 25 km from from the telescope. Every effort will be made to minimize the number of people working at high altitude. The OSF will have shops, labs, offices, and residence facilities. During construction, the antennas will be assembled and outfitted at the OSF then transported along a private road to the array site for integration into the growing array. During operations, an antenna will be transported back to the OSF if it requires major maintenance.

The NRAO is a facility of the National Science Foundation operated under cooperative agreement by Associated Universities, Inc.

0-7803-7846-6/03/$17.00 ©2003 IEEE 

# ALMA Prototype Antennas

Jeffrey S. Kingsley*
National Radio Astronomy Observatory
Stefano Stanghellini
European Southern Observatory
Nobuharu Ukita
National Astronomical Observatory Japan

The Atacama Large Millimeter Array (ALMA) project has procured high performance prototype antennas for evaluation. These revolutionary telescopes will operate at millimeter and submillimeter wavelengths to comprise an array of individual antennas each 12 meters in diameter that work together to make precision images of astronomical objects. The goal of the ALMA Project is an array of 64 antennas that can be reconfigured as needed over an area 10 kilometers in diameter so as to give the array a zoom-lens capability. The site is located in the Andes Mountains of northern Chile at 5,000 meters elevation.

Specifications for these transportable antennas are very demanding, that include sub-arcsecond pointing with high surface accuracy and stringent path length stability. The unique specification of the antennas is the fast switch capabilities that can change antenna position by 1.5 degrees in 1.5 seconds with an accuracy of 3 arcseconds peak pointing error. A fast-switching capability is imposed by the need to rapidly and repeatedly calibrate the phase of the array. The unenclosed antennas make extensive use of carbon fiber reinforced plastic (CFRP) technology in order to maintain a stable parabolic surface in the harsh thermal and wind environment characteristics of the ALMA site. Advance metrology systems are also incorporated into the designs in order to meet the pointing requirements. These antennas must also have the ability to perform full solar observations.

Currently the prototype type antennas are undergoing evaluation and testing at the NRAO VLA site in New Mexico. A selection will be made in 2004 for production of the antennas that will be manufactured and sent to the ALMA site in Chile to compose the array. The design and construction of these antennas have been optimized for quantity production and to operate at the high altitude site. The current status and comparison of the 12-meter prototype antennas and designs will be reviewed.

0-7803-7846-6/03/$17.00 ©2003 IEEE 

**Plans and Progress in the Construction of Receiver Systems for ALMA**

The ALMA system is an interferometer comprising 64 Cassegrain antennas, each twelve meters in diameter, having maximum baseline lengths up to 14 kilometers. Each antenna will be outfitted with a cryogenically cooled heterodyne radio receiver that covers all the atmospheric windows between 30 and 950 GHz in ten bands. In each of these bands the two orthogonal polarizations must be simultaneously detected each in an IF bandwidth of 8 GHz. For frequency bands above 84 GHz SIS junctions, cooled to below 4 Kelvin, will be used to meet stringent performance specifications. Initially just four of the ten bands will be constructed with the balance following at a later date. In addition, a water-vapour radiometer operating at 183 GHz will be incorporated in each front end and used to track atmospheric delay variations. The local oscillator system is a unique design that was developed to meet the difficult phase and amplitude noise requirements required for an interferometer working at such high frequencies and long baselines.
Given the high (> 5000 m) and remote site (Chilean Atacama dessert) and the large number of antennas, special weight has been given to developing a design that is simple, reliable and easy to use. In addition, care has been taken to produce a design that is both suitable for series production and cost-effective.
In this talk technical details of the front end design will be described and the current state of development will be reviewed. Plans for the construction phase will also be presented.

0-7803-7846-6/03/$17.00 ©2003 IEEE

# Band 3 Receiver for ALMA

S. M. Claude, C. C. Chin, P. F. Dindo, D. Erickson, F. Jiang and K. K. Yeung

The Atacama Large Millimetre Array (ALMA) that will be built in the Atacama desert in Chile at 5000 m altitude consists of an array of 64 12 m antennas operating in the millimeter and sub-millimetre range. Out of the 10 bands, band 3, covering 84 – 116 GHz will be one of the 4 day-one bands to be commissioned on ALMA.

Band 3 receivers will operate in spectroscopic and continuum modes. The ground state rotational transition of CO, at 115 GHz will be one of the most important lines to be detected. Astrochemistry studies will be achieved by detecting other lines common to the interstellar molecules. Also, higher excitation lines of CO are redshifted in this band, permitting observations and distance determination of star-forming galaxies to high values of z. Observation of the continuum will be used to determine the thermal dust emission, in order to estimate dust properties.

The band 3 receivers will also be used for pointing checks with the 87 GHz SiO maser line. Holographic setting of the antenna panels will use the SiO maser and continuum emission from compact non-thermal sources.

The receiver consists of a cartridge that can be inserted in the main ALMA front-end receiver. The core of the receiver is a superconductor-insulator-superconductor (SIS) mixer for converting the millimeter signal down to an intermediate frequency (IF) signal centered at 8 GHz with a bandwidth of 8 GHz. The SIS mixers must be operated at 4K. This is done with a close cycle refrigerator on the ALMA receiver providing three cooling stages at 4 K, 15K and 80 K. The input signal is split in two linear polarizations using a waveguide Orthomode Transducer. The down converted IF signal from the mixer is then amplified with a Low Noise Amplifier (LNA) that consists of three stage High Electron Mobility Transistors (HEMT). We will present recent development in the abovementioned critical components. The challenge of this project lies in the fact that not only the detection must be low noise but also, the design must be tailored to a series production of 64 receivers targeting cost and reliability issues.

0-7803-7846-6/03/$17.00 ©2003 IEEE 

# THE BASELINE ALMA CORRELATOR

J. C. Webber*, R. P. Escoffier, C. M. Broadwell, J. Greenberg, R. Treacy
National Radio Astronomy Observatory
2015 Ivy Road
Charlottesville, VA 22903

The status of the baseline correlator being designed by the NRAO for the Atacama Large Millimeter Array (ALMA) radio astronomy observatory is presented here. Also presented is an upgrade path for the correlator under consideration for increasing the spectral performance of the instrument.

The NRAO, in collaboration with other North American and European scientific agencies, is developing the ALMA radio astronomy array, to consist of a main array of 64 12-meter diameter antennas and possibly a compact array of smaller 8-meter antennas. The instrument is to be used for observing astronomical sources at millimeter and submillimeter wavelengths at a 5000 meter elevation site in the Atacama desert of Chile.

The correlator under development will process the outputs of the 64 antennas that are to comprise the main array of the ALMA observatory using a bandwidth of 16 GHz per antenna. The system, designed using a conventional XF architecture, works at a clock rate of 125 MHz. Antenna-based electronics in the correlator include fiber optic receiver cards to recover digitized samples from the remote telescopes, digital FIR filters for bandwidth selection, delay lines, and signal conditioning logic to packetize the output of the high-speed digitizers in order to drive lower-speed correlator circuits.

An application-specific integrated circuit (ASIC) has been designed for use in measuring the cross- and auto-correlation coefficients. Each correlator ASIC has 4096 lags, including 20 bits of integration and 16 bits of secondary storage for the results. Prototype units of this ASIC have been received and tested successfully. Prototype logic cards for both station-based and baseline-based applications in the correlator have been evaluated, including the correlator card with 64 of the 4096-lag ASICs mounted. All cards tested so far have demonstrated acceptable functional and speed characteristics. System testing of a prototype 2-antenna correlator is currently in progress.

A study of implementing an enhanced digital filter card with multiple selectable output bands is in progress. This could increase the spectral resolution at the wider bandwidths and permit operation as a digital hybrid correlator.

0-7803-7846-6/03/$17.00 ©2003 IEEE

## The Submillimeter Array

Ken Young, Smithsonian Astrophysical Observatory, USA

The Submillimeter Array (SMA) is a collaborative project of the Smithsonian Astrophysical Observatory and the Academia Sinica Institute of Astronomy and Astrophysics. When completed the array will be comprised of eight 6-meter antennas which will be deployed among 24 pads arranged in four rings approximating Reuleaux triangles. The antennas will contain cryostats capable of cooling up to eight receiver inserts. The initial suite of receivers will cover three frequency bands: 177 to 240 GHz, 230 to 350 GHz and 600 to 700 GHz. Eventually receivers will be installed to cover all usable atmospheric windows from 177 to 950 GHz. Full polarization measurements will be possible in the 345 GHz band. The IF system and correlator will allow simultaneous observations with two receivers, each with a bandwidth of two GHz.

Because submillimeter observations can only take place in locations were the atmospheric transmission is highest, the array is being constructed at the high, dry site of Mauna Kea in Hawaii. On Mauna Kea, observations in the 230 GHz band are possible 80% of the time, 345 GHz observations may be done 50% of the time, and the atmospheric windows above 400 GHz may be used about 20% of the time. The array is scheduled to be completed in November of 2003. Two neighboring submillimeter telescopes, the JCMT (15-meter) and CSO (10.4-meter) are expected to periodically join the array starting in 2005.

By the beginning of 2003, £ve antennas were deployed in the array at the Hawaii site. Holographic measurements using a 232 GHz beacon at low elevation have allowed the antenna surfaces to be adjusted to an rms accuracy of $\sim$ 15 microns. Monitoring of the surface of one antenna over a period of two years has shown that the surface degrades very slowly and the panels will need to be adjusted only once every few years.

Astronomical observations in the 230 and 345 GHz band have been made with up to £ve antennas, producing maps of star-formation regions, evolved stars and galaxies. As of late 2002, three antennas are working in the 650 GHz band. Observations of a beacon at 682 GHz show that the phase closure error is less than one degree. Molecular emission at 691 GHz (CO(6-5)), 685 GHz (CS(14-13) and 658 GHz ($H_2O$: $\nu_2 = 1$, $1_{10} \rightarrow 1_{01}$) from celestial sources has been detected and in some cases mapped with the array, as have 690 GHz continuum sources as weak as 5 Jy.

0-7803-7846-6/03/$17.00 ©2003 IEEE

# CARMA
# (Combined Array for Research in Millimeter-wave Astronomy)

R. Plambeck
Radio Astronomy Lab, University of California, Berkeley, CA 94720

CARMA is the merger of two university-based arrays, the Caltech OVRO array and the Berkeley-Illinois-Maryland Association array, at a new site in the Inyo Mountains in eastern California. The new site is at an elevation of 2200 m. Tipper data showed that the median 225 GHz opacity was 0.18 in winter 2002.

With 15 antennas and 105 baselines, CARMA will provide excellent snapshot imaging capability. The most extended antenna configuration, with baselines up to 2 km, provides a 0.15″ synthesized beam at 230 GHz. As a heterogeneous array, with both 10.4-m and 6.1-m antennas, CARMA will take advantage of new imaging strategies to map extended sources. Operating CARMA in conjunction with the eight 3.5-m antennas of the University of Chicago SZ array, at the same site, offers the opportunity to produce high fidelity images of even larger sources.

Receivers cover the 80-116 GHz and 215-270 GHz bands. The I.F. bandwidth is 4 GHz. The correlator is based on the OVRO Cobra design, which uses field programmable gate arrays rather than custom correlator chips. The FPGAs can be reprogrammed to obtain new spectral line correlator modes, and can be replaced to upgrade performance as more advanced FPGAs become available.

All communication between the antennas and control building is via optical fiber. A roundtrip phase monitor developed at BIMA tracks the electrical delays through the fiber to an accuracy of 0.1 picosecond, making it feasible to transmit local oscillator reference signals through standard, non-temperature-compensated fiber. Water vapor radiometers at 22 GHz will be used to compensate for atmospheric phase fluctuations. The array is operated with a heterogeneous set of computers communicating via CORBA libraries. Data will be transmitted in near real-time to the NCSA data archive at the University of Illinois for archiving and pipeline processing.

OVRO and BIMA antennas will be moved to the new site in 2004. Combined operations will begin in 2005.

0-7803-7846-6/03/$17.00 ©2003 IEEE

# CARMA Software Development and Data Archiving

Marc W. Pound
Astronomy Department
University of Maryland, College Park

CARMA (Combined Array for Research in Millimeter-Wave Astronomy) will combine the existing BIMA and OVRO mm interferometers into a single array at a new high altitude site ($\sim$ 8000 ft). A third array, the Sunyaev-Zeldovich Array (SZA), will be built in the next 2 years and co-located with the CARMA interferometer. The SZA antennas will be available at times for cross-correlation with the CARMA antennas. This combination of hetereogeneous antennas and their subsytems bring up new challenges not only in hardware, but also in software and in remote collaborations.

The two existing arrays have their own mature operations software, developed over the last decade, and the SZA software will be partially based on the DASI system currently at the South Pole. For CARMA, the situation is not as simple as choosing one over the other. It is further complicated by the fact that the software developers are dispersed among 5 institutions (UC Berkeley, Caltech/OVRO, U. Maryland., U. Illinois, U. Chicago) and 3 time zones. Such multi-institution development requires frequent communication, local oversight, and reliable code management tools.

Timeline has forced us to carefully balance reusing existing software, with perhaps wrappers to a new more object oriented approach, and rewriting from scratch. New hardware, such as the correlator, has already resulted in new software, but we anticipate re-using a fair fraction of the existing telescope software.

Each existing array also has its own visibility data format, storage facility, and tradition of data analysis software. The choice for CARMA was to use one of a number of an existing formats or devise a format that combined the best of each. We describe our solution in which the pipelined data passes through two forms: a low-level database-based format oriented toward engineers and a high-level dataset-based form oriented toward scientists.

We will adopt the BIMA Data Archive at NCSA which has been operating in production mode for a decade and will be reused for CARMA with enhanced search capabilities. The integrated BIMA Image Pipeline developed at NCSA will be used to produced calibrated visibility data and images for end-users. We describe how the data move from the CARMA telescope correlator to delivery to astronomers over the web and show current examples of pipeline-processed images of BIMA observations.

0-7803-7846-6/03/$17.00 ©2003 IEEE

# The Sunyaev-Zel'dovich Array

John E. Carlstrom for the SZA collaboration
University of Chicago

The Sunyaev-Zel'dovich Array (SZA) is an interferometric array consisting of eight 3.5 meter precision (30 $\mu$m rms surface) telescopes equipped with low-noise HEMT amplifier based receivers operating at 26 - 36 GHz and 85 - 115 GHz. A digital correlator will process up to 8 GHz bandwidth for exceptional continuum sensitivity. The project is being led by by the University of Chicago with collaboration with Caltech, NASA/MSFC, Columbia and CARMA. The initial key project of the SZA is a deep survey covering 12 square degrees for galaxy clusters through their Sunyaev-Zel'dovich Effect (SZE). The SZE has the remarkable property that it is essentially redshift independent. Therefore the SZA will find all clusters above the survey mass-limit, independent of redshift. As the abundance of clusters with redshift is strongly dependent on the cosmology, the survey yields will be used to set tight constraints on cosmological parameters. The survey will be done using the 26-36 GHz band. The 85 - 115 GHz band will be used to perform detailed follow up observations of the survey detected clusters. These observations will allow an understanding cluster structure evolution and its effect on using high-redshift clusters for cosmological studies.

The SZA will also be used as a compact sub-array of CARMA creating a unique and powerful heterogeneous array, and thereby greatly increasing its angular dynamic range.

The SZA is currently under construction with first light expected by 2003 January. This presentation will review the scientific motivation for the SZA and the details of the design as well as the status of the project.

0-7803-7846-6/03/$17.00 ©2003 IEEE

## Polarization Studies of Interstellar Clouds

Brenda C. Matthews
Radio Astronomy Lab, University of California, Berkeley, CA 94720

Measurements of polarized emission are often regarded as highly challenging, due to issues of sensitivity, execution and complexity of interpretation. This is particularly true for interferometers, since systematic effects can affect polarized and total intensity data differently. However, polarimetry has been regarded as increasingly important in the study of interstellar clouds as our understanding of the rôle of magnetic fields in the formation and evolution of clouds has progressed. Recent measurements have revealed evidence for ordered magnetic fields on scales both larger and smaller than a single core, and the development of magnetized models for filamentary clouds and collapsing cores has also provided a means to better interpret polarimetry observations, particularly on moderate parsec-scales within molecular clouds.

I will review the existing body of millimeter polarization work on interstellar clouds and star formation with particular emphasis on the results from the Berkeley-Illinois-Maryland Association (BIMA) array, which has done the majority of high resolution polarimetry. Based on BIMA's results and predictions of star formation theories for the formation of disks and outflows, we should expect significant contributions to our understanding of magnetic fields from the new class of millimeter interferometers: the Sub-Millimeter Array (SMA); the Combined Array for Research in Millimeter Astronomy (CARMA); the Atacama Large Millimeter Array (ALMA); as well as the Australian Telescope Compact Array (ATCA) which was recently fitted with 3mm receivers. I will emphasize the particular niches each of these telescopes will fill in frequency, resolution and sensitivity, and how each will contribute through its particular strengths to our understanding of magnetic fields in molecular clouds and star formation.

If time permits, I will explore the potential for these instruments beyond their initial design, such as the SMA's potential combination with the James Clerk Maxwell Telescope, and the implementation of dual-beam polarimetry for CARMA. I will also discuss the many benefits of investing in single dish instruments to provide short spacings information missing from interferometric maps and why this is so important for polarization observations in particular.

0-7803-7846-6/03/$17.00 ©2003 IEEE 

**Measurements of Atmospheric Vapor Above Mauna Kea Using an Infrared Radiometer**

David Naylor, Ian Chapman*, Brad Gom, Robin Phillips
University of Lethbridge, Alberta, Canada

The performance of astronomical interferometer arrays operating at (sub)millimeter wavelengths is seriously compromised by rapid variations of atmospheric water vapour content that distort the phase coherence of incoming celestial signals. Unless corrected, these phase distortions, which vary rapidly with time and from antenna to antenna, seriously compromise the sensitivity and image quality of these arrays. Building on the success of a prototype Infrared Radiometer for Millimeter Astronomy (IRMA I), which was used to measure atmospheric water vapour column abundance, this paper presents results from a second generation radiometer (IRMA II) operating at the James Clerk Maxwell Telescope (JCMT) on Mauna Kea, Hawaii from December, 2000 to March, 2001. These results include comparisons with other measures of water vapour abundance available on the summit of Mauna Kea, including measurements from the Submillimeter Common User Bolometer Array (SCUBA) and from the Caltech Submillimeter Observatory (CSO) opacity meters.

This paper will also discuss the development of a new radiative transfer model, the University of Lethbridge Transmittance and Radiance Atmospheric Model (ULTRAM), in the Interactive Data Language (IDL®). Also included is a comparison of the experimental data from IRMA II with a theoretical curve-of-growth calculated from ULTRAM, which was developed specifically for the purpose of investigating spectra for the atmosphere above Mauna Kea.

ULTRAM has been extended to produce spectra for the atmosphere above the Atacama desert in Chile, future site of the Atacama Large Millimeter Array (ALMA). This paper will discuss the expected performance of a third-generation radiometer (IRMA III), which will be deployed to Chile for site testing as a possible phase correction device for ALMA.

0-7803-7846-6/03/$17.00 ©2003 IEEE

## Wireless Networks and Propagation

**Co-Chairs:** N. Nikolova
M. Bialkowski

1:15 Opening Remarks

67. 1 1:20 Interference Suppression in M-QAM OFDM Mobile Wireless Receivers using Antenna Arrays ..... APS
*R. Czarnecki, I. I. Jouny, Lafayette College, USA*

67. 2 1:40 Study of Instantaneous Variation of OFDM Sub-carrier Spectrum Towards Symbol-by-symbol Quality Control ..... APS
*K. ITOKAWA, N. KITA, A. SATO, Nippon Telegraph and Telephone Corporation (NTT), S. UWANO, NTT Advanced Technology Corporation, D. MORI, NTT Advanced Technology, S. SAITO, DoCoMo Technology Corporation, Japan*

67. 3 2:00 DOA Estimation for Impulsive EM Pulses with a Broadband Interferometry .....320
*T. Morimoto, Y. Hosokawa, A. Hirata, Z. Kawasaki, Osaka University, Japan*

67. 4 2:20 Transmitter with Antenna Array for MC-CDMA Forward Link ..... APS
*Y. Fujino, M. Inada, Y. Kuwahara, Shizuoka University, Japan*

67. 5 2:40 A Study on Reactively Steered Adaptive Array in OFDM Systems ..... APS
*Y. Nakaya, T. Toda, Fujitsu Laboratories, Ltd., S. Hara, Osaka University, Y. Oishi, Fujitsu Laboratories, Ltd., Japan*

67. 6 3:00 BER Performance of a Smart Antenna System for IS-95 CDMA ..... APS
*S. Durrani, M. E. Bialkowski, University of Queensland, Australia*

67. 7 3:20 Video Signal Wireless Distribution using NRD Guide Transmitter and Receiver At 60GHz .....321
*F. Kuroki, Kure Nat'l Coll of Tech, T. Yoneyama, Tohoku Inst of Tech, M. Yamaguchi, K. Yamaoka, Kure Nat'l Coll of Tech, Japan*

67. 8 3:40 The Simulation of Adjacent Channel and Co-Channel Interference To WLAN for Compatibility in the 5GHz Band of Korea by Radar.....322
*S. Kim, H. Lee, ETRI, Korea*

67. 9 4:00 The Characteristics of Radio Noise for Different Traffic Densities .....323
*M. Chang, K. Lin, National Sun Yat-sen University, Taiwan*

67. 10 4:20 Performance Analysis of 802.11a WLAN in Real Indoor Environments ..... APS
*H. K. Son, H. S. LEE, Electronic Telecommunication Research Institute, Korea*

67. 11 4:40 GENETIC OPTIMIZATION of RADIOBASE-STATION SIZING and LOCATION using a GIS-BASED FRAMEWORK: EXPERIMENTAL VALIDATION ..... APS
*B. Di Chiara, University of Lecce , R. Sorrentino, M. Strappini, University of Perugia, L. Tarricone, University of Lecce , Italy*

67. 12 5:00 A Computationally Efficient Optimization Algorithm for Base Station Placement and Frequency Assignment in Urban Environments using Genetic Approach .....324
*G. Moral, C. A. Tunc, Bilkent University, Turkey*

# DOA Estimation for UWB EM Pulses with a Broadband Interferometry

T. Morimoto, Y. Hosokawa, A. Hirata*, and Z. Kawasaki

Dept. of Communications Eng., Osaka Univ., 2-1 Yamada-oka, 565-0871 Osaka, Japan
Fax: +81-6-6879-7690, E-mail:hirata@comm.eng.osaka-u.ac.jp

*Introduction*: Various techniques of direction-of-arrival (DOA) estimation for electromagnetic (EM) waves have been developed in accordance with the spread of wireless communications. Most of the DOA techniques are applicable only for static monochromatic waves. In other words, less attention is paid to the DOA estimation for ultra-wideband (UWB) EM waves. Lightning discharge and electric power equipments are typical sources of impulsive EM pulses, and their DOA estimations are important from the viewpoint of EM compatibility. The frequency spectrum of such EM waves is largely dependent on the kind of sources, temperature, humidity and so forth. Therefore, sufficient intensity of EM power could not be always obtained by using conventional monochromatic approaches. For a class of EM waves with a wideband spectrum, mutual coupling between antennas would not be negligible at the lower frequency band. In this paper, the concept of conventional interferometry for narrow band is extended for UWB signals on the basis of our previous paper (R. Mardiana and Z. Kawasaki, *IEEE Trans. Instrum. & Meas.*, 2000). First, an interferometer under consideration is analyzed by using the FDTD method to calculate the interaction of antennas. Then, a novel signal processing scheme for wideband pulses is presented with the influence of mutual coupling of antennas taken into account.

*Methods*: We consider two circular plate antennas for DOA estimations (See Figure). We pay attention to the frequency band between 25 MHz and 250 MHz. Mutual impedances of the antenna array are calculated using the FDTD method as a pre-processing. For an injection of plane wave, we can calculate induced currents at the feeding point of antennas in the time domain. The induced currents are transformed into the frequency domain by FFT. Then, the induced voltages of the antennas for each Fourier component are calculated. Finally, we can obtain the phase differences between the antennas at each component.

*Results*: For the incidence of EM pulses modulated by sinusoidal waves, the errors between computational and theoretical values are 3.5 degrees at most, although they are dependent on the frequencies of the EM waves. Note that no noise exists except for computational errors. We observe that the errors are mainly caused by the mutual coupling of the antennas. From the results, we find two difficulties left to be overcome. One is the frequency-dependent error in the estimated values for the angles of incidence. The other difficulty is the determination of proper values from the angles of incidence. In order to overcome the former, we propose to use a database that includes the correlation between estimated and theoretical values for the angles of incidence at each frequency. We can handle the latter difficulty by using the weighting function determined on the basis of the intensity of Fourier spectrum. Furthermore, in order to evaluate the general effectiveness of this system, we investigate the behavior of this system for the EM pulse emitted from discharge of needle-plane electrode. Gauss noise is added so that the S/N ratio becomes 5 dB. From numerical investigation, the above-mentioned scheme is found to suppress the estimated angle.

*Conclusion*: In this paper, we have presented a broadband interferometery for the DOA of UWB EM waves. The interaction between the antennas was calculated using the FDTD method, and taken into account in the analysis. We proposed the signal processing scheme for wideband pulse, and confirmed the effectiveness.

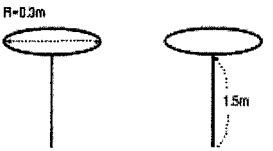

Fig: circular plate antenna array

0-7803-7846-6/03/$17.00 ©2003 IEEE

# Video Signal Wireless Distribution Using NRD Guide Transmitter and Receiver at 60GHz

Futoshi KUROKI, Motofumi YAMAGUCHI, and Kouichi YAMAOKA
Kure National College of Technology,
2-2-11 Aga-Minami Kure 737-8506, Japan

Tsukasa YONEYAMA
Tohoku Institute of Technology.
35-1 Yagiyama-Kasumichou, Taihaku-Ku, Sendai 982-8577, Japan.

NRD guide transmitter and receiver have great advantages such as wide bandwidth operation beyond 4GHz as well as a small size less than that of the name card [1]. By using them, an video signal from digital video camera was distributed successfully at 60GHz. Figure 1 shows the photograph of the transmitter and receiver, which consist of Gunn diode oscillator, up/down converter made by Schottky barrier diode (SBD), 3dB directional coupler, and circulators. The performances of the fabricated two transceivers are summarized in Table 1. Figure 2 shows the system configuration of video signal distribution systems. An NTSC video signal from the video camera is converted to an FM signal with the intermediate frequency (IF) of broadcasting satellite (BS) in Japan, and the IF signal is up-converted to a millimeter wave in the NRD guide transmitter. In the NRD guide receiver, the IF signal is recovered and is inputted to the BS tuner. An example of this system is shown in Fig. 3, where the millimeter wave from the transmitter propagates to the receiver through four reflectors located at the corners in a room to circumvent any obstacles. The usefulness of this system is confirmed since the demodulated picture is quite clear.

Reference [1] F.Kuroki, M.Yanaguchi, and T.Yoneyama, Proc. of IEEE AP/URSI Int. Conf., 2002

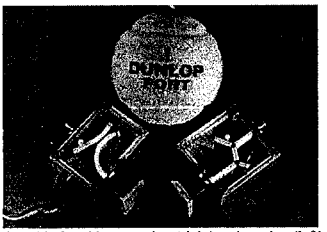


Fig. 1 NRD guide transmitter(right) and receiver(left)

Table 1 Performance of NRD guide transmitter and receiver

| Transmitter | |
|---|---|
| LO Frequency | 58.966GHz |
| Intermediate Frequency | 0.09～1.9GHz |
| Transmitting Power | 0 dBm (Average) |
| Size (Excluding Antenna) | 44×49mm |
| Receiver | |
| LO Frequency | 58.965GHz |
| Intermediate Frequency | 0.09～1.9GHz |
| Conversion Loss | 7 dB (Average) |
| Size (Excluding Antenna) | 39×53mm |

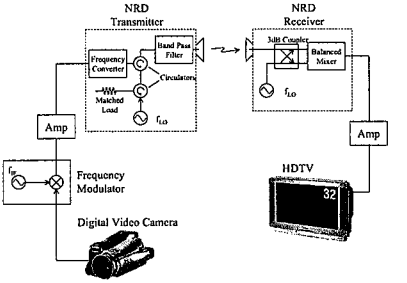


Fig.2 System configuration of video signal wireless distribution

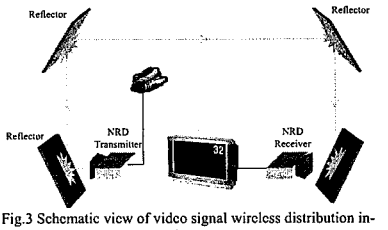


Fig.3 Schematic view of video signal wireless distribution indoors

**The Simulation of Adjacent Channel and Co-Channel Interference to WLAN for Compatibility in the 5GHz Band of Korea by Radar**

**S. J. Kim*, H. S. Lee**

**Radio Resource Team, Radio Broadcasting Lab., ETRI, Korea**

**ABSTRACT**

The following is the adjacent channel and co-channel interference analysis for WLAN; it is presented with PHY (Physical Layer) performance results by software simulation. With this, we made a model of two systems in PHY and scenarios for the interference analysis. The method is achieved by software simulations using MATLAB. By the results, evaluate performance that is based in WLAN standard (IEEE 802.11a) through the parameters, PER (Packet Error Rate) EVM (Error Vector Magnitude, Constellation Error), against signal to Interference Ratio (SIR) and analyze the compatibility for two systems. The result is useful for being compared, considered and referred when WLAN (Wireless Local Area Network) freq. is allocated in Korea.

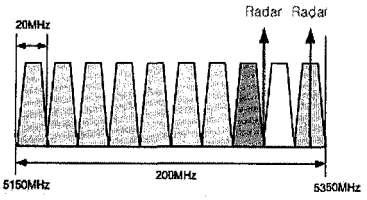


Figure 1: Frequency of Radar

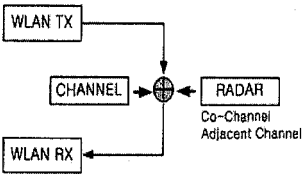


Figure 2: Interference Model

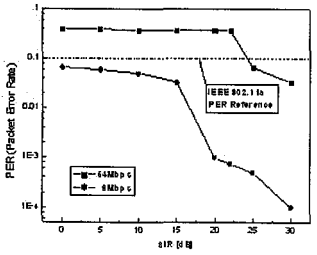


Figure 3: PER Performance

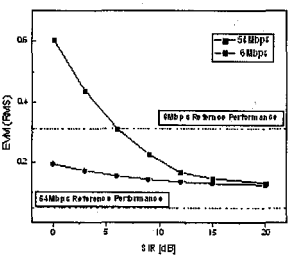


Figure 4: RMS Error of Constellation

* (1) E; Electro magnetic Noise and Interference, E3; Spectrum management and Utilization
(2) Interference Modelling, Analysis of Performance in Spectrum Management
(3) Developing Radio Resource

* This paper must be a poster presentation (Author want this paper to be poster presentation)

# The Characteristics of Radio Noise for Different Traffic Densities

*Ming-Hui Chang[1], Ken-Huang Lin[2]

Department of Electrical Engineering, National Sun Yat-sen University, Kaohsiung, 80424, Taiwan, [1]minghui@pcs.ee.nsysu.edu.tw; [2]khlin@mail.nsysu.edu.tw

**Abstract**

In urban areas, the pollution of electromagnetic environment is mainly due to man made radio noise. Man made radio noise sources may be classified as three types: (a) Incidental radiation: Ignition systems, electric power lines, and electric motors, (b) Intentional radiation: Wireless systems, radio stations, and licensed transmitters, (c) Unintentional radiation: Cable TV systems, microwave ovens, and RF–stabilized arc welders ( John R. Herman, Electromagnetic ambients and man–made noise, Don White Consultants, Inc. 1979). The metropolitan area noise maxima exist at the center of an urban area coincident with the greatest concentration of either vehicular traffic or industrial facilities ( Edward N. Skomal, Man–made radio noise, Van Nostrand Reinhold Company, 1978). The vehicles ignition system radiates highly impulsive noise. This paper presents information on the variation in the radio noise among different vehicles. Taiwan is one of world's most densely populated places and much more motorcycles and cars are used there. The electromagnetic environment is unique and the information about radio noise is not sufficient at this time. The interference which noise environment causes is important to wireless communication system. Thus, we need to consider the influence that the noise causes. In order to obtain the information necessary for evaluating the degradation of the performance of communication system, we measured the statistical distributions of the noise envelope. The most useful parameter for describing ambient electromagnetic environment is noise power. Noise power is usually related to noise figure. This paper describes the method for measuring urban radio noise, the relationship of noise figure between frequencies, the values of standard deviation for observation frequency and the properties of urban radio noise in time domain by the statistical analysis. Because of this paper must take traffic density into account. We measured at different places of the city in Taiwan. Each place for the measurement represents the different noise environment. The difference lies in the number and kinds of vehicles. The purpose of this paper is to provide an overview of the electromagnetic environment in the city. The information is important for design of UHF mobile communication systems.

0-7803-7846-6/03/$17.00 ©2003 IEEE 

# A Computationally Efficient Optimization Algorithm for Base Station Placement and Frequency Assignment in Urban Environments Using Genetic Approach

Gökhan Moral, Celal Alp Tunç*
Communications and Spectrum Management Research Center (ISYAM), Bilkent University, Ankara, Turkey
* Department of Electrical and Electronics Engineering, Bilkent University, Ankara, Turkey
gm@bilkent.edu.tr , celal@ee.bilkent.edu.tr

Since terrain and other factors may result in weak radio signals in certain areas, the position of base stations (BSs) must be changed in order to provide satisfactory coverage. Thus the design of cellular systems needs a way to optimize the placement of BSs. Furthermore, the rapid development of cellular mobile networks increases the need for economic use of the available frequency resource. Frequency assignment problem is the second major issue. The cost for building a mobile network is financial cost. In an extremely competitive market, the financial cost is a key element in determining the economic feasibility of any communication system. A good design method should be able to minimize the financial cost. There are several studies in which genetic approach has been used to optimize the possible base station placement. The studies usually consider the hexagonal cellular rural environment using Hata models. Also, there are indoor transmitter placement studies using ray-tracing model. However, the optimization problem concerning the urban environment is not a common interest. This paper presents urban outdoor propagation simulations and a novel automatic cell planning approach that aims to design a mobile network, which guarantees the system performance i.e. a network which meets the requirements of coverage and interference level, while trying to minimize the spectral and financial costs, for urban areas. Instead of grid-based propagation analysis, we have proposed a pre-processing study that reduces the computational cost drastically. The pre-processing part finds the following values for each combination of two base stations: The number of points in coverage of both base stations, in the coverage of first BS interfered by the second BS, in the coverage of second BS interfered by the first BS, in the intersection of coverage areas. The objective function of the genetic algorithm is a function of coverage, interference, number of base stations and their rent values.

In this work, we have proposed a heuristic search method with a novel and rapid representation for optimizing the base station placement problem. The implementation has been verified with various examples. The implementation can maximize the coverage while maintaining the minimum costs. The simulation results prove that the algorithm gives near-optimum results. In further study, traffic requirements may be considered by modifying the objective function. The points that require more traffic may be given more coverage weights. Moreover, the objective function and the preprocessing part may be expanded to optimize the antenna configuration and transmitter power. Terrain profile may be taken into account. The optimum solution with four frequency sets is given in Figures 1 and 2. The interfered points are indicated with a blue color and the points that are not covered because of weak received power or interference are shown in black contours. The base stations on buildings 72 and 202 have the same frequency set. The total interference free coverage obtained is 96.33%. 0.4% of total environment is interfered.

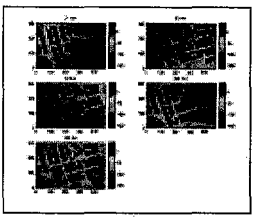

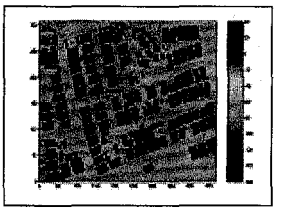

*Special Session*

## Geometric Methods for Discrete Electromagnetics

**Organizer(s):** F. Teixeira, ESL OSU
R. Kotiuga, Boston University

**Co-Chairs:** F. Teixeira
R. Kotiuga

1:15 Opening Remarks

70. 1 1:20 A Novel Technique To Build Constitutive Matrices for Generalized FDTD Algorithms ..... APS
*M. Marrone, DEEI, University of Trieste, Italy*

70. 2 1:40 Construction and Properties of Consistent 3D-Subgrids for FIT / FDTD ..... 326
*R. Schuhmann, F. Mayer, T. Weiland, Technische Universität Darmstadt, Germany*

70. 3 2:00 Stable Space-Time Mortar Finite Element Approach for FDTD Subgridding ..... 327
*M. Wong, France Telecom R&D, M. Bonilla, Université Paris 6, J. Wiart, France Telecom R&D, V. Fouad Hanna, Université Paris 6, France*

70. 4 2:20 FEMSTER: An Object Oriented Class Library of Discrete Differential Forms ..... APS
*P. Castillo, Lawrence Livermore National Lab, R. N. Rieben, UC Davis, D. A. White, Lawrence Livermore National Lab, USA*

70. 5 2:40 A Note on DeRham Diagram, Tree-cotree Splitting, and Schwarz Preconditioners ..... 328
*J. Lee, OSU, USA*

70. 6 3:00 Data Structures for Computational Electromagnetics Inherited from Algebraic Topology ..... 329
*P. Kotiuga, Boston University, Department of Electrical and Computer Eng, USA*

70. 7 3:20 A Discrete Vector Calculus in Tensor Grids ..... 330
*N. Robidoux, Simon Fraser University, Canada, S. Steinberg, University of New Mexico, USA*

70. 8 3:40 On Grid Subdivisions for the Simplicial Discretization of Maxwell's Equations ..... 331
*F. L. Teixeira, B. He, Ohio State University, USA*

70. 9 4:00 A Sub-cellular Algorithm for Wire Transmission Lines in the FDTD Method ..... APS
*C. J. Railton, B. Koh, I. J. Craddock, University of Bristol, United Kingdom*

70. 10 4:20 RF Computations with the Finite Integration Technique (FIT) and the Coupled S-Parameter Calculation (CSC) ..... APS
*U. Van Rienen, H. W. Glock, K. Rothemund, J. Junak, Rostock University,*

70. 11 4:40 Application of the CFS PML to the FDTD Solution of Wave-Structure Interaction Problems ..... APS
*J.-P. Bérenger, Centre d'Analyse de Défense, France*

70. 12 5:00 Simulation of Circular Patch Antenna on a Sphere Using the Conformal Finite Difference Time Domain (CFDTD) Algorithm ..... APS
*K. Du, N. Farahat, H. Abdel-Raoul, T. Su, W. Yu, R. Mittra, The Pennsylvania State University, USA*

## Construction and Properties of Consistent 3D-Subgrids for FIT / FDTD

**Rolf Schuhmann*, Frank Mayer, Thomas Weiland**

Technische Universität Darmstadt
Department of Electrical Engineering and Information Technology (FB18)
Computational Electromagnetics Laboratory (TEMF)
Schlossgartenstr. 8, 64289 Darmstadt, Germany
schuhmann@temf.tu-darmstadt.de

The purpose of so-called subgridding approaches for the FDTD method is to provide a local refinement in a Cartesian grid, either to resolve geometric details or to supply for a finer resolution of the electromagnetic fields e.g. near singularities. Besides this increase of accuracy in the spatial discretization, an important requirement for such subgrids is to preserve the stability and conservation properties of the FDTD method. These properties can preferably be analyzed using the notation of the Finite Integration Technique (FIT, cf. Weiland, *Int. J. Num. Mod.* **9**, 259-319, 1996) which on Cartesian grids and combined with the leapfrog time integration is computationally equivalent to FDTD. The so-called spatial stability of FIT / FDTD can here be easily proven by some elementary matrix properties which have to be preserved also in the subgrid-extension of the method. The consistency of the FIT with the geometric principles of Maxwell's equations have been summarized e.g. in (Schuhmann, Weiland: *PIER Monograph Series* **32**, 301-316, 2001).
In this presentation we explain the systematic construction of an enhanced subgrid scheme which has been first proposed for electrostatic problems by Podebrad (*PhD-Thesis, TU Darmstadt*, 2001). In contrast to former approaches, the basegrid-subgrid interface is located on faces of the dual grid. This new concept is responsible for a considerably increased flexibility of the subgrids, including L-shaped and cascaded subgrids (cf. left Fig.).

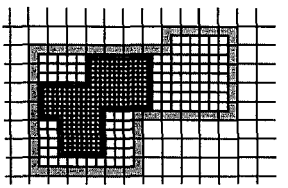

*Flexible and cascaded subgrids.*

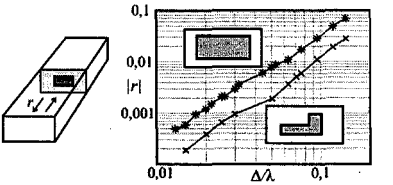


*Reflection at basegrid-subgrid interfaces.*

We present the proof for the long-term stability and the conservation properties of the new scheme and perform a detailed analysis of the parasitic reflections at basegrid-subgrid interfaces in waveguides (cf. right Fig.). It is shown that these reflections, a measure for the accuracy of the subgrid interface, are in the range of the theoretical minimum of a corresponding one-dimensional grid refinement.

0-7803-7846-6/03/$17.00 ©2003 IEEE

# Stable Space-Time Mortar Finite Element Approach for FDTD Subgridding

Man-Faï Wong, Matthieu Bonilla*, Joe Wiart and Victor Fouad Hanna*

France Télécom R&D, DMR/IIM, 92794 Issy Moulineaux, France
* Université Paris 6, LISIF, 75252 Paris, France
manfai.wong@francetelecom.com

The conventional Finite Difference Time Domain (FDTD) scheme is widely used because of its ability to tackle large and complex electromagnetic systems in various applications such as antennas, waveguiding structures, electromagnetic compatibility and biological interactions with human bodies. This powerful feature comes from the very nature of its mesh which is regular and orthogonal. The algorithm is explicit and avoids a linear system solving which occurs for the standard time domain version of the Finite Element Method (FEM). However this kind of mesh could be not suitable to model complex geometries which are not aligned to grid points. Thus, many approaches have been investigated to overcome the problem : how to model arbitrary material properties and geometry shapes while preserving the efficiency of the FDTD ? Among them, subgridding techniques have been developed with focus on the spatial connection or interpolation schemes at the interface and the time stability. In this work, the subgridding in FDTD is derived from a FEM formulation in 3D in the framework of Whitney elements and by knowing that the FDTD can be derived from it using mass lumping techniques. Mortar finite elements are used to glue the non-conforming meshes, a coarse grid and a fine one, in space. The procedure is equivalent to a FEM formulation with a Lagrange multiplier. Applied to cubic grids, the subgridding scheme in space is obtained using mass lumping techniques. Analogy with network equations naturally provided by Whitney elements will be shown. The connection scheme of the problem discretized in space is reciprocal which means passivity in an equivalent circuits model and thus ensures its stability. The subgridding is also performed in time using the usual leap-frog schemes in each mesh domain. The time stepping scheme is derived by verifying a discrete energy conservation which ensures the stability of the fully discretized problem in space and time. The results for a subgridding factor of 3 will be presented. The presented technique is general and can be applied to match different kinds of non-conforming meshes like FDTD/FEM, FEM/FEM or conforming FEM but with different time steps.

0-7803-7846-6/03/$17.00 ©2003 IEEE

# A note on DeRham diagram, tree-cotree splitting, and Schwarz preconditioners

Jin-Fa Lee
ESL, Electrical Engineering Dept.
1320 Kinnear Rd.
The Ohio State University
Lee.1863@osu.edu

In this talk, I shall detail three recent concepts/algorithms that are of paramount importance in solving PDEs efficiently. Two major issues are at the heart of developing robust and efficient FEM solvers for Maxwell equations: The well-posedness of the formulation throughout the frequency range; and, The robust and efficient preconditioner render the system matrix equations easy to solve. To address these two questions directly, I shall discuss in detail three topics that are closely related.

1. Basis functions. An overview of basis functions, employed in vector finite element methods (FEMs) as well as volume integral equations (VIEs), will be described in simple differential forms through the de-Rham diagram. It will be emphasized that in both the FEMs and integral equation formulations, the traditional approaches usually suffer the so-called low frequency instability. The low frequency instability problem results in two important consequences: **a**. The numerical solutions do not improve as the mesh get refined; and, **b**. At very low frequency applications, the numerical solutions are either very wrong or the iterative matrix solution technique fails to converge. Remedies such as tree-cotree splitting (in FEM) and loop-star basis functions (in MOM) will be discussed.
2. Tree-cotree splitting. A very efficient preconditioner based on the multiplicative Schwarz method employed in a p-type environment has been developed in the author's group in recent years. The idea is to derive the higher order basis functions in a hierarchical way, and treating each polynomial function space as a "domain". However, the p-version of the Schwarz methods strongly depend on the basis functions possess the loosely coupled nature. Subsequently, it is of paramount importance in splitting the curl-conforming vector basis functions through an in-exact Helmholtz decomposition process. Namely, the basis functions need to be written explicitly as pure gradient functions and in-exact "curl-like" functions. As it turns out, the splitting of the lowest-order curl-conforming basis functions, edge elements, is also essential. Without the tree-cotree splitting at the edge elements level, the solution process will breakdown due to a low-frequency instability problem suffered by conventional field formulation (R. Dyczij-Edlinger, G. Peng, and J.F. Lee, CMAME, 169, Feb 1999). Details of how to construct the tree-cotree splitting from a basis graph theory will be presented.
3. Schwarz preconditoners. Two types of Schwarz preconditioners are common in recent years in solving PDEs. The additive and the multiplicative Schwarz methods. The multiplicative Schwarz method not only takes fewer iterations to converge (usually ½) than the additive version but also much more robust (it succeeds when additive version fails). A simple error bounds for both the geometric multigrid and the p-type Schwarz method will be presented in the talk.

0-7803-7846-6/03/$17.00 ©2003 IEEE

# Data Structures for Computational Electromagnetics Inherited from Algebraic Topology

**P. Robert Kotiuga (Boston University, ECE Dept.*)**

In both finite element analysis and the study of manifolds, the notion of a simplicial complex has long been used as a basic data structure enabling one to model spaces without making implicit geometric or topological assumptions. In electromagnetics, the basic equations are most naturally stated in terms of differential forms. That is, Maxwell's equations are integral laws and information about the electromagnetic field is obtained by integrating or appealing to the generalized form of Stokes' theorem to deduce differential versions of Maxwell' equations and interface conditions. In the last two decades, within computational electromagnetics, Whitney forms have emerged as an ideal solution to the quest for a discrete model of differential forms phrased in terms of the data structures of simplicial complexes (see, for example A.Bossavit, Computational Electromagnetism, Academic Press Boston, 1998, or P.W. Gross and P.R. Kotiuga, Data Structures for Geometric and Topological aspects of Finite Element Algorithms, Ch. 6 of Geometric Methods for Computational Electromagnetics, PIER Vol.32, EMW Publishing, 2001). The adoption of Whitney forms has resolved many outstanding problems in vector interpolation and riddles such as the computation of spurious modes in cavities.

- Given the success of simplicial data structures and Whitney forms, we examine the roots of simplicial techniques and geometric integration theory within topology, outgrowths, and inevitable technology transfer to computational electromagnetics. Specifically, we will examine the following mathematical milestones in the context of open problems in, and data structures for, 3-d computational electromagnetics:

- De Rham's 1931 thesis and simplicial techniques in developing homology theory in the 1920's. (i.e. first proofs of many statements in Ch.1 of Maxwell's treatise).
- The appearance in the 1940's of Eilenberg-Steenrod axioms for a cohomology theory.
- Reaction to axiomatics; Andre Weil's paper (A. Weil, Sur les Theorems de de Rham, Commentarii Matematicae Helvetici, 1952), developing the formula for Whitney forms, and Whitney's subsequent geometric integration theory.
- Milnor's theorem on CW complexes and the rejection of triangulations by the mainstream of algebraic topology in the late 1950's.
- Subsequent uses of Whitney forms in rational homotopy theory (P.A. Griffiths and J.W. Morgan, Rational Homotopy Theory and Differential Forms, Progress in Math, Vol. 16, Birkhauser Boston, 1981), combinatiorial Hodge theory and the understanding of torsion invariants (W. Muller, Analytic Torsion and R-Torsion of Riemannian Manifolds, Advances in Math., Vol.28, pp 233-305, 1978).
- Semi-simplicial objects in algebraic topology (B. Gray, Bull. AMS, (38)2, 217-220, Review of: Simplicial Homotopy Theory, P. G. Goerss and J .F. Jardine, Progress in Math, vol.174, Birkhauser, Basel, 1999) as a combinatorial abstraction of space.

* 8 Saint Mary's Street, Boston, MA 02215
Tel: +1(617)353-4151, email: prk@bu.edu

URSI Topics, B8, B11.

0-7803-7846-6/03/$17.00 ©2003 IEEE

# A Discrete Vector Calculus in Tensor Grids

Nicolas Robidoux[1] and Stanly Steinberg[2*]

[1]Department of Mathematics
Simon Fraser University
8888 University Drive
Burnaby BC V5A 1S6 Canada

[2]Department of Mathematics and Statistics
University of New Mexico
Albuquerque NM 87131-1141 USA

***Abstract***

The key to the success of mimetic discretization methods is that they discretize some underlying description of continuum mechanics, e.g. in the vector calculus or in the differential forms language. For a discretization to be fully mimetic, it must have exact discrete analogs of the important results or theorems from the continuum theory.

In this paper, we will enumerate exactly which results from vector calculus we need to mimic. We will then produce a discrete vector calculus on uniform tensor product grids in three dimensions that is fully mimetic. The results are useful in extending the mimetic approach to more general structured and unstructured grids in three dimensions.

0-7803-7846-6/03/$17.00 ©2003 IEEE 

# On Grid Subdivisions for the Simplicial Discretization of Maxwell's Equations

F. L. Teixeira[1*] and B. He[1]

[1]ElectroScience Laboratory and Department of Electrical Engineering,
The Ohio State University, Columbus OH 43212 USA

During the discretization of the first-order pair of Maxwell's curl equations on irregular and simplicial (triangular in 2-D, tetrahedral in 3-D) grids, one is confronted with the inherent asymmetry caused by the fact (I) that a dual grid of a simplicial primal grid is not simplicial anymore. Accordingly, the use of dual staggered grids in this case does not retain the symmetry of the hexahedral (cellular) geometry, which impacts the consistent discretization of the first-order curl equations [1]-[3].

In the differential forms framework [1]-[9], each $n$-cell element (node, edges, facets, cells) of the grid is mapped (a bijection) to a basis element on the $n$-cochain space (discrete fields), or equivalently, the space of discrete differential $n$-forms. If one chooses to associate the 1-form $E$ and the 2-form $B$ with the primal grid, then the 1-form $H$ and the 2-form $D$ become necessarily associated with the dual grid. In the discretization of the metric part of Maxwell's equations (Hodge operators) [4], it is necessary to employ an interpolation (continuum representation) of the discrete fields. The interpolants are called *Whitney forms* (for 1-forms in the Euclidean space, they just correspond to the usual edge elements of the finite element literature) [3],[5],[6] which are defined for a simplicial grid only (II). Note that edge elements for non-simplicial grids do exist, but they are not divergence-free interpolants anymore. As a result of (I) and (II), the discretization of the metric part of Maxwell's equations becomes ambiguous.

Here, we discuss the use of grid (lattice) subdivisions to restore the symmetry between the primal and dual grid in simplicial discretizations of the first-order Maxwell's curl equations and allow for the definition of Whitney interpolants in both grids. After such subdivisions, the full discretization can be realized in the (simplicial) first subdivision grid and the symmetry between the fields in the primal and dual grids is fully restored. We discuss the use of both barycentric [7] and standard [8] subdivisions for this purpose.

## References

[1] S. Sen, S. Sen, J. C. Sexton, and D. H. Adams, *Phys. Rev. E*, **61**(3), 3174-3185, 2000.
[2] F. L. Teixeira and W. C. Chew, *J. Math Phys.*, **40**(1), 169-187, 1999.
[3] F. L. Teixeira (ed.), *Geometric Methods for Computational Electromagnetics (PIER 32)*, EMW, Cambridge, Mass., 2001.
[4] C. Kraus and R. Ziolkowski, *USNC/URSI Meeting Digest*, 714, Montreal, 1997.
[5] T.Tarhasaari, L. Kettunen, and A. Bossavit, *IEEE Trans. Magn.*, **34**(5), 2551-2554, 1998.
[6] A. Bossavit, *IEE Proc. A*, **135**, 493-500, 1988.
[7] P. R. Kotiuga, *IEEE Trans. Magn.*, **25**(4), 2813-2815, 1989.
[8] A. Bossavit, IEEE Trans. Magn., **34**(5), 2429-2432, 1998.
[9] H. Whitney, *Geometric Integration Theory,* Princeton Univ. Press, Princeton, 1957.

0-7803-7846-6/03/$17.00 ©2003 IEEE 

*Special Session*

## Propagation Measurements and Validation Efforts

**Organizer(s):** Mike Newkirk
Dan Dockery

**Co-Chairs:** K. Anderson
K. Chamberlin

1:15 Opening Remarks

71. 1 1:20 Coastal Ocean Meteorological Processes Influencing RF Propagation Near the Virginia Eastern Shore ..... 335
*R. E. Marshall, E. H. Burgess III, Naval Surface Warfare Center Dahlgren Division, J. R. Rottier, The Johns Hopkins University Applied Physics Laboratory, USA*

71. 2 1:40 The Rough Evaporation Duct (RED) Experiment: Microwave Propagation Over the Sea ..... 336
*K. D. Anderson, SPAWARSYSCEN SAN DIEGO, USA*

71. 3 2:00 EVALUATION of COAMPS-DERIVED RADAR PROPAGATION PREDICTIONS ..... 337
*K. L. Davidson, P. A. Frederickson, A. Newton, Naval Postgraduate School, K. D. Anderson, Space and Naval Warfare Systems Center, USA*

71. 4 2:20 Comparison of Propagation Coverage from Refractivity from Clutter (RFC) Profiles or Other Refractivity Profiles To Measured Propagation in Surface Bas ..... 338
*R. J. Pawlak, Naval Surface Warfare Center Dahlgren Division, W. D. Thornton, Lockheed Martin Tactical Systems, USA*

71. 5 2:40 Multiple-Source Assimilation and Refractivity Interpolator (MARI) ..... 339
*A. K. Kochhar, G. C. Konstanzer, JHU/APL, USA*

71. 6 3:00 Progress on the Validation of Short-Distance, Ground-to-Ground Propagation Models at VHF Frequencies ..... 340
*K. Chamberlin, M. Khankin, University of New Hampshire, A. Barrios, Spawarsyscen, USA*

71. 7 3:20 Effects of Ducting on GPS Occultations ..... 341
*C. O. Ao, G. A. Hajj, JPL, USA*

71. 8 3:40 A Study of 2.3GHz Bands Propagation Characteristic Measured in Korea ..... APS
*G. S. Bae, H.K. Son*
*Agency for Defense Development, Korea*
*Electronics and Telecommunications Research Institute, Korea*

71. 9 4:00 Outdoor Propagation Analysis of Ultrawide Band Signals ..... APS
*G. Schiavone, R. Palaniappan, P. Wahid, J. Tracy, University of Central Florida, USA*

**Coastal Ocean Meteorological Processes Influencing RF Propagation Near the Virginia Eastern Shore**

Robert E. Marshall* and Edward H. Burgess, III, Naval Surface Warfare Center, Dahlgren Division, J Ross Rottier, The Johns Hopkins University Applied Physics Laboratory

Near surface microwave propagation in the littoral region is a direct result of the spatio-temporal structure of the coastal atmospheric boundary layer. This thermally and frictionally dominated layer of the earth's atmosphere can introduce horizontal and vertical gradients in temperature and water vapor leading to the spatially and temporally heterogeneous development of evaporation ducts in the surface layer and elevated or surface based ducts dependent on the slope of the thermodynamic gradients across the entrainment layer.

This paper will present the results of a study that seeks to correlate the recorded spatio-temporal structure of the refractivity fields to the structure of the coastal atmospheric boundary layer influenced by the multi-scale atmospheric systems during the Wallops 2000 Microwave Propagation Measurement Experiment.

Advecting synoptic scale meteorological circulations can strengthen or weaken vertical thermodynamic gradients in the coastal atmospheric boundary layer. Vertical mixing produced by low-pressure systems tends to lead to near standard refraction. High pressure produces large-scale subsidence that lowers and strengthens elevated ducts.

Mesoscale circulations like the sea-breeze/land-breeze combination can reverse the direction of temperature advection across a marine surface boundary leading to a diurnal impact on the coastal atmospheric boundary layer and subsequent refractivity structure.

During the multi-agency Wallops 2000 Microwave Propagation Measurement Experiment, a wealth of surface and upper air meteorological observations and direct microwave propagation measurements were collected to document the spatial and temporal structure of the coastal atmospheric boundary layer and the refractivity structure near the Virginia Eastern Shore. Standard, superrefractive, and trapping refractivity conditions were documented.

The synoptic scale forcing during the test period from April 5, 2000 through May 12, 2000 has been documented by archived World Meteorological Organization observations. The mesoscale circulations have been recorded by the Office of Coast Survey Chesapeake Bay Local Analysis and Prediction System. Gridded sea surface temperature fields have been archived by NOAA Coastwatch.

0-7803-7846-6/03/$17.00 ©2003 IEEE

# The Rough Evaporation Duct (RED) Experiment: Microwave Propagation over the Sea

Kenneth D. Anderson
SPAWARSYSCEN SAN DIEGO 2858, 53560 Hull St., San Diego, CA 92152
619 553 1420; kenn@spawar.navy.mil

Prediction of microwave and infrared signal propagation over a wind-roughened sea relies on a thorough knowledge of signal interaction with the sea surface, the mean profiles of pressure ($P$), humidity ($Q$), temperature ($T$), wind ($U$), their turbulent fluctuations ($p$, $q$, $t$, $u$), and the vertical distribution of aerosols. Yet, within the marine surface layer, these mechanisms are not sufficiently understood nor has satisfactory data been taken to validate models. The RED experiment was designed to provide first data for validation of both meteorological and microwave frequency propagation models in the marine surface layer for rough surface conditions including the effects of surface waves.

Over the ocean, "smooth-rough" surface similarity theory is often applied to construct profiles of $P$, $Q$, $T$, and $U$ in the surface layer. In this context, the "rough" boundary layer is derived from empirical relations where ocean wave characteristics are neglected. For seas where wind speeds are less than 10 $ms^{-1}$ and wave age near unity, there is excellent agreement for both meteorological and microwave propagation theory and measurements. However, recent evidence indicates that even small waves perturb $P$, $Q$, $T$, and $U$ profiles throughout the surface layer. Indirect evidence of surface induced distortion of $P$, $Q$, and $T$ profiles via modeling of the vertical microwave refractivity profile (*i.e.*, the evaporation duct) is indicated by analyses of previous microwave signal propagation experiments.

The RED experiment was conducted offshore of the Hawaiian Island of Oahu in late summer, mid-August to mid-September, of 2001. *R/P FLIP*, moored about 10 km off of the NE coast of Oahu, hosted the primary meteorological sensor suites and served as a terminus for the propagation links. There were eleven scientists and engineers aboard *R/P FLIP* who installed instruments measuring mean and turbulent meteorological quantities, sea wave heights, directions, and kinematics, upward and downward radiance, near surface bubble generation, atmospheric particle size distributions, laser probing of the atmosphere, and sources for both microwave and electro-optic signals. In addition to *R/P FLIP*, two land sites were instrumented with microwave and electro-optic receivers and meteorological sensors, two buoys were deployed, a small boat was instrumented, and two aircraft flew various tracks to sense both sea and atmospheric conditions. In all, more than 25 people from four countries, six universities, and four government agencies were directly involved with the RED experiment.

0-7803-7846-6/03/$17.00 ©2003 IEEE

# EVALUATION OF COAMPS-DERIVED RADAR PROPAGATION PREDICTIONS

Kenneth L. Davidson*, Paul A. Frederickson and Adam Newton
Department of Meteorology, Naval Postgraduate School, Monterey, CA 93943
Kenneth D. Anderson
SPAWAR Systems Center D858, 49170 Propagation Path, San Diego, CA 92152

Having the capability to operationally predict atmospheric effects on sensors and weapons systems for any region of interest would improve the U.S. Navy's tactical decision making. For example, commanders could position their assets to optimize force protection or strike effectiveness based on the future propagation conditions in the tactical battlespace. In this study propagation predictions derived from the Navy's Coupled Ocean-Atmosphere Mesoscale Prediction System (COAMPS) are evaluated against actual propagation measurements to investigate the current state of such propagation forecasts.

The Roughness and Evaporation Duct (RED) Experiment was conducted off the windward coast of Oahu in 2001. Radar propagation measurements were obtained during RED over a 26 km path between a moored platform and a shore station. Concurrent meteorological measurements were obtained from the NPS "Flux" buoy. These buoy data were input into the Naval Postgraduate School's (NPS) bulk evaporation duct model to compute a refractivity profile, which was then used to run the Advanced Propagation Model (APM) to obtain propagation loss values. COAMPS-predicted surface values of wind speed, air and sea temperature, humidity and pressure were averaged over several grid points in the RED propagation path area and were then input into the NPS model and APM to compute propagation loss predictions. These COAMPS-derived propagation loss predictions where then compared with the flux buoy-derived values and the actual propagation measurements. A time series of the propagation loss values from these three sources is shown below. The black diamonds indicate the initial COAMPS model run value and the green dots are the hourly COAMPS predictions out to 12 hours. This figure indicates that COAMPS shows promise as a tool for predicting propagation conditions over a mesoscale region.

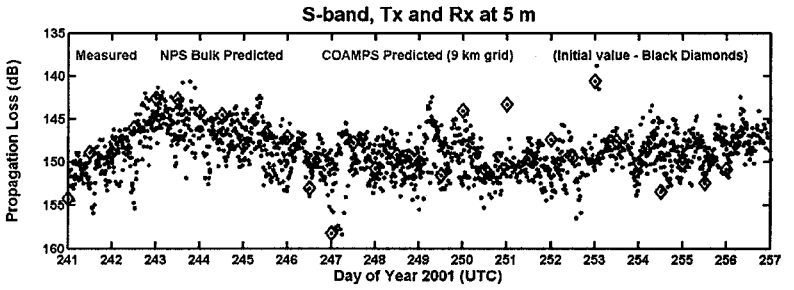


0-7803-7846-6/03/$17.00 ©2003 IEEE

# Comparison of Propagation Coverage Diagrams from Refractivity From Clutter (RFC) Profiles or other Refractivity profiles to Measured Propagation in Surface Based Ducting Environments

R. Pawlak*, Naval Surface Warfare Center Dahlgren Division, Dahlgren VA 22448, pawlakrj@nswc.navy.mil
W. Thornton, Lockheed Martin Tactical Systems, P.O. Box 1570, Dahlgren VA 22448, thorntonwd@nswc.navy.mil

During the spring of 2000, the ONR351 Air and Surface Weaponry Technology Program conducted a Ship Based Defense Demonstration at Wallops Island, VA. A series of experiments designed to show how environmental knowledge could be used to improve shipboard radar performance against cruise missile threats were conducted. A variety of sensors were simultaneously used to collect pertinent data. These included multiple refractivity sounding systems, several bulk meteorological measurement systems including boats and buoys, a direct propagation measurement system operated at three radar frequencies of interest, and sea surface backscatter measurements from both the SPANDAR atmospheric research radar and the AN/SPY-1A radar. The simultaneous measurement of all of these data allowed for a number of studies to be conducted.

This work presents a statistical comparison of Refractivity From Clutter (RFC) propagation predictions with directly measured propagation loss in surface based ducting environments. Statistical summaries were calculated for the on time observations for the RFC, a helicopter based, range dependent sounding system, a rocketsonde system, and single profiles extracted from the helicopter soundings. A Liu-Katsaros-Businger (LKB) evaporation duct, calculated using meteorological measurements from a buoy, was appended to all helicopter and rocket measured refractivity profiles. Analyses of the on-time error statistics for each method showed that the error distributions were not normally distributed, thus indicating the use of robust statistics in the analysis. The analysis also indicated that the helicopter measurements produced more accurate estimates of the propagation than either the RFC or the rocketsondes, which had comparable error magnitudes.

Time lagged results were also analyzed. These statistics show the loss of accuracy of the propagation predictions as a function of time, via a comparison of RFC, helicopter and rocketsonde results to the propagation measurements.

0-7803-7846-6/03/$17.00 ©2003 IEEE 

## Multiple-Source Assimilation and Refractivity Interpolator (MARI)

A. K. Kochhar* and G. C. Konstanzer
The Johns Hopkins University Applied Physics Laboratory, USA

The Multi-source Assimilation and Refractivity Interpolator (MARI) program is being developed to process meteorological measurements to characterize *in situ* atmospheric propagation conditions to better support Navy testing of advanced radars. This will be achieved through a common treatment of meteorological data from any or all of the measurement sources commonly used by JHU/APL to support field tests to characterize atmospheric refractivity. Measurement sources include surface observations from boats, ships, buoys, and helicopters, as well as vertical profiles from balloon-dropsondes, rocketsondes, and helicopters. In addition MARI accommodates a variety of evaporation duct models to characterize refractivity near the surface. The resulting surface layer profiles are merged with processed data from directly measured profiles. The major algorithms from the Rocketsonde Evaporation Duct (RED) and the Large-Scale Atmospheric Refractivity Range Interpolator (LARRI) programs are used to accomplish this. These include a procedure for automatically identifying convective regions based on virtual potential temperature and mixing ratio, which is used to determine variations in mean refractive conditions with range. Existing procedures for assimilating the refractivity profiles from the various data sources are applied to determine a consistent characterization of atmospheric refractivity over the region of interest. Most of the algorithms in MARI derive from programs that have been successfully applied to hundreds of data sets for dozens of tests, which often include comparisons of modeled radar performance to observed performance. Others represent improvements over previously existing capabilities, but are less thoroughly tested. Yet MARI, as it currently exists, appears to have advantages over previous refractivity processing programs in terms characterizing refractivity as well as facilitating data analyses, code maintenance, and development of new capabilities. In this presentation MARI will be described and examples of capabilities will be shown.

0-7803-7846-6/03/$17.00 ©2003 IEEE

# PROGRESS ON THE VALIDATION OF SHORT-DISTANCE, GROUND-TO-GROUND PROPAGATION MODELS AT VHF FREQUENCIES

Kent Chamberlin and Maxim Khankin
Dept. of Electrical & Computer Engineering
University of New Hampshire,
Durham, NH 03824-3591
Kent.Chamberlin@unh.edu

Amalia Barrios
SPAWARSYSCEN SAN DIEGO, 2858
Atmospheric Propagation Branch
49170 Propagation Path
San Diego, CA 92152-7385
barrios@spawar.navy.mil

At the 2002 URSI conference in Boulder, one of the authors gave a presentation entitled "A Streamlined Approach for Collecting Signal Strength Data to Validate a Ground-To-Ground Propagation Model" which describes an approach for collecting a large amount of propagation data for use in model validation. At that time, only preliminary results were reported. The focus of this presentation is to review validation work that has been performed since the last presentation.

Recently, additional VHF signal strength data have been collected over a range of terrain types (from relatively flat terrain to mountainous terrain) and distances (10 to 100 miles) for a fairly low receiver height of 4 feet. In some cases, data were collected repeatedly over the same locations to gain information about measurement repeatability and the relationship between receiver velocity and small-scale fading characteristics. These data have been used to validate a GTD-based ray-tracing model and a model based upon the parabolic wave equation. No meteorological measurements were made during the radio measurement campaign. However, for these low receiver heights the dominant propagation mechanism is diffraction, and for short ranges a standard refractive linear gradient can be assumed. For longer ranges (near 100 miles) non-standard refraction and possibly troposcatter can play a more important role. These effects, along with variations in model predictions due to differences in terrain elevation profiles from different terrain database sources (USGS and DTED) will be investigated in the validation study.

This presentation overviews the data collection hardware and software and then focuses on the results obtained, both measured and modeled. Related topics, such as signal statistics, measurement repeatability, and model operation are also addressed.

0-7803-7846-6/03/$17.00 ©2003 IEEE 

## Effects of Ducting on GPS Occultations

C. O. Ao and G. A. Hajj

Jet Propulsion Laboratory, California Institute of Technology, Pasadena, USA

The Global Positioning System (GPS) satellites continuously broadcast radio signals at 1.57542 GHz and 1.22760 GHz. As these satellites rise or set behind the Earth, the signals as measured by a receiver on a low-earth orbit are directly affected by the index of refraction of the Earth's atmosphere along the signal propagation paths. These events, known as GPS occultations, provide active limb sounding of the Earth's atmosphere, with the advantages of global coverage, high vertical resolution, and the capability to operate under all-weather conditions. The basic observables in the GPS occultation are the phase and amplitude of the carrier signals. The inversion methodology generally relies on the conversion of the observables into ray bending angles and impact parameters, denoted respectively as $\alpha$ and $a$. Under the assumption of local spherical symmetry, the relation $\alpha(a)$ can be integrated using the Abel inversion formula to yield the radial refractivity profile.

Recent improvement in receiver technology has allowed the occultation signal to penetrate more deeply into the lower troposphere. The prospect of using GPS occultation to remotely sense the planetary boundary layer (PBL) from space become increasingly feasible and attractive. However, simulation studies performed with tropical radiosonde profiles show that the refractivity gradient associated with the PBL could be sufficiently large to cause ducting to take place. When this occurs, Abel inversion of the inferred $\alpha(a)$ will lead to incorrect, underbiased refractivity values within and below the ducting layer. In order to accurately sense the PBL, the ducting problem needs to be overcome. At the very least, the occultation data that are significantly affected by ducting should be identified and rejected in any PBL study. In this work, we employ the multiple phase screen forward model to investigate the sensitivity of the occultation observables to the structure of the ducting layer. We consider both the ideal case where the data are noiseless and the more realistic case with different random noise levels. Inversion strategies and identification schemes in the presence of ducting are discussed and assessed.

0-7803-7846-6/03/$17.00 

# EOSTAR: A GEOMETRIC OPTICS APPROACH TO ATMOSPHERIC PROPAGATION MODELS

S. M. Doss-Hammel*, D. Tsintikidis
SPAWAR Systems Center
San Diego, CA 92152 USA
A. M. J. van Eijk, G. J. Kunz
TNO Physics and Electronics Laboratory
P. O. Box 96864
2509 JG The Hague, The Netherlands

Modern surface Navy ships require dependable and predictable communications, surveillance, and tracking systems. The next generation of surface Navy ships will have passive imaging systems operating in infrared wavelengths. In addition to the stealthy detection capability that a passive infrared sensor provides, an imaging sensor can provide superior location and target recognition.

It is important to be able to assess the performance of an imaging infrared sensor in an operational environment. The determination of the propagation environment for surface ships can be a difficult problem. Although the full atmospheric hemisphere surrounding the ship must be characterized, the most critical portion is the 50-meter-thick surface layer containing the ship and extending to the horizon. Extended horizontal propagation paths in the atmospheric surface layer encounter relatively dynamic refractivity conditions. Sub-refractive mirages are common in this environment and they can be exploited to improve detection probabilities.

We will describe work to develop the EOSTAR (Electro-Optical Signal Transmission and Ranging) model suite to provide accurate sensor performance predictions. The EOSTAR model is built upon a geometrical optics approach to infrared propagation: a ray is traced through the propagation environment, and path-dependent perturbations to the signal can be determined. EOSTAR is a valuable tool for prediction and exploitation of several phenomena common to this environment. The multiple-image created by a sub-refractive mirage can be exploited to provide a passive ranging capability. Sub-refractive mirages are responsible for a refractive propagation factor which provides a signal enhancement that can be exploited to extend the detection envelope. Scintillation effects can also be exploited to provide an early detection capability, and we will describe work to predict a signature frequency and variance to enable detection enhancement.

0-7803-7846-6/03/$17.00 ©2003 IEEE 

# Optical imaging through discrete random media based on point source radiative transfer equation: shower curtain effect

Sermsak Jaruwatanadilok*, Akira Ishimaru, Yasuo Kuga
Department of Electrical Engineering, Box 352500
University of Washington, Seattle, WA 98195-2500

Imaging through discrete random media is an important area of research with applications in biomedical diagnoses and atmospheric imaging. It is well known that discrete random media, such as biological tissues and fog and clouds in the air, degrade the quality of images. The main reason is the effect from particle scattering, which causes poor resolution and contrast. Therefore, there is considerable interest in modeling the random media and reducing the effect of scattering from particles.

For the optical imaging problem, radiative transfer theory is predominantly applied because of its simplicity relative to the more complex field scattering solution based on Maxwell's equations. The radiative transfer equation is based on the addition of power; thus, it provides only the intensity information. The equation is an integro-differential equation which cannot be solved analytically. However, for the plane-parallel problem, the equation can be reduced to a form that can be computed numerically.

The plane-parallel problem has been used extensively because it can be applied to many real-world applications. In our previous work (A. Ishimaru, S. Jaruwatanadilok, and Y. Kuga, *Applied Optics*, **40** (30), 5495-5502, 2001), we derived the modified pulse vector radiative transfer equation in the plane-parallel problem with plane wave incidence. Here, we extend our previous work using the same geometry, but consider a point source. The main contribution of this approach is that it provides the dependence on the location of the source, the object, and the random medium, which makes the equation a closer approximation to real imaging scenarios. We explain the assumptions and approximations of this method. We also make numerical simulations of the image through discrete random medium using this point source approximation method and compare the results with those of plane wave incidence. We can also apply the point-source approximation to verify the phenomenon called the *shower curtain effect*, which states that not only the properties but also the *location* of the random medium relative to location of the source and observation affects the quality of the image.

0-7803-7846-6/03/$17.00 ©2003 IEEE

F3: Point to point propagation effects

# Statistics of Fade Slope on a Free-Space Optical Communication System at 0.83μm Operating over Densely Urbanised Terrain

E. Couto de Miranda
R. S. Cole*

Centre for Telecommunication Studies
Pontifical Catholic University of Rio de Janeiro
Rua Marquês de São Vicente 225, Ala K. 7th Floor
Gávea, Rio de Janeiro, RJ
Brazil 22453-900
Tel: +552131141682, Fax: +55212945748, e-mail: erasmus@cetuc.puc-rio.br

*University College London

***Abstract***

A free space optical communication system at 0.83μm operated across central London for 4 years. The 4.1 km link connected the 11th floor of the Engineering building at University College London to the 12th floor of the Imperial College of Science and Medicine. The beam passed over a variety of urban elements such as buildings of different heights, "canyons" formed by flat terrain such as squares and even a small lake at Hyde park (the Serpentine). The system was used to test the viability of a free-space optical communication system over a densely urbanised environment. The study consisted of the analysis of long term measurements of received power scintillations, angle of arrival, attenuation of the received signal and the effects of rain and urban climatology. In this paper, the statistics of fade slope, defined as the rate of change of attenuation, are presented and discussed. Among the results obtained are the distributions of fade slope for the negative and positive values and for the entire data bank. The relationship between the average fade slope and fade depth is also analised.

Several authors who had explored this subject for lower frequencies (mainly for satellite links operating at Ku and Ka bands) found that the distribution of fade slope values follows a gaussian shape, which means that the distributions for negative and positive slopes are mirror images of each other. On the other hand, no general agreement has been reached as to the relationship between the level of attenuation and the average level of fade slope.

With the results from this study of this dynamic aspect of attenuation, designers will be able to build an array of tools for building intelligent fading countermeasures, which may increase the overall quality of the service provided by the link.

The distributions of fade slope values were found in general to be leptokurtic, departing from the expected gaussian bell-shaped curves towards a more pronounced mode on the obtained densities. There seems to be a straight line relationship between fade depth and the average value of fade slope. The descriptive statistics of fade slope values also seem to have well defined relationships with fade depth.

As for the contributions of this work to "new knowledge", this is the first paper (as far as the authors are aware) to explore the characteristics of fade slope at optical frequencies and with a system operating in such an free space optical propagation-hostile (yet realistic for any commercial Free Space Optical Communication System) environment as central London.

This work is part of a series of related studies in the propagation characteristics of a free space optical communication system operating in urban environements, as well as the effects of the urban microclimatology in the reliability of such systems. Several papers, dealing with other aspects of optical propagation such as the effects of scintillations and angle of arrival variations have been produced over the course of the study and are published in journals and conference proceedings.

0-7803-7846-6/03/$17.00 ©2003 IEEE 

***Special Session***

## Higher-Order Basis Functions for Efficient Solution of Large Problem Via Matrix Size Reduction

**Organizer(s):** Raj Mittra, Pennsylvania State University
Guiseppi Vecchi, Polytechnic of Turin

**Co-Chairs:** R. Mittra
G. Vecchi

1:15 Opening Remarks

73. 1 1:20 Use of higher order entire domain basis over electrically large subsectional patches .....347
*T. K. Sarkar, Syracuse University, USA, B. Kolundzija, University of Belgrade, Yugoslavia, M. Salazar-Palma, Universidad Politécnica de Madrid, Spain*

73. 2 1:40 High-Order Integral Equation Solution for Scattering by Composite Materials ..... APS
*S. D. Gedney, C. Lu, University of Kentucky, USA*

73. 3 2:00 Higher-order Vector Bases for Singular Fields on Curved 2D-elements. .....348
*R. GRAGLIA, G. LOMBARDI, Politecnico di Torino, Italy*

73. 4 2:20 Diacoptic Basis Function Grouping Techniques Applied to the Method of Moment Solution of (M)MIC-Structures ..... APS
*T. Vaupel, T. F. Eibert, FGAN-FHR, V. Hansen, University of Wuppertal, Germany*

73. 5 2:40 Synthetic-Function Analysis of Large Printed Structures ..... APS
*L. Matekovits, G. Vecchi, M. Orefice, Politecnico di Torino, Italy*

73. 6 3:00 MATRIX COMPRESSION and SUPERCOMPRESSION TECHNIQUES FOR LARGE ARRAYS ..... APS
*S. Maci, University of Siena, G. Vecchi, Politechnic of Turin, A. Freni, University of Florence, Italy*

73. 7 3:20 The Characteristic Basis Function Method (CBFM) _ an Alternative To FMM for a Class of Antenna and Scattering Problems .....349
*R. Mittra, V. V. Prakash, Penn State University, USA*

73. 8 3:40 Characteristic Basis Function Method for Solving Large Problems Arising in Dense Medium Scattering ..... APS
*Y. Sun, C. H. Chan, City University of Hong Kong, China, R. Mittra, Pennsylvania State University, USA, L. Tsang, City University of Hong Kong, China*

73. 9 4:00 Fast Solution of Electromagnetic Boundary Value Problems by the Characteristic Basis Functions/FEM Approach ..... APS
*M. Kuzuoglu, Middle East Technical University, Turkey*

73. 10 4:20 Nédélec's Element Definition on Simplex Coordinates .....350
*M. Casas, L. E. García-Castillo, Universidad de Alcalá, M. Salazar-Palma, Universidad Politécnica de Madrid, Spain*

73. 11 4:40 A Fast Hybrid MoM/FEM Technique for Microstripline Vertical Couplers with Multiple Identical Cavities ..... APS
*J. Cheng, Chang Gung University, Taiwan*

73. 12 5:00 Convergence Rates of 2D Moment Method Solutions for the MFIE and EFIE ..... APS
*C. P. Davis , K. F. Warnick, Brigham Young University, Provo, UT USA*

# USE OF HIGHER ORDER ENTIRE DOMAIN BASIS OVER ELECTRICALLY LARGE SUBSECTIONAL PATCHES

Tapan K. Sarkar
Department of Electrical Engineering and Computer Science
Syracuse University, Syracuse, New York 13244-1240.
Phone: 315-443-37775, Fax: 315-443-4441
Email: tksarkar@syr.edu; Homepage: http://web.syr.edu/~tksarkar

Branko Kolundzija
Department of Electrical Engineering
University of Belgrade
11120 Belgrade, Yugoslavia
Email: kol@kiklop.etf.bg.ac.yu

Magdalena Salazar-Palma
Departamento de Señales, Sistemas y Radiocomunicaciones, Escuela Técnica Superior de Ingenieros de Telecomunicación, Universidad Politécnica de Madrid, Ciudad Universitaria s/n, 28040 Madrid, Spain,
Phone: +34-91-336-7366, ext: 391, Fax: +34-91-336-7362, E-mail: salazar@gmr.ssr.upm.es

**ABSTRACT:** The use of higher order entire domain basis over large surface patches can be quite advantageous for efficient and accurate solution of electromagnetic field problems. The incorporation of such formulations in WIPL-D has made solution of large problems on desktops a reality.

For example, use of entire domain higher order basis can guarantee continuity of the charge over the surface of the structure and will thus result in a more accurate solution for the input impedance for radiation problems, accurate near field results and faster overall convergence as evidenced in WIPL-D.

In addition, it can reduce the undesired instabilities for solutions of the currents when using an electric field integral equation near internal resonant frequencies. It is well known that the electric field integral equation breaks down at frequencies near the internal resonant frequencies of the structure. However, when using higher order basis over large surface patches it will be demonstrated that the region of instability in the solution is dramatically reduced and can provide quite meaningful solutions without much problem.

Finally, regarding the efficiency of the solution procedure we know that when subsectional basis functions like the triangular patch is used to discretise a surface typically one needs approximately 100-300 unknowns per square wavelength of surface area to approximate the surface current. However, when using higher order basis in conjunction with entire domain functions over large patches that number can be reduced to 10-30 unknowns per square wavelength of surface area. That leads to a dramatic reduction in the size of the matrix and electrically large problems, which for the subsectional basis require a super computer to solve, can now be analyzed on desktop computers. More interestingly as the electrical size of the patch increases, the number of basis functions per unit square wavelength of surface area actually *decreases*!

The presentation will illustrate these points with examples.

0-7803-7846-6/03/$17.00 ©2003 IEEE 

# Higher-order vector bases for singular fields on curved 2D-elements.

Roberto D. Graglia*, and Guido Lombardi

Dipartimento di Elettronica, Politecnico di Torino,
Corso Duca degli Abruzzi 24, 10129 Torino, Italy.
email: graglia@polito.it, fax: (+39)-011-5644099.

Curl-conforming functions are useful in the FEM solution of the transverse vector Helmholtz equation, whereas divergence-conforming functions are used in the Moments Method solution of surface integral equations. This work improves on the results of a previous work (R.D. Graglia, G. Lombardi, *2002 IEEE AP-S Symp. Digest*, vol. I, pp. 62-65) and presents higher-order singular curl- and divergence-conforming bases on curved triangular and quadrilateral elements, directly defined in their parent space. The method used to construct such bases is simple and general, and can be used for any order. Several issues are addressed including completeness of the bases and number of degrees of freedom. Our bases incorporate the edge condition and are able to approximate the unknown field components in the neighborhood of the edge of a wedge for any order of the singularity coefficient $\nu$, that is supposed given and known *a priori*. The wedge can be penetrable in the curl-conforming case, while it is supposed metallic in the divergence conforming case. For metal wedges of aperture angle $\alpha$, one has $\nu = \pi/(2\pi - \alpha)$. Our curl (divergence) conforming singular functions are compatible with standard $p$-th order vector functions in adjacent elements (R.D. Graglia, D.R. Wilton and A.F. Peterson, *IEEE Trans. Antennas Propagat.*, vol. 45, no. 3, pp. 329–342, 1997), and guarantee tangential (normal) continuity along the edges of the elements allowing for the discontinuity of normal (tangential) components, adequate modelling of the curl (divergence), and removal of spurious modes (solutions). The Galerkin form of FEM to study with curl-conforming elements a homogeneous circular waveguide of unit radius with a baffle extending to its center has been implemented. The figure reports the relative errors on $k_z^2$ for the lowest order TE mode, that at the edge vertex supports singular fields with $\nu = 1/2$.

The mesh used for these simulations required to increase only by 20 the number of degrees of freedom in order to switch from regular to singular bases. The results obtained with regular vector functions of order $p = 2$, 3 are less precise than those obtained with singular vector bases of order $[p = 2, 3; s = 0]$. More results will be presented at the Conference.

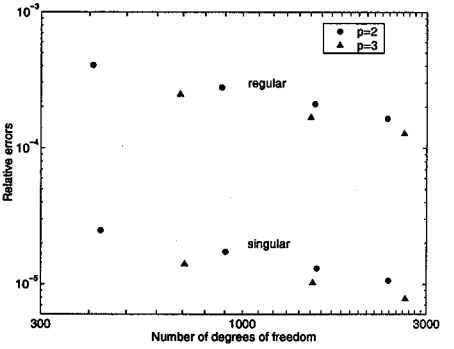


0-7803-7846-6/03/$17.00 ©2003 IEEE

# The Characteristic Basis Function Method (CBFM) – An Alternative to FMM for a class of Antenna and Scattering Problems

Raj Mittra and V.V.S. Prakash

319 Electrical Engineering East,
The Pennsylvania State University, University Park, PA 16802-2705
E.mail: Mittra@engr.psu.edu

The Fast Multipole Method (FMM) and its multilevel variants are very elegant and well-established approaches to fast solution of RCS problems formulated via the Method of Moments (MoM), and the FMM is clearly the chief protagonist in the CEM-solver world today, for attacking the EM scattering problems involving large bodies. The purpose of this paper is to present an alternate approach (CBFM), which is designed to complement the FMM in a whole host of situations. These include the modeling of large antennas and arrays, and the RCS computation of large objects that one might want to handle by using the MoM, FEM, or FDTD, depending upon the nature of the problem (note that the CBFM is not limited to MoM formulation alone).

The core concept in CBFM is the reduction of Degrees of Freedom (DOFs) with which to describe a problem. This reduction is realized by solving a number of sub-problems used to generate what are defined as the *primary* and *secondary* basis functions – which are adequate for many problems, though higher-order functions can be readily added on *as-needed* basis. The reduced matrix in MoM or FEM is typically several orders of magnitude smaller than the size of the original matrix. The principal advantage of the reduction process is that it obviates the need for iterative solution in many practical problems of interest, as for instance a large finite phased array antenna, or FSS radome problem comprising of several thousands of elements, which are not amenable to the analysis by using the conventional approaches, including the FMM.

The presentation will include numerous examples of the application of the CBFM to a wide variety of problems; (a) Two-layer Fractal antenna, which takes several hours to simulate using a commercial MoM code (b) a large phased array with more than 2,500 elements simulated by FDTD; (c) RCS of typical objects at multiple frequencies and look angles by using RWG/MoM code in conjunction with CBFM; (d) a phased array covered by an FSS radome whose periods are dissimilar; (e) modeling of a very large waveguide phased array, whose geometry is quasi-periodic.

We will also present a novel approach for generating the MoM matrix elements, based on their Characteristic Basis Function representation that requires only a few (<10) DOFs to represent the entire impedance matrix of the system.

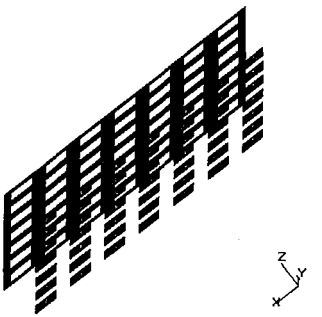


Fig.1. Microstrip patch array with radome cover.

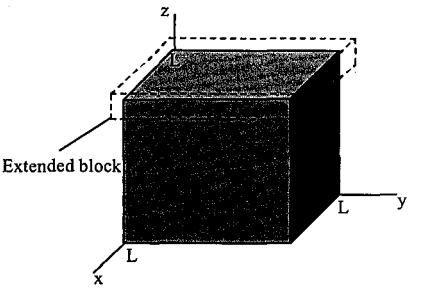


Fig.2. Geometry of metallic cube. Each face of the cube is treated as one block with six CBFs.

0-7803-7846-6/03/$17.00 ©2003 IEEE

# Nédélec's Element Definition on Simplex Coordinates

Miguel Casas[1], *Luis E. García-Castillo[1],
Magdalena Salazar-Palma[2]

[1]Departamento de Teoría de la Señal y Comunicaciones, Universidad de Alcalá
Escuela Politécnica, Campus Universitario, Ctra. Madrid-Barcelona Km. 33.600
28806 Alcalá de Henares (Madrid), Spain. Phone: +34-1-8856720.
Fax: +34-1-8856699. Email: luise.garcia@uah.es

[2]Dep. Señales, Sistemas y Radiocomunicaciones, Universidad Politécnica de Madrid
E.T.S.I. Telecomunicación, Ciudad Universitaria s/n, 28040 Madrid, Spain
Phone: +34-1-3367358, Fax: +34-1-3367362. Email: m.salazar-palma@ieee.org

Among the curl-conforming elements appeared in the Finite Element Method (FEM) literature, it is worth mentioning the so called mixed order elements proposed by J. C. Nédélec (*Numerische Mathematik*, 35, 315–341, 1980). The authors have proposed a methodology for the construction of the $k$-th order finite element vector basis functions over 2D and 3D simplices that follows rigorously the finite element definition given by Nédélec. The finite element is defined in terms of a domain, a space of functions $\mathcal{R}^k$ and a set of degrees of freedom acting as linear functionals on $\mathcal{R}^k$. The vector basis functions are obtained by imposing the interpolatory character of the basis functions with respect to the definition of the degrees of freedom of the element, which act as linear functionals on $\mathcal{R}^k$. The application of this methodology has leaded to a mixed-order curl-conforming family of finite elements (see M. Salazar-Palma et al., *Iterative and Self-Adaptive Finite-Elements in Electromagnetic Modeling*, Artech House, 1988, L. E. García-Castillo et al., *Int. J. Num. Modelling: Elec. Networks, Devices and Fields*, 13, 261–287, 2000, L. E. García-Castillo et al., *IEEE Trans. Magnetics*, 38. 2370–2372, 2002). Higher-order triangular and tetrahedral elements up to third-order, have been implemented using this methodology with cartesian coordinates. Vector basis functions are obtained in the master element and, by means of an affine transformation, are mapped to the real element.

The objective of this paper is to explore the application of the author's methodology with simplex coordinates (also called natural coordinates), i.e., the definition of $\mathcal{R}^k$ on simplex coordinates and the imposition of the definition of the degrees of freedom using simplex coordinates. A comparison between both approaches, i.e., finite element definition using cartesian and simplex coordinates, will be discussed, and the advantages and disadvantages of both approaches will be shown.

0-7803-7846-6/03/$17.00 ©2003 IEEE

*Special Session*

## EBG Surfaces 3: Applications

**Organizer(s):** Per-Simon Kildal
N. Eegheta
**Co-Chairs:** P. S. Kildal
N. Engheta

1:15 Opening Remarks

74. 1 1:20 (Sub)mm-Wave Components and Subsystems Based on PBG Technology ..... APS
*I. Ederra, R. Gonzalo, Universidad Pública de Navarra, Spain, C. Mann, Rutherford Appleton Laboratory, United Kingdom, P. De Maagt, European Space Agency, Netherlands*

74. 2 1:40 Leaky Surface-Plasmon Theory for Dramatically Enhanced Transmission Through a Subwavelength Aperture, Part I: Basic Features ..... APS
*A. A. Oliner, Polytechnic University, D. R. Jackson, University of Houston, USA*

74. 3 2:00 Leaky-Wave Theory for Enhanced Transmission Through Sub-Wavelength, Apertures II. Leaky-Wave Antenna Model ..... APS
*T. Zhao, D. R. Jackson, J. T. Williams, University of Houston, A. A. Oliner, Polytechnic University, USA*

74. 4 2:20 Leaky-Wave Antennas Realized by using Artificial Surfaces..... APS
*S. Maci, R. Magliacani, A. Cucini, University of Siena, Italy*

74. 5 2:40 Advances in Tunable Impedance Surfaces for Leaky Wave Beam Steering and Adaptive Antennas ..... 353
*D. F. Sievenpiper, J. H. Schaffner, HRL Laboratories LLC, USA*

74. 6 3:00 Planar Arrays of Wavy Microstrip Lines As Thin Resonant Magnetic Walls ..... APS
*P. Mladenov, S. Prosvirnin, Institute of Radio Astronomy, Ukraine, S. Tretyakov, Helsinki University of Technology, Finland, S. Zouhdi, Laboratoire de Genie Electrique de Paris LGEP-Supelec, France*

74. 7 3:20 Tunable Millimeter-Wave Band-Stop Filter using Electromagnetic Crystal (EMXT) Surfaces ..... APS
*Hao Xin, J. A. Higgins, Rockwell Scientific Company, USA, M. Kim, Korea University, Korea*

74. 8 3:40 A Uni-Directional Ring-Slot Antenna Achieved by Using an Electromagnetic Bandgap Surface ..... 354
*F. Elek, R. Abhari, G. V. Eleftheriades, University of Toronto, Canada*

74. 9 4:00 The N-Guide: a Novel Miniaturized Hard Quasi-TEM Waveguide ..... APS
*M. N. M. Kehn, P.-S. Kildal, Chalmers University of Technology, Sweden*

# Advances in Tunable Impedance Surfaces for Leaky Wave Beam Steering and Adaptive Antennas

Dan Sievenpiper, Jim Schaffner

HRL Laboratories, LLC.
3011 Malibu Canyon Road
Malibu, CA, 90265

**Abstract:**

Recently, antenna designers have seen an evolution from conventional metal ground planes into engineered ground planes, whose surface wave properties and diffraction characteristics can be tailored to fit a variety of applications. This began with the corrugated structures, now often known as soft and hard surfaces, [1] and eventually progressed into two-dimensional textured surfaces. [2] These materials allow one to define the sheet impedance and other properties of a metal surface using effective lumped circuit parameters.

Several applications have emerged for these new materials, such as low-profile antennas that can lie directly adjacent to a metal surface. While various thin antennas have existed for years, these textured ground planes expand the antenna designer's toolbox, resulting in new concepts such as horizontally polarized, low-angle directive antennas. [3] Many of these can be understood as a manipulation of surface wave modes.

Now, with the development of tunable surfaces, new kinds of active and adaptive antennas are possible. For example, steerable reflectors have been built using mechanically [4] or electrically tunable surfaces, which offer a low-cost alternative to conventional phased arrays, although they typically require illumination by a separate feed.

Recently, steerable leaky wave antennas have been built using these same surfaces, which allow the feed to be conformal with the steerable surface. (See figure 1.) These antennas can steer over a broad range of angles, (See figure 2.) using an entirely planar design, and a single integrated feed. This talk will describe recent advances in tunable surfaces, and will introduce new concepts for steerable leaky wave antennas based on them.

[1] P.-S. Kildal, "Artificially Soft and Hard Surfaces in Electromagnetics", IEEE Trans. Ant. Prop. vol. 38, pp. 1537-1544, 1990

[2] D. Sievenpiper, "High-Impedance Electromagnetic Surfaces", Ph.D. dissertation, UCLA, 1999

[3] J. J. Lee, R. J. Broas, S. Livingston, D. Sievenpiper, "Flush-Mounted Antennas on Hi-Z Ground Planes", IEEE APS Symp. Dig. vol. 3, pp. 764-767, 2002

[4] D. Sievenpiper, J. Schaffner, R. Loo, G. Tangonan, S. Ontiveros, R. Harold, "A Tunable Impedance Surface Performing as a Reconfigurable Beam Steering Reflector", IEEE Trans. Ant. Prop. vol. 50, pp. 384-390, 2002

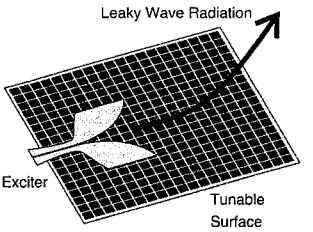


*Figure 1. A steerable leaky wave antenna can be built using a tunable impedance surface. An exciter launches a leaky wave, which then radiates at an angle determined by phase matching on the surface.*

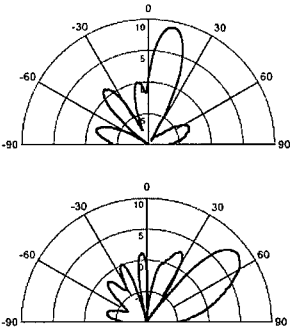


*Figure 2. An example of beam steering using a tunable impedance surface The beam can be steered in the elevation plane by varying the impedance of the surface, and shifting the surface wave band structure. Near-broadside and near-endfire patterns are shown.*

0-7803-7846-6/03/$17.00 ©2003 IEEE

Commission B: Novel Challenges with Electromagnetic Bandgap Surfaces

# A Uni-Directional Ring-Slot Antenna Achieved By Using An Electromagnetic Bandgap Surface

Francis Elek, Ramesh Abhari, and George V. Eleftheriades

The Edward S. Rogers Sr. Department of Electrical and Computer Engineering
University of Toronto, 10 King's College Road, Ontario M5S 3G4, CANADA

Slot antennas offer a number of advantages including low-profile, ease of fabrication, and ease of integration with electronics. Their main drawback, however, is that they are inherently bi-directional radiators. One common technique to redirect the back radiation forward is to place a conducting reflector at a fixed distance away from the antenna. However, in this case the parallel-plate geometry permits the excitation of the dominant TEM mode, which drastically reduces the overall radiation efficiency. Several methods have been shown to successfully reduce the back radiation. One method is to print the slot on a quarter wavelength thick substrate, which gives a gives a front-to-back (F-B) power density ratio at broadside of $\varepsilon_r$. However, slot antennas printed on thick substrates suffer severe surface wave power losses. For an array of slot radiators though, phase cancellation techniques significantly reduce surface wave losses. This is accomplished by properly spacing the array of slot radiators to achieve destructive interference of the surface wave modes (M. Qiu, M. Simcoe, and G.V. Eleftheriades, *IEEE Transactions on Microwave Theory and Techniques*, vol. 50, no. 2, pp. 517-528, Feb. 2002.)

In this abstract we describe how to solve this problem and achieve uni-directional single element slot antennas by using a periodic surface (instead of the uniform conducting reflector) placed behind the slot. The periodic surface is an electromagnetic bandgap (EBG) structure which inhibits the propagation of electromagnetic waves in the region between the slot antenna's ground plane and the periodic surface. An EBG surface which is not prone to radiation leakage and remains compact at low RF frequencies is the mushroom structure described in (D. Sievenpiper, L. Zhang, R.F.J. Broas, N.G. Alexopolous, and E. Yablonovitch, *IEEE Trans. Microwave Theory Tech.*, vol. 47, no. 11, pp. 2059-2074, Nov. 1999.) We will present numerical (FEM) and experimental results which demonstrate the effectiveness of the above described EBG surface in suppressing the back radiation from a CPW-fed ring-slot antenna. The antenna is designed to resonate at 3.7 GHz and is printed on a substrate of dimensions 20 x 20 cm, and the EBG surface is 10 x 10 cm. The gain improvement at broadside in the E and H planes is between 2.5 and 2.9 dB (89-98% efficiency) over a 5% (-10 dB $S_{11}$) bandwidth.

0-7803-7846-6/03/$17.00 ©2003 IEEE

# MODE-MATCHING ANALYSIS OF AN EBG QUASI-TEM CONICAL HORN REALIZED BY STRIPS AND VIAS

**Sergei P. Skobelev**

Joint-Stock Company "Radiophyzika", 10, Geroev Panfilovtsev str.
Moscow 125363, RUSSIA; Fax: +7 095 496 8790
E-mail: jscapex@online.ru

The last decade is characterized by growing interest in research of electromagnetic bandgap (EBG) structures for application in waveguides and horns capable to support the quasi-TEM mode having a uniform field distribution over the cross-section. This feature can be effectively used for development of horn antennas and feeds with high aperture efficiency and low cross-polarization. The quasi-TEM horn exciters also allow enhancing the performance of the quasi-optical grid amplifiers.

A promising realization of the EBG structures for the quasi-TEM horns is a so called hard wall based on an internal dielectric cover loaded with narrow longitudinal strips connected by vias to the basic metallic wall. The purpose of this work is numerical analysis of the horn with the indicated wall, since such a design is of definite practical interest, however its properties have not been studied yet before.

The analysis is based on the mode-matching method, which allows accounting for all the effects associated with the wave propagation and scattering in the horn. The first stage is the representation of the conical surfaces by stepped surfaces formed by a set of cylindrical sections with appropriate flanges. We use a combined hard wall model, where the strip-loaded sections alternate with the longitudinally corrugated sections representing the vias. Further, the mode-matching method is used for calculation of the generalized scattering matrix for each step. The necessary eigenmodes of the strip-loaded and corrugated sections are determined with using the corresponding asymptotic boundary conditions that significantly simplify the analysis. The scattering matrices of the steps are subsequently used for calculation of the scattering matrix of the stepped transition as a whole. The latter matrix together with the open-ended waveguide characteristics calculated with using the factorization method are used for determining the horn reflection coefficient, radiation pattern, aperture efficiency, and cross-polarization level.

In the work, we present the calculated characteristics of the hard strip-loaded horn with vias, discuss the effect of the different parameters of the model, and compare the features of this hard horn with hard horns of other types.

0-7803-7846-6/03/$17.00 ©2003 IEEE

## Finite Difference Time Domain Methods

**Co-Chairs:** J. Kotulski
Q. H. Liu

1:15 Opening Remarks

# The Alternating-Direction Implicit Finite-Difference Time-Domain (ADI-FDTD) Method and its Application to Simulation of Scattering from Highly Conductive Material

Xi Shao[1,2], Neil Goldsman[2] and Omar M. Ramahi[2,3,4]
[1]National Space Science Data Center, Goddard Space Flight Center, NASA
Greenbelt, MD 20771
[2]Electrical and Computer Engineering Department, [3]Mechanical Engineering Department
and [4]CALCE Electronic Products and Systems Center, University of Maryland,
College Park, MD 20742
www.enme.umd.edu/~oramahi

The study of shielding effectiveness of natural and synthetic conductive material requires accurate modeling of the electromagnetic field distribution in the close proximity and within the material. At microwave frequencies, the skin depth of highly conductive materials is in the micrometer range. For accurate modeling, the field within the material must be resolved, which places heavy computational burden on most traditional electromagnetic solvers. The alternating-direction implicit finite-difference time-domain (ADI-FDTD) method offers a unique advantage in comparison to other time-domain volume-based methods in that the time step is not constrained by the smallest space-cell size (i.e., the Courant limit). This lack of time-step constraint is a direct product of the *implicitness* of the ADI-FDTD. However, and as reported in recent works, dispersion can be a direct casualty of time-step relaxation. To investigate the effectiveness of scattering interaction between non-conductive (lossless) and highly conductive media, we developed a multi-grid three-dimensional ADI-FDTD method. As a starting point, we simulated the classical problem of microwave frequency plane wave incidence on a highly conductive half-space. In this simulation, the smallest grid resolution of 0.1 μm was chosen within the material, while a grid resolution of 0.5mm was chosen in the lossless medium. Different time steps were chosen and their effect on the accuracy in general, and dispersion in particular was analyzed. The effect of multi-grid cell structure was also studied and comparison was made to theoretical calculation for simple half-space scattering problems. The current term ($J$) in Maxwell equations was implemented using two different approaches. In the first, the $E$ field was expressed using the Crank-Nicolson method. In the second, the $E$ field was treated implicitly. Discussion of the effect of all these factors will be addressed with the objective of determining the robustness of the ADI-FDTD method for the treatment of general highly conductive natural and synthesized structures.

0-7803-7846-6/03/$17.00 ©2003 IEEE 

# SOME ADVANCES IN THE ADI–FDTD METHOD

R. Godoy Rubio, S. González García*, A. Rubio Bretones, and R. Gómez Martín

Dept. of Electromagnetism and Matter Physics. University of Granada
18071 Granada (Spain). salva@ugr.es

URSI Commission B (Fields and Waves): B6.2 (Time-domain methods)

The unconditionally stable Alternating Direction Implicit Finite Difference Time Domain (ADI–FDTD) method (T. Namiki, *IEEE Trans. on Microw. Theory and Techn.*, **47**, 2003–2007, 1999) (F. Zheng, *et al.*, *IEEE Microw. Guided Wave Lett.*, **9**, 441–443, 1999) is a powerful alternative to the traditional FDTD method. It can be obtained starting from the Crank–Nicolson fully implicit–in–space scheme, by adding a $\Delta t^2$ perturbation term to it, which permits its factorization into a two–substep tridiagonally implicit–in–space scheme. The resulting algorithm advances a single step in roughly 1.5 times the CPU time employed by the classical FDTD, but since the time increment does not need to fulfil the Courant stability criterion, it can be conveniently increased in many practical problems, with which the ADI–FDTD method can achieve significant reductions in CPU time compared to the FDTD method.

In the first part of this work we briefly summarize some new extensions of this method: inclusion of material dispersion, subgridding techniques, hybridizing with other time domain techniques, accurate source implementation, etc.

One drawback of the method is the errors that appear, especially in low frequency problems, and which are not present in the Crank–Nicolson scheme. Using the analytical expression of the truncation error, it has been shown (S. G. García, *et al.*, *IEEE Antennas and Wireless Propagation Letters*, **1**, 31–34, 2002) that the time increment cannot be increased arbitrarily taking into account only numerical dispersion criteria (number of samples per period); it is also limited by the fact that it must accurately *resolve* the spatial variations of the fields as well.

In the second part of this work we further discuss the origin of these errors, analyzing the consistency and convergence of the scheme. Finally, we focus our attention on possible solutions and alternatives to reduce the aforementioned errors.

0-7803-7846-6/03/$17.00 ©2003 IEEE

# A Novel Longitudinal-section FDTD algorithm for Simulating Large-size Electromagnetic Compatibility and Interference (EMC/EMI) Problems

*Hany E. Abd El-Raouf and Raj Mittra*
*Electromagnetic Communication Laboratory, 319 EE East*
*The Pennsylvania State University*
*University Park, PA 16802*

## Abstract

In this paper we present a new Longitudinal-section FDTD algorithm, designed to solve field penetration problems involving electrically large structures that cannot be handled by a direct application of the method. This technique begins by dividing the structure into relatively small sections in the longitudinal direction, and then applying the conventional FDTD, successively progressively along that direction using the field distribution on the last plane of a sub-domain as the field input on the first plane of the following one. The field computation in each sub-region is carried out by terminating it with a PML layer. The magnitude and the phase of the field computed on the plane located at the interface between two slices are stored in the frequency domain. To investigate the problem of penetration inside a building, *i.e.*, to solve an EMI problem, these serial computations are successively applied until the back wall is reached. Following this, similar computations are used--once again--to track the reflected waves until they reach the observation plane. Multiple reflections between the walls are included on 'as needed' basis until the desired accuracy is achieved. Since the slices in the longitudinal dimension can be relatively small, and we place virtually no limits on the number of slices very large problems can be accommodated using a machine with only a moderate-size memory.

To validate the above Longitudinal-FDTD approach, we have investigated the problem of penetration of EM wave inside a room and have compared the results of this approach with the direct application of the FDTD. In this example, the operating frequency of the incident plane wave is 500 MHZ and the outer dimensions of this geometry are 2.25m x 2.25m x 3m. The walls have dielectric constant 6.25 and conductivity 4.17e-2 Mho/m, except the rear wall has a dielectric constant 4.0. We have divided the computational domain into two regions, we added a PML layers at the end of the first computational domain, to absorb the waves traveling in the y-direction at the end of the computational domain of this region. For this test example, the incident field is a plane wave, which impinges upon the room in a direction normal to the aperture in the front wall. Fig. 1 shows a comparison of the $E_z$-field along the central line (x=const) in an observation plane at f=500MHZ, derived by using the first two reflections. It can be noted from this figure that the domain decomposition results using the first two reflections agree well in the region of interest, which is the center region of the room, with those derived via a direct application of the FDTD. We have also used the newly developed serial FDTD technique to solve the problem of penetration of the fields radiated by a broadband antenna into an electrically large building, with a measurement probe located inside the building. In order to deal with wire-type antennas as well as lossy inhomogeneous structures, such as building walls, we have hybridized the FDTD method with the NEC code and have determined the field received by the probe antenna by using the reciprocity theorem. The visualization of the field inside the building and the field received by the probe will be presented.

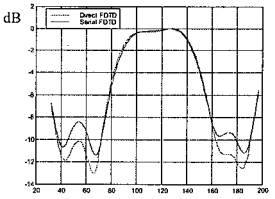


Fig. 1. Magnitude of the field distribution at the center line of the observation plane. The computed field by using two reflections is compared with that of the direct application of the FDTD. $\overline{E}^{inc} = E_0 e^{-j k_0 y} \overline{a_z}$.

# Accurate Metal Edge Processing for Edges Parallel to the FDTD Grid

C. Whelan*, M. Okoniewski, University of Calgary, Canada

Modelling geometries within the Finite Difference Time Domain (FDTD) technique is challenging. Cartesian mesh allows for easy formulation of update equations, yet can cause difficulty when the problem geometry does not coincide with the grid. One particular case is that of a sharp metal edge. Singularities in field exist near the edge and if taken into account, they can increase the accuracy of an FDTD simulation involving flat metals. Currently, static cases, such as metals at a 45° angle to the mesh (Esselle, Okoniewski, and Stuchly *IEEE Microwave and Guided Wave Letters*, Vol. 9, No. 6, June 1999) have been solved. These techniques have been extended using a graded mesh to model metal edges lying at different angles. The drawback with these techniques is the moving of H field components from their cell-centered position, requiring a re-formulation of E and H updates for that cell. While solving the problem of modeling arbitrarily angled flat metals using only altered updates for H fields, equations have been developed which take into account the singularity near the metal edge and can be applied when it runs *parallel but not aligned with* the cartesian FDTD grid. These equations are defined on the transverse electric plane for two cases. The first case occurs when the H field is located on or inside the metal strip; the update equation is:

$$H_z^{i,j,k} = 0 \tag{1}$$

The second case occurs when the metal edge is between the cell edge (E component), and the cell center(H component) with the H component located outside of the metal. The update equation is:

$$H_z^{i,j,k} = H_z^{i,j,k} - \frac{\Delta t}{\mu}\left(\frac{E_x^{i,j+1,k} - E_x^{i,j,k}}{\Delta y(2\sqrt{l^2 - \frac{1}{2}l})} - \frac{E_y^{i+1,j,k} - E_y^{i,j,k}}{\Delta x}\right) \tag{2}$$

where $l$ is the percentage of the cell's perpendicular side that is located outside of the metal. If the metal sheet edge falls directly on the E field component (i.e. $l = 0.0$) then the $2\sqrt{l^2 - \frac{1}{2}l}$ in the denominator becomes $\sqrt{2}$. As the edge approaches the H component in the center of the cell, $l$ approaches 0.5, and the denominator of the corresponding spatial derivative approaches zero, reflecting the singular behaviour of the field in the vicinity of the edge. These update equations have been implemented and applied to a simple microstrip circuit. Without modified update equations, the impedance of the strip is calculated to be approximately 39.54 ohms at 10GHz, 41.4 ohms at 20 GHz, and 41.66 ohms at 30 GHz. With the above equations, the microstrip was shifted across the

Table 1: Impedance results for modified equations at three frequencies.

| $l$ | $Z_{10GHz}$ | $Z_{20GHz}$ | $Z_{30GHz}$ |
|---|---|---|---|
| 0.3 | 42.45 | 41.80 | 40.30 |
| 0.6 | 39.58 | 41.34 | 41.68 |
| 0.9 | 39.58 | 41.36 | 41.72 |

width of one cell and impedance measurements were taken for each shift. The modified equations did not cause instability, and the results in Table 1 show the modified equations' efficacy.

0-7803-7846-6/03/$17.00 ©2003 IEEE

# Backward Differentiation (BDF) - based Numerical Schemes for Efficient Time Integration of Maxwell's Equations

COSTAS D. SARRIS
The Edward S. Rogers Sr. Department of Electrical and Computer Engineering,
University of Toronto, Toronto, ON, Canada
E-mail: cds@waves.toronto.edu

The Finite Difference Time Domain (FDTD) technique presents a versatile and relatively simple way of solving Maxwell's equations in the time-domain, for arbitrary geometries. Yet, two fundamental concerns limit its applicability to multi-wavelength domain problems, of the type that often arise in wireless communication applications. First, numerical dispersion necessitates the use of dense spatial gridding. Second, numerical instability necessitates the use of a dense temporal gridding. An answer to the first concern, comes from the so-called higher order methods, such as S-MRTD [Krumpholz and Katehi, IEEE MTT-T, April 1996]. An important matter that little attention has been given to, is that their combination with low-order time integration schemes (such as the FDTD leap-frog, or midpoint rule), compromises their accuracy [Aidam and Russer, Proc. 15th Annu. Rev. Progress App. Comput. Electromag.].

In this paper, we focus on the initial value problem that comes from the space discretization of Maxwell's equations with higher order functions, namely Battle-Lemarie, biorthogonal and Daubechies scaling functions. Recognizing that what is needed for efficient time integration of the resultant IVP is a stable, higher order method, we adopt an effective class of methods that has been previously employed in the so-called *stiff* problems of fluid dynamics: Backward differentiation methods [Curtis and Hirschfelder, Proc. Nat. Acad. Sci. USA, 1952]. The latter, approximate temporal derivatives at time step $n+r$ by a backward difference approximation, using $r$ additional points going backwards in time. It is noted that the derivation of an $r-th$ order accurate method, using $r$ points is possible. The 1-step BDF is simply the well-known first order accurate, backward Euler method. The highest order of accuracy that can be implemented for a stable BDF is six.

Dispersion analysis of all schemes under consideration is provided and stability conditions are explicitly stated. Derivations of absorbing boundary conditions are presented. Benchmarking applications to cavity problems, as well as real-life applications such as integrated waveguides and antennas are considered.

0-7803-7846-6/03/$17.00 ©2003 IEEE

# Staggered Upwind Embedded Boundary Method for 3D Maxwell's Equations

Tian Xiao* and Qing Huo Liu
Department of Electrical and Computer Engineering
Duke University
Box 90291
Durham, North Carolina 27708

The Yee's finite-difference time-domain (FDTD) algorithm has enjoyed widespread applications in computational electromagnetics. However, in spite of its flexibility and 2nd-order accuracy in a homogeneous medium, the FDTD method suffers from a serious degradation when treating material interfaces, greatly reducing its accuracy in the presence of inhomogeneous media and perfect conductors. Indeed, such a so-called staircasing approximation may lead to local divergence and loss of global convergence. In this work, an embedded FDTD scheme, the staggered upwind embedded boundary (SUEB) method, is developed for the solution of 3D Maxwell's equations. This simple embedded technique uses upwind flux to penalize the numerical jumps of the tangential field components that do not satisfy the boundary conditions. This process makes the location and physical conditions of material and metallic interfaces asymptotically correct, thus eliminating problems caused by the staircasing approximation in the FDTD method. Accuracy analysis has been made to show that the SUEB method maintains a 2nd-order accuracy globally. Since the entire problem has been embedded into the simple staggered grid similar to that employed by the Yee method, an extra effort is only needed when treating the grid points close to the interfaces. Therefore, little additional computational cost is needed over the Yee method. The embedded FDTD scheme has been validated by the analytical solutions for some typical benchmark cases. Numerical examples show that this method is much more efficient than the FDTD method.

0-7803-7846-6/03/$17.00 ©2003 IEEE

# Implementation of a Massively Parallel Hybrid Finite-Element/Finite-Difference Electromagnetic Solver in the NEVADA Framework

J.D. Kotulski*, M.F. Pasik, D.B.Seidel, and C.D. Turner
Sandia National Laboratories
P.O. Box 5800
Albuquerque NM 87185-1152 USA

This presentation describes the implementation of hybrid finite-element/finite-difference algorithms within the NEVADA framework for solving Maxwell's equations in the time domain. The NEVADA framework is an object-oriented time-domain finite-element framework implemented in C++ supported by the Department of Energy's Advanced Simulation and Computing Program (ASCI). The NEVADA framework forms the basis of the well-known h-adaptive finite-element shock-physics code ALEGRA. One of the main reasons for implementing our electromagnetic algorithms in the NEVADA framework was to facilitate coupling with other type of physics analysis.

The finite-element services of the NEVADA framework allowed us to rapidly implement both a conditionally stable coupled first-order and unconditionally stable second order Whitney edge-element based formulations originally developed in the VOLMAX code. Most of the effort involved in adding finite-element based electromagnetic algorithms to NEVADA related to the implementation of specialized communication for sub-cell models such as slots and wires.

To facilitate the implementation of finite-difference algorithms we extended the key NEVADA framework concept of a computation region to include one based on structured mesh topologies. We also extended the framework by encapsulating our proven structured communication plan algorithms and data structures developed for the QUICKSILVER code into general-purpose framework objects. The introduction of another new region type, a region controller (a "smart" container of regions which also encapsulates the necessary data and algorithms used to interconnect the regions) allowed us to implement both multi-block and massively parallel structured mesh capabilities.

In the presentation we will focus on how we further extended the framework communications objects and the controller region concept to support hybrid structured/unstructured mesh connections in parallel. The costs and benefits of the framework implementation will be compared/contrasted to the algorithm development efforts in the VOLMAX and QSVM codes. Practical applications of the implementation will be presented that demonstrate the hybrid capability and sub-cell algorithms.

Sandia is a multiprogram laboratory operated by Sandia Corporation, a Lockheed Martin Company for the United States Department of Energy under Contract No. DE-AC04-94A185000.

# Efficient 3-D Ground Penetrating Radar Simulation with Spiral Antennas and Buried Objects

Mei Chai* and Qing Huo Liu
Department of Electrical and Computer Engineering
Duke University
Box 90291
Durham, North Carolina 27708
Email: mchai@ee.duke.edu, qhliu@ee.duke.edu

In the simulation of ground penetrating radar detection of buried objects such as landmines, one often needs to model the detailed structure of the transmitting and receiving antennas as well as the buried objects. Of particular interest are compact GPR systems with spiral antennas which were designed to operate at an optimal efficiency with a limited dimension. Unfortunately, such antennas may have fine structures well below the wavelength of the transmitted microwaves. Such small structures require fine spatial discretization, and thus a small time step size in the finite-difference time-domain (FDTD) method. This restriction arises because the Courant-Friedrich-Levy (CFL) conditions limits the maximum time-step to minimum cell size in a computational domain. Recently, an unconditionally stable three-dimensional alternating direction implicit (ADI) scheme was investigated. The successful implementation of this scheme has the potential to impact the application of FDTD to the problems where very fine mesh is required over the large geometric area.

For the ADI-FDTD to be applicable to the practical electromagnetic problems, an efficient absorbing boundary condition must be derived to maintain unconditional stability. In this work, a well-posed perfectly matched layer (PML) medium in a non-split form based on the coordinate-stretching technique is applied to the three-dimensional (3-D) ADI-FDTD method. Under this well-posed PML absorbing boundary condition, the ADI-FDTD method remains unconditionally stable. To validate this new method, we compare the ADI-FDTD and the regular FDTD methods for large-scale simulations of ground penetrating radar (GPR) measurements of landmines.

0-7803-7846-6/03/$17.00 ©2003 IEEE

# Application of the Biorthogonal Multi-Resolution Time Domain Method to Study Elastic-Wave Interactions With Buried Land Mines

Xianyang Zhu and Lawrence Carin
Department of Electrical and Computer Engineering
Box 90291, Duke University
Durham, NC 27708-0291

Electromagnetic waves are very effective in detecting buried land mines. However, if the permittivity of the land mine (plastic mines, for example) is very close to the soil permittivity, or the conductivity of the soil is high, the scattered fields will be very weak. It will be very difficult to detect the land mines. In this case, elastic waves are very promising and show great advantages. Elastic waves interact with the land mines and cause the mines and the surface above the mines to vibrate, and the vibration can be detected thus the mines can be located.

The elastic wave motion in a medium can be described by a set of first-order partial differential equations according to the equation of motion and the stress-strain relation. Thus the finite-difference time-domain (FDTD) modeling scheme can be naturally applied for this issue to explore the mine-wave interactions. Similar to the FDTD method for electromagnetic wave applications, the advantage of such implementation is that it can deal with complex-shaped, homogeneous or inhomogeneous targets. Also it has a poor numerical dispersion property, which means the fields must be over-sampled to obtain accurate results.

In this paper we will introduce biorthogonal multi-resolution time domain (Bi-MRTD) method to this field. A perfectly matched layer surrounding the discretized solution space is also implemented to absorb the outgoing waves. Numerical results show that the numerical dispersion properties can be improved significantly by using biorthogonal wavelets as bases, which means larger problem can be considered with the same computational resources.

To further increase the ability of the model, the message-passing interface (MPI) is used to parallelize the algorithm.

0-7803-7846-6/03/$17.00 ©2003 IEEE

# Modelling of Open Boundaries for FIT/FDTD-Simulations of Particle Beams

M.C.Balk*[1], R. Schuhmann, T. Weiland
Technische Universität Darmstadt
Computational Electromagnetics Laboratory (TEMF)
Schlossgartenstr. 8, 64289 Darmstadt, Germany
balk@temf.tu-darmstadt.de

Electromagnetic field simulations with FIT (FDTD-like) provide solutions for a large range of different problems and the corresponding methods are quite sophisticated. However, there still is a need –e.g. in particle accelerator laboratories– of simulating charged particle beams with appropriate boundary conditions.

Existent **P**article **I**n **C**ell (PIC) methods for simulating moving particles are numerically inefficient in case of heavy-ion beams, where the particles show nearly unchanging electromagnetic characteristics throughout the structure. Furthermore, no open boundary condition exists for particles with ($v < c$). Therefore, a method is proposed to simulate charged particle beams in time domain within the Finite Integration Technique (FIT, cf. Weiland, *Int. J. Num. Mod.* **9**, 259-319, 1996).

As first step, the moving charged particles are modeled as a line current along one grid line. This current is implemented using a discrete form of the continuity equation. Hence, the approach ensures the line current to be divergence free and does not introduce unphysical electric charges. At the end of the calculation domain a prediction of the line current via a "Mur"-type open boundary condition is needed.

In the second step – the boundary condition– the electromagnetic field of a charge moving towards the calculation domain has to be considered. Assuming an infinitely long homogeneous beam tube and $v < c$ this field is of infinite extent. Thus, a threshold is discussed, which is a "quasi" limit of the charge's influence on the boundary of the calculation domain.

The electromagnetic field of the moving charge can be found by a combination of a Lorentz transformation and a discrete electrostatic field solution. The Lorentz transformation is applied to the grid where the charge is moving. In the resulting grid, the electric field of the charge can be found by the solution of a discrete Poisson equation. Then this field –after the re-transformation– can be used to impose the boundary fields. The advantage of such a grid based transformation is that the resulting fields obey some consistency laws on the discrete level.

The method will be applied to a typical particle accelerator structure.

[1]The work of M. C. Balk is supported by GSI Darmstadt.

0-7803-7846-6/03/$17.00 ©2003 IEEE

***Special Session***

**Data Assimilation**

**Organizer(s):** Gary Bust
Farzad Kamalabadi, University of Illinois at Urbana-Champaign

**Co-Chairs:** C. Minter
B. Wilson

1:15 Opening Remarks

76. 1 1:20 Validation of a Global Ionospheric Data Assimilation Model ..... 370
*B. Wilson, G. Hajj, Jet Propulsion Laboratory, C. Wang, University of Southern California, X. Pi, Jet Propulsion Laboratory, I. Rosen, University of Southern California, USA*

76. 2 1:40 Validation of the Ionospheric Data Assimilation Three Dimensional (IDA3D) Algorithm ..... 371
*T. W. Garner, G. S. Bust, T. L. Gaussiran, Applied Research Laboratories: The University of Texas at Austin, USA*

76. 3 2:00 Global Assimilation of Ionospheric Measurements (GAIM) ..... 372
*R. W. Schunk, L. Scherliess, J. J. Sojka, D. C. Thompson, Utah State University, D. N. Anderson, M. Codrescu, C. Minter, T. J. Fuller-Rowell, NOAA/Space Environment Center, R. A. Heelis, M. Hairston, University of Texas at Dallas, B. M. Howe, University o*

76. 4 2:20 Using Auxiliary Weighted Least Squareswith the Extended Kalman Filter To Forecast Unobservable Regions in the Thermosphere ..... 373
*C. F. Minter, T. J. Fuller-Rowell, University of Colorado - CIRES, USA*

76. 5 2:40 Multipath Channel Estimation Using Two-Step Maximum Likelihood Method ..... 374
*H. S. Mir, J. D. Sahr, University of Washington, USA*

76. 6 3:00 Isolated Ionospheric Disturbances As Deduced from Global GPS Network ..... 375
*E. L. Afraimovich, E. I. Astafieva, Institute of Solar-Terrestrial Physics SD RAS, Russia*

**Validation of a Global Ionospheric Data Assimilation Model**

B. Wilson (2), G. Hajj (1,2), C. Wang (1), X. Pi (1,2), I.G. Rosen (1)

(1) Department of Mathematics, University of Southern California, CA 90089-1113 (2) Jet Propulsion Laboratory, California Institute of Technology, 4800 Oak Grove Dr. Pasadena, CA 91109, Brian.Wilson@jpl.nasa.gov.

As the number of ground and space-based receivers tracking the global positioning system (GPS) steadily increases, and the quantity of other ionospheric remote sensing data such as measurements of airglow also increases, it is becoming possible to monitor changes in the ionosphere continuously and on a global scale with unprecedented accuracy and reliability. However, in order to make effective use of such a large volume of data for both ionospheric specification and forecast, it is important to develop a data- driven ionospheric model that is consistent with the underlying physical principles governing ionosphere dynamics.

A fully 3-dimensional Global Assimilative Ionosphere Model (GAIM) is currently being developed by a joint University of Southern California and Jet Propulsion Laboratory team. GAIM uses a first-principles ionospheric physics model ("forward" model) and Kalman filtering and 4DVAR techniques to not only solve for densities on a 3D grid but also estimate key driving forces which are inputs to the theoretical model, such as the ExB drift, neutral wind, and production terms. The driving forces are estimated using an "adjoint equation" to compute the required partial derivatives, thereby greatly reducing the computational demands compared to other techniques. For estimation of the grid densities, GAIM uses an approximate Kalman filter implementation in which the portions of the covariance matrix that are retained (the off-diagonal elements) are determined by assumed but physical correlation lengths in the ionosphere. By selecting how sparse or full the covariance matrix is over repeated Kalman filter runs, one can fully investigate the tradeoff between estimation accuracy and computational speed.

Although GAIM will ultimately use multiple datatypes and many data sources, we have performed a first study of quantitative accuracy by ingesting GPS-derived TEC observations from ground and space-based receivers and nighttime UV radiance data from the LORAAS limb scanner on ARGOS, and then comparing the retrieved density field to independent ionospheric observations. A series of such GAIM retrievals will be presented and validated by comparisons to: vertical TEC data from the TOPEX altimeter, slant TEC data from ground GPS sites that were not included in the assimilation runs, and global ionosonde data (F0F2, HMF2, and bottom-side profiles where available). By presenting animated movies of the GAIM densities and vertical TEC maps, and their errors computed as differences from the independent observations, we will demonstrate the reasonableness and physicality of the climatology derived from the GAIM forward model, examine the consistency of the GPS and UV datatypes, and characterize the quantitative accuracy of the ionospheric "weather" specification provided by the assimilation retrievals.

0-7803-7846-6/03/$17.00 ©2003 IEEE

# Validation of the Ionospheric Data Assimilation Three Dimensional (IDA3D) Algorithm

T. W. Garner*, G. S. Bust, and T. L. Gaussiran II
Applied Research Laboratories, The University of Texas at Austin

Submitted to Commission G (Ionospheric Radio and Propagation)
G2. Ionospheric modeling and data assimilation

Ionospheric tomography has been used for several years to create large-scale electron density maps for GPS or radio beacon TEC data. Recently, the computerized ionospheric tomography (CIT) algorithm [Bust et al., *Int. J. Imag. Syst. Technol.*, **5**, 160, 1994] has been adapted into the Ionospheric Data Assimilation Three Dimensional (IDA3D) algorithm. IDA3D is a data assimilation algorithm, which incorporates all available electron density and electron content observations into a coherent picture of the synoptic or global scale ionosphere. IDA3D primarily uses slant total electron content (TEC) measurements from available GPS ground sites and radio beacon receiver arrays operated by the Applied Research Laboratories, The University of Texas at Austin (ARL:UT), but can easily use peak electron density measurements from digasondes, electron density profiles from incoherent scatter radar and satellite-based GPS-occulation measurements of the topside TEC. This study compares different electron density maps for the same time period. Individual maps are created for each data set and combination of data sets (for a total of thirty maps), and compared to those observations that not used in a given map. By comparing the IDA3D maps to withheld observations, this study determines the validity of IDA3D, the usefulness of a given data set, and regions where more observations are needed.

0-7803-7846-6/03/$17.00 ©2003 IEEE 

# GLOBAL ASSIMILATION OF IONOSPHERIC MEASUREMENTS (GAIM)

Robert W. Schunk*, Ludger Scherliess, Jan J. Sojka, Donald C. Thompson
Center for Atmospheric and Space Sciences, Utah State University,
Logan, UT 84322-4405

David N. Anderson, Mihail Codrescu, Cliff Minter, Timothy J. Fuller-Rowell
NOAA/Space Environment Center, Department of Commerce, 325 Broadway,
Boulder, CO 84303

Roderick A. Heelis, Marc Hairston
W B Hanson Center for Space Sciences, University of Texas at Dallas,
PO Box 830688, MS F022, Richardson, TX 75083-0688

Bruce M. Howe
Applied Physics Laboratory, University of Washington, 1013 NE 40th Street,
Seattle, WA 98105

The ionosphere is a highly dynamic medium that can vary significantly from day to day and from hour to hour at a given location, and these variations can have detrimental effects on military and civilian systems. In an effort to minimize or circumvent the detrimental effects, a physics-based data assimilation model of the ionosphere and neutral atmosphere is under development with funding from the Multi-Disciplinary University Research Initiative (MURI) program. Two university consortia are involved, with Utah State University (USU) and University of Southern California (USC) as the lead institutions. When completed, the GAIM model will provide specifications and forecasts on a spatial grid that can be global, regional, or local (25 km x 25 km). GAIM will use a physics-based ionosphere-plasmasphere-polar wind model and a Kalman filter as a basis for assimilating a diverse set of real-time (or near real-time) measurements. The resulting specifications and forecasts are in the form of 3-dimensional electron density distributions from 90 km to geosynchronous altitude (35,000 km). Auxiliary parameters are also available, including $N_mF_2$, $h_mF_2$, $N_mE$, $h_mE$, and slant and vertical TEC. In addition, GAIM will provide global distributions for the self-consistent ionospheric drivers (neutral winds and densities, magnetospheric and equatorial electric fields, and particle precipitation patterns), and in its specification mode, it will provide quantitative estimates for the accuracy of the reconstructed ionospheric densities.

In addition to the physics-based, Kalman filter, data assimilation model, we have also developed a Gauss-Markov Kalman filter model. For both of these models, we have assimilated several data sources, including in situ electron density measurements from the DMSP satellites, bottomside electron density profiles from the Air Force network of digisondes, GPS-TEC data from a world-wide network of more than 100 stations, GPS-TEC data from 332 stations in the CORS network (covering the U.S.), and occultation data. The presentation will first provide a brief description of the two models, and then the focus of the presentation will be on a comparison of the results from the two models and a validation with independent data sources.

0-7803-7846-6/03/$17.00 ©2003 IEEE

# Using Auxiliary Weighted Least Squares with the Extended Kalman Filter To Forecast Unobservable Regions in the Thermosphere

Clifton F. Minter*and Timothy J. Fuller-Rowell
CIRES/University of Colorado
NOAA/Space Environment Center
325 Broadway
Boulder, CO 80305

To determine Global Positioning System corrections and propagation parameters of high-frequency radio waves, an accurate forecast of the ionosphere is desirable. Forecasting the ionosphere, especially during geomagnetic storm times, is strongly dependent on perturbations in the neutral composition. Because of the coupling between the ionosphere and neutral atmospheric chemistry, accurate knowledge of the neutral composition is critical in forecasting the ionosphere. However, changes in the neutral composition may occur suddenly during storm times, and these regions may not be observed due to limited satellite coverage. Additionally, the use of a physical model to propagate the information to the unobservable regions is insufficient due to the comparatively short time period of the storm. Therefore, an alternative method is applied with the extended Kalman filter to estimate these unobservable regions using empirical orthonormal functions (EOF's). The EOF's are calculated in parallel with the extended Kalman filter using an auxiliary weighted least squares method. These EOF's, calculated from the available observations and weighted based on the Kalman state error variance-covariance matrix, are then used to estimate the composition in the unobservable regions. Results show improvements in the composition forecast for these regions and demonstrate a lower overall root mean square error during geomagnetic storm times.

0-7803-7846-6/03/$17.00 ©2003 IEEE 

# Multipath Channel Estimation Using Two-Step Maximum Likelihood Method

Hasan Mir and John Sahr
Department of Electrical Engineering Box 352500
University of Washington, Seattle WA 98195-2500

Channel estimation is an issue of importance to both passive Radar and mobile communication applications. In such scenarios, a signal is sent through a time-varying multipath channel that severely distorts it. The need for channel estimation arises since the response of the multipath channel/transmit-filter cascade (referred to as the "channel response") is assumed to be unknown at the receiving end.

Blind estimation methods attempt to exploit apriori knowledge of both the statistics of the transmitted signal and structure of the channel. Among these methods, the Maximum Likelihood estimators are quite popular, partly due to the fact that they enjoy the property of asymptotically approaching the Cramer bound. Recently, Hua (Y.Hua, IEEE Trans Sig Proc,661-672,March 1996) introduced the two-step Maximum Likelihood (TSML) method for blind channel estimation. TSML is distinctive in requiring only two iterative steps, each involving minimization of a quadratic function.

Like other channel estimation methods, however, TSML in its original formulation does not take into account additional apriori knowledge that is often available at the receiver. Specifically, the transmit filter is often known, and as such, only estimation of the multipath channel rather than the multipath channel/transmit-filter cascade is required.

In this paper, we show how Hua's TSML method may further be extended to incorporate apriori knowledge of the transmit-filter, and assess the resulting improvement in its performance. In particular, we show how this additional knowledge further constrains the overall system model by reducing the dimensionality of the problem. Additionally, through simulations, we demonstrate various cases where TSML fails without knowledge of the transmit-filter, whereas with this knowledge, it yields satisfactory performance.

0-7803-7846-6/03/$17.00 ©2003 IEEE

# Commission G, Session G6

## Isolated ionospheric disturbances as deduced from global GPS network

E. L. Afraimovich, E. I. Astafieva
Institute of Solar-Terrestrial Physics SD RAS,
p. o. box 4026, Irkutsk, 664033, Russia,
fax: +7 3952 511675; e-mail: afra@iszf.irk.ru

**Abstract**

We investigate an unusual class of medium-scale traveling ionospheric disturbances (MS TIDs) of the nonwave type, isolated ionospheric disturbances (IIDs) that manifest themselves in total electron content (TEC) variations in the form of single aperiodic negative TEC disturbances of a duration of about 10 min (the total electron content spikes, TECS). For the first time, we present the TECS morphology for 170 days with a different level of geomagnetic activity and with the number of stations of the global GPS network ranging from 4 to 240. A total number of the TEC series (radio paths) used in the analysis, corresponding to the observation along a single receiver-satellite Line-of-Sight (LOS), with a duration of each series of about 2.3 hours, exceeded 850000. The data were obtained using the technology of global detection and monitoring of ionospheric disturbances (GLOBDET, developed at the ISTP SB RAS) of a natural and technogenic origin using measurements of TEC variations from a global network of receivers of the GPS. It was found that TECS are observed in no more than 1-2% of the total number of radio paths. We present the results derived from analyzing the dependence of TECS parameters on the local time, and on the level of geomagnetic activity. The TECS amplitude exceeds at least one order of magnitude the TEC fluctuation intensity under "background" conditions. The IID-induced TEC variations are similar in their amplitude, form and duration to the TEC response to shock-acoustic waves (SAW) generated during rocket launchings and earthquakes. However, the IID propagation velocity is less than the SAW velocity (800-1000 m/s) and are most likely to correspond to the velocity of background medium-scale acoustic-gravity waves (AGW), on the order of 100-200 m/s.

0-7803-7846-6/03/$17.00 ©2003 IEEE

***Special Session***

**Numerical Methods in Space Physics**

**Organizer(s):** Meers M Oppenheim, Boston University
**Co-Chairs:** M. Oppenheim
E. Bering

3:20 Opening Remarks

# KINETIC SIMULATIONS OF PERPENDICULAR SHOCKS

L. Muschietti
Space Sciences Laboratory
University of California, Berkeley, CA 94720-7450

In order to render the problem computationally tractable, simulation codes make approximations which limit the physics they can represent. Because of the disparity between electron and ion characteristic scales, simulating a fast magnetosonic shock with a full particle electromagnetic code is a daunting task, which requires compromises. We have developed an electromagnetic code in the Darwin approximation, whereby the transverse part of the displacement current is neglected. This neglect affords us a larger timestep than the Courant condition would otherwise impose on a grid resolving the Debye scale length.

We consider a perpendicular geometry, where x points into the shock and the electromagnetic field structure is $\mathbf{E} = (E_x, E_y, 0)$ and $\mathbf{B} = (0, 0, B_z)$. Moderate shocks with Mach number $M_a \sim 2$–4 and isothermal upstream plasma ($\beta_i = \beta_e \sim 0.1$–$0.3$) are addressed. The 1D3V code has open boundaries with upstream and downstream particles traversing the left and right boundaries, respectively. The simulation is carried out in the frame of the shock. We initiate the computation by loading the particles according to profiles of density, temperature, and fields which are modeled consistently with conservation laws (Rankine-Hugoniot). Particles and fields are then left to evolve self-consistently. Importantly, due to the partial decoupling of ions and electrons which occurs in the magnetic ramp, the electrostatic field $E_x$ builds up a large spike whose role is to slow down the ions and reflect a small fraction thereof. The reflected ions are accelerated by the transverse electric field $E_y$, gyrate back into the shock front, and are finally transmitted downstream. After several thousand timesteps a quasi-stationary shock structure is formed.

We discuss the simulation techniques used and compare the results of our shock model with those from a fully electromagnetic particle code [Lembege (2003)]. This is done for a set of parameters accessible to the fully electromagnetic code, such as: a ratio of electron gyro-to-plasma frequency $\Omega_e/\omega_{pe} = 1/2$ and a ratio of the thermal velocity to the speed of light $v_e/c = 1/15$. We then indicate how results change for parameter values which apply more realistically to shocks in the solar wind.

0-7803-7846-6/03/$17.00 ©2003 IEEE

# Gyrokinetic and Gyrofluid Modeling of Low-Frequency Phenomena in Well-Magnetized Space Plasmas

Scott E. Parker, Samuel T. Jones and Yang Chen
Department of Physics, University of Colorado, Boulder, CO 80309

Often, one is interested in frequencies much lower than either the electron or ion cyclotron frequency in well-magnetized regions of the magnetosphere and ionosphere. In such cases, a gyrokinetic (or drift-kinetic) model may be a very useful approximation. There are existing three-dimensional electromagnetic $\delta f$ gyrokinetic turbulence simulations that model both ions and electrons as kinetic using realistic mass ratios. These codes can be used for studying collisionless inner magnetosphere plasmas where $\beta$ is low. Both the benefits of using gyrokinetic simulation methods as well as the approximations and appropriate limits involved will be discussed. We will also discuss both the benefits and limitations of the $\delta f$ method. In addition, a linear one-dimensional gyrofluid model of Alfvén wave propagation in the auroral ionosphere will be discussed. Alfvénic wave packets have dramatic acceleration in phase velocity when entering the auroral acceleration region and resonant electrons can be "picked up" and accelerated to 1-10 keV energies. Finally, we will discuss how these kinetic methods can be used to close macroscopic MHD (or so-called "extended-MHD" models).

0-7803-7846-6/03/$17.00 

Abstract submitted to the 2003 URSI Meeting

**Numerical methods used in the SAMI2/3 ionosphere models**

J.D. Huba and G. Joyce (Plasma Physics Division, Naval Research Laboratory, Washington, DC 20375)

We describe the numerical techniques used in the low- to mid-latitude ionosphere models that have been developed at the Naval Research Laboratory: SAMI2 and SAMI3. SAMI2 is a two-dimensional model while SAMI3 is a three-dimensional model. These models use numerical methods that are very different from most other ionosphere models. First, ion inertia, which is neglected in other ionosphere models, is included in SAMI2 and SAMI3. A semi-implicit scheme is used to advance the densities, velocities and temperatures along the magnetic field direction. Although this requires a small time step (e.g., $\Delta t \lesssim 30$ sec) the numerical scheme is robust. Second, a nonorthogonal Eulerian grid is used. Most other ionosphere models use a Lagrangian grid and track the motion of flux tubes. One axis of our grid is the dipole field. The other two axes are defined numerically to provide high resolution at low altitude and sparse resolution at high altitudes; they are not aligned with the $\mathbf{E} \times \mathbf{B}$ drift of the plasma. The $\mathbf{E} \times \mathbf{B}$ transport is based on a finite volume method using the donor cell method. Finally, both SAMI2 and SAMI3 are fully parallelized using the Message Passing Interface (MPI) method and run on a Linux Beowulf system.

Research supported by ONR

0-7803-7846-6/03/$17.00 ©2003 IEEE

# Vlasov Simulation of Nonlinear Wave Structures in Space Plasmas

David L. Newman* and Martin V. Goldman
Center for Integrated Plasma Studies, 390 UCB,
University of Colorado, Boulder, CO 80309-0390

Robert E. Ergun and Laila Andersson
Laboratory for Atmospheric and Space Physics, 392 UCB,
University of Colorado, Boulder, CO 80309-0392

There are two primary approaches to kinetic simulations of space plasmas: particle-in-cell (PIC) methods and Vlasov methods. Both of these complementary approaches have advantages and disadvantages relative to one another. In the PIC method, a large number of particles from a given plasma species is represented by a single *macroparticle* with the charge-to-mass ratio characteristic of that species. The relatively small number of macroparticles (compared to the number of *physical* particles in the plasma being modeled) makes the evolution of their individual positions and velocities numerically tractable. By contrast, the Vlasov method takes the opposite approach in which the discrete particles are represented by a continuous phase-space fluid, while again maintaining the original charge-to-mass ratio. The Vlasov partial differential equations for each species are then numerically integrated on a phase-space grid. In both methods the evolution is governed by applied and self-consistent fields, with the latter found by solving the Maxwell (electromagnetic) or Poisson (electrostatic) equations.

As a result of the absence of discrete particles, Vlasov simulations are inherently quieter than corresponding PIC simulations. Consequently, simulation diagnostics (especially phase-space diagnostics) are easier to analyze. Implementing non-periodic boundary conditions is also simpler in Vlasov simulations. However, PIC simulations enjoy a major computational advantage when scaling to higher spatial dimensions because the simulation grid is only of dimension $D$ of the physical space whereas the corresponding Vlasov phase space dimension is (in general) $2D$. Thus, for example, a Vlasov simulation of a 3-D plasma in 6-D phase space is numerically impractical—even on today's massively-parallel computers—for physically useful grid dimensions.

The focus of this talk will be an exploration of methods that can be employed to extend Vlasov simulations into higher dimensions without "breaking the computational bank." A primary example will be the extension of 1-D Vlasov simulations of current-driven double layers and associated electron holes (D. L. Newman et al., *Phys. Rev. Lett.*, **87**, 255001, 2001) into a second spatial dimension by restricting consideration to highly-magnetized species. Under this approximation, which is valid for electrons (but not ions) in regions of the auroral ionosphere where double layers and electron holes have been observed (R. E. Ergun, et al., *Phys. Rev. Lett.*, **87**, 045003, 2001), phase space is reduced from 4-D to 3-D because of restricted particle motion perpendicular to **B**. Proposed modifications to the Vlasov algorithm that will accommodate unmagnetized or weakly magnetized ions while keeping the computational demands well within the capabilities of today's computers will also be discussed.

0-7803-7846-6/03/$17.00 ©2003 IEEE

# A Consistent Kinetic Plasma Solver for the Computational Modeling of 2D Conductive Structures in Flowing Ionospheric Plasmas

*Éric Choinière[1] and Brian E. Gilchrist[1]

[1]University of Michigan, Electrical Engineering and Computer Science Department, Ann Arbor, Michigan 48109-2122, USA, echoinie@umich.edu, gilchrst@umich.edu

## 1 Background and Motivation

Current-collecting conductive objects in flowing, collisionless, unmagnetized plasmas are found in several applications, such as plasma diagnostic devices (Langmuir probes, Mach probes), in spacecraft charge control, and for bare electrodynamic space tethers. Space electrodynamic tethers offer the opportunity for propellantless propulsion of near-earth orbiting spacecraft, based on the conversion of the geomagnetic force on an electric current along a tether into a propulsive force. One of the key parameters affecting thrust is the current level flowing through the tether, which in turn is limited by the level of ionospheric electron collection. It is desirable to assess how the electron collection capability of various tether cross-section geometries, immersed in a flowing plasma, departs from that predicted by the Orbital Motion Limit, which is only valid in the case of thin wires in non-flowing plasmas.

## 2 Proposed Kinetic Computational Model

Existing models for the round cylindrical probe in flowing plasmas have assumed a symmetrical sheath potential. In this paper, we present a novel electrodynamic computational model based on kinetic theory that fully accounts for the sheath potential asymmetries induced by plasma flow effects. The model numerically solves, self-consistently, the Poisson and Vlasov equations for arbitrarily-shaped 2D conductive bodies in collisionless, unmagnetized, flowing 2-species plasmas(ions and electrons). The resulting solver allows representation of the complete, non-equilibrium arbitrary velocity distribution of both species within the computational domain, given Maxwellian populations at infinity. It provides an adaptive, unstructured meshing strategy and allows simulation of very large computational domains. Finally, it has a parallel implementation, such that it could be run on either a single host, a parallel architecture, or a scattered network of workstations.

The implementation of the solver consists of successive linearizations of the non-linear Poisson-Vlasov operator, within a Newton iterative process stabilized using the Tikhonov regularization procedure, which handles the numerical instabilities introduced by the use of large grid spacings. The Finite Element Method is used for the Poisson solver, while the inside-out trajectory tracking procedure, also known as the method of characteristics for partial differential equations, is used for the Vlasov solver.

## 3 Theoretical and Experimental Validation

The proposed model was validated against known 1-D results in the non-flowing case, existing approximate models for ion collection in flowing plasmas, published Mach probe simulation and measurements, and experimental data obtained as part of vacuum chamber tests on long collecting probes in a flowing plasma (Gilchrist *et al*, IEEE Trans. on Plasma Science, **30** (5), Oct. 2002).

0-7803-7846-6/03/$17.00 ©2003 IEEE

# RF EFFECTS ON OEDIPUS-C FLOATING VOLTAGES

*J.G. Laframboise
Physics and Astronomy Department, York University
4700 Keele Street, Toronto, ON, Canada M3J 1P3
Tel: 416 736 5621, Fax: 416 736 5516
e-mail: laframboise@quasar.phys.yorku.ca

D.D. Wallis
Magnametrics
2340 Briar Hill Drive, Ottawa, ON, Canada K1H 7A9
Tel: 613 521 4463, e-mail: d.wallis@cyberus.com

H.G. James
Communications Research Centre, Ottawa, ON, Canada K2H 8S2
Tel: 613 998 2230, Fax: 613 990 6339
e-mail: gordon.james@crc.ca

The OEDIPUS-C tethered payload was launched on 7 November 1995 from the Poker Flat Research Range, Alaska. The Tether Current Monitor (TCM) instrument operated the two subpayloads and the conducting tether as a double electrostatic probe. During the part of the experiment discussed here, the flight upleg, the angle between the tether and the geomagnetic-field direction was less than 5 degrees. The TCM configured the payload cyclically as a high-impedance voltage probe and as a low-impedance current probe.

OEDIPUS C also carried a high-frequency exciter (HEX) on its forward subpayload. With the HEX connected to the forward subpayload dipoles and with the frequency swept from 25 kHz to 8.0 MHz, the transient response of the TCM voltage showed a number of reproducible features. At the lowest frequencies of the sweep, the RF pulses drove the forward subpayload potential negative with respect to the aft by several tens of volts. The time-constant of relaxation of the payload's potential between the HEX pulses increased as background density decreased.

The TCM voltmeter data showed a steady rise in the time-averaged floating voltage of the forward subpayload as the HEX transmitter was swept from lower to higher frequencies. This is as expected when ponderomotive effects become relatively more important relative to rectification. Superposed on this was another feature in which the forward subpayload was driven increasingly negative as the frequency approached the electron gyrofrequency from below, and increasingly positive as it approached it from above. This suggests that RF forcing of the electrons counteracted geomagnetic restriction of the electron collection below the gyrofrequency, but enhanced it above the gyrofrequency.

In order to verify this explanation, we have performed a model calculation of electron collection in the combined RF near-field and steady geomagnetic field in the neighbourhood of an antenna element, assumed to be an infinite cylinder perpendicular to the geomagnetic field. Our model includes effects of time-dependent sheath expansion following the start of RF pulses, and of time-dependent sheath collapse following their end.

0-7803-7846-6/03/$17.00 ©2003 IEEE 

## Array Analysis

**Co-Chairs:** R. Acosta
V. Erturk

1:15 Opening Remarks

78. 1 1:20 Analysis and Computation of the Radiation and Mutual Coupling in Large Waveguides Slot Array ..... 386
*P. Mahachoklertwattana, The Ohio State University, USA, D. H. Kwon, Samsung Advanced Institute of Technology, Korea, P. H. Pathak, The Ohio State University, USA*

78. 2 1:40 A DFT Based Accelerated Generalized Forward Backward Method for the Fast Analysis of Two Dimensional, Large Printed Arrays with Arbitrarily Shaped E ..... 387
*V. B. Erturk, Bilkent University, O. Aydin Civi, Middle East Technical University, Turkey, H. Chou, Yuan Ze University, Taiwan*

78. 3 2:00 COMPUTER SIMULATION of PHASED ARRAY ANTENNA PERFORMANCE DEGRADATION AT WIDE SCAN ANGLES ..... 388
*S. K. Johnson, R. Reinhart, R. J. Acosta, NASA Glenn Research Center, USA*

78. 4 2:20 Analysis of Finite Arrays of Circumferentially Oriented Printed Dipoles on Electrically Large Cylinders ..... 389
*B. Guner, V. B. Erturk, Bilkent University, Turkey*

78. 5 2:40 Modeling of a Large Slotted Waveguide Phased Array using the FDTD and Characteristic Basis Function (CBF) Approaches ..... 390
*T. Su, L. Ma, N. Farahat, R. Mittra, Pennsylvania State University, USA*

78. 6 3:00 Genetic Algorithm Radiation Pattern Optimization of Microstrip Patch Antenna Arrays Conformal To the Surfaces of Circular Cylinders ..... 391
*R. Allard, D. Werner, Applied Research Laboratory, The Pennsylvania Stat, USA*

78. 7 3:20 Multimode Equivalent Network for the Analysis of a Radome Covered Finite Array of Open-ended Waveguides ..... 392
*A. Neto, R. Bolt, G. Gerini, TNO-Physics and Electronics Laboratory (TNO-FEL), D. Schmitt, European Space and Technology Centre (ESTEC), Netherlands*

# Analysis and Computation of the Radiation and Mutual Coupling in Large Waveguides Slot Arrays

*P. Mahachoklertwattana[1], D.H. Kwon[2], and P. H. Pathak[3]

[1,3]The Ohio State University, Electroscience Laboratory,
1320 Kinnear Road, Columbus, OH, 43212
[2]Samsung Advanced Institute of Technology,
P.O.Box 111, Suwon, 440-600, South Korea
[1]mahachop@ee.eng.ohio-state.edu, [2]kwon22@samsung.com, [3]pathak.2@osu.edu

Because of their high power capabilities and simple geometrical configuration, rectangular waveguide slot antenna arrays have found relatively broad applications such as in radar and communication systems. There has been an extensive study on the design and analysis methods for a single waveguide slot in a waveguide, as well as on waveguide coupling of a radiating slot to a feeding slot, etc. Among them, the integral equation method using method of moments (MoM) technique has been found to be well-suited for these kinds of problems. However, in the calculation of the MoM operator matrix, the evaluation of internal and external admittance terms involving certain integrals must be done carefully, since one can experience numerical difficulties due to the singularities present in the integrands.

In this study, the method of moments (MoM) has been employed for the analysis of resonant and traveling wave slot antenna array problems involving thousands of slots. The above mentioned numerical difficulties arise in these more complex array type problems as well. Therefore useful, efficient and robust algorithms are developed in this study for the evaluation of all the important internal and external self admittance terms, which correspond primarily to the diagonal elements in the MoM operator matrix. In particular, a hybrid modified ray-mode representation of the dyadic modal waveguide Green's functions is developed for the evaluation of the internal self-admittance terms which can make the summation of modal series within the integrals for the MoM operator matrix converge more rapidly. This approach is an extension of the technique utilized in the MoM analysis of infinite periodic structures and is an extension of the work in [1]. Other approaches for dealing with the convergence problems have also been presented elsewhere for single slots, e.g. [2]. The present MoM method is employed to calculate the radiation patterns of numerous broadwall slot antenna arrays, i.e., both resonant and nonresonant waveguide slot antenna arrays using either offset or inclined slots. The patterns thus computed via MoM account for the array mutual coupling. Numerical results are presented to indicate the utility of the method developed here. In conclusion, the purpose of this work is to arrive at robust numerical procedures to deal with a large number of slots in a rectangular waveguide array that is useful in practical applications, such as those involving a large number of stacked waveguides with each guide containing a large number of slots.

## References

[1] S. Singh, W. F. Richards, J. R. Zinecker, and D. R. Wilton. Accelerating the convergence of series representing the free space periodic Green's function. *IEEE Trans. Antennas Propagat.*, 38:1958–1962, December 1990.

[2] S. R. Rengarajan and G. M. Shaw. Accurate characterization of coupling junctions in waveguide-fed planar slot arrays. *IEEE Trans. Antennas Propagat.*, 42:2239–2248, December 1994.

0-7803-7846-6/03/$17.00 ©2003 IEEE

# A DFT Based Accelerated Generalized Forward Backward Method for the Fast Analysis of Two Dimensional, Large Printed Arrays with Arbitrarily Shaped Elements

V. B. Ertürk[1], Özlem Aydın Çivi[2], Hsi-Tseng Chou[3]
[1]Dept. of Electrical and Electronics Engineering, Bilkent University, TR-06533, Bilkent, Ankara, Turkey e-mail: vakur@ee.bilkent.edu.tr, Tel:++90-312-290 3154
[2]Dept. of Electrical and Electronics Engineering, Middle East Technical University, Ankara, Turkey
[3]Dept. of Electrical Engineering, Yuan Ze University 135 Yuan-Tung Rd., Chung-Li 320, Taiwan

Fast and accurate analysis of electromagnetic radiation/scattering from large, planar, printed arrays over grounded dielectric slabs is of interest to researchers due to their highly flexible commercial as well as military applications. However, majority of these methods suffer greatly from storage requirements and computing time if the analyzed arrays are electrically large.

In this paper, various planar arrays consisting of finite number of printed, arbitrarily shaped patches over grounded dielectric slabs are investigated using a generalized forward backward (GFB) method. Previously, GFB method has been applied to rough surface scattering (M. Pino *et. al.*, *IEEE Trans. Antennas and Propagat.*, **6**, 961-968, 1999). In this method the conventional forward-backward (FB) approach is combined with the Method of Moments (MoM), where only a single arbitrarily shaped patch is solved using a conventional MoM procedure. The solution is then found through an iterative procedure which resembles to the FB method in general concepts, though it exhibits some significant differences. In the FB method, the current computation is swept cell by cell (each cell corresponds to a basis function) whereas, the GFB method sweeps the current computation element by element (each element corresponds to an arbitrarily shaped patch). A simple MoM procedure with few unknowns is employed to obtain the forward current and its backward correction on the selected element. Consequently, sophisticated shaped array elements can be treated accurately. A similar approach was reported previously (H. T. Chou and H. K. Ho, *IEEE AP-S Int. Symp. and USNC/URSI Meeting*, 40, 2001) for linear arrays of elements with arbitrary cross-sections. In this paper, this work is extended to planar arrays.

The computational complexity of this method, which is originally $O(N^2)$ for each iteration, can be reduced to $O(N)$ ($N$ being the number of array elements), assuming that elements are identical and periodic. This is achieved using a DFT based acceleration algorithm which divides the contributing elements into "strong" and "weak" interaction groups for a receiving element in the GFB method. The contributions from the strong group are obtained by conventional element-by-element computation to assure the fundamental accuracy. On the other hand, contributions coming from the weak region are obtained based on a DFT representation of the array current. In general, only a few significant DFT terms are sufficient to provide accurate results due to the fact that they provide minor corrections to the solution in contrast to the dominating strong group.

Various sized periodic arrays with arbitrarily shaped printed patches will be considered and results will be compared with the conventional MoM results to assess the accuracy of this method.

0-7803-7846-6/03/$17.00 ©2003 IEEE

# COMPUTER SIMULATION OF PHASED ARRAY ANTENNA PERFORMANCE DEGRADATION AT WIDE SCAN ANGLES

Sandra K. Johnson*, Richard C. Reinhart, Roberto J. Acosta
NASA Glenn Research Center, Cleveland, Ohio

***Abstract*** – Phased array antennas offer a number of advantages to NASA missions compared to traditional gimbaled reflectors including electronic and vibration free beam steering, graceful degradatrion, smaller volume and multibeams. However, the MMIC-based phased array antennas also present challenges to mission designers because of reduced power efficiency, higher costs, and system effects that result in link degradations. NASA Glenn Research Center (GRC) continues to pioneer aerospace communications technologies to address the challenges of array antennas to improve efficiency, reduce costs, and better understand system effects.

This abstract addresses the degenerative system effects between high-rate modulated data and signal timing delays caused by antenna beam steering at wide scan angles. Conventional phase shifters used in MMIC-based phased array antennas are physically limited to 360 degrees of phase shift. Often, depending on the size of the array or specified beam angle, the required phase shift may exceed 360 degree. In these instances, the actual phase shift obtained is the remainder of the phase request, modulo $2\pi$. The modulo $2\pi$ result causes a delayed carrier signal radiated from the element whose phase shifter requires a phase shift greater than 360 degree. Multiple delayed signals can radiate from the antenna depending on the size of the array and scan angle. For each modulo $2\pi$ wrap, the carrier is delayed one cycle time, resulting in intersymbol interference (ISI).

ISI can be simulated in Matlab/SIMULINK by placing M delay blocks in parallel with the input signal, with M being equal to the number of elements in the plane of the scanned signal being analyzed. The amount of delay configured for each delay block is equal to the number of modulo $2\pi$ wraps that the element would experience at the angle being analyzed, multiplied by the ratio of the data rate to the carrier frequency. This simulates the ISI in the baseband system. The baseband representation of the system in SIMULINK is necessary to reduce computation time. The results of a range of ratios for an 11-element linear array scanned 60 degrees is shown in Figure 1. These results show that at the limit of data rate to carrier frequency ratio of 1/10, there would be a 3.25 dB loss due to ISI for a small array. Measurements are ongoing to determine if the actual system loss is the same as predicted.

0-7803-7846-6/03/$17.00 ©2003 IEEE

# Analysis of Finite Arrays of Circumferentially Oriented Printed Dipoles on Electrically Large Cylinders

B. Güner, V. B. Ertürk*
Dept. of Electrical and Electronics Engineering
Bilkent University, TR-06533, Bilkent, Ankara, Turkey
E-mail: vakur@ee.bilkent.edu.tr, Tel: ++90 312 209 3154

The design and analysis of conformal arrays of printed antennas is of interest in applications ranging from satellite and wireless communications (mobile phone base stations, space division multiple access (SDMA) applications, etc) to military systems (flush-mounted antennas for aircraft and missiles). In these applications, conformality is required either for aerodynamic reasons or to reduce the array's radar cross section. However, the lack of adequate design and analysis tools, in particular for electrically large arrays, is a problem that remains to be solved for conformal printed antenna arrays.

In this paper, several arrays consisting of finite number of circumferentially oriented printed dipoles on electrically large, dielectric coated, circular cylinders are investigated using a hybrid method of moments (MoM)/Green's function technique in the spatial domain. This method is basically an "element by element" approach in which the mutual coupling between dipoles through space wave as well as the surface wave is incorporated. The efficiency of the method comes from the computation of the Green's function, where three types of spatial domain Green's function representations are used interchangeably, based on their computational efficiency and regions where they remain accurate. These representations are (*a*) a steepest descent path (SDP) representation, which is valid everywhere except along the paraxial region and electrically small separations between the source and observation points, (*b*) an asymptotic-based, spatial domain representation which is valid along the paraxial region and complements the SDP representation, and (*c*) an efficient integral representation of the of the planar microstrip dyadic Green's function for the evaluation of self-terms.

Previously, axially oriented printed dipole arrays on electrically large dielectric coated circular cylinders have been investigated, and some of their interesting features have been observed and reported (V. B. Ertürk, K. W. Lee and R. G. Rojas, *IEEE AP-S Int. Symp. and USNC/URSI Meeting*, 23, 2002). However, a full wave analysis for the circumferentially oriented printed dipole arrays has not been reported yet. Therefore, in this paper, our goals are; (*i*) to perform a full wave analysis of large phased arrays of circumferentially oriented printed dipoles on large coated cylinders, and (*ii*) to compare their performances (in the form of current distributions, active reflection coefficient, etc) with axially oriented printed dipoles on the same cylinders, as well as, arrays of printed dipoles on grounded planar slabs.

Several numerical examples, in the form of mutual coupling between two printed dipoles and array current distributions for relatively large arrays, as well as, basic performance metrics for these arrays will be presented. These performance metrics will also be compared with axially oriented printed dipole arrays on similar coated cylinders and printed dipole arrays on grounded planar substrates. Certain similarities and discrepancies will be discussed.

0-7803-7846-6/03/$17.00 ©2003 IEEE

# Modeling of a Large Slotted Waveguide Phased Array Using the FDTD and Characteristic Basis Function (CBF) Approaches

Tao Su*, Laiching Ma, Nadar Farahat and Raj Mittra
EMC Lab, 319 EE East
Pennsylvania State University
e-mail: mittra@engr.psu.edu

Stacked narrow-wall-slotted waveguide phased arrays find widespread use in practice. Modeling these arrays to determine their aperture field distribution is an important part of the design process, not only for predicting their radiation characteristics, but also for estimating the co-site interference problems when the array operates in a complex environment. To compute the aperture field of the slotted waveguide array, we propose to employ the Finite Difference Time Domain (FDTD). However, since the array we are configuration modeling is very large — comprising of more than 8000 elements — it is impossible to simulate even a single row of the array with the FDTD, let alone the compute complete one. Hence, to render the problem manageable we divide it into small sections, find the equivalent circuit model for each section, and finally combine them to solve a circuit problem. The aperture field over each slot is then computed, using the port voltages and currents, in the characteristics basis function formulation (CBF). (1) The use of the CBF method (CBFM) enables one to significantly reduce the number of unknowns, and this render the problem manageable. The details on CBFM, and the procedure for constructing these functions can be found in [V.V.S.Prakash and R.Mittra, Microwave and Optical Technology Letters, Jan. 2003; R. Mittra, Proceedings of IASTED International Conference, Wireless and Optical Communications, July 17-19, 2002, pp. 1-5, Banff, Canada].

In order to taper the aperture field distribution along both dimensions of the array, the feed couplers exciting each of the waveguides as well as the tilt angles of each slot are chosen to be different V.V.S. Prakash, *et al.,* IETE Technical Review, 16, 57-61, 1999]. Hence, we cannot apply the unit cell approach, typically employed to reduce the problem size in large arrays to a manageable size. Instead, we treat each coupler as a four-port network, and compute the coupling coefficients by using the FDTD. Rather them simulating each and every coupler — which will make the process extremely time-consuming — we only perform the simulation for a few selected ones, and use interpolation to determine the couplir.g coefficients for the rest. The same strategy is applied to obtain the circuit parameters of the slots whose number exceeds 8,000. To derive its parameters, we view the slot as a two-port network, which can be represented by an ABCD matrix. To account for the mutual coupling effects, we also include several neighboring slots in the simulation so that we can determine the 'active' circuit parameters for the center element. When the circuit parameters are determined for all the slots and couplers, the port voltage and currents can be calculated by solving the equivalent circuit problem.

To obtain the aperture field distribution above a single slot, we assume that it is a combination of two characteristic basis functions, corresponding to the two traveling waves inside the waveguide. These functions are extracted by solving a set of linear equations once the circuit parameters have been determined. The actual aperture field is represented as a combination of the two basis functions, weighted by the strength of the incident wave. The interpolation of the basis functions as functions of the slot angle is more complicated than that of the circuit parameters. We begin by smoothing the aperture distribution with a low pass filter, while making sure that the far field pattern is unaffected. The reduced sampling rate is approximately 4 samples per wavelength and can be interpolated very easily. This method is valid because, in our application, the scatterers are located sufficiently far from the antenna such that it is in the far field of the sub-array even though it is in the near field region of the entire array.

Extensive numerical results will be presented in the paper to illustrate the application of the method described above.

0-7803-7846-6/03/$17.00 ©2003 IEEE 

# Genetic Algorithm Radiation Pattern Optimization of Microstrip Patch Antenna Arrays Conformal to the Surfaces of Circular Cylinders

R. J. Allard* and D. H. Werner
Applied Research Laboratory
The Pennsylvania State University
P.O. Box 30
State College, PA 16804
rja5@psu.edu and dhw@psu.edu

A Genetic Algorithm (GA) radiation pattern synthesis technique for linear arrays of microstrip antenna elements mounted axially along a PEC circular cylinder was recently introduced in (R.J. Allard, D.H. Werner, and P.L. Werner, *2001 IEEE Antennas and Propagation Society International Symposium,* **2**, 366 - 369, 2001). An extension of this GA radiation pattern synthesis procedure is presented here that is capable of evolving the optimal set of excitation magnitudes and/or phases for the elements of one- or two-dimensional microstrip patch antenna arrays conformal to the surfaces of dielectric-coated PEC circular cylinders. The goals of the optimization include the ability to achieve a desired beam-steering capability as well as to meet specified beamwidth and sidelobe level requirements. A variety of optimization schemes will be considered, including those based on synthesizing an ideal cosine pattern, a Gaussian pattern, or a sector pattern. It will also be shown that a point-by-point weighting function may be defined over critical regions of the radiation pattern in order to improve the convergence properties of the GA. The total fitness of a GA population member in this case is defined to be the combined squared difference between the desired array patterns and the actual array patterns.

This paper presents examples of optimizations performed using this GA procedure for several different one- and two-dimensional conformal microstrip antenna arrays mounted on dielectric-coated PEC circular cylinders. The advantages and disadvantages of using each of the available objective functions for the synthesis of specific classes of radiation patterns are investigated, as well as the possible benefits of optimization scenarios for arrays that employ magnitude-only, phase-only, or both magnitude and phase excitation. In addition to this, an efficient algorithm for use in conjunction with GA optimization procedures will be presented for calculating the gain associated with cylindrically-mounted arrays of arbitrarily shaped microstrip antennas. This algorithm is based on the domain-decomposition/reciprocity technique previously presented in (R.J. Allard, D.H. Werner, and J.S. Zmyslo, *2000 IEEE Antennas and Propagation Society International Symposium,* **1**, 2 – 5, 2000). Some examples where the gain characteristics of cylindrically mounted microstrip antenna arrays are optimized directly will also be presented and discussed.

0-7803-7846-6/03/$17.00 ©2003 IEEE

# MULTIMODE EQUIVALENT NETWORK FOR THE ANALYSIS OF A RADOME COVERED FINITE ARRAY OF OPEN ENDED WAVEGUIDES

**A. Neto[(1)], R. Bolt[(1)], G. Gerini[(1)], D. Schmitt[(2)]**

*[(1)] TNO-Physics and Electronics Laboratory (TNO-FEL), P.O. Box 96864, 2509 JG The Hague, The Netherlands*

*[(2)] European Space and Technology Centre (ESTEC) , P.O. Box 299, 2200 AG Noordwijk, The Netherlands*

The effects of the finiteness of an antenna platform plays an important role in phased array applications as well as the radome coverage of the actual antenna. When low side-lobes are required, this implies accurate modeling of mutual coupling and scattering effects in the feed. In this contribution we present a theoretical model for the analysis of finite arrays of open-ended waveguides on top of finite cylindrical supporting structures and/or radome coverages. This model is based on a Multi-mode Equivalent Network (MEN) (G. Gerini, M. Guglielmi, G. Lastoria, *IEEE MTT-S Digest,* vol.3, 1747-1750, 1998) representation of the radiating waveguides with their tuning elements and a high frequency approach for the external region.

The accessible ports given by the multi-mode network connecting the antenna and feeding waveguides offers the possibility of optimizing the structure looking both at the antenna's radiation characteristics and the matching network inside the waveguides. The effect of the truncated ground plane is derived using a UTD approach (Kouyoumjian, R. G., and P. H. Pathak, *Proc. IEEE* ,62, no.11, 1974, 1448-1461), (Kouyoumjian, R. G., and P. H. Pathak, *Acoustic...and Low Frequency Asymptotics,* vol. II, Varadan and Varadan, Eds. Amsterdam, North Holland. 1986) where the applied ray tracing procedure turns out to be analytical. When also considering a radome coverage, a physical optics algorithm is included in the analysis to quantify the alteration of the multimode impedances.

The first step in the procedure consists in setting up an integral equation that enforces the continuity of the tangential magnetic field on the apertures composing the array. In the waveguide regions, the field is expressed as a superposition of TE and TM modes which can be divided in accessible and non-accessible ones (see ref. MEN). The magnetic current in the apertures can then be conveniently expanded in terms of a set of unknown vector functions weighted by the modal current amplitudes of the accessible modes. We are then left with a set of integral equations where the unknowns are magnetic currents that can be found for each mode assumed to be exciting the structure. Once this set of integral equations is solved with a standard Method of Moments approach, the final multi-mode equivalent network representation can be easily derived by recalling the modal voltage definition based on the orthonormality property of the modes. The magnetic field Green's function used in the integral equations is that of a finite grounded metallic cylinder, that can also operate in the presence of a radome. This Green's function can be expressed as a superposition of the grounded half space Green's function and two separate contributions, one that accounts for the truncation of the ground plane and one that accounts for the radome reflections. The procedure is similar to the one described in (A.Neto, D. Pasqualini, A. Toccafondi, S. Maci, *IEEE Trans. Antennas and Propagat.,* vol.47, no.10, Oct. 1999) for quantifying the impact on the input impedance of slot elements, due to the reflections inside an elliptical dielectric lens antenna. Detailed analysis of the reults and numerical issues will be addressed during the presentation.

0-7803-7846-6/03/$17.00 ©2003 IEEE

***Special Session***

**In Honor of Chalmers Butler**

**Organizer(s):** Robert Nevels, Texas A&M University
**Co-Chairs:** R. Nevels
D. Wilton

7:55 Opening Remarks

# Evaluation Of Singular And Near-Singular Potential Integrals

*Donald R. Wilton*, Michael Amin Khayat*
Department of Electrical and Computer Engineering
University of Houston, Houston, TX 77204-4005
wilton@uh.edu, michael.khayat@mail.uh.edu

The integral equations of electromagnetics often involve singular potential integrals that require special numerical considerations for their evaluation. Unbounded (but integrable) singularities usually occur, for example, in the kernels of so-called self-terms in the method of moments whenever testing and source subdomains coincide. Often no numerical quadrature rules exist for directly handling these singularities. In such situations, the *singularity subtraction* or *singularity cancellation methods* are often used. In the *singularity subtraction* approach, terms having the same asymptotic behavior as the integrand at the singularity are first removed from the integrand, resulting in a bounded difference integrand that is integrated numerically. An analytically performed integration of the subtracted singular term is then added back to the numerically integrated terms to complete the potential evaluation. Despite widespread usage, however, the singularity subtraction method has a number of disadvantages: (1) The integrand's higher order derivatives remain unbounded and limit the convergence rate of the difference integral. (2) The analytical integration becomes increasingly involved as the complexity of bases, geometry, and Green's functions increase. (3) Object-oriented coding approaches are difficult to implement since each analytically-evaluated self term integral links the source subdomain, basis function, and the asymptotic form of the Green's function.

To extend the capabilities and accuracy of general-purpose codes, we have recently abandoned the subtraction method in favor of purely numerical quadrature schemes, which we report here. These schemes employ *singularity cancellation methods*. In contrast to the singularity subtraction method, the resulting integrand is analytic in the transformed variables and hence is amenable to integration by a Cartesian product of Gauss-Legendre rules. An example of the singularity cancellation method is the so-called Duffy method [M. G. Duffy, *SIAM J. Num. Anal.*, **19**, pp.1260-1262, 1982]. The Duffy method, however, has two major drawbacks: (1) It leaves an angular dependence about the singular point in the resulting integrand. (2) It does not work well when applied to *nearly-singular* integrals that occur when an observation point is *near* a source point.

In this presentation we present a purely numerical singularity cancellation method that not only removes the angular dependence about the singular point, but also is effective in computing nearly-singular integrals. We present both analysis and numerical results for wire, triangle, quadrilateral, brick, tetrahedral and prism subdomains.

0-7803-7846-6/03/$17.00 ©2003 IEEE 

# Efficient Generation of Method of Moments Matrices Using the Characteristic Function Method

Raj Mittra*, Junho Yeo and V.V.S. Prakash

Electromagnetic Communication Laboratory
The Pennsylvania State University
Department of Electrical Engineering
University Park, PA 16802
mittra@engr.psu.edu

In the conventional MoM using the sub-sectional basis functions, and a $\lambda/10$ or $\lambda/20$ discretization, the computation of the MoM impedance matrix elements consumes a considerable portion of the total solution time as the problem dimensions become large in terms of the wavelength, because the matrix generation requires $O(N^2)$ operations, where N is the number of unknowns. In this paper, we investigate the Degrees of Freedoms (DoFs) of the MoM matrix elements and show that they can be represented in terms of a very small number of Characteristic Functions. We then take advantage of this fact by generating the elements without having to perform the usual integration involving the basis, testing and Green's functions, except for a few entries that we computed directly. The results below, for a $2\lambda$ square plate as a case example, show that the matrix elements, current coefficients and the RCS all agree very well with the direct calculations, which, of course, are considerably more CPU intensive, both in terms of storage and time.

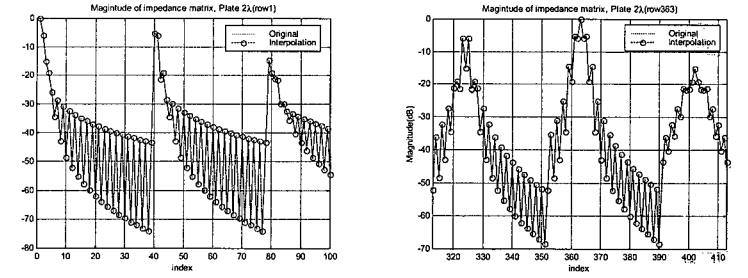


(a) (b)

Fig. 1. Comparison of magnitude of impedance matrix: (a) row 1; and (b) row 363.

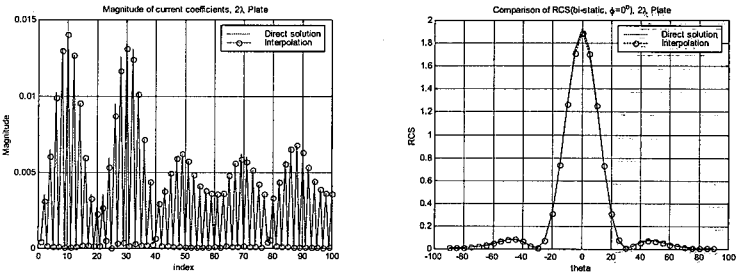


(a) (b)

Fig. 2. Comparison of current coefficients and radar cross section (RCS): (a) current coefficients; and (b) RCS.

0-7803-7846-6/03/$17.00 ©2003 IEEE

# Novel Method for the Analysis of an Antenna Attached to a Planar Surface of a Conducting Body

John C. Young
Holcombe Department of Electrical and Computer Engineering
331 Fluor Daniel EIB Building
Clemson University, Clemson, SC 29634-0915 USA

The traditional method to analyze an antenna attached to a conducting body involves the replacement of the conducting body surface and the wire surface with equivalent currents. An integral equation is then solved for these currents. Often, the current near the antenna-body junction varies rapidly. This is especially true in the case of a wire antenna mounted on a conducting body when symmetry is lacking. In a traditional integral equation/Method of Moment solution of the problem, special care must be exercised in modeling the current near the junction to ensure accurate calculation of matrix elements and continuity of current at the transition between the body and the antenna. One method that is often applied to these structures uses "attachment" modes to model the body current near the wire-body junction. Another method, proposed by Young and Butler (J.C. Young and C.M. Butler, Proceedings of the XXVIIth General Assembly of URSI, p. 1397, August, 2002) for antennas attached to planar surfaces of conducting bodies, applies the equivalence principle to define a surface that divides the original problem into two equivalent models. The two models are coupled together by matching tangential fields across the defined surface. The equivalent models are chosen so that the current on the planar surface of the body to which the antenna is attached does not need to be modeled. In effect, the modeling of the body current on the planar surface is replaced with the matching of tangential fields across a surface remote from the antenna where the fields vary less rapidly. Because the fields vary less rapidly on the chosen surface, one may use conventional Method of Moment techniques to compute matrix elements.

A review of the method of Young and Butler is offered, and a discussion of the equivalence principle as applied to this method is given to show that the method is exact. In addition, because the choice of "dividing" surface and equivalent currents for a particular structure is not unique, advantages and disadvantages of various surfaces and currents are explored. The method is specialized to that of a wire antenna attached to the planar surface of a conducting Body Of Revolution (BOR). In the context of BOR theory, equivalent currents on the various surfaces are expanded in Fourier series, and, boundary conditions are enforced for each Fourier mode. Computed and measured data of the input admittance of a straight-wire antenna mounted at various position on the planar cap of a conducting cylinder are presented. Good agreement is obtained between the measured and computed data. Even when the antenna is close to the edge of the planar surface, only a few Fourier modes are required for convergence of the input admittance.

0-7803-7846-6/03/$17.00 ©2003 IEEE

# Physical Optics for Bodies with Anisotropic Surface Impedance

Piergiorgio L. E. Uslenghi
Department of Electrical and Computer Engineering
University of Illinois at Chicago
851 South Morgan Street, Chicago, Illinois 60607-7053, USA
Email: uslenghi@uic.edu

The physical optics approximation is considered for bodies with an anisotropic surface impedance boundary condition. The far scattered field and the monostatic radar cross section are examined in detail for the case when the illuminated surface of the scatterer is symmetric with respect to a plane parallel to the direction of propagation of the incident wave, under certain symmetric behaviors of the surface anisotropy. Considerations are also developed for bistatic scattering. The analysis is based on the method of stationary phase (see, e.g., M.M. Tenenbaum, *Radiotekhnica i Elektronica*, vol. 5, no. 12, pp. 1909 ff., 1960), and represents a generalization of previously known results for the case of an isotropic surface impedance (see P.L.E. Uslenghi, *Alta Frequenza*, vol. 33, pp.541-546, 1964).

The presence of a nonzero surface impedance leads to a depolarization of the backscattered field whose magnitude is dependent on the surface impedance anisotropy. The anisotropy in the surface impedance may be realized by the use of composite materials (either as bulk materials or coating layers), or surface corrugations. The results obtained are applied to a variety of scattering shapes (both smooth and with edges) and surface anisotropies. The validity of the physical optics approximation for the case under study is checked by comparison with other analytical theories such as the geometrical theory of diffraction, as well as with numerical approaches. General conclusions are drawn on the limits in the applicability of physical optics to the general problem considered.

0-7803-7846-6/03/$17.00 ©2003 IEEE 

# Twenty-Five Years of Potential-Based Electromagnetics

W. A. Johnson*, D. B. Seidel, and D. G. Dudley[1]
Sandia National Laboratories, P.O. Box 5800, Albuquerque NM, 87185-1152 USA
[1]ECE Bldg. 104, University of Arizona, Tucson AZ, 85721 USA

In the academic year 1975-1976 Chalmers M. Butler visited the University of Arizona during a sabbatical and had a profound impact on the authors, who were in Arizona's electromagnetics group at that time. This paper takes a look back at the work ongoing at that time and traces Professor Butler's influence on the authors through the past 25 years in solving computational electromagnetics problems. Topics touched on include use of the potential solution to avoiding confusion on singularities in the electric dyadic Green's function, the problem of a grounding rod penetrating the air-earth interface, a horizontal wire above the air-earth interface, dual series techniques used to benchmark the accuracy of "Mississippi-style computational electromagnetics", sample problems run with Patch (a frequency domain code developed in the 1980's), and EIGER (an object oriented frequency domain electromagnetics code) .

Sandia is a multiprogram laboratory operated by Sandia Corporation, a Lockheed Martin Company for the United States Department of Energy under Contract No. DE-AC04-94A185000.

0-7803-7846-6/03/$17.00 ©2003 IEEE 

# A Hybrid Fast Capacitance Solver

Weng Cho Chew* and Lijun Jiang
Center for Computational Electromagnetics and Electromagnetics Laboratory
Dept. of ECE, University of Illinois at Urbana-Champaign, Urbana IL 61801
(w-chew@uiuc.edu)

In this paper, we discuss a hybrid fast capacitance solver that can be 4 to 30 times faster than using the traditional fast multipole algorithm. This speed up is achieved by drawing ideas from the Appel algorithm, Barnes-Hut algorithm, and the Rokhlin-Greengard multipole algorithm. The combined algorithm is much faster than the Rokhlin-Greengard algorithm as well as being error-controllable.

The Appel algorithm and the Barnes-Hut algorithm were originally written for the calculation of Coulombic forces governing the movement of stars in galaxies. Later Rokhlin and Greengard developed a systematic way to perform these calculations demonstrating that they are error controllable.

The central idea of Appel and Barnes-Hut algorithms was to expand the gravitational field in terms of the center of mass of a cluster of stars. In this manner, the gravitational field can be efficiently represented. This also follows from the physical fact that the gravitational field is a solution of Laplace's equation, and hence, it cannot convey information long range. Consequently, all gravitational fields eventually appear to be coming from a monopole or a single source if one is far enough from the cluster of stars. A monopole representation is an efficient representation of the far field of a cluster of sources.

Recently, Shi, Liu, Kakani, and Yu suggested using Appel algorithm to expedite fast capacitance solution (IEEE Trans. CAD ICS, March 2002). We present an alternate way of expediting FastCap (White) which is based on the Rokhlin-Greengard algorithm. Our algorithm makes a combined use of ideas from Rokhlin-Greengard, Appel, and Barnes-Hut algorithms. It retains the systematic nature of the Rokhlin-Greengard algorithm, but exploits some physics of Laplacian field as was done in the Appel and Barnes-Hut algorithms. In this manner, the algorithm is error controllable, but at the same time, is more efficient than a plain Rokhlin-Greengard algorithm.

0-7803-7846-6/03/$17.00 ©2003 IEEE

# The performance of the Extraction of Wideband Response from Early Time and Low frequency Data and Method to Find the Optimal Parameters

Mengtao Yuan, Tapan K Sarkar, Jinhwan Koh
Department of Electrical Engineering & Computer Science
121 Link Hall, Syracuse University
Syracuse, New York 13244-1240
Phone : 315-443-3775
Fax : 315-443-4441
Email : myuan@syr.edu , tksarkar@mailbox.syr.edu

Extrapolation of wideband response from early time and low frequency data is a good approach to reduce the computational loads for electromagnetic analysis. It has been accomplished by the use of the orthonormal Hermite, Laguerre or Bessel- Chebyshev polynomials. The fact that Fourier transforms of the presented polynomials are analytic functions allows us to work simultaneously with time and frequency domain data. However, the performance of this creative method is sensitive to two important parameters - the scaling factor *11* and the expansion order *N*. It's very significant to find the optimal parameters to achieve the best performance and put this method into practice. In this paper, how the parameters affect the performance of the extraction is carefully discussed. Then a method to find the useful range of the parameters and a numerical and hybrid procedure to search the optimal parameters are promoted. The computation load of this method is not large because we only deal with small matrix and DFT/IDFT of short series of data. The estimated parameters are quite accurate compared with the real optimal ones. In addition, the searching procedure is stable to guarantee a converged extrapolation and a best or near best performance. The searching procedure is automatic and easy to program and can be used in practice. The feasibility of the proposed method is validated by two scattering examples of conductiong or dielectric scatters. Finally the performances using three different polynomials vs. *N* at the optimal *11* are compared and reasons are explained.

0-7803-7846-6/03/$17.00 ©2003 IEEE 

# Application of Equivalence Principle in the Analysis of Buried Objects/Underground Power Transmission Cables

Xiao-Bang Xu
Holcombe Department of Electrical and Computer Engineering
Clemson University
Clemson, SC 29634-0915
Email: ecexu@eng.clemson.edu

One of the most important things I have learnt from Prof. Chalmers Butler, as his former graduate student and current colleague, is the understanding and application of equivalence principle in electromagnetics. In this paper, two examples are presented.

First, we present a hybrid integral equation formulation for determining the scattering from inhomogeneous cylinders buried below a planar interface separating two semi-infinite half-spaces of different electromagnetic properties. The inhomogeneous cylinders of general cross section are of infinite extent, and are illuminated by a plane wave excitation. The hybrid integral equations are formulated by employing both the surface equivalence principle and the volume equivalence theorem. In the formulation, attention is focused on minimizing the Sommerfeld-type integrals that are often encountered in the investigation of buried objects, and on reducing the number of unknowns. The Green's functions of all the volume integrals and part of the surface integrals involved are simply free-space Green's functions. Also, the hybrid integral equations formulated have less unknowns comparing to "pure" volume integral equation formulation.

Second, we present a two-step numerical technique for the investigation of magnetic fields produced by ELF sources enclosed by a ferromagnetic pipe. The first step is to employ the finite element method to solve the differential equations for the magnetic vector potential. From the solution of the magnetic vector potential, the electric and magnetic field can be computed. In particular, the fields on the outer surface of the pipe are obtained. Then, in the second step, employing the equivalence principle, a computational model equivalent to the exterior region is formulated. The equivalent currents can be determined directly from the electric and magnetic fields obtained in the first step. Based on knowledge of the equivalent currents, the magnetic field outside the pipe can be computed in a straightforward manner. To validate the two-step numerical technique, the numerical results of the magnetic field produced by an underground three-phase pipe-type cable are compared with existing measurement data. A good agreement is observed.

0-7803-7846-6/03/$17.00 ©2003 IEEE 

# Aperture Description of Coupling of a Microring Laser to a Fiber

Reyhan Baktur* and L. W. Pearson
Holcombe Department of Electrical and Computer Engineering
J. M. Ballato, School of Material Science
Clemson University
Clemson, SC 29634-0915
grehang@clemson.edu
pearson@ces.clemson.edu

Recently, microring lasers have been formed from optically active polymers formed into a circular band, using an optical fiber as mandrel (see figure at right) [Frolov, *et. al.*, *Appl. Phys. Lett.*, 72(22), pp. 2811-2813]. Gregory has observed that light delivered into the fiber can pump the microring laser [R. V. Gregory, Private Communication]. Indeed, the Frolov paper suggests the possibility of coupling into the fiber by way of evanescent tunneling. Gregory's observation is simply that of the reciprocal path. We note that a gold barrier is present between the band and the fiber.

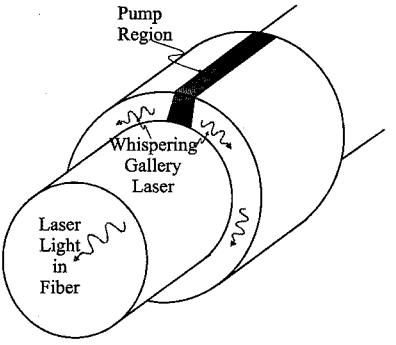


This paper presents a quantitative description of the coupling of electromagnetic energy from the laser into the fiber by way of evanescent tunneling. This description can be deduced from consideration of the field over two aperture planes defined by the end faces of the circular band and penetrating into the fiber. The field of these whispering gallery waves can be described in the band and specifically on the aperture planes defined just at the edges, which are adjacent to the monomode fiber. Thus, equivalent sources on the aperture faces are capable of exciting the fiber mode through the mechanism of evanescent tunneling.

The coupling across the apertures is necessarily weak, else energy would be taken from the laser so quickly that lasing would be quenched. Consequently, it is adequate to view the aperture sources as unperturbed by the loading of the fiber. With in constrains of the weak coupling requirement, one can employ the aperture description to deduce means of optimizing the coupling of light leaking from the edges of the laser into the fiber.

A proposed application of microring laser is as pump sources on erbium-doped fiber amplifiers. A distribution of the rings along the fibers would accommodate pumping in a geometrically simple fashion.

We discuss the aperture model for this structure and our current understanding of means for optimization of the laser/fiber coupling.

*a.k.a. Rehanguli Gayiti

0-7803-7846-6/03/$17.00 ©2003 IEEE 

## Square Kilometer Array

**Co-Chairs:** D. Bock
S. Dougherty

7:55 Opening Remarks

## LOFAR, the Low Frequency Array

Colin J. Lonsdale
MIT Haystack Observatory

The Low Frequency Array (LOFAR) is being designed by a three-partner consortium (ASTRON in the Netherlands, MIT, and the Naval Research Lab) to open up the 10-240 MHz spectral window to high resolution and high sensitivity study. The array is scheduled for initial operations in 2006, with full capability by 2008. Consisting of roughly 100 phased array stations spanning 400km, and targeting an imaging dynamic range of up to $10^6$, LOFAR is in many important ways a precursor of and prototype for SKA technologies and techniques. Of particular note are requirements for methods of solving for time-variable station beam shapes, atmospheric and ionospheric phase delays that are a function of position within the field of view, and signals from strong sources and RFI entering through station sidelobes. Other important considerations include high bandwidth connectivity of a geographically distributed array, criteria for siting of such an array, and approaches for cost-effective maintenance and operation in a situation where much of the equipment is located in a large number of remote sites.

During the design phase of LOFAR, these issues, along with many others specific to the galactic background limited, RFI-contaminated low frequency regime, have been carefully considered, and design choices have been made. In this presentation, the overall design of LOFAR is described, paying particular attention to problems shared by SKA, whose solutions for the LOFAR project may be relevant for SKA. It will be shown how the development of comparatively modest next-generation radio astronomical arrays like ATA and LOFAR can reduce the cost and risk associated with the designing and building of major instruments like SKA.

0-7803-7846-6/03/$17.00 ©2003 IEEE 

# Scientific Goals of The Large Adaptive Reflector (LAR)

P. E. Dewdney* and S. M. Dougherty
National Research Council of Canada

Radio astronomy continues to be an important contributor to the overall growth of astronomical knowledge. Moreover, radio telescopes can be designed with extraordinary capabilities – large imaging fields-of-view, polarization measurement, and high spatial and spectral resolutions. Using recent technologies, all of these attributes can be achieved simultaneously. This is balanced by the general weakness of the flux to be detected, and the need to build very sensitive telescopes to detect emission from sources at distances comparable to the largest scales in the Universe.

The next-generation radio telescope, the Square Kilometer Array (SKA), will have a hundred times more collecting area than our most powerful existing radio telescopes. This telescope will be required to meet the scientific challenges presented by the desire to observe the early stages of the evolution of the Universe. Cost effective, new antenna technology is needed to build such a large collecting area. The Large Adaptive Reflector (LAR) is a new concept in antenna design being developed to address this challenge. The LAR is a long focal-length parabolic reflector that requires an air-borne platform to support the focal receiver. A very large, nearly flat active reflecting surface brings incoming radiation to a focus on the airborne platform. The long focal length permits the reflector to present a very flat profile and therefore the reflector, made up of adjustable panel segments, does not need to be mechanically tilted as in traditional designs. This concept offers the possibility of an order-of-magnitude reduction in the cost per $m^2$ of collecting area for very large antennas.

A prototype telescope is needed to prove the concept under operational conditions. This presentation will outline the specifications envisaged for such a prototype and explore its scientific potential. The prototype will be a 300-m diameter reflector, with an upper frequency of about 2 GHz, an instantaneous bandwidth of 750 MHz, and a wide-field feed (a cluster of ~300 beams on the sky). The reflector will be an offset design, steerable to an Elevation Angle of 30°, and yielding a beam with very low side-lobes, minimal scattering, and high antenna efficiency. Its flux sensitivity will be ~50 $\mu Jy/s^{0.5}$ using room temperature receivers ($T_{rcvr}$ = 18 K; $T_{sys}$ = 30 K); in a 100 kHz line-channel, this corresponds to ~4 $mJy/s^{0.5}$.

Such high sensitivity, combined with the surveying speed enabled by the multi-beam feed, will enable rapid surveys of red-shifted gas, most particularly hydrogen, over a large volume of the Universe. For example, it is expected that this telescope will map, in emission, the small neutral fraction of neutral gas that can now only be detected by Ly$\alpha$ optical absorption. Additionally, this telescope will have an enormous impact on pulsar research.

0-7803-7846-6/03/$17.00 ©2003 IEEE

# Radiation Properties of a Large Faceted Reflector Antenna

Bruce Veidt* and Peter Dewdney
National Research Council of Canada
Box 248
Penticton, British Columbia, V2A 6J9 Canada

A new design for a reflector antenna has been proposed called the Large Adaptive Reflector. This antenna will have a diameter of ~200 metres with a focal length of 500 metres. The primary reflector will consist of reflecting panels supported off the ground by vertical actuators, and the receiver will be supported by a special stabilized airborne platform. The antenna will be steered by moving the receiver and adjusting the shape of the reflector surface to the appropriate section of a paraboloid. This antenna is in general an offset reflector antenna. Because of the long focal length of this antenna, it will be possible to construct reflector panels with a flat (or nearly flat) surface. The radiation properties of this unique faceted reflector antenna have been examined and will be reported in this paper.

Our analysis was based on the Convolution Theorem which allowed us to separate the effects of the radiation pattern of individual panels from the pattern of an assemblage of panels. This greatly reduced the computational complexity of our analysis.

The first part of our analysis was to calculate the reduction in efficiency due to the phase errors resulting from the flat panels. These simulations have shown that flat panels can indeed be used. Operation up to 22 GHz with 80% efficiency is possible with panels as large as 4 metres in diameter. If the panels are constructed with a slight parabolic sag, the diameter can be increased to 5 metres. This amount of sag is ~3 millimetres for a 5 metre panel and the focal length of the panel is the same as for the entire reflector. This is a significant improvement since it would reduce the number of panels and actuators from 2500 to 1600 per antenna.

The second part of our analysis was to consider the radiation pattern of the faceted reflector. We found that the grating response due to the repeating pattern of panels will be suppressed by nulls in the radiation pattern of the individual panels. However, this effect will be compromised if panel size is less than panel spacing, which would reduce the spacing between the nulls of the panel radiation pattern so that they no longer coïncide with the grating responses. This difference in sizes could result from gaps between the panels or if the surface currents are attenuated near the edge of the panels (as will be the case at long wavelengths), reducing the effective size of the panels.

0-7803-7846-6/03/$17.00 ©2003 IEEE 

# Design and Performance of the Tethered Aerostat Subsystem of the Large Adaptive Reflector (LAR)

**M. Nahon[1], D. Chalmers[2] and P. Dewdney[2]**

The proposed Canadian design for the Square Kilometer Array consists of an array of very large antennas, each similar in size to Arecibo. The antenna design, known as the Large Adaptive Reflector (LAR), consists of a ground-supported adaptive parabolic reflector and a receiver suspended in the air by a multi-tethered aerostat, at the focus of the reflector. The location of the receiver can be actively controlled, through 360° of azimuth angle and down to a 60° zenith angle, by winches at the base of the tethers.

In order for the antenna to meet its functional requirements, the receiver must meet certain motion criteria (position, speed), even in the presence of significant wind and turbulence. This is a challenging task, given that the tethers are on the order of 1 km long. Work has been ongoing for the past few years to evaluate the feasibility of the multi-tethered aerostat concept for this task, and this paper describes that investigation. Our initial efforts centered on a computer simulation of this system (which includes the aerostat, tethers and winches) to predict its behavior and which could be used for design tradeoff studies. With encouraging simulation results we undertook the design and construction of a one-third scale proof-of-concept prototype. This scaled system is itself of imposing dimension---it has a footprint of about one half square kilometer.

In the design of the scaled system, Buckingham's Pi theorem was used to identify the relevant non-dimensional parameters, which governed the system's behavior. The scaled system components were then chosen to maintain similarity of these parameters with the full-scale system. Construction of the prototype began in the spring of 2001 and it is now operational, albeit without closed-loop winch control. A number of flights have been made with the open-loop system aimed at quantifying the system's natural motion in response to various wind speeds and turbulence. One key benefit of these flights has been the operational experience gained from them. The computer-controlled winches that will be used to control the system are presently undergoing tests and will be installed in the spring of 2003.

This paper will present some of our measured results from the prototype, as well as similar data from the simulation. It will also discuss our plans for future enhancements of the system to further improve its performance.

[1] Department of Mechanical Engineering, McGill University, Montreal, Canada
[2] National Research Council of Canada, Penticton, Canada

0-7803-7846-6/03/$17.00 ©2003 IEEE

# The Allen Telescope Array as Prototype for the SKA

David R. DeBoer, SETI Institute

The Allen Telescope Array (ATA) is a joint project of the SETI Institute (Mountain View, CA) and the University of California at Berkeley's Radio Astronomy Lab to build a world-class radio telescope facility composed of 350 6.1-meter offset Gregorian antennas. This array incorporates many novel components that allow a high degree of performance and flexibility. The use of commercial-off-the-shelf components where possible, and exploitation of the many new technologies for wide-band applications and manufacturing allow for a very high-performance/cost-effective array to be built. Extensions of these techniques will be required to successfully realize the Square Kilometer Array (SKA).

Some of the particular technologies that we feel are viable candidates for SKA development are: the use of hydroformed, rim-supported dishes; the use of compact drive systems and structural, cast/machined housings; the wide-band, cryogenic log-periodic feed; wide-band low-noise amplifiers; wide-band analog fiber-optic links; a flexible, compact and simple RF/IF signal chain and digital processor; the FX correlator; a robust, component-based software system with TCP/IP connectivity utilizing JAVA.

The ATA will consist of 350 6.1-meter offset Gregorian dishes at the Hat Creek Radio Observatory site arrayed over approximately 1 square kilometer. Given the number of antennas, the large size of the primary beam and the novel signal path implementation, this array will have an unprecedented degree of observing flexibility and excellent sensitivity. A hierarchical assortment of individual users may simultaneously use the array to observe a different part of the sky at independent frequencies and concurrently image the sky at one or more frequencies. Testing is currently underway on the first three elements of the ATA (Figure 1).

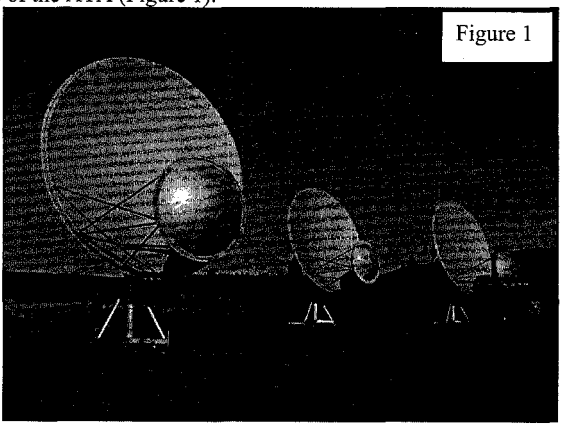

Figure 1

0-7803-7846-6/03/$17.00 ©2003 IEEE

# ATA Optics and Feed

Wm. J. Welch & Greg Engargiola
Radio Astronomy Laboratory
University of California
Berkeley CA 94720

January 21, 2003

**Abstract**

The final design for the reflector optics and feed for the Allen Telescope Array have been selected, and prototype models have been constructed and tested. The frequency coverage of the system is 0.5 - 11.5 GHz, and the feed is a dual linearly polarized log-periodic zig-zag antenna to achieve that bandwidth. The mirror system is an off-set Gregorian with a metal shroud half surrounding the feed between the primary and secondary. The primary is 6.1m and the secondary 2.4m. Spillover to the ground is very small in this design. The low cost of this small antenna matches the receiver cost reasonably well for best economy. Measurements show the feed match to be no worse than -16db at any frequency, and its cross polarization is about -25db. There is no evidence of the sharp drop-outs in transmission at certain frequencies that sometimes plagues log periodic antennas. The principal novel feature of this feed design is that there is a metal pyramid within the feed that provides space for the low noise wide-band amplifier of the system. The balanced feed output is coupled to the LNA through a wide-band tapered microstrip balun. The small primary provides a large field of view. The array is planned to be 350 elements for a total geometric collecting area of 10,000 square meters. At the Hat Creek Observatory, it will be used for both SETI and conventional astronomy. The element is also a possible prototype for the future Square Kilometer Array.

0-7803-7846-6/03/$17.00 ©2003 IEEE 

# Issues for Studies of Radio Transients with the Square Kilometer Array

James M. Cordes
Cornell University

The Square Kilometer Array (SKA) is conceived as the next generation radio telescope for discovery and analysis of the radio universe. A large volume of observational phase space that is only cursorily characterized so far but which will be opened up by the SKA concerns radio transients. Compared to surveys at high energies, the radio transient sky is very poorly known. To unveil the transient radio sky requires specific capabilities of the SKA that influence its design.

Transient sources are expected on all scales, ranging from solar system to Galactic to cosmological. Known radio objects show variations and bursts on time scales ranging from nanoseconds to years. It is almost certain that new classes of sources will be discovered with the SKA. I will discuss the kinds of signals expected, taking into account the differences between coherent and incoherent signals and intrinsic versus extrinsic causes of variability.

Giant pulses from objects such as the Crab pulsar provide one prototype for detection of fast transients on sub-milliscond time scales. I will discuss some of the phenomenology of giant pulses and an attempt (with M. McLaughlin) at detecting giant pulses from pulsars in M33. Radio frequency interference currently limits our ability to detect such extragalactic pulses. I will discuss potential remedies for contamination by RFI involving multibeam and multistation observations. SKA specifications and operating modes for transient surveys will be summarized.

0-7803-7846-6/03/$17.00 ©2003 IEEE 

**Wideband Array Receivers**

*Sander Weinreb and Niklas Wadefalk

California Institute of Technology, Pasadena, CA, 91125

Until recently, almost all receivers in radio astronomy have been limited by both antenna feeds and low-noise amplifiers to bandwidths less than 50% of the center frequency. New developments in log-periodic feeds (G. Engargiola *Proc. IEEE APS/URSI Symp. San Antonio*, 2002) and low noise amplifiers (S. Weinreb, *IEEE MTT Symp. Dig*, 1999) have demonstrated bandwidths with upper frequency to lower frequency ratios of 22:1. This enormous increase in bandwidth has three major benefits:

1) Searches for spectral lines or signals from extraterrestrial civilizations can simultaneously be carried out over the entire microwave spectrum with much greater efficiency.

2) Measurements of continuum sources have increased sensitivity by virtue of the root bandwidth dependence. In addition the spectral index (slope of the continuum spectrum) can be determined.

3) The number, and hence cost, of receivers required to cover a wide spectrum is reduced by an order of magnitude; this is particularly important for large arrays.

On the negative side, wideband receivers have increased susceptibility to interference; have lower aperture efficiency and higher noise temperature due to spillover, and somewhat higher LNA temperature. The Allen Telescope Array mitigates the spillover noise with offset reflector geometry and a ground shield which reduces the spillover noise. Another paper submitted to this conference (D. Ericsson, P-S Kildal, and S. Weinreb) analyzes the efficiency of the Engargiola log-periodic feed and discusses measures to increase efficiency.

A wideband feed has been developed at TRW and is being evaluated at Caltech; test data will be reported at the conference. The feed covers the 0.5 to 11 GHz band with a constant phase center location, is compact, and has terminals within 1cm of a large volume behind a ground plane that can be used to house the low noise receiver.

Both the log-periodic feeds and the TRW feed have balanced outputs with respect to ground and a wideband balanced to unbalanced transformer (balun) is required. An active MMIC balun, a low noise differential amplifier, covering the 0.5 to 11 GHz frequency range has been designed and will be reported at the conference.

It is expected that wideband receivers will be an active research topic for the next several years and a key component of the Square Kilometer Array (SKA) project. The research will include optimization of reflector optics, shields for minimization of spillover, feed design improvements for decreasing impedance variations, higher-temperature operation of the LNA, and configurations which allow cryogenic cooling of the feed, balun and LNA.

*SWeinreb@caltech.edu, 818-354-4065

0-7803-7846-6/03/$17.00 ©2003 IEEE 

# Optimization of the Side Lobes of Antenna Station as an Array Element.

L. Kogan[1]

(1) - National Radio Astronomy Observatory, Socorro, New Mexico, USA

January 6, 2003

Using a group of antennas (antenna station) as an array element is widely discussed now (the projects LOFAR and SKA for example). An antenna station beam usually has high level of side lobes. Thus minimizing side lobes of an antenna station is rather actual.

The AIPS task CONFI has been used to optimize the configuration of the antenna station minimizing the maximum side lobe inside of the antenna primary beam. The hexagon was chosen as an initial configuration for the given number of antennas at the station. For each number of antennas the cell size of the hexagon was chosen as two antenna diameter. The antenna diameter was taken $d = 12m$. The illumination of the antenna dish is considered to be flat. The minimum spacing between antennas is chosen as 15 meters. So the configuration has some freedom at the cost of the shadowing.
The following table gives the achieved side lobes for different number of antennas $N_{ant}$ and the array size $D_{array}$ in comparison with the side lobes of the single dish with flat illumination. As seen from the

Table 1: The side lobes of the antenna station with different number of antennas

| $N_{ant}$ | 13 | 19 | 37 | 61 | dish |
|---|---|---|---|---|---|
| $D_{array}$, m | 83 | 96 | 144 | 192 | |
| Worst Side lobe | 0.04 | 0.028 | 0.019 | 0.013 | 0.017 |

table, the side lobes (worst) of the antenna station beam can be minimized to the level of the single dish beam ($\sim 2\%$). The side lobe of an antenna station beam can be made even better at the cost of more shadowing. The following problems can limit using antenna station as array element.

**A single antenna follows the source always during the observation. Therefore its directivity and collecting area stay the same for all elements of the array and during the whole experiment if the antennas of the array are identical.**

**At the antenna station case the collecting area stays constant during observation but its directivity does not because change of the station projection. Therefore the array is not homogeneous during the observation. For the very large arrays, when the elevation is different for different stations, the directivity can be different for different antenna stations. Effect of mutual shadowing of the station antennas makes additional contribution to the problem.**

0-7803-7846-6/03/$17.00 ©2003 IEEE

# SKA: Configurations and Simulations

Sheperd Doeleman*(dole@haystack.mit.edu)
Colin Lonsdale
Roger Cappallo
Ramesh Bhat
MIT Haystack Observatory, Off Route 40, Westford, MA. 01886

Current SKA designs call for sensitivities at the nano-Jansky level and imaging over wide fields of view. In depth simulations that produce realistic visibility data sets will be required in order to test imaging algorithms and ensure that dynamic ranges of $\sim 10^6$ can be achieved. Haystack observatory has developed an SKA simulator that produces data sets including effects of a turbulent ionosphere, time variable station beams, realistic skies at SKA sensitivities and antenna noise that is dependent on sky position. Though data for any SKA concept can be produced with the simulator, it is tailored for the Large-N case and includes the capability of combining multiple individual receptors into phased stations with realistic beamforming algorithms. A flexible format for describing frequency channels allows general investigation of multi-frequency synthesis issues.

In addition to producing data sets, the simulator can efficiently be used to search through SKA configuration parameter space for optimal designs. Figures of merit including total cable length to connect stations, point spread function sidelobe levels and point spread function shape allow possible configurations to be ranked and filtered using genetic algorithms.

We present results from our initial parameter searches and show imaging results of SKA skies simulated under realistic data gathering conditions. Algorithms used in the simulator will be discussed.

0-7803-7846-6/03/$17.00 ©2003 IEEE 

# SITE SELECTION FOR AN ARRAY OF WIDELY SEPARATED RADIO TELESCOPES

Steven Durand, Peter Napier *, Frazer Owen, Craig Walker
National Radio Astronomy Observatory
Socorro, NM 87801

As part of the EVLA Project NRAO is currently identifying sites for a new interferometric array of radio telescopes, known as the New Mexico Array (NMA), intended to increase the spatial resolution of the VLA. Some of the experience gained in this work may be of use for planning the Square Kilometer Array, which will face many of the same site selection issues as the NMA.

The NMA is an array of ten telescopes surrounding the VLA at distances of 50 km to 250 km from the VLA. One of the telescopes, the VLBA telescope at Pie Town, already exists. Wide bandwidth data from each of the NMA telescopes will be sent via a fiber-optic network to the VLA site for correlation with each of the 27 VLA antennas. With a requirement for a total network fiber length of approximately 1400 km, and a fiber cable installation cost of approximately 20 $K/km, it is not economically feasible to install our own fiber. The array must be designed to use existing fibers owned by commercial communication companies. This consideration has a major impact on the selection of NMA sites. Negotiations with commercial companies have shown that the most economic way to establish the NMA network is to lease "dark fibers" from the companies and to use NRAO-owned equipment to transmit and receive the wide bandwidth data.

In order of decreasing importance, the factors that we have found important in selecting NMA sites are as follows:

Accessibility to optical fiber
Imaging performance of the array configuration
Accessibility to commercial electrical power
Radio frequency interference issues
Land availability and suitability
Environmental impact issues

For the last four of these considerations there is no substitute to making visits to prospective sites to obtain a correct impression of the feasibility of the site. Visits to prospective NMA sites resulted in significant relocations of most of the sites due to one or more of these concerns.

Details of some of these issues will be presented during the talk, as will some of the costing information that has been developed.

0-7803-7846-6/03/$17.00 ©2003 IEEE 

Consensus has been reached by the radio astronomy community around the world that the next major facility in the field should be an array of antennas working at centimetre to meter wavelengths, with one million square meters of collecting area. Designated the Square Kilometer Array (SKA), this extremely sensitive telescope will have 30 times the collecting area of the largest telescope built so far, and will be a key facility in attacking many of the most important questions in astrophysics.

From the start, the SKA has been conceived as a global endeavour. A meeting in Sydney in 1997 signalled the start of a concentrated effort to develop SKA technology. On the organisational side, astronomical institutes in 11 countries (Australia, Canada, China, India, Italy, the Netherlands, Poland, Sweden, UK, and the USA) formed regional consortia and, in August 2000, signed a Memorandum of Understanding to establish an International SKA Steering Committee (ISSC) and carry out cooperative technology development for the SKA. The ISSC coordinates the technical studies and site testing activities around the world, and has initiated preparation of a detailed science case. It meets twice per year and is supported by a secretariat, and a full-time project director.

The ISSC is working to a timeline that includes informing governments of the project (perhaps via the OECD Global Science Forum) and presenting a management plan late this year, an initial selection of promising technological concepts as well as the location of the array in 2005, the final selection of concept in 2007, world-wide coordinated proposals to governments for construction money in 2008, start of construction in 2010, and operational status in 2015.

There are many technological, political, financial and organisational challenges inherent in this international mega-science project. For example, account has to be taken of different funding cycles, different prior investment histories, different scientific interests, different stages of SKA-specific technology development, and different decision-making cultures in the various regions of the world. Radio astronomy does not have the benefit of an inter-governmental organisation like ESO or CERN to coordinate international decision-making and manage the construction and operation of a major facility like the SKA. This presents a challenge to create an organisational and management structure for the SKA that is "light" but sufficient.

## Material Characterization

**Co-Chairs:** V. V. Varadan
C. Baum

10:00 Opening Remarks

88. 1 10:00 In Situ Material Characterization of Curved Samples using Analysis of Gaussian Beam Reflection from a Convex Cylindrical Shell ..... 418
*V. V. Varadan, K. Du, The Pennsylvania State University, USA*

88. 2 10:20 Electromagnetic Material Characterization Using a H-Plane Step Rectangular Waveguide ..... 419
*M. Havrilla, Air Force Institute of Technology, E. Rothwell, Michigan State University, USA*

88. 3 10:40 Quadrupole Terms in Magnetic Singularity Identification, Part 2 ..... 420
*C. E. Baum, Air Force Research Laboratory, USA*

88. 4 11:00 A Comparison of One-Tier and Two-Tier Stripline Calibration Techniques for Applications in Electromagnetic Material Characterization Measurements ..... 421
*A. Bogle, L. Kempel, E. Rothwell, D. Nyquist, Michigan State University, M. Havrilla, Air Force Institute of Technology, USA*

88. 5 11:20 Calibration of RF Power Meters Based on an Isothermal Method ..... 422
*Y. Hsiao, Y. Lu, C. Huang, H.-T. Chou, Yuan Ze University, D. Lin, Chung-Shan Institute of Science and Technology, Taiwan*

88. 6 11:40 AUXILIARY POTENTIALS IN PSEUDOCHIRAL OMEGA MEDIA ..... APS
*R. Saraei, J. Rashed-Mohassel, Tehran University, Tehran, Tehran, Iran*

*In Situ* Material Characterization of Curved Samples using Analysis of Gaussian Beam Reflection from a Convex Cylindrical Shell

Kai Du and Vasundara V. Varadan*
Center for the Engineering of Electronic and Acoustic Materials and Devices
Department of Engineering Science and Mechanics
The Pennsylvania State University
University Park, PA 16802, U.S.A.

ABSTRACT

A method to invert S-parameter data from curved samples is presented using an analysis of Gaussian beam reflection from a convex circular cylindrical shell. The scattering of Gaussian beam by a layered cylinder can be formulated rigorously using the Fourier expansion method. It is proposed here that if only incoming waves, instead of standing waves, are used in the series expansion for the fields in the inner region, the result is a good approximation of the fields scattered by a convex cylindrical shell. Physically this means an infinite sink (perfectly absorbing column) is placed on the axis of the layered cylinder so that the reflection from the far side of the closed cylinder is eliminated. Such a modification is validated by a comparison with the complex ray tracing method for the special case of a Gaussian beam scattering by a half circular cylinder. As another verification, the reflected fields are used to calculate an equivalent "reflection coefficient" as measured in a free space material characterization system using spot-focusing antennas. Computation results are compared with experimental data and the agreement is as expected. The analysis can be used in an inversion algorithm for characterization of material samples in the shape of circular shells.

**Additional Information:**

1. Commission A (Electromagnetic Metrology), A8. Antennas and EM-field metrology
2. Using this formulation, an inversion technique is developed for the electromagnetic characterization of curved samples.
3. In previous work, curved samples were characterized, using the free space method consisting of spot focusing antennas, by assuming that samples were locally flat. These measurements are valid only for samples with large radii of curvature.

0-7803-7846-6/03/$17.00 ©2003 IEEE

# Electromagnetic Material Characterization Using a H-Plane Step Rectangular Waveguide

Michael J. Havrilla*†
Department of Electrical and Computer Engineering
Air Force Institute of Technology
WPAFB, OH 45433

Edward J. Rothwell
Department of Electrical and Computer Engineering
Michigan State University
East Lansing, MI 48824

Rectangular waveguides are frequently used in electromagnetic material characterization measurements due to their general availability and the relative ease in which testing samples can be machined. Measurements involving frequencies $f > 2\ GHz$ require relatively little testing material. In a S-Band waveguide ($2.5\ GHz < f < 4\ GHz$), for example, sample dimensions in the cross-sectional plane are only 2.84 inches wide by 1.34 inches in height. However, for lower-frequency applications, waveguide dimensions can be on the order of 4 feet wide by 2 feet in height. Consequently, large quantities of materials are required, leading to possible sample fabrication difficulties. Under these circumstances, a waveguide sample holder having a reduced height or width may be utilized to accommodate facilities not capable of producing such large sample sizes. This type of holder, however, will cause a disruption in the waveguide-wall currents, resulting in the excitation of higher-order modes and subsequently leading to significant errors in the computed values for the permittivity and permeability of the sample material. This paper will discuss how these higher-order modes can be accommodated in a reduced-width (i.e., H-plane) waveguide sample holder in order that the electromagnetic properties of the material may be accurately determined.

A mode-matching technique will be used to model the effects of a symmetric H-plane step sample holder. If a $TE_{10}$ mode is incident upon the sample holder, then due to the assumed symmetry, only even $TE_{m0}$ higher-order modes will be excited in the waveguide feed and sample holder regions. Enforcement of total tangential electric and magnetic fields at the front and back interfaces of the holder leads to a subsequent expression for the theoretical sample scattering parameters. The electromagnetic properties of the test material can then be determined numerically by comparing these theoretical values with the experimentally-measured S-parameters using a Newton's method root search, that is

$$S_{11}^{thy}(\omega,\varepsilon,\mu) - S_{11}^{exp}(\omega) = 0$$
$$S_{21}^{thy}(\omega,\varepsilon,\mu) - S_{21}^{exp}(\omega) = 0$$

Experimental results for several sample materials will be provided and compared with the ideal case. Experimental plots of permittivity and permeability will be given showing the effects that the number of modal expansion terms have on convergence.

† The views of the co-author expressed in this article do not reflect the official policy of the U.S. Air Force, Department of Defense, or the U.S. Government.

0-7803-7846-6/03/$17.00 ©2003 IEEE

# Quadrupole Terms in Magnetic Singularity Identification, Part 2

Carl E. Baum
Air Force Research Laboratory
Directed Energy Directorate
Kirtland AFB, NM

Abstract

In magnetic singularity identification (MSI) of conducting and permeable scatterers one considers the low-frequency poles with real natural modes and real natural frequencies to represent the magnetic-polarizability dyadic. This is an approximation neglecting the higher-order multipoles.

This paper continues the treatment of the quadrupole terms in magnetic singularity identification (MSI) in [C. E. Baum "Quadrupole Terms in Magnetic Singularity Identification", Interaction Note 569, 2001] which we can conveniently reference as Part 1. In that paper the magnetic-dipole formulae were extended to magnetic-quadrupole terms as certain integrals over the magnetization vector, particularly in the form of natural modes. Then questions were addressed concerning optimal choice of coordinate origin to "minimize" the quadrupole term associated with modes having a magnetic-dipole moment. The present paper (Part 2) further extends this development, including the use of norms and the point symmetry groups.

This paper (Part 2) extends the basic properties of magnetic quadrupoles in MSI. For minimizing such terms associated with natural modes with nonzero magnetic dipoles, the 2-norm over the unit sphere is formed. This leads to the definition of the optimal coordinate center (or center of the natural mode) for minimizing the quadrupole term. This does not necessarily make the quadrupole term zero, only minimum. Depending on various symmetrys of the target it is possible for certain of the natural modes to have a zero quadrupole moment. The case of two displaced magnetic dipole is generalized for zero quadrupole. The symmetry considerations are extended to discrete two-dimensional rotation with a transverse symmetry plane.

There may be other cases to consider, but this should help in optimal employment of MSI.

0-7803-7846-6/03/$17.00 ©2003 IEEE

# A Comparison of One-Tier and Two-Tier Stripline Calibration Techniques for Applications in Electromagnetic Material Characterization Measurements

Andrew Bogle*, Leo Kempel, Edward Rothwell and Dennis Nyquist
Department of Electrical and Computer Engineering
Michigan State University
East Lansing, MI 48824

Michael Havrilla†
Department of Electrical and Computer Engineering
Air Force Institute of Technology
WPAFB, OH 45433

Electromagnetic material characterization is the process of determining the permittivity and permeability of a sample. A stripline field applicator can be utilized to facilitate measurement of these constitutive parameters, especially since it is an inherently broadband device that supports a relatively uniform TEM field distribution, has a larger cross-sectional area than a 7 mm coaxial sample holder, can be clamped (thus eliminating the effects of gaps) and has an easily-machinable sample geometry. A critical part of the material characterization process is achieving an accurate calibration. The goal of this paper is to present and compare two types of frequency-domain stripline calibration schemes, referred to here as one-tier and two-tier techniques, and the resulting effect that these techniques have on measurement accuracy.

The overall objective of the above material measurement process is to experimentally obtain the sample scattering parameters using a network analyzer and compare them with their theoretical expressions, that is

$$S_{11}^{thy}(\omega,\varepsilon_r,\mu_r) - S_{11}^{exp}(\omega) = 0$$
$$S_{21}^{thy}(\omega,\varepsilon_r,\mu_r) - S_{21}^{exp}(\omega) = 0$$

These coupled equations can be solved for $\varepsilon_r$ and $\mu_r$ in closed form using the well-known Nicolson-Ross-Wier procedure. However, the front and back sample planes are not immediately accessible for the measurement of $S_{11}^{exp}$ and $S_{21}^{exp}$, therefore an initial stripline calibration must be performed. In the two-tier calibration scheme, the network analyzer is first calibrated to the end of the network analyzer 7mm cables using the internal network analyzer cal kit and associated 7mm calibration standards. During the secondary stage, specialized stripline standards are utilized to remove the effects of the stripline transition regions. In comparison, the one-tier calibration involves immediate calibration of both the cables and stripline device in one stage. Consequently, the one-tier calibration scheme requires fewer measurements and subsequently leads to enhanced accuracy.

The permittivity and permeability of various samples will be determined and a comparison will be made using both calibration schemes. Details of the stripline calibration techniques and corresponding measurement procedure will be presented and discussed.

† The views of the co-author expressed in this article do not reflect the official policy of the U.S. Air Force, Department of Defense, or the U.S. Government.

0-7803-7846-6/03/$17.00 ©2003 IEEE

# Calibration of RF Power Meters based on an Isothermal Method

Yu-Ting Hsiao*, Yu-Cheng Lu, Chien-Chang Huang and Hsi-Tseng Chou
Dept. of Comm. Eng., Yuan-Ze University, Chung-Li 320, Taiwan
De-Phone Lin
Chung-Shan Institute of Science and Technology, Tao-yuan, Taiwan

Calibration of high frequency power meter with high power input is very important and essential in the development of measurement techniques. Popular methods of measuring power transfer the signal power into other forms of energy such as direct current, potential difference, resistance and heat temperature, and employ a signal bridge to extract the corresponding power level. Among these, heat temperature that indicates a heat power is considered most accurate and reliable parameter to indicate the power level. A calibration procedure and system based on this method is thus employed to provide accurate calibration of RF power meters at high frequency and high power levels. In particular, an isothermal method, which tends to provide accurate measurement of heat power and was firstly employed to measure the efficiency at lower power level, is employed in the system. In the application of this isothermal method to power measurement is found to be very accurate at lower power level, and cause some uncertain factors. In order to improve the accuracy and stability of this method at high power, a RF network analyzer is first employed to study the effects of the calorimeter caused by the mismatch of transmission lines. Correction factors are then obtained based on the measured reflection coefficients, which are then employed in the calibration procedure to provide accurate measurement of actual power levels. Note that an automatic control system is also implemented to further assure the stability. System structure of the calibration procedure as well as its performance evaluations will be presented and validated.

0-7803-7846-6/03/$17.00 ©2003 IEEE

## DOA Estimation

**Co-Chairs:** C. Christodoulou
P. Wahid

7:55 Opening Remarks

89. 1 8:00 A Method for Wideband Direction-of-Arrival Estimation using Frequency-Domain Frequency-Invariant Beamformers ..... APS
*T. Do-Hong, Munich University of Technology, F. Demmel, Rohde&Schwarz Company, P. Russer, Munich University of Technology, Germany*

89. 2 8:20 Applying Direction Finding Algorithms for Obtaining Processing Gains in OFDM System with Multiple Receiving Antennas ..... APS
*H. Lin, K. Ho, M. Tseng, National Taipei University of Technology, Taiwan*

89. 3 8:40 Reactance-Domain MUSIC DOA Estimation using Calibrated Equivalent Weight Matrix of ESPAR Antenna ..... APS
*A. Hirata, H. Yamada, T. Ohira, ATR Adaptive Communications Research Laboratories, Japan*

89. 4 9:00 Argus: an L-Band Array for Detection of Astronomical Transients ..... APS
*S. W. Ellingson, G. A. Hampson, The Ohio State University, USA*

89. 5 9:20 Radio Wave Propagation Over a Rectangular Obstacle ..... APS
*C. J. Coleman, The University of Adelaide, Australia*

89. 6 9:40 Effects of Angle Spread in a Complex Outdoor Environment At 2.4 GHz ..... APS
*S. W. Ellingson, The Ohio State University, USA*

89. 7 10:00 Experimental Study of Near-field Beamforming in Conformal K-band Linear Arrays ..... APS
*R. Tulpule, N. Karnik, B. P. Kumar, California State University, Sacramento, G. R. Branner, University of California, Davis, USA*

89. 8 10:20 New Implementation of the Correlation Function of the PN Code for Application in Automotive Radars ..... APS
*O. Aly, A. Omar, Uni. Magdeburg, Germany*

89. 9 10:40 Fast Minimum Entropy Autofocusing for ISAR Imaging ..... 424
*X. Qiu, Nanjing Univ. of Post and Telecommunication, Y. Zhao, Nanjing Normal Univ., China, A. Cheng, DSO National Lab., Singapore*

89. 10 11:00 A New Criterion for DOA Estimation of Coherent Sources Based on Weighted Spatial Smoothing ..... APS
*B. Wang, Y. Wang, H. Chen, Key Research Lab Wuhan Radar Academy , China*

89. 11 11:20 The Pre-processing Method Based on Signal Conjugate Cyclostationary ..... APS
*C. Hui, W. Yongliang, W. BuHong, Wuhan Radar Academcy Key Lab., China*

89. 12 11:40 A New Adaptive Saptial Smoothing Method ..... APS
*T. Jun, P. Yingning, Tsinghua University, China*

# Fast Minimum Entropy Autofocusing for ISAR Imaging

X. H. Qiu, [1] Y. Zhao, [2], Alice. H. W. Cheng [3]

[1] Department of Information. Eng,

Nanjing University of Post and Telecommunication, Nanjing 210003, China

[2] School of EEE, Nanjing Normal University,Nanjing 210042, China

[3] Radar Research Center, DSO National Lab., 118230 , Singapore

Inverse synthetic aperture radar (ISAR) imaging is a powerful tool in microwave imaging for moving target. It provides high range resolution by transmitting wide-band signal and high cross-range resolution by coherently accumulating echoes, where phase compensation is one core technique for range-Doppler image formation. However, conventional autofocusing methods usually have problems to compensate the translational motion between radar and target with sufficient accuracy when the motion has high order or even random terms. To solve this problem, recently Li proposed a minimum entropy-based autofocusing method (Li et al, IEEE Trans. AES, Vol.35, p1240-1251,1999. ), which can achieve much better aufocusing effect, but it only gives optimization principle theoretically, and no effective implementation is introduced yet about the algorithm. Moreover, it needs a huge computation for multi-dimensional searching and consequently, so it is not available in use. In this paper, we present a two-dimensional fast minimum entropy autofocusing(FMEA) approach. According to non-correlation relationship of phase error between each echo, phase optimization for each echo can be calculated to make two-dimensional entropy minimized. On the other hand from the point of two-dimensional image and entropy of range-Doppler imaging, error phase can be coupled together by image and entropy, and then they become correlative. As a result for each new iteration solution it can skip out from local minimum value of last iteration and approaches to the global minimum value. Simulation and real ISAR data processing have shown the validation and efficiency of our method, especially the algorithm processing is speeded up greatly compared with Li's method, as seen in Table 1. It is a cost-effective way that needs small computation with high convergence speed, good autofocusing effect as well as explicit formulation easily for practical use

Table 1 Computation resource comparison between two methods.

| Method | time for each iteration (sec) | iteration number | total time cost |
|---|---|---|---|
| FMEA(t1) | 1.16 | 50 | 58 |
| Li's (t2) | 242 | 250 | 60500 |
| Data comparison* | 0.48% | 20% | 0.09% |

* Note: Data Comparison means percentage value from (t1 / t2 ) 100%

0-7803-7846-6/03/$17.00 ©2003 IEEE

## Remote Sensing of Ocean Surface and Atmosphere

**Co-Chairs:** D. Trizna
K. Aydin

7:55 Opening Remarks

# Oil Slick Detection on the Ocean Surface

Farshid Aryanfar* and Kamal Sarabandi
Radiation Laboratory, EECS Department
University of Michigan
Ann Arbor, Michigan, USA
Email: faryanfa@eecs.umich.edu, saraband@eecs.umich.edu

Oil spill is the main source of the pollution in the oceans. It reduces ocean interaction with the atmosphere and contributing to the carbon and water cycles and therefore causing harm for the ocean lives. So detection and quantification of oil spills on water is one of the most important issues of environmental protection. As the oil layer above the ocean surface is very thin, the difference in effective permittivity due to it is not significant. However adding a thin layer of oil reduces the surface roughness and consequently the electromagnetic backscattering. There are many algorithms for oil slick detection that has been used such as pattern recognition techniques, frequency spectrum attenuation measurements, neural networks recognition techniques and SAR images detection and characterization (P. Trivero *et al.*, *Int. Journal of Remote Sensing*, **19**, 543-548, 1998).

Most of the reported techniques are useful however complex. In this paper an easy method has been proposed to find oil slicks on the ocean surface by calculating backscattering coefficient. Different types of ocean surfaces (Gaussian surface with band-limited ocean spectrum and Band-limited fractal surface based on the Weierstrass-Mandelbrot function) have been considered for this study. The oil effect on the ocean surface has been modeled as decrease in upper wave-number cutoff. The surface integral equation is solved numerically using the method of moments. Figure 1 shows a random generation of these surfaces and effect of oil on them. The simulation results for back scattering coefficient are shown in Figure 2. As it can be seen for incident angles more than **35** degrees the reduction in back scattering coefficient in both cases is more than **3** dB and easily detectable.

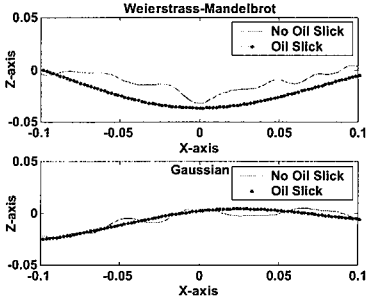


Figure 1. Surface Profiles

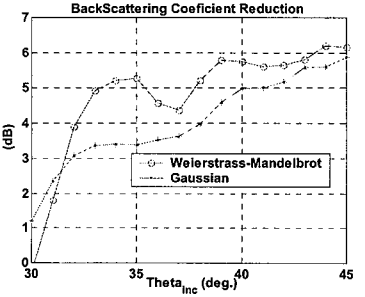


Figure 2. Back-Scattering Reduction

**Abstract**

We present results of an experiment using a digital HF receiver approach to measure the Doppler spectrum of high-frequency back-scattered radar signals in a bistatic mode. The shift of the first order sea scatter Bragg lines from their expected values can be used for radial ocean surface current estimation. Targets appear in the Doppler spectrum with amplitude proportional to radar-cross-section (RCS), while the Doppler shift is proportional to the radial velocity. This is the first experiment that validates the capability of utilizing direct digitization of the radio frequency echo to achieve a minimum of 60-dB dynamic range, and milli-Hertz Doppler shift accuracy for radial velocity resolution, operating in a bistatic mode. Two independent GPS-coupled rubidium oscillators were used to generate the transmitted waveform and A/D timing clock generation, respectively. Data were recorded with four receive loop antenna elements and A/D cards, and data were digitized at a 60 MHz rate and stored for off-line processing. Results of Doppler analysis of ocean sea scatter and target detection for pulse-to-pulse switching of 32 frequencies over the 3-30 MHz band are presented.

The experiment validated a methodology being used in the design of a single real-time eight-channel transceiver PC card. It will allow real time digital down-conversion filtering and recording of data from an eight-element array at the intermediate frequency under Windows OS control. This filtered data will be stored at a rate commensurate with the transmitted bandwidth, thus reducing volume of data significantly from the results presented above. This design utilizes a pair of DDS chips to provide both a variety of transmit pulse waveform generation (simple pulse, FM pulse, FM-CW, noise, phase-coded) and coherent digitization on a single PC card. A separate sister exciter card uses the same PCB footprint of the transceiver, but only exercises the exciter chip component portion, for use with a bistatic transmitter. Each card has capability of a rubidium clock input, under GPS time control, suitable for bistatic radar operation. GPS time allows coordinated interleaved pulsing between sites, for as many bistatic sources as one desires. The transceiver and exciter are in final stages of construction, and prototypes will be available for viewing at the meeting.

0-7803-7846-6/03/$17.00 ©2003 IEEE 

# Microwave Emission of Reproducible Breaking Waves: The POlarimetric Emissivity of Whitecaps EXperiment (POEWEX '02)

S. C. Reising*, S. Padmanabhan, and M. A. Aziz, Microwave Remote Sensing Laboratory, University of Massachusetts, Amherst, MA 01003-4410, USA (Email: reising@ecs.umass.edu, spadmana@ecs.umass.edu, aziz@mirsl.ecs.umass.edu)

W. E. Asher, Applied Physics Laboratory, University of Washington, Seattle, WA 98105, USA (Email: asher@apl.washington.edu)

L. A. Rose and P. W. Gaiser, Naval Research Laboratory, Washington, DC 20375, USA (Email: allen.rose@nrl.navy.mil, peter.gaiser@nrl.navy.mil)

WindSat, the first polarimetric microwave radiometer in orbit, was launched on January 6, 2003, in order to demonstrate the viability of passive sensing of the ocean wind vector from space and to perform risk reduction for the NPOESS Conical Microwave Imager/Sounder. The Naval Research Laboratory and the WindSat Science Team are studying the retrieval of the ocean wind vector using a physically-based approach, which depends upon an accurate forward model of surface emission, as well as of atmospheric emission and its reflection from the surface. Aircraft measurements and model results have shown that the signature in azimuth with respect to the wind direction is much smaller in magnitude (roughly 1-3 K peak-to-peak) than that of wind speed. Therefore, it is necessary to determine the dependence of the surface microwave emission on the wind vector as accurately as possible. The microwave emission of the sea surface depends upon wind roughness, whitecaps, surfactants, temperature and salinity. For moderate wind speeds and greater, the increased ocean surface emission caused by whitecaps and foam due to wave breaking is very significant, relative to the wind direction signal. This increase is the product of foam emissivity and the foam fractional coverage in area. The importance of radiometer measurements with bore sighted video cameras near the sea surface is that they determine the *emissivity* of foam independent of the foam fraction as a function of wind speed that occurs on the open ocean.

The authors have conducted several experiments to measure the microwave emissivity of foam. The first study measured beam-filling foam on a calm water surface, along with microphysical measurements to characterize the artificially-produced foam. Second, open ocean measurements during the FAIRS experiment observed that the foam emissivity changes due to the temporal wave development and the viewing angle of the radiometer. Third, in order to measure the time, polarization, frequency and angular dependence of foam emission on the sea surface, reproducible breaking waves were generated in a saltwater wave tank. Passive polarimetric measurements of the breaking waves were performed at X-band (10.8 GHz), K-band (18.7 GHz), and Ka-band (36.5 GHz). The radiometric emission of the breaking waves was observed as a function of time, polarization, frequency, incidence and azimuth angles. In order to correlate features of individual breaking waves as well as to perform ensemble averages, wave and foam properties were measured concurrently. These include the void fraction and bubble size spectrum of the foam, wave height, Ku-band radar backscatter to infer roughness and turbulence parameters using acoustic Doppler velocimetry. Results of the POEWEX '02 experiment will be reported and discussed.

0-7803-7846-6/03/$17.00 ©2003 IEEE

# An Analysis of the Radar Image from Ocean Scattering near KaoHsiung Harbor Using UTD Model

Eric Chu[1], M. C. Liang[1] and R. J. Burkholder[2]

[1]I-Shou University, Dept. of Electronics Engineering, KaoHsiung 840, Taiwan;
mcliang@isu.edu.tw
[2]The Ohio-State University, ElectroScience Lab., Columbus, Ohio 43212

**Abstract**

When a radar is set up along the coast near KaoHsiung harbor, the radar image shows a peak periodically even without an obvious target on sight. From previous studies, it was found that the effect is from the ocean itself, more specifically, from the scattering of the oceanic wave.

The sea spike scattering can be relatively large. In many instances, it might be higher than the scattering from a small RCS target on the sea. This might significantly limit the detection capability of the coast radar system. A close observation has shown that in order to reduce the problem and increase the sensitivity of the detection capability, the sea scattering effect must be somehow eliminated or reduced.

To understand the problem, series measurements of the sea scattering at different time of the day, day of the month, month of the year, with different wind direction and conditions are recorded. An X-band pulsed radar with PRF approximately 2000 PPS, and transmitted peak-power around 150 KW is used to obtain the data. The radar system is set up near the coast, with antenna direction fixed at preset directions and distances. A statistical analysis of the model is done to find out the sensitivity to different parameters.

An UTD analysis of the scattering from the concave/convex periodic surface is modeled. The effect of the ocean scattering is modeled using UTD analysis. A post processing of the measured radar image by removing the UTD scattering effect is presented.

0-7803-7846-6/03/$17.00 ©2003 IEEE

# Long-term observations of the 3-D wind field by using CLOVAR VHF wind-profiler radar.

Radian G. Belu
College of Engineering
Wayne Sate University,
Detroit, Michigan, USA

and

Wayne K. Hocking
Department of Physics and Astronomy,
The University of Western Ontario,
London, Ontario, Canada

In the past three decades, VHF/UHF radars were used extensively for studying the structure and dynamics of lower and middle atmosphere. Wind-profiler radars offer the capability for measuring atmospheric wind motions with excellent temporal resolution and moderate height resolution. The CLOVAR VHF radar is located at 43°04.44' N, 81°20.20'W, operates at a frequency of 40.08 MHz, peak power of 10 kW (average power of 800 W) and is owned and operated by the University of Western Ontario, London, Ontario, Canada. The VHF MST radars have provided a new tool for continuously monitoring of all three components of the air velocity vector over a single location, and they are relatively unique in their ability to measure and monitor the vertical and horizontal wind velocity components.

The important influence of dissipating and interactions of gravity waves on the circulation of many regions of lower and middle atmosphere is now widely acknowledged. Gravity waves generated by various sources, throughout the atmosphere play an important role to the shaping and structure of atmospheric circulation. The can transport significant momentum and energy from the regions, where they are generated to the other parts of the atmosphere. Analyzing the generation, propagation, and climatology of these waves is important to the understanding of middle and upper atmosphere dynamics. Long-term radar measurements of the tropospheric wind velocities provide considerable insight into gravity wave processes, making it possible to study temporal and spatial variability of these waves. MST radars have proven to be a key tool in providing high-resolution measurements of the wave-induced velocity fields, which in turn have led to advances in our theoretical description of these processes. The seasonal variation of wind velocity and momentum fluxes induced by gravity waves in the troposphere have been studied using wind observations by the CLOVAR VHF radar at London, Ontario, Canada from January 1996 to December 1997. Our wind velocity variance and momentum flux estimates were correlated with information about weather systems taken from daily weather maps. The CLOVAR wind-profiler is located in a flat region of Eastern Canada, so that the gravity wave generation is not affected by orography.

0-7803-7846-6/03/$17.00 ©2003 IEEE

# Spatial structure of RASS signals observed by a UHF Volume Imaging Radar

*Paco López Dekker and Stephen J. Frasier*

An implementation of a Radio Acoustic Sounding System (RASS) using the Turbulent Eddy Profiler (TEP), a UHF volume imaging radar, is presented. TEP makes use of digital beamforming techniques to generate a number of simultaneous beams within its field of view, providing 3-D clear-air radar data of a portion of the atmospheric boundary layer. In RASS mode, TEP can be used to retrieve virtual temperature fields. High resolution time series of vertical profiles of virtual potential temperature are used, in combination with clear-air radar reflectivity images, to validate and interpret the temperature measurements. Here, the system is used to study the spatial structure of the RASS echo by observing the diffraction pattern on the antenna array, or by studying beamformed intensity images of the RASS echo. In low-wind conditions, the time-averaged intensity of the diffraction pattern of the RASS echo shows a well defined structure, which implies that this pattern has a persistent morphology. It is appealing to interpret this structure as the focused spot. In general, the observed structures have scales of one meter, matching the aperture size of the acoustic source. Examples of the volumetric images of the RASS echo are shown, displayed as a stack of horizontal slices of the reflectivity field. While the acoustic beam embedded in the radar field of view can be recognized, these images also suggest more complex patterns like split regions of high reflectivity (see figure). These patterns have been predicted in the literature, and can be related to vertical gradients of temperature and wind velocity.

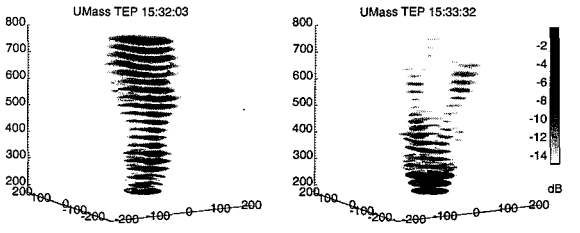


Figure 1: Spatial signature of RASS signal. The images show stacks of horizontal slices showing the radar-reflectivity at each range gate.

# Cloud Ice Crystal Classification Using a 95 GHz Polarimetric Radar

K. Aydin and J. Singh
Penn State University
Department of Electrical Engineering
University Park, PA 16802
Phone: (814)865-2355
Fax: (814)863-8457
E-mail: k-aydin@psu.edu

The identification of various ice crystal types within a cloud, as well as the estimation of their ice water content are important goals with applications to cloud microphysical studies and to understanding the effect of clouds on the Earth's radiation budget. Millimeter wave polarimetric radars have the potential for accomplishing both of these goals. There are several millimeter wave radars operating at 95 GHz for the remote sensing of ice clouds from ground-based and airborne platforms. This paper brings together observations from experiments and modeling studies, and focuses on 95 GHz polarimetric radar signatures of ice crystals. Results from simulations and experimental data for the reflectivity factor $Z_h$, differential reflectivity $Z_{DR}$, and linear depolarization ratio LDR are combined to generate different ranges of values for each observable corresponding to different crystal categories. A fuzzy classification algorithm (including the air temperature to separate columnar crystals from the small aggregates) is developed to classify ice crystals as follows: (i) columnar crystals, (ii) planar crystals, (iii) planar crystals and small aggregates or rimed planar crystals, (iv) planar crystals and large aggregates or densely rimed planar crystals or graupel like snow or small lumpy graupel, and (v) graupel. Measurements with the University of Wyoming's airborne 95 GHz radar system and particle probes (2D-C cloud and 2D-P precipitation probe) obtained in 1997 are used to demonstrate the technique. During these experiments the aircraft penetrated through the clouds and the onboard radar and particle probes collected data. Ice crystals throughout the cloud were classified according to this technique and the closest range gates compared very well with the 2D probe images of the crystals.

1. Commission F : F5 Remote sensing of oceans and atmosphere
2. A new technique for ice crystal classification in clouds using a 95-GHz polarimetric radar is presented.
3. There are a number of papers focusing on 95 GHz polarimetric radars for cloud remote sensing. This paper brings together modeling and experimental results for using such radars to classify ice crystals in clouds.

0-7803-7846-6/03/$17.00 ©2003 IEEE

# On the possibility of rain rate estimation by observation of the scatter of satellite broadcasts

J. D. Sahr, J. W. Diamond, S. Hawk
Department of Electrical Engineering Box 352500
University of Washington, Seattle WA 98195-2500
J. A. Weinman
Microwave Sensors Branch, Code 975
NASA Goddard Space Flight Center, Greenbelt MD 20771

We have investigated the possibility of coherently detecting the scatter of microwave broadcasts from satellites to synthesize Doppler radar measurements of precipitation. This study was motivated by our prior development of a passive VHF system observing commercial FM broadcasts to study plasma turbulence in the ionosphere.

In particular, we have investigated a system consisting of two antennas; one directed towards a Ka-band broadcast from geosynchronous orbit, and one directed to observe bistatic Rayleigh scatter. The first antenna provides a coherent reference which can be used to create very large processing gain to detect the second, much weaker signal. Ka-band is not used in ordinarly weather radar systems because the absorption may be large. In a conventional radar the signal must pass twice through the absorbing medium, while the net path would be approximately half as large for the passive system. In the proposed bistatic geometry the signal strength does not decrease with range.

As one would expect, the performance is severely limited by the low brightness of the illuminators. For time and space resolution that are comparable to NEXRAD, the proposed system would be approximately 50 dB less sensitive than the WSR-88D: the weakest observable signal is about 20-30 dBZ, depending upon choice of frequency, and time and space resolution. Although the RF hardware associated with this system should be inexpensive, the computing task is quite large (tens of Tera operations per second). We will present a short summary of this work, briefly providing an example of our VHF instrument. An extended technical report describing this work may be found at

https://www.ee.washington.edu/techsite/papers/refer/UWEETR-2002-0019.html

0-7803-7846-6/03/$17.00 

F1: Propagation modelling and measurement

# The Estimation of the Cumulative Probability Distribution Function of Rainfall Rate as a First Step Towards a Cost Effective Attenuation Prediction Model

E. Couto de Miranda, L.A.R. da Silva Mello and M.S. Pontes
Centre for Telecommunication Studies
Pontifical Catholic University of Rio de Janeiro
Rua Marquês de São Vicente 225, Ala K. 7th Floor
Gávea, Rio de Janeiro, RJ
Brazil 22453-900
Tel: +552131141682, Fax: +55212945748, e-mail: erasmus@cetuc.puc-rio.br

***Abstract***

At the basis of any attenuation prediction model for satellite communications there is the behaviour of rainfall. Due to the spatial and temporal randomness of rain, the correlation between attenuation and rainfall can only be observed at a statistical level. Therefore, the better the understanding of the statistics of rainfall rate, the better the attenuation models obtained from it.

The statistical modelling of attenuation in an Earth-satellite link requires the joint use of radiometers and satellite beacon receivers. The cost of such a set-up can exceed 40000 US Dollars. In countries with large areas and diverse climates (as is the case of Brazil), the total cost of a widespread coverage is prohibitive. The set-up required for a raingauge does not reach 1000 US Dollars. Therefore, if a model for characterising rainfall-induced attenuation could be obtained from the statistics of rainfall it could greatly improve the mapping of attenuation in countries like Brazil.

The modelling of the cumulative distribution function of rainfall at a given site was achieved by fitting a two parameter Weibull distribution to the empirical cumulative distribution function obtained from the recorded rainfall rates. The Weibull distribution is a generalised form of the exponential distribution and has been found to fit not only rainfall distributions but also the attenuation.

The data used in this study consisted of 93 empirical cumulative distributions of rainfall rate, 73 taken from the ITU-R database and 23 obtained from measurements in several sites in Brazil. The distributions were all obtained from one year of measurements.

The Weibull distribution was found to be an excellent fit to the empirical distributions of rainfall, with explained variances always exceeding 95%. From the statistics of the parameters of the obtained Weibull distribution estimates, it was possible to arrive at the conclusion that the rainfall distributions were in fact Burr Type III. The Burr type III distribution is the result of a Weibull distribution with gamma distributed parameters. This mixture distribution representation makes more physical sense than a single distribution fit since the empirical cumulative probability function of rainfall integrates the effects of stratiform and convective , which are rainfall regimes with totally different dynamics.

This work explores an avenue of research which aims at obtaining a cost effective, yet reasonably accurate, attenuation model and is connected with the overall research objectives and results (extensively published in the literature) of the Propagation Group at the Center for Telecommunication Studies of the Pontifical Catholic University of Rio de Janeiro.

0-7803-7846-6/03/$17.00 ©2003 IEEE 

**Estimation of Effective Raindrop Shape Model from 35 GHz Attenuation and Differential Attenuation**

S. E. A. Daisley and K. Aydin
Department of Electrical Engineering
Penn State University
University Park, PA 16802

Phone: (814) 865-2355
Fax: (814) 863-8457
E-mail: k-aydin@psu.edu

Rainfall measurements using polarimetric radar observables exploit their sensitivity to the shape-size dependence of raindrops. The equilibrium shape-size relationship of raindrops is well established. For radar applications raindrops are modeled as oblate spheroids with size dependent axial ratios. The relationship between size and axial ratio may be altered by oscillations. Furthermore, the drop shape projected on the plane perpendicular to the radar line-of-sight direction is also affected by drop canting. It is of interest to determine whether or not there is a deviation from the equilibrium shape-size model and to estimate an effective shape model for raindrops from measurements during a rainfall event. For this purpose we propose the use of specific attenuation $A_h$ and specific differential attenuation $\Delta A = A_h - A_v$ at 35 GHz, where h and v denote horizontal and vertical polarization. It is shown that raindrop canting and oscillation affect $A_h$ negligibly and $\Delta A$ significantly. Simulations using DSDs from ground based disdrometer measurements indicate that the relationship between $A_h$ and $\Delta A$ is sensitive to the raindrop shape model used. For example, power law relationship of the form $A_h = a(\Delta A)^b$ (with both $A_h$ and $\Delta A$ having units of dB/km) have the following coefficients for an equilibrium drop shape model ($a = 6.78$, $b = 0.889$) and two different oscillation models ($a = 8.25$, $b = 0.873$; and $a = 8.91$, $b = 0.887$). It is suggested that simultaneous measurements of $A_h$ and $\Delta A$ could be used together with simulated $A_h$ - $\Delta A$ relationships for determining the presence of drop oscillations and canting and for estimating an effective raindrop shape model during a given rainfall event.

1. Commission F : F5 Remote sensing of oceans and atmosphere
2. A new technique is presented for determining the presence of drop oscillations and canting and for estimating an effective raindrop shape model during a given rainfall event.
3. The proposed technique can have a significant impact on improving the estimates of rainfall rate using polarimetric radar measurements, which is a topic of current research interest.

0-7803-7846-6/03/$17.00 ©2003 IEEE

# Ka-Band Propagation Experiment at a Tropical Site

**R. Acosta, S. Johnson, W. Feliciano, D. Hilderman**
21000 Brookpark Road, MS 54-6
NASA Glenn Research Center, Cleveland, Ohio 44135, USA
Tel: (216) 433-8016; Fax: (216) 433-6371;
e-mail:Roberto.j.Acosta@grc.nasa.gov

**R. Pollard**
Florida Atlantic University
Boca Raton, Florida 33431
e-mail: rpol6456@fau.edu

**L. A. Gonzalez**
University of Puerto Rico
Humacao, Puerto Rico 00791
e-mail: la_gonzalez@cuhad.upr.clu.edu

***Abstract*** - Results from a tropical Ka-Band propagation measurement experiment conducted with the Global Broadcast Satellite are presented. The measurements were made at a site in Humacao, Puerto Rico. The experiment included Ka-band beacon signals, Ka-Band sky noise and rain rate. The measurements were started in April 2002 and extend to December 2002. Results presented are annual monthly distributions of rain rate, attenuation, fade durations, and inter-fade intervals. The results are compared with available models to ascertain their applicability in tropical climates.

***Introduction*** -Since the early years of satellite telecommunications, the evolution of systems has led to a strong increase in satellite capacity, a decrease of boarded equipment size and a significant cost reduction. From the technical point of view, the congestion of primary allocated frequency bands resulted in the use of higher and higher bands from L, S or C bands to X and Ku bands, and in the near future up to Ka, V and EHF bands. One of the main concerns with these higher frequency bands is the influence of the atmosphere on radio wave propagation. Until now, some studies have shown that the feasibility of such links seems to be guaranteed, especially in the Ka-band. Several propagation experiments have been conducted, mainly in mid-latitude climates, with the OLYMPUS, ITALSAT, and ACTS satellites. However, it is still necessary to determine what service availability will be supplied to the user, and to predict the behavior of these systems when affected by high fading conditions. In particular, the knowledge of propagation issues in wet climates has to be improved.

Satellite telecommunication links in the EHF band are disturbed by troposphere phenomena, which can severely degrade service quality. First, attenuation is caused by atmospheric gases (mainly oxygen and water vapor), by clouds (liquid water and ice particles) and by precipitation (hail, snow and particularly rain). Scintillation appears as rapid fluctuations of signal amplitude or phase caused by tropospheric turbulence in clear sky conditions or by precipitation. Depolarization is due to non-symmetrical particles such as raindrops, snowflakes, and especially ice particles.

The statistical models have been validated up to Ka band (20/30 GHz) in temperate areas, in particular with the OPEX (OLYMPUS Propagation Experiment) campaign. Currently, the ITALSAT propagation experiment studies the validity of these models in the EHF band (40/50 GHz) in European countries. The ACTS campaign was concerned with the Ka-band (20/29 GHz) in the U.S.A.

0-7803-7846-6/03/$17.00 ©2003 IEEE

# Refractivity estimation using multiple elevation angles

**Peter Gerstoft[1], L. Ted Rogers[2], William S. Hodgkiss[1], and Lee J. Wagner [2]**

[1]Marine Physical Laboratory, Scripps Institution of Oceanography
University of California San Diego, La Jolla CA 92093-0238
Email: gerstoft@mpl.ucsd.edu

[2]SPAWAR Systems Center, San Diego
Code D858
San Diego, CA 92152-7385

Estimation of the atmospheric refractivity is important for the prediction of radar performance. Surface or elevated trapping layers formed by the outflow of relatively dry and warm air over a cooler body of water often results in the refractive structure supporting convergence-zone like behavior and multi-modal effects. The propagation under such conditions can be very sensitive to even small changes in the vertical and horizontal structure of refractivity. Obtaining *in situ* measurements of sufficient fidelity to estimate where intensifications in the EM field will occur is difficult.

The authors previously have demonstrated the ability to infer refractivity parameters from grazing-incidence radar sea clutter data. The radar system was the 2.8 GHz Space Range Radar that overlooks the Atlantic Ocean in the vicinity of Wallops Island, VA. The forward modeling consisted of the mapping of an 11-parameter environmental model via an electromagnetic propagation model into the space of the radar clutter observations. A genetic algorithm was employed to optimize the objective function. Ground truth data were atmospheric soundings obtained by a helicopter flying a saw-tooth pattern. The overall result was that the ability to estimate the propagation within the duct itself was comparable to that of in situ measurements, however, the ability to characterize the region above the duct was quite poor.

Modern 3-D radars, however, have relatively narrow beams. Using these narrow beams at multiple elevations might resolve the ambiguity leading to the poor characterization in the region above the duct. Using radar data from the SPANDAR radar it is demonstrated that such an approach is feasible and more robust estimates can be obtained by using two elevation angles and/or by constraining the solution to contain realistic refractivity profiles.

0-7803-7846-6/03/$17.00 ©2003 IEEE

## Special Numeric Methods

**Co-Chairs:** M. Deshpande
M. Carr

7:55 Opening Remarks

# Element-Free Galerkin Method for Solving Wave Equations

* Z. Zeng, L. Xuan†, B. Shanker, L. Udpa and L. Kempel

2120 Engineering Building, Dept. ECE, Michigan State University,
East Lansing, MI 48824, USA, {zengzhiw,bshanker,udpal,kempel}@egr.msu.edu
† Electrical and Computer Engineering, 453 FPAT, Lexington, KY 40506, USA,
lxuan0@engr.uky.edu

The finite element method has found widespread application in computational electromagnetics. While it is a powerful tool, it requires an underlying mesh to describe the structure. However, in many scenarios exact geometric information is unavailable or is time varying. Under such circumstances, it is desirable to develop a formulation that does not depend on the underlying tessellation. Furthermore, it is also desirable to have a technique that is adaptive, i.e., the user increases the density of points in a region to increase the computational accuracy. In this context, meshless methods have found extensive application in both mechanics as well as computational electronics (T. Belytschko, Y. Krongauz, D. Organ, M. Fleming, and P. Krysl, *Comput. Methods Appl. Mech. and Engr.*, **139**, 3-47, 1996; G. Li and N. R. Aluru , *Sensors and Actuators A*, **91**, 278-291, 2001). Meshless methods, also known as finite point cloud techniques, relies on a set of points to describe the underlying function; this coupled with the moving least squares approach for the construction of the interpolation function and Galerkin testing yields the element-free Galerkin (EFG) method.

The EFG method has been successfully applied in static and quasi-static electromagnetic field computation in two and three dimensions. This and all other formulations to date have relied on using scalar basis functions to discretize the solution domain. The main thrust of our work is to extend these approaches to tackle vector problems. To this end, we propose the development of vector basis functions that will then be used in the underlying computational scheme. The resulting algorithm is first validated by determining resonant modes of cavities. This scheme will then be extended to analyze loaded cavities.

0-7803-7846-6/03/$17.00 ©2003 IEEE

# Iterative Preconditioning of Three-Dimensional FE-BI Equation Systems

Thomas F. Eibert
FGAN-FHR
53343 Wachtberg, Germany

The finite element (FE) - boundary integral (BI) technique provides for an exact formulation of three-dimensional (3D) scattering and radiation problems. Early formulations appeared in the late 80es of the last century, however, it was quickly recognized that the equation systems resulting from standard discretizations are rather difficult so solve. Consequently, not many formulations were pursued over the years and later even doubts arose whether standard formulations are capable of producing accurate results at all (X.Q. Sheng, J.-M. Jin, J.M. Song, C.C. Lu, W.C. Chew, *IEEE Trans. AP*, pp. 303–311, Mar. 1998).
In this work, we consider a standard formulation based on the electric field integral equation (EFIE) discretized using a Galerkin procedure involving RWG basis functions on triangular meshes in the BI along with edge elements on tetrahedral meshes in the FE and in previous publications it was shown that the formulation is capable of producing accurate results. However, in the past we solved the linear system of equations by direct LU decomposition techniques restricting applicability of the algorithm to rather small problems. In order to tackle larger problems, the algorithm was extended by an iterative solver in conjunction with the multi-level fast multipole method for the fast evaluation of the BI matrix-vector products. Solving large problems involving irregular FE meshes requires a good preconditioner for the system matrix. Preconditioners are typically generated using a sparse approximation of the system matrix that is factorized by direct LU decompositions. However, during the factorization process new matrix elements (fill-ins) are generated and in order to keep computer resources little, most of these fill-ins must be suppressed. Experience shows that the preconditioner becomes easily useless if too many fill-ins are dropped and consequently the whole procedure may be very inefficient and its behavior is rather unpredictable. To avoid such problems, we employ an iterative preconditioning strategy related to that one proposed by Liu and Jin in (J. Liu and J.-M. Jin, *IEEE Trans. AP*, pp. 1212–1221, Sep. 2002.). In contrast to introducing a further local absorbing boundary condition operator into the formulation, our preconditioner is directly derived from the FE - BI equation system. As usual, we choose a sparse approximation of the FE - BI system and preconditioning operators are generated using a few iterations of the generalized minimal residual (GMRES) algorithm. Overall convergence of the iteration loop is very good and in contrast to incomplete LU decomposition techniques the behavior of the iteration loop can be controlled by adjustment of the iteration count in the preconditioner dependent on the observed convergence. Numerical results will be shown to demonstrate the usefulness of the proposed iterative preconditioning strategy.

0-7803-7846-6/03/$17.00 ©2003 IEEE

## A NEAR-FIELD PRECONDITIONER FOR FAST METHODS

***Michael A. Carr (carr.96@osu.edu) and John L. Volakis (volakis.1@osu.edu)**
ElectroScience Laboratory, EE Dept., The Ohio State University, Columbus, OH 43212

Approaches such as Fast Multipole Method (FMM) and Adaptive Integral Method (AIM) use specialized matrix vector products (MVP) in conjunction with iterative solvers to reduce the complexity of solving an electromagnetic problem directly. As a result, computational complexity is often reduced from the $\mathbf{O}(N^3)$ associated with direct LU factorization to as low as $\mathbf{O}(N \log N)$ while memory requirements are reduced from $\mathbf{O}(N^2)$ to $\mathbf{O}(N)$. The MVPs associated with fast methods, however, are non-trivial and can require significantly more time to compute when compared to traditional Method of Moments (MoM). Since electromagnetic problems typically result in poorly conditioned systems and require solution of many right-hand-sides (RHS), any reduction in the number of MVPs significantly decreases the total computation time required.

In the past, standard preconditioning techniques such as the Incomplete LU (ILU) and Approximate Inverse Preconditioner (AIPC) (Y. Saad. *Iterative Solutions for Sparse Linear Systems*. PWS Publishing Company, Boston. 1996.) have been used to improve the condition of the system matrix and reduce the overall number of MVPs required. While some improvement can be observed with these techniques, neither is specially tailored specifically for electromagnetic problems. Specifically, the ILU suffers from an uncontrollable non-zero pattern while the AIPC requires careful hand tuning for optimum performance. This paper proposes a new approach that uses the physics contained within the near-field (NF) terms of the system matrix to generate a preconditioner that has low computational complexity, requires little storage, and significantly reduces the total of MVPs required for convergence. Several typical electromagnetic examples are shown to validate the performance of the approach and demonstrate how computation of the NF preconditioner can achieve near-linear speedup in either shared- or distributed-memory parallel computing environments.

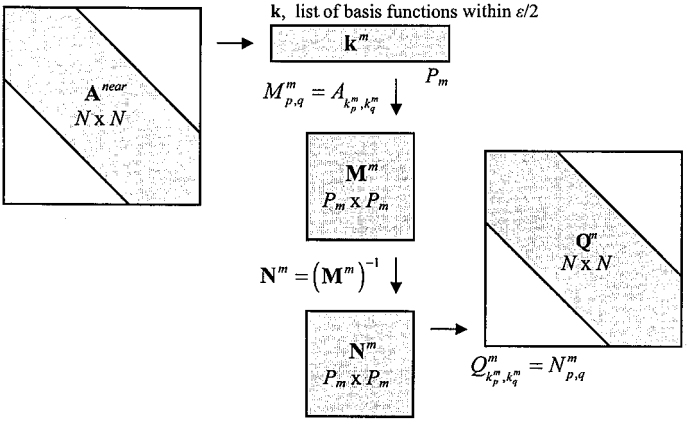


**Figure 1. Assembling the Near-Field Preconditioner Q from the system matrix A**

# An Improved Algorithm for Surface Field Calculations on Large Dielectric Covered Circular Cylinders using Asymptotic Techniques

Patrik Persson[*] [1], Björn Thors[1] and Roberto G. Rojas[2]

[1] Div. of Electromagnetic Theory, Royal Inst. of Technology, SE-10044 Stockholm, Sweden, Email: patrik@tet.kth.se

[2] ElectroScience Lab., Dept. of Electrical Eng., The Ohio State University, Columbus, OH 43212, USA, Email: rojas-teran.1@osu.edu

The analysis and design of conformal antennas is becoming more important as various commercial and military applications for this class of devices become prominent. Although a variety of methods have been proposed, most of them tend to be applicable for electrically small structures.

In a couple of previous papers (V. B. Ertürk and R. G. Rojas, *Trans. AP*, Oct. 2000 and P. Persson and R. G. Rojas, *Radio Science*, in print) an asymptotic Green's function technique has been presented for the calculation of surface fields on a PEC circular cylinder covered with a dielectric layer. The sources may be either waveguide fed apertures or microstrip antennas. The method presented in these papers is an efficient high frequency approximation and, thus, valid for large cylinders in terms of wavelengths. However, the method can be improved even further by modifying the algorithm.

The new method involves a deformation of the integration contour. But this deformation cannot be done arbitrarily since the positions of the Green's function poles $\left[\nu_m(k_z)=\nu'_m(k_z)-j\nu''_m(k_z)\right]$ must be considered. And, as will be explained, some non-trivial positions of the poles make the contour deformation more critical than expected. It turns out that the pole positions in the $\nu$-plane may move from the second/fourth quadrants to the third/first quadrants when evaluating the SDP integral at points away from the saddle point $(k_z \in \mathbb{C})$. However, by following the pole location trajectories, it is possible to find rules for how to navigate safely through the area in which poles can be found. With this information, the integration path can be safely deformed. Thus, the difficulties with highly oscillating and slowly decaying integrands in the old algorithm can be removed. As a result, a much faster and more accurate method is obtained. In addition, a physical interpretation of the poles (surface waves, leaky waves, etc.) can be obtained not only for real $k_z$ but for $k_z \in \mathbb{C}$ as well.

0-7803-7846-6/03/$17.00 ©2003 IEEE

# Comparison of Scattering Coefficients for Tapered Beams Generated Analytically or by Plane Wave Spectrum Decomposition

J.E. Roy

Communications Research Centre Canada
3701 Carling Ave., P.O. Box 11490, Station H
Ottawa, Ontario, Canada, K2H 8S2
jasmin.roy@crc.ca

## 1 Abstract

This presentation shows a comparison between the results obtained for computing the plane wave scattering (reflection and transmission) coefficients of a dielectric slab of known permittivity when the plane wave illumination is implemented by three differents methods. The first method corresponds to the infinite plane wave illumination. Its results are obtained analytically from computing the overall scattering matrix of the slab by cascading the scattering matrices for each interface and the scattering matrix for the transmission line representing the intervening dielectric propagation medium between the two interfaces, as per Reference [1]. The two other methods consist of generating an incident tapered beam as the excitation in FDTD simulations. The beam is tapered to avoid illuminating the edges of the slab and thus, to avoid generating diffracted rays which would otherwise corrupt the results. In the second method, the tapered beam is generated analytically throughout the computational domain. The resulting beam corresponds to an ideal tapered beam with uniform polarization throughout the beam and uniform intensity through the slab, but it is non-Maxwellian according to Reference [2]. In the third method, the tapered beam is generated by summing a finite number of infinite plane waves according to the technique of Reference [3]. The resulting tapered beam is Maxwellian but its polarization and its intensity are not perfectly uniform throughout the beam or through the slab, respectively. We want to see if using a non-Maxwellian tapered beam as the excitation in a FDTD simulation could create spurious responses or instabilities. Furthermore, we want to assess how successfully a tapered beam could be used in place of an infinite plane wave illumination for computing by FDTD simulation the scattering coefficients corresponding to the bulk material of the slab. The presentation shows also in detail the technique for carrying out the measurement of the reflection and the transmissions coefficients of the slab by FDTD simulation.

### REFERENCES

[1 ] J.E. Roy and L. Shafai, "Generalized Scattering Matrix and Symmetry Principles for Infinite Planar Structures", *Can. J. Phys.*, Vol. 75, 1997, pp. 413-431.

[2 ] Henning Braunisch, Yan Zhang, Chi O. Ao, Shih-En Shih, Y. Eric Yang, Kung-Hau Ding, Jin A. Kong and Leung Tsang, "Tapered Wave with Dominant Polarization State for All Angles of Incidence", *IEEE Trans. on Antennas and Propag.*, Vol. 48, No. 7, July 2000, pp. 1086-1095.

[3 ] J.E. Roy, "Tapering an Incident Plane Wave", submitted to *IEEE trans. on Antennas and Propag.*, January 2003.

0-7803-7846-6/03/$17.00 ©2003 IEEE 

# Spectral Methods in General Curvilinear Simplex Grids

Tian Xiao* and Qing Huo Liu
Department of Electrical and Computer Engineering
Duke University
Box 90291
Durham, North Carolina 27708

The ever-increasing need for the modeling of large-scale broadband electromagnetic problems has attracted intensive research in high-order and spectral time-domain methods. Examples of such methods are the pseudospectral time-domain methods, and high-order finite-element time-domain method, high-order discontinuous Galerkin method. Compared to the conventional finite-difference time-domain method, high-order and spectral methods are attractive because of their high efficiency and accuracy. However, so far most spectral methods have only used elements with straight faces, thus limiting the accuracy for curved geometries. In this work, we develop a spectral method based on a high-order simplex grid so that the element faces can be curved. With this discretization, the accuracy of the geometrical representation is compatible with that of the field interpolation scheme. The effects of discretization approximation on the accuracy of spectral penalty methods are studied for general high-order curved elements. For numerical implementation, the spectral method for 3D Maxwell's equations is developed with a quadratic simplex grid. Numerical results show the accurate discretization of the object geometry plays an important role in the simulation with spectral methods. The solution for the second-order discrete approximation of the quadratic simplex grid is much more accurate than that for the first-order discretization approximation of the tetrahedron grid. Furthermore, this quadratic simplex spectral method is more efficient that traditional linear simplex grid since it allows a much coarser grid for curved objects.

0-7803-7846-6/03/$17.00 

# Comparison of Optimum Mutation Rate for Continuous and Binary Genetic Algorithms

You Chung Chung*
youchung@ieee.org
Electrical and Computer Engr.
Utah State University
Logan, UT 84322
435-797-0784

Randy L. Haupt
randy.haupt@ece.usu.edu
Electrical and Computer Engr.
Utah State University
Logan, UT 84322
435-797-2840

## Abstracts

The genetic algorithm (GA) has been applied to many applications of electromagnetic optimization. Based on the complexity of a cost function and the number of a cost function calls, the convergence speed of a GA can be different. The number of cost function calls can be reduced by using an optimum population size and a mutation rate. The optimum mutation rate and population size of GAs have been studied for the binary and continuous parameter GAs. Recent studies show that a small population size with a high mutation rate converges faster than a large population size with a low mutation rate. The reference written by Back suggested a proper mutation rate (1/L) for a GA using binary parameters, where L is the number of bits in a binary chromosome. It is not an optimum mutation rate for all the binary GAs, but it gives rough range of optimum mutation rate generally.

While a continuous GA uses the continuous N parameters in a chromosome directly, a binary GA uses the encoded binary N x K bits in a chromosome where K is the number of bit per parameter. In a population size (P), possibly N x P parameters can be mutated in the continuous GA, and there are N x K x P bits can be mutated with a give mutation rate (M%). While numbers of mutated parameter of the continuous GA will be (N x P x M%/100), the number of mutated bits of binary GA will be (N x K x P x M%/100) bits. There are different numbers of mutated parameters in the GAs due to the different representations with a given mutation rate. Therefore, the mutation rate of a continuous GA should be different from a binary GA with the mutation process explained above.

It is nice to use continuous GA since there is no encoding and decoding processes and it allows a GA to save time to converge without the encoding and decoding process. Based on the statistical analysis among the GAs using binary and continuous representations and simulation of GAs with many EM applications using different cost functions, the relationship between optimum mutation rates for GAs using continuous and binary representation are compared.

0-7803-7846-6/03/$17.00 ©2003 IEEE

**Genetically Optimized Two-Dimensional Fractal-Random Arrays**

Joshua S. Petko* and D. H. Werner
The Pennsylvania State University
Department of Electrical Engineering
University Park, PA 16802
jsp160@psu.edu and dhw@psu.edu

In has been known to antenna engineers that periodic arrays can be used to effectively suppress radiation pattern side-lobes with just a small number of elements but are more susceptible to effects from element failure. Random arrays on the other hand are more robust in terms of element failure but are not typically able to suppress side-lobe levels as effectively as their periodic counterparts. In an effort to design robust arrays which are able to effectively reduce side-lobe levels, a compromise was proposed that included both fractal and random features called the fractal-random array (Y. Kim and D.L. Jaggard, *Proc IEEE.*, **74** (9), 1278-1280, 1996; D.H. Werner and R. Mittra, *Frontiers in Electromagnetics.*, Ch. 3, 96-100, 1999). Fractals are objects that have a self-similar structure repeated periodically throughout their geometry produced by the repeated application of a simple Euclidian structure called the generator. In order to introduce randomness into a fractal-random array, one can randomly choose from several different generators and apply them at different stages of the fractal structure. In this way fractal-random arrays can possess good qualities of both the periodic and random classes of arrays.

Not every fractal-random array configuration is capable of producing radiation patterns that have low side-lobe levels. In fact, often the designs with the most optimal solutions call for unconventional array layouts that may not be obvious to the antenna engineer. A technique based on genetic algorithms will be introduced as a design tool for optimizing the performance of fractal random arrays. Genetic algorithms are useful because they allow antenna designers to optimize radiation parameters by creating a large population of candidate antennas. The laws of natural selection are then applied to the population in order to evolve an effective layout scheme. Fractal-random arrays are ideally suited for optimization via genetic algorithms because their self-similarity can be exploited to reduce the number of calculations needed to be performed for each antenna, thus making it possible to find solutions for much larger antenna arrays. The purpose of this paper is to present a methodology for optimizing the layout of fractal-random arrays by using a novel genetic algorithm technique in conjunction with fractal tree theory. The genetic algorithm breaks the data (chromosome) representing each antenna structure apart into smaller pieces called subchromsomes, which contain the genes for each individual tree branch. This process allows the various genetic manipulations to be performed at a subchromosome level, providing an effective means of evolving optimal fractal-random arrays that vary widely in size, structure, and even number of elements. This genetic algorithm approach shows that fractal-random arrays can be designed to be effective in suppressing radiation pattern side-lobes and yet remain relatively robust with respect to element failure.

0-7803-7846-6/03/$17.00 ©2003 IEEE

## Electromagnetic Coupling through Slot Apertures into Cavities with Loaded Wires

Russell P. Jedlicka*+, Brian A. Lail++, Steven P. Castillo+
+Klipsch School of Electrical & Computer Engineering, New Mexico State University, Las Cruces, NM 88003 {rjedlick, scastill}@nmsu.edu
++School of Electrical Engineering and Computer Science, University of Central Florida, Orlando, FL, 32816, blail@mail.ucf.edu

Electromagnetic coupling is a critical factor in electromagnetic compatibility (EMC) and electromagnetic interference (EMI). The coupling to structures through slot apertures has gained much attention and has been investigated by a variety of authors in the past. The techniques vary but the main goal is to estimate a bound on the signals coupled to a given system. Due to the complexity of real-world systems, it is generally not possible to model the structure in its entirety. Thus, most methods identify the major features of the system and model them using appropriate electromagnetic techniques.

The hybrid method presented here uses the transmission line model of Warne and Chen (IEEE Transactions of EMC, Vol EMC-34, No. 3, August 1992), which is solved via the method of moments (MOM), to model the aperture. This model incorporates slot depth, wall losses and allows gaskets to be incorporated in a simple and straightforward fashion. The interior of the cavity is solved using the finite element method (FEM) (Jedlicka, Castillo and Warne, IEEE Transactions on Antennas and Propagation, Vol AP-48, No. 3, March 2000) – it allows metallic and lossy dielectric objects to be included within the cavity region. Wires within the cavity, which can significantly alter the frequency response and coupling level, are included via a filamentary MOM representation. The model presented here is based upon that of Lail and Castillo (IEEE AP-S International Symposium and USNC/URSI Radio and Science Meeting, Volume III, pp. 290-293, 16-20 June 2002, San Antonio, Texas.); however, the moment method boundary conditions are modified to incorporate loads on and at the ends of the wires.

The basic formulation is predicated on the following integro-differential equation,

$$\left[2H_{1,M,z}(a,z)+\frac{\Delta Y_L}{2}\frac{d^2I_M(z)}{dz^2}-\frac{\Delta Y_C}{2}I_M(z)\right]-H_{2,J,z}(\rho_o,z)-\Delta H_z(\rho_o,z)=-2H_{inc,z}$$

$H_{inc,z}$ is the component of the incident field aligned with the slot (here oriented along the z axis), $H_{1,M,z}$ and $H_{2,J,z}$ are the magnetic fields due to the magnetic current along the equivalent antenna representing the slot aperture and the electric current along the wire, respectively. $\Delta H_z$ is the difference field obtained by solution of the FEM problem.

In addition to the formulation of the problem and computer implementation of the code, an experimental setup was constructed and the electromagnetic coupling to a cavity, through narrow slot apertures, was measured for a variety of wire and load conditions. The presence of an unloaded wire impacts the coupling to the cavity, the variation depends upon the orientation of the wire with respect to the major fields within the structure. Loads on the ends of the wire further modify the result. The numerical computations are compared to measured results for a variety of configurations and load conditions. For example, placing 50 Ω loads on the ends of the wire modifies the peak coupling level by 10 – 15 dB or more.

0-7803-7846-6/03/$17.00 ©2003 IEEE

# Time domain finite element analysis of the transient electric field penetration through thin slit apertures on rectangular enclosures

Daniel L. Faircloth*, Dr. Michael E. Baginski†
Dr. Manohar D. Deshpande‡

Dept. of Electrical and Computer Engineering,
Auburn University, Room 423 Broun Hall,
Auburn, Alabama, 36849, USA

E-mail D. Faircloth:faircdl@eng.auburn.edu

**Abstract**

A time domain finite element technique is presented to determine the transient electromagnetic fields present resulting from thin slit aperture penetration on rectangular conducting enclosures. The purpose of the study is twofold: 1) A comparison of the resulting transient fields is done using a Fourier transform methods of the results and contrasting them to a method of moments solutions (MOM), and other methods for both verification purposes and to investigate the possible presence of highly damped transient evanescent modes. 2) Investigation of the shielding effectiveness of a rectangular enclosures for typical transient events on enclosures with thin slit apertures (e.g., lightning and EMP).

Determination of the electromagnetic fields in within the cavity assumes the electromagnetic wave is normally incident on the enclosure with and has a Gaussian temporal structure but otherwise consistent with standard plane wave excitation. Maxwell's equations are solved with the appropriate boundary conditions for the unknown aperture transient fields. Numerical data of EM shielding effectiveness of a rectangular box with a single aperture and multiple apertures is discussed in addition to earlier published data.

Several simulations forced a restriction that allowed only the dominant modes to develop in the cavity. Both time domain and frequency domain FEM simulations were done and the results of these simulations were found to be in excellent agreement with the published the work of Desphande [*Digital Avionics Systems Conference, 1999*]. An Expansion of this method to investigate the behavior of multiple apertures and aperture sizes is also done and resulting transient field signatures are discussed and compared to previous work and measurements. The complete solution without restrictions allowed the development of higher order modes and showed excellent agreement with corresponding measurements. Analysis of the problem results in a system of time-dependent partial differential equations in Cartesian coordinate forms. The system of equations is solved with the positive definite normal equations of the forms A**T*A*x = A**T*b and a least squares finite element method used for the solution.

*Supported by NASA graduate fellowship
†Supported by a grant form NASA
‡Research scientist at NASA Langley, VA

0-7803-7846-6/03/$17.00 ©2003 IEEE

# ELECTROMAGNETIC SCATTERING DUE TO POLYGONAL SHAPED THIN METALLIC PLATES USING HYBRID ELEMENTS

*M. D. Deshpande, NASA Langley Research Center, Hampton VA*


## SUMMARY

Electromagnetic (EM) scattering analysis of polygonal shaped metallic plates can be accomplished by using various numerical techniques. One of the widely used techniques is the MoM in which a polygonal plate is first discretized into number of triangular patches called subdomain patches. The unknown surface current density on these subdomains is then expressed in terms of well known Rao-Wilton-Glisson (RWG) (S. M. Rao, D. R. Wilton, and A. W. Glisson, IEEE Trans. On Antennas and Propagation , Vol. AP-30, no. 3, pp. 409-418, May 1982) basis functions and determined using the EFIE in conjunction with the method of moments. Although, the triangular meshing and use of RWG basis functions is very popular and matured concept, the non-vanishing normal component of surface current on one of the inclined edges of sub-domain triangles attached to open /boundary edge of polygonal plate will give a non-zero normal component of the surface current. However, the non-zero normal component of the surface current on the boundary edge will approach zero when very fine discretization is used in the region close to the open/boundary edges. This problem will not arise if one uses a subdomain element (near the bounary) whose edges will be either along the boundary or normal to the boundary. For example, a quadrilateral element can be assigned to open/boundary edges of polygonal plate to satisfy such requirement. Use of quadrilateral elements along the open/boundary edges and trinagular elements over the interior region will improve the convergence of the MoM solution.

In this paper a numerical method will be presented to estimate electromagnetic scattering due to polygonal shaped thin metallic plates using 1) trinagular, 2) quadrilateral, and 3) triangular/quadrilateral meshing. Through numerical examples, advantages and disadvantages of each scheme will be demonstarted as far as the numerical convergence is concerned. Figure 1a shows a triangular plate with a triangular hole (a = 5.08cm, b= 2.54 cm, frequency =11.811GHz). Figure 1b shows monostatic EM scattering due to the plate (shown in Fig . 1(a)) illuminated by E-polarized plane wave in the y-z plane using pure triangular and quadrilateral meshing schemes .


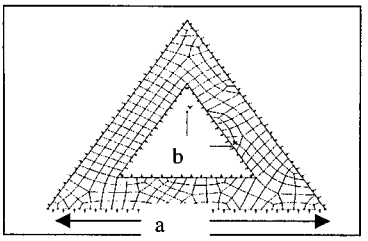


Figure 1(a)

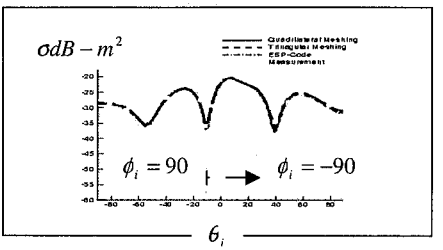


Figure 1(b)

## Scattering and Coupling in Circuits and Components

**Co-Chairs:** V. Jandhyala
W. Davis

10:00 Opening Remarks

93. 1 10:00 Coupled Circuit-Electromagnetic Simulation with Time Domain Integral Equations ..... APS
*C. Yang, V. Jandhyala, University of Washington, USA*

93. 2 10:20 Scattering Parameters for Nonlinear Devices, Measurement and Simulation ..... 452
*W. A. Davis, Virginia Tech, J. B. Call, Silicon Semiconductor Corp, USA*

93. 3 10:40 Evaluation of Green's Function Integrals in Conducting Media ..... APS
*S. Chakraborty, V. Jandhyala, University of Washington, USA*

93. 4 11:00 Coupling in Some Edge-coupled Microshield Transmission Lines ..... APS
*B. Guo, X. Dong, W. Yin, Y. Gan, Temasek Laboratories, Singapore*

93. 5 11:20 Integral Equation-Based Coupled Electromagnetic-Circuit Simulation in the Frequency Domain ..... APS
*Y. Wang, D. Gope, V. Jandhyala, R. Shi, University of Washington, USA*

93. 6 11:40 Electromagnetic Scattering from a Multilayered Cylindrical Waveguide ..... APS
*F. Seydou, University of Oulu, Finland, R. Duraiswami, University Maryland, USA, T. Seppanen, University of Oulu, Finland*

# Scattering Parameters for Nonlinear Devices, Measurement and Simulation

**William A. Davis*** (wadavis@vt.edu), Virginia Tech Antenna Group
Bradley Dept. of Elec & Comp Engr, Virginia Tech, Blacksburg, VA 24061-0111
**John B. Call**, Silicon Semiconductor Corp, Durham, NC 27713

A three-port representation of a nonlinear device as a function of drive level can be obtained with a few relatively simple measurements. This characterization is used to analyze and simulate device performance for a range of large-signal drive levels. Using the three-port model, designers may make use of the results in their circuit simulations rather than depend solely on manufacturer data. The technique is applied to high power transistors in this paper.

The Reflect-Thru-Line (RTL) measurement system was developed by Davis (URSI/USNC, Boulder, 1993) as a 1-way two-port alternative to TRL for scattering parameter measurements on nonlinear devices under high drive-level conditions. This system was used to obtain *S*-parameter measurements on several commercially available power transistors that previously had been considered unmeasurable because of their high gain and capability for large output levels.

Using the three-port model, a device can be characterized using *S*-parameter measurements as a function of drive level. Advantages of a three-port device representation are 1) any two-port nonlinear device dominated by a single non-linearity can be represented — ideal for characterizing devices using new physical structures or exotic materials and RFIC or MMIC devices which are not adequately handled by existing models; 2) most functional RF design labs have the measurement equipment required to extract a three-port model. The extracted three-port model parameters were found to provide an excellent fit to measured power sweep data with only minor limitations. Though the effort required to obtain a three-port model is minimal, the information and insight available from the model make it possible for high-power amplifier designers to adopt tools and techniques that have previously been available only to small-signal circuit designers. The current system does not account for harmonic loading, but no serious variations were found due to this omission.

A simulation of load-pull measurements was run using the three-port model for two high-power devices and compared to measured load-pull data. Gain contours were compared with measured gain contours for three different power levels. At low drive levels the simulation and measured contours were in close agreement. As the power levels increased, the simulated and measured contours began to diverge, most likely due to device heating. The latter device heating problem must also be overcome with existing modeling approaches to account for the thermal properties of the device separately from the RF properties.

0-7803-7846-6/03/$17.00 ©2003 IEEE 

## Electromagnetic Education

**Co-Chairs:** D. Kelley
D. Voltmer

7:55 Opening Remarks

96. 1 8:00 Transformation of Unit Vectors To Facilitate Evaluation of Vector Potentials ..... APS
*S. J. Weiss, US Army Research Lab, USA*

96. 2 8:20 Undergraduate Electromagnetics for the Future: Discrete, Numeric, and Analytic ..... APS
*D. R. Voltmer, Rose-Hulman Institute of Technology, USA*

96. 3 8:40 A Software Tool Based on the Finite Element Method for Electromagnetic Education... APS
*D. Sánchez-Repila, L. E. García-Castillo, Universidad de Alcalá, Spain*

96. 4 9:00 A Matlab Application Programmer Interface For Educational Electromagnetics..... APS
*S. Selleri, University of Florence, Italy*

96. 5 9:20 A PROJECT-BASED GRADUATE ANTENNA COURSE .....454
*E. Arvas, M. Hasanovic, S. Tozin, T. Imeci, S. Arvas, L. Kuzu, Syracuse University, USA*

96. 6 9:40 A Practical Approach To Education of Electromagnetic Compatibility at the Undergraduate Level..... APS
*Y. Zhao, Nanjing Normal University, China, K. See, Nanyang Technological University, Singapore*

# A PROJECT-BASED GRADUATE ANTENNA COURSE

Ercument Arvas, Moamer Hasanovic*, Samir Tozin, Taha Imeci,
Serhend Arvas, and Lokman Kuzu

Dept. of EECS, Syracuse University, Syracuse, NY 13244

A project-based graduate course on Microwave Planar Antennas was developed and taught at Syracuse University twice. A basic antenna course was prerequisite for the course. During the first half of the semester, the theory of the microstrip antennas was studied. Then students were divided into small groups of two or three and each group was required to design, simulate, build and test a microstrip antenna or an array of them. These are typical steps that an antenna engineer follows in industry. Some groups received design specs from local industry while others chose their problems from the literature. The initial design was based on the theory provided in the first half of the course. The simulations were carried out using different commercial software available in our lab. The optimized designs were then built and tested in our microwave lab or in the facilities of local microwave industry. Each group prepared a final report for their projects and presented their results to an audience of experienced antenna engineers from the local industry. One of the projects was an X-Band Quasi Yagi Antenna. The center frequency was 10GHz with 40% bandwidth and 50 Ohm input impedance. An end-fire beam with linear polarization was required. The antenna was built on a 25 mil thick substrate with relative dielectric constant of 10.2 and loss tangent of 0.0023. The antenna was printed on the substrate using a milling machine we have in our microwave lab. The size of the finished product was less than 15mm by 15mm. The simulated and measured results for the VSWR were in excellent agreement. The measured and simulated antenna gain patterns showed satisfactory agreement. Results for this and other projects will be presented during the meeting. This practical, project-based graduate course was very well received by the industry and the students.

0-7803-7846-6/03/$17.00 ©2003 IEEE 

## EMI Measurements

**Co-Chairs:** A. Thansandote
D. Hill

10:00 Opening Remarks

# STATISTICAL PROPERTIES OF FIELDS IN REVERBERATION CHAMBERS

David A. Hill
Radio Frequency Technology Division
National Institute of Standards and Technology
Boulder, Colorado 80305
USA

The use of reverberation chambers (also called mode-stirred chambers) for electromagnetic compatibility (EMC) measurements has increased rapidly during the past decade. Reverberation chambers are electrically large, multimoded cavities that use either mechanical stirring or frequency stirring to create statistically uniform fields. Reverberation chambers are reciprocal facilities that are equally useful for radiated immunity and emissions measurements. They are particularly advantageous for high-power immunity testing because the high Q of the cavity allows the generation of high field strength with modest input power.

The interpretation of reverberation chamber measurements requires a thorough knowledge of the statistical properties of the electric and magnetic fields throughout the chamber. A plane-wave integral representation (D.A. Hill, *IEEE Trans. Electromag. Compat. 40*, 209-217, 1998) has been found useful for predicting field properties and responses of test objects and reference antennas in reverberation chambers. For well-stirred fields, the ensemble averages (obtained from mechanical stirring) of the electric and magnetic fields are zero, and the averages of the squared electric and magnetic fields are spatially uniform with a ratio equal to the square of the free-space impedance. The fields are completely depolarized, and the rectangular components are uncorrelated. All of these properties have been verified by three-axis electric and magnetic field probe measurements. Field probability density functions have also been derived and verified experimentally.

Spatial correlations of the fields and energy density are important in understanding the responses of electrically large antennas or test objects with separated entry points (apertures). Spatial correlation functions have been derived for the total electric (or magnetic) field, electric and magnetic field components, and the energy density. Some of these correlation functions have been verified by measurements with separated receiving antennas (D.A. Hill and J.M. Ladbury, *IEEE Trans. Electromag. Compat. 44*, 95-101, 2002).

Most reverberation chambers are constructed in the shape of a rectangular box. For this shape, it is possible to use multiple image theory to derive the field properties near the chamber walls and corners as well as in the central region of the chamber. Expressions that satisfy the wall and corner boundary conditions (tangential electric and normal magnetic fields equal zero) have been developed. These expressions reduce to the expected uniform-field expressions at large distances from the walls and corners. These results are helpful in determining the useful (uniform-field) test volume of reverberation chambers.

0-7803-7846-6/03/$17.00 ©2003 IEEE 

## RF Field Mapping System for Cellular Base Stations

G. B. Gajda*, A. Thansandote, E. Lemay, P. Lemyre & J. P. McNamee
Consumer & Clinical Radiation Protection Bureau, Health Canada
(Phone: 613-954-0309, e-mail: greg_gajda@hc-sc.gc.ca)

Opposition to cellular base station siting based on concerns about possible adverse health effects persist. Reports of research linking electromagnetic energy from mobile handsets to cancer fuel these fears despite the obvious difference in exposure levels between handset and base station emissions. Allaying these fears using existing data for base station emissions, if available, is difficult since it usually consists of spot measurements taken many months or years previously. The general public's belief that the build-out of additional services is accompanied by a concurrent rise in power levels generally leads to suspicion of the old data. There is a desire to know current emission levels especially in residential areas, school zones and hospitals.

The goal of this work is to develop specialized instrumentation for measuring the patterns of radiofrequency (RF) field intensity in areas near base stations. We have developed low-cost, portable equipment capable of measuring the total RF power density (PD) in the two mobile cellular bands (800 MHz and 1900 MHz) versus geographic position measured with a Global Positioning Satellite (GPS) receiver. The equipment consists of a dual band antenna/diplexer, a direct conversion receiver for each band, an analog-to-digital converter (ADC) and the GPS receiver (Magellan Meridien). A photograph of an early prototype (less the GPS) is shown below along with its block diagram.

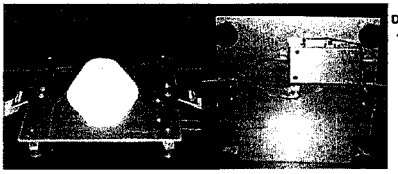

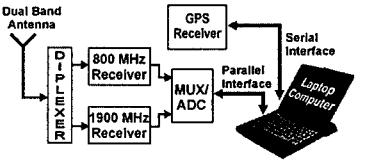


Digitally sampled PD outputs are fed to the parallel port of a laptop computer while the GPS data is read from a serial port. The software controls selection of the band, timing of the readings and storage of the data in text files for later use with a spreadsheet. For vehicle mounted operation, measurements can be taken at either regular time or distance traveled intervals. An example of vehicular measurements (800 MHz) taken in the city of Ottawa is shown in the plot below. All PD levels are referenced to the Canadian Safety Code 6 exposure limit for the 800 MHz band.


0-7803-7846-6/03/$17.00 ©2003 IEEE

# A Measurement Method for Magnetic Antenna Factor of Small Circular Loop Antenna by 3-Antenna Method

Masanori Ishii* Masanobu Hirose Koji Komiyama
National Institute of Advanced Industrial Science and Technology,
National Metrology Institute of Japan

**Background:**

In the field of electromagnetic interference and electromagnetic compatibility (EMI/EMC), it is important to exactly measure the radiating magnetic field. In order to measure the magnetic field strength, a receiving loop antenna's antenna factor must be exactly determined, too. In this paper, a measurement method for the magnetic antenna factor of a small circular loop antenna using a 3-antenna method is described. The frequency range is less than 30MHz. The result of the 3-antenna method on magnetic antenna factor is compared with a theoretical one and it is confirmed that these results agree with each other.

**A proposed 3-antenna method:**

A loop antenna behaves as a small antenna at the low frequency. The magnetic antenna factor is defined as the ratio of the incident plane magnetic field strength to the output voltage of the matched load. However, it is difficult to obtain a quasi far-field condition or apply the plane wave to the loop antenna at the low frequency. So the averaged magnetic field over the aria of the receiving loop is generally used instead of the plane magnetic field. (F. M. Greene, "The Near-Zone Magnetic Field of a Small Circular-Loop Antenna", J. of R. NBS-C, EI, Vol. 71C, No.4, Oct.-Dec. 1967.) A 3-antenna method defined by the averaged magnetic field is expressed as Equation (1).

$$F_m(\omega) = \sqrt{\frac{-A_{32}}{A_{21}A_{13}}\frac{\alpha_{21}\alpha_{13}}{\alpha_{32}}} \quad [S/m], \qquad \cdots \quad (1)$$

where

$$\alpha_{ij} = \frac{\sqrt{1+k^2R_{ij}^2}}{j\omega\mu_0\pi Z_0 R_{ij}^3}\left\{1+\frac{15(r_j r_i)^2}{8R_{ij}^4}+\frac{315}{64}\frac{(r_j r_i)^4}{R_{ij}^8}\right\}, \qquad R_{ij} = \sqrt{d^2+r_i^2+r_j^2},$$

$F_m$ : magnetic antenna factor, $k$ : wavelength constant ($=2\pi/\lambda$), $A_{32}, A_{21}, A_{13}$ : transmission S-parameters between antennas, $\omega$ : angular frequency, $\mu_0$ : permeability of free-space, $Z_0$ : load matched to the line impedance, $r_1, r_2, r_3$ : radiuses of loop antennas and $d$ : distance between the two loops.

**Comparison the result of a proposed 3-antenna method with theoretical one:**

The input impedance of a small loop antenna ($Z_{in}$) is obtained theoretically. ( J. E. Storer, "Impedance of Thin-wire Loop Antennas, AIEE. Trans. Vol. 75, Part1, No.27, pp.606-619, Nov. (1956)) It is possible to calculate the theoretical magnetic antenna factor of a small loop antenna from $Z_{in}$ and Faraday's law. In Fig.1, the magnetic antenna factors by the proposed 3-antenna method simulation and the theory are exactly same. The frequency range is from 10kHz to 30MHz. The radius of the loop is 10cm. The diameter of the antenna element is 3mm. The distance of the two antennas is 2m. For this 3-antenna method, the transmission S-parameters are calculated by the moment method. The difference between these results is 0.13dB at the maximum. The result confirms that the proposed 3-antenna method is effective.

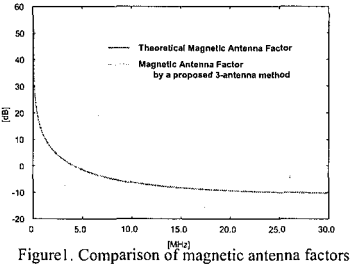


Figure1. Comparison of magnetic antenna factors

# Experiment Study on Performance for LISN-based Networks Applied in EMI Measurement

Yang Zhao
Nanjing Normal University, School of EEE, Nanjing 210042, China
Kye Yak See
Nanyang Technological University, School of EEE, S'639798, Singapore

Currently , the most common test instrument for conducted emission measurement is line impedance stabilization network (LISN). Though LISN is a specified standard EMC measurement instrument , it can only measure the total conducted EMI on the power lines but can not be utilized to detect mode currents like common-mode and different-mode current(CM/DM). Paul. Presented a CM/DM diagnosis network (CM/DM DN) (Paul and Hardin, IEEE Trans. MEC Vol.30, p553-560, 1988 ), but it can only detect single-mode EMI noise with a mechanic switch, which may bring the affects on network performance of discriminating capability at high frequency. Then See presented another network that employs two transformer with center-tapped and no switch appeared in network. (See, Electronic Letter., Vol.35, p1446-1447, 1999). Mardiguian proposed a very simple network which only use one transformer (Mardiguian, IEEE Int.Sym.EMC,Vol.2, p882-886, 1999). However up to date, no complete dada can be found in hand on performance of network for those networks. In this paper, the test setup in laboratory is developed based on splitter as seen in Fig.1. By using this technique, the insertion loss and mode-rejection ability can be measured for both common-mode and differential-mode noise in easy way, and measurement data are obtained in frequency range of 10Khz ~30MHz. Hence, these networks may be compared with each other for bset choice in use. Further, application example for switched mode power supply (SMPS) conductive EMI measurement is done, as illustrated in Fig.2

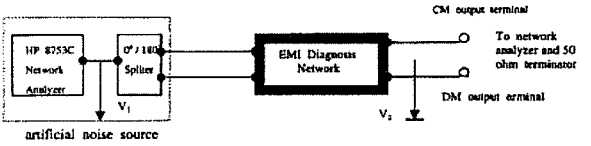


**Fig.1** Test setup for performance testing of CM/DM diagnosis network

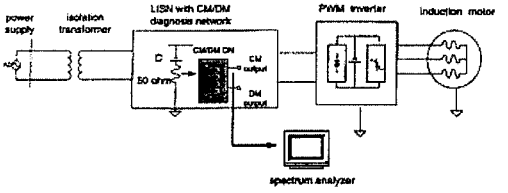


**Fig.2** Conducted EMI measurement for switched-mode power supply by using CM/DM DN

0-7803-7846-6/03/$17.00 ©2003 IEEE

## Propagation and Instabilities in Plasmas

**Co-Chairs:** L. Dyrud
Q. Zhou

7:55 Opening Remarks

98. 1 8:00 Electron Hole Resistivity in Space Plasmas ..... 462
*L. P. Dyrud, M. M. Oppenheim, Boston University, USA*

98. 2 8:20 A Preliminary Investigation of the Pseudospectral Numerical Solution of the Perkins Instability Equations ..... 463
*Q. Zhou, J. Mathews, Q. Du, Penn State University, C. Miller, La Follette School of Public Affairs, USA*

98. 3 8:40 Propagation of EM Waves in a Bounded Plasma Region ..... 464
*A. A. Helaly, E. A. Soliman, A. A. Megahed, Faculty of Engineering, Cairo University, Egypt*

98. 4 9:00 Quasi-Electrostatic Z-Mode Propagation Observed in the Two-Point OEDIPUS-C Experiment ..... 465
*G. James, Communications Research Centre Canada, Canada*

98. 5 9:20 Stochastic Model of Electromagnetic Signal Propagation in the Turbulent Flow with Resonance Absorption ..... 466
*V. G. Spitsyn, L. N. Kudryashova, Tomsk Polytechnic University, Russia*

98. 6 9:40 Noise Radiation of Electron Flow Interacting with Undulator System Electromagnetic Fields ..... 467
*A. N. Jezmer, B. P. Yefimov, Institute if Radiophysics and Electronics of NAS of Ukraine, Ukraine*

# Electron hole resistivity in space plasmas

L. P. Dyrud* and M. M. Oppenheim
Center for Space Physics, Boston University
725 Commonwealth Ave, Boston, MA 02215
(e-mail: ldyrud@bu.edu)

**Abstract**

Phase-space electron holes are seen in simulations, laboratory plasmas, and many regions of the Earth's space environment. We present simulations of beam plasmas showing that the generation and decay of electron holes results in a reduction of electron current, implying a parallel resistivity. This resistivity occurs in simulations where a cold electron beam is coincident with a warmer background plasma, and appears to be mediated by the generation of ion acoustic waves propagating obliquely to the magnetic field. The electron holes initially scatter electrons in the beam direction thus steepening the electron beam distribution, which launches and drives ion acoustic waves that cause resistivity and are also responsible for strong ion heating perpendicular to $\vec{B}$. Resistive effects occur in both strongly and weakly magnetized plasmas. Given that electron holes are observed in many space plasmas, these results have important implications for a number of magnetospheric and auroral ionospheric processes. For auroral plasmas, electron hole resistivity could support parallel electric fields on the order of 10 mV/m, which could account for parallel potential drops of the order of kV. The same simulations replicate a number of additional features observed in the auroral downward current region, including, ion conic distributions, electrostatic whistler waves (thought to be the source of VLF saucers). Turbulent electron hole resistivity also explains the observed non-linear relationship between downward current and potential. For the magnetopause, simulations show effective collision rates of 0.008 per $\omega_{pe}^{-1}$, which could provide dissipation and diffusion across the boundary.

Date: January 15, 2003

Paper Title: Electron hole resistivity in space plasmas

1) URSI Commission: H Plasma Physics of the Auroral Acceleration Region

2) The paper to be presented contains new results from computer plasma simulations of electron holes. We demonstrate that under certain conditions the generation and decay of electron holes induces a parallel resistivity. This resistivity may aid diffusion and support substantial field aligned potential drops along auroral fields lines and other space plasmas.

3) This paper relates to plasma and laboratory simulations of electron holes, but has particular importance for understanding auroral ionosphere observations made by the FAST satellite.

0-7803-7846-6/03/$17.00 ©2003 IEEE

# A Preliminary Investigation of the Pseudospectral Numerical Solution of the Perkins Instability Equations

Qina Zhou* and John D. Mathews
Communications and Space Sciences Laboratory, The Pennsylvania State University, University Park, PA 16802-2707 USA, JDMathews@psu.edu

Qiang Du, Dept. of Mathematics, The Pennsylvania State University, University Park, PA 16802

Clark A. Miller, La Follette School of Public Affairs, 1225 Observatory Drive, Madison, WI 53706. Email: miller@lafollette.wisc.edu

A pseudospectral method code has been developed to simulate the electrodynamic turbulence (spread-F) behavior of the mid-latitude ionosphere by numerically solving two of Perkins' equations (Journal of Geophysical Research, 78, 218-226, 1973). This work follows that of Miller (Ph.D. thesis, Cornell university, 1996) and provides significant extensions in both the solution method and the solution results. For example, in the instability linear-growth stage, the simulation result is very consistent with Perkins' prediction yielding relative differences of less than 0.5%. A random initial condition case like that of Miller (1996) is then carried out and the results agree with Miller's approach. In addition, the effect of non-linearity of the system is observed—the damping region of the linear stage in wave vector space now exhibits growth regions. Results also indicates that over a large wavelength range, self-similar ionospheric structures (Mathews et al., Geophysical Research Letter, 28, 4167-4170, 2001) can be generated in potential and conductivity (the field-line integrated electron concentration is constant). By using two-mode excitation with suitable parameters, saturation of the instability process is observed—an example is presented. We additionally show that some two-mode excitation processes are much different from that of the single mode excitation in many aspects—especially in wavelength dependence. It is found that the saturation state is related to the fundamental mode wave vector, the perturbation amplitudes of the fundamental mode and the secondary mode, electric field, etc. On the other hand, some two-mode excitation processes do not display a saturation state. In this case, the process follows the path of the corresponding single mode excitation. Reasons are discussed.

0-7803-7846-6/03/$17.00 ©2003 IEEE 

# Propagation of EM Waves in a Bounded Plasma Region

A. Helaly*, E. A. Soliman and Adel A. Megahed,
Department of Engineering Physics,
Faculty of Engineering, Cairo University,
Giza 12211, Egypt

- A. Helaly is currently with Phys. Dept., Sohar college of Educ., Sultanate of Oman, P.O.Box : 135, Postal Code : 311

## Abstract

In recent years there has been a definite trend toward using plasmas as absorbers or reflectors of the electromagnetic radiation depending on a specified application. Such study is very important to find out the suitable parameters of the plasma which affect the electromagnetic energy. Studying the electromagnetic waves interaction with a stratified layered media can be carried out using either analytical or numerical methods.

An analytic technique is developed to calculate the reflection, absorption and transmission of electromagnetic waves by a bounded plasma region. The model chosen for this study is a magnetized, cold, steady-state, two dimensional, non uniform plasma slab, which is presented by a number of parallel flat layers. It is assumed that the electron density is constant in each layer such that the overall electron density profile across the slab follows any prescribed distribution function. The proposed technique is referred to as scattering matrix model ( SMM ). The incident wave is a transverse electromagnetic plane wave (TEM ). The fields in each layer are written in the form of summation of the appropriate eigen functions weighted by unknown scattering coefficients. The coefficients are determined via the application of the appropriate boundary conditions at each interface. The effect of varying the wave frequency as well as the plasma parameters on the degree of reflection, absorption and transmission are investigated. Referring to the numerical results, it is found that the main function of plasma slab has been greatly dependent on the wave frequency. Also, the degree of reflection and transmission has been found to be affected by the plasma parameters. A sample of numerical results will be presented and discussed.

0-7803-7846-6/03/$17.00 ©2003 IEEE 

# Quasi-Electrostatic Z-Mode Propagation Observed in the Two-Point OEDIPUS-C Experiment

H.Gordon James
Communications Research Centre Canada
Ottawa, Ontario K2H 8S2 Canada
gordon.james@crc.ca

The OEDIPUS-C rocket double-payload experiment was carried out in the auroral night-side ionosphere. Waves were emitted from a double-V dipole on a transmitting subpayload and received at a distance of about 1200 m on a similar dipole connected to a synchronized receiver. Z-mode waves were observed at frequencies $f$ in $max\{f_c, f_p\} < f < f_{uh}$, where $f_c$ is the electron gyrofrequency, $f_p$ the plasma frequency, and $f_{uh}$ the upper-hybrid-resonance frequency. The separation vector between the transmitter and receiver lay along a direction at about 5° from the axis of the Earth's magnetic field **B**. In addition to ordinary (O) mode pulses with group speeds close to $c$, strong, highly dispersed Z-mode waves were transmitted at frequencies just below $f_{uh}$. These measurements are related to similar observations of strong, highly delayed echoes seen on the ISIS sounders at the same frequencies. An investigation of the quasi-electrostatic Z mode propagation has been carried out using solutions of the complete electromagnetic hot-plasma dispersion. It is found theoretically that there are no solutions at the working frequency with the observed group delays and group directions. So the original assumption of rectilinear propagation from an emitting dipole has been discarded.

A explanation based on incoherent radiation from sounder-accelerated electrons (SAE) has been investigated. Previously published reports [James et al., *Phys. Plasmas, 6(10)*, 4058, 1999; Huang et al., *J. Geophys. Res., 106(A2)*, 1835, 2001] show that the transmitting dipole produces strong SAE at energies from 10 eV up to 10 keV when the transmitting frequency sweeps through the above mentioned frequency range. This model supposes that a field-aligned tube centered on the transmitter confines SAE moving helically downward in the general direction of the receiver. At every instant, each SAE particle creates radiation that obeys the resonance condition $f - mf_c = (nf/c)\cos\theta\, V\cos\alpha$, where $m$ is an integer, $n$ is the Z-mode refractive index, $\theta$ is the angle between the direction of propagation of the radiation and **B**, $V$ is the electron speed and $\alpha$ its pitch angle. Using the reported SAE energies, it is found that the time delays like those observed can be explained with Z-mode $n$ and $\theta$ values, for $m = 0$, 1or 2. The resonance condition and dispersion relation together require $\theta$ values near the upper-oblique resonance cone. Incoherent radiation theory [e.g. McKenzie, *Phys. Fluids, 10(12)*, 2680, 1967] is used to compute the theoretical radiation level created by the SAE flux, for comparison with the observed levels.

0-7803-7846-6/03/$17.00 ©2003 IEEE 

# Stochastic Model of Electromagnetic Signal Propagation in the Turbulent Flow with Resonance Absorption

V.G. Spitsyn*, L.N. Kudryashova
Department of Computer Engineering, Tomsk Polytechnic University,
84, Sovetskaya street, Tomsk, 634034, Russia,
Tel: +7 3822 418912, Fax: +7 3822 419149,
E-mail: spitsyn@ce.cctpu.edu.ru

The purpose of this work is a numerical investigation of the process of electromagnetic signal multiple interactions with moving turbulent inhomogeneous in the flow of slightly ionized plasma with resonance absorption. To the analysis of this problem a method of stochastic modeling is applied (V.G. Spitsyn, IEEE AP-S International Symposium, 1, 288-291, 2002). Here is considered the propagation of waves with arbitrary frequency spectrum in the plane-parallel turbulent flow with inhomogeneous profiles of velocity and concentration of turbulences. The indicatrix of turbulence over-radiation is supposed by isotropic type. In the Figures 1, 2 are presented the computation results of angular and frequency spectrums of scattering signal for case of propagation wave across the axis of flow.

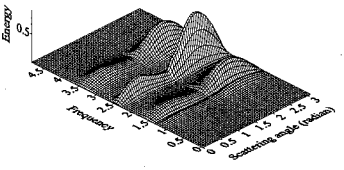


Figure 1

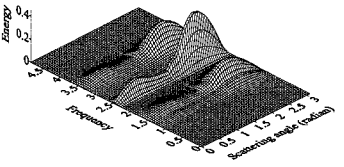


Figure 2

In the horizontal plane in the Figure 1 and Figure 2 are presented the scattering angle, calculated from the direction of incident wave propagation, and the value of dimensionless Doppler shift of frequency. By the vertical axis in this figures are calculated the energy of scattering signal, which is normalized on the maximum of energy in the first frame (Figure 1). There are presented the results of transformation frequency spectrum of incident wave with three Gaussian components in the flow with inhomogeneous profiles of velocity and concentration of turbulences. In the Figure 1 is presented the angular and frequency spectrum scattering signal, which received for case of multiply signal interaction with turbulences. In the Figure 2 is presented the results of signal propagation in the flow for case of only one act of signal scattering on the turbulences. In Figure 1 we can see more strong effect of resonance absorption on the frequency equal 1,4 in comparison with Figure 2. This fact is explained by the large significant of effect of multiply signal interaction with moving turbulences.

0-7803-7846-6/03/$17.00 ©2003 IEEE 

**Topic H3.** Wave interaction and wave-particle interaction.

# NOISE RADIATION OF ELECTRON FLOW INTERACTING WITH UNDULATOR SYSTEM ELECTROMAGNETIC FIELDS

Jezmer A.N., Yefimov B.P.
Institute of Radiophysics and Electronics of NAS of Ukraine, 61085 Kharkov,
Ac. Proscure str., 12. Tel.: 38(0572)448570, Fax.: 38(0572)441105, e-mail:
jean@ire.kharkov.ua.

The experimental results of focusing and transport of electron beam through Motz undulator with small kinetic energy are presented in this paper. It is shown that a use of external leading magnetic field improves inlet conditions in the system and has an influence on spontaneous radiation intensity. Resonance scattering of space charge waves on periodical inhomogeneities of electron beam formed by undulator static magnetic field was obtained in regimes of great current values. A question of possibility of influence of Cerenkov radiation mechanism on undulator system resonance radiation was discussed.

Development of theoretical and experimental researches of physical processes of FEL forms new direction – laser physics and allow physicists to create tunable in a wide wave range, new class of powerful relativistic devices based on stimulated radiation. However we can notice a tendency of carrying out experiments in a region of small energies of electrons and electron flows of high density, and also degree of wave participation in scattering operations on electrons in cyclotron and Cerenkov interaction regimes in undulator space [2],[11-12]. This work is directed on a solving of task in high current density regimes and small accelerating voltages of electron beam (electron velocity is about 0,1 - 0,3 of light velocity). For observation of resonance effects of density wave scattering of electron flow moving in crossed H-fields the model of Motz undulator was made. It was linear chain of constant dipole magnets fabricated from materials inter-metallic material Sm? ? $_5$. Accelerating voltage of electron diode gun was varied up to 6 kV, beam current did not exceed 100 mA. Space amplitude of electron flow motion was operated by ratio $H_? / H_{II}$. In fig.1 typical photo of projection of a beam moving in undulator space is shown. Spontaneous radiation of electron flow was received by dipole antenna of cm-range and registered by receiving apparatus.

Fig.1. The photograph of electron flow motion trajectory.

In accelerating voltage range up to 6 kV several microwave resonances were observed on oscillograph. They appear as strong increase (in 10-50 times) of noise signal amplitude relatively to non resonance case. One of possible variant of resonance radiation excitation explanation by means of synchronization mechanism of electron flow density waves with slow harmonics of undulator periodic structure was considered.

0-7803-7846-6/03/$17.00 ©2003 IEEE

## High Frequency Techniques

**Co-Chairs:** M. Cátedra
E. Heyman

10:00 Opening Remarks

# 3D RAY-TRACING ACCELERATION TECHNIQUE FOR THE ANALYSIS OF PROPAGATION AND RADIATION IN ENVIRONMENTS MODELLED BY SURFACES WITH ARBITRARY FORM

**I. González, C. Delgado, F. Saez de Adana, O. Gutiérrez, M.F. Cátedra**

*Dept. Teoría de la Señal y Comunicaciones*
*Escuela Politécnica, Universidad de Alcalá*
*28806 Alcalá de Henares. Madrid. Spain*
*Fax: +34 91 885 6699. E-mail: felipe.catedra@uah.es*

In electromagnetic asymptotic ray-tracing techniques like GTD/UTD, the electrical field is calculated as the sum of all rays that reach the observation point or the observation direction: direct, reflected, diffracted and combination of them. The most of the CPU time is spent in determining the surfaces that shadows the ray and the searching of the possible points that can contribute by another effect different to direct ray. So, it is necessary to reduce the number of surfaces involves in such process, applying acceleration techniques like Space Volumetric Partitioning, Binary Space Partitioning or Angular Z-Buffer. When it is necessary good accuracy between the real model and the geometrical model, flat faceted models can not be used and arbitrary surfaces like NURBS must be used. The technique proposed is based on the Angular Z-Buffer but developed to the be used with any kind of surfaces: flat and curve.

The shadowing tests are accelerated using a *"shadowing window"* defined for every surface and sources of electromagnetic field defined in the environment. The space is divided into angular regions named anxels *"angular elements"* that contains the surfaces for a certain margin of directions. When the shadowing test is applied, the anxel where the ray lies is determined and the surfaces contained in it are used for the surface-ray intersection tests. Because there is no analytical formula to determine the intersection between a ray and a surface and it is necessary the use of minimization algorithms like Conjugate Gradiente Method (CGM), the CPU-time required is reduced remarkably, as is shown in the results obtained.

The technique above can be extended and easily applied to speed-up the searching of the possible reflection points. Using the possible margin of the reflected fields, a *"reflection window"* from the source is obtained applying the Snell Law to the surfaces visible from the source. The anxels that contains the margins above are updated with the surface. When the reflected rays are calculated for a specific direction, the anxel where the rays lies is located and the surfaces contained in it will be used to serach the reflection points. The procedure above can be extended to the double reflection case, calculating a *"reflection window"* associated to every surface of the model. In that case, the surface is bounded in a parallelepiped box and the 8 vertexes of the box are used as auxiliary sources to determine an absolute margin of reflection directions from the surface.

The technique proposed has been implemented in FASANT, a code based on GTD/UTD to calculate the radiation pattern of antennas on-board complex structures modelled by NURBS surface. The reduced CPU-time is large for instance 1/6 for a case of an airplane modelled by 304 surfaces.

0-7803-7846-6/03/$17.00 ©2003 IEEE

# Evaluation of the Multiplaten Z-Buffer Algorithm for Electromagnetic Ray Tracing in High-Frequency Electromagnetic Scattering Computations

Yong Zhou* and Hao Ling

Dept. of Electrical and Computer Engineering
The University of Texas at Austin
Austin, TX 78712-1084 USA

The shooting and bouncing ray (SBR) technique, proposed in the 1980s, has become a standard approach for high-frequency radar signature prediction. In applying the SBR technique, the total computation time is comprised of the ray-tracing time and the time for carrying out the electromagnetic calculations. A number of techniques have been implemented in the mid-1990s to accelerate the latter. As a result, the total computation time of applying the SBR technique is currently dominated by the ray-tracing time. A faster ray tracer can significantly speed up the SBR algorithm for signature prediction. In this paper, we evaluate the multiplaten Z-buffer ray-tracing algorithm proposed by J.-L. Hu et al (*Elec. Lett.*, **33**, 825-826, 1997) as an alternative to the traditional Binary Space Partition (BSP) tree algorithm. Although it was claimed that the multiplaten Z-buffer algorithm should be superior to the traditional ray-tracing process, no evaluation about its time performance was reported.

In the standard BSP-tree algorithm, a BSP tree is first built based on the facet model of the target by recursively cutting the bounding box of the object along a spatial plane. Ray tracing is then performed by traversing the BSP tree. The BSP-tree based ray tracer is considered the fastest among all of the spatial subdivision approaches. In the multiplaten Z-buffer approach, a multi-layered Z-buffer is first generated from the scan conversion process. Instead of just storing the z-coordinates of the visible pixels as in the traditional Z-buffer process, multiple Z-buffers are created to store the z-coordinates of all of the facets within each pixel during the scan conversion. During the ray trace, a ray is tracked by moving along the ray direction pixel-by-pixel. Within every pixel, the z-depth of the ray is compared to all of the Z-buffer values for that pixel to check for possible intersections. Once an intersection is found, the hit point and the reflection direction can be calculated, and the tracing process is then iterated until the ray departs from the bounding box. We evaluate the computation time performance of the multiplaten Z-buffer ray tracer against that of the BSP tree-based algorithm. Results for a wide range of targets are tested to determine the computational as well as memory complexity as functions of the number of facets and the complexity of the target.

0-7803-7846-6/03/$17.00 ©2003 IEEE

# Fast Analysis of Impedance Surface Reflector Antennas via the Applications of Gaussian Beam Expansions

Shih-Chung Tuan[1]* and Hsi-Tseng Chou[2]
1 Kuang Wu Institute of Technology, Taipei, Taiwan
2 Dept. of Comm. Eng., Yuan-Ze University, Chung-Li 320, Taiwan

Impedance surfaces are employed in the design of reflector antennas in many applications such as being subreflectors in dual reflector configurations, which can be used in frequency selected manners. With the increasing trend of applications in the high frequency, the analysis of radiation from such an antenna system becomes computational inefficient if the conventional approach of physical optics (PO) is employed. Note that PO requires cumbersome numerical integration over the induced currents on the boundaries of the reflector surfaces, and is very inefficient at high frequencies. This paper extends previous work of Gaussian beam (GB) applications in the fast analysis of perfectly conducting reflector antennas (H-T Chou, P.H. Pathak and R.J. Burkholder, IEEE Trans. Antenna Propa., 49(6), pp. 880-893, Jun. 2001) to treat the impedance surface reflector antennas. The GB techniques represent the feed radiations in terms of a set of relatively few and rotationally symmetric GB's that are launched from the phase center of feed and illuminate the reflector surfaces. PO is then employed to treat the scattering of each GB illumination. The advantages of the GB techniques are that closed form solutions based on asymptotic evaluation of PO integral due to each GB incidence can be found in terms of reflection and edge diffraction effects with a transition function in terms of complex parameters, and in most cases only a relatively few GB's are sufficient to provide accurate prediction of radiating fields. Note that the complex parameters completely avoid the ray caustic problems in real space, and since numerical integrations are completely avoided, the efficiency can be therefore achieved. Numerical implementation and examination will be presented to validate the extended GB techniques in terms of accuracy and efficiency.

0-7803-7846-6/03/$17.00 ©2003 IEEE 

# A Study of the Radiation Characteristics due to Sources on Doubly Curved Surfaces

Patrik Persson*[1] and Lars Josefsson[1,2]

[1] Div. of Electromagnetic Theory, Royal Inst. of Technology, SE-10044 Stockholm, Sweden, Email: patrik@tet.kth.se

[2]Ericsson Microwave Systems AB, SE-43184 Mölndal, Sweden, Email: lars.josefsson@ericsson.com.

Today's aircraft, satellites, and launch vehicles are designed to perform diverse and complex tasks. To meet these communication requirements multiple antennas are mounted on the surfaces of aerospace structures. The antenna characteristics for these antennas are important to determine to ensure proper operation of the communication systems.

For conformal arrays numerical solutions of integral equation formulations for the unknown fields can be used, at least for reasonably small antennas. For certain canonical surfaces, e.g. a circular cylinder or an elliptic cylinder it is possible to obtain a modal solution. But for more arbitrarily shaped bodies other methods have to be used. In this paper an asymptotic high frequency method will be used.

With this method it is possible to analyse both singly and doubly curved convex surfaces. Earlier, this method (combined with MoM) has been used for mutual coupling calculations between apertures on PEC (singly and) doubly curved surfaces. The results have been compared against measured results obtained from a test antenna shaped as a general paraboloid of revolution (GPOR) built at Ericsson Microwave Systems AB in Mölndal, Sweden. The agreement was good (Persson et al., *IEEE AP*, Mar. 2003).

In this presentation another part of the analysis of doubly curved conformal array antennas will be considered, namely the radiation problem. The hybrid method will be used to calculate the radiation pattern due to sources (dipoles and apertures) on the general paraboloid of revolution (GPOR). Measurements of the radiation pattern have been performed at Ericsson Microwave Systems AB in Mölndal, Sweden and the calculated results will be verified against the measured results. The polarisation dependence of the radiation pattern will also be discussed.

0-7803-7846-6/03/$17.00 ©2003 IEEE

# A Frame Based Beam Summation Algorithm for Wideband Radiation

Amir Shlivinski,† Ehud Heyman,† Amir Boag,† and Christine Letrou‡
† Faculty of Engineering, Tel–Aviv University, Tel–Aviv, 69978 Israel
‡ I.N.T. SAMOVAR (CNRS FRE 2310), 9 rue Charles Fourier, F-91011 EVRY Cedex, FRANCE

Beam-based discrete phase space algorithms are an important tool for tracking high frequency wave fields since they provide a systematic framework for ray-based solutions in complex configurations, e.g., slowly or abruptly varying inhomogeneous media. In these algorithms a given aperture field is expanded into a set of spatially and spectrally shifted expansion functions. When propagating away from the aperture, each expansion function gives rise to a shifted and tilted beam, which propagates along its corresponding ray trajectory. The radiated field is obtained as a sum of all beam contributions at the observation point.

In a recent paper, we presented a Windowed Fourier Transform (WFT) frame-based wideband beam representation that overcomes the difficulties of the critically complete Gabor expansion (e.g., window's non-locality and a frequency dispersion of the beam lattice). Using an overcomplete set of expansion functions adds a degree of freedom, which makes it possible to use the same beam lattice for all frequencies. The overcompleteness also smoothes out the dual (analysis) function and thereby localizes and stabilizes the expansion coefficients. Using a properly chosen set of iso-diffracting Gaussian-beam basis functions also provides the "snuggest", i.e. numerically, the most efficient and compact representation for all frequencies.

The emphasis in the presentation is on analytical study of the expansion and beam parameters that render the beam representation most effective and localized. It is shown that the frequency band which can be efficiently treated with a given beam lattice is of order of one octave in width. For wider excitation bandwidths, the aperture field is sub-band filtered into a hierarchy of one octave wide frequency bands. Each band is then treated separately with its own beam parameters. The beam parameters of different bands are related by a decimation scheme that leads to a self consistent representation wherein the beam axes of the highest frequency band are partially reused for all the other bands.

These algorithms will be applied to a 3D numerical modeling of a wide-band radiation from a focused aperture. We shall show that a phase-space localization greatly reduces that number of beams contributing to the field at any given location, thus leading to a numerically efficient algorithm. It will also be shown that the field calculated using these algorithms is uniform upon transition through caustics and cusps. A time domain counterpart of the algorithm is presented in a companion paper [1].

[1] A. Shlivinski, E. Heyman, A. Boag and C. Letrou, "A pulsed beam algorithm for transient radiation from extended apertures," *This Session* .

0-7803-7846-6/03/$17.00 ©2003 IEEE

# A Pulsed Beam Algorithm for Transient Radiation from Extended Apertures

Amir Shlivinski,[†] Ehud Heyman,[†] Amir Boag,[†] and Christine Letrou[‡]
[†] Faculty of Engineering, Tel–Aviv University, Tel–Aviv, 69978 Israel
[‡] I.N.T. SAMOVAR (CNRS FRE 2310), 9 rue Charles Fourier, F-91011 EVRY Cedex, FRANCE

The wideband discretized-phase-space beam summation representation introduced in the first part of this sequence [1] has several attractive features that make it amenable for an extension into the time domain (TD): (*a*) The same beam lattice is used for all frequencies; (*b*) The iso-diffracting Gaussian basis provides the "snuggest" frame representation for all frequencies; (*c*) The propagation parameters of the resulting beams are frequency-independent and need to be calculated only once at a reference frequency. These properties have been utilized in a recent paper to derive a new TD representation for radiation from extended apertures, wherein the field is expanded in a discrete lattice of shifted and tilted pulsed beam (PB) propagators. The excitation coefficients of these PBs are extracted from the aperture source distribution via the new "discretized local slant stack transform."

The present theory completes the analogy between the frequency and time domain spectral representations. In the frequency domain, the spectral framework is provided by the spatial windowed Fourier transform formulation which is discretized via the *frame formulation.* In the TD, the non-windowed formulation is based on the *slant stack transform* (SST) where the field is described as an angular spectrum of time-dependent plane waves, while the windowed approach is based on a *local-SST* comprising a phase-pace continuum of PBs that emerge from all points in the aperture and in all directions. In our recent paper, we introduced a *discretized local-SST.* From a broader perspective, it is a new "discrete local Radon transform" in $\mathbb{R}^3$ that may be relevant in other disciplines, such as image processing.

This new TD formulation is further developed here. The emphasis is on an effective treatment of the time coordinate, which may comprise many time scales of variation. This efficacy is achieved using temporal frame based expansion which comprises interpolation kernels. In this procedure the aperture field is analyzed using spatial-temporal window functions comprising a variety space-time scales of variations. Each scale is treated separately using the discretized local-SST in order to define the parameters of the discretization. The hierarchy of temporal and spatial discretizations is such that a set of the PBs trajectories and parameters are constructed first for the highest space-time scale, and then its decimated versions are used for all other scales.

Numerical evaluation of the pulsed field produced by a focused aperture with a transient excitation will be used to demonstrate the new concepts. It will be shown that time and space localization of the emerging PBs fields facilitates numerically efficient field computations in free space and complex environment such as radomes.

[1] A. Shlivinski, E. Heyman, A. Boag and C. Letrou, "A frame based beam summation algorithm for wideband radiation," *This Session* .

0-7803-7846-6/03/$17.00 ©2003 IEEE

## *URSI Student Paper Contest*

Papers from URSI Student Paper Contest are not available.

***Special Session***

## A Memorial to Dr. Walter (Bud) A. Flood, Jr.

**Organizer(s):** G. Brown, Virginia Polytechnic Institute & State University
A. Voronovich

**Co-Chairs:** G. Brown
A. Voronovich

1:15 Opening Remarks

# A Review of Numerical Methods for Rough Surface Scattering

Joel T. Johnson
Department of Electrical Engineering and ElectroScience Laboratory
The Ohio State University
205 Dreese Laboratories, 2015 Neil Ave, Columbus, OH 43210
(614) 292-1593, (614) 292-7297 FAX, email: johnson@ee.eng.ohio-state.edu

Numerical methods allow studies of electromagnetic scattering from rough surfaces without approximation, so that insights beyond those available from traditional approximate theories can be obtained. Although the necessity of Monte Carlo simulations for capturing stochastic effects increases computational demands beyond those of typical numerical electromagnetic applications, recent developments in highly efficient algorithms have made large scale computations possible. For surfaces modeled as being rough only in one direction (two-dimensional scattering problems), the use of numerical methods is reaching a relatively mature state. Computational complexity however still has limited studies in the three-dimensional scattering problem to only a few examples.

In this talk, recent developments in numerical methods for rough surface scattering will be reviewed. Several efficient algorithms will be discussed, and results from previous studies presented. Results in the areas of sea surface remote sensing, ground penetrating radar analysis, target/surface clutter interactions, low grazing angle scattering, radar imaging of surfaces, and backscattering enhancement will be illustrated. Comments on current issues in the area will be provided, along with suggested other applications where numerical surface scattering methods may play an important role. The relative importance of numerical versus approximate methods in differing areas will also be discussed.

0-7803-7846-6/03/$17.00 ©2003 IEEE

# Rough surface scattering: comparison of approximate methods with a boundary integral method

**M. Saillard*, G. Soriano, C. A. Guérin**
Institut Fresnel, UMR CNRS 6133
Faculté St-Jérôme, case 162
13397 Marseille Cedex 20, France
marc.saillard@fresnel.fr

The boundary integral formalism, combined with fast numerical solvers, is among the most efficient ways to deal rigorously with the time-harmonic scattering from a randomly rough surface separating two semi-infinite homogeneous media. However, despite the rapid increase in computer speeds and the recent progress in numerical methods, computation times remain quite long, mainly because the method of moments requires a Monte Carlo process. As a comparison, approximate methods remain very fast, especially when a statistical formula is obtained. But no estimation of the error is provided with such formulas. For validation, approximate results can be compared to measurements, but this requires an accurate knowledge of the surface roughness. Only a few controlled laboratory experiments have been designed with this aim. These remarks have motivated this work, consisting in comparing approximate results with those obtained from the numerical solution of the rigorous integral equation.

Obviously there are too many parameters to derive general rules. Therefore, we have restricted our investigations to a few examples. First, all the random rough surfaces considered here have a Gaussian surface height distribution, since this assumption is often required to get the approximate formulas. The power spectrum $S(K)$ thus completes the description of the surface statistics. Two kinds of spectra have been studied: the Gaussian spectrum, typical of single scale surfaces, and a power law spectrum, because $1/f$ spectra are very popular to describe natural surfaces. A well known example is the sea surface spectrum, which can be well fitted by a $f^4$ law over a wide range of scales. Secondly, considering that surface scattering at grazing incidence angle cannot be accurately solved with our rigorous method, and that, away from grazing, incidence angle is not a critical parameter for approximation validity, we have used a 20° incidence angle only. Thirdly, to save computation time, we have restricted our study to metallic surfaces, or, with remote sensing applications in mind, to low penetrable surfaces like sea surface in the microwave range.

The rigorous model will be compared to approximate methods dedicated to surfaces with small slopes (the Small Slope Approximation, the Kirchhoff approximation, the Meecham-Lysanov approximation). To this end, the same incident Gaussian beam and the same surface samples have been used throughout the whole process.

URSI Commission B. *Reviews of the state of Rough Surface Scattering Analysis and Experimentation*, session organized by A. A. Voronovich and G. S. Brown.

# Direct Numerical Simulations of Pulse Scattering from Evolving Ocean-Like Surfaces: Range-Doppler Analysis

*Jakov V. Toporkov* and Mark A. Sletten*
Naval Research Laboratory, Code 7255, Washington DC. 20375-5320

Over the past several years, a significant progress has been made in developing numerical methods that allow exact evaluation of electromagnetic field scattered from a surface with an arbitrary profile. While techniques for truly three-dimensional (3-D) large-scale geometries are still under development, the 2-D methods have achieved considerable maturity. They offer highly efficient solution of the scattering problem for electrically large surfaces at all incidence angles including the challenging low grazing angle (LGA) regime. With modern high-performance computers, these techniques can be applied to practical problems of interest to radar and remote sensing community.

The presentation reviews the integral equation-based numerical scattering technique and the hydrodynamic surface model that form the basis for this study. The numerical scattering method (originally formulated for monochromatic incident wave and motionless surfaces) is extended to produce a time-varying range-resolved response from evolving ocean surfaces. Processing times are addressed, as the range-Doppler simulations, even confined to a 2-D space, prove to be computationally intensive and require high performance computing (HPC) resources.

To illustrate capabilities of direct numerical simulation technique, scattering of a 5-ns X-band pulse from an evolving 60 m-long realization of non-linear Pierson-Moskowitz surface is calculated. Accounting for non-linear hydrodynamic interactions of surface harmonics was shown to be essential in simulating LGA Doppler spectra (J. V. Toporkov and G. S. Brown, *IEEE Trans. Geosci. Remote Sensing*, **38**, 1616-1625, 2000), and it has significant effect on the range-resolved LGA backscattering signature as well, particularly for HH polarization. The data is calculated at both VV and HH polarizations and the incidence angles of 60° and 85° (5° grazing). The differences in scattering signatures for these polarizations are clearly observed, especially at LGA. Range-resolved Doppler spectra for different incidence angles and polarizations are also compared.

Range-Doppler description of the sea clutter is most detailed, and the ability to benchmark it through direct simulations will benefit the development of Navy radars, as well as remote sensing studies of the surface hydrodynamic processes.

0-7803-7846-6/03/$17.00 ©2003 IEEE

## Inverse Problem in the Theory of Wave Scattering from Rough Surfaces

A.G. Voronovich

NOAA/Environmental Technology Laboratory
325 Broadway, Boulder, CO, 80305-3328
alexander.voronovich@noaa.gov

In the theory of wave scattering from rough surfaces direct problems draw much more attention than the inverse ones. This is, probably, due to the reasonable assumption that solution of the inverse problems should be preceded by an ability to solve reliably a direct problem, which is still not the case in many instances. Nevertheless, practical necessity to approach this problem does exist. There are two basic paradigms here: reconstruction of the roughness through near and far field measurements. Remote sensing applications, in particular, often require retrieval of the properties of scattering surfaces based on measurements of the scattering in the far field. This talk will be devoted to the review of the existing approaches to this problem.

Inversion techniques that allow analytical treatment are immediately related to the approximate methods of solution of the direct problem. One of such techniques is based on small-perturbation method, or Bragg scattering. Scattering cross-section in this case is proportional to the spectrum of surface roughness at a wave-vector equal to the difference of horizontal projections of scattered- and incident wave-vectors, and measurements of scattering cross-section at all scattering angles allow to reconstruct surface roughness for all spectral components in the range corresponding to propagating waves. This approach is used, in particular, for estimation and tuning sea-wave spectrum in the range of centimeter waves.

Another inversion method is based on the Kirchhoff approximation. In the geometric-optics limit scattering cross-section is proportional to the probability density of slopes, which can thus be directly measured by using near-nadir measurements. In the directions far from nadir, this allows to infer probability distribution of steep waves.

There is an interesting possibility to use full-wave Kirchhoff diffraction integral for solution of the inverse problem. This integral generally depends on two parameters, one of which coincides with the Bragg wave-vector, and the other equals to the appropriate sum of the vertical projections of the incident- and scattered wave-vectors. If measurements of scattering cross-sections are made at a sufficiently rich set of the incident/scattering angles, or if backscattering cross-section is measured at different angels and frequencies, one can infer exponential of correlation function by making Fourier transform over a special subset of scattering data. The same approach works in the case of small-slope approximation as well, since to the lowest order scattering cross-section in this case is also proportional to the same Kirchhoff-type diffraction integral. In a deterministic setting solutions based on the small-perturbation and the Kirchhoff approximations were suggested and investigated by R. Wombell and J.A. DeSanto.

If backscattering cross-section is known as a function of incidence angle at a fixed frequency, the inversion problem becomes strongly non-linear even in the case of small slopes. Analytical approach to this problem is not known yet. In this case one can try to treat it numerically using the approach based on different iteration schemes, or on invariant embedding.

0-7803-7846-6/03/$17.00 ©2003 IEEE 

# Inverse Scattering from Rough Surfaces Using Evolutionary Strategies

D. Macías, E. R. Méndez*, and G. Olague

División de Física Aplicada, CICESE,
Apartado Postal 2732, Ensenada, Baja California, México.

The scattering of electromagnetic waves, produced by their incidence on a rough surface, has been widely studied in the past. The inverse scattering problem, on the other hand, that consists of the reconstruction of the profile of a surface from scattering data is more complex and has been less studied.

In this paper, we present a study of inverse scattering from rough surfaces. The goal is to retrieve the unknown surface profile function from scattered intensity data, treating the problem as an optimization problem. The angle-resolved scattered intensity used as input data for the algorithms depends on the surface profile function in a complicated way but, for one-dimensional surfaces, the direct problem can be solved numerically.

The closeness of a proposed profile, $z_c(x)$, to the original one can be estimated through the difference between the measured angular distribution of intensity $I^{(m)}(q|k)$, and the angular distribution of intensity $I^{(c)}(q|k)$, obtained by solving the direct scattering problem with the trial profile $z_c(x)$. The goal then would be to find a surface for which the condition $I^{(c)}(q|k) = I^{(m)}(q|k)$ is satisfied. When this happens, and if the solution to the problem is unique, the original profile has been retrieved. We define our fitness (objective) function as

$$f(\zeta(x)) = \sum_{i=1}^{N_{\text{ang}}} \int \left| I_s^{(m)}(q|k_i) - I_s^{(c)}(q|k_i) \right| dq, \tag{1}$$

where $N_{\text{ang}}$ represents the number of angles of incidence considered. The inverse scattering problem is then reduced to the problem of minimizing $f(\zeta(x))$.

Results for inversion procedures, combining evolutionary strategies (H. P. Schwefel, *Evolution and Optimum Seeking*, Wiley, NY, 1995) and the downhill simplex method (J. Nelder and R. Meade, Computer Journal, **7**, 308, 1965) will be presented. The evolutionary strategies employed are the elitist $(\mu/\rho+\lambda)$ and the non-elitist $(\mu/\rho,\lambda)$ strategies with recombination. Here $\mu$ is the number of parents in the initial population, $\lambda$ is the number of offsprings generated by means of the genetic operators, and $\rho$ is the number of members of the population that generate an intermediate population through recombination. Once the evolution strategies have reached the termination criterion, the downhill simplex algorithm is employed to improve the solution.

The results show that surface profiles can be reconstructed from far-field intensity even in the presence of noise and multiple scattering. Some issues concerning the uniqueness of the solution appear in the results and will also be discussed. The procedure employing the non-elitist strategy with recombination $\rho = 2$, appears to be more stable than the other algorithms studied.

0-7803-7846-6/03/$17.00 ©2003 IEEE

# The Design of Random Surfaces with Specified Scattering Properties

Tamara A. Leskova,[1] Alexei A. Maradudin[1]*, and Eugenio R. Méndez[2]
[1]Department of Physics and Astronomy
and Institute for Surface and Interface Science
University of California, Irvine, CA 92697-4575
Email: leskova@duey.ps.uci.edu, aamaradu@uci.edu

[2] División de Física Aplicada
Centro de Investigación Científica y de Educación Superior de Ensenada
Apdo. Postal 2732,
Ensenada, B.C. 22800, México
Email: emendez@cicese.mx

## abstract

In this paper a novel type of inverse scattering problem is discussed. A description is presented of methods that have been developed recently for designing one- and two-dimensional randomly rough surfaces that scatter waves with a specified angular or spatial distribution of the scattered intensity. These methods are based on the geometrical optics limit of the Kirchhoff approximation. In the case of a one-dimensional random surface the surface profile function is assumed to have the form $\zeta(x_1) = a_n x_1 + b_n$ for $nb \leq x_1 \leq (n+1)b$ with $n = 0, \pm 1, \pm 2, \ldots$; in the case of a two-dimensional circularly symmetric random surface the surface profile function is assumed to be given by $\zeta(x_1, x_2) = H(r) = a_n r + b_n$ for $nb \leq r \leq (n+1)b$ with $n = 0, 1, 2, \ldots$, where $r = (x_1^2 + x_2^2)^{\frac{1}{2}}$. In both cases $b$ is a characteristic length, the $\{a_n\}$ are independent, identically distributed, random deviates, and the $\{b_n\}$ are determined by the requirement that the surface profile function be a continuous function of its argument. It is the probability density function of the $\{a_n\}$ that is sought, from which an ensemble of realizations of the surface is generated. The scattering problem for each realization is then solved numerically. It is shown by computer simulation calculations that the resulting surfaces possess the postulated scattering properties when multiple scattering processes of all orders are taken into account. To illustrate these approaches they are applied to the design of one- and two-dimensional random surfaces that produce a constant scattered intensity within a specified range of scattering angles and produce no scattering outside this range – band-limited uniform diffusers; random surfaces that produce a scattered intensity that is proportional to the cosine of the polar scattering angle – Lambertian diffusers; and random surfaces that produce a specified distribution of scattered intensity along the axis normal to the scattering surface in the absence of the roughness. It is then shown that the results in the last case can be used to generate random surfaces that produce a scattered field that has the nature of a pseudo-nondiffracting beam.

0-7803-7846-6/03/$17.00 ©2003 IEEE

# NEW INTEGRAL EQUATION METHODS FOR SCATTERING FROM DIFFRACTION GRATINGS

John A. DeSanto
Department of Mathematical and Computer Sciences
Colorado School of Mines
Golden, CO 90401

One of the main methods to describe the scattering from rough surfaces is that of integral equations. Here we restrict the type of surfaces to diffraction gratings although the methods we discuss can be extended to arbitrary rough surfaces. The equations can be derived using Green's theorem in a periodic cell. The result is a representation of the field in the domain in terms of a boundary integral on the grating, an integral along a line (or plane) above the highest surface excursion, and side or vertical line integrals which cancel due to Floquet boundary conditions. The usual boundary integral equations in coordinate-space follow by evaluating the domain field on the grating boundary. There are several approaches of this type and we mention some of them.

The main difference in our approach here is that we set the domain field on the line (or plane) above the surface. There are several advantages to this. First, the fields on the line have an exact representation as scattered plane waves. Second, the periodic Green's function G in the grating integrals does not have a vanishing or near-vanishing argument. In coordinate-space, G is time-consuming to compute particularly for small arguments. Our values of G do not have this difficulty. Further, the Weyl representation for G simplifies (since the absolute values drop). This enables us to use spectral methods in a simple manner, and leads to integral equations in mixed spectral- and coordinate-space and fully in spectral-space. These involve topological basis modes. An additional new class of equations arises if we use conjugate topological modes in the analysis.

URSI Commission B
Columbus, OH
June, 2003
Session Title: Reviews of the State of Rough Surface Scattering Analysis and Experimentation
Organizers: G. Brown and A. Voronovich

0-7803-7846-6/03/$17.00 ©2003 IEEE 

# Stochastic Green's Functions for Rough Surface Scattering

Akira Ishimaru*[1], John D. Rockway[2], Seung-Woo Lee[1], and Yasuo Kuga[1]
Department of Electrical Engineering
[1]Box 352500, University of Washington, Seattle, WA 98195-2500
[2]Lawrence Livermore National Laboratory, Livermore, CA 94550

One of the important quantities in rough surface scattering is the scattering amplitude and the scattering cross section per unit area of the rough surface, and this is normally obtained when a plane wave or a tapered beam wave is incident on the surface. However, recent interest in LGA (Low Grazing Angle) scattering and scattering by objects located close to the rough surface has lead to renewed interest in considering incident waves which are more general than a plane wave. This requires the study of Green's functions which contain all propagating and evanescent modes and the coupling between the rough surface and the random current on the deterministic object. This paper presents a review of some recent theoretical developments in rough surface Green's functions as applied to LGA and object scattering.

First, we consider the first and second moments of Green's functions when both the point source and observation point are located close to or on the rough surface. In the perturbation approximation, the coherent Green's function satisfies the Dyson equation and propagates over the effective impedance surface which includes the rough surface effects. The incoherent Green's function satisfies the Bethe-Salpeter equation and gives the effective scattering cross section which includes the propagation characteristics and is distance-dependent. We discuss the HH/VV ratio for LGA, enhanced backscattering, formulation of the surface radiative transfer equation, and scattering by distributed wedges in the high frequency approximation.

If an object is located close to the rough surface, the currents on the object are random and satisfy the stochastic integral equations involving the fourth-order moments, including the coupling between Green's function and the current. Green's function includes the effects of coupling between the object and the rough surface. If we make further assumptions, such as, circular Gaussian, we can decouple Green's function from the current distribution. If the object size is much smaller than the correlation distance of Green's function, the scattered field at the source point is given by the "double passage" Green's function, and the equivalent RCS reveals the enhanced backscattering of a factor of 2 due to multiple scattering. In addition, we discuss several outstanding problems, including the impedance of a dipole above the rough surface, the objects on or below the rough surface, the effects of the object resonance, and the time-domain considerations.

0-7803-7846-6/03/$17.00 ©2003 IEEE 

# A Numerical Method for Rough-Walled Waveguides

Gary S. Brown
ElectroMagnetic Interactions Laboratory
Bradley Department of Electrical & Computer Engineering
Virginia Polytechnic Institute & State University
Blacksburg, VA 24061-0111
(540) 231-4467, (540) 231-3362 (FAX), randem@vt.edu

Propagation in rough-walled waveguides has received a great deal of attention in previous years for many applications in electromagnetics, acoustics, and elasticity. By in large however, little has been done in the way of numerical methods to deal with such problems. With the increased interest in applications involving wave propagation in tunnels, caves, and even the 'urban canyon,' the need for such methods is becoming even more pressing. The purpose of this paper is to apply one particularly successful single-wall method to setting up a numerical scheme for dealing with wave propagation in a parallel plate waveguide.

To simplify the illustration, the problem is taken to be a source exciting the interior of a waveguide formed by two perfectly conducting parallel planes located at $z = 0$ and at $z = a$. The source is assumed to be a line source of current extending to infinity along the y-coordinate and at ($x = 0$, $z = 0$). The waveguide walls are further taken to be rough in the x-direction with the roughness forming a stochastic process having zero mean and a specified probability density function and spectrum. The goal of the research is to find an expression for the scalar field strength at any position x down the rough-walled waveguide. Having found an appropriate numerical method for predicting the field for any realization of the roughness process, Monte Carlo techniques may then be used to generate the statistics of the field at any point in the guide.

The approach we investigate is the *Method of Ordered Multiple Interactions (MOMI),* or also called the *Forward-Backward Method,* which has proven to be very useful for calculating the scattering by an infinite, mean planar, rough surfaces. With the introduction of the second rough wall, there are two multiple scattering processes in force. The first is due to the wall roughness which gives rise to the interaction of one part of the wall with another. The second is the wall-to-wall scattering that reduces to a simple reflection process in the absence of the roughness. MOMI is a method for essentially re-summing the most important orders of roughness induced multiple scattering and doing it in a manner that easily computed with minimum storage requirements. The addition of the second rough wall complicates the simplicity of the basic MOMI method, but it is shown herein how this may be recovered. It is demonstrated how the important orders of roughness and wall-to-wall induced multiple scattering may be reordered and re-summed into a form that retains the easy-to-calculate and minimum storage attributes of the original MOMI. It is particularly easy to see how robust the approach is when the roughness is small in amplitude. Furthermore, the MOMI approach produces a result that is also amenable to application of the fast multipole technique for an additional reduction in computational time.

0-7803-7846-6/03/$17.00 ©2003 IEEE

# Recognizing Non-Bragg Scattering of Microwaves from the Sea Surface

William J. Plant
Applied Physics Laboratory
University of Washington
Seattle, WA USA

Bragg /Composite Surface scattering theory predicts that the average HH cross section is smaller than the average VV cross section. This is found to be true for backscattering from the sea surface if sufficient averaging is carried out. However, if only a small amount of temporal averaging is done, then HH cross sections occasionally exceed those at VV, and a practice has developed of calling such occurrences "Non-Bragg Scattering". In this paper we will show that this label is erroneous. In fact, due to fading, that is the interference of fields backscattered from different locations within the illuminated area of sea surface, Bragg/Composite Surface scattering theory does allow the possibility that HH cross sections will exceed VV cross sections if insufficient averaging is done. We have compared the results of simulations of probability distributions of polarization ratios using Bragg/Composite Surface theory with those actually measured on the ocean. We have made these comparisons for a variety of wind speeds, incidence angles, and averaging times. We find that for incidence angles between about 30 and 50 degrees, Bragg/Composite Surface theory yields distributions that are in very good agreement with measurements. As the incidence angle increases, the agreement degrades due to under-prediction of the HH cross section by the theory. However, probability distributions of cross sections at HH polarization show that this under-prediction is not a result of a few very high HH cross sections but rather due to an under-prediction of cross sections through out the distribution by the theory. Thus the possibility exists that Bragg/Composite Surface theory also does not explain HH cross sections at incidence angles above about 50 degrees. This is in addition to the well known failure of theory at low incidence angles, a failure that is easily remedied by evaluating the complete Kirchoff integral. The occurrence of occasional samples of HH cross sections exceeding those at VV in time series that have been averaged over only short time periods is not sufficient to indicate "Non-Bragg Scattering", however.

0-7803-7846-6/03/$17.00 ©2003 IEEE

# Ultrawideband Radar Backscatter from Breaking Water Waves with Simultaneous Optical and Infrared Imagery

Mark A. Sletten*, Jim C. West**, Xinan Liu***, Jim H. Duncan***, Geoff Smith*

*Naval Research Laboratory,
Code 7255
4555 Overlook Ave SW
Washington DC 20375
(202) 404-7971
mark.sletten@nrl.navy.mil

**Oklahoma State University
School of ECE
202 Engineering South
Stillwater, OK 74078

***University of Maryland
Mech. Engineering Dept
3118 Martin Hall
College Park, MD 20742

This paper will summarize the results of two sets of radar scattering experiments that were carried out at the University of Maryland-College Park wavetank facility. The first set was conducted in September, 2000, and the second is scheduled for February, 2003.

In the September 2000 experiments, spilling and plunging breakers with a water wavelength of approximately 80 cm were generated through dispersive focusing of a chirped wave packet, and were then imaged with a high-speed camera in conjunction with a laser sheet. Simultaneously, the radar backscatter generated by the breakers at a nominal grazing angle of 12 degrees was measured by an ultrawideband, dual-polarized, X-band radar with a range resolution of approximately 4 cm. In addition to providing both quantitative profiles of the evolving water surface and the corresponding ultra-high resolution radar backscatter, this experimental setup also included a moving instrument carriage that allowed the sensors to follow the breakers throughout their entire evolution. Numerical scattering simulations that use the measured surface profiles as inputs complement these experimental investigations by providing a means to investigate the scattering mechanism.

An analysis of the results shows that when the radar views the spilling breaker in the "upwave" direction, over 90% of the horizontally (HH) polarized radar backscatter is generated during the initial stage of breaking by the small bulge near the wave crest. For vertical (VV) polarization, the crest bulge produces about 60% of the total backscattered energy. For VV, the remainder of the backscattered energy is generated by the turbulent, post-breaking surface, and in fact a close correlation is observed between increases in the VV backscatter amplitude and the shedding of vortex ripples after the wave breaks. Agreement between the experimental and numerical results is good, particularly in the Doppler domain. For the plunging breaker, the initial feature on the crest (an overturning jet) generates a lower percentage of the total backscattered energy. In this case, initial Doppler velocities are somewhat higher than the dominant wave phase speed, particularly for HH polarization.

In the experiments scheduled for February 2003, an improved radar system with a wider bandwidth will be used, and waves will be generated by wind forcing as well as by dispersive focusing. An additional camera will also be used to image the surface signatures of these breaking waves in the infrared (wavelength 3-5 micron).

0-7803-7846-6/03/$17.00 ©2003 IEEE

# Non-Gaussian Sea Surface Slope Statistics Observed During SOWEX

E. J. Walsh*, D. C. Vandemark, C. W. Wright
NASA/Goddard Space Flight Center, Code 972, Wallops Island, VA 23337, U.S.A.

M. L. Banner
The University of New South Wales, School of Mathematics, Sydney 2026, Australia

J. Shaw
Depart. Electrical and Computer Eng., Montana State University, Bozeman, MT 59717, U.S.A.

The Southern Ocean Waves Experiment (SOWEX) was conducted in June 1992 (Banner et al., *J. Phys. Oceanog.*, **29**, 2130-2145, 1999; Chen et al., *J. Phys. Oceanog.*, **31**, 174-198, 2001). Backscattered power data at 36 GHz, registered to ocean wave topography, were acquired southwest of Tasmania with the NASA Scanning Radar Altimeter (SRA) (Walsh et al., *J. Geophys. Res.*, **103**, 12,587-12,601, 1998) under a wide range of wind and sea conditions, from quiescent to gale force winds with 9 m wave height. The collection altitude varied from 35 m to 1.4 km, allowing determination of the sea surface mean squared slope (mss), the directional wave spectrum, and mss variation with respect to wind and wave parameters.

Under light wind conditions at low altitude, the reflection of the aircraft, silhouetted against the bright sky, intermittently appeared in the downlooking video, providing a graphic demonstration of the two-scale nature of the scattering. The image was still distorted by surface gravity waves on the order of 10 m, but a simulation of the scattering indicated that the high-contrast nature of the image demonstrated that the contribution to the mss by waves in the typically dominant gravity-capillary region was only about 0.00003, two orders of magnitude below the Cox and Munk (*J. Mar. Res.*, **13**, 198-227, 1954) minimum value of 0.003. As the windspeed at 35 m height fluctuated between 2 and 5 m/s, the aircraft image fluctuated between high contrast and totally faded out.

The non-Gaussian sea surface slope statistics observed by the SRA over the range of sea states agree well with the theoretical developments of other investigators and a simple model to fit them has been developed.

*presenter, presently on assignment at NOAA/Environmental Technology Laboratory, R/ET1, 325 Broadway, Boulder, CO 80305-3328, U.S.A.

0-7803-7846-6/03/$17.00 ©2003 IEEE

## Surveys at Radio Wavelengths

**Co-Chairs:** J. Condon
L. Knee

1:15 Opening Remarks

# The Canadian Galactic Plane Survey

Lewis B.G. Knee
Dominion Radio Astrophysical Observatory, Herzberg Institute of Astrophysics,
National Research Council Canada, P.O. Box 248, Penticton BC V2A 6J9, Canada
lewis.knee@nrc-cnrc.gc.ca

The Canadian Galactic Plane Survey (CGPS) is a large collaboration pursuing high-resolution multiwavelength studies of the interstellar medium (ISM) over wide fields of view in the Galactic plane. The observational component of the CGPS is being carried out primarily by the Synthesis Telescope (ST) at the Dominion Radio Astrophysical Observatory (DRAO). Complementary data sets from other instruments have been integrated with the DRAO data to produce a database which traces all the major components of the ISM. The centrepiece of the CGPS is the first high-resolution interferometric survey of the HI 21-cm line over a significant area of the northern Galactic plane. This unique dataset is leading to scientific discoveries in many areas of ISM studies, the most important of which concern the largely unexplored realm of cold neutral atomic hydrogen, large-scale mass and energy transfers from the plane to high Galactic latitude, and the detailed interaction between stars and HI.

The initial target of the CGPS was a 666 square degree section of the plane 9 degrees wide in Galactic latitude (b) and extending from Galactic longitude (l) 74 degrees to 147 degrees. All of the HI data in this first phase of the CGPS has now been observed and processed, and is being made publically available for research through the Canadian Astronomy Data Centre (CADC). As part of a project to map the majority of the Galactic disk in HI, the International Galactic Plane Survey (IGPS), the CGPS has entered a second phase of observations which will extend the longitude coverage in the plane to 64 degrees in the inner- and 175 degrees in the outer-Galaxy. Also part of the second phase is the imaging of a restricted longitude range ($100 < l < 117$ degrees) up to high latitudes, $b = +17.5$ degrees. This will permit study of the ISM in the Perseus Arm high above the Galactic plane as well as the extended complex of nearby low mass star forming clouds known as the Cepheus Flare.

For more information, see the CGPS public web page at
http://www.ras.ucalgary.ca/CGPS/

For data download from the CADC, go to:
http://cadcwww.hia.nrc.ca/cgps/

0-7803-7846-6/03/$17.00 ©2003 IEEE

# The Power of the Canadian Galactic Plane Survey for Probing the Galactic Magnetic Field

J. C. Brown, University of Calgary, Canada

The plane of polarization of an electromagnetic wave propagating through a magnetized gas of electrons will rotate through the process of Faraday rotation. One quantitative measure of the effect of Faraday rotation on a signal is the Rotation Measure (RM). The RM depends on the signal wavelength, the electron density, and the magnetic field strength and orientation along the path of propagation. By examining radiation from polarized sources at multiple wavelengths, it is possible to obtain information about the magnetic field in the Galaxy along the line-of-sight to a source. The more sources there are with identifiable RMs, the better the sampling of the Galactic magnetic field.

As part of the Canadian Galactic Plane Survey (CGPS), the synthesis array at the Dominion Radio Astrophysical Observatory images full polarization signals (Stokes $I, Q, U, V$) in four closely spaced bands around 1420 MHz. Consequently, these data can be used to obtain unambiguous RMs of compact sources within the CGPS region ($-3.6° \leq b \leq 5.6°$, $74.2° \leq l \leq 147.3°$). From these data, I have determined RMs for roughly 600 extragalactic (EG) compact sources (dark symbols in figure 1). This translates to a source density of roughly one source per square degree and almost equals the number of previously published EG RMs across the entire sky (light symbols in figure 1). Using these RMs, I have been studying the magnetic field in the outer part of the Galaxy. The high source density is revealing structures and detail never before observed, and is allowing me to address unanswered questions. These include 'How many magnetic field reversals are there beyond the solar circle?', 'What is the latitude dependence of the field?', and 'What is the relationship between the small and large-scale components of the magnetic field?'.

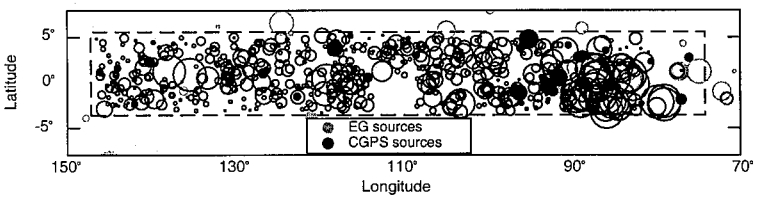


Figure 1: RMs in the CGPS (dashed box). Symbol size is proportional to the magnitude of RM (legend symbols are 250 rad $m^{-2}$); open circles represent negative RMs, and filled circles represent positive RMs.

0-7803-7846-6/03/$17.00 ©2003 IEEE

# A Polarization Survey of the Galactic Plane at 1420 MHz: the Canadian Galactic Plane Survey

T.L. Landecker[1], A.D. Gray[1], R. Kothes[1,2], B. Uyaniker[1,3], J.C. Brown[2], J.L. West, [4], R. Reid[1]

[1]Dominion Radio Astrophysical Observatory, Herzberg Institute of Astrophysics, National Research Council, Penticton, B.C., Canada, V2A 6K3

[2]Department of Physics and Astronomy, University of Calgary, Calgary, Alberta, Canada, T2N 1N4

[3]Max-Planck-Institut für Radioastronomie, D-53121 Bonn, Germany

[2]Department of Physics and Astronomy, University of Manitoba, Winnipeg, Manitoba, Canada, TR3T 2N2

The Canadian Galactic Plane Survey is producing a database of images of the northern Milky Way portraying the major constituents of the Interstellar Medium with arcminute resolution. Among these data products is a survey of Stokes parameters Q and U at 1420 MHz made with the DRAO Synthesis Telescope. Although the nearer supernova remnants can be recognized by their polarized emission, the polarization images are dominated by a widespread chaotic emission with structure on all scales from degrees to arcminutes. There is almost no correlation between regions of polarized emission and features in total intensity. The linearly polarized emission has its origin in synchrotron emission in the Galactic disk and halo, but the appearance of the sky at this frequency is dominated by Faraday rotation in the intervening medium rather than structure in the emission regions. The polarization images are therefore revealing the magneto-ionic medium (MIM), widely distributed ionized gas threaded by magnetic fields. This talk will present results from a number of directions towards the outer Galaxy. These results will be compared with computed polarization images based on models of the synchrotron background and the MIM.

Beam depolarization and depth depolarization are operative, reducing the apparent fractional polarization. Both effects increase with propagation distance, and there is therefore a distance beyond which polarized emission cannot be detected; this is the polarization horizon. At 1420 MHz, the polarization horizon is at 2 kpc in the Cygnus direction ($l \approx 90°$), and we do not "see" structures beyond the Local arm. Towards $l \approx 135°$ the polarization horizon is more distant, at least as distant as the Perseus arm.

The Faraday rotation is produced within the Warm Ionized Medium (WIM). The telescope can more easily detect ionized gas by the Faraday rotation it produces than by its total-intensity emission. The polarized fraction is rapidly reduced if many Faraday rotating regions are superimposed along the line of sight. The very fact that linear polarization can be detected at 1420 MHz means that the filling factor of the WIM must be considerably less than one.

0-7803-7846-6/03/$17.00 

**The International Galactic Plane Survey**

A.R. Taylor
University of Calgary

The Dominion Radio Astrophysical Observatory is nearing completion of an observing project to image the radio emission from the Northern Galactic Plane as part of the Canadian Galactic Plane Survey (CGPS). The DRAO observations provide simultaneous radio continuum images at two wavelengths, 74 cm and 21 cm, and spectral line images of the 21-cm line of neutral atomic hydrogen. This survey forms part of an international collaboration to create a database, within the CGPS region, of arcminute scale resolution, high spatial dynamic range images of all major components of the interstellar medium (ISM). The data have reveal wide-spread features and process in the interstellar medium that are not readily visible by other means, including, for example, unusual atomic hydrogen structures related to the vertical transfer of matter and radiation between the disk and halo of the Galaxy, Faraday rotation structures that allow study of the magnetic field and diffuse ionized component in the plane of the Galaxy, and a highly-structured, cold atomic phase of the neutral medium that may provide a link between global shock phenomena in the Galaxy and the formation of molecular clouds.

A global alliance has now been forged to secure a high resolution 3-D image of the atomic hydrogen emission from the disk of the Milky Way Galaxy. This project, the International Galactic Plane Survey, will combine the CGPS for the northern Plane, with the Australia Telescope, Southern Galactic Plane Survey (SGPS) for the southern Galaxy and the VLA Galactic Plane Survey (VGPS) for the equatorial region. These surveys combined provide arcminute-scale atomic hydrogen images over 90% of the stellar disk of the Milky Way. Complementary surveys of CO(1-0) in the northern plane will be carried out using focal plane array receivers on the Five Colleges Radio Astronomy Observatory and the Onsala Space Observatory. I will review the specifications and scientific highlights of the project.

0-7803-7846-6/03/$17.00 ©2003 IEEE

Title: Galactic Plane Surveys of Molecular Gas at FCRAO
Author: Mark Heyer

High spatial dynamic range imaging of molecular line emission along the galactic plane provides critical input to studies of the physical processes which regulate the evolution of star forming regions. High resolution is required to detect the discrete features within a highly textured medium while large area coverage allows one to place an emission component within an environmental context. With its ability to construct high spatial dynamic range images of the molecular interstellar medium, FCRAO has played an important role in defining the distribution and properties of giant molecular clouds in the Milky Way. I will review recently completed and ongoing surveys of CO emission with the FCRAO 14m telescope. These programs are made possible by the development of focal plane arrays at mm wavelengths and the implementation of On-the-Fly Mapping.

The FCRAO CO Survey of the outer Galaxy covers 330 $deg^2$ at 50″ sampling ($1.7\times10^6$ pixels) and remains the highest spatial dynamic range image of the molecular ISM to date. The Survey reveals the complex distribution of molecular gas generated by gravity, turbulence, UV radiation, and expanding motions driven by HII regions, stellar winds, and supernova. It provides important complementary information to the DRAO HI Galactic Plane Survey. I will highlight some of the most important results derived from the data.

Most of the molecular gas in the Milky Way resides within a ring located between 3.6 and 6 kpc. Describing the interstellar processes in this feature is essential to understanding star formation and the evolution of the Galaxy. The Boston University-FCRAO Molecular Ring Survey is a significant improvement over all previous surveys of the inner Galaxy as it measures the more optically thin tracer $^{13}CO$ J=1-0 emission, sampled at the Nyquist rate (22″) with high spectral resolution. These parameters enable one to gauge the structure *within* GMCs and to more readily associate molecular line emission with star forming regions identified by mid and far infrared photometry to derive distances and protostellar luminosities. Near-far side distance ambiguities are resolved by the presence or absence of HI self absorption at the velocity of the molecular feature allowing one to reliably derive masses and far infrared luminosities of associated protostars and clusters. Initial results from this ongoing survey are presented.

0-7803-7846-6/03/$17.00 ©2003 IEEE

# Recent Radio Searches for Globular Cluster Pulsars

Scott M. Ransom
*McGill University Physics Dept., Montreal, Quebec, Canada*

## Abstract

Globular clusters are ancient spherical systems of $10^5$–$10^6$ stars that orbit the Galaxy. High stellar concentrations in the cores of the clusters cause relatively frequent dynamical interactions between stars that produce large numbers of exotic systems, including Cataclysmic Variables, Low-Mass X-ray Binaries and Millisecond Pulsars (MSPs).

MSPs are neutron stars (compact stellar remnants with radii of only 10–20 km but with more mass than the Sun) that spin hundreds of times per second. Radiation from their magnetic poles is detected as an extremely stable train of radio pulses here on Earth. This stability allows astronomers monitoring the pulse arrival times to use them as high-precision probes of many areas of astrophysics, including stellar dynamics and evolution, the interstellar medium, and relativistic gravity.

In the decade following the discovery of the first globular cluster pulsar (an isolated MSP) in 1987, groups conducting deep searches with the world's largest radio telescopes had managed to uncover more than 30 pulsars. The vast majority of these pulsars were MSPs and almost half were members of binary systems. Long-term timing of these pulsars has provided unique insights into the evolution and dynamics of globular clusters and their component stars.

Due to significant radio telescope upgrades, the development of advanced search algorithms that target compact binary systems, and the widespread availability of high-performance computing resources, the number of cluster pulsars has more than doubled during the last 5 years and currently stands at over 70 known systems. In this talk I will describe the nature of these searches, the most interesting of the newly discovered pulsars, and the initial results from the timing of these systems.

0-7803-7846-6/03/$17.00 ©2003 IEEE 

# The Parkes Multibeam Pulsar Survey

I. H. Stairs*, Dept. of Physics and Astronomy, University of British Columbia, 6224 Agricultural Road, Vancouver, B.C., V6T 1Z1, Canada
R. N. Manchester, G. B. Hobbs, Australia Telescope National Facility, CSIRO, PO Box 76, Epping, N.S.W. 1710, Australia
A. G. Lyne, M. Kramer, M. A. McLaughlin, D. R. Lorimer, A. J. Faulkner, B. C. Joshi, University of Manchester, Jodrell Bank Observatory, Macclesfield, Cheshire SK11 9DL, U. K.
F. Camilo, Columbia Astrophysics Laboratory, Columbia University, 550 W. 120th St., New York, NY 10027, U.S.A.
V. M. Kaspi, S. M. Ransom, Physics Dept., McGill University, 3600 University St., Montreal, Quebec, H3A 2T8, Canada
N. D'Amico, A. Possenti, M. Burgay, Osservatorio Astronomico di Cagliari, loc. Poggio dei Pini, Strade 54, Capoterra, I-09012, Italy

We are carrying out a large-scale survey of the Galactic Plane using the 13-beam 20-cm receiver with 288 MHz bandwidth on the 64-m telescope at Parkes, Australia. The search covers the region $260° < l < 50°$, $|b| < 5°$, and each pointing lasts 35 minutes, leading to a nominal sensitivity of 0.2 mJy for pulse periods in the range 0.1 – 2 s and dispersion measures (DMs) less than 300 pc cm$^{-3}$. The search processing includes the standard elements of summing the data at many trial DMs, taking Fourier Transforms at each DM to search for peaks in the power spectra, and summing harmonics to increase the sensitivity to short-duty-cycle pulsars. As a 35-minute pointing could in principle cover a significant fraction of a binary orbit, an incoherent acceleration search is also employed, in which the pointing is divided into 16 segments and checked for signals that drift in frequency. Other algorithms search for very slow pulsars, strong single pulses, and extremely fast binary systems. Survey observations were taken from 1997 August through 2002 March, and all pointings are currently being reprocessed with the full code including acceleration searches and improved interference excision techniques.

Over 625 pulsars have been discovered to date from this survey, with candidates (including high-quality millisecond and binary candidates) still appearing in the reprocessing outputs. We have adopted the practice of timing each new pulsar for a full year after its discovery, in order to correctly determine positions and period derivatives. Most of this follow-up timing is done at Parkes and the 76-m Lovell Telescope at Jodrell Bank, U.K., with a small number being timed using the 305-m Arecibo Telescope in Puerto Rico. Highlights of the new pulsars include several young objects, some with very high magnetic fields or plausible associations with supernova remnants or unidentified EGRET point sources, and 15 new binary systems, with companion types ranging from white dwarf to neutron star to massive main-sequence star.

0-7803-7846-6/03/$17.00 ©2003 IEEE

# Large-Scale Pulsar Surveys with a Multibeam Feed Array System at Arecibo

James M. Cordes
Cornell University

A new multibeam feed array is being constructed for use on the Arecibo telescope, the Arecibo L-band Feed Array (ALFA). ALFA consists of seven feed horns and dual-polarization receiver systems providing 300 MHz bandwidth from 1225 to 1525 MHz. The beam width of each feed is approximately 3.6 arcmin. ALFA will become available approximately at the end of 2004 and is expected to be used in part for large-scale surveys of neutral hydrogen (Galactic and extragalactic), recombination lines, continuum surveys, rotating neutron stars (pulsars), and extraterrestrial intelligence. I will discuss ALFA pulsar surveys that will include:

1. A deep Galactic plane survey covering Galactic latitudes $|b| \lesssim 5°$ and galactic longitudes accessible to Arecibo. Tentative specifications are a dwell time of 300 sec, 1024 channels across the 300 MHz bandwidth, and a dump time of 64 $\mu s$. The total survey time is $\sim$ 2000 hr and will take at least three years to finish. With these specifications, the ALFA survey will reach a maximum distance (at fixed luminosity) twice as far as that for the very successful Parkes multibeam survey that has discovered more than 600 new pulsars. The ALFA Galactic-plane survey will probe to the edge of the pulsar distribution. Its yield will include rare objects (e.g. relativistic binaries) that serve as laboratories for basic physics and a large pulsar sample that allows tomographic mapping of the Galaxy's spiral arms, ionized gas and magnetic field.

2. An out-of-plane survey optimized for detecting millisecond pulsars, relativistic binary pulsars with neutron-star and black-hole companions, and high-space-velocity pulsars. A shorter dwell time will allow coverarge of a larger total solid angle than in the Galactic plane survey.

3. A shallow, all-Arecibo sky search for bright pulsars and transient sources.

It is expected that many of the ALFA surveys will be conducted in commensal (i.e. "piggy-back") mode where, for example, the Galactic plane pulsar survey takes place simultaneously with three other programs: a search for neutral hydrogen from galaxies in the zone of avoidance, mapping of Galactic hydrogen, and SETI.

Data management of ALFA pulsar surveys presents a formidable challenge because roughly 1 Petabyte of raw data are expected. The plannning process for pulsar surveys includes consideration of management of both the raw data and data products, with timely delivery to the astrophysical community.

Further details on ALFA and science consortia may be found at `http://alfa.naic.edu/` and `http://www.astro.cornell.edu/~cordes/ALFA`.

0-7803-7846-6/03/$17.00 ©2003 IEEE

# An All-Sky Survey at 74 MHz with 80 Arcsecond Resolution

**Richard A. Perley**

*National Radio Astronomy Observatory,*
*1003 Lopezville Road, Socorro, NM 87801 USA.*
*e-mail: rperley@nrao.edu*

## ABSTRACT

The very low frequency portion of the electromagnetic spectrum, despite being the 'birthplace' of radio astronomy, and of radio astronomical interferometric techniques, has received little attention for many years, as most development in radio astronomy has been focussed on higher frequencies. In part, this situation has resulted from the special dif£culties attending coherent interferometric imaging at low frequencies – especially those associated with removing the effects of the highly refractive ionosphere.

Yet the science rewards from high resolution, high sensitivity imaging in the low frequency radio spectrum are very high. Unique information on cluster halos and relecs, on fossil radio sources, high redshift radio galaxies, normal galaxies, pulsars, SNRs, HII regions, the ISM, and extra-solar planets can be obtained only by observations at low radio frequencies.

The VLA has been out£tted at 74 MHz with a modest-ef£ciency feed system, allowing sensitive, sub-arcminute imaging of the radio sky. This system has also permitted development of methodologies for removal of the ionopheric phase screen in some situations, permitting full-beam imaging of the background sky.

A proposal to survey the entire sky visible from the VLA in its B-con£guration has been submitted to the NRAO. As part of the development effort, about 6 days' observing in B-con£guration, covering 0.9 steradians, has been taken and reduced, giving 80 arcsecond resolution, and one-sigma brightness sensitivity of 100 mJy/beam. The proposed observing will provide a set of publicly-available images, and a catalog of nearly 100,000 objects.

0-7803-7846-6/03/$17.00 ©2003 IEEE

# "COSMIC WINDOWS" SKY SURVEYS

J. J. Condon, W. D. Cotton, and Q. F. Yin
National Radio Astronomy Observatory

Astronomical observations are degraded by dust and gas between the source and the telescope, expecially in the far-infrared, ultraviolet, and X-ray portions of the spectrum. The Earth's atmosphere is so bright and/or opaque that such observations must be made from space, and they are still affected by the interstellar medium of our Galaxy, which stands forever between us and all extragalactic sources. Fortunately the interstellar medium is quite patchy, and there are several "cosmic windows" covering $\sim 100$ deg$^2$ of sky having exceptionally low interstellar extinction and cirrus emission. Since the universe is nearly homogenous and isotropic on cosmological scales, these areas contain representative samples of cosmologically distant sources and will be the focus of most future multiwavelength studies. During the next few years, the major space observatories SIRTF, GALEX, and XMM-Newton will detect millions of galaxies, tens of thousands of quasars, and hundreds of clusters of galaxies at cosmological distances in the infrared, ultraviolet, and X-ray bands by making surveys covering the cosmic windows. The survey results will be used for evolutionary studies of star formation, supermassive black holes, and massive galaxy clusters. Complementary optical and radio surveys provide essential source identifications, redshifts, morphologies, and continuum spectra.

The first radio survey of this type complements the First-Look Survey (FLS) of the Space InfraRed Telescope Facility (SIRTF), which will cover about 5 deg$^2$ centered on J2000 $\alpha = 17^{\rm h}\,18^{\rm m}$, $\delta = +59^\circ\,30'$ in order to characterize the extragalactic infrared sky two orders-of-magnitude deeper than the IRAS survey. We expect that most of the FLS far-infrared ($\lambda = 160$, 70, and 24 $\mu$m) sources will be star-forming galaxies obeying the very tight far-infrared/radio correlation and will be continuum radio sources with flux densities $S \gtrsim 100\,\mu$Jy at $\nu = 1.4$ GHz. Conversely, radio sources stronger than $100\,\mu$Jy are usually powered by star-forming galaxies, plus some active galactic nuclei, and most should be detectable by the SIRTF FLS. Thus a sensitive radio survey can be used to select and identify most of the SIRTF FLS source population before launch. We used the B configuration of the NRAO Very Large Array to image the FLS area at $\nu = 1.4$ GHz with $\sigma_{\rm n} \approx 23\,\mu$Jy beam$^{-1}$ noise, $\theta = 5$ arcsec resolution, and $\sigma_{\alpha,\delta} \lesssim 0.5$ arcsec position uncertainties. The resulting radio image and catalog of 3565 radio components brighter than $S_{\rm p} = 5\sigma_{\rm n} = 115\,\mu$Jy beam$^{-1}$ have been posted on the web site `http://www.cv.nrao.edu/sirtf_fls/` to expedite follow-up optical identification and spectroscopy.

0-7803-7846-6/03/$17.00 ©2003 IEEE

# The Radio and Optical Morphologies of Micro-Jansky Radio Sources

E. B. Fomalont
National Radio Astronomy Observatory
Charlottesville, VA 22903

## Abstract

We have imaged a 17′-region in the SSA13 field with the VLA at 1.4 GHz with a resolution of 1.8″, and we have obtained sensitive Subaru images at R-band (0.9 $\mu$m) and Z-band (1.3 $\mu$m) with a seeing of 1.1″. The field center is at RA=13 23 17.4, DEC=42 38 05.0 and we have detected 548 radio sources in the complete sample with image flux density > 27.5 $\mu$Jy. Over 95% are identified on the Z-band image, to a limiting magnitude of 25.8 mag. The major properties of the sources are: (1) Over 30% of the identifications are with Extremely Red Objects; (2) The average radio angular size is 1.35″ and very few sources are larger than 5″, except seven relatively bright extended AGN; (3) The differential count of radio sources has a slope of −2.3, and there is significant difference in the source density of this field compared with other fields; (4) The radio spectral index between 1.4 and 8.4 GHz steepens considerably below 100 $\mu$Jy.

A detailed comparison of the hundreds of radio/optical associations show the following: (1) About 50% of the radio sources are identified with relatively isolated galaxies and 35% with binary systems. (2) The orientation of many radio sources are similar to the optical counterpart or the separation of the binary system if applicable, suggesting that the emission is primarily associated with the star formation process. (3) About 25% of the radio sources are smaller than 1″ and are AGN candidates. However, many of these are probably associated with compact starformation regions. (4) About 20% of the radio sources are considerably displaced from the central regions of the optical counterpart. Thus, a comparison of radio and optical morphologies contain information about the evolution and time-scale of starburst activity and the increases resolution and sensitivity from new instruments will permit modeling of the evolutions and dynamics of starburst and galaxy mergers.

0-7803-7846-6/03/$17.00 ©2003 IEEE

Compact Radio Source: A VLBA Survey of Structure and Kinematics

K. I. Kellermann*, D. Homan, and M. Lister, NRAO
E. Ros and A. Zensus, MPIfR, Germany
M. Cohen, Caltech
R. Vermeulen, ASTRON, the Netherlands

Since 1994, we have been using the NRAO Very Long Baseline Array (VLBA) to study the structure and kinematics of more than 200 quasars and AGN. The observations are made at 2 cm wavelength where the angular resolution is about 0.5 by 1 milliarcseconds. We chose this wavelength as a compromise between the better resolution that is available at shorter wavelengths and the reduced atmospheric effects found at longer wavelengths. Each image is constructed from approximately eight 5 minute observations spread over an hour angle of 8 hours. This results in an image with an rms noise of about 0.3 mJy and dynamic range of about 1000:1. For each source, we have between 3 and 8 epochs of observation spread over up to eight years, providing the most extensive data base on compact source motions.

Most of the sources which we observed show the characteristic asymmetric core-jet appearance, but some, show more symmetric structure. Often the jets appear curved, particularly close to the core component. In general the observed peak brightness temperatures are consistent with synchrotron self absorption, but some sources, especially those associated with AGN appear to have considerable free-free absorption from a surrounding ionized medium,

The interpretation of the motions is difficult due to the rather complex brightness distribution found in most sources in which components brighten and fade with time, sometimes even disappearing and then reappearing at a later epoch. For most sources, the motion appears to be linear and is along a trajectory aligned with the jet orientation. In some sources, however, there is a difference between the direction of motion and the direction defined by the jet. In a few cases where we have particularly good data, there appears to be a changes in the apparent trajectory and velocity.

In most sources the jet components appear to be moving away from an opaque core with apparent velocities ranging up to v □ 30c, but which is, however more typically about 7c, considerably less than indicated by earlier VLBI observations. AGN are generally slower than quasars, while BL Lac objects show a wide range of velocities. Comparison of the apparent velocities with the time scale of flux density variations suggests that there is an intrinsic range of Lorentz factors consistent with a power law distribution with exponent about -1.25. But the analysis is complicated by apparent differences between the pattern velocity, which may be due to the propagation of internal shocks, and the actual flow velocity which determines the Doppler boosting and apparent brightness temperature. We find no defining characteristics of structure, motion, polarization, or optical counterpart of GPS sources other than their peaked spectrum.

Observations now in progress will extend the time frame to a full decade and will include both linear and circular polarization.

0-7803-7846-6/03/$17.00 ©2003 IEEE 

## Antenna Measurements

**Co-Chairs:** S. Mishra
V. Cable

1:15 Opening Remarks

# A Time Domain Antenna Range

Everett G. Farr*†, W. Scott Bigelow†, Lanney M. Atchley†, Leland H. Bowen†,
and Tyrone C. Tran‡
†Farr Research Inc., 614 Paseo Del Mar NE, Albuquerque, NM, 87123
‡Air Force Research Laboratory / Directed Energy Directorate
3550 Aberdeen Ave. SE, Kirtland AFB, NM 87117-5776

We have been developing a time domain antenna range that appears to have a number of advantages over frequency domain systems. In this paper we provide a review of the status of that program.

The system we are developing includes a fast pulser, fast sampling oscilloscope, sensor, azimuth/elevation positioner, computer controller, and software for data acquisition and data processing. It is intended to be stored in a shed and quickly deployable in the field. Such a range is more easily used outdoors than frequency domain ranges, because temperature stability is less of a problem. In addition, the equipment required for a time domain range is considerably less expensive than the corresponding equipment for a frequency domain range.

We have compared the performance of our antenna range to that of a frequency domain range by measuring a number of different antennas on both ranges. In most cases, our time domain range compares favorably to the frequency domain measurements. The time domain range appears to be especially well suited to measuring non-dispersive Ultra-Wideband antennas, such as Impulse Radiating Antennas, because their impulse response dies out quickly. The advantage comes from being able to measure two decades or more of bandwidth with a single waveform. On the other hand, the time domain range may be less well suited to measuring the more dispersive log periodic dipole arrays, whose impulse response is a rather long decaying exponential. In this case, we must use a long time window, which adds ground reflection and noise to the measurements.

We provide here a general status of the hardware and software associated with the time domain antenna range. We also provide preliminary data on the antenna types that the range may be used to measure, and the expected accuracy as a function of frequency. The accuracy of the system appears to be at least as good as that needed for early-stage antenna development, and it may prove to be competitive to that of frequency domain ranges.

0-7803-7846-6/03/$17.00 ©2003 IEEE

# Antenna Range Imaging

Vaughn P. Cable
California Institute of Technology
Jet Propulsion Laboratory
vcable@jpl.nasa.gov

## Introduction

The quality of antenna measurements is important to the success of JPL missions. Most antenna ranges experience some form of multipath as a source of error and uncertainty in the measured data. At JPL, data from these measurements, including measurement uncertainties, are used in spacecraft link budget and sensor performance estimates to help determine optimal mission profiles. The best estimate of this uncertainty is obtained from field probe measurements of amplitude and phase across the quiet zone. These samples provide an accurate map of amplitude and phase ripple and taper and formulas exist [*Standard Test Procedures for Antennas*, IEEE, 1979] that compute the measurement uncertainty for that particular set of data.

These field probe measurements can also be used to locate many of the sources of multipath on the range [e.g., Moghaddar & Walton, AMTA, 1990]. For example, 2D planar field probe data can be mathematically transformed into a map (or image) of the up-range sources illuminating the quiet zone. This includes primary as well as secondary (unwanted) sources. This paper describes a field probe technique and the post processing currently being implemented at JPL to image and locate (and reduce) these secondary sources and, thereby, to improve the quality of JPL antenna measurements.

## Background

The Jet Propulsion Laboratory antenna measurement facility currently uses 9 antenna ranges, including 6 outdoor free space ranges and 3 indoor chambers, for development and testing of spacecraft communications and remote sensing antennas over a wide range of frequencies (VHF through W band). Depending on the wavelength and the range being used, the data from these measurements usually includes some form of multipath, either from ground bounce, surrounding foliage scattering, support tower scattering and scattering from nearby buildings or chamber walls. Some sources of multipath on an antenna range are intuitive (i.e., tower scattering and ground bounce) and placement of absorber is obvious. But others are not so intuitive. For example, measuring low sidelobes in the presence of multibounce, indoors or outdoors.

## Imaging Sources of Multipath

This paper describes a Fourier approach to transforming 2D planar amplitude and phase field probe data into wavenumber and angle space. Windowing functions are used to limit the processing sidelobes and results from simulated as well as measured quiet zone data are presented to demonstrate the usefulness of this technique for imaging and locating range multipath.

0-7803-7846-6/03/$17.00 ©2003 IEEE

# Adjustment of an Active Phased Array Antenna on a Near-Field Range and Determination of it's characteristic Performance Parameter in an Anechoic Far-Field Chamber

Wolfgang Haselwander, Manfred Uhlmann, Markus Böck

EADS Deutschland GmbH, Germany, 89077 Ulm, Wörthstraße 85
Tel. ++49 731 392 3715, Fax. ++49 731 392 5810
E-Mail : wolfgang.haselwander@sysde.eads.net

## ABSTRACT :

**Active Phased Array Antennas especially for use in radar systems ( e.g. Airborne Radars ) have to be adjusted and tested before they can be operated in the radar system. This adjustment process shall guarantee the antenna performance under all operating conditions.**
**Therefore, the Active Phased Array Antenna is measured on a Near-Field Test Range to determine the adjustment corrections to improve the pattern quality.**
**Operating the antenna with the adjustment corrections, it is ready to determine the antenna performance. This will be performed in two steps; on the Near-Field Test Range and within an anechoic chamber.**

**This paper describes the adjustment process and how to determine the performance parameter of the Active Phased Array Antenna. Performance parameter are**

- **Sum and Difference Antenna Patterns ( measured on a Near-Field and Far-Field Range )**
- **Directivity**
- **Average Far SLL**
- **Difference Null Depth**
- **Noise Figure ( described by G/T )**
- **EIRP**
- **and the Antenna Signature.**
- **Electrical Gain**
- **Beam Pointing Resolution**
- **Beam Pointing Accuracy**
- **Pulse Shape**

## TOPIC :

An Active Phased Array Antenna will be a standard equipment of a fighter aircraft in the near future. There it will be used as a front radar antenna with a planar aperture containing a large number of radiating elements , e.g. 1000.
Each radiating element ( RE ) is directly connected to an **active** Transmit / Receive Module ( TRM ), which provides the necessary output power in transmit operation ( TX ) and vice versa amplifies the incoming signal in receive operation ( RX ). TX output power and RX amplificiation can be individually controlled on each TRM over a range of 20 dB below the nominal values and further, the insertion phase of each RF path to the RE can be changed between 0° and 360° in TX and RX mode using a phase shifter within each TRM.
Because the TRMs have an insertion transmission varying between different TRMs, all other RF components have transmission variations as well, there is a strong need to adjust the Active Phased Array Antenna on a Near-Field Test Range to ensure a good antenna performance ( e.g. pattern quality ).
Only one TRM is switched on, all others are switched off ( **Single Element Adjustment** ). A defined digital control state is set at the TRM and the insertion amplitude and phase are measured for TX and RX in the considered frequency band for several frequency points. This procedure is repeated for all other TRMs in the antenna.
Adjustment corrections will be derived and entered in the antenna control process.

Now the Active Phased Array Antenna can be mounted in the Anechoic Far-Field Range on a turntable and the described performance parameter can be determined.

## CONCLUSION :

The Near-Field Range is a fundamental tool for the adjustment of an Active Phased Array Antenna and a valuable tool to evaluate the antenna, especially when full 3D antenna patterns are needed.
The measurement equipment architectures, described in this paper, were proofed during the evaluation of an Active Phased Array Antenna. They fulfil all needs for RX and TX measurements. The wideband detector in the Network Analyser used for pulsed TX measurements has an acceptable dynamic range of 45 dB, this is not a big limiting factor when the power budget of the measurement equipment setup is considered and carefully adjusted.
Pulse Shape measurements are performed with a Peak Power Meter, the Noise Figure is measured with an Average Power Meter.

0-7803-7846-6/03/$17.00 ©2003 IEEE 

# Numerical Study of Broadband Dielectric Rod Probe (DRP) for Near-Field Measurements

Kwan-Ho Lee*, Chi-Chih Chen, Fernando L. Teixeira and Robert Lee

ElectroScience Laboratory
Electrical Engineering,The Ohio State University
1320 Kinnear Rd., Columbus, Ohio 43212
Phone: 614-292-1433, FAX: 614-292-7596
e-mail: khl@esl.eng.ohio-state.edu

In order to be used as a probe for near-field measurements, an antenna must meet basic requirements such as: minimal probe to antenna-under-test (AUT) interaction, isotropic pattern, and adequate polarization properties. Open-end waveguides (OEWG) have been widely used for near-field measurements. However, major disadvantages of OEWG probes include the relatively narrow bandwidth due to the cut-off frequency and large probe-AUT interaction due to the conducting structure of the OEWG. A dielectric rod antenna (DRA), originally developed for landmine detection with reduced antenna/ground interaction and broadband characteristics, has been found to be very suitable for near-field measurements.

The dielectric rod probe (DRP) prototype also exhibits reduced probe-AUT interaction, similar E- and H- plane patterns, and dual polarization capability. The basic DRP probe configuration uses a linear taper with various angles to reduce the RCS level (in general, smaller angles produce lower RCS). In this study, we perform a numerical investigation, using the finite-difference time-domain (FDTD) method, of several different tapers to *simultaneously* reduce the RCS and broaden the beamwidth of such probes. Near field patterns in X-band from various taper models will be presented. Also, electromagnetic wave diffraction and reflection mechanisms caused by the different taper profiles will be discussed.

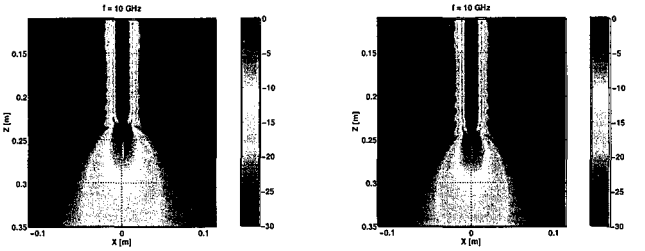


(a) Concave-quadratic profile (b) Concave-cosine profile

Figure 1: Normalized Electric field distribution at f = 10 GHz for different taper profiles.

0-7803-7846-6/03/$17.00 ©2003 IEEE

# High-Power Scanning Waveguide Array

Carl E. Baum
Air Force Research Laboratory
Directed Energy Directorate
Kirtland AFB, NM

Abstract

Microwave antennas for hypoband (narrow band) operation are a well-established subject. For high-power application, with electric fields approaching breakdown in various media of interest, the subject is less well established. However, some basic techniques for radiating high-power microwaves (HPM) have been published in several papers. These have been summarized in a book. [C. D. Taylor and D. V. Giri, *High-Power Microwave Systems and Effects*, Taylor & Francis, 1994] Among other things, these give techniques and canonical designs for HPM antennas systems (including waveguides) for pyramidal-horn fed reflector antennas for both high power and high gain. While these are quite appropriate HPM radiators, it is useful consider other possible types for their advantages/disadvantages.

Array antennas, while more complex, have the advantage of having less depth (and hence less volume) for the same total antenna aperture, and hence similar potential antenna gain. A common form of an array is formed by a set of slots in one or more rectangular waveguides. (However, small holes are not appropriate for high power transmission through them.) Using the dispersive character of the lowest order waveguide mode ($H_{1,0}$) one can steer the antenna beam by changing the microwave frequency. Other types of guiding structures (e.g., dielectrics) have also been used for this purpose. However, for frequencies around a GHz the large size of the waveguide suggests that for low mass a hollow metal pipe has certain advantages.

In [C. E. Baum, "Some Features of Waveguide/Horn Design", Sensor and Simulation Note 314 (section VI), 1988] I have discussed the division of a rectangular waveguide into a set subguides by insertion of metal sheets parallel to the broad wall (and perpendicular to the electric field of the $H_{1,0}$ mode) inside the waveguide and connecting to the side (narrow) walls. There, among other things, I suggested that this technique could be used to divide the power in the waveguide into $N$ subguides which could be used to feed N array elements. The present paper expands on this in one form of such an array.

0-7803-7846-6/03/$17.00 ©2003 IEEE 

*Special Session*

## Asymptotic and Hybrid Methods: In Celebration of Professor R.G. Kouyoumjin's 80th Birthday

**Organizer(s):** Prabhakar Pathak, ESL OSU
**Co-Chairs:** P. H. Pathak
R. Tiberio

1:15 Opening Remarks

# Diffraction in Lossy Media

R. G. Kouyoumjian*

ElectroScience Lab, The Ohio State University
1320 Kinnear Road, Columbus, OH 43212, USA

In this presentation ray methods are used to calculate the high frequency scattering from an object buried in a lossy half space. In general this could be a quite difficult problem, because ray paths connecting real source and observation points in a lossy medium involve complex values of the space coordinates, i.e., complex rays. However in the problem described here, the solution can be obtained using real rays. Furthermore, the solution naturally separates into the solution for the field scattered from the same object located in a lossy medium of infinite extent plus the field of rays introduced by the interface between air and the lossy half space. Interestingly enough the same type of separation occurs when treating the problem by a low frequency approach such as the moment method. The fields scattered through the interface into air as well as the fields scattered into the lossy half space are of interest. In the latter case, the high frequency scattered field is composed of the field of a ray directly radiated from the scatterer plus the field of a ray reflected from the interface together with a lateral wave field guided by the interface.

0-7803-7846-6/03/$17.00 ©2003 IEEE 

# A REVIEW OF FREQUENCY AND TIME DOMAIN HYBRID RAY-MODE REPRESENTATIONS

**Leopold B. Felsen**

*Dept. of Aerospace & Mechanical Eng. and Dept. of Electrical & Computer Eng.*
*Boston University (part-time)*
*Also, University Professor Emeritus, Polytechnic University, Brooklyn, NY 11201, USA*

When time-harmonic wave propagation is spatially (transversely) constrained by physical impenetrable boundaries or by "virtual" boundaries (ducts) established through refraction in transversely inhomogeneous media, the resulting source-excited longitudinally guided (ducted) waves have traditionally been described in terms of two alternative phenomenologies: progressing and oscillatory. The progressing formulation views the wavefields as continuous spectra of waves which propagate away from the source to the receiver, through the guiding environment, via multiple transverse reflections and (or) refractions. The oscillatory formulation views the wavefields as discrete (or discrete-continuous) superpositions of frequency-dependent (guided mode) eigenspectra which are matched to the entire transversely confining cross section, which are individually independent of source and receiver locations, but whose *amplitudes* of excitation and reception do depend on these locations.

At high frequencies (HF) – the "overmoded" regime where the transverse dimensions span many wavelengths and many modes can propagate – the oscillatory formulation becomes unwieldy, and is not well-matched to the wave physics, for *large* source-receiver separations since the lower mode eigenspectra there form closely spaced clusters. Here, the progressing wave spectra can be more efficiently adapted to the wave physics by approximate tracking of *local* plane waves whose constructive interference maxima coalesce around source-receiver dependent "ray" trajectories which are determined via HF asymptotics. On the other hand, at *small* source-receiver separations, the progressing formulation becomes unwieldy because it entails many closely spaced multiple reflections, whereas the oscillatory lower eigenmode spectra are widely spaced and, while excited in their totality near the source, decay exponentially (are evanescent) longitudinally away from the source when the number of oscillations in their transverse profile exceeds a frequency-dependent cutoff threshold.

These circumstances have motivated efforts to combine these two *complementary* spectral methodologies, neither of which is convenient for *all* source-receiver locations, in a manner that seeks to exploit the best features of each. The outcome has been a comprehensive rigorously based, selfconsistent *hybrid ray-mode algorithm*, which has clarified the ray-mode interplay through a series of spectral studies and wide-ranging applications to complex waveguiding environments initiated more than two decades ago. These studies are reviewed here because of their potential relevance to HF interaction with complex "new" environments that combine both ray-adaptable and mode-adaptable constituents. Also discussed are corresponding time domain short-pulse-excited hybrid wavefront-resonance schemes. Illustrative examples are included in the presentation.

0-7803-7846-6/03/$17.00 ©2003 IEEE 

# Applications of the wavefront evolution technique to high-frequency electromagnetic scattering [1]

E. Bleszynski, M. Bleszynski, and T. Jaroszewicz
Monopole Research, Thousand Oaks, CA 91360

We present elements and representative applications of the wavefront (WF) evolution method in describing high-frequency (HF) electromagnetic scattering phenomena. In our approach the WFs (constant phase surfaces) are implemented as well-defined meshed (triangulated) surfaces, orthogonal to rays, the rays being associated with vertices of the mesh. We describe evolution of rays by means of Geometrical Optics and the Uniform Geometrical Theory of Diffraction (UTD), accounting for diffraction processes (the present implementation being limited to edge diffraction on scatterers defined by facetized surfaces). In our implementation, in order to be able to compute diffracted fields with higher accuracy, we use a suitably modified version of UTD, which ensures that the field behavior near diffraction edges is reproduced in agreement with the exact solution to the canonical problem.

The WF method has two advantageous features compared to more conventional ray-tracing techniques:

(a) The *number of rays is adjusted dynamically* in order to maintain an approximately constant resolution as the WF expands or shrinks, and
(b) the WF definition as a surface with connectivity properties enables us to achieve *accurate interpolation of fields associated with rays.*

We describe in more detail two elements of the method:

(1) an algorithm for generating edge-diffracted WFs, and
(2) a procedure for evaluating currents induced on the scatterer surface by incident, reflected, and diffracted WFs, which can be used in the context of integral equation based methods.

(1) In order to generate a diffracted WF, we first construct, by interpolation, rays emerging from a WF and hitting (within the given tolerance) those edges of the (triangulated) scatterer surface which may be considered a source of diffraction (i.e., edges whose adjacent faces are sufficiently non-coplanar). Next, from the edge points hit by the interpolating rays, we launch sets of diffracted rays (with the angular spacing appropriate for the required WF resolution). Finally, we create ray-ray connectivity data to define the triangulated surface of the new diffracted WF.

(2) We parameterize the currents induced on the scatterer surface in terms of "large-support basis functions" (LSBFs) defined on sets of triangles of the scatterer surface mesh of sizes dependent on the scatterer geometry, but independent of the frequency, and, typically, large compared to the wavelength. The LSBFs incorporate the notion that the asymptotic HF solution should be representable as a sum of products of rapidly oscillating exponential factors (due to specific HF scattering mechanisms), and smooth modulating functions.

We evaluate the surface currents by constructing intersections of "ray tubes" with the scatterer surface, and interpolating the field associated with the rays. (Ray tubes are defined here as prisms consisting of triplets of rays emerging from vertices of a triangle belonging to the WF mesh.)

The algorithm elements (1) and (2) allow us to obtain asymptotic solutions to HF scattering problems at a cost independent of the frequency, and dependent only on the complexity of the scatterer geometry.

[1] Supported in part by AFOSR, under contract No. F49620-01-C-0045,

0-7803-7846-6/03/$17.00 ©2003 IEEE 

# Heuristic UTD and ITD for Edges in Penetrable and Coated Planar Screens

Roberto Tiberio*, Alberto Toccafondi and Alessia Polemi
Dept of Information Engineering, University of Siena
via Roma, 56, Siena, Italy

A *revisited* exact solution has been obtained for the electromagnetic problems of edges illuminated at skew incidence, for both an half-plane with surface impedance faces and a surface impedance discontinuity on a plane [R. Tiberio and A. Toccafondi, *IEEE AP-S Symp*, Columbus, OH, June 2003]. Also, an explicit exact spectral integral representation has been obtained for dipole source illuminations and finite distance observations. It is nowadays a simple matter to derive from them the Uniform Geometrical Theory of Diffraction (UTD) formulations for the relevant canonical problems. From these same exact solutions, an Incremental Theory of Diffraction (ITD) formulation has been obtained [R. Tiberio et al., *IEEE AP-S Symp*, Columbus, OH, June 2003] for defining incremental field contributions from local edge discontinuities in planar surfaces with impedance boundary conditions. Of course, both rigorous, high-frequency UTD and ITD solutions have an applicability which is limited to those practical cases that can be modeled by surface impedance boundary conditions. Furthermore, their expressions involve the Malyuzhinets special functions, that are somewhat difficult and time consuming to calculate.

In this paper, first it is shown that both the UTD and ITD formulations can be manipulated to provide rigorous expressions, where the Malyuzhinets special functions are confined into a convenient multiplying term. It is found that this term reduces to unity at both the incidence (SB) and reflection (RB) shadow boundaries and exhibits a slowly varying behavior. Several numerical experiments have shown that, when this term is approximated by unity throughout the calculations, results are obtained that very well compare with those from the rigorous formulations. Thus, it is suggested that this approximation may effectively be employed in most practical applications. Indeed, by introducing this approximation the dyadic diffraction (UTD) and incremental (ITD) coefficients are expressed in closed form.

Next, these formulations are heuristically extended to treat the cases of edges in penetrable and coated planar screens. This is basically achieved by replacing in the rigorous formulation, the reflection coefficients at a planar surface impedance by those at the actual screens. To this end, it is worth pointing out that the heuristic approximations need to be introduced in the relevant 2D rigorous solution. Then, this heuristically modified 2D solution is introduced into the same formulation as that used in the exact solution to obtain the 2D -3D transformation. This is indeed a peculiar property of the formulation of the above mentioned exact solution, in which the 3D solution is obtained as a simple combination, involving only trigonometric functions, of relevant scalar 2D solutions. Thus, after introducing suitable heuristic modifications, closed form high-frequency expressions are obtained that explicitly satisfy reciprocity, rigorously provide the continuity across the shadow boundaries of the GO field and satisfy the boundary conditions at the dominant asymptotic order.

Then, it is shown how surface wave contributions can be included into the simplified treatment of impedance boundary conditions, as well as into its heuristic extension for penetrable and coated screens.

Numerical results from the simplified expressions for impedance boundary conditions are compared with those from the rigorous high-frequency formulations. Also, calculations relevant to penetrable and coated screens are presented and discussed.

0-7803-7846-6/03/$17.00 ©2003 IEEE

# Hybridizing Asymptotic and Numerically Rigorous Techniques for Solving Electromagnetic Scattering Problems using the Characteristics Basis Functions (CBFs)

*G. Tiberi, A. Monorchio, G. Manara*
*Dept. of Information Eng.*
*University of Pisa, Italy*

*R. Mittra*
*EMC Lab*
*Penn State University, USA*

## Abstract

The problem of electromagnetic scattering from large bodies is often addressed by using asymptotic methods such as the GTD, because the size of the problem makes the numerically rigorous techniques either impractical or uneconomical to use. To render the problem manageable, one sometimes employs a numerically rigorous method, e.g., the Method of Moments with subdomain basis functions, on a part of the body to improve the accuracy of the solution, while using an asymptotic scheme—such as Physical Optics (PO)—elsewhere. This type of hybridization approach, though attractive in principle, is often found to be fraught with pitfalls when applied in practice, not only because it is difficult to find a systematic approach by which the two methods can be dovetailed, but also because it often leads to ill-conditioned matrices.

In this paper we describe a novel approach based on the use of the Characteristic Basis Functions (CBFs) [V.V.S. Rakash and Raj Mittra, Microwave and Optical Technology Letters, March 2003], which have the same features as the asymptotic solutions, but are utilized in a Galerkin type of numerically rigorous matrix method to satisfy the boundary condition on the scatterer. We assume that the scatterer can be represented as a faceted structure, and we introduce three types of *primary* CBFs to be used to represent the induced currents on the facets. The first type of the primary CBFs, have characteristics similar to the Physical Optics currents; but, unlike the PO currents, they exist both in the lit and shadow regions. The other two basis functions are similar to fringe currents, and they are either free-edge or corner-fringe types, depending upon the connectivity of the facet. The secondary basis functions are derived next from the primary ones by using the technique given in the reference above. The above basis functions are subsequently used to construct a matrix equation by imposing the boundary condition on the scatterer in a numerically rigorous manner — a feature unavailable in the asymptotic methods. Another useful feature of the CBFs is that, if necessary, they can be readily hybridized with RWG bases for complex objects. Two representative numerical examples involving a 4λ flat plate (left figures) and a 12λ dihedral (right figure) are given below to illustrate the application of the method.

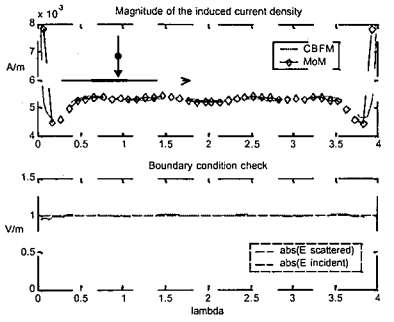


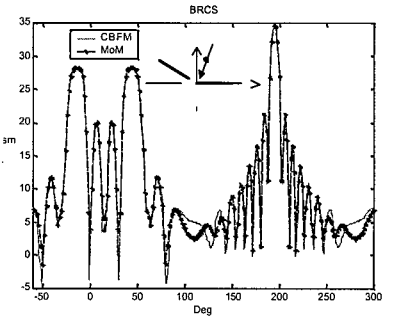


Note: We point out that the slight difference in RCS in the vicinity of the grazing angles stems from the inability of the MoM to satisfy the edge condition accurately, which the CBFs do satisfy rigorously. The difference in the edge behavior is evident from the top left figure, which plots the two current distributions. The number of CBFs are less than 10 in both of these examples.

0-7803-7846-6/03/$17.00 ©2003 IEEE

# Construction of large-support basis functions for rigorous high-frequency integral equations

E. Bleszynski, M. Bleszynski, and T. Jaroszewicz
Monopole Research, Thousand Oaks, CA 91360

During the last decade new matrix compression techniques characterized by the $N \log N$ solution complexity, where $N$ is the number of unknowns, were introduced. Their implementation extended the spectrum of electromagnetic scattering and radiation problems tractable in terms of integral equations methods. These compression techniques require that the geometry discretization (typically about 10 points per wavelength) reproduces accurately variations of the electromagnetic field. Hence the numerical size of the problem increases with the increase of frequency.

Further reduction in the solution complexity constitutes a serious challenge which may be addressed by applying techniques including domain decomposition, preconditioning, asymptotic evaluation of the matrix-vector product, as well as utilization of suitably chosen basis functions in selected areas of the scatterer surface. The latter approach utilizes the fact that, in the high frequency asymptotic, solutions (typically the surface current) can be parameterized as a sum of rapidly oscillating functions multiplied by functions varying slowly on the wavelength scale. The specific objective of these methods is to achieve an integral-equation discretization with a frequency-independent number of unknowns. In some approaches such parameterizations are built on the basis of approximate asymptotic high-frequency solutions, including Physical Optics approximation [1, 4] and multiple reflection effects [5]. In other approaches [2, 3] the known MoM solutions at a lower frequency are analyzed, and the characteristic oscillations are determined. This information is then used to construct basis functions defined on supports large compared to the wavelength and incorporating oscillatory factors. The basis functions are then extrapolated to a higher frequency.

In this contribution we present our recent results on the development of a particular realization of an LSBF based discretization model for solving scattering problem with frequency independent number of unknowns. The model consists of two components,

(i) LSBFs parameterized in terms of suitably chosen oscillatory factors representing contributions of incident, reflected and diffracted waves, coexisting with
(ii) locally confined small support basis functions needed to reproduce rapid variations of the solution near edges and corners.

We present the results of the validity tests of the above-mentioned LSBF model for representative scattering problems involving polygonal plates and their combinations. We find linear combinations of the LSBFs approximating the rigorous MoM solutions, and assess the approximations' accuracy by comparing the resulting scattered fields. We show that, if the relevant scattering mechanisms are incorporated in the LSBF construction, highly accurate approximations can be obtained in large frequency ranges with a frequency-independent number of parameters.

1. K.R. Aberegg and A.F. Peterson, "Application of the integral equation asymptotic phase method to two-dimensional scattering", *IEEE Trans. Antenn. Propagat.*, Vol. AP-43, pp. 534-537, 1995.
2. Z. Altman, R. Mittra, O. Hashimoto, and E. Michielssen, "Efficient representation of induced currents on large scatterers using the generalized pencil of function method", *IEEE Trans. Antenn. Propagat.*, Vol. AP-44, pp. 51-57, 1996.
3. D.-H. Kwon, R.J. Burkholder, and P.H. Pathak, "Efficient method of moments formulation for large PEC scattering problems using asymptotic phase-front extraction (APE)", *IEEE Trans. Antenn. Propagat.*, Vol. AP-49, pp. 583-591, 2001.
4. O. Bruno, A. Sei, and M. Caponi, "High-order high-frequency solutions for rough surface scattering problems", *Radio Science*,Vol. 37, 2002.
5. O. Bruno, "New high-order, high-frequency methods in computational electromagnetism", to appear in *Computational Methods in Engineering and Science*, 2002.

0-7803-7846-6/03/$17.00 ©2003 IEEE

# A Fast Hybrid UTD-PO for the Analysis of Very Large Cylindrical Reflectors with a Linear Feed Array

P. H. Pathak, K. Tap*, T.-H. Lee and T. Lertwiriyaprapa

ElectroScience Lab, The Ohio State University
1320 Kinnear Road, Columbus, OH 43212, USA
E-mail: pathak.2@osu.edu

In some radar applications it becomes necessary to employ a cylindrical reflector, fed by a linear antenna phased array for electronic scanning with a very high gain beam in the plane containing the array, and with a shaped beam in the other, orthogonal, plane. Conventional methods for analyzing such reflector and feed array combinations employ a physical optics (PO) integration over the reflector surface. The current induced on the reflector is calculated within the PO formulation in terms of the field incident from each antenna element of the array. Such a procedure becomes very time consuming and even intractable for electrically very large reflectors because the number of samples in the numerical PO integration increases rapidly with the electrical size.

A method is developed here to overcome the above problem and make the PO integration highly efficient. In particular, a given array distribution is expressed in terms of a very compact Discrete Fourier Transform (DFT) expansion, where each DFT term produces an asymptotic closed form expression for the field of the entire long array. Such an array field can be described via rays that emanate from an interior point on the array, and from the two end points of the array, respectively. This ray description follows the earlier development of (L. Carin, L. B. Felsen, and T.-T. Hsu, IEEE Trans. AP, AP-44, 1, 1-11, Jan. 1996; O. A. Civi, P. H. Pathak, H.-T. Chou, and P. Nepa, Radio Sci., 35, 2, 607-620, Mar.-Apr. 2000; F. Capolino, S. Maci, and L. B. Felsen, Radio Sci., 35, 2, 579-593 Mar.-Apr. 2000). Furthermore, this asymptotic ray field description for the array radiation can be expressed in the format of the uniform geometrical theory of diffraction (UTD). Such a composite UTD array field, which is incident on the cylindrical reflector, can facilitate the PO integral over the reflector surface to be performed essentially in closed form. Thus, one arrives at a highly efficient hybrid UTD-PO approach, utilizing UTD for the feed array together with PO for the cylindrical reflector, which allows one to treat feed array and cylindrical reflector combination that otherwise may become intractable using conventional element by element array field superposition used in conjunction with numerical PO based reflector field calculation. Numerical results will be presented to illustrate the speed and accuracy of the hybrid UTD-PO for treating very large array feed and cylindrical reflector combination.

0-7803-7846-6/03/$17.00 ©2003 IEEE

**How to Use the Method of Moments for Small Scattering Features in Your Physical Optics Code**

Robert J. Burkholder*
ElectroScience Laboratory, Dept. of Electrical Engineering
The Ohio State University, 1320 Kinnear Road, Columbus, OH 43212, USA
rjb@esl.eng.ohio-state.edu

Physical optics (PO) and the method of moments (MoM) both use equivalent currents to represent the electromagnetic (EM) fields scattered or radiated by a physical structure. The currents satisfy a surface integral equation that enforces the appropriate EM boundary conditions. PO finds the currents approximately using only the geometrical optics field and the local properties of the surface, whereas, the MoM solves for the currents via numerical solution of a matrix. It is natural to combine the two methods so that the currents on large, smooth portions of the body may be approximated using PO, and the currents on small features may be found more exactly using MoM. In this paper it is demonstrated how the two methods may be combined first using a hybrid iterative solution that includes the interactions between the PO and MoM regions (R.E. Hodges and Y. Rahmat-Samii, *IEEE Trans. on Antennas and Propagation*, 45(2), pp. 265-276, 1997). Then, to simplify the implementation into an existing PO code, a first-order reciprocity formulation is used to compute the scattered field from the small feature without having to iterate back to the large feature.

The iterative algorithm goes as follows:

1. Find the currents on the large body excited by the incident field using PO.
2. Using MoM, solve for the currents on the small feature excited by the incident field plus the fields radiated by the PO currents of step 1.
3. Find the modified currents on the large body due to the currents radiated by the small feature of step 2.
4. Repeat steps 2 and 3 until converged.
5. Compute the scattered field directly from all currents.

If only one iteration is needed, as is often the case, then step 4 may be omitted and steps 3 and 5 can be combined using reciprocity. The reduced algorithm is:

1. Find the currents on the large body excited by the incident field using PO.
2. Using MoM, solve for the currents on the small feature excited by the incident field plus the fields radiated by the PO currents of step 1.
3. Compute the scattered field using reciprocity.

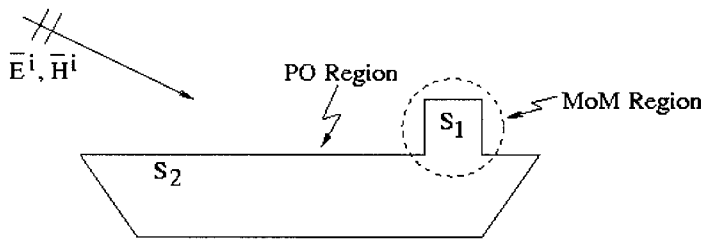


0-7803-7846-6/03/$17.00 ©2003 IEEE

# Analysis of Thick Metallic Dichroic Screens with Arbitrarily Shaped Apertures by a Hybrid Mode Matching - Finite Elements Technique

G. Manara*, A. Monorchio, and P. Grassi

Department of Information Engineering, University of Pisa
Via Diotisalvi 2, 56126 Pisa, Italy
e-mail: g.manara, a.monorchio, p.grassi@iet.unipi.it

Thick conducting screens periodically perforated with apertures are frequently used as inductive Frequency Selective Surfaces (FSSs), i.e., structures with the property of selectively reflecting or transmitting electromagnetic waves at certain frequency bands. The aim of this communication is to present a hybrid Mode Matching (MM) - Finite Elements (FE) technique to analyze inductive FSSs with arbitrarily shaped apertures, illuminated by a plane wave impinging on the structure at oblique incidence, even in the presence of inhomogeneous fillings of the apertures. As a first step, the electromagnetic field in the free-space region is expanded in a complete set of Floquet modal basis functions, with unknown complex coefficients. Next, the transverse electromagnetic fields inside each arbitrarily shaped aperture, considered as a section of a metallic waveguide, are represented by a complete set of waveguide modes obtained via the FE approach. In the case of inhomogeneous fillings, the complete set of complex hybrid modes is taken into account. Moreover, the problem of the spurious solutions is avoided by the use of both Whitney's Edge elements to interpolate transverse field components and Lagrange polynomials to reconstruct the longitudinal ones. Then, boundary conditions are applied at the interface between these two regions. Through the computation of the unknown modal coefficients, the Generalized Scattering Matrix (GSM) of the free-space/waveguide interface is determined. Finally, the GSM of the entire screen is obtained by considering the cascade connection of the lit face, the waveguide section, and the shadow face, then combining the corresponding matrices in accordance with the standard formulas for microwave circuits (A. Monorchio et al., "Analysis of waveguide discontinuities using edge elements in a hybrid Mode Matching/Finite Elements approach", *IEEE Microwave and Wireless Components Letters,* vol.11, pp. 379 -381, Sept. 2001).

The proposed hybrid scheme combines the MM and the FE method in order to retain the advantages of the two techniques, i.e., the numerical efficiency and the accuracy of the MM and the capability of the FE method to analyze complex and irregular structures. Some numerical results will be presented to demonstrate the accuracy and the effectiveness of this hybrid approach, with specific reference to the convergence rate of the technique.

0-7803-7846-6/03/$17.00 ©2003 IEEE

## GENERALIZED HYBRIDIZATION WITH ITERATIVE FIELD REFINEMENT

***Michael A. Carr (carr.96@osu.edu) and John L. Volakis (volakis.1@osu.edu)**
ElectroScience Laboratory, EE Dept., The Ohio State University, Columbus, OH 43212

When applying computational simulation techniques to scattering or radiation problems, it is often possible to decompose a complicated geometry into simpler elemental structures (i.e. a helicopter rotor system into its individual blades). It is then desirable to simulate each element separately, allowing a given problem to be decomposed into smaller and more manageable ones as long as coupling between each component is accounted for. To implement this coupling, we propose and employ in this paper an Iterative Field Refinement (IFR) method. Using IFR, it is then possible to accelerate simulation of geometries made up of rotated, translated, reflected, or replicated versions of a given structure. It is shown that the IFR approach not only reduces total computation time, but also allows for combining different analysis methods in treating each of the separate components comprising the structure.

Our approach differs from previous works by incorporating additional generality to decompose the geometry into a discrete set of smaller problems. One is then free to apply any method(s) of choice to model each of these components. Therefore, with careful selection of the fastest and most suitable method for each structure, the total simulation time can then be significantly reduced. IFR serves to include the coupling interactions among these structures, a process that normally requires interaction matrices (i.e. "coupling" matrices) to be incorporated into a large system matrix along with each of the individual structure matrices.

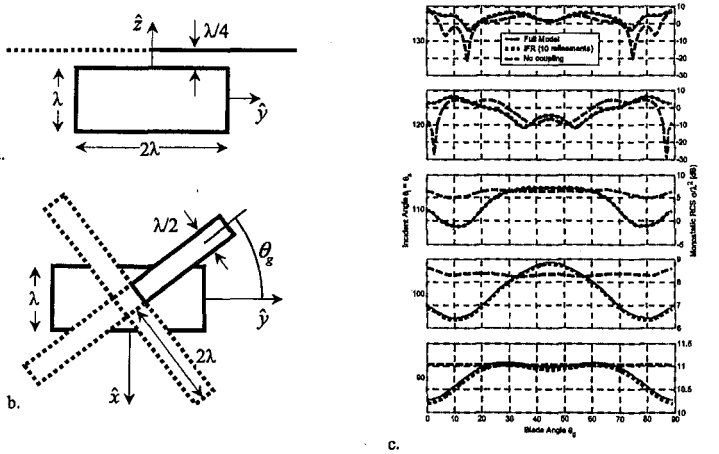


**Figure 1. Side (a) and top (b) views of four rotated helicopter blades in the presence of a fuselage, where three of the blades are replicas of the first; (c) Monostatic RCS vs blade angle ($\theta_g$) for several incidence angles for θθ-polarization. Results are shown for simulation of the full model, with IFR, and with no higher-order interactions.**

## Sources and Discontinuities in PBG and Other Periodic Structures

**Organizer(s):** F. Capolino
D. R. Jackson, University of Houston

**Co-Chairs:** F. Capolino
D. Jackson

1:15 Opening Remarks

119. 1 1:20 Enhanced Performance of a Microstrip Patch Antenna using a High Impedance EBG Structure ..... APS
*M. Fallah-Rad, L. Shafai, University of Manitoba, Canada*

119. 2 1:40 A Compact Microstrip Patch Antenna Having a 2-Dimentional Grounded-Pad Array Embedded in an LTCC Substrate ..... APS
*Y. Horii, Kansai University, Japan*

119. 3 2:00 Frequency Beam Scanning and Gain Enhancement Properties of PBG-Antennas .....526
*H. Boutayeb, K. Mahdjoubi, A. Tarot, IETR - Institut d' Electronique et de Télécommunications de Rennes, France*

119. 4 2:20 Metamaterials with Low Effective Permittivity for Directive Antennas .....527
*S. Enoch, G. Tayeb, P. Vincent, P. Sabouroux, N. Guérin, Institut Fresnel, France*

119. 5 2:40 Radiation from a Short Vertical Dipole in a Disk-Type PBG Material ..... APS
*M. G. Silveirinha, Universidade de Coimbra, C. Fernandes, Instituto Superior Técnico, Portugal*

119. 6 3:00 Theoretical and Experimental Characterization of Focusing in Periodically Loaded Transmission Line Negative Refractive Index Metamaterials .....528
*A. K. Iyer, G. V. Eleftheriades, University of Toronto, Canada*

119. 7 3:20 Full Wave Analysis of Sources Within Periodic Structures .....529
*H. D. Yang, University of Illinois at Chicago, USA*

119. 8 3:40 Field Representation in PBG Waveguides .....530
*F. Capolino, University of Siena, Italy, D. R. Jackson, D. R. Wilton, University of Houston, USA*

119. 9 4:00 Efficient Semi-Analytical Analysis of Two-Dimensional Photonic Crystals ..... APS
*D. Pissoort, D. De Zutter, F. Olyslager, Ghent University, Belgium*

119. 10 4:20 Three-dimensional Analysis of Coupled-cavity Waveguides ..... APS
*M. Vogel, Ansoft Corporation, USA, P. De Maagt, European Space Agency, The Netherlands*

119. 11 4:40 Orthogonal Anisotropy in 2D PBG Structures and Metamaterials .....531
*Christophe Caloz, I-Hsiang Lin, Tatsuo Itoh, UCLA, USA*

119. 12 5:00 Inhibited-Enhanced Spontaneous Emission in 2D Photonic Crystal Waveguides ..... APS
*S. Boscolo, M. Midrio, Università di Udine, C. G. Someda, Università di Udine, Italy*

# Frequency Beam Scanning and Gain Enhancement Properties of PBG-Antennas

H. Boutayeb, K. Mahdjoubi and A.C. Tarot
IETR, University of Rennes 1, Bat. 11D, Campus de Beaulieu, 35042 Rennes - France
mahdjoubi@univ-rennes1.fr

The main purpose of this communication is to present the frequency beam scanning possibility of PBG-antennas and the relationship with high gain property. To this end, we will first remind the gain enhancement phenomenon and then generalize the results to the steered beam antennas.

The first analysis and design of high gain antenna using periodic structures can be attributed to Von Trentini, where he used a simple Fabry-Perot (FP) cavity having a single partially reflecting surface (G.Von Trentini, *IRE Trans. on Antenna and Propagation,* vol. 4, 666-671, 1956). We will show that for FP structures, the angular selectivity $\Delta\theta_{3dB}$, i.e. the antenna half power beam width (HPBW), is related to the to the frequency selectivity, i.e. the quality factor Q of the structure by the following relationship : $\Delta\theta_{3dB} \approx 2/\sqrt{Q}$. More recently the defect mode of multiple layer PBG structures has been used to enhance the antenna directivity gain (M. Thevenot et al., *IEEE Trans., MTT*, vol. 47, no. 11, 1999). However, the frequency beam scanning property of PBG antennas or FP cavities has not been sufficiently emphasized on in the literature and is not well known to the antenna engineers. Hence, we propose here to focus on this aspect of PBG-antennas.

*Figure 1a* presents a simple PBG-antenna where the partially reflecting surfaces are constituted of single row of metallic rods. The beam angle of this structure as a function of frequency is given by the equation $\theta_s = \arccos(\varphi_r c/(4\pi f D))$, where $\varphi_r$ is the phase of the reflection coefficient of the cavity surfaces. In *fig. 2a*, $\theta_s$ is plotted versus the frequency. We present in *fig. 2b-g*, the radiation patterns for the frequencies corresponding to the steered beams $\theta_s$= 10°, 20°, 30°, 40° and 50°. For the steered beam case, the relation between angular and frequency selectivity becomes : $\Delta\theta_{3dB} \approx 2(\arccos(\cos\theta_s - \cos\theta_s/(2Q)) - \theta_s)$.

The second purpose of our communication is to show the effect of multiple layer PBGs on the antenna radiation pattern. Consider the PBG structure 2 (*fig. 1b*). For $D_2$=D, the radiation pattern for broadside beam (*fig. 2h*) seems to be more directive than the previous one (*fig. 2b*). For $D_2$=2D a "double beam" appears due to the coupling between cavities of the same resonance frequencies *(fig. 2i-j)*. This property may be used for "difference pattern" applications.

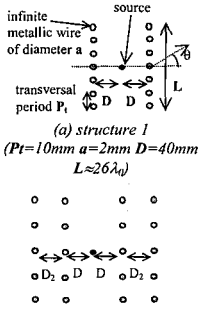


*(a) structure 1 (Pt=10mm a=2mm D=40mm L≈26λ0)*

*(b) structure 2 (Pt=20mm a=2mm D=40mm L≈26λ0)*

*Figure 1: Geometry of PBG-structures*

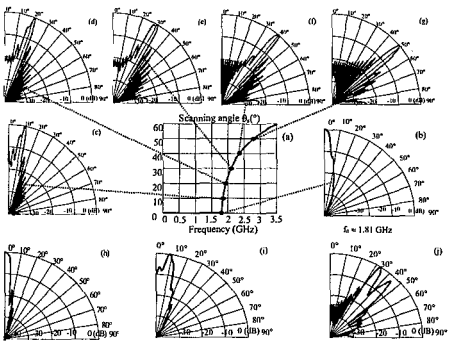


*Figures 2:* (a-g) *Frequency beam scanning with structure 1.* (h) *Broadside radiation pattern for structure 2 where $D_2$=D ($f_0$ ≈1.67GHz).* (i-j) *Broadside and steered patterns for $D_2$=2D. ($f_0$ ≈1.58 & 2.17GHz resp.)*

## Metamaterials with low effective permittivity for directive antennas

**S. Enoch *, G. Tayeb, P. Vincent, P. Sabouroux, N. Guérin**

*Institut Fresnel, UMR CNRS 6133, Faculté de Saint Jérôme, case 161, 13397 Marseille Cedex 20, France*

In this talk we describe our theoretical and numerical work, as well as our experimental results concerning the design of directive antennas. One of the aims is to obtain antennas much more compact than classical solutions. Another interesting feature is that these antennas can be excited by a single feeding device (patch, monopole). Such antennas could be useful for microwave telecommunications.

The behavior of the antenna presented in this talk is based on the properties of a stack of metallic grids, which can be considered as a photonic crystal, a grating, a metamaterial, a complex media, depending on the reader's habits. As well known, these grids have filtering properties. First, they completely filter the low frequencies that cannot propagate inside (low frequency bandgap). We are mainly interested in the small frequency range associated with the transition between the low frequency bandgap and the allowed propagating solutions. Several studies have shown that in this frequency range where the wavelength is much greater than the period of the periodic media, the metamaterial can be homogenized in a material whose relative permittivity has a behavior governed by a plasma frequency in the microwave domain: $\varepsilon_{eff} = 1 - \omega_p^2 / \omega^2$. Of course, using this expression, one can check that the low frequencies see the metamaterial with a negative permittivity, i.e. a pure imaginary optical index, and so the only solutions are evanescent waves. But this expression also tells us that for frequencies just a little bit larger than the plasma frequency, the relative permittivity stays between 0 and 1, and the same is valid for the optical index. In this case where the metamaterial has an effective optical index which can be close to zero, one can expect ultrarefraction phenomena. This remarkable property is the key idea which governs the behavior of the antenna.

The two-dimensional case is used for the preliminary studies. We show that, for thin wires, many properties can be derived from the two-dimensional model. Three-dimensional codes based on Harrington's wire approximation allow us to get a more realistic model, but lead to very large numerical systems.

0-7803-7846-6/03/$17.00 ©2003 IEEE

# Theoretical and Experimental Characterization of Focusing in Periodically Loaded Transmission Line Negative Refractive Index Metamaterials

A. K. Iyer and G. V. Eleftheriades

Department of Electrical and Computer Engineering
10 King's College Rd.
University of Toronto
Ontario, M5S 3G4, CANADA

We have previously shown that a new class of Negative Refractive Index Metamaterials (NRIMs) can be constructed by periodically loading a host transmission line medium with inductors and capacitors in a dual (high-pass) configuration. A 55mm×30mm planar NRIM lens interfaced with a parallel-plate waveguide recently succeeded in experimentally demonstrating focusing of cylindrical waves[1].

In this paper, we present theoretical, simulation, and experimental data describing the focusing and dispersion characteristics of a larger device consisting of a 105mm×200mm NRIM lens interfaced with a 105mm×100mm Positive-Refractive-Index Medium (PRIM), the latter of which is constructed using an unloaded microstrip grid. This new prototype offers significant improvements over the smaller structure originally used to verify focusing; specifically, the edge effects are minimized to more clearly observe the attributes of the focal region; the increased size of the NRIM region permits a closer observation of the spatial evolution of phase and therefore the extraction of more precise dispersion information; and the use of a microstrip grid instead of a parallel-plate waveguide enables the direct measurement of the transmission from the source to the focal region through proximity coupling.

In order to compare the new experimental results with theory, we employ a technique based on the plane wave expansion of cylindrical waves to examine a homogeneous PRIM/NRIM interface excited by an infinitesimal line source oriented vertically to the device plane; this is equivalent to determining the corresponding Green's function. This theory is verified by full-wave electromagnetic simulations conducted on a microstrip implementation of the same structure excited by a shorted vertical dipole source. Supporting experimental data is then presented, revealing vertical electric field distributions consistent with the focusing of cylindrical waves. In particular, the fields at the focal plane exhibit a transmission of nearly unity with respect to the source at 1.8GHz, the frequency at which the theory predicts a relative refractive index of $-1$. The dispersion characteristic of the NRIM is obtained from the experimental data using the average phase shift incurred per unit cell ($\beta d$), and depicts an extremely broadband region spanning approximately 1.5GHz over which the refractive index remains negative. These results are in excellent correspondence with the dispersion characteristics predicted by standard periodic analysis.

[1] G. V. Eleftheriades, A. K. Iyer, P. C. Kremer, "Planar negative refractive index media using periodically L-C loaded transmission lines," *IEEE Trans. on Microwave Theory and Tech.*, vol. 50, no. 12, pp. 2702-2712, Dec. 2002.

0-7803-7846-6/03/$17.00 ©2003 IEEE

# Full-Wave Analysis of Sources within Periodic structures

H.Y.D. Yang
ECE Dept., University of Illinois at Chicago

Electromagnetic wave interaction with periodic structures has significant renewed interest in recent years. Common analytic/numerical methods including plane-wave (Floquet mode) expansion method, integral equation method, time-domain or frequency-domain finite difference method, and finite element method, are more suitable to purely periodic structures. Periodic structures with localized sources or objects are important in many areas of engineering and science. Examples include undesired radar cross section (RCS) in frequency selective surfaces, radiation degradation in phased array, trapped-wave modes in periodic waveguides, and defects or sources within photonic band-gap structures. The implementation of artificial periodic materials into integrated circuit and antenna structures also results in many new applications.

Up to date, Field analysis of source interaction with periodic structures has not received much attention. In principle, discrete methods such as finite difference or finite element method could provide accurate field solutions. However, from the analysis point of view, it is more advantageous to use a continuous method for infinite structures. The fundamental parameters that characterize the devices can be readily and accurately extracted from the numerical results, in spite of the fact that real physical device must be truncated. In this paper, we overview a double-vector integral equation (DOVIE) method, which is efficient, stable, and accurate. This method applies to general infinite periodic structures with anomalies. The method uses an array-scanning method to find the Green's function for sources within general periodic structures. This approach also provides useful information on the field transition into periodic Floquet mode. Subsequently, the moment method is applied to determine the current distribution over the sources. This approach is a continuous method and its accuracy is similar to typical moment method for canonical boundary-value problems. Several examples are given to demonstrate the applicability of the approach. These include microstrip dipole antennas on a planar electromagnetic band-gap substrate, microstrip lines on a planar periodic structure, and source within corrugated parallel-plate waveguides.

0-7803-7846-6/03/$17.00 ©2003 IEEE

# Field Representation in PBG waveguides

**Filippo Capolino*, David R. Jackson**, and Donald R. Wilton****

*Department of Information Engineering, University of Siena, 53100 Siena, Italy
**Department of ECE, University of Houston, Houston, TX 772044005, USA

Photonic band gap (PBG) structures have been used recently to modify the radiation and modal characteristics of sources located near or within them. For example, such structures have been used to suppress surface-wave propagation on dielectric substrates, obtain highly-directive antenna patterns, and achieve low-loss propagation in the millimeter-wave and optical ranges. A PBG material with a row of defects (missing elements) constitutes a waveguiding structure that provides an attractive alternative to conventional waveguides. The applicability of such materials for constructing devices such as switches, multi/demultiplexers, power dividers, couplers, etc., is also receiving increasing interest.

In the present investigation we examine some fundamental properties pertaining to the field representation from a source within a periodic PBG waveguiding structure. The canonical structure that is chosen consists of an infinite 2D PBG structure, with a row of defects that forms the waveguide channel in the $z$ direction. A line source (in the $y$ direction, parallel to the PBG elements) is placed within the channel to form the excitation. One issue in connection with the field representation is completeness; namely, do the modes of the PBG waveguide form a complete set with which to expand the field of the source? Another fundamental issue is the relationship between the nature of the fields inside the PBG waveguide that are excited by the source, and the stopband properties of the surrounding PBG structure.

An exact solution for the field within the PBG waveguide due to the line source can be obtained numerically using a full-wave periodic method of moments. However, the phenomenology is much easier to understand when a simplified model is used, in which the interaction of higher-order Floquet modes between adjacent rows of elements is neglected. For analyzing wave propagation at an arbitrary angle within the PBG structure, the structure on either side of the channel is modeled as a transmission line (in the $x$ direction) with a periodic distribution of shunt loads. This model allows for a Bloch-wave analysis to be used to model the surrounding PBG structure in a spectral-domain analysis for the field excited by the line source. This in turn allows for an analytical representation of the fields within the PBG waveguide so that the field phenomenology can be conveniently studied.

Particular attention is given to the complex longitudinal wavenumber plane (the $k_z$ plane). The poles in the $k_z$ plane determine the modal excitation within the PBG waveguide. The branch points in the $k_z$ plane determine the nature of the continuous-spectrum field that exists within the waveguide, in addition to the modal field. Because of this continuous-spectrum field, the total field within the PBG waveguide excited by the source is never representable solely by the modes of the waveguide (unlike the case of a source within a conventional waveguide of perfectly conducing walls). However, the continuous-spectrum field decays exponentially away from the source when the surrounding PBG structure is operating in a stopband. When the PBG structure is not operating within a stopband, the continuous-spectrum field decays algebraically instead of exponentially.

0-7803-7846-6/03/$17.00 ©2003 IEEE

# Orthogonal Anisotropy in 2D PBG Structures and Metamaterials

Christophe Caloz, I-Hsiang Lin and Tatsuo Itoh

Electrical Engineering Department, University of California, Los Angeles, CA 90095, caloz@ee.ucla.edu

*Orthogonal anisotropy* in 2D PBG structures and metamaterials is explored. Orthogonal anisotropy represents a particular case of anisotropy of a periodic architecture characterized by distinct electromagnetic behaviors along orthogonal directions $x$ and $y$. An example of an orthogonally anisotropic structure is the anisotropic UC-PBG microstrip ground plane consisting of an array of slots with filtering and propagating properties along $x$ and $y$, respectively (C. Caloz, C.-C. Chang, and T. Itoh, "A Novel Anisotropic Uniplanar Compact Photonic Band-Gap (UC-PBG) Ground Plane", European Microwave Conference, vol. 2, pp. 185-187, London, United Kingdom, September 2001).

In this contribution, we focus on anisotropy in *effective periodic structures*, where the lattice constant $a$ is much smaller than wavelength ($a \ll \lambda$), in contrast to typical PBG structures ($a \cong \lambda/2$). In particular, we investigate the existence of an anisotropic structure possessing a "horse saddle" type spectral distribution, as shown in Fig. 1. Such a mode is *propagating forward* (RH) *only in the x direction at frequencies lower than* the center point of the saddle $\omega_0$, and is *propagating backward* (LH) *only in the y direction at frequencies higher than* $\omega_0$. At the $\Gamma$ point, which is the point of "perfect effectiveness" (medium perfectly homogeneous) because the guided wavelength is infinite ($a/\lambda_g = 0$), the group velocity is zero and therefore no propagation occurs. But just above and below $\omega_0$, quasi-effective propagation can occur, with the interesting frequency/spatial anisotropy explained.

2D orthogonally anisotropic structures are demonstrated in lumped-element and distributed configurations

A structure exhibiting a mode of the type shown in Fig.1 could be used in anisotropic waveguide ($\omega$ outside the radiation cone) or antenna/reflector ($\omega$ inside the radiation cone) applications, respectively.

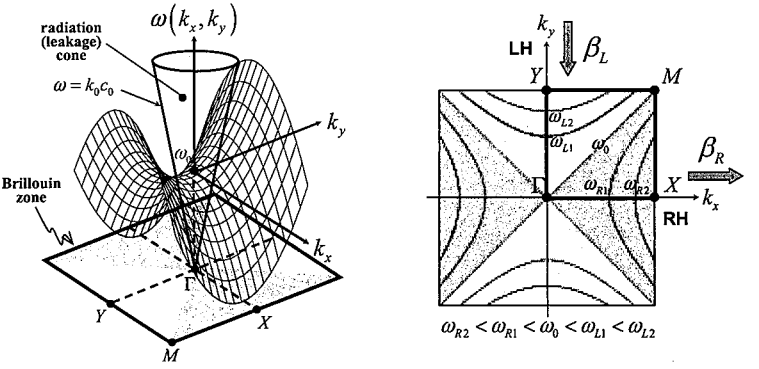


**Figure 1** Spectral distribution for a possible mode $\omega(k_x,k_y)$ in an orthogonally anisotropic 2D periodic structure, characterized by right-handedness along $x$ and left-handedness along $y$. (a) 3D "horse saddle" type configuration of the mode. (b) 2D projection of the mode for different frequencies represented by different contours.

0-7803-7846-6/03/$17.00 ©2003 IEEE

## Wave Propagation in Enclosed Structure and Wall Effects

**Co-Chairs:** H. Y. Pao
K. Casey

1:15 Opening Remarks

120. 1 1:20 Modal Propagation in a Circular Waveguide with a Rough Wall ..... 534
*K. F. Casey, SRI International, USA*

120. 2 1:40 Modelling of Wave Propagation in Rough Mine Tunnels ..... APS
*M. Ndoh, Laval University, G. Y. Delisle, University of Ottawa, Canada*

120. 3 2:00 Simulations and Measurements of Wave Propagations in Curved Road Tunnels for Signals from GSM Base Stations ..... APS
*T.-S. Wang, Chin-Min College, C.-F. Yang, National Taiwan University of Science and Technology, Taiwan*

120. 4 2:20 Analysis of Radio Wave Propagation Characteristics in Rectangular Road Tunnel At 800 MHz and 2.4 GHz ..... APS
*Y. Kim, M. Jung, B. Lee, Kyunghee University, Korea*

120. 5 2:40 The Effect of Different Kinds of Walls on the Attenuation of Radiowaves Indoors ..... APS
*P. Ali-Rantala, L. Ukkonen, L. Sydanheimo, M. Keskilammi, M. Kivikoski, Tampere University of Technology, Finland*

120. 6 3:00 28 GHz Scattering by Brick and Limestone Walls ..... APS
*C. L. Dillard, T. M. Gallagher, C. W. Bostian, D. G. Sweeney, VA Tech, USA*

# Modal Propagation in a Circular Waveguide with a Rough Wall

Kendall F. Casey
SRI International
333 Ravenswood Avenue
Menlo Park, CA 94025 USA

In order to develop an improved understanding of electromagnetic wave propagation in possibly rough-walled regions such as caves and tunnels, we first consider the effects of a randomly rough wall on the propagation of electromagnetic modes in a perfectly conducting quasi-circular waveguide. We wish to determine the utility of a modal field representation, investigate the partitioning of mode power between coherent and incoherent parts of the field, and describe the statistical properties of the modal fields in terms of the statistical properties of the wall roughness.

The field is represented in terms of two scalar functions that satisfy the scalar Helmholtz equation. Forcing the tangential electric field to vanish on the rough wall, we make use of the Wiener-Ito stochastic functional calculus to represent the resulting conditions on the unknown functions that describe the field. We show that the problem becomes one of solving an infinite set of coupled stochastic integral equations for these functions. We develop an approximate solution to the coupled integral equations by using an iteration scheme that is initialized to represent a mode in an equivalent smooth-walled guide. The radius of this smooth-walled guide is less than the average radius of the rough-walled guide, the reduction depending on the variance of the wall roughness, and the modal cutoff frequency is correspondingly higher.

It is shown that this process yields a representation for the modal field that comprises a coherent part similar to the modal field in an equivalent smooth-walled guide of reduced radius, and an incoherent part whose expected value is zero and whose variance depends on radial position within the guide. The variance is largest near the rough wall and decreases as the observation point moves toward the axis of the guide. Representative numerical results are presented to illustrate the analysis; and inferences are drawn regarding the problem of wireless communication in tunnels with rough walls.

0-7803-7846-6/03/$17.00 ©2003 IEEE 

*Special Session*

## Lightning Effects in the Upper Atmosphere

**Organizer(s):**

**Co-Chairs:** S. Cummer
E. Bering

1:15 Opening Remarks

122. 1 1:20 Lighning Effects on the Radiation Belts and the Lower Ionosphere ..... 537
*U. S. Inan, Stanford University, USA*

122. 2 1:40 Sprites Produced by Positive and Negative Lightning Discharges Above Haiti/Dominican Republic Thunderstorms ..... 538
*V. Pasko, Penn State University, S. Cummer, Duke University, M. Stanley, Los Alamos National Laboratry, J. Mathews, Penn State University, U. Inan, T. Wood, Stanford University, E. Williams, R. Boldi, Massachusetts Institute of Technology, USA, M. Sato, Y*

122. 3 2:00 THE RESULTS from the 1999 SPRITES BALLOON CAMPAIGN ..... 539
*E. A. Bering, L. Bhusal, J. R. Benbrook, J. A. Garrett, A. P. Jackson, University of Houston, E. M. Wescott, D. R. Moudry, D. D. Sentman, H. C. Stenbaek-Nielsen, University of Alaska, W. A. Lyons, FMA Research, Inc., USA*

122. 4 2:20 First Results from the 2003 Brazil Sprite Campaign ..... 540
*M. P. McCarthy, R. H. Holzworth, J. N. Thomas, T. Chinowsky, University of Washington, M. J. Taylor, D. Pautet, Utah State University, USA, O. Pinto, Jr, I. Pinto, DGE/INPE, Brazil*

122. 5 2:40 What Are the Differences Between Sprite-producing and Non-sprite-producing Lightning? ..... 541
*S. A. Cummer, W. Hu, Duke University, W. A. Lyons, T. E. Nelson, FMA Research, Inc., USA*

122. 6 3:00 Development of High Speed Spectrograph for Sprite Observations ..... 542
*M. G. McHarg, R. K. Haaland, United States Air Force Academy, USA*

122. 7 3:20 Non-standard Sprites At 1 Ms Time Resolution ..... 543
*D. R. Moudry, H. C. Stenbaek-Nielsen, D. D. Sentman, Geophysical Institute, University of Alaska Fairbanks, USA*

122. 8 3:40 Telescopic Imaging of Upper Atmospheric Streamer and Diffuse Glow Dynamics ..... 544
*E. A. Gerken, U. S. Inan, STAR Laboratory, Stanford University, USA*

122. 9 4:00 Effects of Photoionization on the Dynamics of Positive and Negative Streamers in Sprites ..... 545
*N. Liu, V. Pasko, T. Heffner, Penn State University, USA*

122. 10 4:20 Finite Element Modeling of the Vertical and Horizontal Electric Field Signatures in the Presence of a Sprite ..... APS
*M. E. Baginski, Auburn, University, M. D. Desphande, NASA, Langley, D. L. Faircloth, Auburn, University, USA*

122. 11 4:40 A New FDTD Model for Lightning Generated EM Wave Simulation ..... APS
*W. Hu, S. A. Cummer, Duke University, USA*

122. 12 5:00 DEFORMATION of the SPATIAL SPECTRUM of SCATTERED RADIATION in ABSORPTIVE MAGNETOACTIVE PLASMA ..... APS
*G. V. Jandieri, Georgian Technical University, V. G. Gavrilenko, Nizhny Novgorod State University, Russia V. V. Jandieri, N. M. Daraselia, Georgian Technical University, Georgia, USA*

**LIGHTNING EFFECTS ON THE RADIATION BELTS AND THE LOWER IONOSPHERE**

Umran S. Inan
STAR Laboratory, Stanford University, Stanford, CA 94305

Energy released in lightning discharges affect the lower ionosphere and the radiation belts in a multiplicity of ways, including directly through heating of ambient electrons via quasi-static and electromagnetic fields, production of upward going energetic electron beams, and indirectly through the precipitation of energetic radiation belt particles. In this paper we review some of these phenomena emphasizing the direct comparison of theoretical predictions and experimental data. The impulsive and transient nature of the causative lightning discharge, especially the fact that it often can be definitively measured, located and characterized, allows such comparison between experiment and measurement in ways that are typically not possible in investigations of other space plasma phenomena. For example, the precise timing of the rapid lateral expansion of elves (as measured from the ground) was first predicted and then measured using the Stanford Fly's Eye instrument, allowing the definitive determination of electron-heating by impulsive electromagnetic signal (EMP) as being the root cause. More recently, the spatial morphology of elves were measured from space, once again with a precision and resolution allowing direct comparison with predictions. Concerning lightning-induced precipitation of energetic radiation belt electrons, satellite measurements in the 1980s allowed direct comparison of theoretically predicted energy spectra, temporal profile, and pitch angle distribution with that measured on a low altitude satellite. Since then, the temporal profile of lightning-induced precipitation events have been regularly measured with ground-based sub-ionospheric VLF technique and comparison of the timing measurement with predictions have allowed the discovery and classification of different types of precipitation involving ducted, non-ducted, and magnetospherically reflecting waves. We present an overview of the direct comparisons between experiment and measurement in the context of lightning-driven effects on the radiation belts and the lower ionosphere, including a discussion of the outstanding (i.e., not yet measured) prediction of the production of upward moving energetic electron beams, driven by intense quasi-static fields.

0-7803-7846-6/03/$17.00 ©2003 IEEE 

# SPRITES PRODUCED BY POSITIVE AND NEGATIVE LIGHTNING DISCHARGES ABOVE HAITI/DOMINICAN REPUBLIC THUNDERSTORMS

Victor Pasko*[1], Steve Cummer[2], Mark Stanley[3], John Mathews[1], Umran Inan[4], Troy Wood[4], Earle Williams[5], Robert Boldi[5], Mitsuteru Sato[6], Yukihiro Takahashi[6]
[1]Penn State University, University Park, PA 16802, USA
[2]Duke University, Durham, NC 27708, USA
[3]Los Alamos National Laboratory, Los Alamos, NM 87545, USA
[4]Stanford University, Stanford, CA 94305, USA
[5]Massachusetts Institute of Technology, Cambridge, MA 02139, USA
[6]Tohoku University, Aramaki-aoba, Sendai 980-8578, Japan

In August-September 2001 an experimental campaign has been conducted in Puerto Rico to perform correlative studies of lightning and lightning-induced ionospheric effects. The campaign, which was sponsored by a Small Grant for Exploratory Research from the National Science Foundation to Penn State University, had a broad range of scientific goals including studies ionospheric effects of thunderstorms, studies of VHF-quiet positive leaders and studies of large scale optical phenomena above ocean thunderstorms in tropics. As part of this program we conducted night time video recordings of lightning and large scale luminous phenomena above thunderstorms using a SONY DCR TRV 730 CCD video camera equipped with a blue extended ITT Night Vision GEN III NQ 6010 intensifier with 40 deg field of view. The intensifier provided a monochrome (predominantly green) image output. The video system was deployed at the Lidar Laboratory on the grounds of Arecibo Observatory, Puerto Rico (18.247 deg N, 66.754 deg W, elevation 305 m above the sea level).

We report here low light video and ELF recordings of 8 sprite events observed above a Haiti/Dominican Republic thunderstorm from Arecibo Observatory, Puerto Rico between 01:10 and 02:51 UT on September 3, 2001. The sprite producing thunderstorm system was located approximately 700 km from the observational site and had the cloud area exceeding $10^4$ km$^2$. Morphological features of the observed events closely resemble those observed in other parts of the globe and include, in particular, isolated columns, groups of two or more columns, 'dancing sprites', and small impulsive glows confined to higher altitudes. ELF recordings, performed at Duke University, at Rhode Island MIT site, and at Palmer (Stanford University) and Syowa (Tohoku University) Antarctic stations, identified the 7 of the observed events as to be clearly associated with positive cloud to ground lightning discharges (+CGs) involving the vertical charge moment changes ranging between +143 C km to +2520 C km. The observed QL=143 C km for the weakest sprite event is consistent with the experimentally established 120 C km minimum lightning charge moment change required for the initiation of a sprite [Hu et al., GRL, 29, 10.1029/2001GL014593, 2002]. One sprite event (02:05:49.561 UT) was confirmed in ELF records collected at all four observational sites as being produced by an impulsive CG lightning with negative polarity. The associated vertical charge moment change was estimated to be -278 C km in 1.2 ms.

0-7803-7846-6/03/$17.00 ©2003 IEEE 

# THE RESULTS FROM THE 1999 SPRITES BALLOON CAMPAIGN

E. A. Bering, III[1]*, L. Bhusal[1], J. R. Benbrook[1], J. A. Garrett[1], A. P. Jackson[1], E. M. Wescott[2], D. R. Moudry[2], D. D. Sentman[2], H. C. Stenbaek-Nielsen[2], and W. A. Lyons[3]

[1]*Physics Department, University of Houston, 617 Science & Research, I, Houston, TX 77204-5005, USA*

[2]*Geophysical Institute, University of Alaska, Fairbanks, Alaska, USA*

[3]*FMA Research, Inc., Yucca Ridge Field Station, 46050 Weld County Road 13, Ft. Collins CO 80524, USA*

A balloon campaign was conducted in summer, 1999, to measure the stratospheric electromagnetic fields associated with sprites. This paper will summarize some of the salient results this work. The balloon payloads were instrumented with electric field detectors, magnetometers, an upward looking photometer, and other instruments. Ground observations for detection of sprites included low light level TV (LLTV) observations from three sites, Jelm Mt., WY, Bear Mt., SD, and Yucca Ridge, CO. The disagreements between models and these data will be discussed. The all-sky upward looking photometer data was examined by checking the trace at the times of cloud to ground (CG) strokes reported by the US National Lightning Detection Network (NLDN) to find transient luminous events (TLE's) that were missed visually. In total numbers, the number of -CG TLE's (presumably all halos) predominates over the number of +CG TLE's. 3602 events were analyzed in 4.1 hours of storm time. Threshold current moments of ~50 kA-km for the positive cloud to ground (+CG) TLE's and ~-5 kA-km for negative cloud to ground (-CG) TLE'S are found. Inclusion of the -CG events that are not seen from the ground raises mesospheric power input estimates by a factor of ~5-7. Including the mesospheric effect of CG's not associated with TLE's increases this estimate by a factor of 20.

0-7803-7846-6/03/$17.00 ©2003 IEEE 

## First Results from the 2003 Brazil Sprite Campaign

Michael P. McCarthy*, Robert H. Holzworth, Jeremy N. Thomas
and Timothy M. Chinowsky; *University of Washington*
Michael J. Taylor and Dominique Pautet; *Utah State University*
Osmar Pinto, Jr. and Iara Pinto; *INPE, Sao Jose dos Campos*

We will present and discuss new observations from the 2003 Brazil sprite campaign. This campaign combined low light video equipment and a balloon instrument payload to study sprites. Near sunset on 6-December-2002, a balloon was launched from Cachoeira Paulista, Brazil during a period of local active thunderstorms in order to obtain *in situ* electrodynamic, optical, and x-ray measurements of sprites. The balloon flew within 50 km of 279 lightning network cataloged strokes and within 50–100 km of another 379 detected strokes. The instrumentation consisted of optical flash detectors, x-ray spectrometers, and vector electric and magnetic field probes covering the frequency range from DC–10 kHz. Two different electric field instruments were used in order to cover a wide dynamic range of 0.001–250 V/m.

Following the University of Houston campaign in the United States during summer 1999, this campaign is the second effort to make near measurements of conductivity, the quasi-static electric field environment, and electromagnetic changes at sprite-producing thunderstorms. An unexpectedly high and extensive cloud cover blocked views of high altitudes from the aircraft and prevented camera confirmation of sprite activity during the first balloon flight. Nevertheless, instrumentation on the balloon functioned nominally and we obtained good measurements. Specific new observations include the first ground and aircraft sprite images from Brazil, and stratospheric electric fields an order of magnitude larger than has been previously reported.

0-7803-7846-6/03/$17.00 ©2003 IEEE 

# What Are the Differences Between Sprite-producing and Non-sprite-producing Lightning?

Steven A. Cummer*, Wenyi Hu, Electrical and Computer Engineering Department, Duke University, Durham, NC 27708, USA (email: cummer@ee.duke.edu)

Walter A. Lyons, Thomas E. Nelson, FMA Research, Inc., Fort Collins, CO 80254, USA

Ongoing measurements have shown that the relationship between lightning and sprites is be complicated. To be sure, lightning discharges with large charge moment changes, which create relatively strong electric fields at mesospheric altitudes, do preferentially generate sprites. However, it is known experimentally that exceptionally few sprites are created by negative cloud-to-ground (CG) lightning, despite measurements showing similar occurrence rates between large +CG and -CG lightning in many circumstances [e.g., Huang et al., JGR, 1999]. This polarity asymmetry is not well-understood. Moreover, a preliminary analysis of charge moment changes in many North American sprite-producing discharges during the summer of 2000 has indicated that similar discharges sometimes do and sometimes do not make sprites [Hu and Cummer, GRL, 2002], suggesting at a minimum some day-to-day variability in the ability of lightning to generate sprites. We will present a systematic study of the lightning in individual thunderstorms to determine the differences between lightning that does and does not generate sprites. Local video and remote extremely low frequency (ELF) magnetic field measurements were made during the Severe Thunderstorm Electrification and Precipitation Study (STEPS) in the summer of 2000. These measurements are a relatively complete set of sprite occurrences and lightning charge moment changes spanning many days and individual storms. Specific issues that will be addressed include a comparison in individual storms of charge moment changes in positive cloud-to-ground (CG) lightning that did and did not generate sprites, and a determination of the distribution and limits of charge moment changes in negative CG lightning throughout the entire campaign period. An improved understanding of why some lightning discharges do generate sprites and others do not should expand our knowledge of sprites processes and their global implications.

0-7803-7846-6/03/$17.00 

# Development of High Seed Spectrograph for Sprite Observations

Matthew G. McHarg, Ryan K. Haaland
*United States Air Force Academy*

We describe a high speed spectrograph being developed for sprite observations. The spectrograph is based around a 16 channel multi-anode photo-multiplier array which can be run at 20kHz per channel. The spectral range of the instrument will cover the 400-500nm, thus making it possible to track the temporal evolution of both neutral and ionized Nitrogen emissions from sprites. Calibration results on optical emissions from streamers in low pressure gasses in a large plasma chamber will be presented.

0-7803-7846-6/03/$17.00 

"Non-standard sprites at 1ms time resolution"

Dana R. Moudry, Hans C. Stenback-Nielsen, and Davis D. Sentman
Geophysical Institute drm@gi.alaska.edu
University of Alaska Fairbanks +1(907)474.7410
Fairbanks, AK 99775-7320 elf.gi.alaska.edu/~drm

In 1999 the University of Alaska Fairbanks deployed a 1-ms high speed imager to Wyoming to observe sprites above thunderstorms as part of the 1999 NASA Sprite Balloon Campaign [Bering et al, 2002, Geophys. Res. Lett. 29(5), 10.1029/2001GL013267]. During the night of August 17-18 (August 18 Universal Time), a thunderstorm over Nebraska produced many upper atmospheric optical events, with 26 sequences imaged using the high speed imager. The events covered a range of sprite types, and also some unusual examples, which will form the basis of this presentation. While the examples are unusual in that we have only one or few examples of each, they contain clues to sprite mechanisms. Previous work [Stenback-Nielsen et al, 2000, Geophys. Res. Lett. 27(23), 3829] has shown examples where new sprite tendrils are initiated from beads leftover from a previous sprite. In this presentation, a similar example is presented, where the new sprite tendril appears initiated from the upper end of an upward branch of the previous sprite. Two examples are presented of puffs forming on top of sprite branches, and subsequently the puffs rebrightening during the next halo occurrence approximately 60 ms later. Examples of long-duration (¿50 ms) sprites will also be presented: some include multiple temporally-separate sets of downward moving tendrils, others include only one set of downward tendrils followed by long-duration beads. In one sprite, beads left at two different altitudes move towards each other and, upon reaching the same altitude, create a new carrot sprite. This occurs during continued lightning activity in the underlying thundercloud which is visible as Rayleigh-scattered light above the cloudtops. All of these examples point to additional processes occurring in sprites besides the conventional breakdown and streamer processes suggested in the past decade [Barrington-Leigh et al., 2001, J. Geophys. Res. 106 (A2), 1741; Liu et al., Eos Trans. Suppl. - Amer. Geophys. Union, 2002, 83(47), A11C-0108].

0-7803-7846-6/03/$17.00 ©2003 IEEE

# Telescopic imaging of upper atmospheric streamer and diffuse glow dynamics

Elizabeth A. Gerken and Umran S. Inan
STAR Laboratory, Stanford University

Telescopic imaging shows that decameter-scale structure in luminous lightning-related discharges above thunderclouds (known as "sprites") covers a wide range of morphologies and time scales. Hundreds of sprites have been observed by the Stanford University telescopic imager. Certain categories of structures have been found to occur such as upward and downward branching, beading, propagating diffuse glow striations and streamer/diffuse glow transition regions. During the summers of 1998-2000, Stanford University deployed a telescopic imaging system, consisting of a ~41 cm diameter, f/4.5 Dobsonian-mounted Newtonian reflecting telescope with an intensified CCD camera attached to its eyepiece, a bore-sighted wide field of view (FOV) camera mounted on its top, and both telescopic and wide field of view photometers. The FOV of the telescope (0.5 in CCD) was ~0.7 degrees by ~0.92 degrees while that of the bore-sighted camera (.33 in CCD, 50 mm lens, f/1.4) was ~9 degrees by ~12 degrees. The system was deployed in both New Mexico and Colorado. Electromagnetic signatures of causative lightning discharges known as radio atmospherics (or sferics) were recorded using crossed-loop magnetic antennas and an ELF/VLF receiving systems located at Stanford and in Colorado. Using the telescopic imaging system we find that sprite structure can assume a wide variety of shapes, sizes, and time scales, but certain structures such as beading, faint downward branching, bright upward branching, propagating diffuse glows, and columns appear repeatedly. Propagating diffuse glow striations are observed to move slowly and are similar to the phenomenon observed in glow discharge tubes. While many streamers move at velocities greater than the time resolution of regular video rate imaging, some have been found to move as slowly as 10^4 m/s. Fine beading exists in many negative streamers and may possibly be a result of meteoric dust particles in the upper atmosphere. Columniform sprites may originate from positive branching streamers. Beads at the base of columns can glow for over 100ms while slowly drifting upward. Faint positive streamers are observed at the base of large bright sprites. Some sprites having branching positive streamers and non-branching negative streamers may be double-headed streamers initiated from plasma enhancements. A transition region between streamer formation and diffuse glow is observed at ~ 80km altitude.

Commissions H and G: Lightning Effects in the Upper Atmosphere

# EFFECTS OF PHOTOIONIZATION ON THE DYNAMICS OF POSITIVE AND NEGATIVE STREAMERS IN SPRITES

Ningyu Liu*, Victor Pasko, Tom Heffner
The Pennsylvania State University, University Park, PA 16802, USA

Sprites are large luminous discharges, which appear in the altitude range of ~40 to 90 km above large thunderstorms [e.g., Sentman et al., GRL, 22, 1205, 1995]. Recent telescopic imaging of sprites revealed an amazing variety of generally vertical fine structure with transverse spatial scales ranging from tens to a few hundreds of meters [Gerken et al., GRL, 27, 2637, 2000; Gerken and Inan, 107, 10.1029/2002JA009248, 2002]. Also recently, it has been demonstrated that sprites often exhibit a sharp altitude transition between the upper diffuse and the lower highly structured regions [Stenbaek-Nielsen et al., GRL, 27, 3827, 2000; Pasko and Stenbaek-Nielsen, GRL, 29, 10.1029/2001GL014241, 2002; Gerken and Inan, 2002]. The appearance of the fine structure and the vertical stratification in sprites has been interpreted in terms of positive and negative streamer coronas, which are considered as scaled analogs of small scale streamers, which exist at high atmospheric pressures at ground level [e.g., Pasko et al., GRL, 25, 2123, 1998; Raizer et al., J. Phys. D Appl. Phys., 31, 3225, 1998; Petrov and Petrova, Tech. Phys., 44, 472, 1999; Pasko et al., GRL, 28, 3821, 2001; Pasko and Stenbaek-Nielsen, 2002].

In this talk we report results from a new two-dimensional model recently developed at Penn State for studies of dynamics of positive and negative streamers for a wide range of air pressures corresponding to streamer dominated regions of sprites. The model utilizes a modified Scharfetter-Gummel algorithm for solution of electron convection-diffusion equation [Kulikovsky, J. Comput. Phys., 119, 149, 1995] and accounts for effects of photoionization on the streamer dynamics [e.g., Kulikovsky, J. Phys. D: Appl. Phys., 33, 1514, 2000, and references therein]. Using the model, we studied double-headed streamers initiated at sprite altitudes from single electron avalanches and calculated the full time dynamics of optical emissions (without the steady state assumption) from 1st and 2nd positive bands of $N_2$, 1st negative and Meinel bands of $N_2^+$ and 1st negative bands of $O_2^+$. The model results indicate that the effects of photoionization significantly modify the streamer scaling properties as a function of air pressure, leading in particular, to a factor of three wider streamer structures at altitudes >30 km, when compared to the previously discussed similarity laws [Pasko et al., 1998]. The primary reason for the observed differences is that the effective quenching altitude of the excited states that give photoionizing radiation is about 24 km. The quenching of these states is therefore negligible at altitudes >30 km, leading to a substantial enhancement of the electron-ion pair production ahead of the streamer tip due to the photoionization, when compared to the ground level, and resultant widening of the streamer filaments. In our talk we will present results of a comparison of the model outputs with the recent telescopic imaging of sprites [Gerken et al., 2000; Gerken and Inan, 2002] and discuss parameterizations allowing the evaluation of the effective streamer radius at different altitudes in the streamer dominated regions of sprites.

0-7803-7846-6/03/$17.00 ©2003 IEEE 

## Medical Applications and Safety Assessment

**Co-Chairs:** T. Ibrahim
S. Hagness

1:15 Opening Remarks

123. 1 1:20 A Study on the Receiving Signal Level in Relation with the Location of Electrodes for Wearable Devices Using Human Body as a Transmission Channel ..... APS
*K. Fujii, K. Ito, Chiba University, S. Tajima, Sony Computer Science Laboratories, Inc., Japan*

123. 2 1:40 Analytical Analysis of the Nuclear Magnetic Resonance Signal with Experimental and Numerical Validation ..... 549
*T. S. Ibrahim, The University of Oklahoma, C. A. Mitchel, R. Lee, P. Schmalbrock, The Ohio State University, USA*

123. 3 2:00 SAR Distribution and Thermal Elevation in a Human Head Model Due To the Operation of the Data Telemetry Link and Implanted Chip in a Retinal Prosthesi..... APS
*K. Gosalia, G. Lazzi, NC State University, USA*

123. 4 2:20 Internal Distributions of the Local SAR in the Human Abdomen Measured by a Split Phantom and Small Helical Antennas At 150 MHz ..... APS
*Y. Koyanagi, Panasonic Mobile Communications Co., Ltd., H. Kawai, Chiba University, K. Ogawa, Matsushita Electric Industrial Co., Ltd., K. Ito, Chiba University, Japan*

123. 5 2:40 E.M.-Wave Characterization of Tumor Morphology ..... APS
*O. Cohen, F. R. Zypman, Yeshiva University, USA*

123. 6 3:00 A Study on the Evaluation of the Electromagnetic Exposure in the Human Fetus Model at 150 MHz ..... APS
*H. Kawai, Chiba University, Y. Koyanagi, Panasonic Mobile Communications Co., Ltd., K. Ogawa, Matsushita Electric Industrial Co, Ltd., K. Saito, K. Ito, Chiba University, Japan*

123. 7 3:20 In Vivo Dielectric Characterization of Normal Breast Tissue: a Pilot Study ..... 550
*C. Beasley, S. C. Hagness, University of Wisconsin-Madison, T. Breslin, F. Xu, University of Wisconsin Hospital, M. Lindstrom, J. Booske, University of Wisconsin-Madison, USA*

123. 8 3:40 Microwave Breast Cancer Detection Via Space-time Beamforming: A Computational and Experimental Study of Breast Phantom and Sensor Design Parameters ..... 551
*X. Li, L. Palmer, S. Hagness, B. Van Veen, D. Van der Weide, University of Wisconsin-Madison, USA*

# Analytical Analysis of the Nuclear Magnetic Resonance Signal with Experimental and Numerical Validation

Tamer S. Ibrahim*+, Chad A. Mitchel [I], Robert Lee [II], and Petra Schmalbrock [I]

School of Electrical and Computer Engineering[II]
The University of Oklahoma, Norman, Oklahoma, 73019-1023

Department of Radiology[I] and Electrical Engineering[II]
The Ohio State University, Columbus, Ohio 43210

Ever since MRI was introduced as a medical diagnostic tool, there has been a constant drive towards operating at higher frequencies. There are many advantages to operating at higher frequencies, including the potential of exquisite resolution, reduced scan time, and increases in signal to noise ratio. At the same time, however, MRI at higher frequencies add significant technical complexities to the NMR experiment including difficulties in fabricating suitable RF coils. Understanding the source of the MR signal is a must in order to design a robust high-performance RF coil that can be utilized for high-field imaging. In this work, an analytical approach based on the principle of reciprocity for driving the NMR signal is presented with experimental and numerical validations at 8 Tesla (340 MHz).

An analytical model using the principle of reciprocity was developed to calculate the received signal in MRI. The analytical model was realized for general RF transmit and receive coils' geometries. To verify the analytical model, an experiment was conducted using an 8 Tesla clinical system. A 16-strut capped TEM resonator loaded with an 18.5 *cm* sphere filled with 0.5 *mM Gd DTPA* and 0.125 *M NaCl* was used. A nominal 90° flip angle was defined for a 1 *cm* voxel near the isocenter of the phantom using *STEAM* voxel spectroscopy. Magnitude images for 18 flip angles were obtained and subsequently fit pixel by pixel such that the transmit and the receive fields were experimentally extracted.

For the numerical analysis, a 3D FDTD model was developed such that the RF coil (TEM resonator) and the phantom were modeled as a single system. This approach permits the electromagnetic interactions between excitation source and the sphere, which are easily observed form the results obtained in this study, to be rigorously included. The coil was numerically tuned by adjusting the gap between the TEM stubs until any of the modes of the TEM resonator is resonant at the desired frequency of operation.

An excellent agreement between the experiment and the simulated results was achieved. The results demonstrate the effectiveness of the developed FDTD model and the need for the rigorous modeling of the excitation source. It is concluded that optimizing both the transmit and the receive fields is necessary to achieve homogeneous and high signal to noise image. Therefore, it is imperative to design the transmitter and receiver coils accordingly.

0-7803-7846-6/03/$17.00 ©2003 IEEE

# *In Vivo* Dielectric Characterization of Normal Breast Tissue: A Pilot Study

**C. Beasley[1]*, S. C. Hagness[1], T. M. Breslin[2], F. Xu[3], M. J. Lindstrom[4] and J. Booske[1]**
Department of (1) Electrical and Computer Engineering
University of Wisconsin-Madison, 1415 Engineering Drive, Madison, WI 53706-1691
Departments of (2) Surgery, (3) Pathology, and (4) Biostatistics and Medical Informatics,
University of Wisconsin-Madison, 600 Highland Ave., Madison, WI 53792
email: hagness@engr.wisc.edu

A number of microwave technologies are currently under development for breast cancer detection and treatment. Examples include microwave beamforming (see, for example, E. Bond, X. Li, S. C. Hagness, and B. D. Van Veen, *IEEE Trans. Antennas and Propagation*, April 2003, in press), microwave tomography (e.g. P. Meaney, M. Fanning, D. Li, S. Poplack, and K. Paulsen, *IEEE Trans. Microwave Theory Tech.*, 48:1841-1853, Nov. 2000), microwave-induced thermoacoustic tomography (e.g. M. Xu and L. Wang, *Medical Physics*, 29:1661-1669, Aug. 2002), and microwave phased-array hyperthermia (e.g. R. Gardner, H. Vargas, J. Block, C. Vogel, A. Fenn, G. Kuehl, and M. Doval, *Annals of Surgical Oncology*, 9:326-332, May 2002). The physical basis for these technologies is the dielectric properties contrast between malignant and normal breast tissue, as suggested by relatively sparse amounts of published data.

The engineering of these non-invasive, non-ionizing microwave technologies can be greatly facilitated by a complete understanding of the dielectric properties of malignant, benign, and normal breast tissue. For this reason, the University of Wisconsin in collaboration with the University of Calgary is conducting a comprehensive NIH-funded experimental study of the dielectric properties of malignant, benign, and normal breast tissue at microwave frequencies (100 MHz – 20 GHz). The majority of these measurements are being conducted on freshly excised breast biopsy, mastectomy, lumpectomy, and reduction mammoplasty specimens. Our research protocol has been designed to preserve as much as possible the physiological temperatures and moisture content of the *ex vivo* tissue. Nonetheless, it is of interest to establish the extent to which the measured dielectric properties of excised breast tissue differ from those *in vivo*.

In this paper, we present preliminary results from a pilot study of the dielectric properties of normal breast tissue *in vivo*. This study has been approved by the institutional review board at the University of Wisconsin and all subjects undergo an informed consent process. During an excisional biopsy, the dielectric properties of normal tissue surrounding the suspicious breast lesion are measured using an open-ended coaxial probe technique with an Agilent 8720ES vector network analyzer. The special-purpose probe is manufactured from stainless steel and borosilicate glass with a hermetically sealed tip. (Further discussion of the calibration procedures developed for this probe will be presented at this conference by the Univ. of Calgary.) After the tissue is excised, measurements are repeated *ex vivo* until the tissue has reached room temperature. Afterwards, the measured dielectric properties are correlated with the results from the histopathology, yielding *in vivo* and *ex vivo* dielectric-properties data as a function of normal breast tissue composition and temperature. These results provide the baseline data needed to accurately interpret *ex vivo* measurements.

0-7803-7846-6/03/$17.00 ©2003 IEEE

# Microwave breast cancer detection via space-time beamforming: A computational and experimental study of breast phantom and sensor design parameters

**X. Li*, L. O. Palmer, S. C. Hagness, B. D. Van Veen, D. van der Weide**
Department of Electrical and Computer Engineering
University of Wisconsin-Madison
1415 Engineering Drive, Madison, WI 53706-1691 USA
xuli@students.wisc.edu

We have recently proposed a method of microwave imaging via space-time (MIST) beamforming for detecting and localizing backscattered energy from small malignant breast tumors (E. Bond, X. Li, S. C. Hagness, and B. D. Van Veen, *IEEE Trans. Antennas and Propagation*, April 2003, in press). In our MIST approach each antenna in an array sequentially transmits an ultrawideband microwave pulse into the breast and receives the backscatter. Robust space-time beamforming algorithms are applied to the recorded signals to provide an image showing backscattered energy as a function of location. Malignant tumors produce localized large backscatter energy in the image due to their significant dielectric-properties contrast with normal breast tissue. In our previous computational studies, we applied the beamforming algorithms to simulated backscatter waveforms generated from 2-D MRI-derived FDTD breast models. In previous experimental studies, we tested the MIST approach using a simple first-generation breast phantom comprised of a water-based synthetic tumor suspended in a homogeneous normal breast tissue simulant. The imaging results demonstrated the theoretical and experimental feasibility of the MIST breast cancer detection method.

In this paper, we present in-depth computational and experimental investigations of the MIST beamforming approach using a second-generation breast phantom. Here, a layer of skin simulant is introduced at the surface of the breast phantom and alternative materials are used for the synthetic tumors to more realistically represent the predicted dielectric contrast between normal and malignant breast tissue. 3-D FDTD models of the improved breast phantom including the ultrawideband transmitting/receiving antenna are also developed. The simulated time-domain tumor response observed a single antenna location is compared to the measured tumor response for several cases where the dielectric-properties parameters of the synthesized tumors are varied. The excellent agreement between the simulated and measured tumor responses confirm the accuracy of the FDTD models.

We have conducted a comprehensive parametric study using both measurements and simulations for a variety of breast phantoms. Tumor response strength and signal-to-clutter-ratios of the images are presented as functions of breast phantom parameters, such as the dielectric properties of the breast-tissue simulants and the tumor shapes and sizes. The results of this study provide guidelines for determining dynamic range requirements of the imaging system, as well as image quality for detecting malignant tumors in these different scenarios. The impact of the sensor design on the observed tumor response is also investigated through simulation by changing the antenna geometry and immersion medium in the FDTD models of the system.

0-7803-7846-6/03/$17.00 ©2003 IEEE

# RF Modeling of a Prototype Phased Array Applicator Designed for Thermal Therapy in the Breast

Sandra Soto-Caban[†], Leo Kempel[†], Thaddeus V. Samulski[‡], and Robert J. McGough[†]
[†] Department of Electrical and Computer Engineering, Michigan State University
[‡] Department of Radiation Oncology, Duke University Medical Center

## Abstract

Thermal therapy kills tumor cells with the cytotoxic effects of heat. Thermal therapy simultaneously sensitizes otherwise resistant cells to the effects of radiation therapy, which motivates the use of thermal therapy as an adjuvant to radiation therapy. Thermal therapy techniques are also employed in heat-mediated drug delivery, where the contents of encapsulated drugs are released within a tumor volume once the threshold temperature is exceeded.

In a collaborative effort between Michigan State University and Duke University Medical Center, prototype Radio Frequency (RF) phased array applicators are being designed and characterized for thermal therapy in the breast. This effort, which models RF fields with the finite element method, incorporates the boundary conditions imposed by the walls of the treatment room, the geometry of the prototype RF array, and a 3-D description of patient anatomy. The room is, as a first approximation, a Faraday cage so all RF radiation outside of the room is ignored. The RF phased array prototype is intended for regional heating and therefore operates in the frequency range of 130-160MHz. In this numerical model, a description of the breast anatomy is extracted from Computed Tomography (CT) or Magnetic Resonance (MR) scans, and this information is combined with the material properties of normal and tumor tissue for finite element calculations. The geometrical and material descriptions are entered into FEMLAB, which defines the finite element mesh for all numerical simulations of the prototype RF applicator. After the mesh is defined, finite element results are computed for each antenna and then superposed. Results of simulated power depositions in a 3-D breast model containing a tumor and normal tissue will be presented for a 4-channel RF array prototype. In the breast model, the penetration depth will be evaluated for both single-channel and phased array configurations. Ultimately, the power depositions computed from the RF model will be combined with thermal modeling, and the results of the numerical modeling effort will impact future array designs and treatment strategies.

0-7803-7846-6/03/$17.00 ©2003 IEEE 

# On the Use of Numerical Phantoms in the Study of the Human-Antenna Interaction Problem

*L. Catarinucci[1], P. Palazzari[2], L. Tarricone[1]
[1] DII, University of Lecce, Via Monteroni 73100 Lecce – Italy - luciano.tarricone@unile.it
[2] ENEA – HPCN Project - C.R. Casaccia -- S. Maria di Galeria (Rome - Italy)

## Abstract

The use of numerical methods and phantoms is a common way to attack complex dosimetric problems, such as the near-field interaction between human and radiobase antennas (RBA), which is a relevant topic for employees involved in RBA maintenance. The rigorous problem solution, however, is difficult, both using experimental methods, where the use of homogeneous phantoms deserves a careful estimation of the introduced approximation error, and using numerical methods, where a huge memory and CPU time requirement must be satisfied and accurate numerical phantoms are needed. In this framework, the authors have recently developed an FDTD parallel method, described in (Catarinucci, Palazzari and Tarricone, IEEE Trans. MTT, March 2003). In the present work, this FDTD approach is adopted to compare dosimetric evaluations attained by using different numerical phantoms. The effects of the phantom shape and structure are studied, as well as the error induced by the use of homogeneous phantoms, instead of accurate heterogeneous ones.

For the sake of brevity only the results for six different phantoms are shown here: the well known Yale and Brooks Phantoms (YP and BP), and two couples of homogeneous phantoms, with the same shape of respectively YP and BP, and attained by using the averaged YP parameters on the former couple ($YH_1P$ and $BH_1P$, with $\varepsilon_r$ =46.33 and $\sigma$=0.73 S/m) and the averaged BP ones on the latter ($YH_2P$ and $BH_2P$, with $\varepsilon_r$ =34.32 and $\sigma$=0.63 S/m). Thus, for instance, $BH_1P$ has the shape of Brooks phantom, and $\varepsilon_r$ and $\sigma$ attained as average values inside Yale phantom. The phantoms have been exposed to the same source, the Kathrein RBA 730678 (working frequency 900 MHz), varying the human-RBA distance and using emitted power of 32 W.

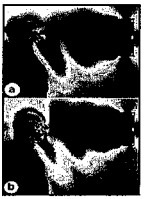

| 1-g SAR and 10-g SAR: peak values [W/Kg] | | | | | | | |
|---|---|---|---|---|---|---|---|
| Dist | type | YP | $YH_1P$ | $YH_2P$ | BP | $BH_1P$ | $BH_2P$ |
| 20 | 1g | 30.3246 | 29.5250 | 27.8730 | 18.4290 | 27.6260 | 25.7077 |
| cm | 10g | 15.3094 | 16.6297 | 15.2104 | 11.8857 | 18.8416 | 17.2059 |
| 30 | 1g | 12.6115 | 11.7294 | 11.4564 | 13.3806 | 19.5851 | 17.8272 |
| cm | 10g | 6.3243 | 6.6411 | 6.2494 | 8.6443 | 13.4448 | 12.0284 |
| 40 | 1g | 10.6837 | 9.9847 | 9.6198 | 6.1333 | 9.6302 | 9.1622 |
| cm | 10g | 5.3198 | 5.6239 | 5.2419 | 4.1630 | 7.1555 | 6.5020 |
| 50 | 1g | 5.3187 | 4.8766 | 4.7711 | 4.7905 | 7.0089 | 6.7971 |
| cm | 10g | 2.6331 | 2.7527 | 2.5955 | 3.1065 | 5.2943 | 4.7935 |

Fig. 1: YP (a) and BP (b) exposure and the obtained peak SAR for 6 different numerical phantoms

From Fig. 1 it is quite apparent the different shape between Yale and Brooks phantoms, and the consequent differences in the field distribution. This causes relevant differences in the SAR estimation, as evidenced in the table, where the peak values of 1-g and 10-g SAR are reported for the six phantoms. From the reported results, it can be summarised that:

- differences of up to 40 % are observed when comparing the two heterogeneous phantoms;
- small differences are observed on the peak SAR when comparing YP with $YH_1P$ and $YH_2P$; nonetheless, larger differences are observed when comparing local SAR value (results not here shown);
- differences of up to 40 % are observed when comparing BP with $BH_1P$ and $BH_2P$;

In conclusion, substantial differences are observed when estimating the peak values for SAR with two different accurate numerical phantoms. A substantial error is also induced when each heterogeneous phantom is approximated by a homogeneous one (as in many experimental set-ups), thus requiring a special care when performing such simplifications.

0-7803-7846-6/03/$17.00 ©2003 IEEE

# Temperature Increase in the Heads of Adult and Children due to Dipole Antenna

M. Fujimoto, A. Hirata*, and T. Shiozawa

Dept. of Communications Eng., Osaka Univ., 2-1 Yamada-oka, 565-0871 Osaka, Japan
Fax: +81-6-6879-7690, E-mail:hirata@comm.eng.osaka-u.ac.jp

Abstract: In recent years, there has been an increasing public concern about health implications of electromagnetic (EM) wave exposures with the use of mobile telephones. For this reason, various organizations in the world have established the safety guidelines for EM wave absorption. For near RF field exposures, these standards are based on the spatial peak SAR (specific absorption rate) for any 1 or 10g of tissues of the body. However, possible physiological damage in humans for EM wave exposures is induced by the temperature increase. The temperature increase of 4.5 [°C] in the brain has been remarked to be an allowable limit, which does not lead to any physiological damage (for exposures of more than 30 minutes). Additionally, the pain in skin is induced at the temperature increase around 10 °C. In our previous paper, we attempted to correlate the maximum temperature increase in the head and brain with the peak SAR value due to handset antennas. For investigating these correlations thoroughly, the total of 660 situations was considered. Then, the numerical results were analyzed on the basis of statistical inference. The maximum temperature increases in the head and brain were found to be estimated linearly in terms of peak SARs averaged over 1g and 10g of tissue in these regions (A. Hirata et al, *URSI GA*, 2002).

In this paper, we investigate this correlation for models of 3 year-old and 7 year-old children. It should be noted that the models of children are developed from our adult head model in the same manner as in the previous paper (J. Wang and O. Fujiwara, *URSI GA*, 2002). The material constants of tissue in the children are larger than those of the adult by 20-50 % (A. Peyman, A. A. Rezazadeh, C. Gabriel, *Phys. Med. Biol.*, 2001). In our calculation, the dependency of material constants on the age is also taken into account. The numerical investigations with corresponding figures reveals that the slope correlating the peak 10-g SAR in the head and the maximum temperature increase in the head is not much affected by the models, while the correlation between the peak 1-g SAR in the brain and the maximum temperature increase in the brain is affected by the models (at most 30 %). Additionally, the effect of the material constants on them is not large, although it is not shown here because of the lack of space.

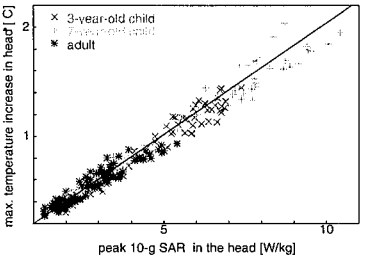


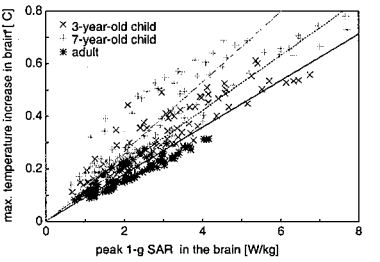

## Electromagnetic Theory

**Co-Chairs:** R. Collin
T. Senior

1:15 Opening Remarks

# Maxwell's Demon and Reciprocity

**Hans Gregory Schantz**

Q-Track Corporation
315 North Main Street
Tennille, GA 31089
h.schantz@q-track.com

**Background:**

In 1867, Peter Guthrie Tait asked his friend, James Clerk Maxwell, for his assistance in explaining the second law of thermodynamics. Just then coming into vogue, scientists recognized that the second law of thermodynamics placed fundamental limits on the availability of energy in thermodynamic systems. One disturbing implication is the inevitable "heat death" of the universe, as the universe irreversibly winds its way down to a state of thermal equilibrium.

Maxwell offered an intriguing thought experiment to "refute" the implications of the second law. Suppose a "very observant and neat fingered being" controlled a frictionless passageway between two chambers of gas in a thermal equilibrium. This being, or "demon," could selectively open and close the passageway to concentrate "hotter" molecules of gas in one chamber and colder molecules of gas in the other chamber.

Maxwell's demon is an example of what is called a "perpetual motion machine of the second kind." A perpetual motion machine of the second kind (PMM2) violates the second law of thermodynamics. It decreases the net entropy of the universe, creating order from disorder. Today, it is generally recognized that any physically realizable demon requires input work to acquire the information on which it acts. Thus the second law of thermodynamics is ultimately upheld. Nevertheless, Maxwell's demon continues to excite imaginations to the present day

**Thermodynamics and Fundamental Antenna Physics:**

Thermodynamic reasoning can be used to establish fundamental principles governing the behavior of antennas. For instance, Slater demonstrated the equivalence of the radiation and absorption patterns of a point dipole by a detailed calculation of their power flow [J.C. Slater, ***Microwave Transmission***, (New York: McGraw-Hill Book Company, Inc., 1942) pp. 235-245.]. He further argued from the statistical principle of detailed balance that absorption and radiation of a dipole in thermal equilibrium with its surroundings must exactly balance in any particular infinitesimal solid angle.

The present paper will use the concept of Maxwell's Demon to provide a simple and sweeping proof of the principle of reciprocity. The equivalence of transmit and receive antenna patterns will be discussed, as well as the equivalence of transmit and receive antenna efficiencies. Finally, this paper will argue that thermodynamic considerations allow limits to be placed on the scattering and reflection of antennas, as well as the efficiency of frequency multipliers.

0-7803-7846-6/03/$17.00 ©2003 IEEE 

# Understanding the Self-Acceleration Paradox

**Hans Gregory Schantz**

Q-Track Corporation
315 North Main Street
Tennille, GA 31089
h.schantz@q-track.com

**Background:**

In a classical electrodynamic calculation, the acceleration of a moving charge is "damped:" the charge loses energy via radiation. The damping force (**F**) is proportional to the rate of change of the acceleration $(\dot{\mathbf{a}})$:

$$\mathbf{F} = \frac{q^2}{6\pi\varepsilon_0 c^3}\dot{\mathbf{a}}, \tag{1}$$

where $q$ is the charge, $c$ is the speed of light, and $\varepsilon_0$ is the permittivity of free space. If no other external forces are applied, the equation of motion for the charge may be written:

$$\mathbf{F} = m\mathbf{a} = \frac{q^2}{6\pi\varepsilon_0 c^3}\dot{\mathbf{a}}. \tag{2}$$

A solution to this differential equation is:

$$\mathbf{a}(t) = a_0 e^{\frac{t}{\tau}} \tag{3}$$

where:

$$\tau = \frac{q^2}{6\pi\varepsilon_0 mc^3}. \tag{4}$$

This "runaway" solution describes an exponential increase in acceleration with time, a result that is decidedly unphysical. A great many attempts have been made to understand and resolve this paradox. A good starting point is the discussion and references provided by Smith [Glenn S. Smith, An Introduction to Classical Electromagnetic Radiation, (New York: Cambridge University Press: 1997), pp. 436-446].

**Action-Reaction:**

Elsewhere, the author has argued that the source of energy radiated from an accelerated charge lies in the energy of the static field which is the cause of the acceleration [H. Schantz, "On the Localization of Electromagnetic Energy," EuroEM 2000 (May 2002)]. If this is the case, then the traditionally accepted classical analysis rests on a false premise: that action-reaction must be considered only for ***two*** entities, the charge and the radiation.

The present paper will review prior understanding of the self acceleration paradox and re-consider the problem of charge self-acceleration explicitly including all three participants: 1) the charge, 2) the radiation, and 3) the applied field responsible for the charge's acceleration.

0-7803-7846-6/03/$17.00 ©2003 IEEE

# *Generalization of Green's Theorem with Fractional Differintegration*

Eldar I. Veliev
*Institute of Radiophysics and Electronics*
*National Academy of Sciences of Ukraine*
*Kharkov 61085, Ukraine*
*E-mail: veliev@kharkov.ua*

Nader Engheta
*University of Pennsylvania*
*Department of Electrical and Systems Engineering*
*Philadelphia, Pennsylvania 19104, U.S.A.*
*E-mail: engheta@ee.upenn.edu*

Some of the potential mathematical applications of fractional calculus in electromagnetic theory have been recently explored by Engheta [see, e.g., N. Engheta, "Fractional Paradigm in Electromagnetic Theory" a chapter in *Frontiers in Electromagnetics*, D. H. Werner and R. Mittra (eds.), IEEE Press, New York, chapter 12, pp. 523-552, (2000)], and certain tools of fractional differintegration have been applied in some EM problems, resulting in interesting outcomes. Fractional calculus deals with mathematical operators involving fractional (non-integer, or even complex) order differentiation and integration.

In the present study, we consider possibility of generalizing the Green's theorem using the concept of fractional differentiation and/or fractional integration. It is well known that in the conventional Green's theorem for a scalar potential function $\phi(x,y,z)$ satisfying the Helmholtz equation, the value of the function $\phi$ at any given point inside a closed mathematical volume can be expressed in terms of the values of $\phi$ and $\partial\phi/\partial n$ over the boundary of this closed volume and in terms of the source inside this volume. This involves the standard Green function for the Helmholtz operator. However, if one wants to use fractional differintegration on this function, how can this relation be generalized? Starting from the basic principles, we develop mathematical steps that include fractional differintegration operators towards obtaining Green's theorem with these operators. Our analysis shows that using such generalization the $\nu^{th}$-order differintegration of function $\phi$ at any point inside a close volume can be expressed in terms of $\mu^{th}$-order differintegration of $\phi$ and $\partial\phi/\partial n$ over the boundary of this region, where $\nu$ and $\mu$ are two arbitrary non-integer constants. This also involves $\nu^{th}-\mu^{th}$ order differintegration of the Green function for the Helmholtz operator. This can lead to an interesting possibility for a novel alternative way of defining the fractional order differintegration of function in terms of the values of the function and its spatial normal derivative over a closed boundary.

In this talk, we will present our mathematical steps in developing the generalized Green's theorem using fractional differentiation and integration.

0-7803-7846-6/03/$17.00 ©2003 IEEE

# Generalization of a Fundamental Theorem for the Scattering from a Receiving Antenna

R.E.Collin
Department of Electrical Engineering and Computer Science
Case Western Reserve University
Cleveland, OH 44106
EMAIL: rec2@po.cwru.edu

The scattering properties of a receiving antenna is important for the determination of the radar scattering cross section of a receiving antenna, and also for the evaluation of local interference effects.

An old fundamental theorem, derived more than half a century ago, states that the electric field $\mathbf{E}_s(Z_L)$ scattered by a receiving antenna terminated in a load impedance $Z_L$ is given by

$$\mathbf{E}_s(Z_L) = \mathbf{E}_s(Z_L = 0) + \frac{Z_L}{Z_L + Z_A} I_{sc} \mathbf{E}_r \tag{1}$$

where $\mathbf{E}_s(Z_L=0)$ is the field scattered when the receiving antenna is terminated in a short circuit, $Z_A$ is the antenna input impedance when it is transmitting, $I_{sc}$ is the current that flows into the shorted termination when it is receiving (Norton equivalent circuit current source), and $\mathbf{E}_r$ is the field the receiving antenna radiates when it is transmitting with unit current at its input. Aharoni (J. Aharoni, "Antennas", Clarendon Press, Oxford, 1946, pp.164-176) calls the second term on the right hand side in (1) the re-radiated field. In this paper we derive a generalized form of this scattering formula which is given by

$$\mathbf{E}_s(Z_L) = \mathbf{E}_s(Z_r) + I(Z_L = Z_r) \frac{Z_L - Z_r}{Z_L + Z_A} \mathbf{E}_r \tag{2}$$

In this formula $\mathbf{E}_s(Z_r)$ is the field scattered by the receiving antenna when it is terminated in the reference impedance $Z_r$ , and $I(Z_L=Z_r)$ is the current flowing into $Z_r$ . When $Z_r=0$ (2) reduces to (1). A case of special interest is when the antenna is connected to a transmission line with characteristic impedance $Z_c$ and the reference impedance is chosen equal to $Z_c$. For this case (2) becomes

$$\mathbf{E}_s(Z_L) = \mathbf{E}_s(Z_c) + I(Z_L = Z_c) \frac{Z_L - Z_c}{Z_L + Z_A} \mathbf{E}_r \tag{3}$$

If now $Z_L=Z_c$ the re-radiated portion of the scattered field vanishes. There is no power flow in the transmission line towards the antenna input so physically it is easy to understand that there will be no re-radiated field. We propose to call the residual scattered field $\mathbf{E}_s(Z_c)$ the intrinsic scattered field. In general the far zone radiation pattern of the intrinsic scattered field is not the same as the radiation pattern of the receiving antenna when it is used to transmit. The generalized scattering formula (2) was derived using the fundamental principles of uniqueness and superposition for electromagnetic fields.

0-7803-7846-6/03/$17.00 ©2003 IEEE

# A New Solution for Diffraction by an Anisotropic Impedance Half Plane at Oblique Incidence

T.B.A. Senior*
University of Michigan
Ann Arbor, MI 48109-2122 USA

S.R. Legault
Defence R&D Canada
Ottawa, Ont. K1A 0Z4 Canada

A problem of continuing interest is the diffraction of a plane electromagnetic wave at oblique (skew) incidence on a half plane subject to anisotropic impedance boundary conditions at its faces. When Maliuzhinets' method is employed, linear combinations of the spectra representing the $z$ components of the total electric and magnetic fields satisfy second order difference equations. When the impedances are the same on both faces, an approximate solution was obtained by Senior and Legault (*Electromagnetics*, **18**, 207-225, 1998) that appeared to produce expressions for the total fields that are reasonably accurate for all angles of incidence. However, on closer study it is found that the coefficients of reflection off the lower surface agree with their optics values only for normal incidence, showing that the method is flawed. The error can be traced to a connection between the spectra that is forced by the boundary conditions at the lower face and that no longer permits the normalization that was carried out to produce the incident field.

The correction for the error is not trivial but can be performed. The revised solution is presented and it is verified that it now produces the correct reflection coefficients and is in agreement with the known exact solutions for normal incidence and for an isotropic half plane at all angles of incidence. Numerical data are given for specimen impedances and a variety of incidence angles.

---

*Corresponding author

(1) URSI Commission B: em theory/diffraction
(2) New solution
(3) Correction of published results

0-7803-7846-6/03/$17.00 ©2003 IEEE 

# The Impact of Evanescent Waves on the Time-Average Power for Intersecting Beams

**L. E. Rickard Petersson* and Glenn S. Smith**
School of Electrical and Computer Engineering
Georgia Institute of Technology
Atlanta, GA 30332-0250

In this talk, we will revisit the topic of orthogonality of the total time-average power passing through a plane transverse to the direction of propagation for two electromagnetic field distributions traveling in opposite directions. The time-average powers contained in the two separate field distributions, in the absence of the other field, are orthogonal if they add up to the total time-average power. In general, this is not the case and there exists an additional term that we refer to as the cross term between the two field distributions. In D. M. Kerns' monograph, *Plane-Wave Scattering-Matrix Theory of Antennas and Antenna-Antenna Interactions*, a general formula is presented for the total time-average power for the situation described above. We will present a slightly different formula that is equivalent to Kerns'. For both formulas, it is clear that the cross term only contains evanescent waves of the two electromagnetic field distributions, and the cross term is zero if one or both of the field distributions do not contain any evanescent waves. An additional case will be presented when the cross term is zero when both distributions contain evanescent waves. This topic is worth revisiting because of the recent interest in near-field applications, such as near-field scanning optical microscopy, where the evanescent waves are significant.

A line source above a dielectric slab is a practical example where two electromagnetic fields propagate in opposite directions, i.e., the incident and reflected fields. In this talk, we will use the formula discussed above for this example. We will show that the cross term for the total time-average power passing through a plane between and parallel to the slab and the source is equivalent to the total time-average power contained in the guided modes of a lossless dielectric slab.

0-7803-7846-6/03/$17.00 ©2003 IEEE

# Dyadic Eigenfunctions and Natural Modes for Hybrid Waves in Planar Media

George W. Hanson
University of Wisconsin-Milwaukee
3200 N. Cramer Street
Milwaukee, WI 53211
george@uwm.edu

The typical analysis of waveguiding problems in electromagnetics involves the formulation of differential equations. Eigenvalues and eigenfunctions of the resulting differential operators are sometimes studied. More often, one considers the natural modes of the structure, which are the homogeneous solutions of the differential equation, and can be considered as eigenfunctions corresponding to zero eigenvalues (at least in a generalized sense).

For planarly-layered media, it is well-known that TE, TM, and hybrid modes may exist, depending on the excitation. The usual analysis consists of analyzing the TE and TM natural modes by reduction to scalar equations, and considering these (uncoupled) solutions as the fundamental modes of the structure. If a source excites a hybrid mode, it is constructed out of a linear combination of the fundamental TE and TM modes.

In this paper a alternative method is developed. The governing eigenvalue equations are elevated to the dyadic level, leading to dyadic eigenfunctions and dyadic natural modes. In particular, the dyadic natural modes are generally hybrid, and, as special cases, decouple to result in the familiar TE and TM independent modes. In the general case, the natural relationship between hybrid mode components is obtained via the corresponding relationship between scalar components of the dyadic natural mode. Dyadic adjoint modes and dyadic associated functions are also discussed, and orthogonality properties of the dyadic modes are obtained.

0-7803-7846-6/03/$17.00 ©2003 IEEE 

# Accurate Closed-Form Solution of Vertical Dipoles above a Semi-Infinite Ground

R. M. Shubair
Communication Engineering Department
Etisalat College of Engineering
P.O.Box 980, Sharjah, UAE
E-mail: rshubair@ece.ac.ae

Using the induced EMF method, the input impedance of a vertical antenna in *homogeneous free-space* can be obtained in closed-form in terms of Sine and Cosine integrals. In doing this, the induced EMF method assumes a sinusoidal current distribution along the vertical dipole and uses the free-space potential Green's function expressed as a spherical wave.

This paper extends the use of the induced EMF method for vertical antennas *above a Semi-infinite ground.* To do this, we must first obtain a spherical-wave representation of the half-space potential Green's function. This is done using the simulated complex image technique which was introduced to model microstrip and multilayered structures (R. M. Shubair, *Proc. IEEE AP-S*, 838-841, 2001). Using this technique here allows us to model the effect of the lower dielectric half-space by introducing a finite set of simulated image antennas. The result is an equivalent problem in which the lower dielectric half-space has been replaced with free-space so that the simulated image antennas form a simulated image array located in homogeneous free-space. The derivation of this simulated image array allows for the use of induced EMF method to calculate the input impedance of the original vertical antenna. This results in a *closed-form expression* which represents the superposition of the antenna's self-impedance, and the mutual impedances due to the presence of image antennas within the derived simulated image array. It should pointed out that as one simulated image array is found for a given height above the dielectric half-space, then for a different antenna height, say upwards, the image array remains unchanged except that it is bodily translated downwards by the same distance. This means that as the induced EMF method is applied *only once*, then at other heights the convergence is even faster since the simulated image antennas need not to be recalculated.

To verify the accuracy and convergence of method, numerical results are obtained showing the complex coefficients of the simulated image antennas, as well as, the input impedance as a function of height above the dielectric half-space, with or without loss.

0-7803-7846-6/03/$17.00 ©2003 IEEE 

# Time-Domain Characterization of Straight Thin-Wire Antennas

Colin C. Bantin

The time-domain response of a straight thin-wire antenna can be represented by the convolution of three functions, a $y$-function, which is the Fourier transform of the admittance at the feed point, an **h**-function, which is the Fourier transform of the time derivative of the effective length, and the source excitation voltage. The first two functions, when convolved together, form a response or **r**-function. This function gives the electric field due to an impulse voltage source and therefore characterizes the antenna as a transmitter. It also gives the time derivative of the received current due to an incident electric field impulse, and therefore characterizes the antenna as a receiver. A link between two such dipoles is characterized by a convolution of the respective transmit and receive **r**-functions, an integration with respect to time, and multiplication by a scale factor inversely proportional to the separation. This gives the impulse response of the entire link, which, when convolved with the source function, gives the received current in the load. It is instructive to explore these $y$, **h** and **r**-function characterizations for different wire lengths, and to predict the response for an infinite wire. We can do this analytically for simple cases, or by using detailed moment method modeling in other cases. To simplify the presentation of the results we consider the functions at an observation point normal to the axis of the wire.

An isolated **current element** has, by definition, a $y$-function that is a delta function. The **h**-function is the time derivative of a delta function, which can be deduced from the Fourier transform of the frequency-domain expression for the electric field. Therefore the **r**-function of a current element is the time derivative of a delta function. A **short dipole**, which has a triangular current distribution at all frequencies, has an admittance dominated by capacitance, therefore the $y$-function is the time derivative of a delta function. The **h**-function, also deduced from the frequency-domain electric field expression, is again the time derivative of a delta function. Therefore the **r**-function of a short dipole is the second time derivative of a delta function. A **finite length dipole**, with a reflection-matched source resistor, has a $y$-function that is essentially a positive impulse function followed by a lesser magnitude negative impulse function separated by the source-to-tip travel time. The **h**-function is a series of impulses of alternating sense and decreasing amplitude (due to radiation damping). Therefore the **r**-function of a finite length dipole, by convolution, is a triplet of impulse functions, two positive pulses separated by twice the source-to-tip travel time, and one negative pulse in the centre. The sum of the positive and negative values equals zero. The response approaches that of a short dipole as the length decreases. An **infinite length dipole** has $y$, **h** and **r**-functions consisting of only a single impulse, in each case equivalent to the first of the pulses for a finite length dipole. This is an exact representation for a tapered thin-wire and approximate for a constant (thin) radius wire. The impedance of an infinite wire dipole can be deduced by taking the inverse Fourier transform of the $y$-function pulse. A **sinusoidal current filament dipole** cannot be evaluated directly, but functions related to the $y$ and **h**-functions illustrate the impossibility of achieving this case physically.

0-7803-7846-6/03/$17.00 ©2003 IEEE 

# Surface Current Second-Order Differential Equation For a Radiation Problem

Y. W. Liu* and K. K. Mei
eeliuy@cityu.edu.hk, (852) 2788 – 7791 (fax)
**Department of Electronic Engineering, City University of Hong Kong**

**Abstract**– For a radiation problem rather than a scattering problem, the technique of measured equation of invariance (MEI) is used to convert a MoM full matrix to a tri-diagonal matrix with an unchanged excitation vector. From a finite difference point of view, the tri-diagonal matrix is equivalent to the discrete form of the finite difference (FD) for a second-order differential equation. Thus, the surface current second-order differential equation for a radiation problem like a thin wire antenna can be obtained from its corresponding tri-diagonal matrix. A mathematical significance of this kind of transformations is that for an arbitrarily shaped wire antenna, there equivalently exists a lowest-order (the $2^{nd}$ order) surface current differential equation. In other words, for a radiation problem, there exists the relationship between a surface integral equation and an equivalent second-order differential equation. Furthermore, the physical meaning of this kind of transformations is that a global relationship between discrete nodes could be simplified into a local relationship between just neighboring nodes. Finally, the computation speed to solve a tri-diagonal matrix generated by the $2^{nd}$ order differential equation is much faster than to solve a full matrix generated by the integral equation. The numerical examples for a straight dipole and a loop antenna show that the results obtained by the $2^{nd}$ order differential equation remains the same accuracy as the results obtained by the integral equation.

0-7803-7846-6/03/$17.00 ©2003 IEEE

# APPROXIMATE RECIPROCAL PHYSICAL EQUIVALENT: WHY NOT USING IT?

Roberto Tiberio*, Alberto Toccafondi and Alessia Polemi
Dept. of Information Engineering, University of Siena
Via Roma, 56. Siena. Italy

The Physical Optics (PO) approximation is still one of the most widely used high-frequency technique. Although PO is based on one of the crudest approximations of the equivalent current density on the surface of a scatterer, it has been providing effective results in a wide variety of practical engineering applications. However, it is well known that the estimate of the scattered field provided by the PO approximation does not satisfy the reciprocity theorem. Although in several practical instances this problem may not cause severe impairments, reciprocity is still a desirable property for any field approximation since it is a fundamental property imbedded in Maxwell's equations. Introducing a similar crude (image) approximation into the induction equivalent for scattering by a perfectly conducting object, provides an estimate that is in general different from that by PO, but does not yet satisfy reciprocity. An interesting and profound discussion about the accuracy and applicability of these above approximate physical and induction equivalents may be found in [R.F. Harrington, *IRE Trans. Antennas Propagat.*, AP-7, 2, 150-153, 1959]. There, the reciprocity issue was also addressed. This discussion has neatly been resumed in [C.A. Balanis, *Advanced Engineering Electromagnetics*, Ch.7, 1989]. Also, an interesting discussion on the possible approximate formulations for physical equivalents was presented in [S.W. Lee et al., *IEEE AP-S Int. Symp.*, 24-1, 408-411, 1988].

In focusing on the reciprocity issue, it should be noted that when considering a scattering problem and its reciprocal configuration, the relevant distributions of the exact equivalent surface currents are in general very different and there is no simple relationship between them. Therefore, when introducing any approximation in calculating them, the subsequent field estimates are expected to violate reciprocity. Indeed, reciprocity is a peculiar property of the field that does not explicitly provide any guidance on how to enforce approximate equivalent currents to satisfy this property. As a consequence, it is believed that it may be extremely difficult to achieve reciprocity by resorting to strictly source based approximations. At a variance, this property may more easily be preserved by resorting to a more field based approximation. Enforcing reciprocity by averaging the two PO solutions obtained by interchanging the transmitter and the receiver is a quite often used practice. However, most of the engineers are reluctant to admit that they have used it; sometimes, this practice is looked upon as a *dirty trick*.

In order to emphasize that this is not the case, a specific rigorous formulation of the reciprocity theorem is presented, and the relevant PO -based approximation is introduced therein to provide an approximate, reciprocal physical equivalent field representation. Explicit formulations for both perfectly and non perfectly conducting scatterers are discussed. Relationships with conventional, approximate physical and induction equivalents are also discussed. The reciprocal field representation referred to here is based on the same crude approximation as PO; thus, its formulation and related implementation are more or less as simple as those of commonly used in standard PO. Its accuracy and applicability, as well, are expected to be comparable. However, this field representation may be more appealing when considering its additional property of explicitly satisfying reciprocity. This property may also be relevant when considering those techniques that have been proposed for improving the accuracy of the PO approximation, such as PTD and its more recent developments or ITD in its fringe formulation; indeed, this augmentations do not guarantee a rigorous remedy for the non reciprocity introduced by PO.

0-7803-7846-6/03/$17.00 ©2003 IEEE

***Special Session***

**Large Finite Arrays and Periodic Structures**

**Organizer(s):** J.L. Volakis, ESL OSU
Raj Mittra, Pennsylvania State University
R. Gilbert

**Co-Chairs:** J. Volakis
R. Gilbert

7:55 Opening Remarks

125. 1 8:00 The Array Decomposition-Fast Multipole Method ..... APS
*R. Kindt, University of Michigan, J. Volakis, University of Michigan/Ohio State University, USA*

125. 2 8:20 A Fast Hybrid DFT-MoM for the Analysis of Large Finite Periodic Antenna Arrays in Grounded Layered Media ..... APS
*P. Janpugdee, P. H. Pathak, P. Mahachoklertwattana, ElectroScience Lab, The Ohio State University, USA, P. Nepa, University of Pisa, Italy*

125. 3 8:40 Solution of Large Array and Radome Problems using the Characteristic Basis Function Approach ..... 569
*R. Mittra, Penn State University, USA*

125. 4 9:00 Fast MOM Solutions for Large Array Via Green's Function Interpolation and Physical Preconditioning ..... 570
*F. Capolino, University of Sienna, Italy, D. Wilton, B. Fasenfest, D. Jackson, University of Houston, N. Champagne, Lawrence Livermore National Lab., USA*

125. 5 9:20 A Wave-Based Model for Mutual Coupling and Truncation in Finite Tapered-Slot Phased Arrays ..... APS
*A. O. Boryssenko, D. H. Schaubert, Antenna Laboratory UMass, USA, C. Craeye, Laboratoire de Télécommunications et Télédétection, Belgium*

125. 6 9:40 A Multi-Cell Array Decomposition Approach To Composite Finite Array Analysis..... APS
*R. Kindt, University of Michigan, J. Volakis, University of Michigan/Ohio State University, USA*

125. 7 10:00 Fast Computation and Extrapolation of the Effects of Array Truncation in Broadband Antenna Arrays ..... APS
*C. Craeye, Université catholique de Louvain, Belgium*

125. 8 10:20 MLFMA Analysis of Finite Aperture Arrays Including Reflector ..... APS
*I. Rullhusen, F. Arndt, University of Bremen, Germany*

125. 9 10:40 On Finite Frequency Selective Surfaces ..... APS
*B. Munk, J. B. Pryor, The Ohio State University, D. Jansen, Air Force Research Laboratory, USA*

# Solution of Large array and Radome Problems using the Characteristic Basis Function Approach

*Raj Mittra*

Electromagnetic Communication Laboratory, 319 EE East
The Pennsylvania State University, University Park, PA 16802
Email: rajmittra@ieee.org

## Abstract

Although the asymptotic methods, such as the GTD or PTD are well suited for computing the RCS of large objects such as aircrafts, they are not very convenient for analyzing antenna arrays, Frequency Selective Surface (FSS) Radomes, or combinations thereof, and it is necessary to resort to numerically rigorous techniques for simulating such problems. There are two major roadblocks to solving large array and radome problems using the MoM, FEM or the FDTD algorithm

First of all, the number of unknowns that we need to deal with becomes very large, even for isolated array and radome problems, when their size becomes greater than 10 or so wavelength, which is very often the case in practical applications. Analyzing an array-radome composite becomes even more burdensome on the CPU, both in terms of memory and solve time, especially when the antenna is operating in close proximity of the radome and the periods of the two systems are dissimilar.

Since both of the situations are encountered frequently in many practical applications, it is evident that an efficient numerical technique for addressing the large array, radome and composite (antenna + radome) problems is highly desirable.

Our objective in this paper is to present a technique we have developed for both of the problems described above. To solve the large array problem we begin by modeling a moderate-size (say 9x9) problem by using the MoM or the FDTD. We run the simulation wilth all the elements excited simultaneously, and compute the **E** and **H** fields on a virtual surface (Huyghens' box) enclosing the array. We then generate the characteristic Basis Functions (CBFs) corresponding to the center, edge and corner regions. Our next step is to express the aperture field of a larger array, which we wish to analyze, in terms of these CBFs and compute the desired radiation pattern. Some representative results for a 21x21 and a 51x51 of the approach as well as the extension to the composite problem will be presented.

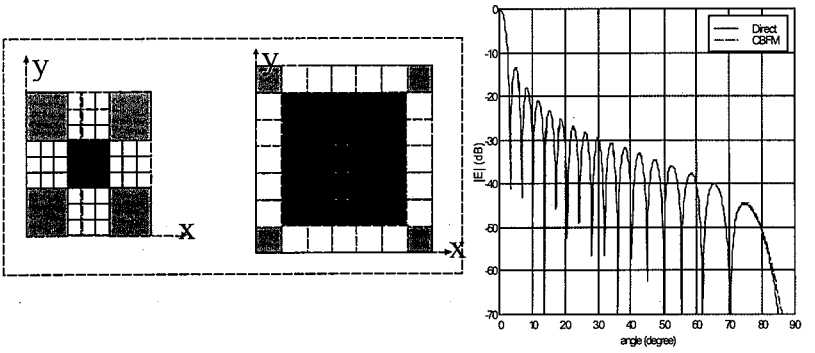


Fig.1. Left: Illustration of the mapping from 9x9 (left) into 21x21(right) sub-surfaces. Clusters of 3x3 are used to fill the center, edge and corner regions. Similar mapping is used for x-z and y-z sides. Right: E-plane far-field pattern of 51x51 array—direct (blue) and CBFM (red).

0-7803-7846-6/03/$17.00 ©2003 IEEE

# Fast MoM Solutions for Large Arrays Via Green's Function Interpolation and Physical Preconditioning

F. Capolino*, D.R. Wilton**, B. Fasenfest**, D.R. Jackson**, N. Champagne***

*Dept. of Information Engineering, University of Sienna, 53100 Siena, Italy
**Dept. of ECE, University of Houston, Houston, TX 77024-4005, USA
***Lawrence Livermore National Laboratory, Livermore, CA 94550, USA

This presentation focuses on numerical procedures that address the difficulties of dealing with large, finite arrays while preserving the generality and robustness of full-wave methods. First we review a method presented recently [F. Capolino, D. R. Wilton, D. R. Jackson, *URSI General Assembly,* Maastricht, 2002] that uses a physically-based preconditioner to accelerate the iterative solution process, generally reducing to a handful the number of iterations required. There, a preconditioner was obtained based on an identity relating the impedance and admittance operators for infinite and finite periodic structures. In particular, the identity relates the inverse of the impedance operator for the actual array problem to a windowed admittance operator for the infinite array and an operator representing mutual coupling between the array and a virtual array formed by extending the actual array to form an infinite array. Here we propose an alternative way to construct the preconditioner based on an FFT transform applied to blocks of the original impedance matrix; comparisons between the two methods will be provided. In many practical cases the preconditioning is sufficiently effective that the preconditioned right hand side alone serves as an excellent approximation to the solution of the full MoM system.

Secondly, we examine a fast method for solving array problems. We present a method based on approximating interactions between sufficiently separated array elements via a relatively coarse interpolation of the Green's function on a uniform grid commensurate with the array's periodicity. The interaction between the basis and testing functions is reduced to a three-stage process. The first stage is a projection of standard (e.g., RWG) subdomain bases onto a set of interpolation functions that interpolate the Green's function on the array face. This projection, which is used in a matrix/vector product for each array cell in an iterative solution process, need only be carried out once for a single cell, and results in a low-rank matrix. An intermediate stage matrix/vector product involving the uniformly sampled Green's function is of convolutional form in the lateral directions so that a 2D FFT may be used. The final stage is a third matrix/vector product involving a matrix resulting from projecting testing functions onto the Green's function interpolation functions; the matrix is the same (Galerkin's method) or a similar low-rank matrix as for the bases projection. Insertion of the physical preconditioner discussed above into this fast solution scheme and its effect on overall matrix/vector product construction time will be analyzed.

0-7803-7846-6/03/$17.00 ©2003 IEEE

# Efficient Asymptotic Closed Form Evaluation of the MoM Impedance Matrix for Antennas and Large Antenna Arrays in a Grounded Multilayered Medium

C. W. Chuang, P. H. Pathak and P. Janpugdee*

ElectroScience Lab, The Ohio State University
1320 Kinnear Road, Columbus, OH 43212, USA
E-mail: pathak.2@osu.edu

The conventional procedure for the evaluation of MoM impedance matrix arising in the integral equation solutions for antennas in grounded multilayered medium generally involves a numerical treatment of the Sommerfeld-type integral representation for the field. The latter integral exhibits pole and branch cut singularities in the integrand; also, the integrand oscillates very rapidly with increasing separation between the source and field points, thus making the computation of the off-diagonal impedance matrix elements very time consuming or even intractable. To overcome the problems in computing the Sommerfeld-type integral, an asymptotic closed form solution was obtained for the integral pertaining to a single layered structure (M. Marin, S. Barkeshli and P. H. Pathak, IEEE Trans. MTT, 4, 669-679, 1989; S. Barkeshli, P. H. Pathak and M. Marin, IEEE Trans. AP, 9, 1374-1383, 1990; G. A. Somers and P. H. Pathak, Radio Sci., 29, 465-481, 1994; P. R. Haddad and D. M. Pozar, IEEE Trans. AP, 11, 1545-1549, 1994). These asymptotic closed form solutions are seen to be accurate not only for lateral separations of the source and field points which are large, but also for separations which are as small as half a free space wavelength. This technique was also extended to a double-layer medium (M. A. Marin and P. H. Pathak, IEEE Trans. AP, 11, 1357-1366, 1992). Unfortunately, at that stage, the extension to multilayered structures appeared formidable due to its mathematical complexity. In particular, the leading term in the asymptotic expansion vanishes in all of these cases so the evaluation of the second term becomes necessary. The second term in the asymptotic expansion is generally far more cumbersome to evaluate than the first term, and this is even more so for the multilayered case. However, recently it was discovered that despite the formidable expression in the integrand for the multilayered case, a simplification does occur toward the end of the development leading to a relatively simple scheme to obtain the second order term. The latter development of the asymptotic solution for the multilayered case is reported in this paper. Numerical results for the multilayered case show that the asymptotic closed form solution obtained also remains accurate for source and field point separations as small as half the free space wave length. In addition, the results also compare very well to those presented in the above references for the special cases of single and double layers. The present asymptotic solution is applicable and useful to the analysis of large finite arrays in multilayered structures, where it will significantly reduce the computational time by one or more orders of magnitude depending on the size of the array. In addition, numerical results for printed crossed dipole arrays in a grounded multilayered medium will be shown to demonstrate the efficiency of the present asymptotic solution.

0-7803-7846-6/03/$17.00 ©2003 IEEE

*Special Session*

## Dielectric Measurements and Sensors

**Organizer(s):** Samir Trabelsi
Omar Ramahi

**Co-Chairs:** S. Trabelsi
O. Ramahi

7:55 Opening Remarks

126. 1 8:00 Dielectric Measurements and Sensors: the Excitement and Challenges Ahead ..... 575
*O. M. Ramahi, University of Maryland, S. Trabelsi, USDA-ARS, USA*

126. 2 8:20 Measurement of the Dielectric Properties of Arbitary Shaped Samples in Waveguides ..... APS
*M. Anis, A. Joestingmeier, T. Meyer , A. S. Omar, University of Magdeburg, Germany*

126. 3 8:40 Use of Microstrip Patch Antennas in Grain and Pulverized Materials Permittivity Measurement ..... APS
*M. A. El Sabbagh, USDA, O. M. Ramahi, University of Maryland, S. Trabelsi, S. O. Nelson, USDA, L. Khan, Illinois State Geological Survey, USA*

126. 4 9:00 Measuring Dielectric Properties of Fresh Fruits and Vegetables ..... APS
*S. O. Nelson, U. S. Department of Agriculture, USA*

126. 5 9:20 Dielectric-based Multiparameter Microwave Sensor ..... 576
*S. Trabelsi, S. Nelson, U. S. Dept. of Agriculture, USA*

126. 6 9:40 Determination of Transmission Coefficients from Finite Planar Composites using Spatial Averaging ..... APS
*J. T. Rockway, R. J. Marhefka, The Ohio State University, USA*

126. 7 10:00 Response Characterization of the Precision Open-Ended Coaxial Probe for Dielectric Spectroscopy of Breast Tissue ..... APS
*D. Popovic, M. Okoniewski, University of Calgary, Canada*

126. 8 10:20 Sensing Volume of Open-Ended Coaxial Probes for Dielectric Characterization of Breast Tissue At Microwave Frequencies ..... APS
*D. Popovic, University of Calgary, Canada, D. Hagl, C. Beasley, University of Wisconsin-Madison, USA, M. Okoniewski, University of Calgary, Canada, S. C. Hagness, J. H. Booske, University of Wisconsin-Madison, USA*

126. 9 10:40 Ex-Vivo Dielectric Characterization of Normal, Benign, and Malignant Breast Tissue At Microwave Frequencies: Preliminary Results from a Multi-Institu ..... 577
*C. Beasley, S. Hagness, J. Booske, T. M. Breslin, F. Xu, M. J. Lindstrom, University of Wisconsin-Madison, USA, D. Popovic, M. Okoniewski, W. Temple, A. Magliocco, T. Ogilvie, University of Calgary, Canada*

126. 10 11:00 Measuring Edge Scattering From Finite-Sized Samples Using a Gaussian Beam ..... APS
*L. E. R. Petersson, G. S. Smith, Georgia Institute of Technology, USA*

126. 11 11:20 Material Measurements of Absorbers with Magnetic Losses ..... APS
*A. Joestingmeier, T. Meyer, A. S. Omar, University of Magdeburg, Germany*

126. 12 11:40 Planar Near-Field Measurements of Microstrip Array Antenna using Photonic Sensor At X Band ..... APS
*M. Hirose, AIST, T. Ishizone, Toyo University, J. Ichijoh, S. Torihara, NEC TOKIN, K. Komiyama, AIST, Japan*

# Dielectric Measurements and Sensors: The Excitement and Challenges Ahead

Omar M. Ramahi[1,2,3] and Samir Trabelsi[4,5]
[1]Mechanical Engineering Department, [2]Electrical and Computer Engineering Department, and
[3]CALCE Electronic Products and Systems Center
2181 Glenn L. Martin Hall, James, University of Maryland, College Park, MD, USA
e-mail: **oramahi@calce.umd.edu**
[4]USDA-ARS, Richard B. Russel Agricultural Research Center, Athens, GA 30604, USA
[5]University of Georgia, Athens, GA, 30604, USA
e-mail: strabelsi@qaru.ars.usda.gov

The field of electromagnetics has experienced a dramatic growth during the past 50 years. Driven largely by military-related factors since the inception of the radar until the recent innovations in stealth technology. The revolution in communications was also, in part, made possible by the remarkable innovations in antennas and transmissions systems. It is perhaps safe to assert that the paradigm of electromagnetic problems of "how can I solve for or predict the field-matter interaction" is approaching its classical stage. Leaving efficiency considerations aside, it is possible now to find electromagnetic field solvers that can address the most challenging field-matter interaction. Does this maturity imply stagnation in the field of electromagnetics? While for many selfish reasons, many would predict and hope otherwise, the good news is that a new paradigm is emerging. How can we leverage the high maturity and advances in the field of electromagnetics to create advances in other fields. How can the field of electromagnetics play and be an integral part in the new age of information that will most likely characterize the 21st century. The answer lies in *electromagnetic-field-based sensors*.

Sensors are the link between information and electromagnetics. Microwave based sensors (and possibly millimeter wave based sensors) are becoming a highly desirable, mobile, versatile, and highly-reliable tools to gather information from afar as in the example of remote sensing, to very close proximity of the sensed object, as in mine and tissue detection or even near-field microscopy. Microwave-based sensors can even be placed on "small" objects to be sent for detection of harmful substances and events. Clearly, sensors represent an integral part of an information gathering system. However, sensors need to know what they are sensing. Electromagnetic fields are color-blind. They can only discriminate based on dielectric properties. If these properties are not understood correctly, the sensing system is rendered useless (as the old saying goes, garbage-in-garbage-out). This is no more important than in the area of microwave-based cancer detection where determining accurate benign and malignant tissue properties presents a challenge that is, arguably, greater than the formidable task of designing the sensor in the first place. Another area that has recently witnessed significant activities is multi-function sensing where multi-parameter calibration becomes essential. Multi-function microwave sensing is expected to play a strong role in a wide range of technologies from grain moisture and temperature sensing to detection of impurities in pharmaceutical products.

In this presentation, we present an overview of current applications of microwave-based sensors. We discuss current research trends in dielectric measurements and address some of the system integration challenges that are critical to making robust and reliable sensors.

0-7803-7846-6/03/$17.00 ©2003 IEEE

# DIELECTRIC-BASED MULTIPARAMETER MICROWAVE SENSOR

Samir Trabelsi*, and Stuart O. Nelson
U. S. Department of Agriculture, Agricultural Research Service, Richard B. Russell Agricultural Research Center, P. O. Box 5677, Athens, GA 30604-5677, U.S.A. Phone: +1 706 546 3157; Fax: +1 706 546 3607, E-mail:strabelsi@qaru.ars.usda.gov

In the last few decades, microwave dielectric-based sensors were mainly developed for sensing moisture in different materials (Nyfors E. and Vainikainen P., Industrial Microwave Sensors, 1989). The fact that these sensors rely on measurement of dielectric properties, which are also dependent on other physical properties of the material, make them potentially multiparameter sensors, provided that appropriate correlations are established between measured dielectric properties and physical properties of interest. At microwave frequencies, dielelectric properties of moist granular materials depend on frequency, moisture content, bulk density and temperature (Nelson S. O, Trans. ASAE, 16, 384-400, 1973). In fact, at these frequencies, water is the dominant factor because of its polar nature, and hence effects of both bulk density and temperature are water-related effects. Decoupling these effects for purpose of determining one parameter at a time is not obvious. This explains the difficulty encountered in the early use of microwave moisture sensors. For moisture to be determined accurately, effects of bulk density and temperature have to be accounted for by means of additional measurement and compensation, or eliminated by identifying density-independent and temperature-insensitive permittivity functions. In the last three decades, efforts have been dedicated mainly to density-independent measurements of moisture content.

In this paper, different approaches are examined for determining bulk density, moisture content and temperature of cereal grain and oilseed. In the first approach, and the most straightforward, direct relationships are established between the dielectric constant, $\varepsilon'$, and dielectric loss factor, $\varepsilon''$, and bulk density, moisture content, and temperature. In the second approach, bulk density and moisture content are determined simultaneously from new correlations between the dielectric properties, $\varepsilon'$ and $\varepsilon''$, and the water partial density ($m_w/v$) and dry matter partial density ($m_d/v$). Effectivenes of each approach is compared to previously used methods (Meyer W. and Schilz W. M., IEEE Trans. Microwave Theory Techn., 29, 732-739, 1981; S. Trabelsi et al., IEEE Trans. Instrum. Meas, 47, 1, 127-132, 1998). Since both approaches are based on measurement of $\varepsilon'$ and $\varepsilon''$, combined together, they constitute the basis for the development of a multiparameter microwave sensor. The principles and feasibility of such a sensor are demonstrated through measurement of the dielectric properties of three major commodities, wheat, corn and soybeans at microwave frequencies. The methods presented in this paper, along with the availability of microwave components at affordable prices, constitute incentives for the development of a new generation of versatile microwave sensors that can be used for real-time determination of physical properties of granular materials.

0-7803-7846-6/03/$17.00 ©2003 IEEE

# Ex-Vivo Dielectric Characterization of Normal, Benign, and Malignant Breast Tissue at Microwave Frequencies: Preliminary Results from a Multi-Institutional Study

**C. Beasley, S. C. Hagness*, J. Booske**
Department of Electrical and Computer Engineering
University of Wisconsin-Madison, 1415 Engineering Drive, Madison, WI 53706-1691

**T. M. Breslin[1], F. Xu[2], M. J. Lindstrom[3]**
Departments of (1) Surgery, (2) Pathology, and (3) Biostatistics and Medical Informatics
University of Wisconsin-Madison, 600 Highland Ave., Madison, WI 53792

**D. Popovic, M. Okoniewski**
Department of Electrical and Computer Engineering
University of Calgary, 2500 University Drive, Calgary N.W., Alberta, T2N 1N4

**W. Temple[4], A. Magliocco[5], T. Ogilvie[5]**
(4) Department of Surgery and Oncology, (5) Department of Pathology
University of Calgary, 1331 29th St NW, Calgary N.W., Alberta, T2N-4N2

Several dielectric spectroscopy studies of breast tissue reported in the literature over the past 50 years suggest that the dielectric-properties contrast between malignant and normal breast tissue is greater than 2:1 in the microwave frequency range. Recognition of the potential diagnostic value of such a contrast has fueled a number of recent investigations of novel microwave breast cancer detection and treatment technologies. However, there is little or no dielectric-properties data above 3 GHz – a region of practical importance since shorter wavelengths offer higher spatial resolution. More importantly, the existing data does not cover all of the possible tissue types present in the heterogeneous normal, pre-cancerous, or cancerous breast. Furthermore, the different dielectric-properties data sets are not all in agreement. In fact, Hurt et al (*IEEE Trans. Biomed. Eng.*, 1:396-401, March 2000) recently pointed out that out of 18 human tissue types, the greatest uncertainty in dielectric properties at microwave frequencies currently exists for normal breast tissue. Consequently, a number of important questions remain.

To fill in the gaps in our understanding, the University of Wisconsin (UW) and the University of Calgary (UC) are conducting a comprehensive NIH-funded prospective study of the dielectric properties of malignant, benign, and normal breast tissue at microwave frequencies (up to 20 GHz). We are characterizing freshly excised tissue specimens from excisional biopsy, mastectomy, lumpectomy, and reduction mammoplasty surgeries at the UW Hospital and Clinics and the UC Tom Baker Cancer Centre. The dielectric properties of selected regions of each tissue specimen are measured using an open-ended coaxial probe technique with a special-purpose probe and Agilent vector network analyzer. Each measurement is carefully correlated with the histopathology of the region of the specimen "sensed" by the probe.

In this talk, we will present preliminary results from our multi-year study. These results begin to provide answers to questions of engineering importance for future microwave technology developments related to the detection, diagnosis, monitoring, and treatment of breast cancer.

0-7803-7846-6/03/$17.00 ©2003 IEEE

## Novel Circuits and Devices for High-Speed Applications

**Co-Chairs:** S. El-Ghazaly
R. Cicchetti

7:55 Opening Remarks

# THE IMPACT OF FLIP-CHIP PACKAGING ON RF MONOLITHIC INDUCTORS

Mostafa Abdulla and Qing-Lun Chen
Intel Corporation
9750 Goethe Road, LOC4/19
Sacramento, CA 95827, USA
Email: mostafa.abdulla@intel.com

**ABSTRACT**

Recently, Flip-Chip (FC) package technology has become popular for RF applications. The main reason for that is the shorter interconnects length of the bumps compared to wire bond technology which enhances the interconnect performance at high frequency.

On the other hand, monolithic inductors are important and performance-limiting components in Radio Frequency Integrated Circuits (RFIC's), such as voltage control oscillators (VCO's) and low noise amplifiers (LNA's). The most important parameter of monolithic inductor is its quality factor. Inductor quality factor is limited by the losses. The metal and substrate losses mechanisms have been reported and studied in many literatures. To the best of our knowledge, no literature has reported the effect of package losses on the inductor quality factor.

Although reducing the FC bump height enhances the frequency reponce of the package interconnects, it will results in proximity coupling between the package and upper metal layers of the inductor. This coupling produces additional losses and reduces the quality factor of the inductor.

In this paper, we investigate the effects of the FC packaging on the monolithic inductor quality factor. We evaluate the inductor electrical parameters using full-wave electromagnetic field solver. We present the inductor parameters with and without FC package (see Fig.1). Our investigation helps RF designer to predict accurately inductors parameters including package assembly effects and to reduce redesign cycles.

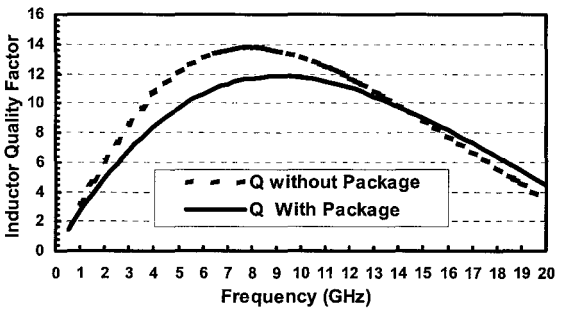


**Fig. 1 Example of the package assembly impact on typical inductor quality factor**

0-7803-7846-6/03/$17.00 ©2003 IEEE 

# Modeling of Planar Inductors in IC's at X-Band

Kevin Idstein*[1], Roberto G. Rojas[1] and Gregory Creech[2]
[1]The Ohio State University, Electrical Engineering, ElectroScience Laboratory
Columbus, OH 43212
[2]AFRL/SNDM, Wright Patterson AFB, Dayton, OH 45433

Microwave integrated circuits today demand low power dissipation and a high level of integration. To meet these requirements, engineers must design low-loss passive devices on-chip. However, at X-Band frequencies, passive components suffer significantly from skin-effect losses, conductive substrate losses, and field coupling in an inhomogeneous substrate. These parasitic effects cannot be neglected when designing passive components to operate at high frequencies.

To investigate the various models available for IC inductors, six inductors ranging from 0.75 nH to 1.00 nH were designed with an emphasis on maximizing the Q factor. The technology is Fully Depleted Silicon on Insulator (FDSOI) with a silicon resistivity of 2000 Ohm-cm. Figure 1 shows a popular circuit model for this inductor. Unfortunately, there is little consensus from the literature as to how the circuit components of this model are derived. Frequently, these components are found by data fitting the measured or simulated S-Parameters. Data fitting is not beneficial for design purposes, however. There are analytical formulas for these component values, but they do not provide sufficient accuracy.

The inductors were simulated using three simulation tools: a standard full wave Method of Moments (MOM) simulator, a MOM simulator using electrostatic approximations (RF MOM), and a Partial Element Equivalent Circuit (PEEC) simulator using electrostatic approximations. Furthermore, after making some rough approximations of the current distribution and charge distribution, the PEEC technique was also used to analytically calculate the component values of Figure 1. Once the component values were calculated, the Q and effective inductance of the model circuit were calculated. These two parameters are compared to the MOM simulation, the RF MOM simulation, the electrostatic approximate PEEC simulation, and measured data.

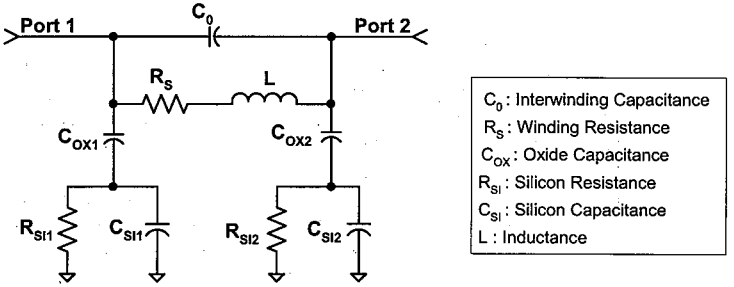


Figure1: Generic circuit model for a spiral inductor on an IC substrate.

0-7803-7846-6/03/$17.00 ©2003 IEEE

## A New Class of Interdigital Capacitors for Planar Integrated Circuits

*G. Bit-Babik[1], D. Caratelli[2], R. Cicchetti*[2], and A. Faraone[1]*
*[1]Motorola Corporate EME Research Lab, Fort Lauderdale, Florida, USA*
*[2]University of Rome "La Sapienza", Department of Electronics Engineering, Italy*

A new class of planar interdigital capacitors (*IDCs*) useful to be employed in wireless communication systems are presented and analyzed in detail. The electromagnetic characteristics of the proposed structures, derived by means of a new locally conformal *FDTD* scheme, are compared in order to establish their circuital and *EMC* performances. Interdigital capacitors having zig-zag and sinusoidal shape fingers are analyzed and a new frequency-independent equivalent circuit, which includes surface and volume waves effects, useful to be employed in *CAD* tools, has been introduced. The particular form of the capacitor's fingers has been chosen so to obtain compact structures with a higher value of the series capacitance. To establish the main characteristics of the proposed structures circuital and *EMC* characteristics are compared with those obtainable using *IDCs* having straight fingers. As an example, in Fig. 1a the geometry of an *IDC* structure having zig-zag finger is shown.

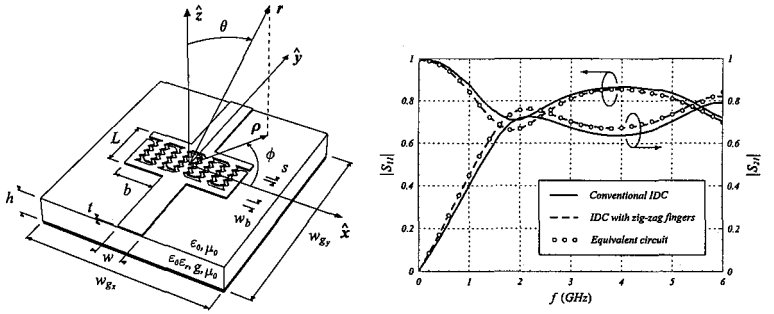


*Fig. 1 Geometry (a) and magnitude of the scattering parameters versus frequency (b) of a planar interdigital capacitor having zig-zag fingers. Substrate parameters: h=1.27 mm, $\varepsilon_r$=10.2.*

The magnitude of the scattering parameters in the frequency range *0-6 GHz*, obtained employing the *FDTD* technique, is given in Fig. 1b. From Fig. 1b, it is evident that a stronger coupling between the input and output ports of the devices appears in the structure having zig-zag fingers. It can be demonstrated that this particular behaviour is due to the higher reactive energy stored between the zig-zag fingers, which results in a higher value of the series capacitance. Finally, from the same figure it appears the good numerical accuracy obtainable using the proposed frequency-independent equivalent circuit of the device. Details concerning the analysis model, the equivalent circuits, the circuital and the emission characteristics of the proposed structures, will be given during the symposium presentation.

0-7803-7846-6/03/$17.00 ©2003 IEEE

# THE EFFECT OF PACKAGE CAVITY ON THE WIREBOND HIGH FREQUENCY PERFORMANCE

Xiang-Yin Zeng[1], Mostafa Abdulla[2] and Qing-Lun Chen[2]

[1]Intel China LTD
2299 Yanan Road (west), Shanghai Mart Tower
Shanghai, China 200336
xiang.yin.zeng@intel.com

[2]Intel Corporation,
9750 Goethe Road, LOC4/19
Sacramento, CA 95827, USA
mostafa.abdulla@intel.com

**ABSTRACT**

Nowadays, package-interconnects is performance–limiting components in RF, and high-speed applications. The high frequency discontinuity introduced by wirebond inductance could affect the high frequency circuit performance significantly. However, wirebond technology is still attractive due to its reliability and cost effectiveness.

To reduce the wire bond inductance, wire length is minimized as possible. Recently, UltraBGA package technology was introduced to minimize bond wire length and therefore increase the package bandwidth. This is achieved by putting the bare die inside a grove (cavity), which formed inside the metallic package ground (Fig 1.).

Since package substrate thickness is less than the bare die thickness and the die is inside a metallic cavity, a high frequency effect is expected. Changing the ground height will affect bond wire characteristic impedance and cause high frequency discontinuity and limit the package bandwidth. So far, no work reports the effect of the change of ground plan height on the wirebond performance and bandwidth.

In this presentation, the impact of package cavity on the package bandwidth will be discussed. The insertion and return losses of different wire bond schemes and package configurations are evaluated using finite element method and de-embedding techniques. An optimized layout and design recommendations will be presented. This technique will help wirebond packages to achieve wider bandwidth to accommodate high-speed applications.

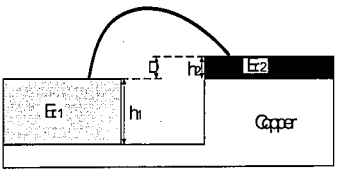


**Fig.1 Wire bond interconnect structure**

# Signal Integrity Issues for Package Level Discontinuities and RF Chip-Package Interconnects Using FDTD Analysis and Equivalent Circuit Modeling

Jeffrey McFiggins*, Maulin Bhagat, Jayanti Venkataraman, Rochester Institute of Tech., NY

As on-chip frequencies move into the gigahertz region a need exists to gain an understanding of how interconnects impact signal integrity. Signals can be degraded by discontinuities along the signal path as well as coupling from adjacent circuits. There are several established methods to analyze the effects of discontinuities and coupling. These include both full wave simulations and equivalent circuit models. These circuit models are typically developed for a particular layout and are optimized to obtain element values to match the response of a full wave simulator. One drawback of this method is re-optimization is required for a different geometry. The current work develops an equivalent circuit model to estimate coupling using closed form equations. The major advantage is that changes in the geometry are accounted for in the equations and no tedious re-optimization is required. Insight into signal integrity issues can be obtained through time domain analysis. To facilitate this a Finite Difference Time Domain (FDTD) code was written implementing a UPML absorbing boundary for lossy materials.

The structure used for this work is shown in fig. 1, where two vias, rectangular in cross section, are placed a distance d apart (center to center). These vias connect transmission lines of length $l_1$ and width $w_1$, on the top layer (solid lines), to transmission lines of length $l_2$ and width $w_2$ on a lower layer (dotted lines). This structure was chosen because it exhibits both discontinuity and coupling effects. To develop the equivalent circuit model the length of the coupled vias were divided into two segments. The circuit model for each segment is shown in fig. 2, where L represents self-inductance, R is the losses associated with the vias, and Ca and k represents coupling between the vias.

The S-parameters obtained from the circuit model are compared with that obtained from FDTD and are shown in fig. 3. The model shows very good agreement. Figure 4 shows coupling from port 1 to port 3 and 4 in the time domain, for a 10GHz sinusoidal (2 Vp-p) input applied at port 1. These results show that coupling from neighboring circuits can be significant enough to impact signal integrity thereby degrading system performance.

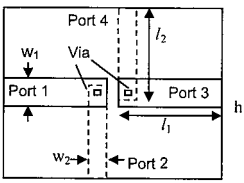


Fig. 1. Coupled via structure. (a) top view (b) side view, $w_1 = 11.58$ mils, $w_2 = 5.79$ mils, $l_1 = 33$ mils, $l_2 = 37.89$ mils, h = 2.46 mils, D = 7.79 mils, via dimensions = 2 × 2 × 2.46 mil

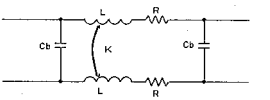


Fig. 2. Equivalent circuit model for a coupled via subsection

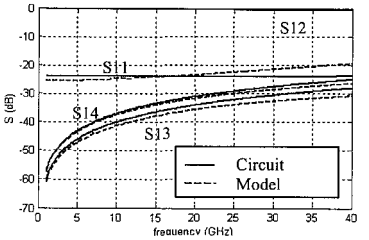


Fig. 3. Comparison of S-parameters for Coupled via structure

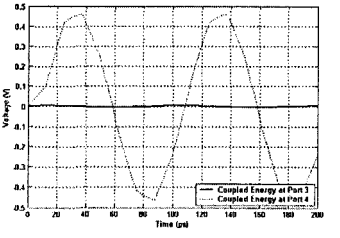


Fig. 4. Time domain coupling for port 3 and 4

0-7803-7846-6/03/$17.00 ©2003 IEEE

# Mitigation of PCB Radiation through Novel Mesh Fencing Techniques

Xin Wu[1,3] and Omar M. Ramahi[1,2,3]
[1]*Mechanical Engineering Department,* [2]*Electrical and Computer Engineering Department, and* [3]*CALCE Electronic Products and Systems Center*
*2181 Glenn L. Martin Hall, James Clark School of Engineering, University of Maryland, College Park, MD, USA*
*e-mail: xwu@glue.umd.edu*

In printed circuit boards (PCB), as the frequency increases, the PCB dimension becomes electrically long, and the clock harmonics can lead to resonances, which in turn makes the PCB an efficient radiator. Essentially, the multi-layer PCB structure behaves in a manner identical to that of a microstrip patch antenna, where the radiation is a result of the field accumulation at the edges of the board. The radiated emission occurs at the microstrip line or strip lines under fast switching, which becomes one of the primary electromagnetic interference (EMI) sources. Moreover, the transient currents associated with fast switching produce simultaneous switching noise (SSN), which can significantly compromise the power distribution integrity on the boards, leading to crosstalk and false logic.

Via fencing, an edge treatment that consists of adding a string of vias around the periphery of the PCB effectively shorting out common voltage reference planes, was proposed in previous works to reduce the electromagnetic radiation. It has been demonstrated that closely spaced fencing vias can reduce the radiation from the board edge effectively. However, the energy radiated is partially reflected back into the PCB by fencing vias, therefore enhancing the power plane resonance with consequential adverse signal integrity implications.

In this work, we review via fencing techniques. We then present a quantitative study to determine via fencing effects on enhancing power plane resonance. It is known that RC termination is an effective method to dampen the power plane resonances. In this work, we suggest the addition of "equivalent capacitance" through the use of strip lines (open-ended on both ends). These strips will be perpendicular to the propagating electric field and will act as a capacitive load. With this mesh fencing approach, i.e., a combination of the via fencing and capacitive strip lines, we expect to reduce the radiated emission from PCB while dampen enhanced resonances.

0-7803-7846-6/03/$17.00 ©2003 IEEE

# Junction Circuit Using NRD Guide / Vertical Strip Line Transformer at 60GHz

**Futoshi KUROKI and Makoto KIMURA**
Kure National College of Technology. 2-2-11 Aga-Minami Kure 737-8506, Japan

**Tsukasa YONEYAMA**
Tohoku Institute of Technology. 35-1 Yagiyama-Kasumichou, Taihaku-Ku, Sendai 982-8577, Japan.

Since the transverse field distribution of the NRD guide is similar to that of the TE01 rectangular hollow metal waveguide, a mode transition between the NRD guide and vertical strip line can be constructed by making the right angle corner in the same manner as the rectangular hollow metal waveguide / coaxial line transition [1]. With this in mind, we developed the new type of right angle corner using the NRD guide / vertical strip line transition as shown in Fig. 1. The dielectric strip of the NRD guide is made by low loss Teflon with the relative permittivity of 2.04, and the cross sectional dimensions are 2.25mm in height and 2.5mm in width. The vertical strips consist of metal strips etched on a glass Teflon substrate having the cross sectional dimensions of 2.25mm in height and 0.256mm in width. The width of the metal strip is decided to be 1.8mm so as to be characterized by the impedance of 50 Ω. This substrate is transversely inserted in the cross-sectional plane of the NRD guide and are supported by the Teflon piece with the length of L, where the metal strips are inserted in the dielectric by the depth of D. In order to optimize the performance, the length L and depth D were decided by using HFSS. The calculated scattering parameters of the right angle corner are shown in Fig. 2. It is obvious that a good performance can be obtained. By using the right angle corners, a new type of junction circuit was fabricated as shown in Fig. 3. Figure 4 shows the calculated and measured scattering parameters. Low loss and well balanced output level, which were measured to be 4dB ± 1dB in the bandwidth of 4GHz around a frequency of 60GHz, can be obtained, though there is slight discrepancy between theory and measurement because the scattering parameters were calculated in loss less condition. Next step of this research is to apply the junction circuit to semiconductor devices.

**Reference** [1] F. Kuroki and T. Yoneyama, "Junction Circuits Using NRD Guide at Millimeter-Wavelengths", Proceeding of IEICE, Vol.75-C-I, No.1 (1992)

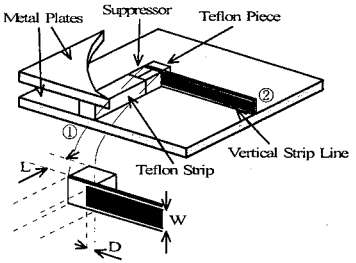


Fig. 1 Structure of right angle corner

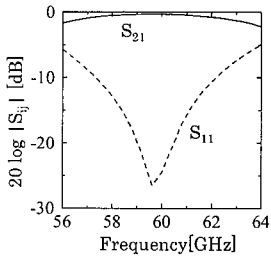


Fig.2 Calculated scattering parameter of right angle corner

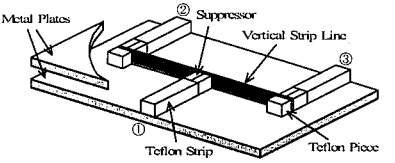


Fig.3 Structure of junction circuit

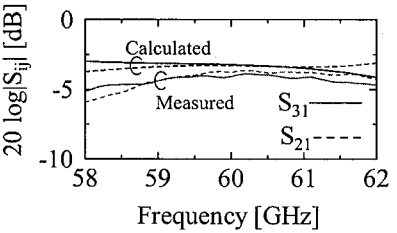


Fig.4 Calculated and measured scattering parameters of junction circuit

# Comparative Studies on the Capacitive Coupling in 3D Interconnects Embedded in LTCCs

*W. Y. Yin, B. Guo, X. T. Dong, and Y. B. Gan*

Temasek Laboratories, National University of Singapore (NUS), 10 Kent Ridge Crescent, Singapore 119260, E-mail: tslyinwy@nus.edu.sg

***Abstract***: It is known that high-performance printed circuit boards (PCBs) consist of multi-layer materials with multiple signal microstrips embedded within. The high-density integration has made the overall signal integrity analysis a very important work. Signal integrity usually include signal delay, distortion, and crosstalk, which are the manifestation of the mutual inductive and capacitive couplings among all microstrips.

To the authors' best knowledge, till now much work has been done for extracting the microstrip capacitances and inductances in three-dimensional (3D) interconnects. Some empirical capacitance models for 2D and 3D interconnects are developed ( T. Sakurai, *IEEE Trans. Electron Device*, **ED-40**, 118-124, 1993; S. –C. Wong *et al*, *IEEE Trans. Semi. Manufact.*, **SM-13**, 108-111 and 219-227, 2000). However, most of these work was focused on the interconnects fabricated in U(V)LSIs, and only Sohn *et al* have given a set of empirical equations on electrical parameters of coupled microstrip lines for crosstalk estimation in normal printed circuit boards(Y. S. Sohn *et al*, *IEEE Trans. Advanced Packaging*, **AP-24**, 521-527, 2001).

In this work, comparative studies on the capacitive coupling in 3D-interconnects embedded in LTCCs (Fig. 1) are done, including the hybrid effects of various geometrical parameters of both microstrips and LTCC superstrate-substrates. The accuracies of different empirical formulas for predicting the capacitive coupling in 2D and 3D interconnects on PCBs are examined and compared. Some conclusions are drawn, which are very useful for practical PCBs design for improving the signal integrity.

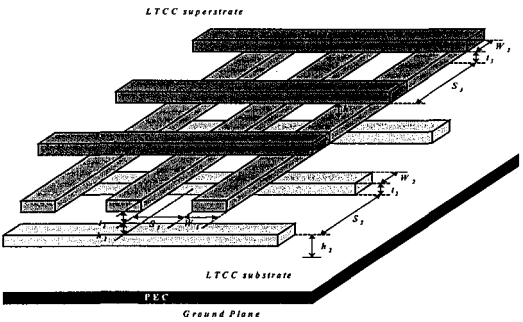


Figure 1. Three-dimensional interconnect embedded in a LTCC superstrate-substrate.

# SCATTERING PARAMETERS OF MAGNETOSTATIC SURFACE-WAVE TRANSDUCERS: THEORY AND EXPERIMENT

Manuel J. Freire, Ricardo Marques*, Francisco Medina
Dept. of Electronics and Electromagnetics, University of Seville
Ave. Reina Mercedes s/n 41012 Seville, Spain

The theoretical and experimental study of the excitation of magnetostatic-surface waves (MSSW) by microstrip transducers was first reported by Ganguly and Webb in [IEEE MTT-23, 998-1006, Dec. 1975] and [IEEE MTT-26, 444-447, June 1978]. In these works, the input impedance of MSSW transducers is calculated assuming two hypothesis: uniform fields along the width of the YIG film and uniform current distribution across the strip. Later, in [T. W. O'Keeffe and R. W. Patterson, J. Appl. Phys., 49, 4886-4895, Sept. 1978], nonuniform fields are considered in an analysis based on a superposition of modes to include the effect of the finite width of the YIG film in the calculation of the delay time of a MSSW delay line. In [J. C. Sethares, IEEE MTT-27, 902-909, Nov 1979] and [S. N. Bajpai, IEEE MTT-36, 132-136, Jan. 1988] it is reported the calculation of the input impedance and the insertion loss of MSSW transducers, respectively, assuming a nonuniform current distribution on the strips. However, uniform fields are assumed in these works when the transmission line theory is applied in the analysis. In the present work, the authors show a method for the calculation of the input impedance (i.e., return loss) and the insertion loss of two-microstrips MSSW transducers not assuming the above two hypothesis. This method has two parts. In the first part, the transmission line theory is applied without disregarding the variation along the width of the YIG film and the telegrapher's equations are solved analytically. The insertion loss is then derived from the closed-form solution of the telegrapher's equations and it is obtained as a function of the width of the YIG film and the following transmission line parameters: the complex propagation constant, the complex characteristic impedance of the YIG-loaded microstrip line and the mutual inductance between the two microstrips. The input impedance (return loss) is obtained from the complex characteristic impedance, the complex propagation constant and the width of the YIG film by using an exact traslation impedance formula without approximations, that is, not assuming uniform fields. In the second part of the method, the transmission line parameters are numerically computed by applying a full-wave method of moments technique. Although a transmission line model is used, the final solution does not correspond to a quasi-TEM approach since the parameters of the model are obtained following a full-wave treatment. Thus, the scattering parameters of two-microstrips MSSW transducers comprising metal-dielectric-YIG-GGG can be computed without restrictions in the dimensions. Theoretical results are found to be in good agreement with measurements for different microstrip structures.

0-7803-7846-6/03/$17.00 ©2003 IEEE

# A Photonic Bandgap Antenna Reflector for PCS Applications

*Dowon Kim[1], M. Kim[1], H. Lee[2], B. Oh[2]

[1]Korea University, EE Department, Seoul, 136-701, Korea, woneeee@hotmail.com
[2]LG Electronics Institute of Technology, Seoul, 137-724, Korea

Photonic bandgap substrates possess a property unattainable from ordinary metal plates and present a large surface impedance near the resonant frequency. They could be placed inside a waveguide to obtain a desired electromagnetic field distribution or in the ground plane of microstrip circuits to form bandpass filters. The radiation pattern in open space could also be enhanced with the use of the PBG substrates as the antenna ground plane. In this paper, we propose the idea of using a small antenna reflector to purposely create a near-field null behind the reflector while maintaining a relatively uniform radiation pattern in the far field. Positioning a metal reflector near the transmitting antenna blocks the radiation itself. The PBG reflector, on the other hand, has little affect on the amount of total radiated power while reducing the near-field power potentially harmful to mobile phone users in personal communication systems. In our experiment, the two-layered thumb-tack approach proposed by Sievenpiper was initially used to fabricate the PBG substrate with the resonant frequency of 2.0GHz. Several different PBG reflector sizes were tested by placing them 3mm away from a simple monopole antenna. In the near field, the PBG reflector with the width of a half free-space wavelength provided an effective shielding with the front-to-backside radiation ratio of almost 20dB. However, the radiation pattern in the far field showed less than 8dB deviation from the pattern measured without any reflectors.

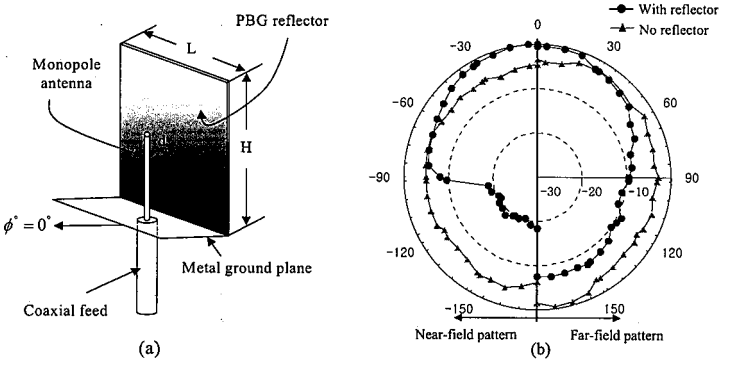


**Figure1.** (a) Reflector antenna test setup, and (b) normalized H-plane patterns measured at 0.2λ and 13λ away from the monopole, respectively. The PBG reflector, λ/2 by λ/2 in size, was placed 0.03λ away from the transmitting monopole antenna to provide the near-field shielding. The far-field pattern shows only 10dB peak-to-null ratio and a smaller field distortion compared to the near-field case.

0-7803-7846-6/03/$17.00 ©2003 IEEE

# Model Establishment and Crosstalk Analysis of the Common-Leg Multiconductor Transmission Line

Chi-Fang Huang* and Yun-Chih Chao
Graduate Institute of Communication Engineering, Tatung University
40, Chungshan N. Rd., 3rd Sec., Taipei 104, TAIWAN
TEL: +886-937-008-883; FAX: +886-945-868-442, , Email: ras@ttu.edu.tw

## I. INTRODUCTION

Due to that the differential transmission line has the effect of "common-mode rejection" to the noise signal, it is suitable for signal of high speed and low voltage to propagate for long distance. However, in the high-speed digital system, for instance, the equipments of telecommunication transmission, the number of kinds of address/data bus will increase along with the raise of complexity, among which the differential signal line structures are much more complicated. Furthermore, in the system of high density, a large amount of the transmission line will lead to huge number of I/O pins in package of semiconductor devices, for example, of 500 ~ 600 pins. To overcome this problem, in other words, to cut down the pin number of ASIC, a new method in engineering is to combine one of each pair of the differential transmission line from transmitter to receiver in the light of one group of differential transmission address/data bus, refer to Fig. 1.

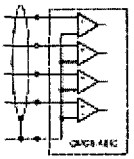

Fig. Circuit representation of a common-leg multiconductor transmission line

The purpose of this paper is to put forward the model establishment and crosstalk analysis for this kind of transmission line structure. In the experiment, the prototypes of different length and line spacing are made for analyzing the relation between the parameters of the structure and the coupling of signals. In the simulation, to economize the calculated memory of computer and simulated time, lumped element equivalent circuit is applied for the establishment of model. At the last, the results of simulation will be proved by the result of measurement.

## II. TEST BED AND MODELLING

Referring to the profile of the structure, the Fig. 2, when the common-leg multiconductor transmission line are realized in a multiplayer PCB, the signal path of the common one is named as the 'reference', and the other signals are shielded by it as well. However, all of them are covered shielded by the ground planes.

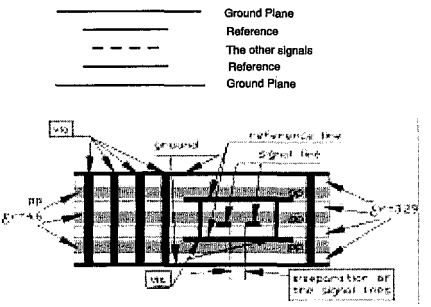


Fig. 2 Cross-section of the transmission line

Consequently, the reference line is to act as a low impedance line. This structure is surely operating as a heavily coupled one. There are two kinds of test bed with different signal path lengths under study, namely, short line of 61.195 mm length and long line of 130.6232 mm length. Both of them have three line spacing cases: s = 1w, s = 1.5w, and s = 2w with w = 0.1584mm (signal line width).

## New Developments in Cosmology

**Co-Chairs:** J. Carlstrom
B. Netterfield

7:55 Opening Remarks

# The Cosmic Background Imager Experiment

C. .R. Contaldi for the CBI Collaboration
Canadian Institute for Theoretical Astrophysics
University of Toronto, Canada

**Abstract**

The Cosmic Background Imager (CBI) is a 13-element interferometer array operating in the 26-36 GHz frequency band situated at an altitude of 5080 metres in the Chilean Andes. The CBI is designed to study the Cosmic Microwave Background Radiation (CMBR) from the early universe. The Angular power spectrum of fluctuations in the CMBR provides a unique testing ground for models of structure formation in the universe. We describe the experiment and observations being carried out. We report on new determinations of cosmological parameters using data from extended mosaic observations. The three extended mosaics cover an area of about 80 $\deg^2$ and comprise observations of the total intensity of the CMBR carried out in the 2000 and 2001 observing seasons. For the 2002–2003 season the instrument has been upgraded for measurement of polarized radiation. We report on the ongoing observations and on the prospects for measurements of peaks in the Cosmic Microwave Background polarization power spectra.

0-7803-7846-6/03/$17.00 ©2003 IEEE

## The Arcminute Cosmology Bolometer Array Receiver

W.L. Holzapfel*[1], P.A.R. Ade[2], R.S. Bhatia[3], J.J. Bock[4], M.D. Daub[1], J.H. Goldstein[5], C.L. Kuo[1,6], A.E. Lange[7], M. Lueker[1], M. Newcomb[1], J.B. Peterson[8], J. Ruhl[9], E. Torbet[5], D. Woolsey[1]

[1]Department of Physics, University of California at Berkeley, Berkeley, CA 94720
[2]Department of Physics and Astronomy, Cardiff University, CF24 3YB Wales, UK
[3]European Space Agency, 2200 AG Noordwijk, The Netherlands
[4]Jet Propulsion Laboratory, Pasadena, CA 91125
[5]Department of Physics, University of California, Santa Barbara, CA 93106
[6]Department of Astronomy, University of California at Berkeley, Berkeley, CA 94720
[7]Department of Physics, Math, and Astronomy, California Institute of Technology, Pasadena, CA 91125
[8]Department of Physics, Carnegie Mellon University, Pittsburgh, PA 15213
[9]Department of Physics, Case Western Reserve University, Cleveland, OH 44106

The Arcminute Cosmology Bolometer Array Receiver (ACBAR) is a novel instrument designed specifically for observations of fine scale cosmic microwave background (CMB) anisotropy and the Sunyaev-Zel'dovich effect. The instrument is a 16 element 230 mK bolometer array that is presently being used to produce images the CMB in three millimeter wavelength bands with approximately 4′ resolution.

The receiver is designed to observe from the 2.1 meter off-axis Viper telescope located at the South Pole. A chopping tertiary mirror sweeps the 16 ACBAR beams 3 degrees across the sky in a fraction of a second without introducing excessive modulated telescope emission or ground radiation pickup. The signals produced as the beams sweep across the sky correspond to sensitive measurements of differences in the sky temperature. The large chop of Viper results in high resolution ($\Delta\ell \sim 120$) measurements of the recovered power spectrum over the range from $\ell \sim 120 - 3000$.

Under the low background conditions available at the South Pole, the ACBAR detectors become background limited at a temperature of approximately 300 mK. The noise equivalent temperature of the 2.1 mm wavelength detectors is measured to be $300\,\mu\mathrm{K}\sqrt{s}$. ACBAR makes use of a self-contained 3-stage Helium sorption refrigerator to reach a temperate of 230 mK with a hold time of 36 Hours. The fridge is periodically recycled with an automated system resulting in a duty cycle of $\sim 90\%$.

The ACBAR frequency bands are optimized to achieve maximum signal to noise while observing the SZ effect and CMB anisotropies in the presence of atmospheric emission. We use a combination of black polyethylene, Yoshinaga, Pyrex, and resonant mesh filters to precisely define the passbands and block high frequency leaks. The band averaged optical efficiencies for the 2.1, 1.4, and 1.1 mm passbands range from $31 - 40\%$.

ACBAR was deployed to the South Pole in December 2000 at has operated continuously for the past two years. The deepest ACBAR observation has produced a 6 deg$^2$ map with a RMS noise in a 4′ pixel of $\sim 10\,\mu$K at 150 GHz and $25\,\mu$K at 220 GHz. This is the most sensitive image of the CMB produced to date and has been used to determine the power spectrum of the fine angular scale CMB with unprecedented accuracy. We have also produced images of the Sunyaev-Zel'dovich effect in a sample of low redshift clusters of galaxies and performed a search for distant unknown clusters. ACBAR is presently being prepared for a third season of winter observations.

0-7803-7846-6/03/$17.00 ©2003 IEEE

**Design and Performance of a Balloon-borne Bolometric Cosmic Microwave Background Polarimeter**

John Ruhl

Physics Department
Case Western Reserve University
Cleveland, OH 44106

Boomerang is a balloon borne millimeter-wave telescope and radiometer, used to study features in the Cosmic Microwave Background (CMB). The receiver is a bolometric instrument, with a focal plane cooled to 285mK. It is coupled to a 1.3m diameter telescope via a series of feeds and filters at 0.3 and 4 Kelvin. The focal plane array of eight horns feeds a total of 12 detectors in three bands, centered at 150, 250 and 350 GHz. The high frequency bands are made sensitive to a single linear polarization by the placement of a wire grid over each feedhorn; the lowest frequency channels use a new technology where both linear polarizations are preserved through the feed optics; the two orthogonal polarizations are absorbed by two separate detectors at the end of the optical chain.

In January 2003, Boomerang flew for 15 days over Antarctica, gathering information on the temperature and polarization anisotropies of the CMB. I will describe the receiver technology and testing, as well as discuss the methods by which these data will be used to characterize the CMB.

0-7803-7846-6/03/$17.00 ©2003 IEEE 

## CMB Polarization with MAXIPOL and POLARBEAR, and Sunyaev-Zel'dovich observations with APEX-SZ

M. Abroe[1], P. Ade[2], F. Bertoldi[3], J. Bock[4,5], J. Borrill[6], H.-M. Cho[7], J. Clarke[7], J. Collins[7], M. Dobbs[8], P. Ferreira[9], R. Guesten[3], S. Hanany[1], N. Halverson[7], W. Holzapfel[7], A. Jaffe[10], B. Johnson[1], E. Kreysa[3], T. Lanting[7], A.T. Lee*[7,8,11], T. Matsumura[1], J. Mehl[7], K. Menten[3], D. Muders[3], M. Myers[7], R. O'brient[7], B. Rabii[7], A. Ranccanelli3, P.L. Richards7,11, T. Renbarger3, P. Schilke3, D. Schwan7, G. Smoot[7,8,11], H. Spieler[8], R. Stompor[6], H. Tran[7], C. Winant[7], P. Wu[12]

[1]Physics Dept., University of Minnesota, Minneapolis, Minnesota
[2]Cardiff University, Cardiff, Wales
[3]Max Planck Institute for Radioastronomy, Bonn, Germany
[4]Jet Propulsion Laboratory, Pasadena, California
[5]California Institute for Technology, Pasadena, California
[6]NERSC, Lawrence Berkeley National Laboratory, Berkeley, California
[7]Physics Dept, University of California, Berkeley, California
[8]Physics Division, Lawrence Berkeley National Laboratory, Berkeley California
[9]Oxford University, Oxford, UK
[10]Imperial College, London, UK
[11]Space Sciences Laboratory, University of California, Berkeley, California
[12]National Taiwan University, Taipei, Taiwan

We will discuss the balloon-borne CMB polarization experiment MAXIPOL, which is an evolution of the MAXIMA CMB experiment. It uses a rotating half-wave plate to modulate the polarization signal onto 16 single-polarization bolometric photometers. The first scientific flight in planned for 2003.

The POLARBEAR experiment is a proposed ground-based experiment with sufficient sensitivity to characterize the E-mode and lensing B-mode polarization and perform a deep search for the possible gravity-wave B-mode signal. It will be deployed in stages eventually building to a 3000 element transition-edge sensor bolometer array with four frequency bands. The array will be built with planar-antenna coupled bolometers with on-wafer band-defining filters. Systematic error controls include two layers of full ground shields and multiple modulations of the sky signal.

The APEX-SZ experiment will search for galaxy clusters over ~100 sq. deg. of sky using a 300 element horn-coupled bolometer array and the 12m APEX telescope to be sited in Atacama Chile. Several thousand clusters should be discovered which will provide a powerful probe of cosmology. The bolometers will have spiderweb absorbers, transition-edge sensors, and SQUID preamplifiers.

0-7803-7846-6/03/$17.00 ©2003 IEEE

# CAPMAP: A Multipolarimeter Experiment for Measuring the Cosmic Microwave Background

S. T. Staggs

Physics Department
Princeton University
Princeton, NJ, 08540

**Abstract**

CAPMAP comprises multiple correlation receivers at 90 and 40 GHz making observations of the cosmic microwave background radiation from the 7 m Bell Labs telescope in Crawford Hill, NJ. In the winter of its first year (2003), four W-band polarimeters were deployed with 3′ beams. This resolution provides sensitivity to the maximum signal in the angular power spectrum of the CMB polarization anisotropy.

Performance of the CAPMAP instrument and initial results from its first season of data will be discussed. We will include techniques of calibration and verification of data quality, as well as details of the polarimeter design. The polarimeters use MMIC HEMT amplifers provided by JPL in a heterodyne, analog correlator. The bandwidth is 16 GHz, broken into three equal-sized band for better phase tuning. The total power in each arm of the receivers is also monitored. Noise performance and polarization offsets will be presented.

0-7803-7846-6/03/$17.00 

## Measuring CMB polarization with DASI

John Kovac for the DASI collaboration
University of Chicago

The Degree Angular Scale Interferometer (DASI) has recently detected polarization of Cosmic Microwave Background using data from 270 days of dedicated observations during its second and third seasons at the Amundsen-Scott South Pole research station. Interferometric observations in all four Stokes parameters were obtained within two 3.4 degree FWHM fields separated by one hour in Right Ascension, over a frequency range of 26 - 36 GHz. The observed polarization is found to have an amplitude and spatial pattern consistent with predictions, offering a validation of the standard theoretical framework of CMB physics and lending confidence to the values of cosmological parameters that have been derived from CMB measurements.

The DASI instrument is currently undertaking its fourth season of operation at the South Pole, and in this talk we discuss the current status of results from previously reported and ongoing CMB polarization observations. We review the instrumental techniques used by DASI to achieve the sensitivity and control over systematics necessary to measure the extremely faint, extended CMB polarization pattern from a terrestrial site. These techniques are relevant to facing the next set of experimental challenges, which include making precision measurements of the polarization power spectra and searching for new cosmological physics in B mode polarization patterns.

0-7803-7846-6/03/$17.00 

# Initial Results from the Microwave Anisotropy Probe

N. C. Jarosik

Department of Physics
Princeton University
Princeton, NJ 08544

The Microwave Anisotropy Probe (MAP) is a NASA sponsored Medium Class Explorer mission designed to produce full sky maps of the cosmic microwave background (CMB) radiation. MAP simultaneously observes in five frequency bands, spanning 20 - 106 GHz. Twenty differential microwave radiometers observe the sky in two orthogonal linear polarizations, allowing reconstruction of maps in Stokes I, Q, and U parameters. The satellite operates from a Lissajous orbit around the second Earth-Sun Lagrange point (L2) that keeps the Earth, Moon and Sun far from the telescope boresites. The radiometers are built with high electron mobility transistor (HEMT) amplifiers and utilize passively cooled input stages to reduce radiometer noise. The broad frequency coverage allows separation of the CMB signal from foreground emission based on their differing spectral properties. Angular resolutions are different in each frequency band and range from $0.^{\circ}82$ to $0.^{\circ}21$ in the lowest and highest frequency bands respectively. MAP has completed the first of four years of planned science observations.

In this talk I review the instrumental and observational aspects of the MAP mission, stressing the characteristics required for high quality CMB observations. Design features and analysis techniques used to minimize and assess systematic error levels are discussed. On-orbit characterizations of the radiometer performance, including sensitivity, short term and long term stability are presented. The characterization of the optical system, including main beam and sidelobe response, is given, derived from a combination of pre-launch and on-orbit measurements.

I also review the publicly available data products, comprising intensity maps at five frequencies, calibrated time ordered data, and beam and radiometer bandpass characteristics. Derived data products, including the angular power spectrum of the CMB, values of cosmological parameters, and maps of foreground emission components, are also presented.

0-7803-7846-6/03/$17.00 ©2003 IEEE

# The QUEST Experiment

Sarah Church (on behalf of the QUEST collaboration}
Department of Physics, Stanford University, Stanford, CA 94305-4060

The QU Extragalactic Survey Telescope (QUEST) is designed to search for polarization of the Cosmic Microwave Background (CMB) radiation at millimeter wavelengths. The instrument comprises an array of 62 polarization-sensitive bolometers mounted on a 2.6m telescope that will be located on the Chajnantor Plateau in the Chilean Andes. The QUEST receiver is designed to operate at frequencies of 100 and 150 GHz to allow CMB polarization to be distinguished from astrophysical foregrounds. We expect QUEST to begin operations in early 2004. In two years QUEST will complete two surveys – a shallow survey of 500 square degrees will allow a precise determination of the power spectrum of E-mode polarization caused by density fluctuations, and a deeper survey of 30 square degrees will detect B-modes produced by gravitational lensing and could also detect, or set strong limits on, B-mode polarization from gravitational waves.

A major challenge for CMB polarization experiments will be to distinguish the tiny polarized signal from systematic effects, astrophysical foregrounds and, for ground-based experiments, atmospheric effects. I will describe how the design of QUEST is intended to minimize these effects. I will also argue that ground-based experiments such as QUEST are an essential precursor to any CMB polarization satellite, and that they offer a valuable opportunity to develop the necessary hardware and techniques for such a mission.

0-7803-7846-6/03/$17.00 ©2003 IEEE 

# The Study of the Anisotropy of the Cosmic Infrared Background at Sub-MM Wavelengths: The EDGE Project

Stephan S. Meyer, Edward S. Cheng, David Cottingham, Dale Fixsen, Peter Timbie, Robert Silverberg, Grant Wilson

**Abstract**

The Cosmic Infrared Background (CIB) is likely to be the integrated emission from stars and galaxies. In the sub-mm the emission comes from galaxies at redshift from 0.5 to 2 and above. Spatial variation in the CIB surface brightness at large angular scales are sourced by variations in the galaxy density which in turn responds to large-scale matter density variations. The CIB anisotropy is thus sensitive to the history of structure growth and galaxy bias at high redshift. The EDGE instrument measures the spatial variation at low angular resolution and can sample much larger volumes than galaxy counting experiments. Redshift determination of structure is obtained at low resolution using submillimeter color information. We discuss the nature of the measurement, the instrumentation and the astrophysical goals of the experiment.

0-7803-7846-6/03/$17.00 

## Array Receivers for CMB with MMIC Technology

Todd Gaier, Michael Seiffert, Charles Lawrence, Douglas Dawson, Mary Wells
Jet Propulsion Laboratory

Low noise coherent receivers have been extensively used for measurements of the cosmic microwave background (CMB). Recent experiments using low noise, high electron mobility transistor amplified front-ends include WMAP, BEAST, DASI, CBI, CAPMAP. Coherent detection offers several advantages for CMB measurement, including the ability to modulate signals after amplification, simultaneous measurements of multiple Stokes parameters and direct imaging through interferometry. Advances in monolithic microwave integrated circuit (MMIC) technology have enabled multifunction receiver component integration at the chip or compact module level. This has in turn, created the possibility of array receivers for CMB measurements.

We will discuss the state-of-the-art in MMIC amplifier based technologies as well as instruments under development which will use MMIC integration. We will also discuss the prospects for massive receiver arrays using coherent detection for deep CMB polarization measurements.

0-7803-7846-6/03/$17.00 

# CMB Polarimetry with Bolometers

James J. Bock, Jet Propulsion Laboratory, Pasadena, CA, 91109

The polarization of the Cosmic Microwave Background promises a wealth of cosmological information. In particular, a curl-mode polarization signal, induced by the gravitational wave background from the inflationary epoch, may be detectable if inflation occurs at the GUT energy scale. However, deep searches for CMB polarization require significant advances in instrument sensitivity and unprecedented control of systematic errors. We describe the development of the BICEP (Background Imaging of Cosmic Extragalactic Polarization) receiver, designed to deeply probe CMB polarization on degree angular scales at 100 and 150 GHz using polarization-selective bolometers. We are developing new bolometer technology with phased superconducting slot-line antennas, transition-edge superconducting sensors, and integral stripline filters. Large arrays of antenna-coupled bolometers, operating over a wide range of wavelengths, will provide significant gains in system sensitivity compared to current capabilities.

0-7803-7846-6/03/$17.00 

# Measuring Magnetic Fields in Interstellar Molecular Clouds

Richard M. Crutcher
Astronomy Department, University of Illinois

The role of magnetic fields in the physics of dense molecular clouds and in the star formation process remains unclear. If sufficiently strong, magnetic fields may support clouds against gravitational collapse and thus prevent or delay star formation. They appear to provide the only viable mechanism for transporting angular momentum from collapsing cores – necessary for subsequent star formation. Finally, magnetic fields may play a significant role in the physics of bipolar outflows that accompany protostar formation. All techniques available for probing the strength and morphology of magnetic fields in molecular clouds involve measuring the polarization of continuum or spectral-line radiation. Such polarization observations are non-trivial because this polarization is typically only a few percent of the strength of the total intensity, and because instrumental polarization is often significant.

Techniques that may be used for molecular clouds are measurement of the Zeeman effect in molecular spectral lines, measurement of the Goldreich-Kylafis effect (linear polarization in spectral lines due to anisotropic radiative transfer), and linear polarization in dust emission or absorption. Although only the Zeeman effect directly yields magnetic field strengths, a statistical method first proposed by Chandrasekhar and Fermi can yield field-strength estimates with the other techniques. I will briefly review these techniques and the instrumental requirements that radio telescope systems must meet. Data for DR21OH will be presented to illustrate study of magnetic fields in one dense molecular cloud. SCUBA dust-emission polarimetry has mapped the large-scale morphology of the field while BIMA synthesis imaging of dust polarization has mapped the small-scale field morphology in the high-mass double core of DR21OH. BIMA has mapped a double CO bipolar outflow originating in the double core; its relation to the magnetic field will be discussed. The Goldreich-Kylafis effect has been mapped in both the CO J = 2 - 1 and 1 - 0 transitions; polarization directions are orthogonal in the two transitions. Finally, the Zeeman effect has been measured in CN N = 1 - 0 transitions with the IRAM 30-m telescope. Thus, a fairly complete picture of the magnetic field strength and morphology is available, making it possible to discuss the role of the magnetic field in the physics and evolution of this dense molecular cloud core.

0-7803-7846-6/03/$17.00 ©2003 IEEE 

## Wireless Communications

**Co-Chairs:** J. Wang
D. Filipovic

7:55 Opening Remarks

133. 1 8:00 Analysis of using Multiple Reader Antennas in RFID Communication ..... 607
*K. Penttilä, M. Keskilammi, M. Kivikoski, Tampere University of Technology, Finland*

133. 2 8:20 Circular Polarization for Antenna Polarization Diversity To Overcom Deep Fading in Terrestrial Wireless Telecommunications ..... 608
*J. J. H. Wang, Wang Electro-Opto Corporation, USA*

133. 3 8:40 Wideband CPW-Fed Slot Antennas on Finite Ground Planes ..... 609
*M. Ali, R. Usaha, University of South Carolina, USA*

133. 4 9:00 Design and Tolerance Analysis of a 5.7 GHz Chip-Size Microstrip Antenna on High Resistivity Silicon ..... 610
*P. M. Mendes, J. H. Correia, Minho University, Portugal, M. Bartek, J. N. Burghartz, Delft University, Netherlands*

133. 5 9:20 LOW PROFILE UNCONVENTIONAL MULTI BAND INTERNAL ANTENNAS ..... 611
*G. R. Kadambi, S. Yarasi, T. S. Hebron, J. L. Sullivan, Centurion Wireless Technology, Inc., USA*

133. 6 9:40 A Flush-Mounted Multiband/Broadband Sinuous-Like Slot Antenna for Terrestrial Communications ..... 612
*M. Buck, A. Bhobe, D. S. Filipovic, University of Colorado, USA*

133. 7 10:00 Folded Dipole Antenna Above EBG Surface ..... 613
*P. Raumonen, P. Salonen, L. Ukkonen, L. Sydänheimo, M. Kivikoski, Tampere University of Technology, Finland*

133. 8 10:20 Dual Band Film Type Antenna for Mobile Devices ..... 614
*M. Ikegaya, T. Sugiyama, H. Tate, Hitachi Cable, Ltd., Japan*

133. 9 10:40 Triple Band Built-in Antenna for Clamshell Type Mobile Phones ..... 615
*T. Sugiyama, M. Ikegaya, H. Tate, Hitachi Cable, Ltd., Japan*

133. 10 11:00 Dual Polarized Reader Antenna Array for RFID Application ..... APS
*S. K. Padhi, CSIRO, Australia, N. C. Karmakar, C. L. Law, Nanyang Technological University, Singapore*

133. 11 11:20 Patch Antenna Over the RIS Substrate: A Novel Miniaturized Wideband Planar Antenna Design ..... APS
*K. Buell, University of Michigan, D. Cruickshank, Trans-Tech Incorporated, H. Mosallaei, K. Sarabandi, University of Michigan, USA*

133. 12 11:40 Development of Two Kinds of UWB Sources for Propagation, EMC and Other Experimental Studies: Impulse Radio and Direct-sequence Spread Spectrum ..... APS
*T. Ogawa, A. Tomiki, T. Kobayashi, Tokyo Denki University, Japan*

# Analysis of Using Multiple Reader Antennas in RFID Communication

K. Penttilä*, M. Keskilammi, M. Kivikoski
Rauma Research Unit, Institute of Electronics, Tampere University of Technology.
Kalliokatu 2, FIN-26100 Rauma, Finland
katariina.penttila@tut.fi

## Introduction

Radio frequency identification (RFID) systems consist of Radio Frequency (RF) transponders, or tags, RF transceivers, or readers, and a host. Readers are strategically placed to communicate with tags, which are attached to objects identified. The host is a data processing unit, which may be connected to database via Internet. RFID technology, its components and functionality have been reviewed and analysed in several publications of TUT, Institute of Electronics. Several different communication methods exist for RFID. This paper focuses to communication in far field, using backscatter technology. The communication link and the size of identification zone are remarkably dependant on, besides the frequency used, the antenna functionalities. It also depends on is environmental reflections and absorptions, which will be issued in the future. In the following section, the influence of using multiple reader antennas is analysed. The concept of multiple reader antennas, which are expected to be similar and having the same operating frequency, may be realised both having multiple readers with one antenna each and having only one reader with multiple antennas with same phase.

## Multiple Reader Antennas

Several applications need the ability to identify large areas. To fill this demand several reader antennas must use. As Fig.1. shows the influence of the reader's functionality to another reader is remarkable. The antennas used for all simulations were patch antennas, with Teflon substrate (Rogers 5870, with dielectric constant of 2,33). The use of several transmitters at the same place at the same time will lead to collision and signal disappearing. The changes of antenna radiation pattern and –3dB beam width are significant when bringing another antenna close to the first one. Radiation patterns are illustrated in Fig.2 and Fig.3. The distance between antennas was 50 cm in Fig.3. Since the backscattered power from tags is much weaker than the power transmitted by readers must this phenomenon been considered very carefully when using multiple antennas in the same near space.

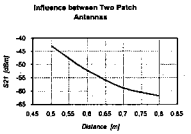


**Figure 1. Influence between two patch antennas**

**Figure 2. Radiation pattern of one patch antenna**

**Figure 3. Radiation pattern of two patch antennas having same phase**

## Conclusions

To solve the collisions between readers the division of time slots or frequency channels or both may be used. The solution is always an application-based choice. Environmental reflections and absorptions are problems issued in the future. Following un-ideal environments the reading zone will be shortened. New antenna structures and very carefully considered antenna placements are some key solutions to solve the problems caused by environmental absorptions and reflections. These features will be researched in the future publications.

0-7803-7846-6/03/$17.00 ©2003 IEEE

# Circular Polarization for Antenna Polarization Diversity To Overcome Deep Fading in Terrestrial Wireless Telecommunications

Johnson J. H. Wang
Wang Electro-Opto Corporation
Marietta, Georgia USA

The performance of terrestrial wireless communications link is mainly limited by deep fading and interference. To overcome the problem, diversity techniques have been employed, among which polarization diversity is noted to be about as effective as conventional spatial diversity yet provides space and cost savings (Dietrich et al, *IEEE AP Trans.*, **49**-9, 1271-1281, 2001). However, polarization diversity has largely been employed at the receive side, and focused on dual orthogonal linear-polarizations (LP) in the form of either V/H (vertical/horizontal) or slanted $\pm 45^{\circ}$.

In this paper, polarization diversity on the transmit side is emphasized. Furthermore, the potential advantage of circular polarization (CP) on the transmit side in overcoming deep fades will be discussed.

A CP wave is in effect an LP vector rotating about the direction of propagation every $360^{\circ}$ for each period of the carrier wave, thus completely spanning the polarization subspace over any time period equal to or longer than the period of the carrier wave. A dual-LP antenna is equivalent to a single LP antenna unless the two orthogonal LP components of identical amplitude are $90^{\circ}$ apart in phase (time). This may explain why the diversity gain of slanted $\pm 45^{\circ}$ was observed to be slightly higher than that of V/H (Lempiainen, *IEEE Veh. Tech. Trans.*, **47**-3, 1087-1092, 1998) while being equal in other analysis (Nilsson, *1998 Int. Symp. Adv. Radio Tech.*, Boulder, 1998).

In radar and other line-of-sight paths, performance merits of CP over LP have been well established. In terrestrial telecommunications, a channel can be segmented into two categories: pseudo-line-of-sight sub-channels and polarization-sensitive scatterers. Scatterers on earth, whether man-made or natural, cause deeper fading to LP than to CP; more generally, the higher the axial ratio of an elliptically polarized wave, the deeper the fading.

On the receive side, dual-CP and dual-LP are equally effective as a polarization diversity scheme. In case no polarization diversity is implemented in the receive antenna, a CP receive antenna (of the same sense CP as the transmit antenna if applicable) is less vulnerable to deep fades than an LP receive antenna. This is because the channel is extremely unlikely to fully convert a signal to the opposite-sense CP to cause deep polarization-mismatch of 30-40 dB.

0-7803-7846-6/03/$17.00 ©2003 IEEE 

# Wideband CPW-Fed Slot Antennas on Finite Ground Planes

R. Usaha and M. Ali*

Department of Electrical Engineering, University of South Carolina, Swearingen Building, Columbia, SC, 29208. Email: alimo@engr.sc.edu.

Slot antennas are finding increasing applications in microwave and mm-wave wireless applications for their wideband characteristics compared to microstrip patches. Slot antennas have bi-directional radiation patterns. Unidirectional patterns can be achieved with the use of a reflector. This includes the cavity-back slot design or more recently slot antennas on PBG (photonic bandgap) substrates.

Recently CPW-fed slot antennas have been investigated by Hall *et al.* [A.U. Bhobe, C.L. Holloway, M. Piket-May and R. Hall: "Coplanar waveguide fed wideband slot antenna", *Electronics Letters*, Vol.36, No.16, pp 1340-1342, 3rd August 2000] among many other researchers. They have proposed an antenna that can provide 49% impedance bandwidth for a 40.3 mm by 27.5 mm by 1.58 mm antenna on a substrate with $\varepsilon_r$=4.3.

In this paper we focus on miniaturized slot antenna design (21 mm by 7.9 mm by 1.5 mm). We propose a design that has an operating bandwidth of 5.5-7.5 GHz (31%). The proposed antenna consists of a folded slot and an additional adjacent slot. The combination of the two slots results in wideband characteristics. The antenna has been simulated using IE3D, a Method of Moments (MoM) based simulation software from Zeland. The antenna operates on 1.5 mm thick Rogers (RO4003) substrate ($\varepsilon_r$=3.38).

Compared to other slot design in the literature our proposed design is much smaller in size and thus can reduce the size of an array significantly. We also present a detailed parametric study of the antenna including current distribution, input impedance, radiation pattern, and gain. In addition we also present antenna performance variation as function of ground plane size. This is of particular significance for portable wireless devices since device miniaturization necessitates reduced PCB size. It has been observed that the PCB ground plane has significant impact on both the input impedance and radiation pattern of the antenna. Further detail will be presented during the conference.

0-7803-7846-6/03/$17.00 ©2003 IEEE

# Design and Tolerance Analysis of a 5.7 GHz Chip-Size Microstrip Antenna on High Resistivity Silicon

P. M. Mendes*, M. Bartek[(1)], J. N. Burghartz[(1)], J. H. Correia,
Dept. of Industrial Electronics, University of Minho, Portugal
[(1)]Lab. of ECTM/DIMES, Delft University of Technology

This paper reports the FEM model, design, fabrication and characterization of a square patch antenna built on high-resistivity silicon (HRS) for operation at 5.7 GHz [Figure 1]. The HRS high dielectric constant of 11.7 leads to antenna size reduction enabling the antenna direct coupling on a chip with RF electronics, which offers potential of low cost, low profile and simplified assembly. The metal patch was made using a 2-μm layer of aluminium and has an area of 7.7x7.6 mm$^2$. The operating frequency and bandwidth were obtained from reflection measurements and are shown in Figure 2. The efficiency of 18.6% was measured using the Wheeler cap method [Figure 2]. The antenna operates at a center frequency of 5.705 GHz, providing a –10 dB return loss bandwidth of 90 MHz. Far-field gain patterns measurements were done using an anechoic chamber and results compared simulations [Figure 3]. The measured gain is ~0.3 dB. Also, FEM analysis was used to study the tolerance of the substrate thickness, substrate resistivity, oxide thickness and metal conductivity in order to predict the antenna behavior [Figure 4]. It was observed that varying the substrate thickness from 500 μm to 550 μm and oxide thickness from 1 μm to 10 μm the operating frequency changes from around 5.7 GHz to 5.85 GHz. Changing the substrate conductivity from 0.02 S/m to 0.05 S/m we found that efficiency changes from 19.6 % to 30.1 %. A wireless link between two prototypes was established and a power of –50 dBm was received when they were placed one meter apart and the transmitting antenna was fed with 0 dBm.

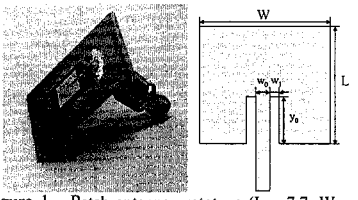


Figure 1 - Patch antenna prototype (L = 7.7, W = 7.6, $y_0$ = 3.1, $w_0$ = 0.36, $w_1$ = 0.32, in mm).

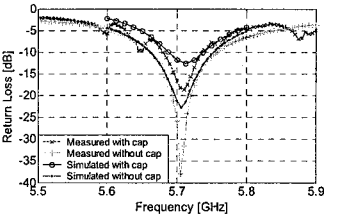


Figure 2 - Co-polar and cross-polar far-field gain patterns obtained at 5.705 GHz.

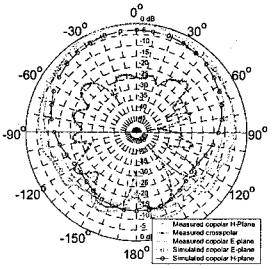


Figure 3 - Return loss used to obtain the antenna operating frequency, bandwidth and efficiency.

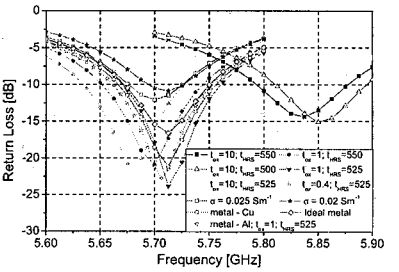


Figure 4 - Influence of wafer parameters ($t_{ox}$, $t_{HRS}$ – oxide and wafer thickness; σ - wafer conductivity).

# LOW PROFILE UNCONVENTIONAL MULTI BAND INTERNAL ANTENNAS

Govind R. Kadambi*, Sripathi Yarasi , Ted S. Hebron,
and Jon L. Sullivan
Centurion Wireless Technologies, Inc.
3425 N. 44th Street, Lincoln, NE 68504, U.S.A.
*E- Mail : govindk@centurion.com*

In the rapidly expanding mobile and data communication technology, apart from the multi band and multi systems capabilities, the miniaturization of the size of the radio device is foremost in the system design consideration. For the evolving technology of internal antennas, the reduction in the size of the radio device has imposed a severe constraint on available volume earmarked for the radiating element. For PIFA, which is a most commonly used internal antenna in the commercial mobile communication applications, the reduction in the available overall volume for its radiating element has profound negative impact on both the realizable bandwidth as well as the gain of the antenna. With the growing trend of restricting the allowable height for the cellular internal antenna to 3-5 mm, the prospect of successful multi band PIFA design with requisite bandwidth and the gain tends to be an involved task. Therefore alternative antenna configurations featured with some or most of the advantages of the PIFA and yet requiring a smaller volume than a PIFA are of great interest to antenna and system designers. This paper proposes several configurations of single feed multi band planar and printed antennas of extremely compact as well as low profile.

In the multi band planar antenna category, the antenna structure facilitates the formation of the radiating element on the top surface of a dielectric carriage. In particular, the case studies proposed in this paper cover the design of single feed Tri or multi band planar antennas whose height can even be of the order of 3 mm. Unlike PIFA, the antenna configurations proposed in this paper warrants the absence of ground plane directly underneath its radiating element. The profile of the radiating element of the multi band antenna of this paper closely resembles the conventional meander line with the following distinction. The radiating element of the proposed antenna has a shorting strip connecting it to the ground plane. As is well known, the radiating element of the meander line type of antenna will not involve connecting short. The design embodiments of the multi band planar antenna of this paper include the radiating element whose surface profile can be either parallel or perpendicular to the ground plane. The technique proposed in this paper has been implemented in the successful design of single feed multi band antenna (33(W) x13 (L) x3 (H) mm) that simultaneously covers the Tri cellular (AMPS/PCS/DCS) as well as non cellular (Bluetooth) frequency bands.

In an alternative antenna configuration, this paper presents the design of multi band printed antenna whose radiating element can be formed on the printed circuit board (PCB) of the radio device itself. Similar to the above planar antennas, the design of printed multi band antennas proposed in this paper has been optimized for unbalanced condition. In an unbalanced condition, the design of the proposed multi band printed antenna is realized with the direct connection between the segment of a radiating element and the ground plane. The multi band printed antenna proposed in this paper can be classified as a multi band printed IFA. Since the radiating element has been formed on the printed circuit board, the profile of the above referred printed antenna tantamount to be of zero height or thickness. The realized Tri band (AMPS/PCS/BT) performance of a printed antenna with a radiating element of cross sectional area of 37(w) X12 (L) mm substantiates the proposed novel concept. This paper also deals with the realizable bandwidth as well as the gain characteristics of the proposed low profile multi band planar and printed antennas.

0-7803-7846-6/03/$17.00 ©2003 IEEE 

## A Flush-Mounted Multiband/Broadband Sinuous-Like Slot Antenna for Terrestrial Communications

Michael Buck*, Alpesh Bhobe, and Dejan Filipoviæ
University of Colorado
Department of Electrical & Computer Engineering
Boulder, CO 80309-0425

The sinuous antenna was designed to fulfill the need for a broadband antenna that could sense orthogonal states of polarization and be flush mounted, having an overall low physical profile. Originally devised by R. H. DuHamel in 1982, the sinuous antenna satisfied the need with a design whose operation bandwidth was determined by the inner and outer antenna diameters.

Sinuous antennas have since been investigated as a flush-mountable means of achieving multiple polarization states while possessing significantly broad bandwidth. This research has mainly been focused on the traditional, non-slot mode microstrip antennas having high input impedances of several hundred Ohms. The high input impedance and the multi-band operation of this antenna make matching and balancing measures more difficult. Using slot-mode excitation, the input impedance of the same antenna can be lowered (X. Begaud, et al., *Ant. & Prop. Conf.*, 2000), allowing improved matching to feed lines.

This paper will discuss the initial experimental performance of a slot-mode type cavity-backed antenna fabricated on a Duroid® 5880 substrate (shown in Figure 1). An odd-mode pattern, favorable for terrestrial communications, with a null at broadside and maxima at acute angles off broadside (shown in Figure 2) is achieved by appropriate feeding of the input. Return loss, input impedance, and far-field power patterns are examined and will be discussed for this mode at various microwave operating frequencies. Suggestions for possible modifications to improve bandwidth and increase gain including cavity dimensions, antenna dimensions, feeding point location, and feeding point geometry will also be discussed.

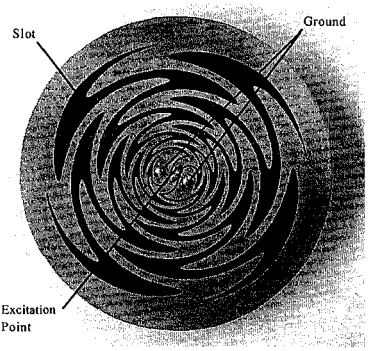


**Figure 1** – Photograph of realized antenna

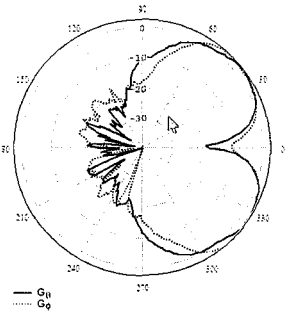


**Figure 2** – Power Pattern at 2.5 GHz

# Folded Dipole Antenna Above EBG Surface

Pasi Raumonen*, Pekka Salonen, Leena Ukkonen, Lauri Sydänheimo, Markku Kivikoski
Tampere University of Technology, Institute of Electronics
Rauma Research Unit, Kalliokatu 2, 26100 Rauma, Finland
Phone: +358-2-5341509, email: pasi.raumonen@tut.fi

Product identification requires modern techniques where RFID (radio frequency identification) has become a promising method recently (P.R. Foster and R.A. Burberry, IEE Colloquium on, 1999 pp. 3/1 -3/5). Therefore, new antennas need to be designed for that purpose. In this paper, the effects of an EBG (electromagnetic band-gap) surface (Fan Yang and Y. Rahmat-Samii, AP-S int. symposium, 2002. IEEE vol.3, pp. 744-747) and the same sized metal plate (or PEC) on a folded dipole antenna are studied. The antenna is placed horizontally very near the surface. Radiation efficiency, antenna impedance, impedance matching and radiated power are simulated as function of antenna height.

When an antenna is close to a metal plate, its surface will reflect all the radiation from the antenna, therefore, it acts like a reflector or mirror. The consequence of this is that the antenna becomes more directive. And this is the case of EBG-surface also, because most of its area is metal. But when the antenna is very near to the metal, its surface will affect to other antenna parameters as well. At least antenna impedance, impedance matching and radiation efficiency will change, even dramatically, and so radiated power will change. The purpose of this study is to find out how the antenna works, when it is placed very near to the EBG surface or the metal surface (PEC). Distance or antenna height is varied from 0.2mm to 10mm. Because the simulation problem is complex, especially for EBG case, analytical solutions for these situations are probably impossible. So simulation is only alternative to find out the effects of the surfaces, if measuring is out of count. This study is carried out with (Ansoft HFSS) Finite Element Method (FEM).

The folded dipole antenna is made of copper and is very thin like tape and the tape is 1mm wide. Its resonance frequency is 2350MHz (wave-length is 128mm) in free space and also all the results of this paper will concern that frequency. In addition, the antenna impedance is approximately 265+j3Ω in free space, so there is very good matching without any extra matching circuit, if 300Ω feeding cable is in use (S11 is then –24dB). The EBG surface and the metal plate are not groundplanes for the antenna, because folded dipole does not need one, but they work as reflectors. The EBG surface consist of 4x6 little square patches, which are joined to ground through the substrate via tiny ducts. The dimensions of the patches are designed for frequency 2350MHz and they depend on dielectric constant of the substrate, substrate height and gap between the patches. The metal plate is copper (conductivity 58MS/m), which works as reflector nearly as good as PEC would work.

When the antenna distance from the metal plate approaches zero (from 10mm to 0.2mm), its impedance changes dramatically. Resistive part becomes very small and it approaches to zero, also reactive part becomes much higher (55->95Ω). So if the impedance of the feed line is 300Ω, the matching is very poor (-2.6->-0.06dB). Actually 50Ω feed provides much better matching (app. –6dB), but it is still very poor (<-1.7dB), when the antenna is close to (0.2-4mm) the metal. Radiation efficiency is reasonably good (>92%), when distance is 4mm or more. If the distance is less than 4 mm, the efficiency is very low and approaches to zero. With 1W feed power, the radiated power is 0.45-0.0002W and 0.76W-0.001W in 300Ω and 50Ω case, respectively. In the EBG case, when antenna distance from the metal plate approaches zero, the resistive part of the antenna impedance becomes little lower (app. 150Ω) and reactive part becomes very high (200->800Ω). Matching to 300Ω is much better than in the metal case (-6,7->-1.3dB), but it still needs extra matching. Matching to 50Ω is as good as in the metal case when antenna is very near (0.2-4mm). Actually the metal case performs much better when distance is longer (app. –1.7dB). The radiation efficiency remains suitable (88%) even when antenna is almost in touch (0.2mm) with the EBG surface, which is wilfully better than in the metal case (1%). And thus, radiated powers are 0.78-0.23W in 300Ω case and 0.35-0.05W in 50Ω case.

As for conclusion one can say that EBG surface provide much better efficiency and matching, compared to the metal plate surface (PEC), when the folded dipole antenna is very near the surface. And consequence of this is more radiated power and/or lower profile antenna designs.

0-7803-7846-6/03/$17.00 ©2003 IEEE

# Dual Band Film Type Antenna for Mobile Devices

Morihiko Ikegaya*, Takahiro Sugiyama*, Hisashi Tate**
* Advanced Research Center, Hitachi Cable, Ltd.,
3550 Kidamari-cho, Tsuchiura, Ibaraki 300-0026, Japan
Fax: +81-29-826-6411; E-Mail: ikegaya@arc.hitachi-cable.co.jp
sugi@arc.hitachi-cable.co.jp
** Hitaka Works, Hitachi Cable, Ltd.,
880 Isagosawa-cho, Hitachi, Ibaraki 319-1418, Japan
Fax: +81-294-42-4483; E-Mail: tate.hisashi@hitachi-cable.co.jp

The dual band antenna for mobile devices has been developed for such a Laptop PC. It is an original Film Type Antenna, which corresponds to the operating frequency of two Wireless LAN standards, the 2.4GHz band (IEEE 802.11b) and 5.2GHz band (IEEE 802.11a). It is of made into the 30.0mm x 30.0mm x 0.3mm thin shape in order to realize easy installation into small devices. Furthermore, unidirectional functionality has been incorporated on each band.

Fig.1 – General view of the Dual Band Film Type Antenna

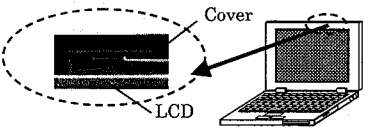


Fig.2 – Built-in state Dual Band Film Type Antenna for the LCD case.

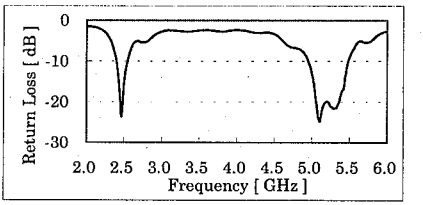


Fig.3 – Resonation property of Dual Band Film Type Antenna when being built-in in the LCD case.

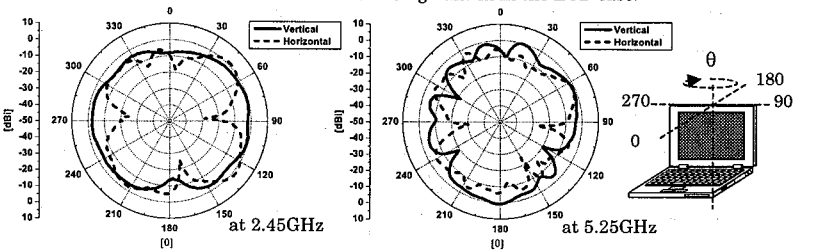


Fig.4 – Radiation directivity of Dual Band Film Type Antenna when being built-in in the LCD case.

Information
(1) B1.2. Antennas for wireless communications
(2) Developed a new concept structure makes easy installation of a dual band antenna into a conventional Laptop PC structure.
(3)

0-7803-7846-6/03/$17.00 ©2003 IEEE

# Triple Band Built-in Antenna for Clamshell Type Mobile Phones

Takahiro Sugiyama*, Morihiko Ikegaya*, Hisashi Tate**
* Advanced Research Center, Hitachi Cable, Ltd.,
3550 Kidamari-cho, Tsuchiura, Ibaraki 300-0026, Japan
Fax: +81(29) 826-6411; E-Mail: sugi@arc.hitachi-cable.co.jp
ikegaya@arc.hitachi-cable.co.jp
** Hitaka Works, Hitachi Cable, Ltd.,
880 Isagosawa-cho, Hitachi, Ibaraki 319-1418, Japan
Fax: +81(0294) 42-4483; E-Mail: tate.hisashi@hitachi-cable.co.jp

A planer inverted-F antenna (PIFA) for clamshell type Mobile phones, which operates in the 900, 1800 and 1900MHz bands, has been developed. To achieve the same size triple antenna as dual-band PIFA ($3cm^3$), the relationship between the bandwidth and the area of ground-plane under the PIFA was studied. Removing a part of the GND plane of the PIFA improves the bandwidth in the 1900MHz band. Moreover, the antenna properties were investigated both "OPEN" and "CLOSED" positions of the clamshell. It appeared that the resonance frequency of the antenna when "CLOSED" depends on the length of the flexible printed circuit (FPC) connecting both circuit boards. Extending the length of FPC reduces interaction of the induced currents on both circuit boards. As result the resonance frequencies of this antenna when "OPEN" can be made to coincide with when "CLOSED".

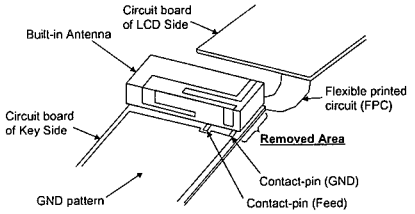


Fig.1 Triple Band Antenna

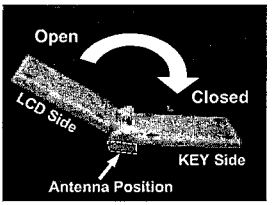


Fig.2 Clamshell type mobile phone

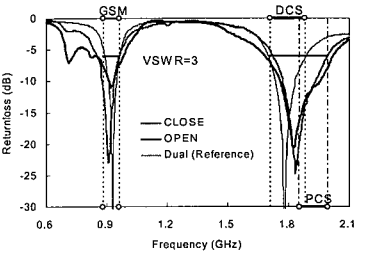


Fig.3 Return-loss of Triple-band Antenna in Clamshell Type Mobile Phone

Information
(1) B1.2. Antennas for wireless communications
(2) Developed antenna structure provides for more stable operation of Clamshell Mobile Phones.

0-7803-7846-6/03/$17.00 ©2003 IEEE

*Special Session*

## EBG Surfaces 2: Modeling

**Organizer(s):** Per-Simon Kildal
N. Eegheta
**Co-Chairs:** N. Engheta
P. S. Kildal

7:55 Opening Remarks

138. 1 8:00 In-phase Reflection and EM Wave Suppression Characteristics of Electromagnetic Band Gap Ground Planes ..... APS
*A. Aminian, F. Yang, Y. Rahmat-Samii, UCLA, USA*

138. 2 8:20 Artificial High-impedance Surfaces: Theoretical Analysis for Oblique Incidence ..... APS
*S. A. Tretyakov, Helsinki University of Technology, Finland, C. R. Simovski, St. Petersburg Institute for Fine Mechanics and Optics, Russia, P. de Maagt, European Space Research and Technology Centre (ESTEC), Netherlands*

138. 3 8:40 USE of ASYMPTOTIC BOUNDARY CONDITIONS on the DESIGN of ANTENNAS with SOFT and HARD SURFACES ..... 618
*A. A. Kishk, University of Mississippi, USA*

138. 4 9:00 Asymptotic Analysis of Periodic Strips on Spherical Structures ..... 619
*Z. Sipus, R. Zentner, University of Zagreb, Croatia*

138. 5 9:20 Modal Propagation in Ideal Soft and Hard Waveguides ..... APS
*G. Ruvio, University of Siena, Italy, P. S. Kildal, Chalmers University of Technology, Sweden, S. Maci, University of Siena, Italy*

138. 6 9:40 Development and Application of Physics-based Compact Models for High-Impedance Electromagnetic Surfaces Integrated in a Power Plane Configuration ..... APS
*T. Kamgaing, Motorola, O. M. Ramahi, University of Maryland, USA*

# USE OF ASYMPTOTIC BOUNDARY CONDITIONS ON THE DESIGN OF ANTENNAS WITH SOFT AND HARD SURFACES

**Ahmed A. Kishk**
**Department of Electrical Engineering and Center for Applied Electromagnetic Systems Research (CAESR), University of Mississippi, University, MS 38677**

Recently, asymptotic boundary conditions (ABC) are used to treat corrugated surfaces and surfaces loaded with periodic narrow metallic strips with period, P, much smaller than the wavelength. These surfaces have been classified as artificially soft or hard surfaces under certain conditions related to the dielectric thickness or the corrugation depth with the strips direction or corrugation directions along the wave propagation direction (hard surface) or in the transverse direction of the wave propagation direction (soft). If the surface is corrugated, the boundary conditions are referred to as the asymptotic corrugation boundary condition (ACBC). If the surface is loaded with periodic strips, the boundary conditions are referred to as asymptotic strips boundary conditions (ASBC). Lately, an idealization for these surfaces in the soft and hard conditions are looked at as a periodic structure with each period made of perfect electric conducting (PEC) strip attached to a perfect magnetic conducting (PMC) strip with P approaching zero (PEC/PMC surface). In this case, the boundary conditions in the asymptotic form are defined as the tangential electric field along the strips is zero and the tangential magnetic filed along the strips is zero. The PEC/PMC boundary conditions are implemented in a general 2D code and a general body of revolution (BOR) code. The codes are based on the surface integral equations and the method of moments. These codes allow the use of the asymptotic boundary conditions with other conventional boundary conditions. These implementations expand the use of these codes to analyze problems that could not be analyzed in a simple form such as the use of hard surfaces in axi-symmetric horns.

The BOR code using the asymptotic PEC/PMC boundary conditions is verified with some special cases of soft horns with the corrugations replaced by PEC and PMC rings of finite width to model ideal soft surface with finite period P. In addition, the 2D code using the asymptotic PEC/PMC boundary conditions is verified with a cylindrical structures that are made of PEC and PMC longitudinal strips of finite period. In the BOR, when the strips are oriented along the body axis, the ideal PEC and PMC strips can't be analyzed with this code, but the asymptotic PEC/PMC boundary condition can be implemented and analyzed. In such a case, the impedance boundary condition model is used for verification because both models can be analyzed by the same code. This allows the analysis of the hard horns with the ideal hard condition.

Several examples will be presented indicating the usefulness of using the asymptotic boundary conditions in the analysis of these antennas efficiently.

0-7803-7846-6/03/$17.00 ©2003 IEEE

# ASYMPTOTIC ANALYSIS OF PERIODIC STRIPS ON SPHERICAL STRUCTURES

Zvonimir Sipus, Radovan Zentner

University of Zagreb, Faculty of Electrical Engineering and Computing,
Unska 3, HR-10000 Zagreb, Croatia
e-mail: *zvonimir.sipus@fer.hr, radovan.zentner@fer.hr*

Strip gratings are well known for their polarization properties. Incident waves with the electric field parallel to the strips are reflected, and incident waves with the electric field orthogonal to the strips pass through the strips. Strip-loaded substrates can be used among others as wave polarizers (e.g. in reflector antenna systems), in horn antennas to improve cross-polar and back-radiation characteristics, or as struts with smaller equivalent blockage width.

Strip-loaded surfaces can be rigorously analyzed by applying the moment method (MoM) to determine the unknown strip currents. The analysis of planar and circular-cylindrical strip-loaded surfaces can be simplified by using the periodical property of the structure, i.e. by expanding the E- and H-fields in Floquet modes. However, if the source excites a full spectrum of plane or cylindrical waves, such as a dipole, the Floquet-mode expansion/MoM is a laborious process. The implementation of asymptotic strip boundary conditions (ASBC) avoids complexity of MoM approach (P.-S. Kildal et.al, *Microwave and Optical Technology Letters*, Vol. 14, pp. 99-101, Feb. 1997). The accuracy of ASBC for planar and circular-cylindrical geometries is discussed in Z. Sipus et.al, *Microwave and Optical Technology Letters*, Vol. 7, No. 3, pp. 173-178, Feb. 1998, where it is shown that for small distance between strips (less than 0.2 $\lambda$) the agreement between ASBC and rigorous MoM results is good.

The purpose of this paper is to extend the previous work to spherical geometry, i.e. to implement the ASBC to spherical structures. The spectral-domain technique is used to expand the electromagnetic field in spherical modes. Since the problem is defined in the spherical coordinate system we apply the vector-Legendre transformation to the E- and H-fields (W.Y. Tam, K.M. Luk, *IEEE Trans. Microwave Theory Tech..*, Vol. 39, pp. 700-704, 1991.). The boundary conditions cannot be satisfied separately for each spherical mode, thus the ASBC are applied to the total field. As an example the scattered field from a strip-loaded dielectric sphere is calculated and compared with the scattered field from equivalent planar and cylindrical structures.

0-7803-7846-6/03/$17.00 ©2003 IEEE

## Analytical and Computational Scattering Analysis

**Co-Chairs:** P. Persson
R. Graglia

7:55 Opening Remarks

# Polarimetric Scattering from Dielectric Targets Buried Beneath 2-D Randomly Rough Surfaces

[1]Magda El-Shenawee, [2]Carey Rappaport and [2]Eric Miller
[1]University of Arkansas
Department of Electrical Engineering
Fayetteville, AR 72701
magda@uark.edu

[2]Northeastern University
Department of Electrical and Computer Engineering
Boston, MA 02115
rappaport@neu.edu, emiller@neu.edu

**Abstract**

The three-dimensional scattering problem solver, the Steepest Descent Fast Multipole Method (SDFMM), is used to calculate the equivalent electric and magnetic surface currents on the random rough ground interface and the buried targets. The fully polarimetric scattering matrix $S$ is evaluated for hundreds of computer generated rough surface realizations. The modified Mueller matrix relates the incident with the scattered waves, which is defined in terms of the modified Stokes vector $I = \left[|E_v|^2 \quad |E_h|^2 \quad 2\mathrm{Re}\left(E_v E_h^*\right) \quad 2\mathrm{Im}\left(E_v E_h^*\right)\right]^T / \eta$. This implies that the Mueller matrix has sixteen complex elements representing all combinations between real and imaginary parts of co- and cross-polarized waves. The co and cross polarized waves are the elements of the polarimetric scattering matrix $S$, i.e. the *vv*, *hh*, *vh* and *hv*. The polarization of the incident or scattered waves is denoted by *h* or *v*, for horizontal or vertical polarization, respectively, while $\eta$ is the intrinsic impedance of the surrounding medium. Using the SDFMM made it possible to compute hundreds of Monte Carlo simulations for scattering from dielectric objects buried under the random rough ground. The statistical average of each element in the Mueller matrix is computed for two cases; rough ground only and rough ground with buried targets. In the current work, the statistical average of the scattered electric fields from one and from two buried objects is calculated in the far-zone. It is important to emphasize that the subtraction process often used to obtain the target signature is not used in the current work. In other words, the far-fields scattered from the rough ground with the buried objects are directly compared with those scattered from the rough ground with no buried objects. The numerical results clearly show that if one relies only on the co- or the cross-polarized intensities (i.e. the magnitude of the four elements in the polarimetric scattering matrix $S$); it is very difficult to sense the buried objects. However, investigating all the sixteen Mueller matrix elements significantly help in detecting these objects. This phenomenal was persistent in the results of statistical averages and in the results of individual rough surface realizations as well.

0-7803-7846-6/03/$17.00 ©2003 IEEE

# Axial Scattering from Thin Cones

Carl E. Baum
Air Force Research Laboratory
Directed Energy Directorate
Kirtland AFB, NM

Abstract

A recent paper [C. E. Baum, "The Physical-Optics Approximation and Early-Time Scattering", Interaction Note 53, October 2000.] considers the physical-optics (PO) approximation for early-time scattering. For axial backscattering examples of perfectly conducting bodies of revolution (BOR), including paraboloids and circular cones, seem to have good PO results as compared to exact and asymptotic results. However, the perfectly conducting angular sector is not approximated at all by PO (giving zero axial backscattering) for the case of the incident electric field parallel to the plane of the angular sector.

It would then seem useful to understand scattering from cones of various cross sections and compare the results to the PO approximation [T. B. A. Senior, private communication]. The general problem with arbitrary interior cone angle has not been solved. However, we know the exact form the solution must take [C. E. Baum, "The Physical-Optics Approximation and Early-Time Scattering', Interaction Note 563, October 2000; C. E. Baum, "Continuous Dilation Symmetry in Electromagnetic Scattering", Ch. 3, pp. 143-183, in C. E. Baum and H. N. Kritikos (eds.), *Electromagnetic Symmetry*, Taylor & Francis, 1995.] which factors the angular dependence from the temporal/frequency dependence. This applies to various types of cone (e.g., dielectric), but our examples here are for perfectly conducting cones.

A model is developed for axial scattering form thin cones of arbitrary cross section based on the electric- and magnetic-polarizability dyadics per unit length. This is later specialized to perfectly conducting cones for axial backscattering. For circular cones it its shown to agree well with exact and physical-optics results. Applying the model to elliptic cones the disagreement with physical-optics results is clear. In the limit this gives the nonzero results for a thin angular sector.

Noting that the present model is appropriate only for thin cones (small $\psi$), we still need accurate calculation for fat cones (large $\psi$, but $<\pi/2$) for further comparison to the PO approximation [T. B. A. Senior, private communication.]. In its own right, however, this small-$\psi$ model can now be applied to various thin structures, including ones that are not conical.

0-7803-7846-6/03/$17.00 ©2003 IEEE 

# Scattering from a cylindrical array antenna coated with a dielectric layer.

*Björn Thors[1], Lars Josefsson[1,2] and Roberto G. Rojas[3]

[1]Royal Institute of Technology, SE-100 44 Stockholm, Sweden, thors@tet.kth.se
[2]Ericsson Microwave Systems AB, SE-431 84 Mölndal, Sweden,
lars.josefsson@emw.ericsson.se
[3]The Ohio State University, Dept. of Electrical Engineering, The ElectroScience Laboratory, Columbus, OH 43212, USA, rojas-teran.1@osu.edu

In this paper the scattering properties of a dielectric coated conformal array antenna are investigated. The array antenna consists of $4 \times 32$ rectangular apertures placed in a rectangular grid on the surface of an infinitely long circular cylinder (See Figure 1).

The problem is formulated in terms of an integral equation for the aperture fields which is solved with the method of moments using rectangular waveguide modes both as basis and test functions. An efficient uniform asymptotic technique is used to calculate both the excitation vector and the backscattered far-field. The asymptotic solution is valid for large cylinders, coated with thin dielectric layers, away from the paraxial (*i.e.* near axial) region. A similar asymptotic solution is used to calculate the mutual coupling in the non-paraxial region. For the self coupling terms and for the mutual coupling in the paraxial region a planar approximation is used with a corresponding spectral domain technique. The planar approximation is very accurate for large cylinders coated with thin dielectric layers if the distance between the source and field points is not too large.

Numerical results are presented as a function of frequency, angle of incidence, cylinder radius and electrical thickness of the coating. Of particular interest is how the dielectric coating will affect the backscattered field. The results are verified against an independent numerical technique valid for non-coated arrays. The individual subroutines that calculate the mutual coupling, the excitation vector and the backscattered far field have all been verified against results found in the literature and/or using other numerical techniques.

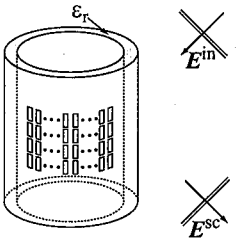


Figure 1: The geometry.

0-7803-7846-6/03/$17.00 ©2003 IEEE

# PSTD Simulation of Two-Dimensional Scattering by a Random Cluster of Electrically Large Dielectric Cylinders

**Snow H. Tseng*, Jed Greene, and Allen Taflove**
ECE Department
Northwestern University,
Evanston, IL 60208

**Joseph T. Walsh, Jr.**
Biomedical Engineering Department
Northwestern University,
Evanston, IL 60208

**Duncan Maitland**
Lawrence Livermore National Laboratory
Livermore, CA 94550

The goal of this research is to investigate the two-dimensional (2-D) electromagnetic wave scattering properties of a random cluster of electrically large dielectric cylinders. This problem arises in the study of the passage of a laser beam through biological tissues containing tubules, fibrils, and collagen fibers. We seek to determine the relative impact upon the scattering cross-section of the cluster's global geometry versus the distribution, composition, and geometry of the cylinders comprising the cluster.

In principle, finite-difference time-domain (FDTD) methods can be used to model this problem. However, the spatial resolution requirements of FDTD limit are applicability to clusters having a relatively small number of electrically large cylinders. A more promising approach is the pseudo-spectral time-domain (PSTD) technique, which permits the use of much lower-resolution grids than FDTD. This allows 2-D clusters having hundreds or even thousands of electrically large cylinders to be modeled using available computers.

In this paper, we report the application to this problem of PSTD with the UPML absorbing boundary condition. Using a parallel-processing computer at Lawrence-Livermore National Laboratory, simulation results have been obtained for the optical scattering properties of random clusters of thousands of ~10-μm diameter dielectric cylinders. Each cluster modeled has macroscopic overall dimensions in the order of 1 mm × 1 mm.

Our research provides perhaps the first results for the electromagnetic scattering properties of a large-scale random system of particles obtained by rigorously solving Maxwell's equations with subwavelength resolution. In addition to this potential theoretical advance, this work may provide practical means to apply optical technology to diagnose pathological conditions such as cancer and to track tissue changes during therapeutic interventions.

0-7803-7846-6/03/$17.00 ©2003 IEEE

# Determination of the Shielding Effectiveness of an Aluminum Honeycomb Panel Modeled as an Array of Cylindrical Waveguides

D.C. Love*, E.J. Rothwell
Electrical and Computer Engineering Department
Michigan State University
East Lansing, MI 48824
rothwell@egr.msu.edu

Aluminum honeycomb panels are widely used for structural support on NASA spacecraft projects. These panels provide a combination of relatively low mass and high strength, which is highly advantageous in space applications. While the mechanical features of these panels are well known, the electrical characteristics are not well understood. This paper investigates the shielding effectiveness of aluminum honeycomb panels. This is done by modeling the panel as an array of cylindrical waveguides and determining the penetration of an incident electromagnetic (EM) field. If the panels are found to perform well as EM shields, future NASA projects might use that feature to address electromagnetic compatibility (EMC) issues.

A model for determining the shielding effectiveness of an aluminum honeycomb panel is presented. The reflected field above the panel and the transmitted field below the panel are represented with Floquet modes (B. Widenberg, S. Poulsen, and A. Karlsson, *J. Electro. Waves Applic.*, **14**, 1303-1328, 2000). The fields within the panel are modeled using cylindrical waveguide modes. Enforcing boundary conditions on tangential fields at the interfaces gives an infinite system of equations describing the unknown Floquet mode and waveguide mode coefficients. The system of equations is then truncated and solved using standard techniques.

This paper considers two cases for the cross-section of the cylindrical waveguides: rectangular and circular. Future work will consider the use of waveguides with hexagonal cross-section. It is anticipated that while the hexagonal case most clearly resembles the physical structure of the panel, the circular or rectangular results may prove equally reliable in the determination of shielding effectiveness.

0-7803-7846-6/03/$17.00 ©2003 IEEE

# Electromagnetic scattering from a curved faces wedge via the Parabolic Equation Method

*R.D. Graglia[1], G. Pelosi[2], S. Selleri[2]**
*[1]Department of Electronics Polytechnic of Turin*
*Corso Duca degli Abruzzi 24, I-10129, Torino - Italy*

*[2]Department of Electronics and Telecommunications*
*University of Florence – Via C. Lombroso 6/17, I-50134 Florence - Italy*

The Parabolic Equation (PE) method is a High Frequency technique for the evaluation of the diffracted field from wedge shaped region. It consists in a very efficient numerical solution of an approximate, Parabolic, differential equation derived from the original, Elliptic, Helmholtz equation. The Parabolic equation contains the slowly variable envelope of the diffracted field as unknown, and implicitly include the radiation conditions at infinity, hence allowing for a very efficient marching-in-space numerical solution.

The PE has shown to be able to treat very complex problems, as anisotropic impedance wedges (Pelosi, Selleri, Graglia, *IEEE Trans. Antennas Propagat.*, 45(5), 1997) and even transparent wedges (Graglia, Pelosi, Selleri, *IEEE Trans. Antennas Propagat*, 49(12), 2001), as well as wedges with complex illuminations (Pelosi, Selleri, *IEEE Trans. Antennas and Propagat.*, 47(10), 1999).

Being the method based on the scattered field alone, it can be applied only if the Geometrical Optics (GO) field is known and if a suitable starting point for the marching in space solution can be obtained. In this contribution the PE will be applied to a perfectly conducting wedge exhibiting curved, convex faces. This is a field of remarkable interest since many structures, like the edges of parabolic antenna reflectors, are better modeled with wedges delimited by curved faces than by wedges delimited by straight faces.

While in previous works the main issue was the computation of both the GO field and the starting conditions here the main issue lies in the domain shape. Straight faces wedge regions have, in a cylindrical reference centered on the edge of the wedge, a width in the $\phi$ co-ordinate which is constant with the distance from the edge $\rho$. This allows for a very easy numerical solution. In the problem at hand, on the contrary, the width in $\phi$ increases as a function of $\rho$, and greater care must be put into the numerical solution. The choice of convex wedge faces is bound to the need to avoid whispering gallery modes.

This work is supported in part by the Italian Ministry of University and Scientific Research under Grant MM09327718: "New analytical and numerical models of electromagnetic scattering and diffraction," and by the Microwave Engineering Center for Space Applications (MECSA) - Italy.

0-7803-7846-6/03/$17.00 ©2003 IEEE 

# Electromagnetic Scattering from a Gap in a Magneto-Dielectric Coating on an Infinite Ground Plane

G. R. Simpson* and W. D. Wood
Air Force Institute of Technology Graduate School of Engineering and Management
2950 P Street, Wright-Patterson AFB, OH, 45433-7765
E-mail: george.simpson@wpafb.af.mil

The electromagnetic scattering from a gap in a magneto-dielectric coating on an infinite ground plane is analyzed. In this context, the gap forms a break only in the material slab coating while the ground plane is continuous and unbroken. The volume equivalence principle is used to convert the gap region to one containing unknown volumetric equivalent currents. The equivalent problem then is one of determining equivalent currents radiating in the presence of an unbroken grounded magneto-dielectric slab. A Green's function for this geometry is developed which consists of two terms: a direct coupling term and correction term to account for the multiple reflected wave series resulting from the grounded-slab geometry. The second term is formulated using periodic array theory and is derived using the Array Scanning Method (ASM). A set of coupled integral equations based on the equivalent currents is then solved via the Method of Moments (MoM) using point matching.

The model can represent a gap that is of a general two-dimensional (2D) shape and can be filled with an inhomogeneous material possessing isotropic magnetic and dielectric constitutive properties different from those of the slab coating. The properties of both the gap filler and the slab coating materials can be complex in representation of lossy materials. The scattering from the gap is evaluated for plane wave illumination that is either TM or TE polarized.

This hybrid Green's Function / MoM technique is validated using a general-purpose MoM reference code and measured data obtained on an RCS measurement range. The results show the hybrid method is accurate and more time efficient than methods relying on general-purpose codes.

New Knowledge: Extends ASM to application of surface feature scattering

Relation to previous work: ASM developed by Munk and Skinner for finite periodic array transmission, reflection, and scattering.



0-7803-7846-6/03/$17.00 ©2003 IEEE 

# Study of Electromagnetic Field Radiation from Apertures using the Alternating-Direction Implicit Finite-Difference Time-Domain (ADI-FDTD) Method

Xi Shao[1,2], Omar M. Ramahi[2,3,4], Lin Li[3,4], Baharak Mohajeriravani[2] and Neil Goldsman[2]
[1]National Space Science Data Center (NSSDC), Goddard Space Flight Center, NASA
Greenbelt, MD 20771, USA
[2]Electrical and Computer Engineering Department, [3]Mechanical Engineering Department,
and [4]CALCE Electronic Products and Systems Center, University of Maryland,
College Park, MD 20742, USA
www.enme.umd.edu/~oramahi

Metal enclosures with apertures are typically used as chasses for high-speed computer systems. As the clock frequency increases, the metal wire and interconnects on printed circuit boards can act as antennas or radiators, whose radiation intensity increases with frequency. Apertures present on the enclosures are primarily intended for thermal management. Li and Ramahi [IEEE APS/URSI Symposium, 2002] proposed a novel structure to reduce field leakage from apertures by coating a layer of conducting material (of much smaller conductivity) on top of the metallic aperture. The coating works to reduce radiation, especially at frequencies at or close to the natural resonance of the aperture. In this work, we developed an alternating-direction implicit finite-difference time-domain (ADI-FDTD) method that is capable of providing a more accurate definition of the electromagnetic fields within the very thin coating layer surrounding the aperture. This multi-grid ADI-FDTD algorithm can efficiently model the problem of a radiating object in the presence of an aperture coated with a thin film material. The thickness of the film can be substantially smaller than that of the metallic surface. We validated our algorithm by comparison to results using other well-established commercial tools. We investigated the effect of textured and/or thin-film material inclusion on the enhancement or reduction of the field in the exterior of an enclosure containing the aperture. Mitigation of transmitted radiation sees critical applications in the field of electromagnetic interference, enhancing radiation, on the other hand, is important in a wide range of applications form maximizing efficiency of antennas to improving the effectiveness of near field optical microscopes. We will present results showing current distribution on the material surrounding the aperture, and present a discussion on the physical aspects of the aperture radiation phenomenon.

0-7803-7846-6/03/$17.00 ©2003 IEEE 

# Analysis of Transient Scattering from Multiregion Bodies Using the Plane Wave Time Domain Algorithm

* J. Gao †, B. Shanker†, D. S. Weile§ and E. Michielssen‡

†2120 Engineering Building, Dept. ECE, Michigan State University,
East Lansing, MI 48824, USA, {gaojun, bshanker}@egr.msu.edu
‡Center for Computational Electromagnetics, 1406 W.Green St., Dept. ECE,
University of Illinois, IL, 16801, USA, emichiel@uiuc.edu
§140 Evans Hall, Dept. ECE, University of Delaware
Newark, DE 19716, weile@ece.udel.edu

Integral equation based methods for time domain scattering analysis are computationally intensive with a cost scaling of $\mathcal{O}(N_t N_s^2)$, where $N_s$ represents the number of surface unknowns modeling the current on the body, and $N_t$ denotes the number of time steps in the analysis. The PWTD algorithm considerably alleviates this cost, and has been used in accelerating the analysis of scattering and radiation from perfect electrically conducting (B. Shanker, A. A. Ergin and E. Michielssen, *Proceedings of IEEE Antennas and Propagation Society International Symposium*, **2**, 1342-1345, 1999) and penetrable bodies (B. Shanker, A. A. Ergin, and E. Michielssen, *J. Opt. Soc. Am. A*, **19**, 716-726, 2003).

In this paper, a novel time domain integral equation technique for analyzing transient scattering from arbitrarily shaped bodies that comprise of different regions will be presented. These regions could be conducting or penetrable. In each region, the time domain Stratton-Chu integral equations are reduced to a set of matrix equations by (i) expanding currents in space and time in terms of Rao-Wilton-Glisson and approximate prolate spheroidal basis functions, respectively, and (ii) by Galerkin testing in space and point matching in time. Our earlier efforts in analyzing this problem suffered from two deficiencies: (i) Despite being implicit, the procedure was unstable for several geometries, (ii) when it was stable, it often was inaccurate as the degree of implicitness increased. Recent work has shown that use of bandlimited functions for representing temporal variation considerably alleviates this problem when analyzing scattering from PEC objects (D. S. Weile, N. W. Chen, B. Shanker and E. Michielssen, *Proceedings of IEEE Antennas and Propagation Society International Symposium*, 162-165, 2002). This paper extends the proposed scheme to multiply connected domains. Boundary conditions between regions are enforced using the algorithm proposed by Medgyesi-Mitschang *et. al.* (L. N. Medgyesi-Mitschang, J. M. Putnam, and M. B. Gedera, *J. Opt. Soc. Am. A*, **11**, 1383-1398, 1994). The set of equations thus obtained is solved using a MOT scheme that is augmented with the PWTD algorithm. To implement the latter, multiple trees and interaction lists are necessary (one for each region) as the wave speed is different in each domain. The proposed technique has been applied to the analysis of scattering from electrically large bodies. Details of the method and numerical results that demonstrate its efficiency will be presented.

0-7803-7846-6/03/$17.00 ©2003 IEEE

# Scattered Fields Computed from the Ramp Response

**Leon Peters, Jr.**

The use of Ramp Response to compute the back scattered fields (*D.L. Moffatt, IEEE Trans AP-17, 299-307, 1969*) from conducting targets represents a long neglected technique. This has now been improved by including penetrable targets and refining the contribution from the shadowed part of the target. The accuracy of this ramp computation has been demonstrated for dielectric and conducting targets including spheres, cones, double backed cones , an ogive, blocks and a pyramid. This approach has also been used to develop an image of a buried A.P. mine (*S. Nag and L. Peters, IEEE Trans. AP-49, 32-40, 2000*).

The ramp response was derived from Physical Optics to obtain

$$f_r^m(t) = -\frac{1}{\pi v^2}\int A\left(\frac{vt}{2}\right)dt \qquad (1)$$

where A is the transverse cross sectional area of the target at the position $z = \frac{vt}{2}$, where the incident ramp waveform becomes non zero, and $v$ is the phase velocity in the ambient medium. The time $t$ is modified in the shadowed region of the target since the path is now along the surface of the target and the magnitude of the incident wave is adjusted to account for focusing. Eq. (1) is modified by including a reflection coefficient for penetrable targets. Finally $f_r(t)$ is Fourier transformed and multiplied by $(jw)^2$ to obtain the usual scattered fields in the frequency $(jw)$ domain. This approach is far simpler than the usual Physical Optics computation.

Recent results show that this approach gives very accurate results in the Rayleigh region and the early time scattering at higher frequencies. It is only required that scattered fields from creeping waves, multiple edge diffraction, etc., be added to obtain the late time response as will be discussed.

Finally, this modified approach results in an improved version of Physical Optics as will be demonstrated using the nose-in incidence case for a conducting cone. The ramp response from the wedge on the back of the cone (shadow region) is accurately predicted via this ramp approach whereas Physical Optics needs to use the Physical Theory of Diffraction for this task.

0-7803-7846-6/03/$17.00 ©2003 IEEE 

**Integral equation methods for solving problems of scattering on an unclosed cone structure**

**Vladimir A. Doroshenko**
Kharkov National University of Radioelectronics
14, Lenin av., Kharkov, 61166, Ukraine
E-mail: vlad_doroshenko@yahoo.com

The method based on using the integral Kontorovich-Lebedev transforms and the semi-inversion method is a successful one for studying boundary electrodynamics problems with single periodical slotted cone geometry(there is one cone strip in the period). Taking into consideration a multi-element cone structure(there are several strips in the period) makes applying the above mentioned method extremely tedious. The task of this work is to find a method that uses singular integral equation to solve an excitation problem for a periodic cone structure with any number of strips($S$) in the period.

Let a semi-infinite perfectly conducting infinitely thin circular cone $\Sigma$ with $N$ equally spaced slots cut along the generatricies be excited by a radial harmonic electric or magnetic dipole. The angular width of the slots and the period of the cone are $d$ and $l = 2\pi/N$ respectively. By virtue of introducing Debye potentials and the integral Kontorovich-Lebedev transforms the electrodynamics boundary problem is reduced to solving dual series equations for unknown Fourier coefficients $\hat{y}_{m,n}^{(j)}$ of electromagnetic field components. The dual series equations are equivalent to singular integral equations like these:

1) for electrical dipole excitation, $j$=1,

$$\frac{1}{2\pi}\int_S \hat{F}(\psi-\alpha)\Phi_1(\alpha)d\alpha + \frac{1}{2\pi}\int_S\left[\hat{A}_{m\pi}^{(1)} - \hat{K}_1(\psi-\alpha)\right]\Phi_1(\alpha)d\alpha = e^{im_0\psi},$$

$$\psi \in S: \frac{\pi d}{l} < |\psi| \le \pi,\ \hat{F}(\psi-\alpha) = \sum_{n\ne 0}\frac{1}{N(n+\nu)}\frac{|n|}{n}e^{in(\psi-\alpha)},$$

$$\hat{K}_1(\psi-\alpha) = \sum_{n\ne 0}\frac{1}{N(n+\nu)}\frac{|n|}{n}\hat{\varepsilon}_{m,n}^{(1)}e^{in(\psi-\alpha)};$$

2) for magnetic dipole excitation, $j$=2,

$$\frac{1}{\pi}\int_S \frac{\Phi_2(\xi)}{\xi-\psi_1}d\xi + \frac{1}{\pi}\int_S K(\xi-\psi_1)\Phi_2(\xi)d\xi = ie^{im_0\psi_1},\ \psi_1 \in S,$$

$$K(\xi-\psi_1) = \frac{1}{2}ctg\frac{\xi-\psi_1}{2} - \frac{1}{\xi-\psi_1} - \frac{i}{2N}\left(\frac{\pi e^{i\nu\xi}}{\sin\pi\nu} - \frac{1}{\nu}\right)\frac{1}{A_{m\pi}^{(2)}} - \frac{i}{2}\sum_{n\ne 0}\frac{|n|}{n}\hat{\varepsilon}_{m,n}^{(2)}e^{in(\psi_1-\xi)};$$

$$\Phi_j(\psi) = \sum_{n=-\infty}^{+\infty}\hat{y}_{m,n}^{(j)}e^{in\psi},\ \psi\in[-\pi,\pi],\ \hat{\varepsilon}_{m,n}^{(j)} = O\left(\frac{\sin^2\gamma}{N^2(n+\nu)^2}\right),\ -1/2 \le \nu < 1/2,$$

$m, m_0 \in Z$, $\hat{A}_{m\pi}^{(1)}$, $A_{m\pi}^{(2)}$ are known.

These integral equations can be solved numerically by the descrete singularities method.

0-7803-7846-6/03/$17.00 ©2003 IEEE

*Special Session*

## Identification and Mitigation of Radio Frequency Interference

**Organizer(s):** Geoffrey Bower, University of California, Berkeley
**Co-Chairs:** G. Bower
K. Tapping

1:15 Opening Remarks

148. 1 1:20 Radio Interference Excision: A Pulsar Observer's Perspective ....636
*D. J. Nice, Princeton University, USA*

148. 2 1:40 Radio Frequency Interference Mitigation Techniques for Pulsar Observations....637
*S. Ransom, McGill University, Canada*

148. 3 2:00 Characterization & Mitigation of L-Band Ground-Based Aviation Radars ....638
*S. W. Ellingson, G. A. Hampson, The Ohio State University, USA*

148. 4 2:20 Design of an L-Band Microwave Radiometer with Active Mitigation of Interference....639
*G. A. Hampson, S. W. Ellingson, J. T. Johnson, The Ohio State University, USA*

148. 5 2:40 Radio Frequency Interference Measurement and Mitigation with the Production Test Array ....640
*G. C. Bower, UC Berkeley, USA*

148. 6 3:00 Real-Time Adaptive Cancellation of GLONASS Interference in OH Signal Observations at the Green Bank Telescope ....641
*A. J. Poulsen, B. D. Jeffs, C. Hansen, K. Warnick, Brigham Young University, R. Fisher, National Radio Astronomy Observatory, USA*

148. 7 3:20 Adaptive Interference Cancellation using an Array Feed Design for Radio Telescopes....642
*C. Hansen, K. F. Warnick, and B. Jeffs, Brigham Young Unversity, Provo, UT,*

148. 8 3:40 Wide Band Nulling with a Single-Tap Beamformer ....643
*G. R. Harp, SETI Institute, S. W. Ellingson, The Ohio State University, USA*

148. 9 4:00 Attenuation of RFI by Interferometric Imaging Arrays....644
*R. A. Perley, National Radio Astronomy Observatory, USA*

148. 10 4:20 How To Keep Computer and Digital Signals Out of Your Radio Telescope: Interference Suppression Begins At Home....645
*T. Landecker, R. Casorso, National Research Council of Canada, Canada*

148. 11 4:40 RFI Tight Modules and Enclosures for the EVLA Project ....646
*S. J. Durand, J. Jackson, R. Ridgeway, National Radio Astronomy Observatory, USA*

148. 12 5:00 Spectrum Management: the First Step in Interference Avoidance ....647
*K. F. Tapping, National Research Council, Canada*

148. 13 5:20 A Spectrum Study of Usage in and Adjacent to Passive Scientific Bands....648
*A. Petrin, P. G. Steffes, Georgia Institute of Technology, USA*

## Radio Interference Excision: A Pulsar Observer's Perspective

David Nice
Physics Department, Princeton University

The temporal and frequency variability of pulsar signals make their observation particularly vulnerable to radio frequency interference. Pulsar observations are made over wide bandwidths at low frequencies (typically between 0.4 and 2.4 GHz), often outside the protected bands. Interference from radar installations, television stations, and other terrestrial sources are a perennial problem.

From an RFI perspective, the most challenging pulsar observations are searches in which neither the pulsar rotation frequency nor its dispersion measure (chirp rate) are known. The data sets are time series of $10^6$ to $10^8$ spectra, sampled at intervals under 1 ms, each with $10^2$ to $10^3$ spectral channels. Fourier and other techniques are used to detect swept periodic signals within the data set. Several steps must be taken to mitigate RFI:

1. Monitor the passband in real time with a spectrometer and chart recorder. In cases of severe interference, reallocate the telescope time to some other project.
2. Search for and remove broadband spikes in power with time resolution of order 0.1 second. The most prominent such sources are radar transmitters and lightning.
3. Examine spectra for excess power in single channels on time scales of seconds or minutes. The most prominent sources are communications carriers.
4. After Fourier transforming the time series, excise known RFI frequencies such as the 60 Hz power line, 1.2 Hz cryogenic pumps, etc.
5. Delete RFI-prone portions of the data at long periods (greater than a few seconds) and small dispersion measures.
6. If the observations cover a series of different telescope pointings made in sequence, search for (and remove) repeated detections of the same candidate pulsar frequency at different sky locations.
7. Manually examine the data after the fact for repeated detections of the same frequency at widely separated points.

All of these steps hinge on the assumption that RFI is confined to particular ranges of frequency and/or time. Increased use of spread spectrum techniques will make RFI more difficult to remove.

Searches for single (non-periodic) pulses are particularly difficult because single pulses are easily mimicked by RFI. Dispersion of astronomical signals is key to distinguishing them from (un-dispersed) terrestrial signals.

Observations of pulsars with known periods are somewhat less vulnerable to RFI (since the signal is naturally "switched"), and steps 4 through 7 above are typically not needed. Still, we have found basic time and frequency domain RFI excision leads to distinct improvement in the quality of such observations. Data acquisition systems based on baseband detection and software analysis are particularly well suited to this task.

0-7803-7846-6/03/$17.00 ©2003 IEEE

# Radio Frequency Interference Mitigation Techniques for Pulsar Observations

Scott M. Ransom
*McGill University Physics Dept., Montreal, Quebec, Canada*

## Abstract

Radio Frequency Interference (RFI) has become a tremendous problem for radio pulsar astronomers over the past decade. Since pulsars are intrinsically weak radio sources that show significant flux variations over timescales of several microseconds, their observation requires large telescopes with sensitive receivers, long integration times, wide bandwidths, and fast sample rates. Additionally, the dispersive effect of the ionized interstellar medium necessitates maintaining high frequency resolution across the bandwidth as well. Unfortunately, these characteristics of pulsar observations make them extraordinarily sensitive to interference as well as to pulsars.

Sensitive searches for new pulsars are especially vulnerable to interference. In general, a pulsar searcher must contend with three basic forms of RFI during a search observation: 1. narrow bandwidth but long duration signals (*i.e.* television and radio stations), 2. strong broadband but short duration events (*i.e.* lightning, garage door openers, microwave ovens), and 3. low-level broadband emissions (*i.e.* unshielded electronics). Each of these interference forms must be dealt with – and hopefully removed – in a different manner.

Over the past several years, I have developed a suite of pulsar analysis software designed specifically for high sensitivity searches of long duration radio observations. RFI mitigation was designed into the system at a fundamental level and has proved essential in today's noisy interference environment. The software removes each of the three main types of interference mentioned above using a series relatively simple time- and frequency-domain algorithms. In this talk I will describe the RFI mitigation algorithms used in this software, their effectiveness at removing interference in data of widely varying quality, and the potential interference issues pulsar astronomers will face in the coming years.

0-7803-7846-6/03/$17.00 

# Characterization & Mitigation of L-Band Ground-Based Aviation Radars

S.W. Ellingson* & G.A. Hampson
*The Ohio State University*, ellingson.1@osu.edu

The 1100–1400 MHz band is important for spectroscopy of HI at high redshift, pulsar work, and SETI. Observations at these frequencies are complicated by pulsed interference from ground-based aviation radars. These radars typically transmit pulsed fixed-frequency or chirped sinusoidal waveforms with pulse lengths of 5–75 $\mu$s, 1–27 ms between transmitted pulses, and bandwidths on the order of 1 MHz. Transmit powers range from $10^3$ W to $10^6$ W into a highly-directional antenna which rotates in azimuth with period on the order of 10 s. Pulses are easily detected through the sidelobes of radio telescopes at least 100 km away, and further when the radar beam is directly pointed at the receiving site or a reflecting object, such as an aircraft. The carrier frequency separation between radars detected at any given site can be 10 MHz or less, making observations in larger bandwidths (desirable for pulsar work, for example) a challenge. The spectrum between carrier frequencies is also corrupted to some degree due to the extended sidelobes associated with the pulse edges, which distorts noise baselines and overwrites spectral features. Pulsar surveys are affected because radar pulses tend to saturate dedispersion/periodicity searches (especially at low dispersion measures), masking pulsar candidates.

We have analyzed several radars received at the Arecibo Observatory using datasets obtained during recent observations. These datasets reveal information about the waveforms and propagation characteristics that can be exploited for mitigation purposes. Using this data, we discuss some simple methods for detection and removal of the radar pulses. Also, we present a coherent subtraction technique that has not previously been applied to the radar problem. This new technique provides an alternative to blanking, which is undesirable in pulsar and SETI work. Using a very crude implementation of the coherent subtraction approach, we show that a radar can be suppressed by at least 16 dB in integrated spectra, and that the maximum single-pulse power observed at the output of the canceler is $\sim$ 15 dB less. We find that the primary limitation is the performance of the pulse *detector*, not that of the canceler. As a result, the performance using blanking turns out to be about the same. Also, we demonstrate that the matched detector for pulses from this radar is relatively insensitive to astronomical transients (e.g., giant pulses), and quantify the risk of such transients being falsely identified as radar pulses.

0-7803-7846-6/03/$17.00 ©2003 IEEE

# Design of an L-band Microwave Radiometer with Active Mitigation of Interference

G.A. Hampson*, S.W. Ellingson, & J.T. Johnson
*The Ohio State University*, hampson.8@osu.edu

Radio frequency interference (RFI) impairs L-band radiometry outside the protected 20 MHz frequency band around 1413 MHz. However, bandwidths of 100 MHz or more are desired for certain remote sensing applications as well as certain astronomy applications. Because much of the RFI in this band is from radars with pulse lengths on the order of microseconds, traditional radiometers (i.e., those which directly measure total power or power spectral density integrated over time scales of milliseconds or greater) are poorly-suited to this task. Simply reducing integration time and discarding contaminated outputs may not be a practical answer due to the wide variety of modulations and pulse lengths observed in L-band RFI signals, the dynamic and complex nature of the associated propagation channels, and the logistical effort associated with post-measurement data editing. This motivates the design and development of radiometers capable of coherent sampling and adaptive, real-time mitigation of interference.

Such a radiometer will be described in this presentation. This design is capable of coherently-sampling up to 100 MHz bandwidth at L-band. RFI mitigation is implemented in FPGA components so that real-time suppression is achieved. The system currently uses a cascade of basic time- and frequency-domain detection and blanking techniques; more advanced algorithms are under consideration. The modular FPGA-based architecture provides other benefits, such as the ability to implement extremely stable digital filters and the ability to reconfigure the system "on the fly". An overview of the basic design along with on-the-air results from an initial implementation will be provided in the presentation. Related L-band RFI surveys will be described to illustrate the relevance of this approach in a variety of operating conditions.

0-7803-7846-6/03/$17.00 ©2003 IEEE

# Radio Frequency Interference Measurement and Mitigation with the Production Test Array

Geoffrey C. Bower
UC Berkeley Radio Astronomy Laboratory
gbower@astro.berkeley.edu

January 15, 2003

The Production Test Array is a three element interferometer that prototypes systems for the Allen Telescope Array. The PTA uses the 6.1-m offset Gregorian antenna, log-periodic feed, broadband LNA and optical signal path of the ATA. The system has continuous frequency coverage from 500 MHz to 11 GHz. We are using the PTA to test the capability of the ATA to implement radio frequency interference mitigation schemes in the environment of Hat Creek Radio Observatory.

Initial results from optical pointing indicate that the PTA antennas have a pointing stability of $\sim 10$ arcsec, which is substantially better than the specification. This is important, though, because amplitude miscalibration is a critical failure mode in interferometric nulling schemes.

We are also making measurements of the interference environment. This includes the effects of self-interference. We intend to make angular RFI patterns that will allow us to determine the location of interferers. We can compare these results with interference measurements made with an isotropic antenna also located at Hat Creek. These measurements permit us to test the frontend for saturation in the presence of powerful interferers.

A test correlator will be installed in the Spring which will allow us to do high throughput RFI experiments, as well. The four-station correlator will process 100 MHz of bandwidth continuously. Earlier experiments with the software correlator of the Rapid Prototyping Array were limited by low bandwidth, low throughput and unstable bandpasses. We expect to see the limits of algorithms such as the postcorrelation method much more readily.

0-7803-7846-6/03/$17.00 

# Real-Time Adaptive Cancellation of GLONASS Interference in OH Signal observations at the Green Bank Telescope

*Andrew Poulsen*[1], *Brian D. Jeffs**[1], *Chad Hansen*[1], *Karl Warnick*[1], *and Rick Fisher*[2]
Brigham Young University[1], bjeffs@ee.byu.edu, and
National Radio Astronomy Observatory[2], rfisher@nrao.edu

This paper reports on development and experimental evaluation of a real-time DSP-based adaptive canceller used to remove orbital satellite RFI from radio telescope observations. Effective operation in driving GLONASS interference well below the integrated noise floor has been demonstrated at both the Green Bank Telescope (GBT), and at the Very Small Array (VSA) of four 3 meter dishes located at Brigham Young University. The system is implemented as an LMS adaptive canceller filter with complex coefficients and a programmable delay line for bulk phase shift correction. The canceller's primary channel input is the corrupted telescope signal, and the high interference to signal ratio (ISR) reference source is obtained from a low-cost dish steered to track the offending satellite. At the GBT, this reference antenna is a 3.7 m dish on a AZ-EL mount driven by commercial satellite tracking software. This antenna is located more than a kilometer from the GBT primary. Since the interfering signal is strong at the reference, we were able to use off-the-shelf commercial low noise amplifiers and a simple receiver design.

The programmable DSP platform uses four 200 MHz, high-end Texas Instruments floating point processors and custom digital receiver front-ends. This system performs the following real-time functions: sampling up to four signal channels at 65 MS/s, complex basebanding, band selection, decimation, bandpass filtering, two channel 1024 point power spectrum estimate and accumulation, and 20 complex tap FIR LMS adaptive filter. As compared to a post processing approach to cancellation, the real-time DSP system has several advantages. It can easily be inserted as a transparent front-end process in an existing telescope system, as we have demonstrated at the GBT. No long-duration, high data rate recording is needed, which is particularly useful if the desired output is just the result of a long integration. Post processing adaptive filtering requires huge data storage. DSP hardware (programmable and FPGA based) are now fast enough to support most desired bandwidths (we have demonstrated 1 to 4 MHz BW operation with our system).

The figures below illustrate real-time cancellation performance with a 12 tap FIR. Processing bandwidth is 1 MHz, with 1 kHz bin width for the 1024 point power spectral estimates, which are also computed in real time over 27 seconds of integration. In the left figure, the GBT signal is corrupted by a sidelobe of the GLONASS transmission band. The adaptive filter removes this interference and corrects the noise floor. No OH signal was present. The right figure shows GLONASS cancellation at the VSA. A simulated OH source (FM sweep) obscured in the primary, is clearly visible between 1608.7 and 1608.9 MHz after filtering.

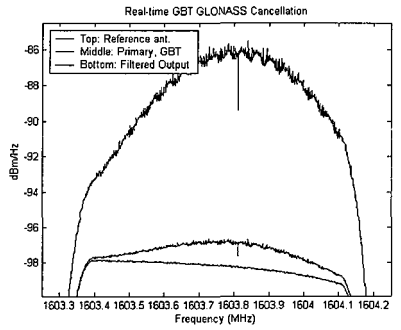


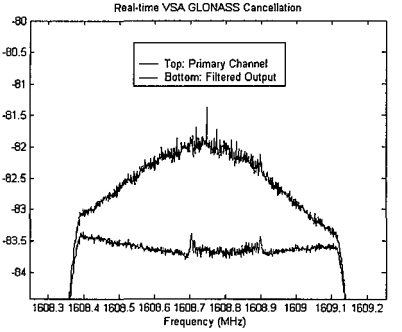


0-7803-7846-6/03/$17.00 ©2003 IEEE

# Adaptive Interference Cancellation Using an Array Feed Design for Radio Telescopes

*Chad Hansen, Karl F. Warnick,* and Brian Jeffs*
Department of Electrical and Computer Engineering
Brigham Young University
Provo, UT 84602

There has been a great deal of work in the past to eliminate or reduce radio frequency interference (RFI) in radio astronomy observations due to satellite systems such as the Russian Federation Global Navigation Satellite System (GLONASS), which operate near radio astronomy frequency bands of interest. These sources are difficult to deal with because they are non-stationary and emit high power signals. Current approaches to this problem are adaptive filtering, adaptive nulling, and blanking of intermittent interferers. Adaptive filtering and adaptive nulling require at least one auxiliary antenna. For applications where multiple antennas are undesirable, adaptive cancellation can be done on a single dish antenna using an array feed.

Phased array feeds have been used on radio astronomy antennas in the past to compensate for reflector aberrations, improve the efficiency of off-axis beams, and to electronically synthesize multiple scanned beams for rapid sky coverage. Full-sampling focal plane arrays have also been designed using electrically small elements, such as dipoles. This type of an array is a good candidate for use with RFI mitigation because it allows many degrees of freedom. Simulations of an array feed in conjunction with a very large array (VLA) model antenna show that the signal-to-interference ratio can be significantly improved using adaptive beamforming techniques such as linear constrained minimum variance (LCMV). We are also studying how the array design can be optimized for both adaptive cancellation and maximum receiver sensitivity (gain/system temperature).

0-7803-7846-6/03/$17.00 ©2003 IEEE

# Wide Band Nulling with a Single-Tap Beamformer

G. R. Harp*, SETI Institute, S. W. Ellingson, The Ohio State University

We investigate the capabilities of the proposed Allen Telescope Array (ATA) for flexible beamforming with a focus on wide-bandwidth pattern nulls co-existent with high point source sensitivity. The ATA is a new radio interferometer dedicated to SETI and radio astronomical observations under construction in Hat Creek, California. As designed, ATA comprises N = 350 6-meter dishes operating over a frequency range of 0.5-11 GHz. The large N of this array offers unique opportunities for beamforming in radio astronomical applications, some of which are explored here.

Because of ATA's large analyzed bandwidth (100 MHz), the beamformers are constrained to a simple design. Each signal entering the beamformer is delayed to form a simple beam at the point of observation. Additionally, each signal may be multiplied by a complex coefficient before summation, corresponding to a single-tap FIR filter. Despite the fact that each signal is manipulated with only a single coefficient, we show that pattern nulls can be created with surprisingly large bandwidth (e.g. > 100 MHz).

For the purposes of this demonstration we introduce a new iterative approach for the calculation of beamformer coefficients consistent with the given constraints. The main appeal of this approach is heuristic; it is easy to see how narrow-band pattern nulls are generalized to the wide-band case. The main exposition of this work uses the iterative technique, but the same concepts are also demonstrated using conventional linearly-constrained methods.

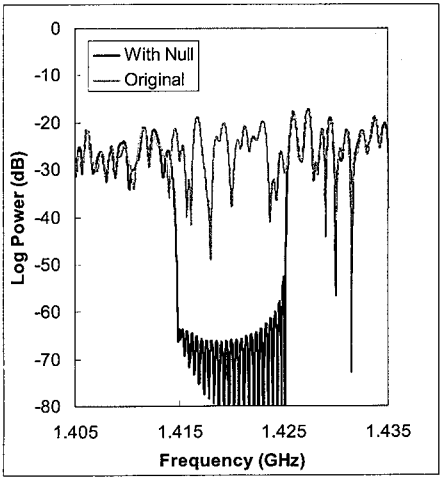


A 10 MHz null is formed in a region far from the beam pattern maximum. The figure compares the frequency dependence of the pattern gain as a function of frequency.

Focusing on the design of a "complete" ATA (scheduled 2005) we study the point source signal to noise ratio (SNR) as it varies with null bandwidth. For a single point null the SNR varies linearly with bandwidth, dropping to zero for BW ~ 250 MHz. We also explore narrow band, large solid angle nulls and similarly find a uniform decrease in SNR with increasing solid angle (SNR approaches zero for solid angles ~ 300 square arc min.). For nulls with both finite solid angle and finite bandwidth, we introduce a single parameter which can be used to predict SNR for the general case.

0-7803-7846-6/03/$17.00 ©2003 IEEE

# ATTENUATION OF RFI BY INTERFEROMETRIC IMAGING ARRAYS

**Richard A. Perley**

*National Radio Astronomy Observatory,*
*1003 Lopezville Road, Socorro, NM 87801 USA.*
*e-mail: rperley@nrao.edu*

## ABSTRACT

Attenuation and/or removal of extraneous signals is critical in radio astronomy, where the spectral ¤ux density of extraterrestrial radiation is many orders of magnitude less than that of nearby, man-made emissions. With the increased demand for wide bandwidths – in part due to tuning requirements, and in part due to the need for increased sensitivity – and at the same time with the increased commercial use of radio frequencies, current and future radio astronomical telescopes must pay special attention to mitigation of unwanted emissions.

It has long been known that imaging interferometers have an advantage over total-power ('single-dish') telescopes, due to their use of the phase of the correlated signals. As the interfering signal originates from a different location than the desired signal, the phase properties of the correlated signal are distinctively different than that of the desired astronomical signal. Averaged over time, a signi£cant attenuation of the unwanted signals will occur, relative to desired signals.

The amount of attenuation is a complicated function of many variables – frequency, baseline length, sky location, and the durations of the interference and/or observation. Past work on the response of an interferometer to RFI have given functional forms permitting calculation of the expected attenuation, these are not explicitly cast in a useful form allowing easy estimation of the attenuation.

The current work derives the attenuation of unwanted signals by a phase-tracking imaging interferometer from the point of view of astronomical imaging. So far as the correlator and imaging processes are concerned, a local source of unwanted emission is no different from the emission from a strong astronomical source located in a far sidelobe. A practical expression allowing calculation of interferometric attenuation as a function of source location, baseline length, frequency, and duration is derived, and its predictions compared to detailed simulations.

Ongoing work on the practicality of accurate interfering signal subtraction from post-correlation data, using methods well known to radio astronomers who remove interfering background sources, will also be described.

0-7803-7846-6/03/$17.00 ©2003 IEEE

# How to Keep Computer and Digital Signals out of your Radio Telescope: Interference Suppression Begins at Home

T.L. Landecker[1], R.V. Casorso[1]

[1]Dominion Radio Astrophysical Observatory, Herzberg Institute of Astrophysics, National Research Council, Penticton, B.C., Canada, V2A 6K3

The high sensitivity of modern radio telescopes derives from low-noise receivers supplemented by clever signal processing algorithms, inevitably carried out with computers and digital-signal processing equipment. The march of technology brings these influences into conflict. As digital signal processing proliferates and operates at higher speeds it generates ever more spurious signals which are picked up by increasingly sensitive front ends.

This talk describes techniques and policies developed at the Dominion Radio Astrophysical Observatory for suppressing interference from digital equipment. Every device that enters the Observatory buildings is tested. The test equipment consists of a broadband antenna with pre-amplifier, feeding onto a spectrum analyzer. One antenna/amplifier pair covers 50 to 1000 MHz and another covers 1000 to 2000 MHz. Amplifier gains and spectrum analyzer setting are standardized. Testing is on a go/no-go basis. If emissions exceed the level in the middle of the screen, the device must be shielded. If emissions are below this level, the device can be used without shielding. The pass/fail level has been calculated by estimating (and measuring) the tolerable level of an interfering signal continuously present, given the particular telescopes in use at the Observatory.

Modern personal computers fail the test, almost without exception, and must be shielded. We have developed a standard enclosure based on a box fabricated from sheet aluminum. All peripheral interconnection lines and power lines are filtered. A similar enclosure is used for laser printers. This computer enclosure costs about Can$1000. It is much cheaper than the additional cost of a Tempest specified computer because we do not attempt to shield frequencies below 100 MHz. At frequencies up to 3 GHz the enclosure delivers a shielding effectiveness of about 50 dB. We have been forced to modify the design as computer clocks have climbed past 400 MHz.

There are some costs, other than the purely financial. It is generally advisable to build the computer enclosure considerably larger than the computer to avoid overheating. This uses office space, and we may be shortening the life of the computer slightly by raising its operating temperature. Some computer enclosures need extra fans, which make noise. It is generally not necessary to shield computer monitors. Digital LED displays cannot be shielded and are not permitted.

To shield large digital systems, it is worth buying commercial enclosures, either shielded individual racks or shielded rooms. There is no cost advantage in attempting to build such devices on your own.

0-7803-7846-6/03/$17.00 ©2003 IEEE

# RFI TIGHT MODULES AND ENCLOSURES FOR THE EVLA PROJECT

Steven Durand*, Jim Jackson, and Robert Ridgeway
National Radio Astronomy Observatory
Socorro, NM 87801

The EVLA Project expands the operating range of the present VLA receivers to cover frequencies from 1 to 50 GHz. This enhancement increases the antenna's susceptibility to internal and external Radio Frequency Interference (RFI). Also, the baseline plan moves the samplers, the digital transmission system, and the monitor and control ethernet switches into the vertex room of each antenna. These requirements necessitate the use of RFI-tight enclosures for all analog and digital electronics.

Astronomical data will be sampled using four sets of 4-GHz and 1-GHz digital samplers. These samplers will provide high-speed parallel data to the Digital Transmission System (DTS) operating at 10 Gigabits/second. The digital clock rates and signal levels present a strong interference source. Successful shielding was obtained by building a double wall aluminum enclosure. Each set of samplers and DTS circuit cards are placed in a 10" x 6" x 20" module enclosure. This enclosure has ½-inch thick brass honeycomb air filters on the top and bottom. Four of these module-enclosures are placed in an RFI tight bin. The bin also has multiple 1-inch thick brass honeycomb air filters on the top and bottom. Two-inch thick RFI absorbing foam sheets line the bin, and RFI gaskets are used between the modules and the bin. The resulting enclosure provides over 90dB of shielding from 0.2 GHz to 20 GHz, and provides refrigerated airflow through each module.

The monitor and control enclosure-shielding requirement is less demanding since the selected commercial ethernet switch clock rate is lower. Preliminary test data indicates the switches radiate from 0.5 to 6 GHz. Additionally, fifty fiber pairs are required to interconnect the switches to the antenna modules. Although the optical connectors can be installed and polished in the field, it would be preferable to use pre-manufactured cables. To accommodate the fiber-optic cables, ten ½" diameter by12" long wave-guides were installed in the top of the enclosure. Honeycomb air filters, RFI foam and gaskets are used in this enclosure. This enclosure provides over 90 dB of shielding from 0.1 to 8 Ghz.

Performance details of these enclosures will be presented during the presentation, along with cost information.

0-7803-7846-6/03/$17.00 ©2003 IEEE 

# Spectrum Management: The First Step in Interference Avoidance

**Ken Tapping**

**Herzberg Institute of Astrophysics**
**PO Box 248**
**Penticton, BC, V2A 6J9**
**Canada**
*Ken.Tapping@nrc-cnrc.gc.ca*

The best time and place to avoid interference problems to radio astronomical observations is in Geneva, at meetings of the International Telecommunications Union. Mitigation of interference during the observations or when analyzing the data involves departure from optimal conditions for observing efficiency, with the concomitant restrictions as to observation planning or possibly having to accept some data degradation.

Ideally, interference problems are avoided by not allocating to active radio services (those involving the transmission of signals) frequency bands that have the potential to give rise to interference problems with radio astronomical observations. Unfortunately, what were good allocations in the past are now, thanks to increasing spectrum use, the implementation of space radio services and many other radio services, now very unsatisfactory, but due to massive capital investments by operators of radio services are not easy to change.

This has led to the complicated and difficult situations we are faced with now, with discussions of band sharing, guardbands, collaborative scheduling, and the *equivalent power flux density model* for estimation of potential interference problems. It is more important than ever that radio astronomers participate strongly in the management of the radio spectrum: in special-interest groups such as the IAU, URSI and IUCAF, national discussions and being members of national delegations to the International Telecommunications Union.

In this talk we'll discuss the processes whereby the spectrum is managed, what is going on now, and what we need to do to ensure that there will be the minimum number of interference problems in the future, with as many of those as possible being addressable through other mitigation methods.

URSI Commission J: Special Session on Radio Frequency Interference Mitigation

0-7803-7846-6/03/$17.00 ©2003 IEEE 

# A Spectrum Study of Usage in and Adjacent to Passive Scientific Bands

**Allen Petrin***
Georgia Institute of Technology, 324341 GA Tech Station, Atlanta, GA, USA, 30332-1005, me@allenpetrin.com

**Paul G. Steffes**
Georgia Institute of Technology, School of Electrical and Computer Engineering, 777 Atlantic Dr., Atlanta, GA, USA, 30332-0250, ps11@prism.gatech.edu

1.) Commission & Session: J7 Radio Astronomy Spectrum protection and interference mitigation

2.) New results of spectrum usage from a recently developed advanced broadband spectrum search system.

3.) This provides actual measured data on potential sources of interference presented previously.

**Abstract:**

A Radio Spectrum Evaluation System (RSES) has recently been constructed at the Georgia Institute of Technology. This system provides coverage from 500 MHz to 6 GHz and provides both azimuthally-resolved power flux density (PFD) data, as well as the omnidirectional incident power flux density. This system provided the capability to observe and analyze spectra in multiple dimensions: frequency, location, space, azimuth, polarization and time.

In this presentation measurements and analysis of spectrum usage in the 608 – 614 MHz, 1395 – 1430 MHZ, and 4950 – 5000 MHz bands currently used for radio astronomy and passive sensing will be presented. The measurement of these bands was undertaken in an urban area, saturated with spectrum users, to increase the probability of intercepting spurious emissions. Such emissions are a common source of interference for passive sensing and other sensitive spectrum users. This study will be focus on establishing a baseline for determination of the future interference potential of systems such as WMTS (Wireless Medical Telemetry Service) or fixed and mobile services in shared or adjacent bands.

0-7803-7846-6/03/$17.00 ©2003 IEEE

## Efficient Techniques for Integral Equations

**Organizer(s):** B. Reinisch, University of Massachusetts Lowell
G. James, Canadian Research Council
**Co-Chairs:** R. Mittra
M. Cátedra

1:15 Opening Remarks

150. 1 1:20 Computing the Impedance Matrix Elements Using Line Integrals ....650
*J. S. Asvestas, NAVAIR, H. J. Bilow, NRL, USA*

150. 2 1:40 A New Matrix-free Approach To the Computation of Electromagnetic Fields Generated by a Surface Current Distribution....651
*S. Rosace, A. Monorchio, G. Manara, University of Pisa, Italy, R. Mittra, Penn State University, USA*

150. 3 2:00 Multilevel Non-uniform Grid Algorithm for Fast Iterative Solution of Scattering Problems ....652
*A. Boag, Tel Aviv University, Israel, E. Michielssen, University of Illinois at Urbana-Champaign, USA*

150. 4 2:20 Efficient Analysis of Electromagnetic Problem Involving Large Bodies using Current Modes ....653
*F. Cátedra, C. Delgado, S. Luceri, F. Saez de Adana, Universidad de Alcalá, F. Rivas, EUP Linares, Spain*

150. 5 2:40 Fast Computation of Radar Cross Section for Multiple Incident Angles by using Characteristic Basis....654
*V. V. Surya Prakash, R. Mittra, The Pennsylvania State University, USA*

150. 6 3:00 A Novel Single-Level SVD To Compress RWG EFIE Matrix for Scattering Problems ....655
*S. Seo, J. Lee, The Ohio State University, USA*

150. 7 3:20 An O(N3/2) MoM Computation of Electromagnetic Radiation and Scattering Problems using a Novel Single Level IE-SVD Algorithm ....656
*K. Zhao, J. Lee, The Ohio State University, USA*

# COMPUTING THE IMPEDANCE MATRIX ELEMENTS USING LINE INTEGRALS

John S. Asvestas*
NAVAIR
RF Sensors Division 4.5.5
B2187, S2190 48110 Shaw Rd.
Patuxent River, MD 20670

Henry J. Bilow
Naval Research Laboratory
Code 5314
4555 Overlook Ave. SW
Washington, D.C. 20375

It was shown in a recent article (W. B. Gordon and H. J. Bilow, *IEEE Trans. Antennas Propagat.*, **50**, 308-311, 2002) that, given a planar surface and a vector-valued function tangential to it, then the integral of this vector over the surface can be expressed as a line integral over the boundary of the surface. The vector in the line integral is not the same as in the original integral. What in effect has been done through this transformation is to, in a way, perform one of the integrations in the surface integral and reduce it to a single integral over the boundary of the surface. Where numerical evaluation of integrals is involved, it is usually easier to deal with single (line) integrals than double (surface) integrals.

With this as the motivation, and also in the hope of reducing the computational load for the same level of accuracy, we use the approach of Gordon and Bilow (G&B) to calculate the elements of the impedance matrix for the case when the integration surface is made of triangular facets and the Rao-Wilton-Glisson functions are used as basis and testing functions. For this case, the integral that represents the vector in the line integral can be evaluated analytically. We are especially interested in the case when the observation point is close enough to the integration triangle so as to cause numerical instabilities. In a typical fashion, we extract the static part of the integrand in the surface integral, and evaluate it exactly using the approach of Gordon and Bilow rather than triangle coordinates. We then reduce the remaining integral to a line integral around the triangle's perimeter. For the observation point near the triangle, this integral can be computed using a Gauss-Legendre quadrature (GLQ) over each side of the triangle. We consider a worst-case scenario and compute this integral. We compare the results with those obtained using the traditional approach of a seven-point GLQ for the surface integral over the surface of the triangle. As a reference ("exact") solution we use one where the integral is computed in double precision via a Simpson Rule over a very fine mesh. We compute Gaussian quadrature results in both single and double precision arithmetic to allow separation of the errors due to round-off and cancellation from the errors due to approximating the integral via GLQ.

Commission and Session: Commission B7 (Numerical methods: int. eq. based)
What new knowledge is contributed by this paper? This study is conducted in the interest of increasing the accuracy of the impedance matrix elements and decreasing the computational load.
Relationship to previous work: See reference above.

0-7803-7846-6/03/$17.00 ©2003 IEEE

# A New Matrix-free Approach to the Computation of Electromagnetic Fields Generated by a Surface Current Distribution

*S. Rosace, A. Monorchio, G. Manara*
*Dept. of Information Eng.*
*University of Pisa, Italy*

*R. Mittra*
*EMC Lab*
*Penn State University, USA*

A major step in the numerical solution of electromagnetic scattering problem entails the computation of the electric field generated by a surface current distribution. The scattered electric field, thus computed, is used to derive the total tangential electric field on the surface of the scatterer, upon which the boundary condition is imposed to solve the scattering problem. Typically, the scattered field computations involve a matrix-vector product, with the matrix generated by using the RWG bases and the vector representing the induced current on the surface of the scatterer. This process can be highly CPU-intensive, both in terms of time and memory, especially when the object size is large. Although the Fast Multiple Method (FMM) has been introduced to speed up the required product, the near-field interaction matrices, which must be stored in the CPU, can still burden the memory quite considerably for large problems, and the matrix-vector operation can be costly despite the application of FMM to off-diagonal blocks.

For planar structures, such as thin plates, an FFT approach has been successfully employed to reduce the memory and CPU time considerably. In this approach, the convolution operation between the induced current **J** and the Green's function **G** is transformed in a product in the spectral domain by first sampling the **J** in a uniform Cartesian grid. The electric field is subsequently derived over the entire surface via an inverse transform operation on $(\tilde{J} \cdot \tilde{G})$, again using the FFT. To the best of our knowledge this procedure has not been extended to the case where the surface on which the E-field is desired is not coplanar with that of the current distribution **J** (or parallel to it), except via the use of multiple inverse FFT's of $(\tilde{J} \cdot \tilde{G})$ for different values of z, a procedure that is numerically very inefficient.

In this paper, we show how the desired $\overline{E}$ -field can be computed over the entire surface in one step, rather than one point at a time, in a highly efficient manner by using a spectral domain technique combined with an analytic continuation procedure. The procedure is valid for all distances and angles between the planes and totally bypasses both the matrix generation as well as evaluation of matrix-vector products employed in conventional schemes. The procedure is well suited for use in the Characteristic Basis Function Method (CBFM) for solving EM scattering problems, which has been recently introduced in the literature by a number of workers for efficient solution of the problem of EM scattering from large scatterers. These functions are often analytically transformable, and their use obviates the need to carry out the FFT of the current distribution, a procedure that can suffer from aliasing and discretization problems.

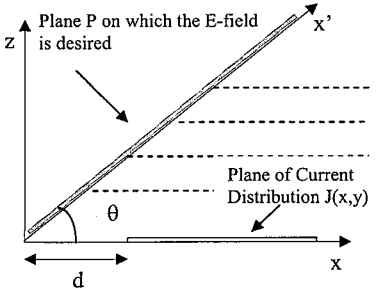


Fig.1. Geometry of System

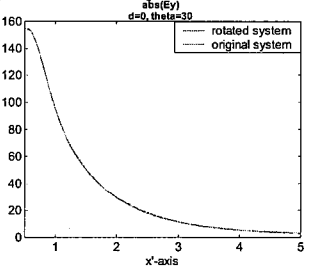


Fig.2. Comparisons of Fields computed by two different methods

0-7803-7846-6/03/$17.00 ©2003 IEEE

# Multilevel Non-uniform Grid Algorithm for Fast Iterative Solution of Scattering Problems

Amir Boag[(1)*] and Eric Michielssen[(2)]

[(1)] Department of Physical Electronics, Tel Aviv University, Tel Aviv 69978, Israel

[(2)] Department of Electrical and Computer Engineering, University of Illinois at Urbana-Champaign, 1406 W. Green Street, Urbana, IL 61801, USA

Rigorous analysis of scattering by arbitrary shaped bodies is often effected via numerical solution of pertinent integral equations. For simplicity, we consider a two-dimensional scattering by an open perfectly conducting surface analyzed via the Electric Field Integral Equation (EFIE). The number of field and current sampling points on the surface is proportional to its electrical dimensions, i.e., of $O(N)$, where $N = kR$, $R$ being the radius of the smallest circle circumscribing the scatterer and $k$ - the wavenumber. Due to $O(N^3)$ computational complexity of conventional direct solvers, iterative approach becomes a necessity for analysis of electrically large problems. Solving EFIE, each iteration requires evaluation of the electric field due to a given surface current. Straightforward evaluation of the field at $O(N)$ points by surface integration involving summation of $O(N)$ terms amounts to $O(N^2)$ operations. This high computational burden underlines the need for using fast field evaluation techniques.

In this paper, we develop a novel non-uniform grid (NG) technique that facilitates the numerically efficient evaluation of the field produced by a given current distribution (A. Boag, et al., *IEEE Antennas Wireless Propagat. Lett.*, vol. 1, no. 7, pp. 142-145, 2002). The algorithm is based on the observation that, locally, the phase compensated field radiated by a finite size source is an essentially bandlimited function of the angular and radial coordinates of the source centered spherical coordinate system. The angular bandwidth is proportional to the linear dimensions of the source, while the local bandwidth with respect to the radial distance decreases rapidly with the distance. Therefore, the radiated field can be sampled on a non-uniform spherical grid with radial density decreasing with the distance from the source. The total number of grid points is proportional to the source region dimensions.

With this in mind, we introduce a multilevel algorithm based upon a hierarchical decomposition of the scatterer surface into subdomains. At each level, the domain decomposition proceeds by subdividing each parent domain into a number of subdomains. At the finest level, for each small subdomain, radiated fields are computed directly at a small number of points of a very coarse non-uniform spherical grid. Next, the fields of each group of adjacent subdomains are aggregated into those of the parent subdomain and defined over a finer non-uniform grid. Transition from coarse to fine grids is effected by interpolation. The phase common to all source points in a given subdomain is removed from the field prior to interpolation, thus rendering the field a slowly varying function of the spatial variables. Following the interpolation step, the phases are restored and partial fields aggregated. At the highest level, the fields are interpolated to the scatterer surface. The proposed multilevel algorithm attains an asymptotic complexity of $O(N \log N)$. A multilevel implementation of the NGTD scheme will be presented along with numerical examples demonstrating its efficacy.

0-7803-7846-6/03/$17.00 ©2003 IEEE

# Efficient analysis of electromagnetic problem involving large bodies using current modes

Felipe Cátedra*, Carlos Delgado*, Stefano Luceri*, Francisco Saez de Adana*, Fernando Rivas**

**Departamento de Electrónica. EUP de Linares. Universidad de Jaén, SPAIN
*Departamento de Teoría de la Señal y Comunicaciones.
Universidad de Alcalá ,28806 Alcalá de Henares (MADRID), SPAIN
Fax: + 34 91 885 66 99, email: felipe.catedra@uah.es

## ABSTRACT

It has been shown that the current in large bodies can be efficiently represented by means of current modes, each one of them defined by means of an exponential function which amplitude and exponent change slowly along the smooth areas of the body (Z. Altman, R. Mittra. *IEEE Transactions on Antennas and Propag.*, pp 744-751, April 1999). Recently it has been shown that the amplitude and phase functions of the modes can be interpolated efficiently from a reduced set of sampling points using splines functions like NURBS (Non-Uniform Rational Bi-splines Surfaces), (O. Gutierrez, F. Saez de Adana, F. Rivas, I. Gonzalez, M.F. Cátedra: "Method to interpolate the induced current with a low amount of sample points by means of Bézier surfaces", *Electronics Letters*, to appear. 2003). In this communication a very efficient way to compute the far or near field due to a current mode is presented. In the computation of the integrals that appear in the field evaluation the integrand function is traditionally sampled at a rate in accordance with the Nyquist criterion, say at least twice the maximum spatial frequency, that represents a minimum of four samples per wavelength, although many times a rate of eight or ten samples per wavelength is used. In the approach that will be presented the phase variation of the mode is extracted, reducing by order of magnitude the sampling rate required to compute the integrals. This means an spectacular reduction in the CPU-time evaluating the field. The approaches described can be combined in an iterative approach to find the induced current solving integral equations because the current is represent efficiently using current modes and the iteration between modes are evaluated considering very small and frequency independent sampling rates.

0-7803-7846-6/03/$17.00 ©2003 IEEE 

# Fast Computation of Radar Cross Section for Multiple Incident Angles by using Characteristic Basis

V.V.S.Prakash and Raj Mittra

121 Electrical Engineering East,
The Pennsylvania State University, University Park, PA 16802-2705
E.mail: vvp2@psu.edu

Conventional approaches to solving scattering problems by using the Method of Moments (MoM) involves the geometry discretization with a size ranging from $\lambda/10$ to $\lambda/20$. Thus, as the object becomes large in terms of the wavelength, the size of the associated MoM matrix grows very rapidly, and this, in turn, places an inordinately heavy burden on the CPU in terms of memory and time. One of the promising techniques that utilizes higher level basis functions to reduce the size of the MoM matrix is the recently introduced Characteristic Basis Function Method (CBFM) [V.V.S.Prakash and R.Mittra, "Characteristic basis Function Method: A new technique for fast solution of integral equations", Microwave Opt. Tech. Lett., Jan. 2003]. The CBFs are specially constructed to fit the object geometry by incorporating the physics of the problem into the basis functions, and the domain spanned by these functions can be many wavelengths. However, these CBF's depend on the excitation vector, and hence, must be regenerated anew for each change of the incident angle. This poses a problem when the response of the structure needs to be computed for a large number of incident angles. The present study is focused to alleviate the aforementioned problem by employing a set of basis functions that are invariant to the angel of incidence, and are derivable from the original CBF's. Also, we present a systematic way of improving the accuracy of the solution by using these new invariant basis.

In order to derive a set of basis that are invariant of the angle of incidence, we first analyze the geometry for a small number of incident angles, say K, for which we construct the CBF's. For a given block 'i', the set of vectors $\{J_j^{(i)}\}_k$ with k = 1,2, .., K define a reduced order subspace $\Xi_i$ of the original Hilbert space. These basis vectors define a subspace $\Xi$ containing the CBF's, but one has to decide how many of them are necessary. In order to define an orthonormal basis of $\Xi_i$, vectors $\{J_j^{(i)}\}_k$ are arranged column wise in a matrix Y, which is subjected to the singular-value decomposition (SVD). Since the singular values typically range over several orders of magnitude, not all of them are needed to achieve a desired accuracy level. Let 'L' be the number of significant singular values that need to be retained. We make use of the L left singular vectors to construct basis for each of the blocks. The original matrix is then reduced to a size of ML x ML. It is possible that the number of significant singular values L be greater than M, in which case the size of the reduced matrix is slightly greater than that obtained with the original CBFM. However, this is offset by the fact that the same set of basis functions can now be used over the entire range of incident angles, and, hence, a numerically efficient solution to the scattering problem can be obtained by using these in place of the conventional CBF's.

The numerical accuracy and the computational advantages of the proposed technique are illustrated by studying the problem of plane wave scattering from PEC objects, while varying the incident angle over a wide range. Our numerical experiments reveal that the results obtained from the proposed approach are even closer to those of the rigorous MoM simulation, than when the original CBFM is used, including the grazing angle cases, which are difficult to simulate accurately.

0-7803-7846-6/03/$17.00 ©2003 IEEE

# A Novel Single-Level SVD to Compress RWG EFIE Matrix for Scattering Problems

Seung-Mo Seo*, Jin-Fa Lee

The ElectroScience Laboratory
The Ohio State University
1320 Kinnear Rd, Columbus, OH 43212
e-mail: sms@esl.eng.ohio-state.edu

An electric field integral equation (EFIE) using RWG basis functions is formulated to solve electromagnetic scattering problems by perfect conducting objects. The solution of large-scale electromagnetic scattering problems using the method of moments (MoM) suffers both the storage and computational complexity of a dense impedance matrix. For a general MoM problems using N basis functions, the computational complexity is $O(N^2)$ for storing and solving the impedance matrix via an iterative algorithm. There have been a number of successful algorithms that reduce the numerical complexity such as the fast multipole method (FMM) (R. Coifman, V. Rokhlin, and S. Wandzura, " The Fast Multipole Method for the Wave Wquation: A Pedestrian Prescription", IEEE AP, pp7-12, 1993) and singular value decomposition (SVD) based algorithms (S. Kapur and D. E. Long, "$IES^3$, IEEE/ACM, 448-455, 1997).

This paper descibes a novel single-level dual rank SVD algorithm to reduce the memory usage and computational complexity for solving PEC scattering problems. The algorithm shows that the memory usage and computational complexity are both $O(N^{3/2})$ with the number of groups chosen to be proportional to $N^{1/2}$ where N is the number of unknowns. The system matrix are divided into two categories: self and coupling matrix blocks. The group self matrix blocks is assembled as a dense matrix. As for the group coupling blocks, the SVD compression scheme is applied except the touching groups which will be assembled as a dense matrix. The SVD algorithm can be divided into four parts: grouping, initialization, construction of Q by dual ranking in an iterative scheme and computation of R by LU decomposition. The unique feature of the proposed approach is that the compression is achieved without assembling the entire matrix. The paper also describes "geo-neighboring" preconditioner. The preconditioner when used in conjunction with GMRES is proven to be both efficient and effective for solving the compressed matrix equations. Details of algorithm and some examples will be presented and discussed at the presentation.

0-7803-7846-6/03/$17.00 ©2003 IEEE

# An $O(N^{3/2})$ MoM Computation of Electromagnetic Radiation and Scattering Problems Using A Novel Single Level IE-SVD Algorithm

Kezhong Zhao* and Jin-Fa Lee
1320 Kinnear Rd., Columbus, Ohio 43212
ElectroScience Lab., Dept. of Electrical Engineering, The Ohio State University
*(Summit to URSI Commission B: B7-Numerical methods: integral-eq. Based)*

Solving large-scale electromagnetic problems by integral equation methods suffers from $O(N^2)$ numerical complexity of memory requirement and CPU time, where $N$ is the number of basis functions. A novel single level dual rank IE-SVD algorithm efficiently compresses the system matrix to reduce the memory requirement and CPU time for both matrix assembly and matrix-vector multiplication to $O(N^{3/2})$. The algorithm forms the $Q-R$ factorization of rank deficient local matrices due to non-self group interactions by ranking the most linearly independent basis functions in the transmitting group and the most significant ones in the receiving group. There have been a number of successful algorithms that reduce the numerical complexity of IE methods such as the fast multipole method (FMM) [1] (R. Coifman, V. Rokhlin, and S. Wandzura, *IEEE AP. Mag*, 7-12, 1993) and the SVD based algorithms presented in [2] (S. Kapur and J. Zhao, *DAC*, 141-146, 1997) and [3] (S. Kapur and D. E. Long, *ICCAD*, 448-455, 1997). The 2-level FMM combined with the iterative techniques has reduced the numerical complexity to $O(N^{3/2})$ to solve dense integral equation matrices that arise from the Helmholtz equation. One major drawback of this approach is its dependence on the integral equation kernel. For complex Green's functions, such as the layered medium Green's function, the application of FMM is much more involved than the surface scattering problems where the free space Green's function can be employed. The SVD algorithm presented in [2] reduces the numerical complexity of the matrix-vector multiplication to $O(N \log N)$, but its matrix assembly stage, which requires the construction of the impedance matrix prior to its factorization, has $O(N^2)$ computational cost. The integral equation solver IES$^3$ given in [3] reduces the numerical complexity of both the matrix assembly and solution to $O(N \log N)$ by using an adaptive grouping of basis functions and an interpolation-based construction of the $Q-R$ matrices in SVD, which assumes that the integral equation kernel is smooth over local regions of space. The key step in [3], the matrix assembly process without the knowledge of the full MoM matrix, is very vague. The method presented in this paper tends to overcome the above drawbacks of the previous algorithms such that: It is independent of the integral equation kernel, or it does not depend on the exact knowledge of the Green's function; It assembles the local Q and R matrices without a priori knowledge of the local matrix itself; It is free of the previous assumptions about the kernel of the integral equation, namely, the smoothness of the kernel to implement reduced sampling procedure in [3].

0-7803-7846-6/03/$17.00 ©2003 IEEE

## Finite Element Methods

**Co-Chairs:** B. Stupfel
R. Gordon

3:20 Opening Remarks

# On the Application of Wavelet-Like Basis Functions in Finite Element Algorithms

W. Elliott Hutchcraft(*), Richard K. Gordon
Department of Electrical Engineering(*)
University of Mississippi
Anderson Hall Box 7
University, MS 38677
Phone: (601) 234-4912
Fax: (601) 232-7231
Email: eeweh@olemiss.edu

Wavelets and wavelet techniques have become important topics in the computational sciences in recent years. Their application in the area of research in computational electromagnetics has only occurred rather recently; however, wavelets have received abundant attention in the scientific literature. Wavelets have been used in many different algorithms. For example, wavelet methods for differential equations have been developed by Jaffard and Laurencot (S. Jaffard and Ph. Laurencot, Wavelets: A Tutorial in Theory and Applications, pp. 543-601, 1992). The use of wavelet-like basis functions in the finite element solution of one-dimensional electrostatics problems in which either Dirichlet or Neumann boundary conditions are enforced at each endpoint of the interval has been discussed by Gordon (R. Gordon, *Proc. of the 11th Annual Review of Progress in Applied Computational Electromagnetics*, pp.559-567, 1995). Although the methods discussed above were using wavelets in frequency domain approaches, they have also been used in time domain techniques. Krumpholz and Katehi have used wavelet expansions in the multiresolution time domain (MRTD) method (M. Krumpholdz and L. P. B. Katehi, *IEEE Trans. on Microwave Theory and Techniques*, vol. 44, no. 4, pp. 555-571, April 1996).

In this presentation, wavelet-like basis functions will be incorporated into several different differential equation based algorithms. A two-dimensional time domain algorithm employing wavelet-like basis functions will be used to solve electromagnetics problems. One difficulty with the traditional FETD method is that it can require the solution of a large matrix equation for each time step; however, in the time domain approach presented here, the solution of a matrix equation for each time step is not required. In this sense, it is more like the traditional FDTD technique originally developed by Yee (Yee, *IEEE Trans. Antennas Prop.*, vol. AP-14, pp. 302-207, 1966). To generate the wavelet-like functions, a variation of the technique presented by Jaffard will be used. Following Jaffard, Hutchcraft, Harrison, and Gordon have previously generated two-dimensional wavelet-like basis functions by beginning with the traditional tetrahedral basis functions. But in this presentation, instead of pursuing this more time consuming approach, a combination of one-dimensional wavelet-like basis functions will be used to generate the two-dimensional basis. First, Neumann and Dirichlet basis functions will be developed for both the x and y directions. For each field component, the two-dimensional basis functions will be derived from combinations of two sets of the one-dimensional basis functions. Finally, these new basis functions are employed in an FETD algorithm. This method will be used for the solution of several problems; comparisons with analytical and FDTD results will be presented. Also, two-dimensional electrostatics problems will be solved using the same technique described above to derive the two-dimensional basis set. Comparisons of the number of steps required for convergence will be made between the traditional finite element algorithm, the previous method for developing wavelet-like basis functions, and the new method for generating two-dimensional wavelet-like basis functions. Finally, higher order wavelet-like basis functions will be discussed. These basis functions are generated from the higher order finite element basis functions. Comparisons between first order and higher order traditional and wavelet-like basis functions will be presented.

0-7803-7846-6/03/$17.00 ©2003 IEEE

# On Improving the Efficiency of the Use of Wavelet-Like Basis Functions in Finite Element Algorithms

Suppakiat Tuksinvarajan, W. Elliott Hutchcraft, Richard K. Gordon(*)
Department of Electrical Engineering(*)
University of Mississippi
Anderson Hall Box 41
University, MS 38677
Phone: (601) 234-5388
Fax: (601) 232-7231
Email: eegordon@olemiss.edu

Wavelet analysis has recently begun to attract widespread interest in the computational sciences. In computational electromagnetics, wavelet bases have been used in both partial differential equation approaches and integral equation techniques.

In this presentation, techniques for improving the efficiency of the use of wavelet-like basis functions in the finite element method will be discussed. Although the use of wavelet-like functions has advantages such as the lowering of the condition number of the system matrix, there are also some drawbacks related to their use. One of the main disadvantages involves the time required to generate the wavelet-like basis. When wavelet-like basis functions are used, time must first be spent in generating these functions. Orthogonalization is required during the generation of the basis, and the orthogonalization process requires the calculation of the square root of a large matrix. Previously, this has been done using a procedure that requires the determination of the eigenvalues and eigenvectors of the large matrix. However, the square root of this matrix can also be found using an iterative technique. A discussion of the advantages and disadvantages of the utilization of this iterative procedure will be presented.

Another disadvantage of the use of wavelet-like basis functions is that it yields a fully populated system matrix rather than the sparse system matrix that is obtained when traditional finite element basis functions are used. This can lead to an increase in the memory and computational requirements of the solution procedure. An investigation of the deletion of insignificant elements from the system matrix will be presented.

When a convergence study is conducted using wavelet-like basis functions, it is easy to use solutions obtained at earlier steps of the study as starting points for solutions at later steps. This can result in a significant reduction in the amount of time required to conduct the convergence study. This technique will also be discussed in detail.

0-7803-7846-6/03/$17.00 ©2003 IEEE

# Solution of Electromagnetic Boundary Value Problems by the Plane Wave Enriched Finite Element Approach

*Mustafa Kuzuoglu (*)*
*Department of Electrical Engineering*
*Middle East Technical University*
*06531, Ankara TURKEY*

*Raj Mittra*
*EM Communication Laboratory*
*319 EE East, Pennsylvania State University*
*University Park, PA 16802 USA*

The numerical solution of electromagnetic boundary value problems by the Finite Element Method (FEM) yields reliable results with a moderate number of degrees of freedom for low and medium frequencies when the well-known 'resolution rule' is satisfied. According to this rule, for an accuracy of 1 %, around 10 nodes per wavelength are required. Therefore, if the wavelength is small with respect to the physical dimensions of the computational domain, the matrix resulting from the FEM discretization becomes huge especially for 3D problems. In this case, the problem becomes unmanageable even with very powerful computers.

In this paper, we present a new approach for the FEM solution of high frequency problems by defining new basis functions for the representation of field quantities. The basic idea is to incorporate the known behavior of the solution in a rational way to improve the performance of standard FEM models. To this end, the finite element space is constructed by multiplying the standard shape functions with a space of functions having good local approximation property. This seems to be a natural way to include 'a priori' information about the local behavior of the solution.

In 2D applications, the finite element basis functions are obtained by multiplying the standard finite element shape functions $N_i$ by a set of functions $p_m(\vec{r}) = \exp(-jk\hat{u}_m \cdot \vec{r})$, which represent plane waves propagating in the direction of the unit vector $\hat{u}_m$. The standard basis functions are 'enriched' by the plane wave solutions. It should also be mentioned that each $N_i$, having a compact support, acts as the 'windowing function' of the plane wave solutions. In this way the conformity of the FEM formulation is preserved. In 2D, we seek a solution to the Helmholtz equation of the form

$$\varphi(\vec{r}) = \sum_{i=1}^{N} \sum_{m=1}^{M} \varphi_{im} N_i(\vec{r}) \exp(-jk\hat{u}_m \cdot \vec{r})$$

This expression is substituted in the weak variational formulation to yield the FEM matrix equation. The elements are no longer subject to the 'resolution rule', and it is possible to handle high frequency problems by a relatively reduced number of unknowns. A higher order Gaussian quadrature is used to evaluate the oscillatory integrals appearing in the calculation of the FEM matrix entries. In addition, owing to the special form of the FEM representation, PML mesh truncation is successfully applied in the plane wave enriched FEM formulation for the truncation of the unbounded computational domain.

In spite of the increased number of degrees of freedom per node, this approach results in a considerable decrease in the computational burden, realized by representing the fields in the domain by a reduced number of 'electrically large' elements.

0-7803-7846-6/03/$17.00 ©2003 IEEE

# Frequency-domain Concurrent Complementary Operators Method (C-COM) for Finite Element Simulations

Xin Wu[1, 3] and Omar M. Ramahi[1, 2, 3]
[1]Mechanical Engineering Department, [2]Electrical and Computer Engineering Department, and [3]CALCE Electronic Products and Systems Center
2181 Glenn L. Martin Hall, James Clark School of Engineering,
University of Maryland, College Park, MD, USA
e-mail: xwu@glue.umd.edu

The Complementary Operators Method (COM) and its concurrent version, the Concurrent Complementary Operators Method (C-COM) have been shown to provide very high degree of absorption even for angles incident on the computational boundary at near grazing incidence. In previous works, the C-COM was applied to the finite-difference time-domain (FDTD) method and to the finite-difference frequency-domain (FDFD) method. The strength of the COM and C-COM is that they can fully cancel the first-order reflections that arise when the computational domain is terminated with an absorbing boundary condition (ABC). The cancellation results from the averaging of the two solutions arising from the two independent but complementary operations. The C-COM is more effective because the averaging can be done concurrently. Because of their high accuracy and implementation simplicity, the COM and C-COM operators have been successfully applied to open-region electromagnetic scattering problems, radiation problems and optical beam propagation problems. In this work, we extend the theory of the C-COM to two-dimensional finite element algorithms. We present the formulation of the complementary operators in a finite element paradigm and discuss mesh shape constraints that are relevant to the application of the averaging perimeter. We present numerical results and comparison with other boundary conditions including the perfectly matched layer (PML). Finally, we discuss computational burdens associated with the implementation.

0-7803-7846-6/03/$17.00 ©2003 IEEE 

# ON THE CONDITION NUMBER OF VARIOUS FINITE ELEMENT MATRICES INVOLVED IN THE NUMERICAL SOLUTION OF ELECTROMAGNETIC RADIATION OR SCATTERING PROBLEMS

Bruno Stupfel
CEA/CESTA, Commissariat à l'Énergie Atomique, B.P. 2, 33114 Le Barp, France

The finite element method (FEM) is a powerful numerical technique for solving scattering problems involving inhomogeneous penetrable 3D objects. For open region problems, the radiation condition may be rigorously taken into account by prescribing either an exact radiation condition (e.g., an integral equation) on the outer surface of the object, or approximately by implementing an absorbing boundary condition (ABC) or a perfectly matched layer (PML) on the outer boundary terminating the FE mesh. The whole set of equations may be solved either directly, or iteratively by using, e.g., a domain decomposition method that reduces the memory storage requirements.

All of these techniques imply the solution of one or several linear systems that result from the FE discretization of Maxwell's equations inside a given (here simply connex) computational domain, on the boundary of which various boundary conditions (BC's) are prescribed. If the electrical size of this domain is large, then the number of unknowns may be such that iterative solvers are needed to reduce the computing time and memory storage. In this case, the number of iterations and, hence, the computational time required to achieve a given numerical accuracy are known to increase with the condition number $\kappa$ of the FE matrix.

In this paper, we attempt to draw the rules that govern the behaviour of $\kappa$. To this effect, an eigenmode technique is proposed that allows us to dissociate the influence of the FE mesh and FE bases fuctions from the one of the actual physical cavity, i.e., the computational domain with its constitutive materials and BC's. We introduce the eigenmodes associated with this cavity, and establish the relationship between the eigenvalues of the FE matrix and those of the matrix of the same FE variational formulation written in the basis of these eigenmodes. Numerical examples are provided for 1D and 3D problems that illustrate the results so obtained. For example, $\kappa$ increases with the number of unknowns $N$; for fixed $N$, it increases when the order of the FE bases functions increases, or when the frequency decreases. Also, regarding the PML, we have come to the conclusion that the ill-conditioning of the FE matrices reported in the literature does not stem from the characteristics of the physical cavity, but from the FE mesh indeed.

0-7803-7846-6/03/$17.00 ©2003 IEEE 

*Special Session*

## Forward and Inverse Algorithms for Subsurfaces

**Organizer(s):** 'F. Teixeira, ESL OSU
L. San Martin

**Co-Chairs:** F. Teixeira
L. San Martin

1:15 Opening Remarks

152. 1 1:20 Numerical Evaluation of the Drill Collar, Borehole, and Invasion Effects on Tools for Oil and Gas Exploration ..... 664
*Y.-K. Hue, B. Donderici, F. L. Teixeira, Ohio State University, L. San Martin, M. Bittar, Halliburton Energy Services, USA*

152. 2 1:40 Full 3D Modeling of LWD Resistivity Tools ..... 665
*D. Omeragic, Schlumberger Oilfield Services, USA, J. Schöberl, University of Linz, Austria, G. N. Minerbo, S. Davydycheva, Schlumberger Oilfield Services,*

152. 3 2:00 FDTD Simulations of Multiple GPR Systems ..... APS
*U. Oguz, L. Gurel, Bilkent University, Turkey*

152. 4 2:20 The BCGS-FFT Method for 3-D Objects in Subsurface Layered Media ..... 666
*X. Millard, Q. H. Liu, Duke University, USA*

152. 5 2:40 Precorrected-FFT Solution of the Volume Integral Equations for Inhomogeneous Dielectric Bodies ..... APS
*X. Nie, L. Li, N. Yuan, T. Yeo, Y. Gan, National University of Singapore,*

152. 6 3:00 Breaking the Diffraction Limit in Wave Physics ..... 667
*F. Chen, Kyocera Wireless Corp., A. A. Aydiner, W. Chew, University of Illinois, USA*

152. 7 3:20 Adaptive B-Spline Approach for Inverse Scattering Problems ..... APS
*A. Baussard, SATIE, France, E. Miller, X. Li, CenSSIS, USA, D. Premel, SATIE, France*

152. 8 3:40 Super Resolution Phenomenon in the Detection of Buried Objects ..... APS
*T. Cui, Southeast University, China, W. Chew, University of Illinois at Urbana-Champaign, USA, X. Yin, Q. Jiang, W. Hong, Southeast University, China*

152. 9 4:00 EV6: Experimental Validation of Sensor Interaction Compensation Scheme for Microwave Imaging ..... APS
*O. Franza, Intel Corporation, USA, N. Joachimowicz, J. Ch. Bolomey, Supelec-CNRS, France*

152. 10 4:20 Synthetic Aperture Imaging Through a Dispersive Dielectric Layer ..... 668
*M. Cheney, Rensselaer Polytechnic Institute, USA, C. J. Nolan, University of Limerick, Ireland*

152. 11 4:40 3D Modeling of Geoelectromagnetic Fields using a Fast Integral Equation Approach ..... APS
*D. Avdeev, A. Kuvshinov, O. Pankratov, Russian Academy of Sciences, Russia*

# Numerical Evaluation of the Drill Collar, Borehole, and Invasion Effects on MWD Tools for Oil and Gas Exploration

Y.-K. Hue[1*], B. Donderici[1], F. L. Teixeira[1], L. San Martin[2], and M. Bittar[2]

[1]ElectroScience Laboratory and Department of Electrical Engineering,
The Ohio State University, Columbus OH 43212

[2]Halliburton Energy Services, Houston TX 77032

The neglect of the effect of the drill collar, antenna geometry, borehole and invasion in the modeling of wave propagation measurement-while-drilling (MWD) tools for oil and gas exploration in dipping and horizontal wells has been motivated, in addition to the inherent technical difficulty, by the realization that in oil-based mud these effects are known to be very small. However in conductive mud, the combined effect of the metal collar, antenna geometry, the borehole fluid and invasion on the measurement can become significant. The 1-D approximation is no longer acceptable in this situation.

A systematic study in horizontal wells of these effects is presented. This study is carried out with a 3-D PDE-based code in cylindrical coordinates that is tested by comparison with analytic and semi-analytic solvers. This 3-D EM solver is matrix-free and has a low, $O(N)$ computational complexity (where $N$ is the number of unknowns) both in terms of CPU time and memory requirements. The 3-D cylindrical grid is made quite compact around the tool by implementing a PML absorbing boundary condition directly in cylindrical coordinates. The new 3-D code incorporates the effect of the metal collar and the exact antenna geometry. This code has enabled us, for the first time, to evaluate systematically the combined effect of the drill collar, antenna geometry, borehole conductivity and invasion on the measurement in horizontal well environments.

We first evaluate the results in oil-based mud and compared the results against 1-D code results. Next, we evaluate a vertical well case and compared the results with a 2-D semi-analytic code. These two cases serve to establish the accuracy of the new approach. We then study the effect of mud conductivity and tool standoff on the MWD measurements in a horizontal well. After that, the effect of invasion is included. Symmetrical and non-symmetrical circular and elliptic invasion, in horizontal wells, are evaluated.

0-7803-7846-6/03/$17.00 ©2003 IEEE 

# Full 3D Modeling of LWD Resistivity Tools

Dzevat Omeragic[1]*, Joachim Schöberl[2], Gerald N. Minerbo[1] and Sofia Davydycheva[1]
[1] Schlumberger Oilfield Services, Sugar Land Technology Center
110 Schlumberger Dr., Sugar Land, TX 77478
[2] University of Linz, Spezialforschungsbereich SFB F013
Freistädter Strasse 313, 4040 Linz, Austria
Phone: (281) 285 8150 Fax: (281) 285 4321 Email: omeragic@slb.com

Accurate EM modeling of Logging-while-drilling (LWD) resistivity tool responses is key in the interpretation process. Existing modeling codes typically use point magnetic dipole approximation. However, if the inhomogeneities are close to the tool and comparable to the tool size it may be necessary to include the tool details in the model.

In the past decade significant progress has been made in solving tool responses in complex 3D environment using the point dipole model approximation. Most commonly used software is based on finite-difference approximation, optimal gridding and efficient material averaging schemes. Although there is a need for more efficient modeling at propagation tool frequencies (400 kHz and 2 MHz), that is considered to be mature technology, and such codes are highly efficient and often are even run in the inversion loop.

For proper characterization of "near effects" such as borehole effect it is necessary to include the tool details in the model. Very often that becomes a challenging modeling problem, primarily because of the problem scales, conductivity contrast up to $10^5$ and necessity to handle tool details of order of mm, as well as formation features. The goal is to compute induced voltages at receivers accurate within a fraction of a percent. The difficulties are following: (1) generating and discretizing the 3D tool/formation model, (2) solving the resulting, usually ill-posed, system of equations, which typically has millions of unknowns, (3) evaluating the accuracy of results, and (4) refining the problem if necessary in order to get the required accuracy.

Two approaches for efficiently solving 3D LWD tool responses are presented. Finite-difference technique is developed in cylindrical coordinate system, using Spectral Lancosz Decomposition method (SLDM) and material averaging scheme. The program allows computation of multiple frequency responses in one step. Material averaging is an effective way of reducing the size of the problem and it may be used in non-metallic domain.

The second approach is based on finite element method (FEM). The program uses multi-grid preconditioning and algebraic multigrid (AMG) solver, combines prismatic and tetrahedral elements, taking special care of anisotropic meshes. The unique feature of the program is dual (goal-driven) adaptive technique, where mesh adaption process is guided in order to get the most accurate solution in the most important part of the domain.

Modeling results are presented for three cases: (1) borehole eccentering responses; (2) responses of the tool to the boundary with the presence of the borehole, and (3) how the presence of nearby metallic objects affect the air-cal. All responses are computed for an array resistivity tool operating at 2 MHz, having transmitter-receiver spacing up to 43".

0-7803-7846-6/03/$17.00 ©2003 IEEE 

# The BCGS-FFT Method for 3-D Objects in Subsurface Layered Media

Xuemin Millard and Qing Huo Liu
Department of Electrical and Computer Engineering
Duke University
Box 90291
Durham, North Carolina 27708

Scattering of electromagnetic waves by penetrable, inhomogeneous objects of arbitrary shape embedded in a planarly layered background is an important research area in subsurface sensing. In particular, such near-surface applications are common to geophysical exploration, environmental characterization, and detection and identification of landmines, unexploded ordnance and underground structures. Simulation of an arbitrary object in such a layered medium is a challenging task because of the complex background and the large number of unknowns associated with realistic targets.

In this work we focus on subsurface sensing of inhomogeneous objects buried in a layered medium. Since the scattering object has an arbitrary inhomogeneity, volume integral equation methods are more suitable (the surface integral equation methods which are amenable to the fast multipole acceleration are in general more appropriate for homogeneous or perfectly conducting objects). Unfortunately, until very recently there has been little progress in the development of fast algorithms for such complicated environment. Most previous efforts have focused on the method of moment (MoM), which requires $O(N^2)$ computer memory, and $O(N^3)$ (direct inversion) or $O(N^2)$ (iterative inversion) CPU time, where $N$ is the number of unknowns.

To solve the volume electric field integral equation for electromagnetic scattering from inhomogeneous objects in a layered medium, we have recently developed the stabilized biconjugate-gradient (Bi-CGSTAB) iterative solver combined with the fast Fourier transform (FFT) (Xu and Liu, *IEEE Antennas Wireless Propagat. Lett.*, vol. 1, pp. 77–80, 2002). This technique is thus called the BCGS-FFT method; it can solve the volume integral equation in the layered medium with $O(N \log N)$ CPU time and $O(N)$ computer memory. We have demonstrated that the BCGS-FFT method is much more efficiently than the CG- and BCG-FFT methods in a homogeneous background. In this presentation, the main theory of the BCGS-FFT method will be summarized and its applications in subsurface measurements of electromagnetic scattering from inhomogeneous objects in planarly layered media will be illustrated.

0-7803-7846-6/03/$17.00 ©2003 IEEE

# Breaking the Diffraction Limit in Wave Physics

Fu-Chiarng Chen*, Allaeddin A. Aydiner, and Weng Cho Chew
*Kyocera Wireless Corp., 10300 Campus Point Drive, San Diego, CA 92121
Center for Computational Electromagnetics and Electromagnetics Laboratory
Dept. of ECE, University of Illinois at Urbana-Champaign, Urbana IL 61801
(fchen@ieee.org*, aydiner@uiuc.edu, w-chew@uiuc.edu)

Recently, there has been a renewed research interest on breaking the diffraction limit in wave physics. The diffraction limit (or Rayleigh criterion) describes that we cannot inscribe a feature or see a feature smaller than half-wavelength of the exposing wave. In this talk, we will review and discuss two different experimental verifications to overcome the diffraction limit reported previously in two different regimes. In the acoustics regime, sub-wavelength focusing has been achieved using a time-reversal mirror and an acoustics sink (J. de Rosny and M. Fink, Physcial Review Letters, vol. 89, no. 12, pp. 124301-1 – 124301-4, 2002). In the above paper, the investigators presented an experiment where an ultrasonic source is time reversed and a focal spot size is achieved much less than the diffraction limit. The investigators brought up the possibility of focusing towards a sub-wavelength spot underlines the issue of the time reversal of a field containing evanescent waves. In the electromagnetics regime, we have experimentally demonstrated super-resolution imaging in nonlinear inverse scattering (F.-C. Chen and W. C. Chew, Applied Physics Letters, vol. 72, no. 23, pp. 1284-1287, 1998). The inverse scattering imaging experimental setup was based on a time-domain ultra-wideband microwave imaging radar system. The experimental data were processed with the distorted Born iterative method (DBIM), and showed that it could resolve features smaller than the half-wavelength dictated by the Rayleigh criterion for limited angle tomography. We have attributed the phenomenon to the multiple scattering effect within an inhomogeneous body. The high spatial frequency (high resolution) information of the object is usually contained in the evanescent waves when only single-scattering physics is considered. Multiple scattering converts evanescent waves into propagating waves and vice versa. Hence, in an inverse scattering experiment, even though an object has to be interrogated with a propagating wave, and that only scattered waves corresponding to propagating waves can be measured, the scattered waves contains high resolution information about the scatterer because of the evanescent-propagating waves conversion. Therefore, an inverse scattering method that can unravel the multiple scattering information can extract the high-resolution information on a scatterer. Note that DBIM can be regarded as an extended form of a time-reversal mirror. In this talk, we will re-examine the physics behind the nonlinear inverse scattering approach to achieve the super-resolution imaging.

0-7803-7846-6/03/$17.00 ©2003 IEEE

# Synthetic Aperture Imaging through a Dispersive Dielectric Layer

*Margaret Cheney[1] and Clifford J. Nolan[2]

[1]Rensselaer Polytechnic Institute, Department of Mathematical Sciences, Troy, New York 12180, USA, cheney@rpi.edu
[2]University of Limerick, Department of Mathematics and Statistics, Ireland, clifford.nolan@ul.ie

We consider the problem of synthetic aperture imaging through a known homogeneous layer of (temporally) dispersive material. We seek to make an image of a ¤at earth under the layer from backscattered waves emitted from an antenna following an arbitrary ¤ight path.

We use a linearized scalar model for the wave propagation, namely

$$\nabla^2 E^{sc} - \partial_{tt}(c_0 \varepsilon_r *_t E^{sc}) = -V \partial_{tt} E^{in}, \tag{1}$$

where

$$\varepsilon_r *_t E(t,x) = \int_0^\infty \varepsilon_r(s,x) E(t-s,x) ds, \tag{2}$$

$\epsilon_r(s,x)$ being known and $V(x)$ being unknown. We use any one of a number of formulas for $\varepsilon_r$ that may be appropriate (causal) effective-medium models for vegetation. Much of the analysis could also apply to imaging through soil.

Analysis of the problem requires a number of steps:

1. Use an explicit representation for the half-space Green's function in terms of its Fourier transform in time and in the lateral variables.
2. Use 1) to £nd the £eld $E^{in}$ emanating from the antenna. This involves a rudimentary model for the antenna as well as the signal waveform sent to the antenna.
3. Combine 1) and 2) to obtain a mathematical model for the signal received at the antenna.
4. Estimates on $\varepsilon_r$ show that the expression obtained in 3) is in the form of a Fourier integral operator $F$ applied to the unknown $V$.
5. Apply a £ltered backprojection operator $Q$ to the data to make an image. The form of the £lter is obtained from analysis of the composition $QF$. The theory shows that the resulting image preserves the visible singularities (edges) in the original scene.

0-7803-7846-6/03/$17.00 ©2003 IEEE

## Computational Electromagnetics: Specialized Techniques

**Co-Chairs:** R. Kastner
B. Shanker

1:15 Opening Remarks

154. 1 1:20 An Efficient Approach for the Analysis of Printed Geometries with Multiple Vertical Metallizations and Their Optimization ..... 670
*M. E. Yavuz, I. M. Aksun, Koc University, Turkey, N. Kinayman, M/A-COM, A Tyco Electronics Company, USA*

154. 2 1:40 An Integral Equation Based Algorithm for Analysis of Surface Plasmon Polaritons ..... 671
*C. Trampel, G. Kobidze, B. Shanker, Michigan State University, USA*

154. 3 2:00 A Simple, Nearly Perfectly Matched Layer for General Electromagnetic Media ..... 672
*S. A. Cummer, W. Hu, Duke University, USA*

154. 4 2:20 Parallel Iterative Solution Techniques for Integral Equation Methods ..... 673
*J. D. Kotulski, Sandia National Laboratories, USA*

154. 5 2:40 Fast Global Radiation Boundary Conditions Based on Non-uniform Grid Approach ..... 674
*A. Boag, U. Shemer, R. Kastner, Tel Aviv University, Israel*

154. 6 3:00 Numerical Evaluation of the Polarizabilities of Complex Scatterers with High-order Boundary Element Model ..... 675
*S. Jarvenpaa, P. Yla-Oijala, A. Sihvola, Helsinki University of Technology.*

# An Efficient Approach for the Analysis of Printed Geometries with Multiple Vertical Metallization and their Optimization

*M. Emre Yavuz[1] ,Noyan Kinayman[2] and M. Irsadi Aksun[1]*

*1: Koc University. Dept. of Electrical &Electronics Eng., 34450 Sarıyer İstanbul-Turkey*
*e-mail, memre@ku.edu.tr, iaksun@ku.edu.tr*
*2: M/A-COM, A Tyco Electronics Company,Corporate R&D,1011 Pawtucket Blvd. M/S 261*
*Lowell, MA 01853 e-mail: kinayman@tycoelectronics.com*

Introduction of the closed-form Green's functions into the Method of Moment (MoM) formulation results in a significant improvement in the computational efficiency of the MoM. However, the application of the MoM using the closed-form Green's functions to geometries consisting of vertical metallization is not as straightforward as its applications to geometries consisting only horizontal conductors. It is demonstrated that the computational cost of the approach does not increase with the number of vertical metallization, providing the vertical strips employ the same number of basis functions. This is because the MoM matrix entries corresponding to the basis functions on a vertical strip are obtained as a function of $\rho$ and because the domains of the integrations along the vertical strips are the same. Once the relation between a basis and testing function on a vertical strip is found, the same expression can be used for different values of $\rho$ where the other vertical metallization are located.

Since the closed-from Green's functions are generally obtained at fixed z points, to handle the integrations along the z axis encountered in the inner product terms, the spectral-domain Green's functions and vertical portion of either the testing or basis function or both are integrated along the z-axis analytically, then, the resulting function is approximated using the GPOF method. According to this scheme, the GPOF method is to be used as many times as the combinations of testing and basis functions along the vertical metallization. Therefore, to obtain efficient operation, the vertical strips are required to have the same number of basis functions, allowing less number of calls for the GPOF method. However, for general geometries, it may be difficult to have the same number of basis functions for each vertical strip. To improve its efficiency and eliminate its restriction of using the same number of basis functions, the number of GPOF call must be decreased and the integration along the z-axis should be performed accurately. This goal is achieved by obtaining the closed-form spatial-domain Green's functions at different z values and employing a numerical integration method for the integration along z-axis.

In this work, the operations of both techniques for different geometries involving different number of vertical metallization are studied, and comparative efficiencies are presented. Then, these approaches are combined with an optimization algorithm, Genetic algorithm, to optimize the performance of microwave circuits and antennas.

0-7803-7846-6/03/$17.00 ©2003 IEEE

# An Integral Equation Based Algorithm for Analysis of Surface Plasmon Polaritons

C. Trampel*, G. Kobidze, and B. Shanker

2120 Engineering Building, Dept. ECE, Michigan State University,
East Lansing, MI 48824, USA,{trampelc,kobidze,bshanker}@egr.msu.edu

Surface plasmons are charge density oscillations that occur at metal-dielectric interfaces. The periodic surface charge density creates a quasi-planar two dimensional electromagnetic waves that propagates along the interface, a surface plasmon polariton (SPP). Surface plasmon polaritons that occur at interfaces between two infinite media do not couple to external radiation. Periodicity in the metal layer facilitates coupling to the incident field. Interactions between SPPs and a periodic array of scatterers have been explored analytically (M. Kretschmann and A. A. Maradudin, *Phys. Rev. B*, **66**, 245408(8), 2002). The dispersion relation for SPPs was derived by Kretschmann *et al.* via a homogenous form of the reduced Rayleigh equation. Enhanced transmission properties of surface plasmons have been studied experimentally (H. F. Ghaemi, Tineke Thio, and D. E. Grupp, *Phys. Rev. B*, **58**, 6779-6782, 1998). Peaks in transmission are observed at wavelengths corresponding to surface plasmon polariton modes on both surfaces of a metal film with holes.

In this paper, we propose a frequency domain integral equation (FDIE) based technique for analyzing surface plasmon polaritons supported by a metal film perforated with a array of subwavelength cylindrical holes. The metal film is modelled via the Drude nearly-free-electron form of the dielectric function. The properties of the metal are accounted for explicitly by using the Stratton-Chu equations for the interior domain. The resulting equations are then reduced to a set of matrix equations by representing the equivalent electric and magnetic current in terms of RWG basis functions. Periodic green's functions are used to enable the analysis of infinitely long perforated structures. In the conference, we shall report our findings on (i) different metals and their response; (ii) the effect of period and perturbations to these; (iii) the effect of thickness of the film; and (iv) response as a function of frequency.

0-7803-7846-6/03/$17.00 ©2003 IEEE

## A Simple, Nearly Perfectly Matched Layer for General Electromagnetic Media

Steven A. Cummer*, Wenyi Hu, Electrical and Computer Engineering Department, Duke University, Durham, NC 27708, USA (email: cummer@ee.duke.edu)

A new implementation of the perfectly matched layer (PML) absorbing boundary condition is presented [Cummer, IEEE Microwave and Wireless Components Lett., in press, 2003]. This formulation is designed such that the partial differential equations in the PML are identical to those in the regular medium for any linear electromagnetic material. Only simple first order ordinary differential equations that relate various field components are added to the PML system of equations. This property makes this method particularly simple to implement, especially in complex dispersive and anisotropic materials, because explicit partial difference equations (which can be tedious to derive) do not need to be rederived for the PML.

We call this method the nearly perfectly matched layer (NPML) because it employs variable changes that are not strictly exact when the PML conductivity is spatially varying, as it normally is for maximum absorbing performance. Such inexact coordinate stretching has been used in other apparently effective PML formulations [Tentzeris et al., IEEE Trans. Antennas Propagat., 1999]. Comparisons of the NPML with the convolutional PML [Roden and Gedney, Microwave Opt. Tech. Lett., 2000] in a dispersive dielectric show that the NPML is as effective an absorber as exact PML formulations, and we also demonstrate its performance in truncating a domain containing anisotropic and dispersive magnetized plasma. This indicates that the details of the numerical implementation, rather than the exactness of the analytical formulation, dominate the absorbing performance when the PML layer parameters are nearly optimal. We further analyze the NPML formulation to demonstrate why it performs numerically as well as an exact PML, despite its theoretical inexactness.

0-7803-7846-6/03/$17.00 ©2003 IEEE 

# Parallel Iterative Solution Techniques for Integral Equation Methods

Joseph D. Kotulski
Sandia National Laboratories
P.O. Box 5800
Albuquerque, NM 87185-1152 USA

Integral equation methods together with sub-cell algorithms have been an extremely useful tool in addressing many complicated, realistic problems. The solution process for integral equation methods result in the construction of a linear system of equation cast a matrix equation. The solution of this matrix equation can be done directly via LU decomposition using iterative techniques. When the iterative technique is chosen an appropriate method has to be used as well as a preconditioner. Alternatively, fast methods (such as FMM and AIM) require the use of iterative schemes since the entire matrix is not computed directly.

There is a large repository of parallel iterative solvers that are available but they are normally appropriate for real sparse matrices. By recasting the complex formulation into an equivalent real formulation real-valued parallel solvers can then be applied to the original complex problem. Depending on the equivalent real formulation the spectral properties will vary which will affect convergence. By using appropriate preconditioners this convergence will be accelerated. The solver package that is used is Trilinos, which an object –oriented solver package written in C++.

This presentation will examine preconditioner strategies that will be exercised on a number of different types of problems with different field formulations (EFIE, CFIE). The spectral properties of the matrix will be examined before and after preconditioning. In addition, different Krylov solvers will be used and the results compared to the direct solution method (LU decomposition). The parallel implications and efficiency will also be described and discussed.

Sandia is a multiprogram laboratory operated by Sandia Corporation, a Lockheed Martin Company for the United States Department of Energy under Contract No. DE-AC04-94A185000.

0-7803-7846-6/03/$17.00 ©2003 IEEE 

# Fast Global Radiation Boundary Conditions Based on Non-uniform Grid Approach

Amir Boag, Uri Shemer, and Raphael Kastner
Department of Physical Electronics, Tel Aviv University, Tel Aviv 69978, Israel

Differential equations based techniques, such as finite element and finite difference methods, are often preferred for analyzing electromagnetic problems including inhomogeneous materials. For configurations defined in unbounded domains, these techniques must be augmented by absorbing boundary conditions, which allow for the truncation of the computational domain. Conventional local Absorbing Boundary Conditions (ABCs) including the Perfectly Matched Layer (PML) type absorbers facilitate such mesh truncation as long as the boundary surface is convex. The convexity requirement translates into a significant additional computational cost when treating an essentially concave geometry since a relatively large "white space" must be meshed in order to obtain a convex exterior boundary. Alternatively, boundary integral formulations allow for arbitrary shaped exterior boundaries, however at the cost of making the boundary conditions global. Therefore, in order to be computationally competitive, the boundary integral operators must be evaluated invoking fast algorithms.

In this paper we propose the use of the recently proposed Non-uniform Grid (NG) approach (Boag et al., *IEEE Antennas Wireless Propagat. Lett.*, vol. 1, no. 7, pp. 142-145 2002.) for a fast evaluation of the boundary integrals. As an example we consider a two-dimensional scattering by a thin concave shell forming a large open-ended cavity. In addition, we assume the usage of a generic iterative solver that becomes a necessity for analysis of electrically large problems. With a conventional ABC approach requiring a convex exterior boundary, the entire interior of the cavity is meshed resulting in a number of unknowns proportional to the electrical dimensions of the scatterer squared, i.e., of $O(N^2)$, where $N = kR$, $R$ being the radius of the smallest circle circumscribing the scatterer and $k$ is the wavenumber. A conventional approach would require $O(N^2)$ operations at each iteration step. On the other hand, if the computational domain is confined by a conformal boundary, the number of unknowns and boundary points is proportional to the electrical dimensions of the scatterer, i.e., of $O(N)$. Clearly, direct evaluation of the boundary integral would then require $O(N^2)$ operations, i.e., the same order as the ABC based approach. This high computational burden underlines the need for using fast field evaluation techniques.

We will demonstrate that the usage of the two-level NG algorithm reduces the computational cost of evaluating the boundary integrals (a single iteration) from $O(N^2)$ to $O(N^{3/2})$. The multilevel algorithm attains an asymptotic complexity of $O(N \log N)$.

0-7803-7846-6/03/$17.00 ©2003 IEEE

# Numerical Evaluation of the Polarizabilities of Complex Scatterers with High-order Boundary Element Model

Seppo Järvenpää*, Pasi Ylä-Oijala, Ari Sihvola

Electromagnetics Laboratory, Helsinki University of Technology
P.O. Box 3000, FIN–02015 HUT, Finland

When a dielectric inclusion is put into a homogeneous electric field, it causes a perturbation to the total electric field distribution. The perturbation is concentrated in the neighborhood of the inclusion. The dipole moment induced in such a scatterer can be identified with the source of the dipolar component in the scattered field, and it is proportional to the external electric field. The ratio between these two, the induced dipole moment and the external field is called polarizability of the scatterer and it is an important parameter in electrostatics, quasistatics, and also in electrodynamics and in modelling of materials.

The polarizability can be calculated by solving boundary integral equation

$$\phi_e(\mathbf{r}) = \frac{\tau+1}{2}\phi(\mathbf{r}) + \frac{\tau-1}{4\pi}\int_S \phi(\mathbf{r}')\frac{\partial}{\partial n'}\left(\frac{1}{|\mathbf{r}-\mathbf{r}'|}\right) dS', \quad \mathbf{r} \text{ on } S \qquad (1)$$

for the unknown potential function $\phi$. In this equation, $S$ is the surface of the inclusion, $\phi_e = -E_e z$ is the potential of the incident field, and $\phi$ is the total potential on the surface. The ratio of the permittivities is denoted by $\tau = \epsilon_i/\epsilon_e$, where $\epsilon_i$ is permittivity of the inclusion. The outward normal to the surface is $\mathbf{n}'$ at point $\mathbf{r}'$.

Equation (1) is solved in this work by the Galerkin method. The surface is discretized with planar triangles, and the potential and the test functions are spanned with third order piecewise polynomial basis functions. In order to ensure accuracy of the solution, the inner integrals of those terms where $\mathbf{r}$ and $\mathbf{r}'$ are close to each other are evaluated analytically.

In the talk, results will be shown for the polarizability of dielectric polyhedra (cube, tetrahedron, octahedron, dodecahedron, icosahedron) and also for the response of clusters of two spheres which are used for the dielectric modelling of dry snow.

0-7803-7846-6/03/$17.00 ©2003 IEEE

## Fast Multipole Methods

**Co-Chairs:** W. Chew
K. Sertel

3:20 Opening Remarks

# Fast Multipole Algorithm Frame Analysis

L.J. Jiang*, and W.C. Chew

Center for Computational Electromagnetics and Electromagnetics Laboratory
Department of Electrical and Computer Engineering
University of Illinois at Urbana-Champaign
Urbana, IL 61801-2991

FMA (Fast Multipole Algorithm) is becoming popular with the increasing computer capabilities and complex electromagnetics requirements. Its principles, cost and memory distributions have an important impact on the efficiency of the applications based on it. A careful FMA frame analysis can guide researchers to develop an optimized algorithm. This study is meant to analyze how FMA distributes the computational loads, and find the ways to improve the FMA performance.

The most popular FMAs focus on the static cases and high-frequency dynamic cases. In principle, they are all based on the addition theorem, albeit with different implementations. The far-field interactions are computed through aggregating the outgoing waves, translating the outgoing waves into the incoming waves, and disaggregating the incoming waves. The near-field interactions are evaluated directly. The speedup of FMA over MoM comes from the off-diagonal matrix-vector product approximated by error-controllable factorized far-field interactions. At least one buffer box is necessary to make the error controllable. So there are MoM (near field) and FMA (far field) parts in a complete FMA procedure. The cost balance between them is important and needs to be optimized.

Since the static Laplacian equation is scale invariant, the multipole expansion of the static Green's function can be scaled so that all levels share the same translators. However, these translators are dense matrices. Then most computational time is spent on the outgoing-wave to incoming-wave translation stage. Of all levels, the finest level has the heaviest load. As a result, the total cost of the static FMA is $O(N)$ (where $N$ is the basis function number).

For the dynamic case, the wave equation is scale variant. In contrast, the dynamic translators are diagonal and cannot be shared between levels. Since the radiation and receiving patterns only compose of propagating waves, the dynamic FMA suffers from low-frequency breakdown. Because of the oscillatory field, the radiation patterns of different levels in the dynamic FMA have different bandwidth. So interpolations and anterpolations are needed in the aggregations and disaggregations to reduce the workload. Analysis shows that when the level number is large, the computational cost of aggregation and disaggregation will become very large. The load of every level is of the same order, which means that the FMA frame shifts the cost to different levels to improve the general performance. As a result, the total dynamic cost will be $O(N \log N)$.

Cost estimation equations and simulation data will be presented in the conference to support the above statements derived from the FMA frame analysis. Suggestions on how to improve the efficiency of FMA will be provided.

0-7803-7846-6/03/$17.00 ©2003 IEEE

# Multi-Level Fast Multipole Algorithm for Dielectric Targets in the Presence of a General Layered Background

Wenbin Lin and Lawrence Carin
Department of Electrical and Computer Engineering
Duke University
Box 90291
Durham, NC 27708-0291

There are many radar-sensing applications for which one is interested in electromagnetic scattering from general dielectric targets embedded in a multi-layered medium, including scattering from buried pipes and land mines. Such a analysis may also be applied to analyze scattering from a model tree and general surface and subsurface inhomogeneities (*e.g.* rocks). Despite this wide range of applications, there has been relatively little research published on rigorously analyzing scattering from general dielectric targets embedded in a layered medium, especially for electrically large targets. With regard to an integral-equation analysis, the principal challenge in a surface-integral-equation analysis involves efficient computation of the layered-medium Green's function, this representing a problem of long-term interest. We consider several different techniques for evaluating the layered-medium Green's function for dielectric targets, particularly with regard to their applicability for the multi-level fast multipole algorithm (MLFMA).

In this talk we consider the MLFMA analysis of a general dielectric target situated in an arbitrary layered medium. Several example results are presented, with comparison to reference solutions. Moreover, careful attention is given to the approximations employed when evaluating the layered-medium Green's function. In particular, we carefully consider the importance of the surface-wave poles and their importance as a function of target and layered-medium type.

0-7803-7846-6/03/$17.00 ©2003 IEEE

# Multi-Level Fast-Multipole Analysis of Induction Problems

Xiaolong Dong and Lawrence Carin
Department of Electrical and Computer Engineering
Duke University
Box 90291
Durham, NC 27708-0291

The sensing of buried unexploded ordnance is typically performed with magnetometers and via electromagnetic induction (EMI). Magnetometers are passive, sensing the presence of a subsurface ferrous target by detecting subtle local changes in the earth's magnetic field. EMI represents an active sensor, in which low-frequency fields are emitted and the scattered fields measured. To mitigate losses in the soil, EMI sensors typically operate at kilohertz frequencies. If a buried target is non-ferrous, as are many buried unexploded ordnance, for example, then EMI is required (such targets are invisible to a magnetometer).

It is of significant importance to understand the EMI signature of buried metal targets, since such a signature is ultimately used for inversion (to determine whether the subsurface target is a UXO, or clutter). In this paper we consider the numerical analysis of EMI sensing of general conducting and ferrous targets. A frequency-domain volumetric integral equation formulation is employed. Since EMI frequencies are considered, the target may not be modeled as a perfect electric conductor (e.g. the properties of the metal play an important role in the target's EMI signature).

Although the UXO are typically very small with respect to the EMI wavelength, the numerical analysis is very expensive computationally. In particular the size of the volumetric basis functions must be small relative to a skin depth. Since the skin depth is typically very small relative to the size of the target, the number of unknowns N may become quite large, significantly taxing memory and computational resources. We therefore analyze the volumetric integral equation by an extension of the fast-multipole method to low frequencies.

The numerical formulation is discussed in detail, and the results of the model are compared to measurements.

0-7803-7846-6/03/$17.00 ©2003 IEEE 

# Fast High-Order Solutions for Electromagnetic Scattering from Three-Dimensional Bodies

K. C. Donepudi, X. Wang, W. C. Chew, and J. M. Jin*
Center for Computational Electromagnetics
Department of Electrical and Computer Engineering
University of Illinois
Urbana, Illinois 61801-2991

Recent advances in the development of computational methods have made it feasible to obtain fast and accurate solutions for electromagnetic scattering from composite scatterers. The multilevel fast multipole method (MLFMA) is an $O(N \log N)$ algorithm used for reducing the computational complexity of integral equation-based methods. Using computers commonly available today, this method can be employed to solve large problems in the range of hundreds of thousands of unknowns. The main purpose of this paper is to summarize our research in the developement of fast and accurate scattering solutions for composite scatterers. Towards this purpose, we have developed two sets of higher-order MLFMA solutions. The first set of higher-order solutions are the traditional higher-order solutions employing higher-order forms of Rao-Wilton-Glisson (RWG) basis functions that guarantee the normal continuity of the expanded unknown current density and the Galerkin's method. Consequently, this method can be applied only to well-connected meshes. The second set of solutions are based on a set of novel higher-order basis functions known as the grid-robust basis functions. These basis functions represent the unknown electric current density within each patch using the Lagrange interpolation polynomials. The Lagrange interpolation points are chosen to be the same as the nodes of the higher-order Gaussian quadratures. As a result, the evaluation of the integrals in the method of moments (MoM) is greatly simplified when using point-matching technique. More importantly, these basis functions do not require the side of a triangular patch to be entirely shared by another triangular patch; hence, the resultant MoM is applicable even to defective meshes.

The salient features of the two higher-order, MLFMA solutions can be summarized as following: higher-order basis functions are employed in conjuction with higher-order geometry description, the Poggio-miller-Chang-Harrington-Wu-Tsai (P -MCHW) surface integral formulation is used to handle different dielectric materials, the impedance boundary conditon (IBC) and resisitive sheet condition (RS) are incorporated, the MLFMA solutions are MPI-based implementations and hence capable of working on distributed memory systems, and an highly efficient preconditioner such as an incomplete LU (ILU) preconditoner is interfaced through a standard software package. The higher-order solutions are also applicable to the case when mixed-order basis functions (with low-orders on small patches and high-orders on large patches) are employed.

0-7803-7846-6/03/$17.00 ©2003 IEEE 

# Error Optimization in Fast Multipole Algorithm

**Tetsuya YAMAMOTO*, Shinichiro OHNUKI and Weng Cho CHEW**
*Center for Computational Electromagnetics and Electromagnetics Laboratory,*
*Department of Electrical and Computer Engineering,*
*University of Illinois at Urbana-Champaign*
*1406 West Green Street, MC-702, Urbana, IL 61801-2991, U.S.A.*
*Tel:+1 (217) 333-4207; Fax:+1 (217) 244-7345; E-mail:tyama@uiuc.edu*

**Abstract**

Electromagnetic wave scattering problems involving electrically large complex objects, for example, aircraft, rocket, automobile and spacecraft have been intensively investigated with the advancement of the computer. In order to solve large complex objects using method of moments (MoM), a surface is discretized into finite elements and the integral equations with the unknowns on each finite element are formulated. The resultant matrix equation comprises all interactions between field and source points is often solved by iterative method like the Conjugate Gradient (CG) method-it takes an extremely long time if especially large scattering objects with a large number of unknowns are solved.

The fast multipole algorithm (FMA) and multilevel fast multipole algorithm (MLFMA) are methods to remedy the unprecedented time-consuming calculation by diagonalizing the matrix elements expressed by interactions between the field and the source points with the assistance of the addition theorem in MoM. In this algorithm, the Green's operator is factorized and expressed in more than three steps; aggregation $\beta_{li}$, diagonal translation $\alpha_{l'l}$ and disaggregation $\beta_{jl'}$ processes.

$$H_0^{(1)}(k\rho_{ji}) = \frac{1}{2\pi}\int_0^{2\pi} d\alpha \tilde{\beta}_{jl'}(\alpha)\tilde{\alpha}_{l'l}(\alpha)\tilde{\beta}_{li}(\alpha) \tag{1}$$

where

$$\tilde{\alpha}_{l'l}(\alpha) = \sum_{p=-P}^{P} H_p^{(1)}(k\rho_{l'l}) e^{-ip\left(\phi_{l'l}-\alpha+\frac{\pi}{2}\right)} \tag{2}$$

and

$$\tilde{\beta}_{jl'}(\alpha) = e^{-ik\rho_{jl'}\cos(\alpha-\phi_{jl'})} \qquad \tilde{\beta}_{li}(\alpha) = e^{-ik\rho_{li}\cos(\alpha-\phi_{li})} \tag{3}$$

Since the Hankel functions have the tendency of divergence, the truncation number $P$ of the diagonal translation operator $\alpha_{l'l}$ must be determined carefully in the numerical implementation. In order to calculate faster with high precision, the optimum truncation number $P$ should be determined as small as possible. The truncation number $P$ is conventionally determined by the number of digits of accuracy $d_0$.

Ohnuki and Chew have proposed the novel expression of the number of digits of accuracy that is defined by $d_0$-$d_1$. The $d_0$ part stands for the convergence rate of the Bessel functions in the multipole expansion. Therefore, this value is determined by the element location. For conventional use, the maximum box size equals to the diagonal length of the box is chosen to predict the error bound. On the other hand, the $d_1$ part stands for the divergence rate of the Hankel function of the diagonal translation operator. This is determined by the distance between the two box centers.

This paper clarifies the relation between the various parameters, for instance, truncation number, buffer number, box number, element location, element number. The novel truncation number $P$ is determined as the function of not only the element location but also the buffer number. The novel truncation number defined by the novel rule is smaller than the conventional truncation number. Time reduction by adopting the novel rules together with the excellent calculation precision is expected.

0-7803-7846-6/03/$17.00 ©2003 IEEE 

# Computing the Translation Operator by Sampling the Green Function at Low Frequencies

Liang Xuan* and Robert J. Adams
Electrical & Computer Engineering
University of Kentucky
Lexington, KY 40506-0046
lxuan@uky.edu

Efficient numerical simulation of integral formulations of electromagnetic problems entails the use of a compression algorithm for the underlying Green function. If a simulation domain is subdivided into N elements, a traditional discretization of the integral equation leads to a linear system of the form $Ax = b$ where $A$ contains $O(N^2)$ nonzero elements. Several methods have been developed to reduce this cost scaling to $O(N \log N)$ or less. An important group of these techniques are the Fast Multipole Methods (FMMs). The earliest form of the FMM algorithm (Greengard and Rokhlin, *J. Comp. Phys.*, 1985) is applicable to low-frequency problems. A more recent FMM algorithm, based on a diagonalization of the translation operator, is efficient at higher frequencies (Rokhlin, *J. Comp. Phys.*, 1990).

An important feature of these FMMs is their dependence on a detailed analysis of the underlying Green function. The analysis facilitates the numerical implementation of a compressed representation of the free-space kernel without sampling the underlying, dense operator. Unfortunately, this feature of the FMM also makes it difficult to directly extend the method to Green functions which satisfy more general boundary conditions.

As discussed in separate papers presented at this meeting, a technique has been developed which determines a compressed, plane wave representation of the Green function at high frequencies using only sparse numerical samples of the Green function. In this presentation we will discuss an analogous procedure for compressing the Green function at low frequencies. As in the high-frequency algorithm discussed elsewhere, the low-frequency algorithm discussed here is based on an asymptotic expansion of the Green function. The low frequency translation operator is subsequently determined from sparse numerical samples of the underlying Green function.

Asymptotic matching of the high-frequency and low-frequency expansions will be shown to yield a uniform compression algorithm for the free-space Green function based only on asymptotic representations satisfying the wave equation. The extension of these results to Green functions satisfying more general boundary conditions is discussed in a separate presentation.

0-7803-7846-6/03/$17.00 ©2003 IEEE

## Transient/Frequency Measurements and Processing

**Co-Chairs:** W. Davis
C. Furse

1:15 Opening Remarks

# Non-Destructive Fault Location on Aging Aircraft Wiring Networks Part 1 – Cost-Optimized Solutions

By: You Chung Chung**, Chet Lo**, John Mahoney**, Jeremy Pruitt**, Ryan Hanks**, Santi Basava**, Cynthia Furse*

Center of Excellence for Smart Sensors
University of Utah* and Utah State University**
50 S. Campus Drive4120 Old Main Hill
Salt Lake City, Utah 84112Logan, Utah 84322-4120

Age-related malfunctioning of wiring infrastructure in aircraft, space vehicles, trains, nuclear power plants, high speed data networks, and even the family home and car is an area of critical national and international concern. As these networks age, the wires become brittle and crack, break, or short circuit, sometimes dangerously, sometimes with annoying intermittents. Millions of man hours are spent each year trying to locate these faults, and costs from this maintenance and the associated down time run into the billions of dollars. The problem of locating the faults is notoriously frustrating. When a car will not start in the morning, is it a dead battery, corroded connector, broken battery cable, alternator, or electrical connection to the alternator? Merely debugging this very simple system will take a significant amount of time and a few cases of trial and error. Imagine when the complexity of this system is multiplied a hundred-fold, and the fault is buried deep within several miles of power distribution wire on an aircraft scheduled to depart for Chicago in twenty minutes.

This paper describes a set of cost-effective sensors that are being applied to handheld fault location meters and in situ testing systems for pre-flight fault detection and location. Three specific sensor families are described – a Frequency Domain Reflectometer, a set of Capacitance sensors, and a new class of Correlation sensors. Several advanced signal processing methods are compared for accuracy, efficiency, and applicability to realistic, noisy, ill-matched, lossy aircraft cables with complex loads. A comparison of accuracy, cost, complexity, and functionality reveals the most cost-effective solution depending on the system requirements.

These sensors and associated algorithms are tested and compared on a variety of realistic wiring platforms including the US Navy's F-18, P3, E-2C, and C2 aircraft. The system-level design considerations are included to begin to understand the most effective method of deploying an in situ network health monitoring system.

0-7803-7846-6/03/$17.00 ©2003 IEEE 

# Non-Destructive Fault Location on Aging Aircraft Wiring Networks Part 2 – Live Wires in Flight

By: Paul Smith**, Alyssa Magelby*, Deekshit Dosibhatla**, Chet Lo, Cynthia Furse*, Jacob Gunther**

Center of Excellence for Smart Sensors
University of Utah* and Utah State University**
50 S. Campus Drive4120 Old Main Hill
Salt Lake City, Utah 84112Logan, Utah 84322-4120

Aging aircraft wiring has been identified as an area of critical national concern. As the system ages, the wires become brittle and crack, break, or develop short circuits. Short circuits, in particular, have been implicated in a variety of smoke incidents, in-flight fires, and crashes. Some of these faults are intermittent, occurring only sporadically as the physical vibration, stresses, temperatures, electrical loads, moisture condensation, etc. change throughout the flight. When the plane is on the ground, no fault can be found. These types of problems are among the most frustrating for aircraft maintainers, resulting in a typical "no fault found" incident taking tens or even hundreds of hours to locate. Some planes even remain grounded for extended periods of time until basic electrical systems can be fully replaced at great cost and labor. One of the greatest hazards of these systems is that they may foreshadow a more serious in flight hazard as a small fault grows, yet for all intents and purposes, the system checks out OK.

This paper describes two systems based on spread spectrum technology that are the first known sensors that can actively locate faults on live wires in flight without disrupting or interfering with existing 400 Hz power or 1553 data bus signals. These systems are found to be highly robust to in-line noise, connection mismatches, etc. They provide measurements accurate to within inches or feet over several hundred inches of both shielded and unshielded cables. They can function accurately within a realistic network environment, and can locate intermittent short circuits (wet or dry arc events) in flight. The sensor development and testing for realistic situations, algorithms for enhanced data processing, and real-time analysis methods are described.

0-7803-7846-6/03/$17.00 ©2003 IEEE 

# Coupled Transmission Lines as a Time-Domain Directional Coupler

Carl E. Baum
Air Force Research Laboratory
Directed Energy Directorate
Kirtland AFB, NM

Abstract

Directional couplers are a well-established microwave subject, various bibliographies and texts being available. Here our attention is limited to TEM transmission-line couplers for their potential time-domain application. This is further restricted to *uniform* two-conductor plus reference transmission lines of finite length because, as we shall see, the coupler samples the waveform of interest over a time window of twice the transit time in the coupler without distorting the waveform. This can be compared to another type of directional coupler which senses the time derivative of the waveforms [C. E. Baum, "A Sensor for Voltage, Current and Waves in Coaxial Cables", Sensor and Simulation Note 447, 2000]. These kinds of directional couplers have application to various measurement situations, including measuring the returning transient signal in a radar antenna which is also used for transmission of the radar pulse. Our general derivation covers previous work with some extension. Note that some authors refer to this type of device as a contra-directional coupler.

Here we show that a traditional type of transmission-line directional coupler can be made to operate for temporal waveforms as well. There is a time-window of width $2t_\ell$ during which the coupled waveform is the same as the incident waveform times a constant. This requires that, in the simplest operation, $2t_\ell$ be longer than the time duration of the pulse of interest. One can extend this to longer times by appropriate data processing, noting the more complete description of the scattering-matrix elements. Our general approach to the theory has revealed various cases of potential interest. The fully symmetric case (symmetry between wires 1 and 2 as well as source and load impedances) with identical resistive impedances (cable characteristic impedances) on all four ports gives rather simple final answers. There are, however, more general cases that still lead to zero transmission form port 1 to port 4 (the directional-coupler criterion) in 4.

Noting that a transmission-line model is used for the coupler, there are some errors in modeling a real such device. In particular, at frequencies high enough that radian wavelengths are not large compared to the cross-section dimensions, a full wave analysis may be required. Near the ports the abrupt changes in the cross-section geometry may make evanescent modes significant there.

0-7803-7846-6/03/$17.00 ©2003 IEEE 

# EXTRACTION OF COMPLEX NATURAL RESONANCES FROM RADAR SIGNATURES MEASURED IN TIME DOMAIN

**R. Toribio[(1)], J. Saillard[(1)], P. Pouliguen[(2)]**

*[(1)]Laboratoire IRCCyN, UMR CNRS 6597, division SETRA, Ecole Polytechnique de Nantes,*
*bât. IRESTE, La Chantrerie 44306 Nantes cedex 3*
*Raphael.Toribio@polytech.univ-nantes.fr*

*[(2)]DGA/CELAR, BP 7419, 35174 Bruz Cedex*

Radar signatures, in the resonance region, can be recognized thanks to their Complex Natural Resonance's (CNR's), in the context of the Singularity Expansion Method (S.E.M). Hence the time domain response $r_t(t)$ of a target, illuminated by an E.M. wave, can be written as the sum of two terms:

$$r_t(t) = f_e(t) + \sum_{i=1}^{N} R_i e^{\sigma_i t} \sin(\omega_i t) \qquad (1)$$

The first term $f_e(t)$ represents the impulsive behaviour of the signal.
The second term is the "late time response" which describes all the phenomena occurring on the object surface (e.g. creeping waves). It represents the time domain area used to determine the CNR's.
$\sigma_i$ and $\omega_i$ are respectively the damped coefficient and the resonance pulsation of the $i^{th}$ CNR. $R_i$ is the corresponding residue of the $i^{th}$ CNR.

CNR's can be extracted in the time domain thanks to some improved versions of Prony method, such as TLS Prony or TSD-TLS Prony. In practice all these formalisms still remain sensitive to important additional noise. A new approach consists in considering a pre-conditioned signal. It can be shown, with analogy of High Resolution Techniques, that the use of the auto-correlated signal after filtering keeps the late time response properties (sum of damped sinusoids) and reduces effects of additional noise. Then, the use of improved Prony methods with auto-correlated measured signals increases the accuracy of CNR's extraction.

The presentation will show the benefits of using auto-correlated measured signals in order to improve CNR's extraction. The results will be presented mainly for conducting canonical targets (dipole, sphere, cylinder, ...). The signatures have been recorded using an UWB laboratory measurement system developed by CELAR (French defense organization) in an anechoic chamber.

0-7803-7846-6/03/$17.00 ©2003 IEEE

# Sequential Quarter-Wave Transmission-Line Transformers

Carl E. Baum
Air Force Research Laboratory
Directed Energy Directorate
Kirtland AFB, NM

Abstract

A recint paper [C. E. Baum, "Nonumiform-Transmission-Line Transformers for Fast High-Voltage Transients", Circuit and Electromagnetic System Design Note 44, 2000] considers a quarter-wave trasmission-line transformer for improving the matching of a switched oscillator to an antenna with an input impedance in the 100 $\Omega$ range. There it was observed that a significant increase could be made in the peak voltage (or equivalently, peak power) delivered to the antenna. The stored energy in the switched oscillator is, of course, then delivered in a shorter time while still approximately maintaining the basic oscillator frequency.

In stepping up the voltage delivered to the antenna we have the associated problem of insulating the antenna input so as to withstand the higher voltage. Perhaps it would be better to step up the voltage in a more gradual way so that as one progressed away from the reflector focus and the feed arms became farther apart the voltage could be allowed to be larger without breakdown. As we shall see, this is accompanied by an increase in the transmission-line characteristic impedance as one progresses away form the switched oscillator.

A sequence (cascade) of quarter-wave transmission-line transformers can then have some advantages over a single transformer. The voltage is allowed to more gradually increase throught the sequence, potentially giving better insulation characteristics in some applications. In the limit of a large number of cascaded transformers the ensemble gives a version for discrete frequencies comparable to a continuously varying transmission-line characterisitc impedance as used for a pulse transformer.

0-7803-7846-6/03/$17.00 ©2003 IEEE 

## Planar Antennas

**Co-Chairs:** G. Thiele
J. Williams

3:20 Opening Remarks

# Analysis and Optimal Design of Vertically and Horizontally Corrugated Monopole Antenna

Dazhi Yang, Yilong Lu *
School of Electrical and Electronic Engineering
Nanyang Technological University
Nanyang Avenue, Singapore 639798
email: eylu@ntu.edu.sg

**Abstract**

This paper presents the analysis and optimal design of two new types of broadband antennas, a vertically corrugated monopole antenna and a horizontally corrugated monopole antenna by using the modal expansion analysis and genetic algorithm. The structures of these two antennas are shown in Fig. 1. The antennas are fed through infinite grounding plane by coaxial cables with the monopole shaped in corrugated form to broaden the bandwidth. Most traditional analyze of monopoles are based on method of moments (MOM), for which the impedance results and the accuracy are often not satisfactory. The modal expansion analysis technique (Z. Shen and R.H. MacPhie, *Radio Sci.*, 5, 1037-1046, 1996 & Z. Shen and R.H. MacPhie, *IEEE Trans. on Antennas and Propagat.*, Vol. 49, No. 11, 1525-1531, 2001) is a more accurate and efficient method for axis-symmetric cylindrical antenna structures. It is applied in this paper to compute the electromagnetic fields and input impedance response of the proposed antennas. To achieve better

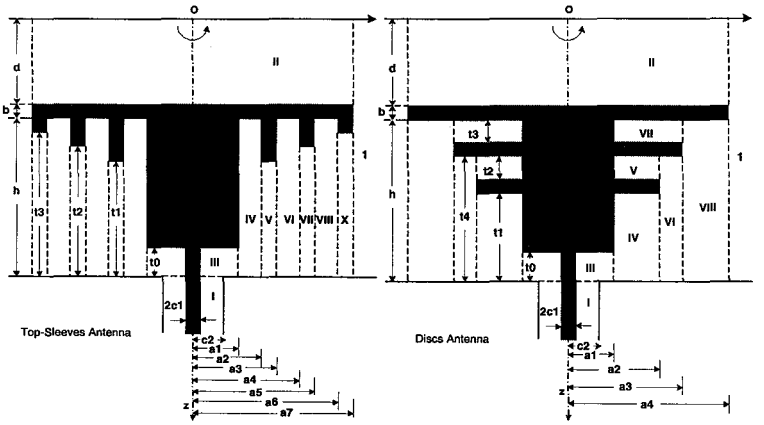


(a) Structure of Vertical Corrugated Monopole Antenna

(b) Structure of Horizontal Corrugated Monopole Antenna

Figure 1: Two Corrugated Monopole Antennas Fed by Coaxial cable

and more stable bandwidth performance of the desired antennas, the effective Emperor-Selective genetic algorithm (EMS-GA)(B K Yeo and Y Lu, *IEEE Trans. on Antennas and Propagat.*, Vol. 47, No. 5, 823-828, 1999) is applied for automatical optimization. Genetic Algorithms are stochastic search and optimization techniques modelled on the mechanics of biological genetics and natural evolution. It becomes very popular in optimization of many engineering problems today. In EMS-GA, real number vectors associated with the proposed antennas' geometrical dimensions are used as the chromosomes. The optimally designed antennas can achieve very wide bandwidth. The performance of these two proposed antennas are compared. The effects due to the vertical and horizontal corrugates are analyzed and discussed.

0-7803-7846-6/03/$17.00 ©2003 IEEE

## Design and Radiation Characteristics of Low Profile TM21 Ring Antenna and Concentric Linear Monopole Assembly

**Author:**
Court Rossman*, Centurion Wireless Technologies, Scotts Valley, CA.

This report presents the design considerations for a low profile TM21 mode satellite-radio antenna at 2.3GHz. A low profile antenna assembly, intended for installation on top of an automobile, is created to generate a circular polarized (CP) conical pattern for satellite reception (optimized for geosynchronous satellites) and a linear monopole radiation pattern for terrestrial reception. The CP conical pattern is generated using a two wavelength ring tuned for the TM21 mode (fig. 1) (R. Garg, P. Bhartia, I. Bahl, A. Ittipiboon, "Microstrip Antenna Design Handbook", Artech House). A simple low profile CP patch does not have a broad enough beamwidth to serve as a satellite antenna for lower elevations. A helix or crossed dipole can be used to generate cardioid patterns, but these are taller antennas.

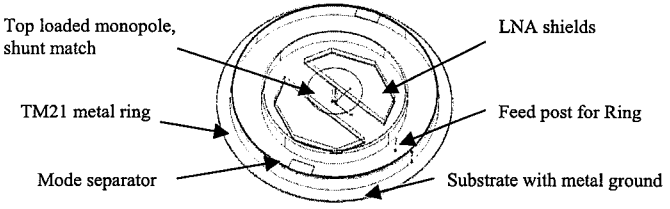


**Fig. 1**: CP TM21 ring / linear monopole (satellite/terrestrial) antenna assembly.

A design parameter is the width of the ring. Wider is better than thinner for four reasons: First, the radiation from a wide-trace ring is dominated by the E fields on the outer edge of the ring, and the gain closer to the horizon is greater. The feed point impedance is reduced to a reasonable design value, due to the ability to move the feed point inwards from the outer circumference. Finally, the bandwidth is larger and the efficiency is better due to the larger effective antenna volume.

The TM21 ring antenna needs a ground plane. A very small ground plane is better than an infinite ground plane for low elevation gain (fig. 2). An infinite ground plane prohibits CP radiation along the horizon. Smaller ground planes can be used on fiberglass trucks or front dashboards. The gain at low elevation can also be increased (better than most other antennas) by placing the ring on a metal pedestal, due to imaging effects (fig. 3).

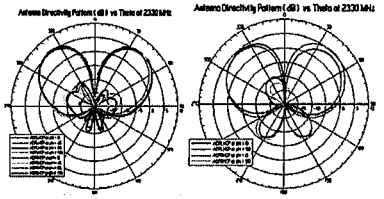

**Fig. 2**: Satellite pattern using 20 inch and 4.4 inch diameter ground plane.

**Fig. 3**: Satellite pattern when the ring antenna is placed on a 0.8inch high, 4.4 inch diameter metal pedestal. This is a great pattern for the far Northern States.

# Wideband Low-Profile Canted Antennas for Array Applications

J. T. Bernhard*, B. Herting, P. Mayes, N. Chen, and E. Michielssen
Electromagnetics Laboratory and Center for Computational Electromagnetics
Department of Electrical and Computer Engineering
University of Illinois at Urbana-Champaign, Urbana, IL 61801
jbernhar@uiuc.edu

Planar microstrip antennas revolutionized phased array technology decades ago. To enable the next levels of array functionality, however, new array elements with expanded capabilities and appropriate array strategies are required to operate over wide frequency bands. While patch antennas have many desirable characteristics, their narrow impedance bandwidths make them unsuitable for wideband applications. Common wideband antennas, on the other hand, promise increased bandwidth, but at the expense of greater physical size and/or reduced gain. This situation captures a fundamental physical limitation analogous to the gain-bandwidth tradeoff in electrical networks. In the case of antennas, this limitation is defined by gain-bandwidth and size. Therefore, in order to increase significantly the bandwidth of low-profile antennas, the effective volume occupied by the antenna structure must be increased. There are two alternatives: (a) increase the height, or (b) increase the lateral dimensions. These choices have implications not only for antenna design but also attainable array performance.

A number of groups are pursuing wideband and ultra-wideband antenna arrays. The motivation for this research is the ability to use one antenna aperture for a number of applications across a large frequency spectrum, reducing the number of antennas on platforms such as satellites, vehicles, and ships. Most often, variants of TEM horns or Vivaldi tapered slot antennas are implemented and do provide very wide band operation. However, these antennas are not applicable in many scenarios due to their large thickness, complicated and labor-intensive feed networks, and considerable weight.

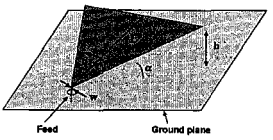


Figure 1: Non-resonant canted sector antenna.

In this presentation, we will describe experimental and simulation results on a family of low-profile antennas (non-resonant canted sectors – a single element is depicted in Figure 1) intended for wideband applications where traditional periodic patch antenna arrays severely limit performance. The results will illustrate compromises between the total height of the antenna above the ground plane, achievable impedance bandwidth, and radiation characteristics. Current designs show promise with over 40% instantaneous bandwidths that maintain useful broadside radiation performance. Simulation strategies, solutions for fabrication of these low-profile structures (similar to those described in J.-C. Langer et al., *IEEE Microwave and Wireless Components Letters*, **3**, 2003) and the development of related structures that ameliorate the poor broadside radiation characteristics as frequency increases will also be discussed.

0-7803-7846-6/03/$17.00 ©2003 IEEE

# SLOTTED PATCH ANTENNAS FOR SPACE APPLICATIONS

**Salvatore Contu[1], Claudio Vegni[1], Filiberto Bilotti[2], Lucio Vegni[2]**

[1]Alenia Spazio S.p.A.
Via Saccomuro n°24 – 00131 – Rome – Italy
Phone: +39.06.41514451 – E-mail: c.vegni@roma.alespazio.it

[2]University of Roma Tre – Department of Applied Electronics
Via della Vasca Navale n°84 – 00146 – Rome – Italy
Phone: +39.06.55177003 – E-mail: vegni@uniroma3.it

The present work has been developed in a recent cooperation between the University of ROMA TRE and Alenia Spazio (ALS).
ALS has been and is currently involved in National, European and International programs on Remote Sensing, Telecommunications and Science applications from UHF up to Ka band frequencies. In that frame, one of the main activities of the ALS Antenna Department is the design of planar array antennas using microstrip technology. Typical antenna designs for space applications have to match the following requirements: impedance bandwidth, gain, radiation pattern polarization purity or ellipticity bandwidth (in case of circular polarization), coverage requirements (shaped beams), port-to-port isolation (mutual coupling in case of arrays), low weight and low profile, structure stiffness, thermal stability, easy technology and manufacturing repeatability. In order to accomplish the previous constraints, a wide typology of patch antennas can be designed and the choice of the final radiator has been derived after a trade-off evaluation. For example, impedance bandwidth requirements can be achieved in some cases using a stacked patch configuration through direct feeding, aperture feeding (COSMO-SKYMED program), electromagnetic coupling feeding (WRAS and LAGRANGE programs); weight requirements can be matched using Kapton–Kevlar materials (MARE-SS, SICRAL program); polarization purity can be optimised with sequential rotation techniques (WRAS program). In that scenario, the design of new patch antenna layouts exhibiting *enhanced* electrical and mechanical performances with respect to *standard* microstrip radiators can be considered as a challenging aspect for the electrical engineer. From that point of view, the present work deals with the design of a novel patch radiator for both array and "stand-alone" configuration. More in detail, the design refers to slotted patch antennas, with linear or circular polarization features and fed by probes or microstrip lines. The slots etched on the patch surface increase the design freedom degrees (shape, allocation and size of the slots) with respect to *standard* microstrip radiators and permit the control of the antenna resonant frequencies, impedance bandwidth, surface current densities, radiation pattern, through a proper design. Particularly, the obtained features of the proposed antennas are broadband or multi-frequency operation, working frequency shift, antenna compactness and mass saving.
The electrical design of such radiators have been performed by a numerical code implemented by the University of Roma Tre. This tool is based on a rigorous full-wave Electric Filed Integral Equation (EFIE) approach developed in the spectral domain and assisted by a combined Genetic Algorithm (GA) - Method of Moments (MoM) optimisation module allowing a very fast, easy and accurate design of slotted patches matching some prescribed requirements. The numerical results obtained through this code have been compared with those of commercial software employing the same theoretical method (e.g. Ensemble) and with measured data.

0-7803-7846-6/03/$17.00 ©2003 IEEE

# A Planar Dual-Band Reduced-Surface-Wave GPS Antenna

Lorena I. Basilio, Richard L. Chen, Jeffery T. Williams, and David R. Jackson

Applied Electromagnetics Laboratory
Department of Electrical Engineering
University of Houston
Houston, Texas 77204-4005

A significant contributor to positioning errors in GPS systems is the interference caused by multipath reflections. Particularly problematic are multipath signals that impinge on the antenna at low elevation angles and those that are a result of ground reflections or scattering from the supporting structure of the antenna. Attempts to reduce these effects by using "choke-ring" ground planes, coating the ground plane with resistive or absorbing materials, and using sophisticated signal-processing techniques have proved to be only moderately successful and often introduce significant cost or weight.

Recently, a single-band GPS microstrip antenna design, based on the Reduced-Surface-Wave (RSW) concept, was introduced. This RSW-GPS antenna *significantly* reduces the deleterious effects of low-angle and ground-bounce multipath signals. In addition to having the advantages common to microstrip antennas, this GPS antenna design provides performance comparable to or better than most commonly used high-precision GPS antennas, including choke-ring and pinwheel designs.

For many high-precision GPS applications it is necessary to simultaneously receive the coded GPS signals at both the L1 and L2 frequency bands. In addition, with the emergence of other GPS bands and the Galileo global positioning system, dual-system/band receivers and, hence, suitable dual-band antennas are required. Unfortunately, the narrow bandwidth of the single-band RSW-GPS antenna is not sufficient to cover the multiple bands. In this presentation a planar dual-band RSW GPS microstrip patch design is introduced for high-precision dual-system/band applications. This antenna integrates two RSW elements, each operating at different bands, to realize dual-band performance.

The integration is achieved by the development of a new inverted RSW element (IRSW) that is complimentary in geometry to the original RSW structure (the radiating edge of the IRSW is the inner edge, and a short-circuit boundary is used at the outer edge). As with the original RSW design, this new IRSW element is based upon the reduced surface wave principle. The RSW antenna is placed inside the IRSW antenna, allowing for a completely planar design that can be fed by a single feed network. Due to the inherent reduced surface wave properties of both elements, the impedance and radiation properties of the individual elements are largely unaffected by the presence of the other. In this presentation, the RSW design principles will be reviewed and specifically applied to the new IRSW element, for which impedance and radiation properties will be shown. The integrated dual-band RSW GPS antenna will then be introduced and characterized.

0-7803-7846-6/03/$17.00 ©2003 IEEE 

# A Comparison Between the Currents of a Multi-Mode Spiral on Planar and Curved Surfaces

G. A. Thiele*, R. P. Penno, and S. W. Schneider
AFRL/SNRR, WPAFB, OH

A planar 4-arm spiral is capable of multi-mode operation (i.e., 3 modes). It has been previously shown that a single planar multi-mode spiral can be used for angle of arrival (AOA) estimation. Comparison of the phases of the mode-former outputs produces an estimate of the azimuth, which is often the primary angle of interest. Best phase accuracy is obtained when the highest order mode (e.g., mode 3) is used because it has the highest rate of phase change with angle. However, mode three phase has a phase ambiguity and that is resolved using the mode 1 (lowest order mode) phase output. Comparison of the magnitudes of the various modal outputs yields an estimate of the elevation angle.

For a planar multi-mode spiral, the magnitude and phases of the modal outputs have been accurately calculated and confirmed by measurement over a hemispherical range of angles. However, in many applications it is desirable, if not necessary, to conform the spiral to a curved surface such as that of a cylinder with circular cross-section. In order to use the multi-mode spiral for AOA in this situation, the changes in the magnitudes and phases of the modal outputs, from those in the planar case, must be known or predictable. It is the purpose of this paper to show such changes and how they affect the usefulness of the multi-mode spiral for AOA when conformed to the surface of a circular cylinder.

To be presented at the 2003 URSI North American Radio Science Meeting, June 22-27, Columbus, OH

1) Commission B, suggested Session B1.5, Mechanical Distortion Effects in Arrays and Reflectors

2) New knowledge: How conforming a multi-mode spiral to a curved surface affects its performance in an AOA application.

3) Relationship to previous work: It is an extension of recent work at WPAFB in the development of a wideband AOA system.

0-7803-7846-6/03/$17.00 ©2003 IEEE

## Time Domain Techniques

**Co-Chairs:** T. Sarkar
T. Rylander

1:15 Opening Remarks

158. 1 1:20 Stability of the Time Domain Finite Element Method ..... 700
*T. Rylander, J. Jin, University of Illinois at Urbana-Champaign, USA*

158. 2 1:40 Solving Radiation Problem with EFIE in Time Domain Using Laguerre Polynomials..... 701
*Z. Ji, T. k. Sarkar, Syracuse University, USA, B. Jung, Hoseo University, Korea*

158. 3 2:00 Time Domain Finite Element Method using Laguerre Polynomials As Temporal Basis Functions ..... 702
*Y. Chung, Myongji University, Korea, T. K. Sarkar, Syracuse University, USA, B. Jung, Hoseo University, Korea*

158. 4 2:20 Temporal Basis of Weighted Laguerre Polynomials in Finite Element Method ..... 703
*S. Llorente-Romano, M. Salazar-Palma, Universidad Politécnica de Madrid, Spain, T. K. Sarkar, Y. Chung, Syracuse University, USA*

158. 5 2:40 A Penalty Method for Multidomain Pseudospectral Time-Domain (PSTD) Algorithm..... 704
*G. Zhao, Q. H. Liu, Duke University, USA*

158. 6 3:00 Comparison of High-order Spectral Element and Finite Difference Methods for Electromagnetic Wave Propagation ..... 705
*M. Sjögren, J. Nordström, Uppsala University, Swedish Defence Research Agency, Sweden*

# Stability of the Time Domain Finite Element Method

Thomas Rylander* and Jian-Ming Jin
Center for Computational Electromagnetics
Department of Electrical and Computer Engineering
University of Illinois at Urbana-Champaign
Urbana, Illinois 61801-2991

The finite element method (FEM) formulated in the time domain is attractive for devices with complex geometry in three dimensions where an accurate result is required in a wide frequency band. For time domain computations in general, it is well known that a numerically stable time-stepping scheme is necessary for reliable results. This talk features stability issues related to the time domain FEM.

The talk will include a review of some recent results on the stability of explicit-implicit hybrid time-stepping schemes for Maxwell's equations (Thomas Rylander and Anders Bondeson, "Stability of explicit-implicit hybrid time-stepping schemes for Maxwell's equations," *J. of Comput. Phys.*, vol. 179, no. 2, pp. 426-438, July, 2002). The recently developed and new hybrid scheme combines the efficiency of the finite-difference time-domain (FDTD) scheme with the ability of the FEM to model complex boundaries. In fact, the FDTD scheme can be deduced by FEM techniques, i.e. edge elements on cubes with lumping by trapezoidal integration, and consequently the hybrid method can be considered as a pure FEM. The hybrid method is derived by applying the Galerkin's method to the self-adjoint Maxwell's equation. This implies that the discretized "$\nabla \times \mu^{-1} \nabla \times$"- and "$\epsilon$"-operators are real symmetric semi-positive definite and positive definite matrices, respectively. The eigenvalues $k^2$ of the corresponding eigenvalue problem are therefore real and non-negative which is necessary for stability. In fact, the hybrid algorithm is stable for time steps up to the stability limit of the FDTD without added dissipation and the proof of stability will be presented during the talk. The hybrid scheme is free from spurious solutions.

We are currently working toward a generalization of this proof of stability, which is intended to include the recently developed conformal perfectly matched layers for the time domain FEM (Thomas Rylander and Jian-Ming Jin, "Conformal Perfectly Matched Layers for the Finite Element Method in the Time Domain," submitted to *2003 IEEE AP-S International Symposium*). The status of this work will be reported during the talk.

0-7803-7846-6/03/$17.00 ©2003 IEEE

# Solving Radiation Problem with EFIE in Time Domain Using Laguerre Polynomials

[1]Zhong Ji, Tapan K. Sarkar , and [2]Baek Ho Jung

[1]Department of Electrical Engineering and Computer Science
Syracuse University, Syracuse, NY 13244
E-mail: zji@syr.edu, tksarkar@syr.edu
[2]Department of Information and Communication Engineering
Hoseo University, Asan 336-795, Korea
E-mail: bhjung@office.hoseo.ac.kr

A time-domain electric field integral equation (TD-EFIE) is presented to obtain the radiation from arbitrarily shaped three-dimensional (3D) open conducting bodies.

The most popular method to solve a TD-EFIE is the marching-on in time (MOT) method using triangular patches and vector basis functions. The TD-EFIE with the MOT method suffers from its late-time instability, which usually takes the form of an exponentially increasing oscillation that alternates in sign at each time step. Instead, we solve the wave equation by expressing the transient behaviors in terms of Laguerre polynomials. By using these orthonomal basis functions for the temporal variation, the time derivatives can be handled analytically. Since these weighted Laguerre polynomials converge to zero as time progresses, the induced electric currents when expanded in a series of weighted Laguerre polynomials also converge to zero. In order to solve the wave equation, we introduce two separate testing procedures, a spatial and temporal testing. By introducing first the temporal testing procedure, the marching-on in time procedure is replaced by a recursive relation between the different orders of the weighted Laguerre polynomials. The other novelty of this approach is that through the use of the entire domain Laguerre polynomials for the expansion of the temporal variation of the current, the spatial and the temporal variables can be separated.

In this paper, an unconditionally stable solution for the TD-EFIE algorithm has been proposed for calculating radiation of 3D arbitrarily shaped open conducting structures. To model arbitrarily shaped structures, triangular patch modeling has been employed to provide more flexibility. A marching-on-in-order method is used to solve the TD-EFIE with weighted Laguerre polynomials. Numerical results are presented, which show the validity of the presented methodology.

0-7803-7846-6/03/$17.00 ©2003 IEEE 

# Time Domain Finite Element Method using Laguerre Polynomials as Temporal Basis Functions

Young-Seek Chung[§], Tapan Kumar Sarkar*, and Baek Ho Jung**

[§] Department of Communication Engineering, Myongji University, Yongin, Kyunggi 449-728, Korea
*Department of Electrical Engineering and Computer Science, Syracuse University, Syracuse, NY 13244
**Department of Information and Communication Engineering, Hoseo University, Asan, Chungnam 336-795, Korea

E-mail: ychung05@syr.edu, tksarkar@syr.edu, bhjung@office.ho seo.ac.kr

In recent times, the finite element method in time domain (FETD) has been introduced to analyze transient electromagnetic problems. By introducing triangular or tetrahedral elements in two or three-dimensional problem, it is easy to apply the FETD method to highly complex shaped models. And by using the Newmark-Beta method, one can obtain an unconditionally stable FETD formulation. By introducing the Newmark-Beta method, although one can eliminate the limitation of time step, the larger value of the time step causes larger numerical error.

In this paper, we propose a new unconditionally stable solution procedure for the FETD method using weighted Laguerre polynomials as temporal basis and testing functions. By introducing the temporal testing procedure, instead of the marching-on in time technique, we introduce the marching-on in order of the temporal functions. Therefore, we can obtain the unknown coefficients for the basis functions from the $0^{th}$ order to the $N_L^{th}$ order by solving recursively the proposed new FETD. And also, the proposed method produces the same banded sparse system matrix as the conventional FETD method, which is independent of the order of temporal basis functions. So, assembling this sparse system matrix only once as like the conventional FETD method with the Newmark-Beta method, we can obtain the transient electromagnetic fields. Considering the bandwidth and the time interval, we can calculate the minimum number of the temporal basis functions. Numerical results are presented to illustrate the validity of this algorithm.

0-7803-7846-6/03/$17.00 ©2003 IEEE 

# Temporal Basis of Weighted Laguerre Polynomials in Finite Element Method

Sergio Llorente-Romano*[1], Magdalena Salazar-Palma[1]
Tapan K. Sarkar[2], Young-seek Chung[2]

[1] Universidad Politécnica de Madrid (Dpto. SSR)
ETSI Telecomunicacion, Ciudad Universitaria s/n, 28040 Madrid, Spain.
llorente@ieee.org

[2] Syracuse University
121 Link Hall, Syracuse, NY 13244, USA

The finite element method in time-domain (FETD) provides a direct way of solving transient electromagnetic problems. Also, FETD allows analysis of complex structures better than other numerical methods. The time-domain analysis has been usually done with a marching-on time scheme that requires much computation time if the electromagnetic problem is large and many time steps are required.

In this work, a scheme based on temporal basis functions is presented. By using a temporal basis, the transient behavior of the unknown function of the electromagnetic problem is described by a set of coefficients. In this paper the chosen basis functions are weighted Laguerre polynomials with increasing orders. The advantage of this election is that the coefficients of the derivative of a function can be handled analytically from the coefficients of the original function. This fact allows the replacement of the marching on time schemes of classical FETD methods by a recursive relation between the coefficients of different orders. The result of this procedure is a matrix linear system with different right hand vectors for each coefficient of the unknown function but with the same matrix of the linear system. Therefore the computation of all coefficients can be done very efficiently.

Two-dimensional and three-dimensional scattering problems are presented in order to show the efficiency and the accuracy of this numerical technique. Among the two-dimensional problems the incidence of a planar wave over a metallic and dielectric cylinder of infinite length is studied. The scattered electromagnetic field produced by the incidence of a planar wave over a metallic and dielectric cube is studied in order to test the numerical procedure in three-dimensional problems. In all cases a gaussian pulse is used to model the temporal variation of the incident electromagnetic wave.

The results are compared with other electromagnetic analysis tools and the agreement is excellent.

0-7803-7846-6/03/$17.00 ©2003 IEEE 

# A Penalty Method for Multidomain Pseudospectral Time-Domain (PSTD) Algorithm

Gang Zhao* and Qing Huo Liu
Department of Electrical and Computer Engineering
Duke University
Durham, North Carolina 27708

The pseudospectral time-domain (PSTD) method has demonstrated significant advantages over the finite difference time-domain (FDTD) method due to its less sampling density and higher-order accuracy. However, traditional pseudospectral methods with a fixed global distribution of grid points suffer from an intensive computational burden and severe time-step ($\Delta t$) restriction when solving problems with strong internal inhomogeneities. This leads to the need for development of multidomain approaches.

Previously, we have implemented the 3-D multidomain PSTD algorithm built on a 3-D hexahedral mesh accurately conformal to the problem geometry. The multidomain strategy allows for a flexible treatment of strongly localized features and avoids the intensive operations on the global domain. We have shown the versatility of the multidomain PSTD method for the simulation of inhomogeneous and conductive media (G. Zhao and Q. H. Liu, *IEEE Microwave Wireless Compon. Lett.*, in press).

In spite of its flexibility, the multidomain scheme requires an extra computational step, namely subdomain patching, to reconcile the field values at the interface of nonoverlapping subdomains. To this end, the characteristic and physical boundary conditions have been developed for the multidomain PSTD algorithm. However, none of these techniques naturally guarantees that the updated fields at the interface still satisfy the original Maxwell's differential equations. Besides, the sequence of patching is dependent on the indexing of subdomains, which can incur singularity problems at the locations of edge and corner, resulting in a potential accuracy and stability degradation. Therefore, a stable and accurate patching technique is called for to bring the advantage of the PSTD method into full play.

The penalty method (J. Hesthaven and D. Gottlieb, *SIAM J. Sci. Comput.*, **17**, 579-612, 1996) seeks for the compromise between the boundary conditions and the equation itself by weakly enforcing the boundary conditions as a penalty term to the equation. This approach has been proved to be asymptotically stable, and has been successfully applied to the finite element method. In this work, we apply the penalty method to our previously developed multidomain PSTD algorithm, to achieve a stable and accurate interface patching technique. This will increase the robustness of the PSTD method, and further broaden its application areas.

0-7803-7846-6/03/$17.00 ©2003 IEEE

# Comparison of High-order Spectral Element and Finite Difference Methods for Electromagnetic Wave Propagation

Martin Sjögren, Jan Nordström, Uppsala University, Swedish Defence Research Agency

As the demands on accuracy increase for complicated problems in electromagnetics, the focus naturally turns to higher-order numerical methods, two of which have been validated, evaluated and compared in this paper.

The first time-domain method is the unstructured spectral element method, a type of discontinuous Galerkin method based on a collection of elements, on which Lagrangian polynomials of varying order act as basis functions. The second type of method is the finite difference time domain scheme. This method is based on a structured grid, and deals with discontinuities by means of a penalty procedure similar to the one used in the spectral element method. In both cases, a high-order Runge-Kutta scheme is implemented for the time development.

Emphasizing efficiency and long-time stability, a comparison of the spectral element and finite difference methods has been carried out in a two-dimensional reflection-refraction situation where a plane electromagnetic wave encounters a dielectric material discontinuity. In the paper, this comparison is discussed in detail.

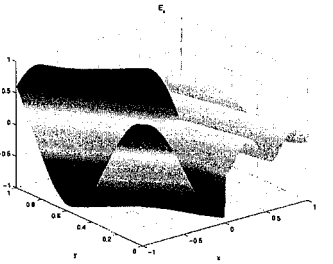

For both methods, the use of proper characteristic boundary conditions ensures an error-boundedness in time which is necessary in calculations that run over long periods of time. The finite difference scheme also proves to be about a factor of 5 more efficient than the spectral scheme. However, this Cartesian sample problem is more or less tailored for finite differences. A more complicated geometry would favor the spectral scheme, mainly because of the relative ease of constructing an unstructured grid for such a geometry.

We also relate this comparison to problems closer to real life by considering a full-size radar scattering calculation on a 7 $m$ generic missile. With the spectral element method and an incoming radiation of 1 $GHz$, the calculation took about 30 CPU-hours. This and corresponding calculations are also discussed in the paper.

0-7803-7846-6/03/$17.00 ©2003 IEEE

## Time Domain Integral Equations

**Co-Chairs:** A. Boag
J. M. Jin

3:20 Opening Remarks

159. 1 3:20 Transient Electromagnetic Scattering from Dielectric Objects using Laguerre Polynomials As Temporal Basis Functions ..... 708
*B. Jung, Hoseo University, Y. Chung, Myongji University, Korea, T. Sarkar, Z. Ji, Syracuse University, USA*

159. 2 3:40 Non-uniform Grid Time Domain Approach For Fast Multilevel Evaluation of Transient Fields ..... 709
*A. Boag, Tel Aviv University, Israel, E. Michielssen, V. Lomakin, University of Illinois at Urbana-Champaign, USA, E. Heyman, Tel Aviv University, Israel*

159. 3 4:00 Fast Integral-Equation-Based Analysis of Transient Scattering from Doubly Periodic Perfectly Conducting Structures ..... 710
*N. Chen, M. Lu, University of Illinois at Urbana-Champaign , B. Shanker, Michigan state university , E. Michiellsen, University of Illinois at Urbana-Champaign , USA, F. Capolino, Università di Siena, Italy*

159. 4 4:20 Efficient Solution of Time Domain Volume Integral Equations using the Adaptive Integral Method ..... 711
*A. E. Yilmaz, University of Illinois, B. Shanker, Michigan State University, J. M. Jin, E. Michielssen, University of Illinois, USA*

159. 5 4:40 Discrete Wavelet Transform Compression for Time Domain Integral Equations ..... 712
*A. E. Yilmaz, J. Jin, E. Michielssen, University of Illinois, USA*

159. 6 5:00 A Parallel Marching on in Time Solver Accelerated by Plane Wave Time Domain Algorithm ..... 713
*N. Liu, M. Lu, A. E. Yilmaz, K. Aygun , University of Illinois at Urbana-Champaign, B. Shanker, Michigan State University, E. Michielssen, University of Illinois at Urbana-Champaign, USA*

# Transient Electromagnetic Scattering from Dielectric Objects Using Laguerre Polynomials as Temporal Basis Functions

[1]Baek Ho Jung, [2]Young-Seek Chung, [3]Tapan Kumar Sarkar, and [3]Zhong Ji

[1] Department of Information and Communication Engineering
Hoseo University, Asan, Chungnam 336-795, Korea
[2] Department of Communication Engineering
Myongji University, Yongin, Kyunggi 449-728, Korea
[3] Department of Electrical Engineering and Computer Science
Syracuse University, Syracuse, NY 13244

e-mail: bhjung@office.hoseo.ac.kr, ychung05@syr.edu, tksarkar@syr.edu, zji@.syr.edu

Several time domain formulations have been presented for the solution of the electromagnetic scattering from arbitrarily shaped 3-D structures using triangular patch modeling technique. For the solution of a time-domain integral equation, the marching-on in time (MOT) method is usually employed. A serious drawback of this algorithm is the occurrence of late-time instabilities in the form of high frequency oscillation. In this paper, we present a new technique to obtain stable responses of the time-domain electric field integral equation (TD-EFIE) for arbitrarily shaped 3-D dielectric objects using Laguerre polynomials as temporal basis functions.

The Laguerre series are defined only over the interval from zero to infinity, and hence, are considered to be more suited for the transient problem, as they naturally enforce causality. Using the Laguerre polynomials, we construct a set of orthonormal basis functions. Transient quantities that are functions of time can be spanned in terms of these orthogonal basis functions. The temporal basis functions used in this work are completely convergent to zero as time increases to infinity. Therefore, transient response spanned by these basis functions is also convergent to zero as time progresses. Using Galerkin's method, we introduce a temporal testing procedure, which is similar to the spatial testing procedure of the method of moments. By applying the temporal testing to the TD-EFIE, we can eliminate the numerical instabilities. Instead of the MOT procedure, we employ a marching-on in-degree procedure by increasing the degree of the temporal testing functions. Therefore, we can obtain the unknown coefficients of the expansion by solving a matrix equation recursively with a finite number of basis functions.

Transient equivalent currents and far field obtained by the method presented in this paper are accurate and stable. The agreement between the solutions obtained using the proposed method and the IDFT of the frequency-domain solution is excellent.

0-7803-7846-6/03/$17.00 ©2003 IEEE

# Non-uniform Grid Time Domain Approach for Fast Multilevel Evaluation of Transient Fields

Amir Boag[†*], Eric Michielssen[‡], Vitaliy Lomakin[‡], and Ehud Heyman[†]
[†] Department of Physical Electronics, Tel Aviv University, Tel Aviv 69978, Israel
[‡] Electrical and Computer Engineering Dept., University of Illinois at Urbana-Champaign, 1406 W. Green Street, Urbana, IL 61801, USA

We consider the problem of analyzing scattering from an open three-dimensional perfectly conducting surface through the Marching On in Time (MOT) based solution of a time domain electric field integral equation. Each MOT step requires evaluation of the electric field generated by all historic surface currents. The number of field and current sampling points on the surface is proportional to its electrical dimensions, i.e., of $O(N)$ where $N=(kR)^2$, where $R$ denotes the radius of the smallest sphere circumscribing the scatterer and $k$ is the wavenumber at the highest frequency present in the incident field. The straightforward evaluation of the instantaneous field at $O(N)$ spatial observation points by surface integration, which requires the summation of $O(N)$ partial fields for each observer, amounts to $O(N^2)$ operations. This high computational burden underscores the need for using fast field evaluation techniques.

In this paper, we develop a novel non-uniform grid time domain (NGTD) technique that facilitates the numerically efficient evaluation of the field produced by a given current distribution. The algorithm is based on the observation that, locally, the delay compensated field radiated by a finite size source is an essentially bandlimited function of the angular and radial coordinates of the source centered spherical coordinate system. The angular bandwidth is proportional to the linear dimensions of the source, while the local bandwidth with respect to the radial distance decreases rapidly with the distance. Therefore, the radiated field can be sampled on a non-uniform spherical grid with radial density decreasing with the distance from the source. The total number of grid points is proportional to the source region dimensions.

With this in mind, we introduce a multilevel algorithm based upon a hierarchical decomposition of the scatterer surface into subdomains. At each level, the domain decomposition proceeds by subdividing each parent domain into a number of subdomains. At the finest level, for each small subdomain, radiated fields are computed directly at a small number of points of a very coarse non-uniform spherical grid. Next, the fields of each group of adjacent subdomains are aggregated into those of the parent subdomain and defined over a finer non-uniform grid. Transition from coarse to fine grids is effected by interpolation. The time delay common to all source points in a given subdomain is removed from the field prior to interpolation, thus rendering the field a slowly varying function of the spatial variables in the retarded time domain. Following the interpolation step, delays are restored and partial fields aggregated. At the highest level, the fields are interpolated to the scatterer surface. The proposed multilevel algorithm attains an asymptotic complexity of $O(N\log N)$.

A high-order accurate multilevel implementation of the NGTD scheme will be presented. Its performance will be compared to that of the established plane wave time domain algorithm in terms of both CPU time and memory consumption.

0-7803-7846-6/03/$17.00 ©2003 IEEE

# Fast Integral-Equation-Based Analysis of Transient Scattering from Doubly Periodic Perfectly Conducting Structures

Nan-Wei Chen[†], Mingyu Lu[†], Balasubramaniam Shanker[‡], Filippo Capolino[††] and Eric Michielssen[†]

[†]Center for Computational Electromagnetics
University of Illinois at Urbana-Champaign
Urbana, IL 61801, USA

[‡]Dept. ECE, Michigan State University
East Lansing, MI 48824, USA

[††]Dipartimento di Ingegneria dell'Informazione
Università di Siena
53100 Siena, Italy

A fast time domain integral equation (TDIE) based solver pertinent to the analysis of transient scattering from doubly periodic, perfect electrically conducting (PEC) structures, is presented. The proposed solver relies on a fast scheme for evaluating transient electromagnetic fields generated by doubly periodic and temporally bandlimited source distributions that hinges on Floquet decomposition concepts as well as more classical accelerators.

Transient scattering from doubly periodic structures traditionally has been analyzed using finite difference methods. Unfortunately, when the structure under study is obliquely excited, classically constructed finite-difference solvers require future fields values, i.e., noncausal data, to update current ones, and therefore cannot be applied. Most fixes to this problem are either hard to implement or limited in scope. A recently developed TDIE-based solver resolved the issue of noncausality through the introduction of time-shifted temporal basis functions and a prolate-like extrapolation scheme for bandlimited signals [N.-W. Chen, B. Shanker and E. Michielssen, *IEE Proceeding-Microwaves Antennas & Propagation.*, 2002, in press]. Unfortunately, this solver is computational expensive in the sense that its computational cost scales as $O(N_s^2 N_t^2)$, where $N_s$ and $N_t$ denote the number of spatial basis functions describing the currents on PEC elements in the mothercell—viz. where the integral equation is being enforced—and the number of time steps in the analysis, respectively. This scaling law precludes the application of this solver to the analysis of complicated structures.

The computational cost of this solver can be attributed largely to its need to evaluate the scattered field, viz. the field radiated by the currents on the periodic structure, for every time step. The proposed fast TDIE-based solver reduces this cost by expressing the scattered field in terms of time domain Floquet waves. Only a small number of Floquet waves suffices to represent the field provided that it is generated by quiescent bandlimited sources. The Floquet waves therefore cannot account for fields produced by sources in the immediate vicinity of the mothercell. As a result, fields in the mothercell are split into two components. First, there are the fields associated with sources in cells in its immediate vicinity: they are evaluated classically, using a low-frequency plane wave time domain algorithm [K. Aygün et al., *Proc. Int. Conf. in Electromagnetics in Advanced Applications*,769-782, 2002], or by a time domain AIM scheme [A. Yilmaz et al., *IEEE APS Symp. Dig.*, 166-169, 2002]. Second, there are the fields produced by sources that do not reside in the immediate vicinity of the mothercell: they are evaluated using the aforementioned Floquet expansion. By doing so, the computational complexity of the scheme scales as $O(N_{\text{mode}} N_s N_t \log^2 N_t)$ where $N_{\text{mode}}$ denotes the number of modes used in the Floquet expansion. Numerical results that demonstrate the efficiency and accuracy of the proposed scheme will be presented.

0-7803-7846-6/03/$17.00 ©2003 IEEE

# Efficient Solution of Time Domain Volume Integral Equations Using the Adaptive Integral Method

Ali E. Yılmaz[1]*, Balasubramaniam Shanker[2], Jian-Ming Jin[1], and Eric Michielssen[1]

[1] Center for Computational Electromagnetics, Department of Electrical and Computer Engineering, University of Illinois at Urbana-Champaign, Urbana, IL 61801, USA

[2] 2120 Engineering Building, Department of Electrical and Computer Engineering, Michigan State University, East Lansing, MI 48824, USA

While time domain surface integral equation formulations typically lead to the most efficient methods for analyzing scattering from nonpenetrable or homogenous penetrable objects, their volume extensions are required when modeling inhomogenous scatterers (N. T. Gres et al., *Radio Sci.* **36**(3), 379-386, 2001). When compared to differential equation solvers, such as those based on the finite-difference time-domain (FDTD) method, volume integral equation solvers inherit most advantages of their surface counterparts. In particular, they (i) implicitly impose the radiation condition, (ii) do not discretize space around the scatterer, (iii) do not suffer from phase dispersion errors, (iv) do not constrain the time-step size by the spatial discretization dimensions (K. Aygün et al., *Int. J. Num. Mod.: Elect. Net. Dev. & Fields* **15**, 439-457, 2002), and (v) because of all of the above, typically require fewer unknowns for a given accuracy. Despite all these features, the high computational complexity and memory requirements of classical marching-on-in-time algorithm (MOT) based integral equation solvers render them unpopular compared to differential equation solvers. Indeed, classical MOT computational complexity and storage requirements scale as $O(N_t N_v^2)$ and $O(N_v^2)$, whereas FDTD simulations typically require $O(N_t' N_v')$ operations and $O(N_v')$ storage. Here $N_t$ and $N_v$ are the number of MOT time steps and spatial vector basis functions (typically the volumetric rooftop basis functions), and $N_t'$ and $N_v'$ are the number of FDTD time steps and grid points such that both solvers simulate fields throughout the scatterer for the same duration and with similar accuracies.

Recently, the time domain counterpart of the adaptive integral method (TD-AIM) for accelerating the solution of time domain surface integral equations has been developed. TD-AIM pre-corrects near-field interactions and efficiently computes far-field interactions through multilevel space-time fast Fourier transforms. The fast Fourier transforms are facilitated by an auxiliary (volumetric) uniform mesh that contains the scatterer (unlike the FDTD grid, this mesh does not extend beyond the scatterer since there is no explicit termination by absorbing boundary conditions). When applied to quasi-planar scatterers the TD-AIM algorithm achieves linear complexity (within a logarithmic factor) for surface integral equations. In this work, TD-AIM is extended to volume integral equations, where it also achieves near-linear complexity. Specifically, the computational complexity and memory requirements of TD-AIM for the solution of volume integral equations are $O(N_t N_c \log(N_g N_c) \log N_g)$ and $O(N_g N_c)$, respectively, where $N_c$ is the number of nodes on the uniform mesh and $N_g$ is the maximum transit time in time steps across the scatterer (i.e., the length of the current history that has to be stored). For volume integral equations, $N_g \sim N_v^{1/3}$ and $N_c \sim N_v$.

0-7803-7846-6/03/$17.00 ©2003 IEEE

## Discrete Wavelet Transform Compression for Time Domain Integral Equations

Ali E. Yılmaz*, Jian-Ming Jin, and Eric Michielssen
Center for Computational Electromagnetics
Department of Electrical and Computer Engineering
University of Illinois at Urbana-Champaign, Urbana, IL 61801, USA

In recent years, various fast algorithms for accelerating the solution of time domain integral equations (TDIEs) have been proposed. Multilevel space-time FFT-based algorithms for accelerating TDIE solution schemes are particularly promising because they apply not only to free-space problems, but also, with minimal modifications, to layered, lossy, and dispersive media problems without significant increase in computational complexity. Whenever the Green's function has a temporal tail, the classical marching-on-in-time (MOT) analysis of a scattering problem requires $O(N_t N_s^2)$ memory and $O(N_t^2 N_s^2)$ operations for $N_t$ simulation time steps and $N_s$ spatial samples. FFT-based algorithms, on the other hand, exploit the space-time translational invariance of the integral kernel and reduce this memory requirement to $O(N_t N_c)$ and the computational complexity to $O(N_t N_c \log(N_t N_c) \log N_t)$. Here $N_c$ is either $N_s$ for uniform scatterer discretizations, or the numbers of nodes on an auxiliary projection mesh for nonuniform discretizations.

In practice, when the scatterer grows electrically large, the bottleneck of FFT-accelerated TDIE solvers is their storage requirement. While the overall memory requirement is better than that of classical MOT solvers ($N_c$ grows as at most $N_s^{3/2}$), the dependence on $N_t$ limits the duration of the analysis, thereby constraining the applicability of these methods to nonresonant scenarios. Here, we report on a discrete wavelet transform-based compression scheme that reduces the memory appetite of both classical MOT solvers and their FFT-based accelerators. In contrast to previous efforts to reduce the memory requirements of TDIE solvers—in which wavelets were used to compress either the MOT spatial memory demands or the spatio-temporal memory demands of global solvers—here, *wavelets are used to efficiently compress temporal waveforms within an MOT framework.* Such compression is possible because, for example, typical MOT solvers require the current waveforms to be heavily oversampled to obtain accurate solutions. However, this high sampling rate is not required to store past current values; in the end, they are represented by bandlimited waveforms. Specifically, while $O(N_t N_c)$ distinct values are required by the FFT-accelerated TDIE solvers (to store the impedance matrices, current history, and partially computed future field values), these values are *not* needed at all $N_c$ space- and $N_t$ time-points *simultaneously*. For example, at each spatial point the known current values can be uncompressed right before they are needed and compressed right after they are used. If this procedure were repeated at each time step, however, its complexity would be of $O(N_c N_t^2)$. Rather, a multilevel compression scheme is used that in structure matches the treatment of temporal FFTs in FFT-accelerated solvers: progressively larger blocks of currents are compressed at larger time-steps, and the larger the block the less often it is compressed. This leads to a complexity of $O(N_c N_t \log N_t)$ for the compression scheme.

0-7803-7846-6/03/$17.00 ©2003 IEEE

# A Parallel Marching on in Time Solver Accelerated by the Plane Wave Time Domain Algorithm

N. Liu[1]*, M. Lu[1], A. E. Yılmaz[1], K. Aygün[1], B. Shanker[2], and E. Michielssen[1]

[1] Center for Computational Electromagnetics, Department of Electrical and Computer Engineering, University of Illinois at Urbana-Champaign, Urbana, IL 61801, USA

[2] 2120 Engineering Building, Department of Electrical and Computer Engineering, Michigan State University, East Lansing, MI 48824, USA

nliu@emlab.uiuc.edu

Time domain integral equation (TDIE) solvers, while ideal candidates for analyzing broadband/nonlinear electromagnetic phenomena, rapidly become impractical for large-scale simulations because of their high computational complexity and memory requirements. Various fast algorithms have recently been proposed to overcome the computational burden of classical marching-on-in-time (MOT) solution of TDIEs. One such algorithm, the multilevel plane wave time domain (PWTD) method dramatically accelerates the solution for analysis of arbitrarily shaped scatterers (B. Shanker et al., *IEEE Trans. Antennas Propagat.*, to appear in Jan. 2003). In a PWTD enhanced MOT solver, at each time step, the computation of the fields (due to the previously calculated currents) is performed in two stages: The "near-field" interactions are evaluated directly; the "far-field" interactions are calculated by the PWTD algorithm by expressing the fields in terms of plane waves and efficiently propagating them using diagonal translation operators. To date, the PWTD-augmented MOT solvers have been successfully applied to accelerating analysis of large-scale scattering, radiation, electromagnetic compatibility, etc. on serial computing platforms.

Here a parallel paradigm is proposed to further increase the capabilities of the PWTD-accelerated MOT solvers. The efficiency of the parallel solver is directly related to the balanced distribution of the computational load and memory requirements among multiple processors. In the proposed scheme, the near-field computations are evaluated in parallel in a straightforward manner, whereas the far-field computations are distributed using a hybrid spatial/angular partitioning scheme. At the lower levels of the PWTD algorithm, the unknowns are divided among the processors according to their spatial locations, whereas higher-level plane waves are distributed according to their angles. The proposed scheme has been implemented on a distributed memory parallel cluster using the massage passing interface (MPI) for inter-processor communication and applied to a range of transient scattering problems to verify its accuracy and efficiency. Computational complexity, parallel speed-up, and timing results of these problems will be presented at the conference. In parallel to the above effort, a parallel FFT-based algorithm, the time domain adaptive integral method (TD-AIM), has been developed (A. E. Yılmaz et al., *URSI Digest*, 319, 2002). The second goal of this study is to give a thorough comparison of the TD-AIM and the multilevel PWTD algorithms in terms of their parallelization, and their theoretical and practical limitations.

0-7803-7846-6/03/$17.00 ©2003 IEEE

*Special Session*

**Remote Sensing from Space**
**Organizer(s):**
**Co-Chairs:** B. Reinisch
G. James

1:15 Opening Remarks

# An Ionospheric Topside-Sounder Investigation in Search of Unique Ionospheric Signatures of Earthquake Precursors

**R.F. Benson, J. M. Grebowsky, H. G. Mayr**
**NASA/Goddard Space Flight Center**

**S. Dent**
**Penn State University**

There have been published reports, received by the scientific community with considerable skepticism, of ionospheric electron-density ($N_e$) signatures associated with earthquake precursors. The signatures are attributed to a quasi-static electromagnetic coupling between enhanced atmospheric electric fields, which have been observed in seismoactive regions, and the ionosphere. A major problem in this research is to discriminate such effects from alternative causes of ionospheric variability. Intensive research efforts have been performed in Japan and Russia. Proponents claim that ionospheric signatures associated with seismic activity exist days before the main shock event. Here we report the results of an independent investigation of this topic based on ionospheric topside-sounder data available from the National Space Science Data Center (NSSDC), including newly-available ISIS-2 digital ionospheric topside-sounder data. While there were some suggestive trends observed in one case, in general no obvious ionospheric signatures of earthquake precursors were detected.

0-7803-7846-6/03/$17.00 ©2003 IEEE 

**Accuracy of the RPI plasmaspheric electron density profiles**

Xueqin Huang[1], Bodo W. Reinisch[1], Gary Sales[1], and James L. Green[2]
[1]University of Massachusetts Lowell Center for Atmospheric Research
600 Suffolk Street, Lowell MA 01854
[2]Goddard Space Flight Center, NASA

Profile inversion techniques have been developed to derive electron density profiles in the plasmasphere [Reinisch et al., GRL, 28, 1167, 2001] and the polar cap [Nsumei et al., JGR, in press, 2003] from echo traces on the plasmagrams recorded by the radio plasma imager (RPI) on the IMAGE satellite. Our analysis of the long-range discrete echo traces indicates propagation of the electromagnetic waves along the magnetic field line through the satellite location. This field-aligned propagation for frequencies above the electron plasma frequency could be caused by refraction and/or ducting due to field-aligned irregularities. To investigate which of these mechanisms dominates the guiding process, we are using ray-tracing techniques and simple duct shapes with adjustable parameters. The simulations are then compared with the discrete X-mode echo traces observed on the RPI plasmagrams, and the absence of O-mode echoes. If the refraction in a medium of changing electron density and magnetic field strength is the dominant guiding factor, the wave will be reflected at the location where the wave frequency equals the cutoff frequency of the magneto-plasma. If ducting is responsible for the field-aligned propagation, reflection will occur slightly before this location, depending on the percentage density enhancement of the duct walls. Results of these simulations and reference to the observed echoes will provide answers regarding the accuracy of the RPI electron density profiles, explain the observed field guidance, and, if applicable, determine the duct shape parameters.

1) Commission: G/H
Session: Remote Sensing from Space

2) New knowledge:
New ray-tracing program for the magnetosphere to simulate RPI observations

3) Relationship to previous work
a) Ray-tracing determines actual ray paths while previous work assumed field-aligned propagation
b) Objective is to explain the observed field-aligned propagation for $f > f_N$

0-7803-7846-6/03/$17.00 ©2003 IEEE 

RPI sounding as IMAGE skims the plasmapause: Ne from direct & ducted echoes and plasma resonances

R. F. Benson, P. A. Webb (NRC), J. L. Green, S. F. Fung
NASA/Goddard Space Flight Center
Greenbelt, Maryland

B. W. Reinisch, X. Huang
Center for Atmospheric Research
University of Massachusetts, Lowell
Lowell, Massachusetts

D. L. Carpenter
STAR Lab
Stanford University
Stanford, California

In early January 2003 the Radio Plasma Imager (RPI) on the Imager for Magnetopause-to Aurora Global Exploration (IMAGE) satellite performed numerous soundings in the plasmapause region as the outbound IMAGE skimmed along the dawn-side plasmapause boundary. Under these conditions it is possible for the electron cyclotron frequency at the satellite to decrease by an order of magnitude, while the electron plasma frequency fluctuates by less than 50%, over a 3/4 hr time interval along the IMAGE orbit. These values can be accurately determined from the RPI-stimulated electrostatic-wave plasma resonances and electromagnetic-wave cutoffs. The soundings in this region reveal a striking sequence of short-range diffuse echoes and long-range discrete echoes. These echoes have been interpreted as direct signal returns from the nearby plasmasphere and guided signals along the magnetic-field direction from the distant denser plasma region below the satellite, respectively [Reinisch et al., GRL, 28, 1167, 2001; Fung et al., Adv. Space Res., 30, 2259, 2002, Carpenter et al., JGR, in press, 2003]. The latter have been used to determine the electron-density ($N_e$) distribution along the magnetic-field direction [Reinisch et al., GRL, 28, 4521, 2001] and to make $N_e$ contours along the orbital path [Nsumei et al., JGR, in press, 2003]. Here we present results using plasma resonances and both the diffuse and discrete echoes to obtain local and remote $N_e$ information during outbound IMAGE dawn-side plasmapause skimming conditions.

0-7803-7846-6/03/$17.00 ©2003 IEEE 

# Measurement of the Direction of Arrival of Transionospheric HF Propagation

H.Gordon James
Communications Research Centre Canada
Ottawa, Ontario K2H 8S2 Canada
gordon.james@crc.ca

It is planned to observe waves from ground HF transmitters such as the Super Dual Auroral Radar Network (SuperDARN) radars and the Canadian Advanced Digital Ionosondes (CADI). The waves will be measured with the Radio Receiver Instrument (RRI) on the enhanced Polar Outflow Probe (e-POP) small satellite when it makes an orbital pass through the nearby topside ionosphere. One objective will be to use measurable quantities, such as the direction of arrival (DOA) and the signal delay time, to "image" the ionospheric structures that produce backscattered or reflected signals observed at those ground facilities. Such measurements would be coordinated with simultaneous recordings at the ground facilities.

Four monopoles connected to the 4-channel RRI will be used to record incident waves originating from the coordinated ground transmitters. Two components of the electric field are to be measured using the RF voltage induced on each of four crossed monopoles connected to high-impedance preamplifiers. Signals from opposite monopole pairs normally will be combined differentially and processed as a dipole signal.

This paper is concerned with the measurement of one important wave characteristic: the DOA. An important issue in the analysis of the received antenna signals is the computational method of determining the DOA from the amplitudes and relative phase of two dipole signals. The NEC4 electromagnetic model of the spacecraft with antennas provides values of the dipole effective lengths. These, in turn, are the basis of the technique for inverting the amplitude and relative phase of voltages induced on the monopoles to the DOA of the wave. This computation is required for elliptically polarized plane CW incident waves. The polarization of the wave electric field is provided by the cold-plasma theory. Expressions have been developed for the induced dipole voltages as functions of the wave-vector azimuthal and polar angles. A numerical approach is generally required for the DOA angles inversion. It is under-specified for only two dipoles, and requires selecting the true solution from two or more possible azimuth-polar pairs throughout the $4\pi$ sr solid-angle space surrounding the spacecraft. The selection of the solution will be guided by values expected for the known ground-transmitter and satellite positions, and by other wave parameter measurements.

0-7803-7846-6/03/$17.00 ©2003 IEEE 

# Magnetospheric Radio Tomography Experiments using IMAGE, WIND, and Cluster

S. A. Cummer*, Electrical and Computer Engineering Department, Duke University, Durham, NC 27708, USA (email: cummer@ee.duke.edu).

J. Green, Space Science Data Operations Office, NASA Goddard Space Flight Center, Greenbelt, Maryland, USA.

B. Reinisch, Center for Atmospheric Research, University of Massachusetts-Lowell, Lowell, Massachusetts, USA.

M. Kaiser, Laboratory for Extraterrestrial Physics, NASA Goddard Space Flight Center, Greenbelt, Maryland, USA.

M. Reiner, Physics Department, Catholic University of America, Washington, DC, USA.

R. Manning, Late of Observatoire de Paris, Meudon, France.

K. Goetz, School of Physics and Astronomy, University of Minnesota, Minneapolis, Minnesota, USA.

I. Christopher, R. Mutel, J. Pickett, D. Gurnett, Dept. of Physics and Astronomy, University of Iowa, Iowa City, Iowa, USA.

C. P. Escoubet, ESA/ESTEC,Noordwijk,The Netherlands.

To validate and demonstrate the potential of magnetospheric radio tomography, we have performed three separate experiments using the Radio Plasma Imager (RPI) on the IMAGE spacecraft as the signal source. The WAVES instrument on WIND and the WBD instruments on the four Cluster spacecraft were used as the wave receivers. These experiments were designed to measure the Faraday rotation of the transmitted wave electric field polarization due to propagation through a magnetized plasma. In the proper frequency range, Faraday rotation is proportional to the path-integrated product of the magnetospheric electron density and magnetic field, enabling large-scale measurements of these quantities on the propagation paths in each of these experiments. In August 2000, WAVES received a single frequency (828 kHz) RPI transmission. In October through December 2001, WAVES received two frequency (508 and 828 kHz) RPI transmissions. And in April 2002, WBD on Cluster received stepped frequency (between 100 and 500 kHz) RPI transmissions. Some of the RPI signals have been measured on propagation paths longer than 10 Re. By exploiting the time variation and frequency dependence of Faraday rotation, the integrated electron density/magnetic field product has been measured, with some limitations, in each of these experiments. We report on the novel large scale measurements of magnetospheric plasma and magnetic field generated by each of these radio propagation experiments. We also demonstrate, through these measurements, what quantities can be measured and how best to measure them on a dedicated radio tomography mission. These experiments have also shown that magnetospheric radio tomography can be implemented with existing instrument technology.

0-7803-7846-6/03/$17.00 ©2003 IEEE 

# Remote Sensing of Magnetospheric Plasma Density from the Analysis of Whistler Mode Echoes Received by RPI on IMAGE

V. S. Sonwalkar*, Electrical and Computer Engineering Department, University of Alaska Fairbanks, Fairbanks, AK 99775, USA (email: ffvss@uaf.edu)

D. L. Carpenter, Electrical Engineering Department, Stanford University, Stanford, CA 94305, USA (email: dlc@nova.stanford.edu)

J. Li, Electrical and Computer Engineering Department, University of Alaska Fairbanks, Fairbanks, AK 99775, USA (email: fsjl3@uaf.edu)

A. Venkatasubramanian, Electrical and Computer Engineering, University of Alaska Fairbanks, Fairbanks, AK 99775, USA (email: ftav@uaf.edu)

M. Spesojevic, T. F. Bell, Electrical Engineering Department, Stanford University, Stanford, CA 94305, USA (email: mystical@stanford.edu)

T. F. Bell, Electrical Engineering Department, Stanford University, Stanford, CA 94305, USA (email: bell@nova.stanford.edu)

U. S. Inan, Electrical Engineering Department, Stanford University, Stanford, CA 94305, USA (email: inan@nova.stanford.edu)

B. Reinisch, Center for Atmospheric Research, University of Massachusetts at Lowell, Lowell, MA 01854, USA (email: bodo_reinisch@uml.edu)

Whistler mode wave injection and reception using the RPI instrument on IMAGE satellite has led to a new remote sensing method to measure the plasma density and to locate and identify plasma density structures in the magnetosphere. During May – August 2000 period, RPI recorded discrete and diffuse whistler mode echoes on a number of days when IMAGE was in the inner plasmasphere and at moderate to low altitudes (<1500-6000 km) near its perigee in the southern hemisphere. The discrete echo is characterized by lightning-whistler-like discrete form whereas the diffuse echo is characterized by multiple echoes from a single transmission. Ray tracing simulations indicate that discrete echoes may result from reflections of RPI signals from the Earth-ionosphere boundary and diffuse echoes may result from scattering of RPI signals from small scale plasma density irregularities, commonly found in the high latitude magnetosphere. By comparing measured dispersion of RPI signals with those from ray tracing simulations it is possible to determine (1) the plasma density and (2) location and spatial size of irregularities responsible for diffuse echoes. The ray tracing analysis of observed dispersion of discrete echoes from several cases leads to electron density of ~500-1000 el/cc at ~4000 km with a $R^{-N}$, where N ~ 4-5, dependence in the auroral and polar magnetosphere. Analysis of diffuse echoes indicates presence of ~10-100 m scale plasma irregularities within ~1000 km of the IMAGE satellite at the time of observation. These results are in general consistent with previous observations of plasma density in the magnetosphere.

0-7803-7846-6/03/$17.00 ©2003 IEEE 

Radio sounding within Z-mode propagation "cavities" by the RPI instrument on the IMAGE satellite

D. L. Carpenter, T. F. Bell, U. S. Inan, Space, Telecommunications and Radioscience Laboratory, Stanford University, Stanford, California

R. F. Benson, NASA Goddard Space Flight Center, Greenbelt, Maryland

B. W. Reinisch, Center for Atmospheric Research, University of Massachusetts, Lowell, Massachusetts

When the Radio Plasma Imager (RPI) on the IMAGE satellite operates in the inner plasmasphere and at moderate to low altitudes over the polar regions, pulses emitted at the low end of its 3 kHz to 3 MHz sounding frequency range can propagate in the Z mode as well as the whistler mode. The Z mode is efficiently excited during almost all soundings in which all or part of its locally allowed frequency range falls within the band of transmitted frequencies. At medium altitudes within the plasmasphere, where the condition $f_{pe}>f_{ce}$ usually obtains, discrete Z-mode echoes are observed, analogous to the regular and oblique Z-mode echoes found on topside sounder records. Z-mode echoes from RPI can provide diagnostic plasma density information that is complementary to the information acquired by RPI from passive measurements of local plasma resonances and cutoffs and by inversion of O- and X-mode echoes. Within certain low to medium altitude regions, we find a Z-mode "cavity" within which discrete Z-mode echoes can be trapped as they propagate along field-line paths between upper and lower altitude reflection points. The echoes present unique forms, depending upon whether IMAGE is located above or below a minimum in the altitude profile of the Z-mode cutoff frequency. Through an inversion process, such echoes make possible remote determination of the field-line electron density profile in regions where that profile is poorly known. In an example, the electron density distribution along the field lines was determined to a distance of about 10,000 km above the location of IMAGE, all on the basis of echo delay information within a frequency band only ~ 40 kHz wide.

0-7803-7846-6/03/$17.00 ©2003 IEEE 

# Fast Z-Mode Propagation Observed on OEDIPUS C

Robert E. Horita
Department of Physics and Astronomy, University of Victoria
Victoria, British Columbia V8W 3P6, Canada
horita@phys.uvic.ca

H.Gordon James*
Communications Research Centre Canada
Ottawa, Ontario K2H 8S2 Canada
gordon.james@crc.ca

The OEDIPUS-C (OC) rocket double payload carried a transmitter High-frequency Exciter (HEX) on its forward subpayload and a synchronized Receiver for EXciter(REX) on its aft subpayload. The HEX and REX had three different frequency modes: a 0 - 8 MHz sweep, a 0.5 - 2.1 MHz sweep and fixed-frequency operation at 4.5 MHz. For the measurements discussed here, the separation vector between the transmitter and receiver had a magnitude of about 1200 m and lay along a direction at about 5° from the axis of the Earth's magnetic field **B**. Whistler, ordinary and extraordinary waves modes were propagated between the two subpayloads. One important feature was that fast Z-mode signals, left-hand polarized propagation occurring in CMA region 4, were strong compared to the adjacent wave modes. In particular, the intensity of the Z-mode signals was enhanced at frequencies just below the plasma frequency $f_p$ for low $f_p$ values but enhanced at frequencies just above the Z-mode cut-off frequency $f_Z$ for high $f_p$. Calculations were made combining the fast Z-mode dispersion relation for a cold plasma, HEX and REX characteristics, and theories for dipole radiation and impedance. Calculated values of transmitted electric fields are presented for zero and non-zero values of stray capacitance, with better agreement with observations with zero stray capacitance.

The relatively strong Z-mode transmissions on OC may have some relevance to other space radio research. The ability of sounders like the IMAGE/RPI to stimulate guided propagation giving rise to "epsilon" echo signatures may be explained with reference to the antenna properties in CMA4. Antenna matching to the plasma may be aided by the dipole's inductive impedance in CMA4. The Z-mode refractive index surfaces have points of inflection. These lead to three separate wave vector directions for a single group direction, which may also play a role in enhancing Z-mode signals through a dispersion-based focusing of rays near the inflection point.

0-7803-7846-6/03/$17.00 ©2003 IEEE 

# The USE OF RF WAVES IN SPACE PROPULSION SYSTEMS

Edgar A. Bering, III[1,2] *, Franklin Chang-Díaz[2], and Jared Squire[2]
[1]*University of Houston, Departments of Physics and Electrical and Computer Engineering, 617 Science and Research I, Houston, TX 77204-5005*
[2]*Advanced Space Propulsion Laboratory, NASA Johnson Space Center, 13000 Space Center Blvd., Houston, TX 77059*

This paper will review the ways in which rf and microwave radiation may be used in the design of electric propulsion systems for spacecraft. Rf power has been used or proposed in electric propulsion systems to ionize, to heat, and to accelerate the propellant, or to produce plasma used to inflate a magnetic field for solar sail purposes. Direct Rf propulsion using radiation pressure or ponderomotive forces is impractical owing to efficiency considerations. Examples of various systems that have been developed or proposed will be reviewed. The Variable Specific Impulse Magnetoplasma Rocket (VASIMR) uses RF for producing, heating and accelerating plasma. Inductive rf and microwave ion thruster schemes use e-m waves to ionize the plasma, which is then accelerated by use of dc grids. The details of the VASIMR and a microwave ion thruster will be discussed and contrasted with related RF systems.

0-7803-7846-6/03/$17.00 ©2003 IEEE 

**Numerical Analysis of Mechanisms of Spacecraft - Ionospheric Plasma Interaction**

V. G. Spitsyn
Department of Computer Engineering, Tomsk Polytechnic University,
84, Sovetskaya street, Tomsk, 634034, Russia,
Tel: +7 3822 418912, Fax: +7 3822 419149,
E-mail: spitsyn@ce.cctpu.edu.ru

We consider the disturbances of ionospheric plasma, created of spacecraft moving on the altitudes $\approx 200$ *km* from the earth surface. There is developed the method of numerical modeling of interaction of equilibrium ions of media with disturbed neutral particles (V.G. Spitsyn, *Modeling of radiowave scattering on the ionospheric plasma disturbances, created of space vehicle*, Tomsk: Publishing House "STT", 2002). On the base of solution of system kinetic equations for spacecraft disturbed neutral particles and ions ionosphere are received the numerical results of ionosperic plasma disturbances magnitude. These results are showing the initiation of concentration ions disturbance in a view of weakly shock wave.

The mechanism of ionospheric ionization produced of neutral particles reflected from moving spacecraft is investigated. In the result of solution the kinetic equation for born ions is received that for case of moving the spacecraft across the magnetic field the pattern of concentration ions disturbance is anisotropic. For the spacecraft with across dimension is equal to 2,4 *m* the maximum eventual value of ionization is 30000 $cm^{-3}$.

The process of ionospheric plasma interaction with spacecraft exhaust jet is investigated. There is modeling the process of ion ionospheric plasma diffusion in the exhaust jet of spacecraft. The results of computation are shown that the maximum of relative number of ionospheric ions disturbances is disposed in the area of near boundary of jet and consist of the value $\cong 5$. The effect of ion accumulation in this area is explained of ions braking in the gas jet. On the base of these results is developed a model of electron concentration disturbances, created of spacecraft exhaust jet.

0-7803-7846-6/03/$17.00 ©2003 IEEE

# Author Index

## C

## D



## E



## F

## G



## H

## I



## J



## K

## L

## M



## N

## O



## P



## Q



## R

## S

## T



## U



## V

## W



## X



## Y



## Z


2003

U.R.S.I.

A P S

IEEE